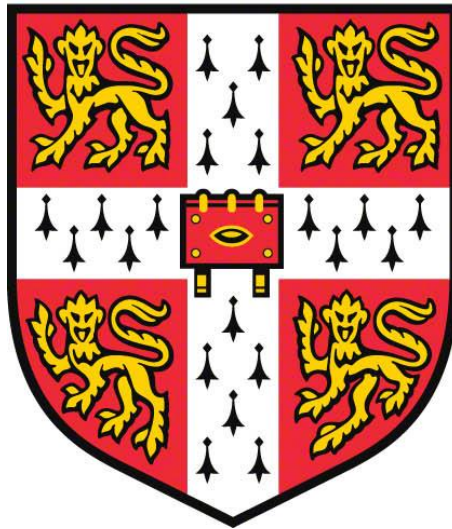


Inhibition of enzymes from mycobacteria using fragment-based approaches



Andrew John Whitehouse

Girton College

University of Cambridge

This dissertation is submitted for the degree of Doctor of Philosophy

June 2019

Declaration

This dissertation is the result of my own work and includes nothing which is the outcome of work done in collaboration except as declared in the Preface and specified in the text.

It is not substantially the same as any that I have submitted, or, is being concurrently submitted for a degree or diploma or other qualification at the University of Cambridge or any other University or similar institution except as declared in the Preface and specified in the text. I further state that no substantial part of my dissertation has already been submitted, or, is being concurrently submitted for any such degree, diploma or other qualification at the University of Cambridge or any other University or similar institution except as declared in the Preface and specified in the text.

It does not exceed the prescribed word limit for the relevant Degree Committee.

Summary

Inhibition of enzymes from mycobacteria using fragment-based approaches

The work described in this thesis is focused on the application of fragment-based approaches for two essential mycobacterial target proteins, fumarate hydratase (fumarase) from *Mycobacterium tuberculosis* (*Mtb*) and tRNA (m¹G37) methyltransferase (TrmD) from *Mycobacterium abscessus* (*Mab*). With *Mtb* fumarase a high-throughput screening (HTS) hit was used to design a small library of fragments in a deconstruction-reconstruction approach. These fragments were screened using a range of both biochemical and biophysical methods. The resultant fragments showed evidence of weak protein binding. As an alternative strategy, derivatives of the HTS hit were synthesised and screened by a biochemical assay, which identified nanomolar inhibitors of this enzyme. In addition, X-ray crystallography was also carried out with a range of these compounds. Selected compounds were subsequently screened by collaborators at the NIH against *Mtb*.

With the enzyme TrmD from *Mab*, the fragment hits identified were used as the basis of a fragment-merging approach to develop potent inhibitors, guided by structural biology. In the implementation of this approach, synthesis and biophysical techniques were extensively utilised, including both differential scanning fluorimetry and isothermal titration calorimetry. This approach led to the development of novel inhibitors with low nanomolar affinity. Select compounds were screened by collaborators against both *Mab* and *Mtb in vitro*. In light of encouraging activity against *Mtb*, the TrmD homolog in *Mtb* was expressed and screened against select compounds to demonstrate the broader applicability of the lead series.

Andrew John Whitehouse

June 2019

Acknowledgements

Firstly, I would like to thank my cosupervisors Prof. Chris Abell and Dr Anthony Coyne. I am grateful to Chris for providing me the opportunity to work in his research group and the freedom to learn and develop, whilst Anthony has been a consistent supportive presence in the laboratory and office over the course of my PhD. I am also grateful to the many members of the Abell and Leeper research groups that have come and gone over the past 4 years, providing an interesting and unique environment in which to work. In particular, I would like to highlight Dr Mohammad Sabbah, Dr Jeannine Hess, Dr Sitthivut Charoensutthivarakul, Dr Glyn Williams and Dr Martyn Frederickson for their tolerance and support in my day-to-day life.

Outside of the Chemistry Department, I would like to thank Prof. Tom Blundell and Prof. Andres Floto for providing me the opportunity to work on the TrmD project, and Dr Sherine Thomas for being a pleasure to collaborate with and producing an impressive amount of structural biology. I am grateful to Dr Marko Hyvönen for allowing me to work in his laboratory, and Dr Gerhard Fischer and Dr Paul Brear for providing help and training on X-ray crystallography for the fumarase project. I really appreciate the generosity of Prof. Angelika Gründling in the provision of material for *Mtb* TrmD studies, and Charlotte Millership for responding to my many questions. I would also like to thank Dr Karen Brown, Dr Daben Libardo and Dr Helena Boshoff for the screening of compounds against mycobacteria, which made a significant contribution to the narrative of my research.

Whilst several years have now passed, I would like to once again thank Dr Zoë Harrison and the other members of the RRI DPU at GlaxoSmithKline, in addition to Dr Elizabeth Grayson at Durham University, for support during my undergraduate studies that made the transition to PhD life possible.

Finally, I would like to thank the select group of family and friends who have been there for me over the years and made life more bearable. Hopefully the future will be better.

This work would not be possible without funding from the EPSRC.

Abbreviations

| | |
|---------|--|
| 7H9 | Middlebrook 7H9 broth |
| Ac | acetyl |
| ASL | anticodon stem loop |
| BSA | bovine serum albumin |
| CCP4 | collaborative computational project number 4 |
| CF | cystic fibrosis |
| cLogP | partition coefficient |
| CoA | coenzyme A |
| COMU | 1-cyano-2-ethoxy-2-oxoethylideneaminoxy)dimethylamino-morpholino-carbenium hexafluorophosphate |
| CPMG | Carr-Purcell-Meiboom-Gill |
| CTD | C-terminal domain |
| d | day(s) |
| Da | dalton |
| DCM | dichloromethane |
| DIBAL-H | diisobutylaluminium hydride |
| DIPEA | <i>N,N</i> -diisopropylethylamine |
| DMAP | 4-dimethylaminopyridine |
| DMF | <i>N,N</i> -dimethylformamide |
| DMSO | dimethyl sulfoxide |

| | |
|----------------------|--|
| DPPC | dipalmitoylphosphatidylcholine |
| DSF | differential scanning fluorimetry |
| <i>E. coli</i> | <i>Escherichia coli</i> |
| EDC | 1-ethyl-3-(3-dimethylaminopropyl)carbodiimide |
| ESI | electrospray ionisation |
| EtOAc | ethyl acetate |
| FBDD | fragment-based drug discovery |
| GAST-Fe | low-iron glycerol-alanine-salts |
| GE | group efficiency |
| h | hour(s) |
| <i>H. influenzae</i> | <i>Haemophilus influenzae</i> |
| HA | non-hydrogen ('heavy') atom |
| HEPES | 4-(2-hydroxyethyl)piperazine-1-ethanesulfonic acid |
| HIV | human immunodeficiency virus |
| HTS | high-throughput screening |
| IC ₅₀ | half-maximal inhibitory concentration |
| IMPDH | inosine-5'-monophosphate dehydrogenase |
| IPTG | isopropyl β-D-1-thiogalactopyranoside |
| ITC | isothermal titration calorimetry |
| K _d | equilibrium dissociation constant |
| LDA | lithium diisopropylamide |

| | |
|---------------------|---|
| LE | ligand efficiency |
| Lp-PLA ₂ | lipoprotein-associated phospholipase A2 |
| <i>Mab</i> | <i>Mycobacterium abscessus</i> |
| MDR | multidrug-resistant |
| Me | methyl |
| MIC | minimum inhibitory concentration |
| min | minute(s) |
| <i>Mj</i> | <i>Methanocaldococcus jannaschii</i> |
| <i>Mtb</i> | <i>Mycobacterium tuberculosis</i> |
| <i>Mth</i> | <i>Mycobacterium thermoresistibile</i> |
| NAD ⁺ /H | nicotinamide adenine dinucleotide oxidised/ reduced |
| ND | not determined |
| NMR | nuclear magnetic resonance |
| NOE | nuclear Overhauser effect |
| NTD | <i>N</i> -terminal domain |
| NTM | non-tuberculous mycobacteria |
| PDB | protein data bank |
| PEG3350 | polyethylene glycol (average M _n 3,350 Da) |
| PET | petroleum ether |
| PI3K | phosphoinositide-3-kinase |
| RNA | ribonucleic acid |

| | |
|----------------|---|
| RR | rifampicin-resistant |
| rt | room temperature |
| SAH | S-adenosyl-L-homocysteine |
| SAM | S-adenosyl-L-methionine |
| SAR | structure-activity relationship |
| SPOUT | SpoU-TrmD |
| STD | saturation transfer difference |
| T3P® | propylphosphonic anhydride |
| TB | tuberculosis |
| TBAF | tetra- <i>n</i> -butylammonium fluoride |
| TBDMS | <i>tert</i> -butyldimethylsilyl |
| TBDPS | <i>tert</i> -butyldiphenylsilyl |
| TCEP | tris(2-carboxyethyl)phosphine |
| TFA | trifluoroacetic acid |
| TFAA | trifluoroacetic anhydride |
| THF | tetrahydrofuran |
| THP | tetrahydropyranyl |
| T _m | thermal melting temperature |
| Tris | tris(hydroxymethyl)aminomethane |
| TrmD | tRNA (m ¹ G37) methyltransferase |
| tRNA | transfer ribonucleic acid |

| | |
|------------|---|
| Ts | <i>p</i> -toluenesulfonyl |
| XDR | extensively drug-resistant |
| w | week(s) |
| waterLOGSY | water-ligand observed via gradient spectroscopy |

Contents

| | |
|--|-----|
| Declaration..... | i |
| Summary..... | ii |
| Acknowledgements | iii |
| Abbreviations | iv |
| 1: Introduction | 1 |
| 1.1: Mycobacterial Infection | 1 |
| 1.1.1: <i>Background</i> | 1 |
| 1.1.2: <i>Mycobacterium tuberculosis</i> | 1 |
| 1.1.3: <i>Mycobacterium abscessus</i> | 2 |
| 1.2: New Targets of Interest..... | 5 |
| 1.2.1: Fumarate hydratase | 5 |
| 1.2.2: tRNA (m ¹ G37) methyltransferase | 11 |
| 1.3: Fragment-based Drug Discovery | 16 |
| 1.3.1: Background | 16 |
| 1.3.2: Biophysical Techniques | 17 |
| 1.3.3: Fragment Elaboration..... | 20 |
| 1.4: Project Aims..... | 23 |
| 2: Fumarate Hydratase | 25 |
| 2.1: Project Setup | 25 |
| 2.1.1: Synthesis and Screening of High-throughput Screening Hit 2 | 25 |
| 2.1.2: X-ray Crystallography | 28 |
| 2.2: Defragmentation of High-throughput Screening Hit 2 | 30 |
| 2.2.1: Library Design | 30 |
| 2.2.2: Library Synthesis | 31 |
| 2.2.3: Library Screening..... | 34 |

| | |
|---|-----|
| 2.3: Structure-activity Relationship Study of 2 | 37 |
| 2.3.1: Analogue Synthesis | 37 |
| 2.3.2: Screening against Target Protein | 41 |
| 2.3.3: Screening against <i>Mycobacterium tuberculosis</i> | 52 |
| 2.4: Summary and Future Work | 54 |
| 3: tRNA (m ¹ G37) methyltransferase..... | 56 |
| 3.1: Fragment Hits and Initial Elaboration Approaches..... | 56 |
| 3.1.1: Fragment-growth Approach with Hit 50 | 58 |
| 3.1.2: Fragment-merging Approach with Hits 53 and 59 | 60 |
| 3.1.3: Synthesis and Screening of 62 and 66a | 64 |
| 3.2: Development of the 3-Aminopyrazole Lead Series | 67 |
| 3.2.1: Optimisation of the Phenyl Ring of 66a | 68 |
| 3.2.2: Exploration of Substitution from the Pyrazole 4-Position..... | 73 |
| 3.2.3: Structure-activity Relationship Study of 71f and Pyridyl Isomers | 76 |
| 3.2.4: Incorporation of Increased sp ³ -content in the Scaffold | 85 |
| 3.2.5: Structure-activity Relationship Study of 103a | 97 |
| 3.2.6: Screening against Mycobacteria and Optimisation for Activity | 102 |
| 3.3: Investigation of <i>Mycobacterium tuberculosis</i> tRNA (m ¹ G37) methyltransferase | 106 |
| 3.3.1: Protein Expression and Screening by Isothermal Titration Calorimetry | 107 |
| 3.3.2: Screening by Differential Scanning Fluorimetry | 108 |
| 3.4: Summary and Future Work | 109 |
| 4: Experimental Methods | 111 |
| 4.1: Synthetic Chemistry | 111 |
| 4.1.1: General Chemistry | 111 |
| 4.1.2: Methods and Characterisation Data for Screened Compounds..... | 112 |
| 4.2: Protein Expression and Purification..... | 154 |

| | |
|--|-----|
| 4.2.1: <i>Mycobacterium tuberculosis</i> fumarate hydratase | 154 |
| 4.2.2: <i>Mycobacterium abscessus</i> tRNA (m ¹ G37) methyltransferase | 155 |
| 4.2.3: <i>Mycobacterium tuberculosis</i> tRNA (m ¹ G37) methyltransferase..... | 155 |
| 4.3: Biochemical Assay with <i>Mycobacterium tuberculosis</i> fumarate hydratase..... | 156 |
| 4.4: Biophysical Techniques | 156 |
| 4.4.1: Differential Scanning Fluorimetry | 156 |
| 4.4.2: Isothermal Titration Calorimetry | 157 |
| 4.5: X-ray Crystallography with <i>Mycobacterium tuberculosis</i> fumarate hydratase | 157 |
| 4.5.1: Seed Stock..... | 157 |
| 4.5.2: Crystal Growth and Soaking..... | 158 |
| 4.5.3: X-ray Data Collection and Processing..... | 159 |
| 4.5.4: Structure Solution and Refinement | 159 |
| Appendix: Supporting Data | 160 |
| A.1: Methods and Characterisation Data for Non-key Compounds..... | 160 |
| A.2: Biochemical Assay Dose-response Curves | 214 |
| A.3: Isothermal Titration Calorimetry Traces..... | 221 |
| A.4: X-ray Crystallography Statistics | 228 |
| References | 229 |

1: Introduction

1.1: Mycobacterial Infection

1.1.1: *Background*

The genus *Mycobacterium* comprises a large number of diverse bacterial species, ranging from the well characterised slowly-growing pathogens *Mycobacterium tuberculosis* (*Mtb*) and *Mycobacterium leprae*, to the non-tuberculous mycobacteria (NTM) that are the focus of increasing scientific study.¹ Mycobacteria are characterised by a complex cell envelope, with hydrophobic mycolic acids attached to the underlying peptidoglycan layer through a branched arabinogalactan polysaccharide network.² These long chain fatty acids intercalate with other lipids to form an outer membrane that provides a permeability barrier for mycobacteria.^{3, 4} If compounds do traverse the mycobacterial cell envelope, efflux pumps are extensively utilised to actively transport toxic molecules out of the cell,^{5, 6} making the targeting of mycobacteria a challenging task.

1.1.2: *Mycobacterium tuberculosis*

Mtb is the causative agent of the disease tuberculosis (TB), which maintains a significant global impact in the 21st century with 10 million new cases diagnosed annually, 9% of which are in combination with HIV. With 1.3 million directly attributed deaths in 2017, in addition to 300,000 associated deaths in HIV-positive individuals, TB remains the leading worldwide cause of death due to a single infectious agent.⁷

TB infection begins with the inhalation of *Mtb*-containing aerosol into the alveoli of the lungs where resident macrophages internalise the bacteria through phagocytosis, however *Mtb* is capable of interfering with the fusion of the phagosome with the lysosome and avoiding degradation. Disruption of the enclosing phagosomal membrane enables the release of material into the cytosol, with subsequent spread of the infection beyond the alveoli to the lung parenchyma initiating the recruitment of immune cells.⁸ These cells aggregate to form granulomas, organised and compact structures that surround the infected cells in a necrotic centre, in which *Mtb* can persist in a contained state.⁹ The possession of these structures is a hallmark of asymptomatic and non-transmissible latent TB infection,¹⁰ a condition that is exhibited by 1.7 billion people worldwide.¹¹ In the event that granuloma-mediated containment fails, active TB disease can disseminate throughout the body with the symptoms of fatigue, fever, weight loss and coughing, which can transmit infectious material to new hosts, commonly observed.⁸ In the absence

of chemotherapy, active TB disease is associated with high mortality rates in patients even without the additional complication of HIV,¹² underlining the essentiality of effective anti-TB treatments.

The standard recommended treatment regimen for TB includes an initial intensive phase of isoniazid, rifampicin, ethambutol and pyrazinamide over 2 months, followed by 4 months of continuation therapy with isoniazid and rifampicin (Figure 1).¹³

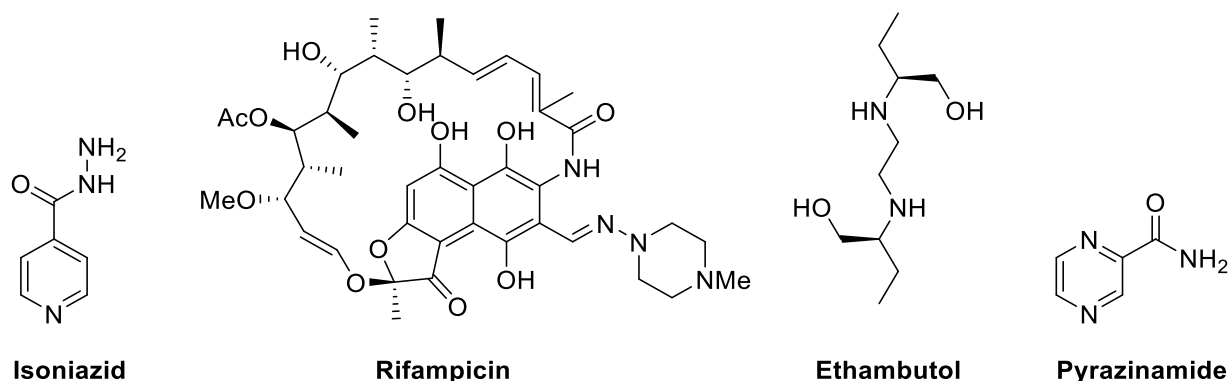


Figure 1: First-line drugs recommended for the treatment of drug-susceptible TB infection.¹³

Worryingly, the effectiveness of antibiotics against TB is in decline with increasing worldwide prevalence of rifampicin-resistant (RR) and multidrug-resistant (MDR) TB, the latter possessing resistance to both rifampicin and isoniazid, with 558,000 cases and 230,000 deaths reported in 2017 due to RR- and MDR-TB.⁷ The treatment of these drug-resistant strains requires longer regimens with additional second-line anti-TB drugs, with conditional recommendation provided for the use of pyrazinamide in combination with a fluoroquinolone, an injectable agent and two alternative antibiotics.¹⁴ However, as with the first-line anti-TB drugs, extensively drug-resistant (XDR) TB strains are now also emerging that display additional resistance to the second-line drugs.⁷ In light of the worsening issue of drug-resistant strains of TB, the development of novel antibiotics with orthogonal mechanisms of action to current anti-TB drugs is urgently required.¹⁵

1.1.3: *Mycobacterium abscessus*

Mycobacterium abscessus (*Mab*) is an NTM that derived its name by its discovery from a knee abscess in 1952. This infection had persisted for 48 years in a semi-dormant state after the initial trauma in a farmyard, with surgical intervention in the patient leading to reactivation and dissemination to other parts of the body.¹⁶ *Mab*, which is characterised by rapid growth and a rod-like profile of 1.0 to 2.5 μm in length by 0.5 μm in width, was considered a subspecies of *Mycobacterium chelonae* before being reclassified as

an independent NTM species in 1992.¹⁷ The species can itself be divided into the subspecies *abscessus*, *bolletii* and *massiliense*,¹⁸ which have been shown to exhibit similar clinical behaviour albeit with some difference in antibiotic susceptibility.¹⁹ This behaviour is reflected in the *Mab* genome, with a bias towards genes involved in intracellular parasitism and survival in soil and water, in addition to displaying evidence of horizontal gene transfer from pathogens associated with cystic fibrosis (CF) including *Pseudomonas aeruginosa* and *Burkholderia cepacia*.²⁰

Mab is an opportunistic pathogen that can cause a variety of disease types in humans, including infection of the eyes, bloodstream and central nervous system. It is however most commonly associated with skin and soft tissue infections, induced either directly through the contact of wounds with contaminated material or indirectly by disseminated disease, in addition to infection of the respiratory tract in patients with preexisting pulmonary disease.²¹ In general, *Mab* pulmonary disease results in the observance of chronic coughing and a susceptibility to fatigue in patients,²² with imaging of the lungs revealing bronchiectasis and the development of nodules.²³ When present in patients with underlying CF, this infection is correlated with an accelerated decline in lung function over time and therefore an impaired quality of life.^{24, 25} This phenomenon is of increasing concern in light of indirect transmission of *Mab* infection occurring between CF patients in hospitals despite the enforcement of segregation, potentially through the ability of *Mab* to persist both on surfaces (fomite) and within aerosols.^{26, 27} These transmitted infections, which are more virulent than those acquired from the environment due to prior genetic adaptation within hosts, worryingly constitute the majority of *Mab* infections in CF patients.²⁷

Mab possesses high intrinsic resistance to chemotherapy, including anti-*Mtb* drugs, making the treatment of infection particularly challenging relative to other mycobacteria. This intrinsic resistance is caused by the confluence of a variety of features in the species, including the impermeable mycobacterial cell envelope, efflux mechanisms, antibiotic- and target-modifying enzymes and the genetic polymorphism of target genes, in addition to *Mab's* ability to acquire resistance through the spontaneous mutation and modification of these genes.²⁸ As a result, treatment of *Mab* infection requires the sustained use of combination therapy with multiple antibiotics taken in parallel over long periods of time.²² This is reflected in the current recommended treatment regimen for *Mab* infection in CF patients, which supports prolonged implementation with the aim of improving symptoms and inducing regression of the disease. This regimen begins with an initial intensive phase lasting up to 3 months, depending on patient tolerance, that includes the oral macrolide azithromycin in combination with intravenous application of

the aminoglycoside amikacin and at least one of the antibiotics cefoxitin, imipenem or tigecycline (Figure 2).²⁹

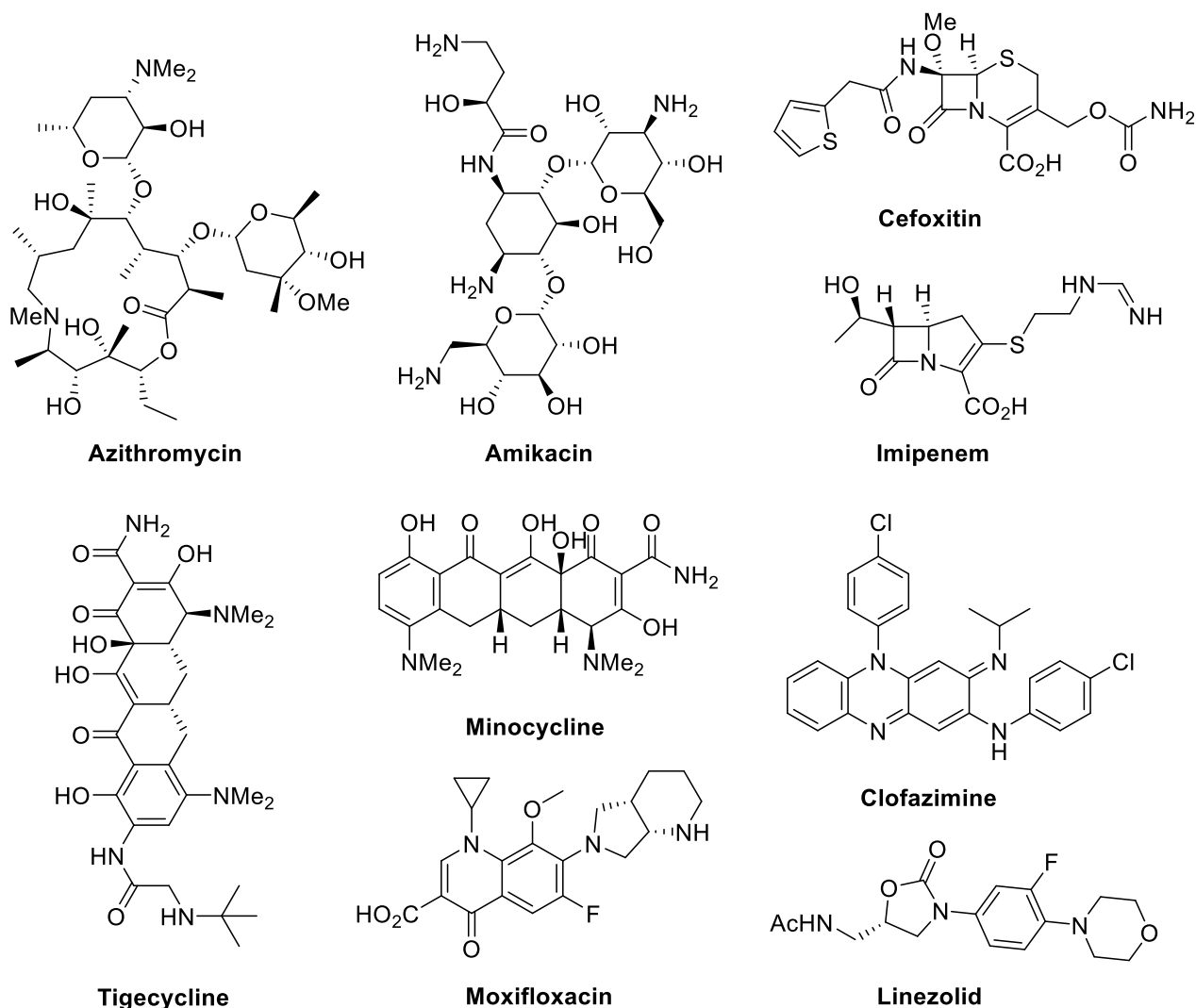


Figure 2: Drugs recommended for inclusion in combination therapy for the treatment of *Mab* infection in CF patients.²⁹

The intensive phase of treatment of *Mab* infection in CF patients is followed by a continuation phase over the long term, with further azithromycin in combination with inhaled amikacin and 2 to 3 of the oral antibiotics minocycline, moxifloxacin, clofazimine or linezolid (Figure 2). In the event that success in disease eradication is suggested, continued application of antibiotic therapy is still recommended for a year.²⁹ This outcome though is not guaranteed and numerous side effects are associated with the antibiotics in this therapy,²⁹ which can result in the modification or cessation of treatment.³⁰ Hence, there is a need for the development of novel antibiotics with improved efficacy against *Mab* infection, particularly for the treatment of afflicted CF patients.

1.2: New Targets of Interest

1.2.1: Fumarate hydratase

Fumarate hydratase (fumarase) is an enzyme in the citric acid cycle, a system that is utilised in energy generation and the connection of numerous biosynthetic pathways in aerobic organisms including mycobacteria, where it catalyses the reversible interconversion of L-malate and fumarate (Figure 3a).^{31, 32}

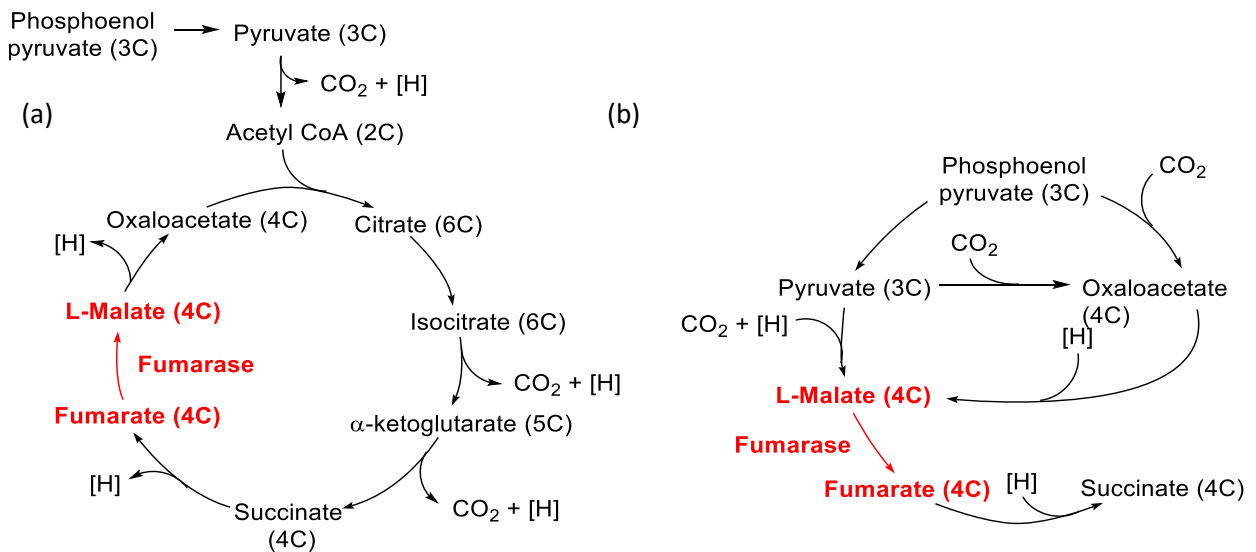


Figure 3: Proposed operation of the citric acid cycle in *Mtb* with involvement of *Mtb* fumarase during (a) aerobic conditions,³² and (b) anaerobic conditions.³³

The citric acid cycle has also received attention for its role in facilitating *Mtb* survival in a non-replicating state under hypoxic conditions through operating in the reverse direction. Reduced cofactors accumulate within *Mtb* cells in the absence of oxygen as a terminal electron acceptor, with relief provided through the excretion of succinate produced by reductive derivatives of the citric acid cycle (Figure 3b).^{33, 34} Under these conditions, which closely mimic the hypoxic conditions of granulomata in latent TB infection, expression of *Mtb* fumarase is upregulated,³³ making it a potential target of interest for treatment of latent infection.

Mtb fumarase is a vulnerable target as it is the only protein that *Mtb* expresses to carry out its function in direct contrast to other sections of the citric acid cycle,^{31, 33} a situation that is not guaranteed in bacteria,³⁵ and has been shown to be essential for *Mtb* survival.³⁶ This essentiality was determined in a conditional knockdown mutant of *Mtb* to be linked to intracellular accumulation of fumarate, which can

react as an electrophile with cysteine thiols of proteins and metabolites. The inactivation of antioxidants catalase and mycothiol by covalent modification with fumarate induces hypersensitivity to oxidative stress in *Mtb* (Figure 4), leading to impaired growth and cell death *in vitro* and in mouse infection models.³⁷

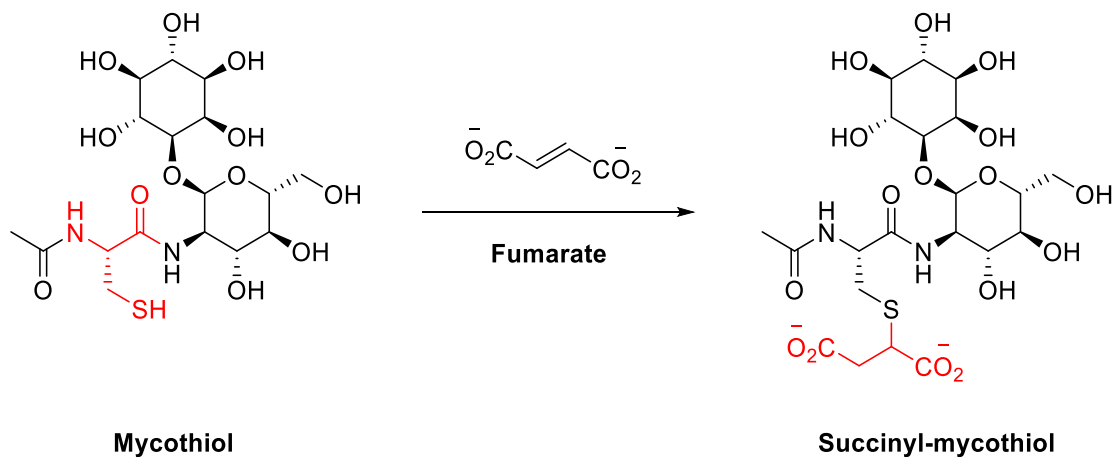


Figure 4: Covalent modification of mycothiol by fumarate.³⁷

Bacteria have been observed to express fumarases from structurally distinct protein families, with homodimeric Class I fumarases exhibiting thermolability and iron-dependence in contrast to those belonging to Class II that are homotetrameric and thermostable.³⁵ *Mtb* fumarase belongs to Class II,³⁸ with a structure consistent with previously characterised bacterial fumarases of this class (Figure 5a).³⁹ The *N*-terminal domain (NTD) of the subunits in the *Mtb* fumarase homotetramer begins with a 2-stranded antiparallel beta sheet, followed by a compact collection of 5 alpha helices up to residue 137. This is succeeded by a central domain from residues 138 to 393, including 5 alpha helices oriented parallel to each other over ~ 40 Å, and a conformationally flexible assembly of 6 short alpha helices in the *C*-terminal domain (CTD) from residue 394 onwards (Figure 5b).³⁸

The homotetramer of *Mtb* fumarase can be considered to be assembled from two dimers, each consisting of two subunits in a ‘head-to-head’ orientation joined by contacts at the top of the central domain with the central and *C*-terminal domains of the other subunit (Figure 5c). The arrangement of these dimers in a ‘head to tail’ orientation then completes the homotetramer, which is held together by extensive interactions between the alpha helices of the central domains in an elongated 20-helix bundle (Figure 5d).^{38, 39} The complex quaternary structure is essential for catalytic activity, with *Mtb* fumarase possessing 4 symmetry-related active sites located in clefts each with contributions from 3 subunits (Figure 5a and Figure 6a).^{38, 40}

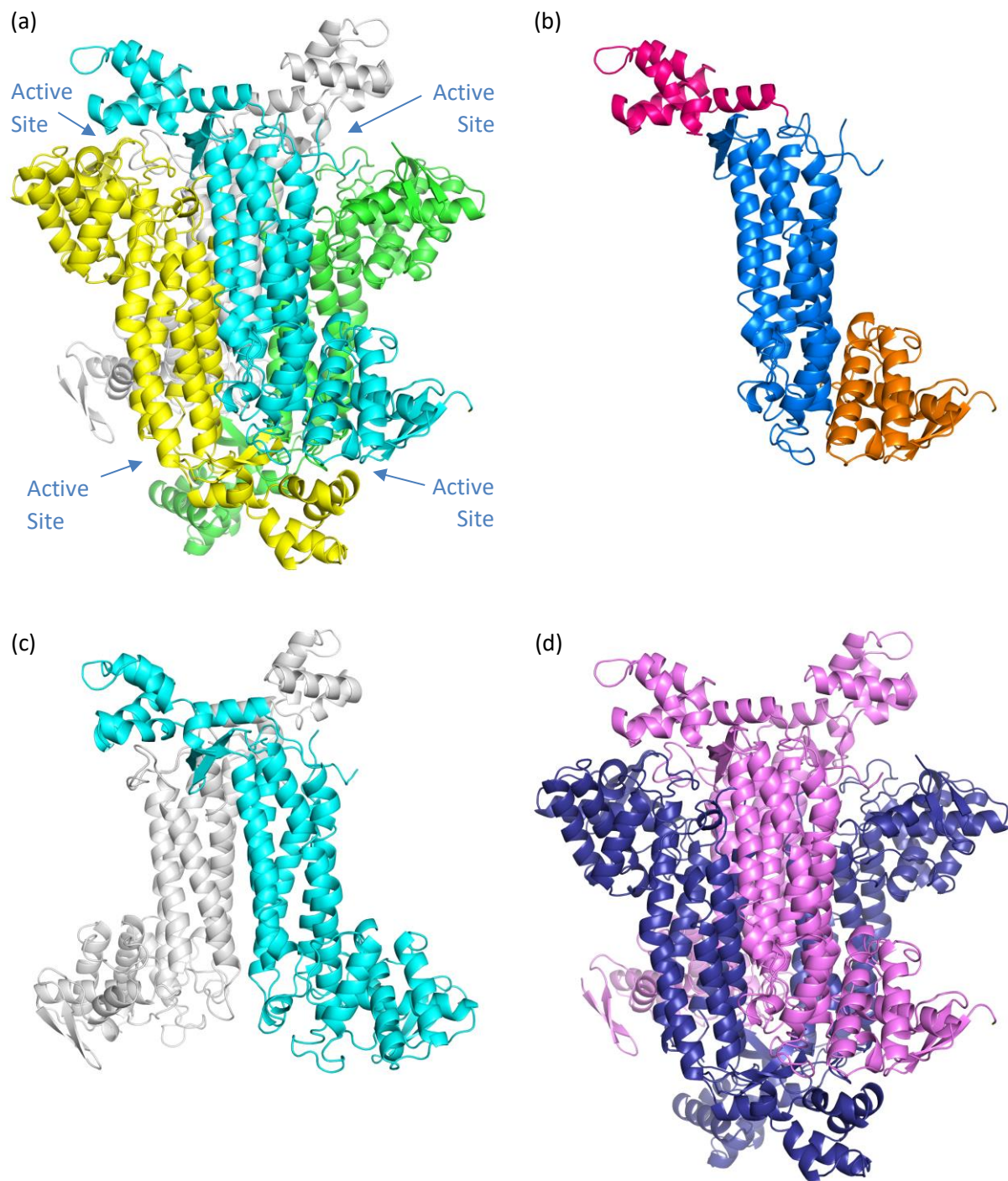


Figure 5: X-ray crystal structure of *Mtb* fumarase bound to formate (PDB code 5F92, 1.86 Å), illustrating (a) the four subunits of the homotetramer (subunit A = white, subunit B = green, subunit C = cyan, subunit D = yellow), (b) one of the subunits further subdivided into three domains (NTD = orange, central domain = blue, CTD = red), (c) the head-to-head arrangement of two subunits (subunit A = white, subunit C = cyan), and (d) the head to tail arrangement of subunit pairs in the homotetramer (dimer 1 = pink, dimer 2 = purple).⁴¹

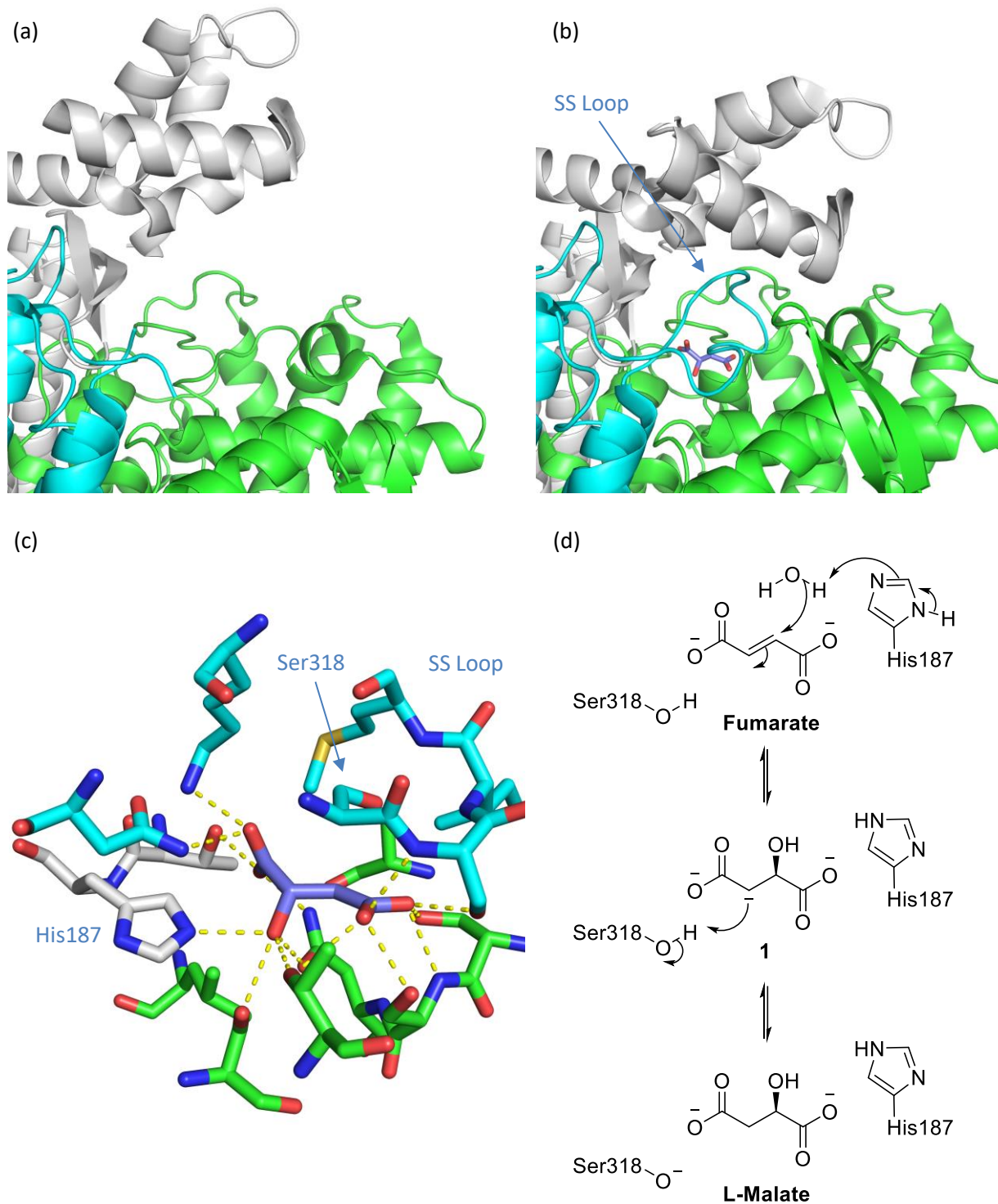


Figure 6: X-ray crystal structures of Mtb fumarase (subunit A = white, subunit B = green, subunit C = cyan, subunit D not visible), with the apo form (PDB code 4APA, 2.04 Å) illustrating (a) the active site in the open conformation, and the L-malate bound form (PDB code 4ADL, 2.20 Å, L-malate = lilac) illustrating (b) the active site in the closed conformation, and (c) the residues surrounding L-malate;³⁸ (d) a proposed mechanism of catalysis for Mtb fumarase.³⁸

The active sites of *Mtb fumarase* share sequence identity and a similar mechanism of action with other members of the wider aspartase/fumarase superfamily that release fumarate as a product.^{38, 42} In the event of substrate binding the loop from residues 316 to 325, the 'SS' loop, undergoes movement from an 'open' state, where the active site is exposed and accessible (Figure 6a), to a 'closed' state that covers the site and brings several residues in contact with the substrate (Figure 6b). When this state is reached the conversion of substrate is suggested to proceed through a two-step acid-base process with the generation of an enediolate intermediate **1**, utilising the conserved residues Ser318 and His187 that are in close proximity to the C α and C β atoms of the substrate (Figure 6c and d).^{38, 42} Further, in *Mtb fumarase* the movement of the 'SS' loop, which is disordered in the open state, has been shown to be dependent on the flexibility of the CTD, which exhibits significant rotation on substrate binding (Figure 6a and b).³⁸

Inhibitors of fumarase have previously been found that demonstrated dose-dependent effects on cell growth,⁴³ underlining its vulnerability, however a key concern in its use as a target for the development of antibacterial compounds is selectivity against the human homolog. Human and *Mtb fumarase* share the same quaternary structure and around 52% sequence identity, which increases to complete conservation of residues in the active site.^{38, 44} This issue was recently circumvented with the discovery of an inhibitor **2** (Figure 7a) of *Mtb fumarase* that binds twice in an allosteric site at the subunit head-to-head interface (Figure 7b and c) (Monica Kasbekar, Department of Chemistry, University of Cambridge), locking the neighbouring CTDs in place and preventing SS loop movement on substrate binding (Figure 7c).⁴¹

The residues to which **2** binds in *Mtb fumarase* are not conserved with the human homolog, conferring demonstrable selectivity. Unfortunately **2** was not able to induce a measurable minimum inhibitory concentration (MIC) against *Mtb* growth *in vitro*, however its selectivity against human fumarase,⁴¹ in conjunction with the essentiality of fumarase to *Mtb*,^{36, 37} supports further study.

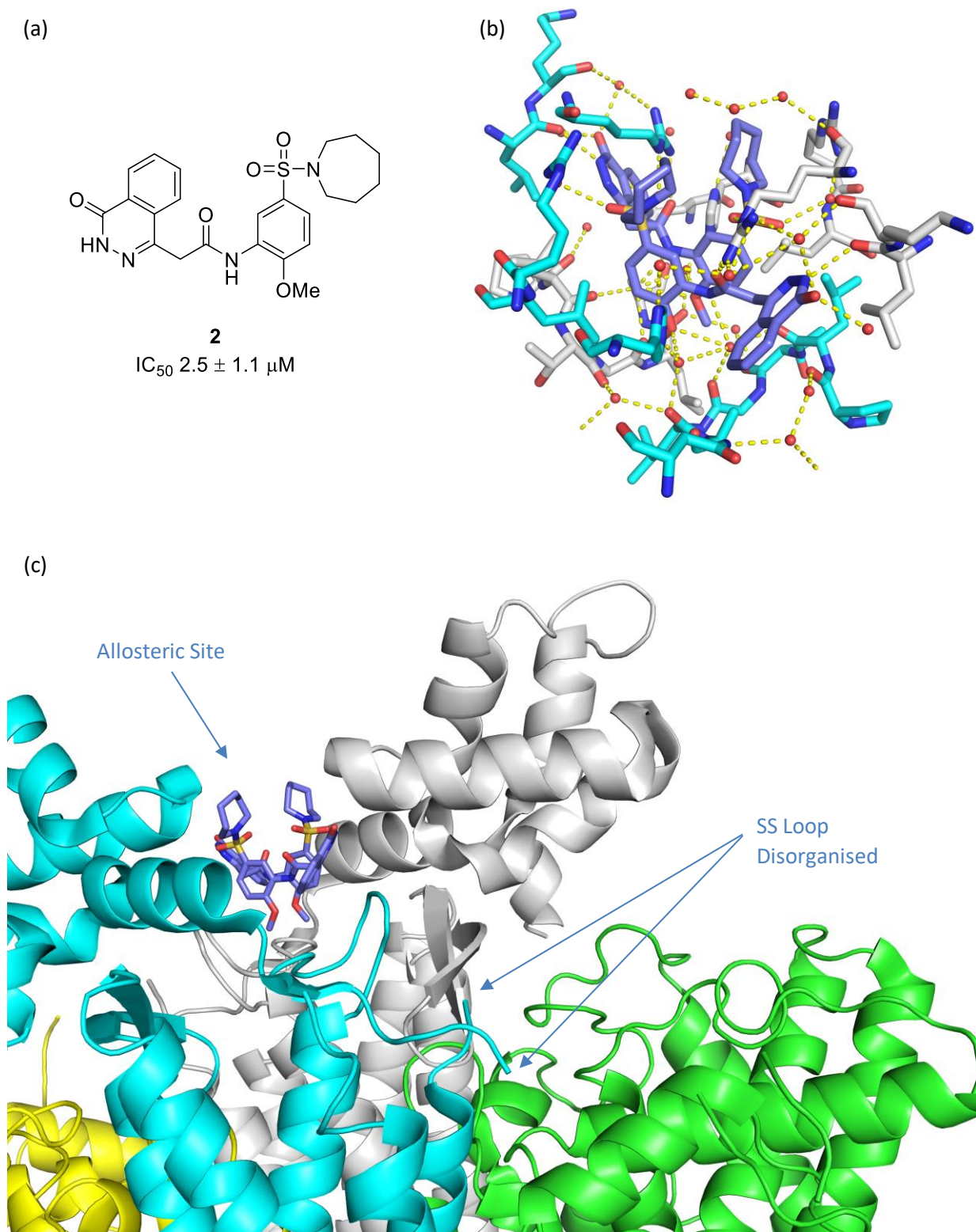


Figure 7: (a) Inhibitor **2**, identified by HTS of fumarase from Mtb;⁴¹ X-ray crystal structure of Mtb fumarase bound to **2** (PDB code 5F91, 2.00 Å, subunit A = white, subunit B = green, subunit C = cyan, subunit D = yellow, **2** = lilac), illustrating (b) the dual binding mode of **2** in the allosteric site and (c) the location of the allosteric site and the open conformation of the adjacent active site.⁴¹

1.2.2: tRNA (m¹G37) methyltransferase

tRNA (m¹G37) methyltransferase (TrmD) is a bacterial protein that belongs to the SpoU-TrmD (SPOUT) superfamily of RNA methylases.⁴⁵ TrmD is responsible for post-transcriptional modification of tRNA molecules containing the sequence G36 – G37,⁴⁶ catalysing the addition of a methyl group from the cofactor *S*-adenosyl-L-methionine (SAM) to the N1 atom of G37 (m¹G37) (Figure 8).

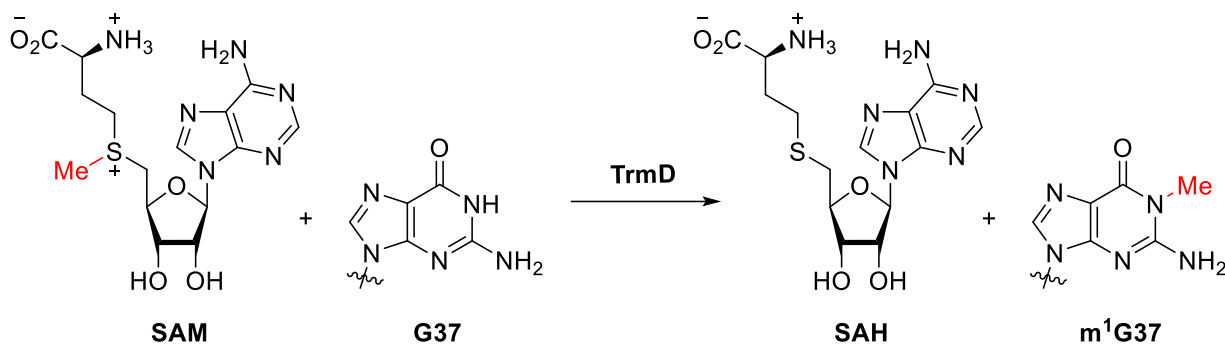


Figure 8: Transfer of the methyl group of SAM by TrmD to G37, forming *S*-adenosyl-L-homocysteine (SAH) and m¹G37.

The nucleotide G37 lies immediately 3' to the anticodon in these tRNA molecules, and its methylation increases the efficiency of protein translation through a reduction in the frequency of +1 frameshifting errors on the ribosome that result in inactive peptides.⁴⁷ This has been shown to occur through suppression of two mechanisms depending on both the identity of the tRNA molecule and the position of the codon in the open reading frame. These involve a +1 frameshift of tRNA during translocation between the A and P sites of the ribosome, and whilst stalled on the P site during a delay in occupation of the A site by a new molecule.⁴⁸ The molecular basis of the effect of m¹G37 on these mechanisms has been suggested by X-ray crystal structures of the ribosome in complex with the anticodon stem loop (ASL) of tRNA^{Pro}. When m¹G37 is present an intramolecular base pairing between U32 and A38 is observed in the ASL, however this is not visible in its absence due to poor density at nucleotides 30 to 32.⁴⁹ Hence, the m¹G37 modification could be reducing the risk of frameshifting through the promotion of preorganisation within the tRNA ASL, which could lead to improved intermolecular interactions on the ribosome.^{48, 49} Importantly, the presence of a functional TrmD gene has been demonstrated to be essential for normal cellular function in mycobacteria, including *Mtb* and *Mab*,^{24, 50} making TrmD an attractive target protein for further study.

Members of the SPOUT superfamily are dimeric in nature, with significant buried surface area, and share conserved structural features. These include a 'common core' in each subunit consisting of a 5-stranded parallel beta sheet flanked by two layers of alpha helices, in addition to deep active sites defined by a

complex arrangement of loops termed a 'trefoil knot'.⁵¹ These are represented in the TrmD homodimer, with SPOUT common cores in the NTDs oriented antiparallel to each other around a 2-fold rotation axis (Figure 9a).^{52 - 54}

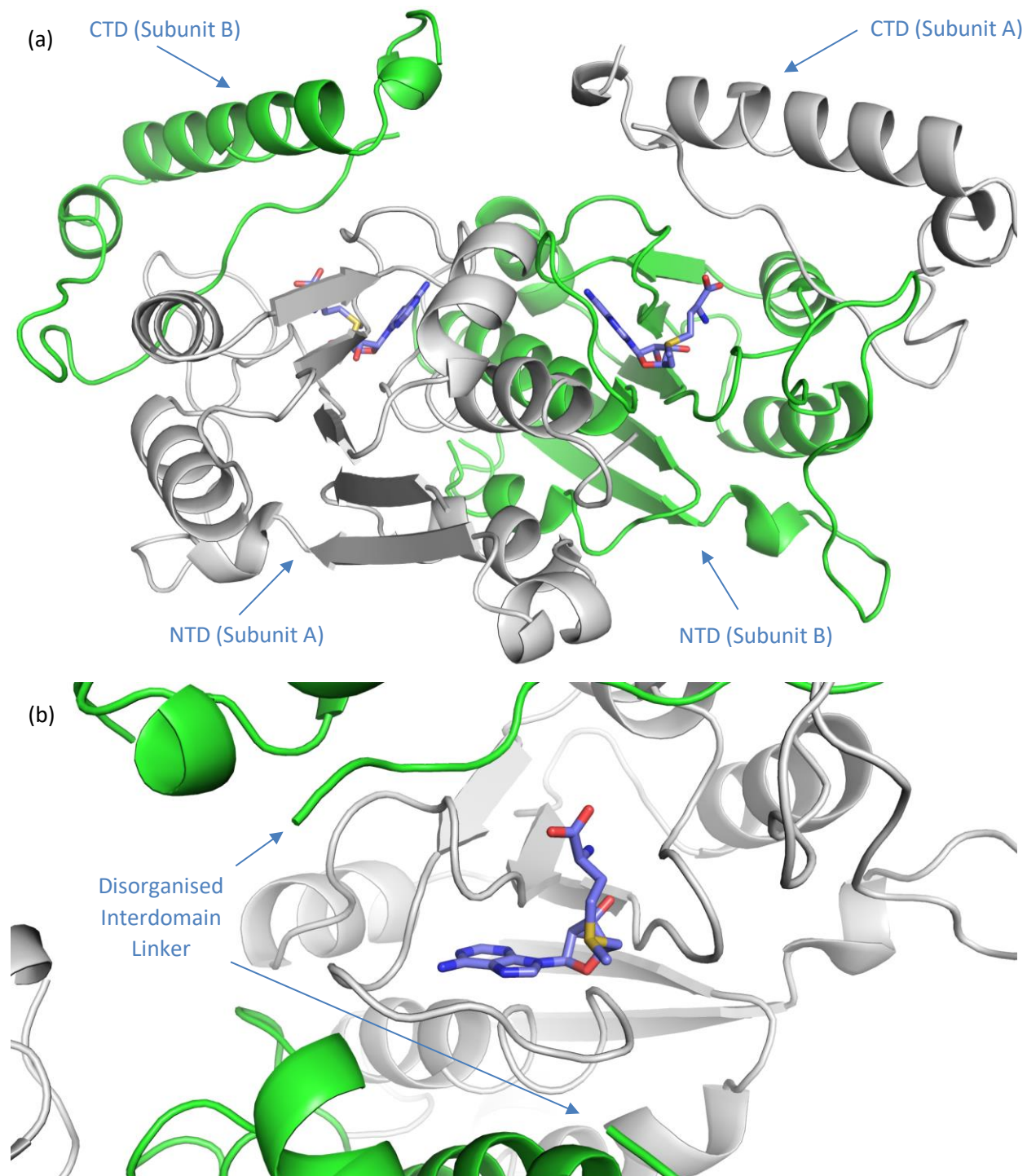


Figure 9: X-ray crystal structure of Mab TrmD bound to SAM (PDB code 6NW6, 1.67 Å, subunit A = white, subunit B = green, SAM = lilac), illustrating (a) the whole homodimer and (b) one of the active sites.⁵⁰

Within each monomer a flexible interdomain linker connects the NTD to a smaller CTD, however these domains are held away from each other with no contact, instead interacting with domains of the other subunit (Figure 9a).^{52 – 54} TrmD possesses two symmetry-related active sites with trefoil knots, formed by loops connecting the beta strands and alpha helices of the common core from one NTD, holding SAM in a bent 'L-shaped' orientation. Each site is located at a subunit interface, with the other subunit making a direct contribution through its CTD and interdomain linker in addition to indirectly stabilising the trefoil knot structure through interactions with its NTD (Figure 9b).^{52, 53}

The trefoil knot facilitates communication between the active sites through the subunit interface, with subunit asymmetry and differences in conformational freedom evident on substrate binding.⁵⁵ As a result, whilst the active sites in TrmD can both bind SAM simultaneously, only one of the sites can be catalytically active at any time and bind tRNA.⁵⁶ A notable manifestation of this asymmetry between the active sites is the organisation of the interdomain linker, which is ordinarily not visible in X-ray crystal structures (Figure 9b), into an alpha helix at the tRNA-bound active site (Figure 10a).⁵⁷

In the tRNA - *Haemophilus influenzae* (*H. influenzae*) TrmD complex the guanine base of G37 is 'flipped out' towards the cofactor, leaving space at the tRNA anticodon for G36 to adopt a *syn* conformation and form π -stacking interactions with the bases of nucleotides 35 and 38. The base of G36 also hydrogen bonds to the side chain of the conserved residue Asp50, which smaller pyrimidine bases would not be able to achieve, providing selectivity for tRNA molecules with a G36 – G37 sequence (Figure 10a).⁵⁷ In the active site the flipped out base of G37 interacts with Arg154 and Asp169 (Figure 10b),⁵⁷ which have been shown to be essential for TrmD catalytic activity in site-directed mutagenesis studies.⁵³ Asp169 engages the N1 atom of G37, and could function as a general catalytic base to abstract its proton and facilitate nucleophilic attack on the methyl group of SAM, with Arg154 stabilising any developing negative charge through its interaction with the carbonyl oxygen of G37 (Figure 10b).⁵⁷ A magnesium(II) cation has also been shown to be essential for catalysis, with evidence suggesting a role in coordination to the oxygen of G37 alongside Arg154 in addition to aiding the orientation of Asp169.⁵⁸ A full catalytic cycle for TrmD has been proposed that begins with 'loosening' of the trefoil knot, allowing SAM to move into the active site, followed by 'tightening' to a state that can bind tRNA through interactions of the phosphates with surface residues before active site insertion of G37. In this model organisation of the interdomain linker, which contains the catalytic residue Asp169, occurs following recognition of G36 by TrmD, allowing methyl transfer and release of the reaction products.⁵⁷

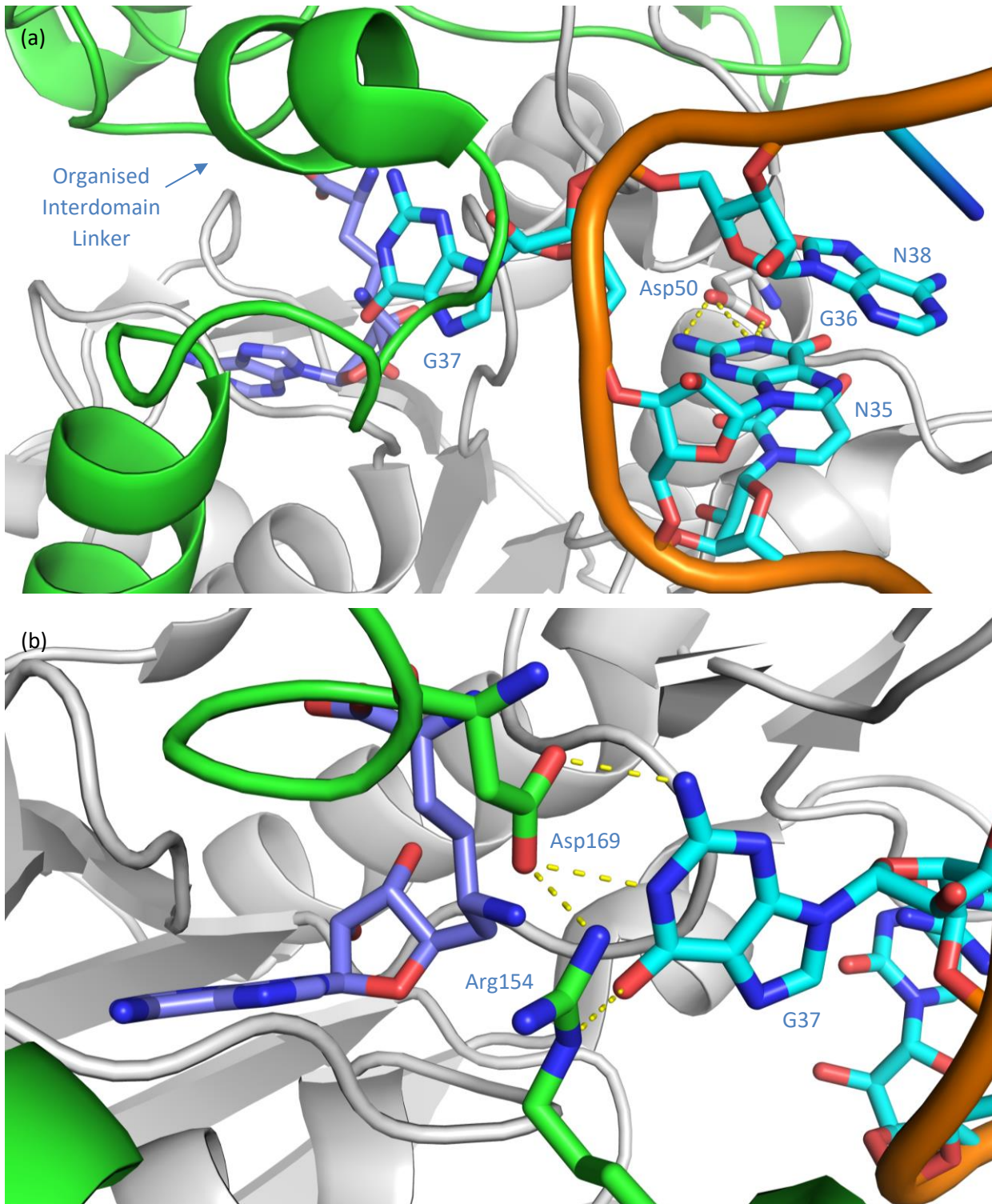


Figure 10: X-ray crystal structure of *H. influenzae* TrmD bound to tRNA and the SAM-analogue sinefungin (PDB code 4YVI, 3.01 Å, subunit A = white, subunit B = green, sinefungin = lilac, tRNA = cyan), illustrating (a) the anticodon region of the bound tRNA and (b) the interaction of G37 with catalytic residues near sinefungin with the alpha helix of the organised interdomain linker removed for clarity.⁵⁷

The m¹G37 tRNA modification has been shown to be essential for normal cellular function in organisms spanning all three domains of life, including archaea and eukarya in addition to bacteria.⁵⁹ Hence, a potential concern could be the interference of a bacterial TrmD inhibitor with the human equivalent. The protein responsible for m¹G37 modification in archaea and eukarya is Trm5, and whilst structural information is not currently available for human Trm5 the archaeal ortholog from *Methanocaldococcus jannaschii* (*Mj*) has been characterised.⁶⁰ *Mj* Trm5 is considered to provide a useful replacement model for the human ortholog,⁶¹ and is structurally distinct from bacterial TrmD with an alternative SAM binding mode.⁶⁰ This was illustrated in the screening of nucleoside and amino acid fragments against *Escherichia coli* (*E. coli*) TrmD and *Mj* Trm5, including adenosine and methionine, which afforded different results for each protein.⁶² Further, *H. influenzae* TrmD was recently used as the target of a fragment-based study based on the development of thienopyrimidone **3** (Figure 11). Whilst the compounds in this study demonstrated weak antibacterial activity, with **4** only possessing an MIC of 3.1 μM against a recombinant *H. influenzae* strain with debilitated AcrAB TolC efflux pumps *in vitro*, the compounds showed selectivity for TrmD when screened against a Trm5 surrogate.⁶³ As a result, selectivity for bacterial TrmD against human Trm5 would probably not be an issue in inhibitor development.

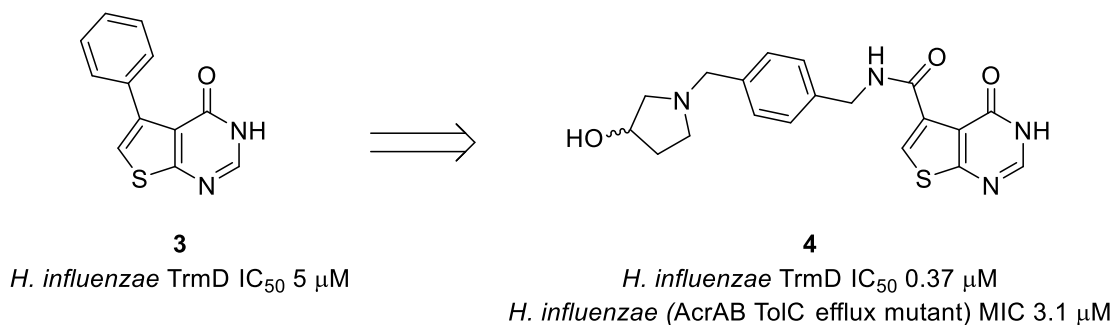


Figure 11: The application of a fragment-based study against *H. influenzae* TrmD.⁶³

The demonstrated essentiality of TrmD in mycobacteria,^{36, 50} the existence of structural data for the *Mab* ortholog,⁵⁴ and low risk of selectivity issues with the human equivalent,^{60 - 63} supports the use of a fragment-based approach against *Mab* TrmD to develop compounds with antimycobacterial properties. To this end, the Abell research group fragment library was recently screened against *Mab* TrmD by Dr Sherine Thomas (Department of Biochemistry, University of Cambridge), affording 27 fragment hits for subsequent elaboration.⁵⁰

1.3: Fragment-based Drug Discovery

1.3.1: Background

Over the past 30 years, high-throughput screening (HTS) has been the primary method used by pharmaceutical companies to identify leads for drug discovery programmes. The HTS approach requires the automated screening of large libraries of compounds, typically 300-500 Da in size, against biological targets with the most attractive hits subsequently optimised for potency and 'drug-like' physicochemical properties. Whilst these libraries often contain millions of compounds they can at best sample an insignificant proportion of the over 10^{63} molecules of this size that are estimated to comprise 'lead-like' chemical space.⁶⁴ Since its first successful utilisation by Fesik *et al.* in 1996,⁶⁵ fragment-based drug discovery (FBDD) has been gaining traction as both an alternative and complementary approach to HTS.⁶⁶ The increasing use of FBDD is exemplified by the FDA approval in recent years of the FBDD-developed drugs Vemurafenib and Venetoclax as treatments for late stage melanoma and chronic lymphocytic leukaemia respectively.^{67, 68} These were joined in 2017 by the cyclin-dependent kinase 4/6 inhibitor Ribociclib as a first-line drug for the treatment of breast cancer (Figure 12).^{69, 70}

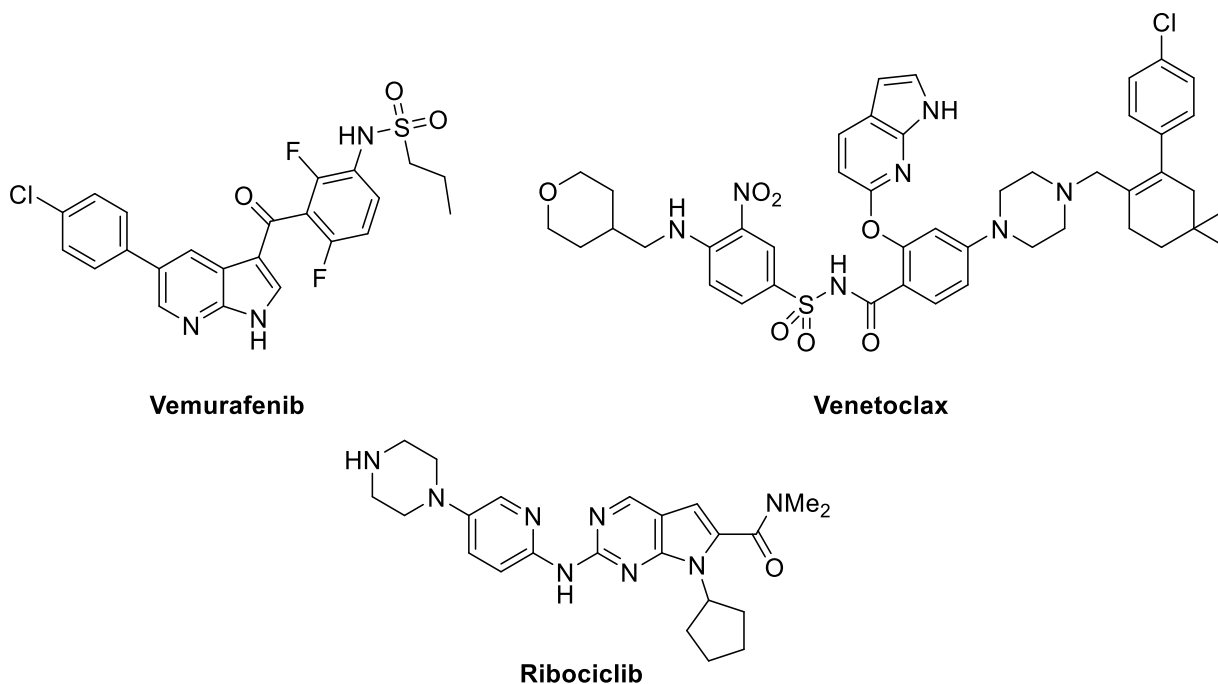


Figure 12: FDA-approved drugs developed using a fragment-based approach.^{67, 70, 71}

In FBDD weakly binding small molecules, fragments with affinity in the 10 mM to 100 μ M range, are identified and subsequently elaborated into potent small-molecule ligands.⁷² Fragments typically comply

with 'Rule of Three' guidelines,⁷³ analogous to Lipinski's 'Rule of Five' for orally bioavailable drug candidates,⁷⁴ with molecular weights below 300 Da, limits of 3 hydrogen bond donors and 3 hydrogen bond acceptors, and a maximum partition coefficient (cLogP) of 3.⁷⁵ Computational chemistry analysis has placed the total number of lead-like molecules at up to 17 carbon, nitrogen, oxygen, sulfur or halogen atoms in size at 10^{11} in magnitude,⁷⁶ therefore a library of only 1000 fragments can sample a higher proportion of chemical space than a larger HTS library. However, careful consideration of fragment library composition is essential to effectively sample chemical space with focus on molecular complexity, diversity and stability in addition to synthetic tractability and the availability of commercial analogues.^{77, 78}

In addition to their improved sampling of chemical space, fragments are more capable than fragment-sized moieties in HTS hits of probing ligand-binding sites without interference from unfavourable steric or electronic matches, forming high-quality interactions due to their reduced molecular complexity.⁷⁹ The presence of these high-quality interactions is essential for a fragment's intrinsic affinity for a protein to overcome the loss of its rigid body translational and rotational entropy on binding, 15-20 kJ mol⁻¹ or 3 orders of magnitude of binding affinity at 298 K as for a larger HTS hit.⁸⁰ The elaboration of a high-quality fragment can present less challenge than the optimisation of an HTS hit with multiple sub-optimally aligned moieties, and ligands derived by FBDD have been shown to display improved physicochemical properties in relation to HTS-derived leads.⁸¹

1.3.2: Biophysical Techniques

In contrast to HTS, the weak binding affinities of fragments necessitate the use of sensitive biophysical techniques. Each technique presents a unique mixture of strengths and challenges, and the use of several in combination is frequently required.⁸² Flexibility in the utilisation of biophysical methods in a FBDD project is desirable, and it has been demonstrated that the use of multiple screening techniques in parallel can minimize the proportion of false negatives,⁸³ however throughput and time constraints are important considerations and the prioritisation of fragment hits is generally of more concern than their availability. Hence, the use of a biophysical screening cascade can be useful, with an initial preliminary screen followed by validation with lower-throughput techniques. After validation, characterisation of the structural features, thermodynamic parameters and stoichiometry of the ligand-protein interaction is essential.^{84, 85}

Differential scanning fluorimetry (DSF) is a high-throughput technique that allows rapid testing of a fragment library, providing enrichment of hits and allowing assessment of target ligandability in the absence of structural information.⁸⁶ The technique is dependent upon analysis of a protein's thermal melting temperature (T_m), the temperature at which its Gibbs free energy of unfolding (ΔG_u) is zero and the concentrations of folded and unfolded states equal in a reversible two-state equilibrium.⁸⁷ This is carried out through the monitoring of the fluorescence of an environmentally sensitive dye with affinity for the hydrophobic interior of proteins, which are typically exposed upon protein unfolding. Sypro Orange[®] is commonly used due to its favourable signal-to-noise ratio in addition to possessing a high wavelength of excitation, minimising the risk of interference by tested ligands in the dye's optical behaviour.⁸⁷ The binding of the dye to the protein results in an increase in the fluorescence signal with T_m corresponding to the inflection point of the sigmoidal curve. The binding of a fragment to a protein is typically associated with stabilisation of the folded protein state, resulting in an increase of the T_m with a reproducible ΔT_m of two to three standard deviations often classified as a hit.⁸⁷ Whilst the ΔT_m values of similar compounds within a series can be utilised to an extent in affinity ranking, their dependence on the relative contributions of entropy and enthalpy to the thermodynamics of binding limits this application, with entropically driven binding affording higher ΔT_m values whilst also providing interference through binding to the unfolded protein state.⁸⁸ Preferential binding of ligands to the unfolded protein state results in the common observance of negative ΔT_m values that are usually discounted in hit selection, but have shown some use in the development of tool compounds against certain targets.^{89, 90}

Several ligand-observed ¹H NMR techniques are available for validation of fragment-protein interactions as part of a screening cascade with saturation transfer difference (STD), water-ligand observed via gradient spectroscopy (waterLOGSY) and Carr-Purcell-Meiboom-Gill (CPMG) NMR utilised in the Abell research group.⁸⁴ In comparison to protein-observed NMR alternatives, ligand-observed NMR techniques are faster, require no protein isotopic labelling or resonance assignment, tolerate lower protein concentrations, impose no restraints on protein size and allow direct ligand quality control.⁹¹ STD NMR involves the selective saturation of protein resonances that rapidly diffuse throughout the protein. In the event of fragment binding, intermolecular magnetisation transfer through the nuclear Overhauser effect (NOE) results in the appearance of a difference spectrum for the fragment.⁹² WaterLOGSY NMR utilises NOE transfer of magnetisation from water molecules to the fragment, with transfer from waters at the protein binding site of opposite sign to that from bulk water due to the different tumbling regime. As a result, non-binding fragments show no change in signal upon addition of protein whilst binding fragments

exhibit dominance of the negative signals.⁹³ In contrast to STD and waterLOGSY, CPMG NMR utilises an acquisition delay to filter out signals from rapidly relaxing molecules. Fragments bound to proteins exhibit increased relaxation rates, hence the signals from fragments hits are reduced in intensity in the presence of protein.⁹⁴

Structural information on the protein-ligand complex is crucial for the development of FBDD projects, and is commonly provided by X-ray crystallography through high concentration soaking of protein crystals with ligand solution and the processing of diffraction data through molecular replacement.⁸⁴ X-ray crystallography is a time-consuming technique, and compromises are often required in the selection and prioritisation of ligands for the acquisition of structural information. Despite the relatively low-throughput of X-ray crystallography, it is also utilised in FBDD as a screening technique in its own right.⁹⁵

Full determination of the thermodynamic parameters of ligand binding can be obtained by isothermal titration calorimetry (ITC) through injection of ligand into a sample cell containing protein within an adiabatic enclosure. The operation of a differential cell feedback system between the sample and reference cells during injections allows the direct measurement of the enthalpy of binding (ΔH_B) and estimation of the equilibrium dissociation constant (K_d) and stoichiometry of the interaction, from which the Gibbs free energy (ΔG_B) and entropy (ΔS_B) of binding can be calculated.⁹⁶ Whilst ITC suffers from low-throughput and high protein requirements, it is utilised for its sensitivity in ligand affinity determination.⁷² The thermodynamic parameters of enthalpy and entropy of binding are attributed in general to specific binding interactions and non-specific hydrophobic effects respectively, hence the selection of starting points with enthalpically-dominated binding and minimisation of entropic increases during a project could be beneficial.⁹⁷ However, due to the nature of these values as the net sums of many competing aspects of ligand-protein interactions that can be challenging to control, as reflected in the commonly observed phenomenon of enthalpy-entropy compensation, over interpretation and their use as endpoints in and of themselves is discouraged.⁹⁸ The high-quality interactions of fragment hits though are reflected in favourable enthalpic profiles, and the use of thermodynamic data in combination with structural information can lead to the development of ligands with desirable physicochemical properties.⁹⁹

1.3.3: Fragment Elaboration

Following screening and characterisation, fragment hits are elaborated into ligands with improved potency through an iterative cycle of synthesis and testing, guided by the strategies of linking, growing and merging.⁷² Fragment-linking, the connection of fragments with non-overlapping binding poses through a linker that allows the resultant ligand to recapitulate the original fragment binding modes without hindrance, can result in large gains in affinity (Figure 13).¹⁰⁰

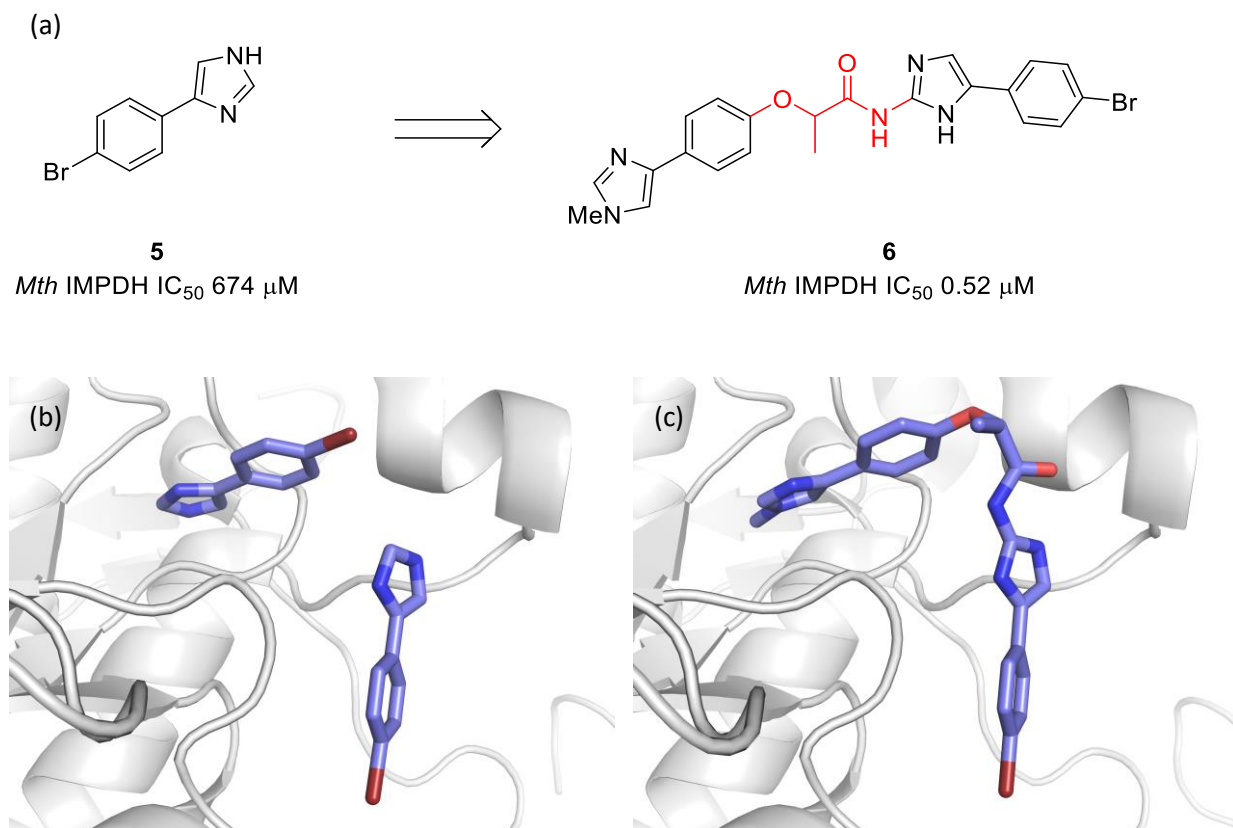


Figure 13: (a) The application of a fragment-linking strategy against *Mycobacterium thermoresistibile* (*Mth*) inosine-5'-monophosphate dehydrogenase (IMPDH) to a fragment **5** bound twice in the active site to achieve a ~1300x potency improvement in **6**, illustrated in X-ray crystal structures of *Mth* IMPDH (*Mth* IMPDH = white, ligand = lilac) bound to (b) **5** (PDB code 5OU2, 1.45 Å), and (c) **6** (PDB code 5OU3, 1.60 Å).¹⁰⁰

The affinity gains that are achievable in a fragment-linking strategy are due to the effective independence of ligand molecular weight and the rigid body entropic penalty of binding, which allows the combination of two fragments to afford a greater increase in the free energy of binding than would be suggested by simple addition of their individual energies.¹⁰¹ However, despite its conceptual appeal, this approach is not commonly used due to the inherent difficulty of developing an ideal linker with appropriate flexibility and geometry in addition to providing favourable interactions with the protein.¹⁰² In contrast to

fragment-linking, when fragments exhibit overlapping binding poses a fragment-merging strategy can be beneficial where portions of the fragments, particularly those with the highest contribution to binding, are incorporated into one ligand with improved affinity (Figure 14).¹⁰³

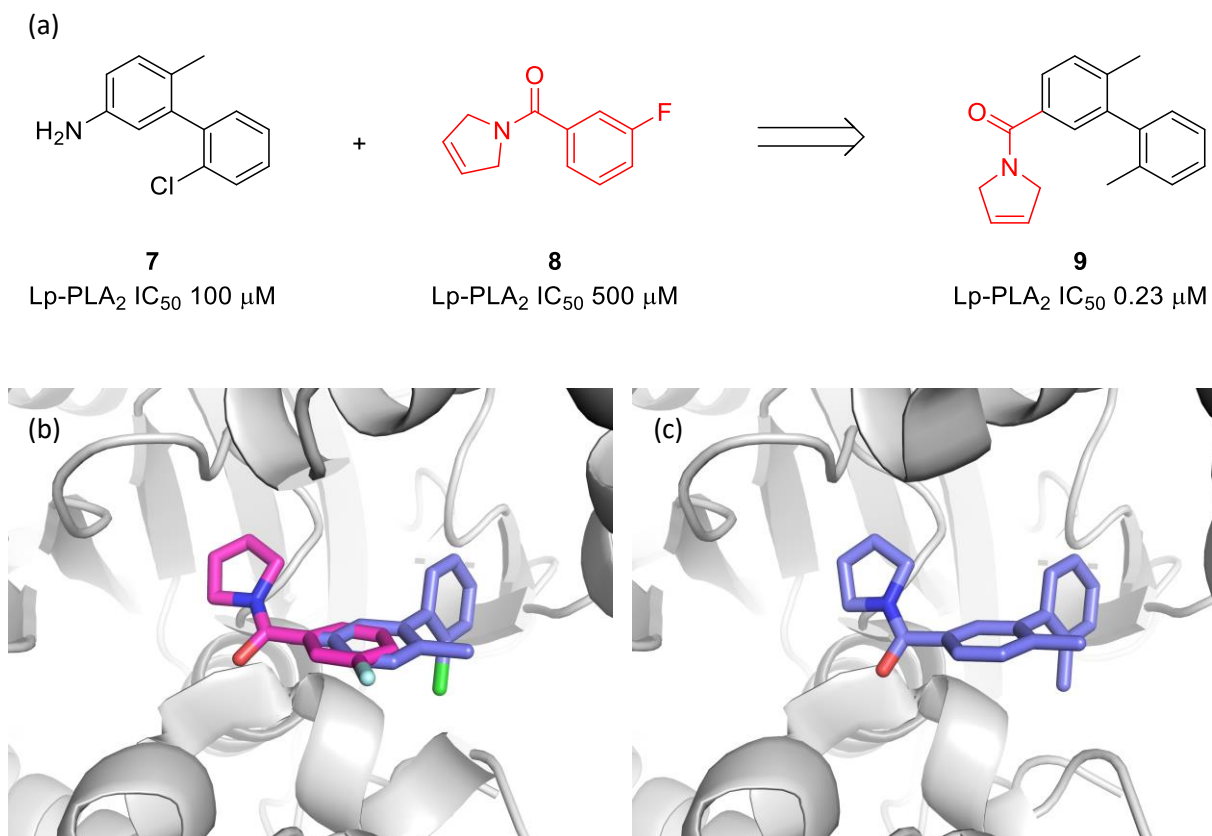


Figure 14: (a) The application of a fragment-merging strategy against human lipoprotein-associated phospholipase A2 (Lp-PLA₂) to fragments **7** and **8** bound in the active site to achieve a ~400x potency improvement in **9**, illustrated in (b) an overlay of X-ray crystal structures of human Lp-PLA₂ bound to **7** or **8** (overlay of PDB code 5JAO and PDB code 5JAL, human Lp-PLA₂ = white, **7** = lilac, **8** = pink) and (c) an X-ray crystal structure of human Lp-PLA₂ bound to **9** (PDB code 5JAP, 2.46 Å, human Lp-PLA₂ = white, **9** = lilac).¹⁰³

The modification of fragment scaffolds based on a fragment-merging approach can provide new possibilities for elaboration however, as in fragment-linking, conceptually appealing changes can be challenging to apply in practice.^{104, 105} In the event of success in carrying out a fragment-linking or merging exercise, new functionality can be added to the scaffold based on structural information. Due to the challenges presented by fragment-linking and merging, the direct addition of new functionality to a fragment hit with the goal of increasing affinity, the fragment-growth approach, is the most common route taken in FBDD projects.⁷² Based on analysis of published X-ray crystallographic data the addition of

new functionality to a fragment generally does not significantly change its binding mode,¹⁰⁶ and significant increases in affinity are frequently published.¹⁰⁷

During the elaboration of fragment hits it is essential that efficiency metrics are utilised in the decision-making process, maximising the benefits of the high-quality fragment starting points and increasing the probability of obtaining potent ligands with 'drug-like' physicochemical properties.¹⁰⁸ A key efficiency metric in FBDD is ligand efficiency (LE), the Gibbs free energy of binding per non-hydrogen or 'heavy' atom (HA) (Equation 1), which allows the assessment of ligand affinity with respect to molecular weight.¹⁰⁹

$$LE = \frac{-RT \cdot \ln K_d}{HA} = \frac{-\Delta G_B}{HA}$$

*Equation 1 : Ligand efficiency.*¹⁰⁹

The maintenance of LE during fragment elaboration prevents excessive increases in molecular mass in the goal of improved affinity. A value of at least 0.3 kcal mol⁻¹ HA⁻¹ is recommended, corresponding to a K_d of 10 nM in a ligand with a molecular weight below 500 Da.¹⁰⁹ Further, LE is often utilised in conjunction with the more sensitive metric of group efficiency (GE), the change in the Gibbs free energy of binding per added HA (Equation 2).¹¹⁰

$$GE = \frac{-\Delta\Delta G_B}{\Delta HA}$$

*Equation 2: Group efficiency.*¹¹⁰

The use of GE analysis in FBDD allows assessment of the contributions of individual moieties to the ligand's free energy of binding, facilitating the development of potent and ligand-efficient compounds.^{111, 112}

Finally, if 'lead-like' ligands are already reported for the target in question, the trial of a deconstruction-reconstruction approach could be beneficial rather than starting a new fragment screening exercise.¹¹³ This approach would involve defragmentation of the ligand scaffold, breaking it down conceptually into smaller fragments, with derivatives that show evidence of binding elaborated to new ligands with improved properties (Figure 15).¹¹⁴ However, such a strategy may not succeed as the individual moieties of lead-like ligands are not guaranteed to be able to either exhibit detectable binding on their own as fragments or bind with the same pose as the parent ligand.¹¹⁵

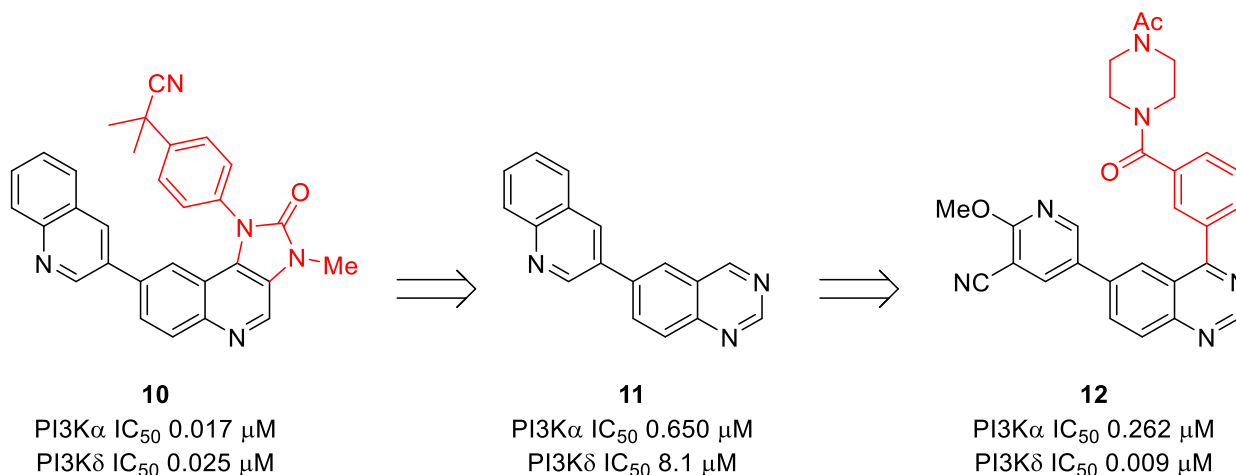


Figure 15: The application of a deconstruction-reconstruction approach against human phosphoinositide-3-kinase (PI3K) for selectivity between the α and δ isoforms using the unselective ligand **10**, with the fragment-like ligand **11** still exhibiting PI3K inhibition and the resultant ligand **12** affording selective inhibition of the δ isoform.¹¹⁴

1.4: Project Aims

The aim of this project is to utilise fragment-based methods to develop ligands with high affinity against *Mtb* fumarase and *Mab* TrmD. These could then be utilised as tool compounds to evaluate the potential of these enzymes as drug targets for the development of novel antimycobacterial treatments.

With regards to *Mtb* fumarase, an HTS hit **2** was previously discovered, and a deconstruction-reconstruction approach will be explored to develop fragments with high quality interactions with the enzyme that could be elaborated into ligands with improved affinity. Facilities and expertise in structural biology will be provided by the Hyvönen research group at the Department of Biochemistry, to aid in the performance of X-ray crystallography with *Mtb* fumarase.

With regards to *Mab* TrmD, the use of a fragment screening cascade has identified 27 fragments with associated structural information on the protein-ligand interaction. The aim will be to obtain affinity data for these fragments and use the most promising hits as starting points for multiple elaboration programmes, taking advantage of the large diversity of binding modes to identify novel compounds for the treatment of *Mab* infection. The work will be performed in collaboration with the Blundell research group at the Department of Biochemistry, with Dr Sherine Thomas providing structural information on ligand binding modes with *Mab* TrmD by X-ray crystallography, and the Floto research group at the Department of Medicine with Dr Karen Brown screening compounds against *Mab* *in vitro*.

Compounds synthesised against both protein targets will be sent to the group of Dr Helena Boshoff at the Tuberculosis Research Section, National Institutes of Health, for screening against *Mtb in vitro* by Dr Daben Libardo.

2: Fumarate Hydratase

2.1: Project Setup

The application of a deconstruction-reconstruction approach to the allosteric inhibitor **2** of *Mtb* fumarase required the ranking of compounds. The use of a biochemical assay to achieve this was dependent on both the acquisition of *Mtb* fumarase, whose activity would be monitored, and the synthesis of **2** to determine a reference IC₅₀ value for comparison to subsequent derivatives.

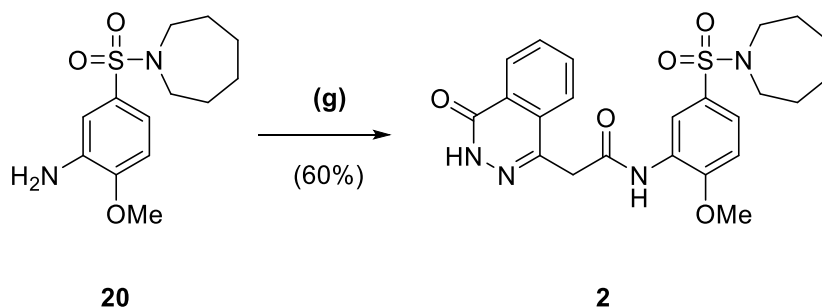
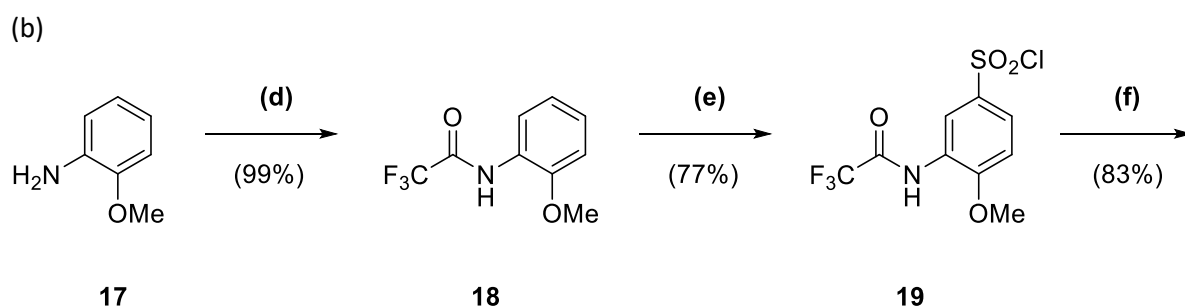
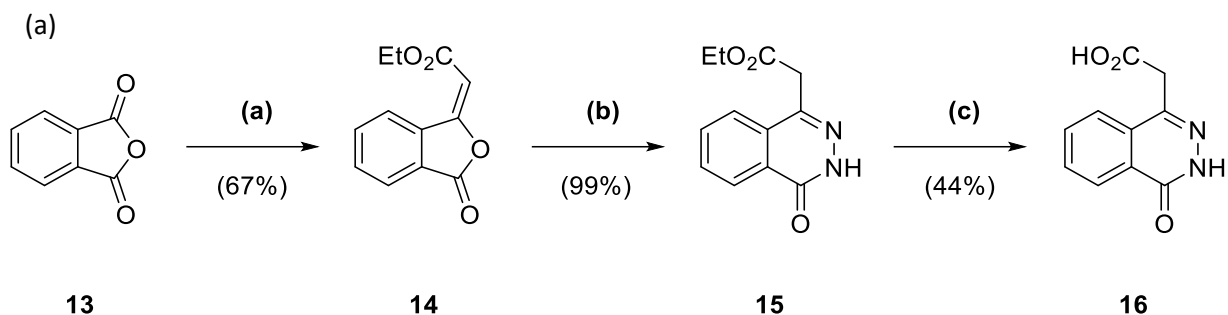
2.1.1: Synthesis and Screening of High-throughput Screening Hit **2**

Synthesis of the allosteric inhibitor **2** was based on a convergent route requiring the synthesis of carboxylic acid **16** (previously developed by Monica Kasbekar, University of Cambridge) (Scheme 1).⁴¹ The synthesis of **16** involved the Wittig reaction of phthalic anhydride **13** and ethyl (triphenylphosphoranylidene)acetate to afford the unsaturated intermediate **14** (67% yield). Heating under reflux with hydrazine in ethanol converted **14** to the phthalazinone ester **15** (99% yield), with subsequent hydrolysis providing **16** (44% yield) (Scheme 1a).

The route also focused on the synthesis of aniline **20**,⁴¹ starting with the addition of a trifluoroacetyl protecting group to *o*-anisidine **17** (99% yield). The protected amide **18** was then treated with chlorosulfonic acid to introduce a sulfonyl chloride group on its phenyl ring through electrophilic aromatic substitution, affording **19** (78% yield) (Scheme 1b). The addition of this electrophilic functional group allowed the synthesis of a sulfonamide, which in the case of **20** was carried out with azepane and NaH, followed by heating under reflux under acidic conditions to remove the trifluoroacetyl protecting group (83% yield). This was achieved in the original synthesis with the isolation of the trifluoroacetyl-protected sulfonamide intermediate,⁴¹ however for expediency this was combined into a two-step reaction with the dropwise addition of acid under cooled conditions to the basic reaction mixture, which also resulted in an improvement in yield (Scheme 1b).

With **20** and **16** successfully obtained, attention could shift to the synthesis of **2**, which was previously achieved through COMU-mediated amide coupling.⁴¹ This was attempted, however this gave a poor yield, therefore an alternative amide coupling reagent propylphosphonic anhydride (T3P®) was utilised (60% yield) (Scheme 1b). T3P®, a water-soluble reagent originally developed for the coupling of peptides

under mild conditions without racemisation,¹¹⁶ was utilised throughout the remainder of the project for the synthesis of most amides.



Reagents and Conditions: (a) (Carboxymethylene)triphenylphosphorane, CHCl_3 , reflux, 3 h; (b) $\text{N}_2\text{H}_4 \cdot \text{H}_2\text{O}$, EtOH, 50 °C, 2 h; (c) NaOH (10% w/v), THF, reflux, 1 h; (d) TFAA, pyridine, DCM, 0 °C to rt, 3 d; (e) HSO_3Cl , DCM, 0 °C to rt, 16 h; (f) (i) hexamethylenimine, NaH, DMF, 0 °C to rt, 3 h (ii) EtOH, H_2O , HCl (37.5% w/v), reflux, 20 h; (g) **16**, T3P® (50 wt. % in DMF), DIPEA, DMF, 70 °C, 1 h.

Scheme 1: Synthesis of (a) 16 in three steps from 13, and (b) 2 in four steps from 17, including 16.

Following the synthesis of **2**, the determination of its IC_{50} against *Mtb* fumarase was carried out using a biochemical assay based on the oxidative citric acid cycle (previously optimised by Monica Kasbekar, University of Cambridge) (Figure 16a), which monitors the production of reduced nicotinamide adenine dinucleotide (NADH) (Figure 16b).¹¹⁷

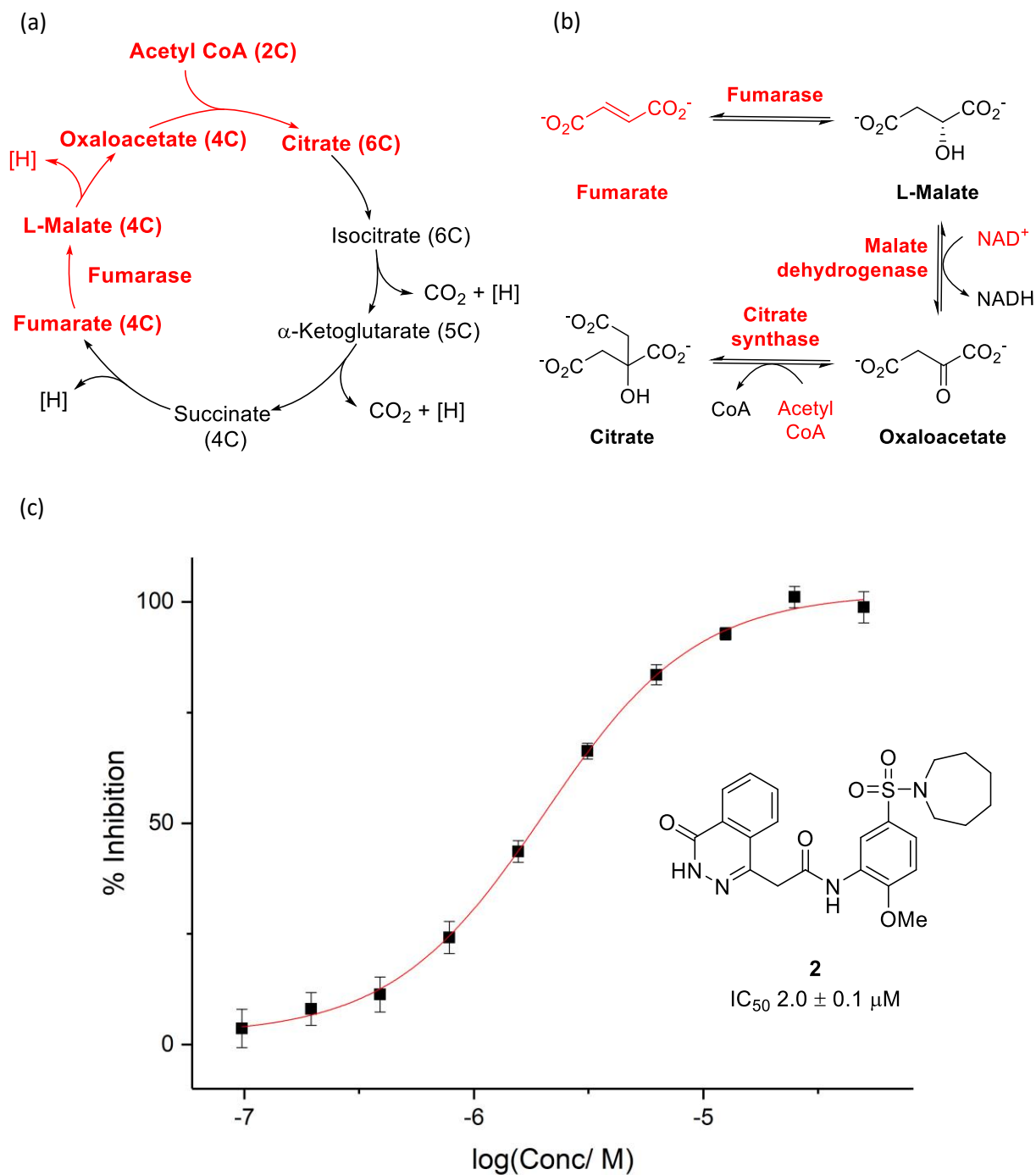


Figure 16: The biochemical assay utilised for the monitoring of *Mtb* fumarase activity, (a) illustrating the relevant portion (red) of the oxidative citric acid cycle and (b) illustrating the reactions of the assay and required materials (red);⁴¹ (c) dose-response curve for **2** obtained from the biochemical assay, with data points representing an average of replicates ($n = 6$) and error bars indicating standard errors of the mean.

The components of the biochemical assay were obtained from commercial sources, except for *Mtb* fumarase itself. The target protein was expressed and purified with a yield of 24 mg L⁻¹ by the transformation of *E. coli* BL21(DE3) strain (plasmid provided by Monica Kasbekar, University of Cambridge). The screening of **2** against *Mtb* fumarase afforded a mean IC₅₀ of 2.0 ± 0.1 μM (Figure 16c), which is consistent with the previously determined value of 2.5 ± 1.1 μM.⁴¹

2.1.2: X-ray Crystallography

In addition to the quantification of inhibition through biochemical assays, the acquisition of structural information on protein-ligand interactions is considered essential for subsequent elaboration, with X-ray crystallography the most widely used technique for this purpose. A successful crystallisation protocol was previously described for *Mtb* fumarase, utilising sitting drop vapour diffusion with the combination of 2 μL protein solution (14 mg mL⁻¹ *Mtb* fumarase, 0.15 M NaCl, 10 mM Tris pH 8.0 and 0.5 mM TCEP) and 1 μL reservoir solution (17% w/v PEG3350, 5% DMSO and 0.20 M magnesium formate).⁴¹ This protocol was used as a starting point for the acquisition of new *Mtb* fumarase crystals.

A sitting drop plate was set up with concentration gradients in PEG3350 (12 – 19% w/v) and magnesium formate (0 – 0.28 M) to account for differences in laboratory technique that could have a significant influence on crystallisation outcome. Crystal quality in this plate was higher at lower levels of PEG3350 and the highest concentration of magnesium formate, therefore a new sitting drop plate was established with a reduced PEG3350 concentration gradient (10 – 17% w/v) and an increased single concentration of magnesium formate (0.30 M). Whilst the crystals were of improved quality, they were generally too small and numerous for practical use, therefore the well with the highest quality crystals was removed (Figure 17a), diluted and sonicated to produce seed stock, which was further diluted (17% w/v PEG3350, 5% DMSO and 0.30 M magnesium formate) to afford 100, 1,000, 5,000 and 10,000x solutions.

The seed stock solutions were applied to a new plate (10 – 12.8% w/v PEG3350, 5% DMSO and 0.30 M magnesium formate) with three ratios of protein, reservoir and seed stock solution. The wells arising from the combination of protein, reservoir and seed stock solution in a 3 : 1 : 0.5 ratio by volume afforded the best quality *Mtb* fumarase crystals (Figure 17b) and were taken forward for soaking trials.

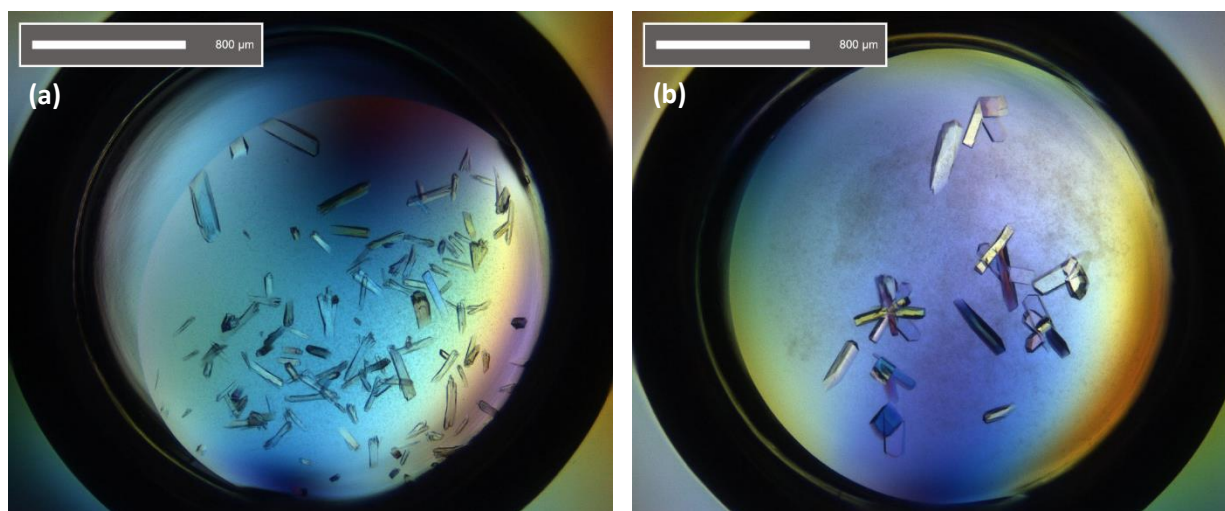


Figure 17: Images of wells from sitting drop plates, with (a) 2 μL protein solution (14 mg mL^{-1} *Mtb fumarase*, 0.15 M NaCl, 10 mM Tris pH 8.0 and 0.5 mM TCEP) + 1 μL reservoir solution (10% w/v PEG3350, 5% DMSO, 0.30 M magnesium formate), 2 w, and (b) 3 μL protein solution (14 mg mL^{-1} *Mtb fumarase*, 0.15 M NaCl, 10 mM Tris pH 8.0 and 0.5 mM TCEP) + 1 μL reservoir solution (10% w/v PEG3350, 5% DMSO, 0.30 M magnesium formate) + 0.5 μL seed stock solution (10,000x dilution), 5 d.

Three solutions of **2** (1 mM) with the same concentration of DMSO (7.5%) and magnesium formate (0.20 M) but differing PEG3350 and glycerol contents (19% w/v PEG3350 and 0% glycerol, 19% w/v PEG3350 and 14.5% glycerol, or 26.25% w/v PEG3350 and 0% glycerol) were applied to crystal-containing drops from the seeding trial (2 μL), representing alternative cryoprotectant strategies. The application of these solutions to crystals with overnight incubation induced a degree of cracking, however crystals were successfully mounted into loops and flash frozen in liquid nitrogen.

X-ray data were collected at a wavelength of 0.9795 Å at the Diamond Light Source synchrotron (Oxfordshire, United Kingdom). Diffraction was best observed with a drop representing the 26.25% w/v PEG3350 cryoprotectant strategy, which was used in all subsequent protocols. Molecular replacement was carried out on this dataset of spacegroup C121 and 1.59 Å resolution using PHASER,¹¹⁸ accessed through the Collaborative Computational Project Number 4 (CCP4) software suite,¹¹⁹ with the previously published **2**-bound *Mtb fumarase* structure used as a search model after removal of ligand and water molecules (PDB code 5F91).⁴¹ The dataset was compatible with this model, with clear density corresponding to dual-bound **2** visible at one of the head-to-head subunit interfaces of *Mtb fumarase*. Molecules of **2** were fitted to this density using the COOT molecular graphics software package,¹²⁰ and the new model (Figure 18) refined with REFMAC5,¹²¹ accessed through CCP4.¹¹⁹

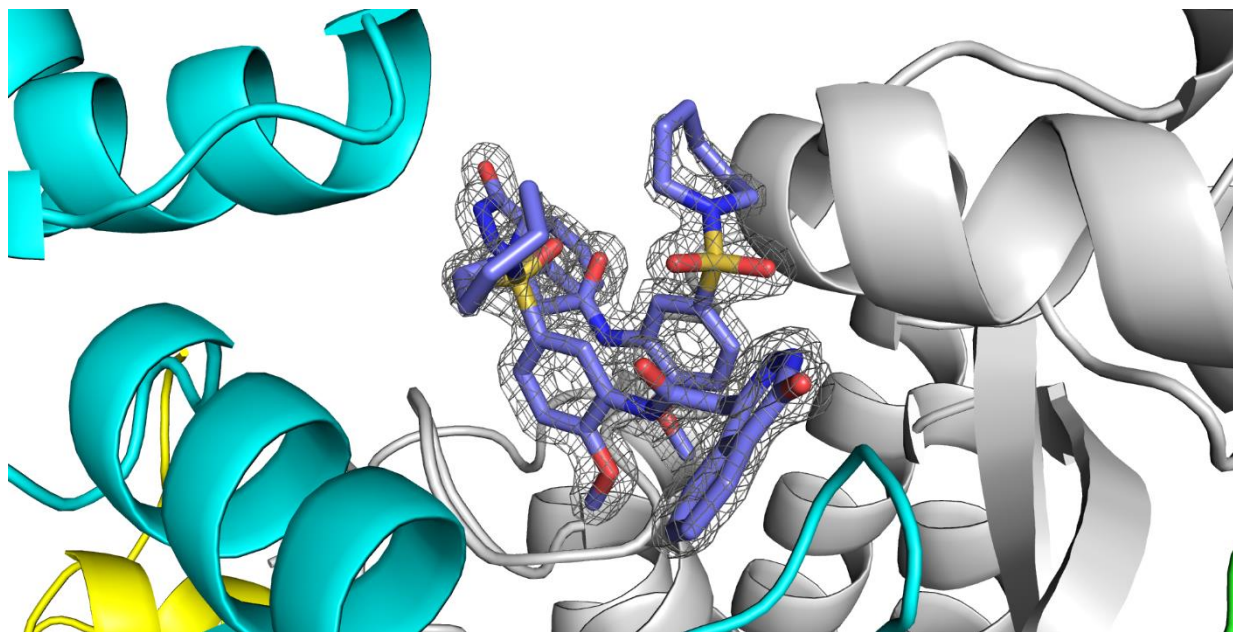


Figure 18: X-ray crystal structure of *Mtb* fumarase bound to **2** (1.59 Å, subunit A = white, subunit B = green, subunit C = cyan, subunit D = yellow, **2** = lilac) after molecular replacement and refinement of a dataset obtained from a crystal of *Mtb* fumarase soaked with **2**, with a $2F_o-F_c$ mesh at 2.0 Å of resolution surrounding **2**.

2.2: Defragmentation of High-throughput Screening Hit **2**

With the inhibition of *Mtb* fumarase by **2** successfully reproduced, the deconstruction-reconstruction strategy was initiated. This would entail the design and synthesis of a focused library of ‘fragment-like’ molecules based on the structure of **2**, and their screening against *Mtb* fumarase.

2.2.1: Library Design

The structure of **2** was used to design a focused library of 10 ‘fragment-like’ molecules of varying molecular weights, including compounds both with and without inclusion of the phthalazinone ring system (Figure 19). Fragments **16** and **20** represent cleavage of the amide bond of **2** into a carboxylic acid and amine, with additional functionality provided by **21** and **22** respectively in case these fragments were unable to bind at a detectable level. This eventuality was suspected to be possible with **16** due to the absence of the central phenyl ring associated with the π -stacking interaction that facilitates the dual binding mode of **2**.

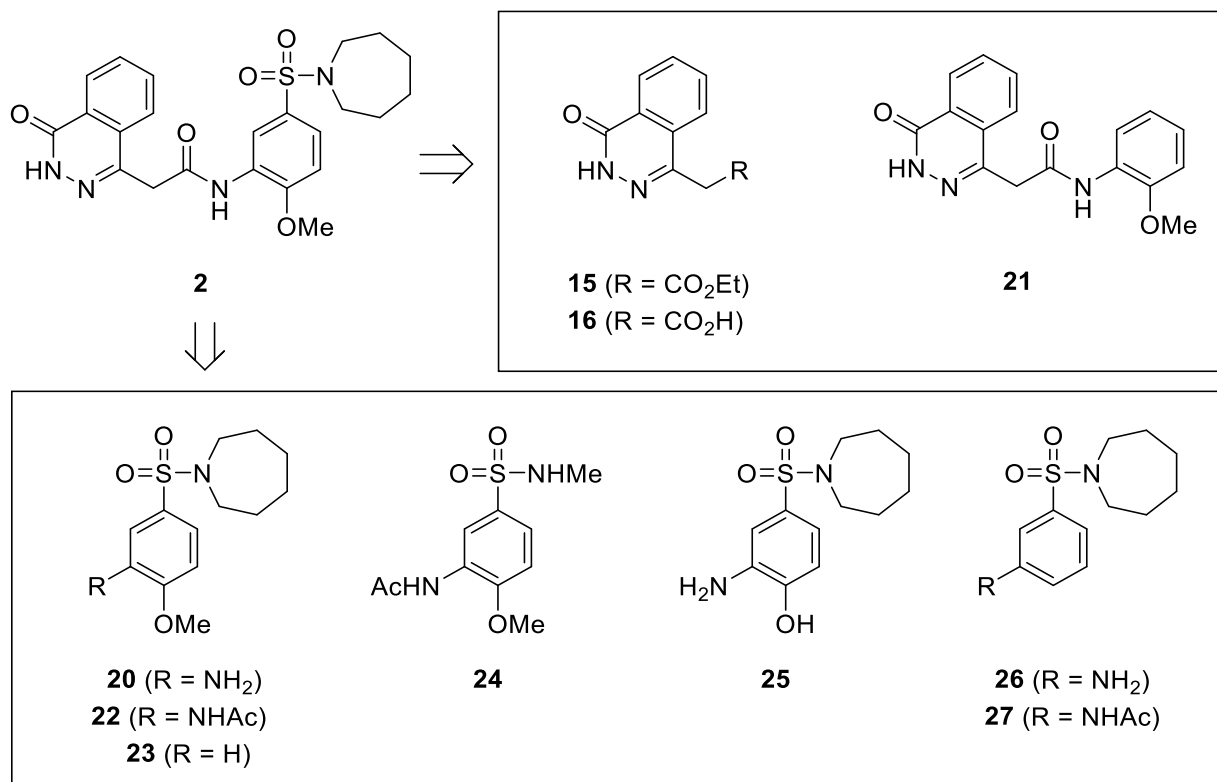
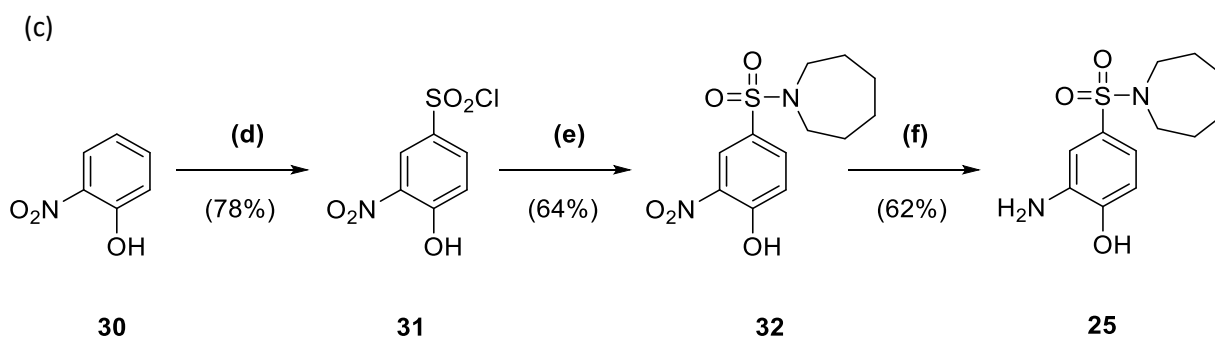
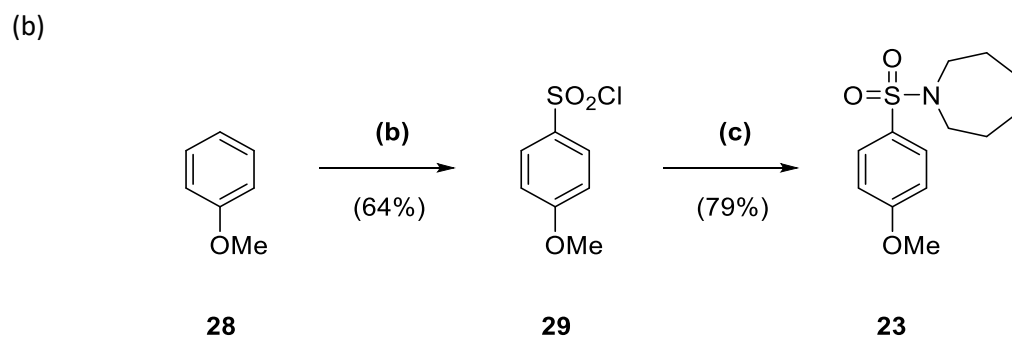
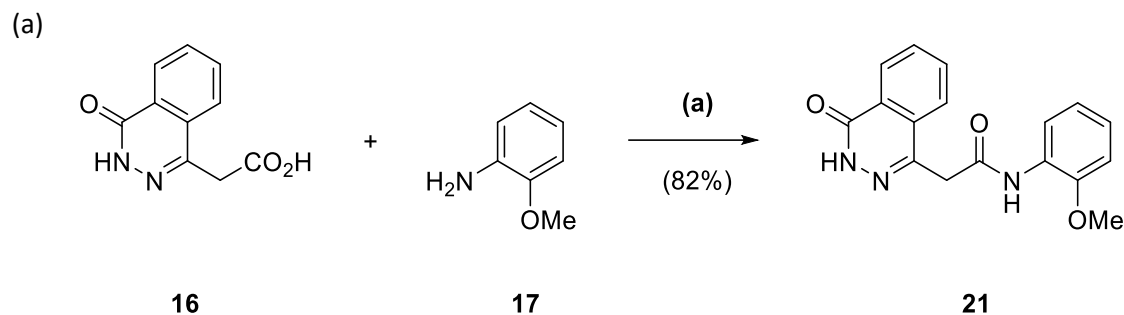


Figure 19: Focused library of fragment-like molecules produced from defragmentation of **2**.

The ester **15** was included in the focused library to insure against the carboxylic acid of **16** not being tolerated in the allosteric site, with similar reasoning behind **23** for the aniline functionality of **20** (Figure 19). The truncation of **22** to the *N*-methyl sulfonamide **24** was to allow investigation of alternatives to the 7-membered azepane ring with retention of the sulfonamide, which is absent in **21**, whilst also providing a new hydrogen bond donor at the nitrogen atom. In contrast, fragments **25**, **26** and **27**, with modification or removal of the methoxy group of **20**, were intended to provide variety in substitution of the phenyl ring (Figure 19).

2.2.2: Library Synthesis

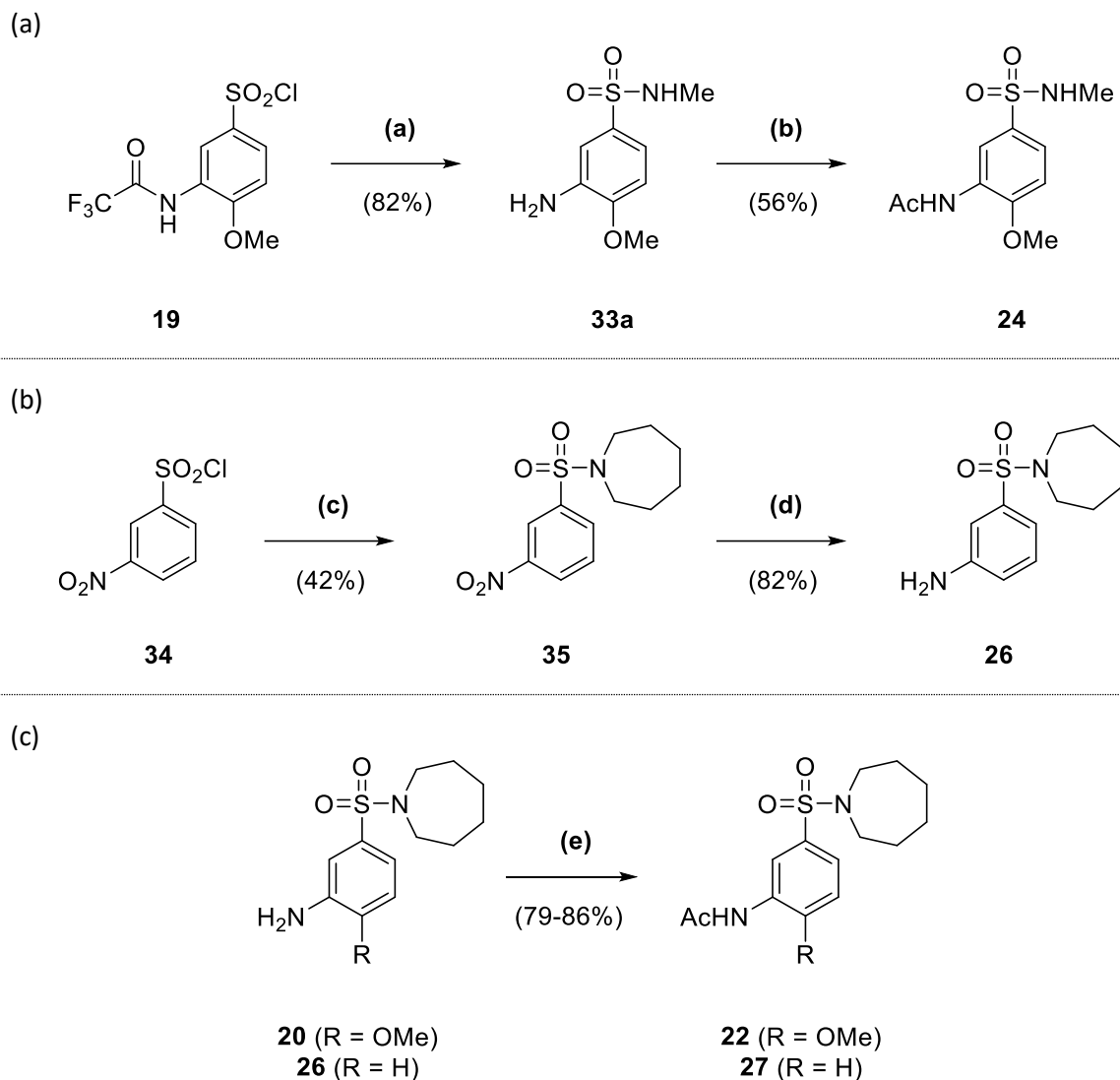
Whilst fragments **15**, **16** and **20** were accessible by the synthetic route for **2**, further synthesis was required for the other members of the focused library. Fragment **21** was produced in one step by the T3P[®]-mediated coupling of **16** with **17** (82% yield) (Scheme 2a). Synthesis of **23** began with the reaction of anisole **28** with chlorosulfonic acid (64% yield), followed by the application of the conditions for the first step of the conversion of **19** to **20** to sulfonyl chloride **29** (79% yield) (Scheme 2b).



Reagents and Conditions: (a) T3P® (50 wt. % in DMF), DIPEA, DMF, 40 °C, 2 h; (b) HSO₃Cl, CHCl₃, 0 °C to rt, 30 min; (c) hexamethylenimine, NaH, DMF, 0 °C to rt, 1 h; (d) HSO₃Cl, CHCl₃, 0 °C to reflux, 90 min; (e) hexamethylenimine, DIPEA, DCM, 15 h; (f) NaBH₄, NiCl₂·6H₂O, MeOH, 0 °C to rt, 2 h.

Scheme 2: Synthesis of (a) 21 in one step from 16 and 17, (b) 23 in two steps from 28, and (c) 25 in three steps from 30.

In contrast to **29**, sulfonyl chloride **31**, itself produced by treatment of **30** with chlorosulfonic acid (78% yield), was reacted with azepane under milder conditions due to its acidic phenol functionality (64% yield). The nitro group of the resultant **32** was then reduced to the aniline **25** using a mixture of NaBH₄ and NiCl₂ (62% yield) (Scheme 2c). A third method for the conversion of a sulfonyl chloride to a sulfonamide was applied in the synthesis of *N*-methyl sulfonamide **33a**, with the heating under reflux of **19** with methylamine in THF prior to acidic trifluoroacetyl deprotection (82% yield). The free aniline of **33a** was then acetylated with acetic anhydride and pyridine to give **24** (56% yield) (Scheme 3a).



Reagents and Conditions: (a) (i) Methylamine (2 M in THF), THF, reflux, 90 min (ii) EtOH, HCl (37.5% w/v), H₂O, reflux, 3 h 30 min; (b) Ac₂O, pyridine, DCM, 2 d; (c) hexamethyleneimine, NaH, DMF, 0 °C to rt, 90 min; (d) NaBH₄, NiCl₂, MeOH, 0 °C to rt, 45 min; (e) Ac₂O, pyridine, DCM, 90 min to 5 h.

Scheme 3: Synthesis of (a) 24 in two steps from 19, (b) 26 in two steps from 34, and (c) 22 and 27 in one step from 20 or 26.

Aniline **26** was synthesised by the initial treatment of sulfonyl chloride **34** with azepane and NaH (42% yield), followed by reduction of the nitro group of **35** in the same manner as **32** with NaBH₄ and NiCl₂ (82% yield) (Scheme 3b). As with **33a**, **20** and **26** were reacted with acetic anhydride to give the acetylated derivatives (79-86% yield) (Scheme 3c).

2.2.3: Library Screening

With the synthesis of the focused library completed, the majority of the fragments were screened using the biochemical assay, with negligible inhibition values afforded at 1 mM concentration (Table 1).

| Compound | Inhibition (%) at 1 mM | ΔT_m (°C) at 5 mM | Compound | Inhibition (%) at 1 mM | ΔT_m (°C) at 5 mM |
|-----------|---------------------------|------------------------------|-----------|---------------------------|------------------------------|
| 15 | < 10 | -0.6 | 23 | ND | +0.1 |
| 16 | < 10 | -0.4 | 24 | < 10 | -0.4 |
| 20 | < 10 | -0.7 | 25 | ND | -1.6 |
| 21 | 13 | -0.4 | 26 | < 10 | -1.2 |
| 22 | 12 | -0.6 | 27 | < 10 | -0.4 |

Table 1: The results from the screening of the focused library from defragmentation of **2** against *Mtb* fumarase using both the biochemical assay and DSF.

Due to the lack of measurable inhibition from screening of the fragments with the biochemical assay, the use of sensitive biophysical techniques was explored. A protocol for the application of DSF against *Mtb* fumarase (previously optimised by Monica Kasbekar) was subsequently utilised for the screening of the focused library (Table 1).¹¹⁷ In contrast to **2**, which gave a ΔT_m of +3.9 °C at a ligand concentration of 0.63 mM, DSF screening of the focused library against *Mtb* fumarase at 5 mM afforded negative ΔT_m values for the majority of fragments, with a ΔT_m of -1.6 °C induced by **25** (Table 1). Whilst negative values, which are associated with preferential binding to the unfolded state of the protein,⁸⁸ are usually discounted, the investigation of fragments that afford these values has yielded useful information in previous studies.^{89, 90} Hence, further characterisation was sought.

Ligand-observed NMR is a technique in FBDD that can provide validation of fragment-protein interactions,⁹¹ and was previously applied against *Mtb* fumarase.¹¹⁷ The same conditions were adopted for use with selected fragments of the focused library, **22** and **26**, the largest and smallest molecules by molecular weight possessing the central phenyl ring (Figure 20).

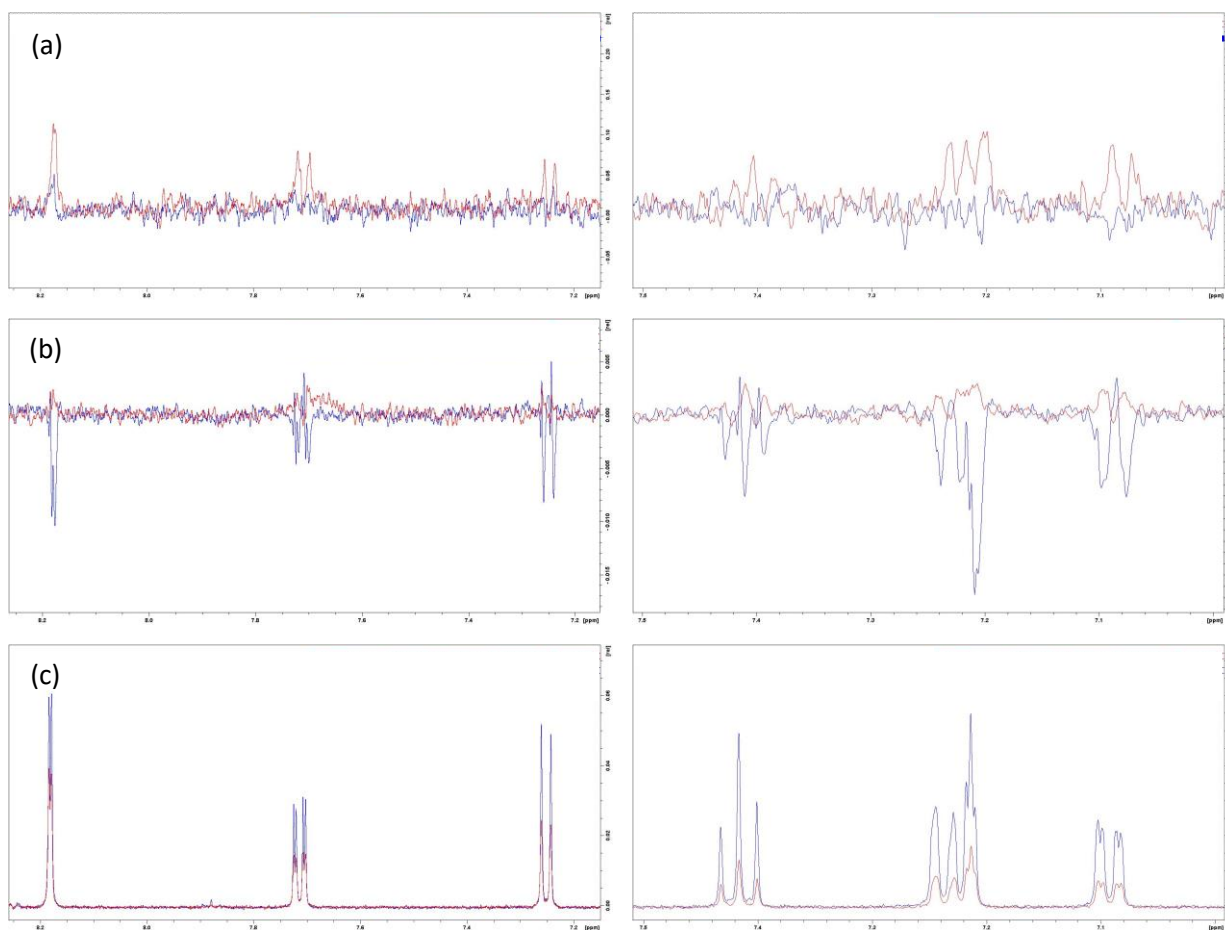
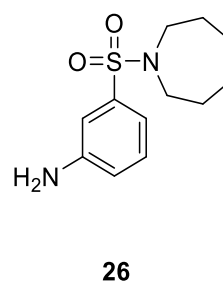
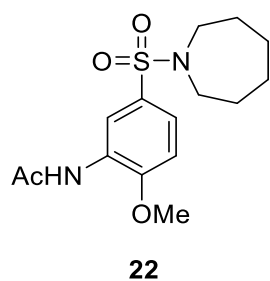


Figure 20: Ligand-observed NMR experiments (fragment-only = blue, fragment + protein = red) for **22** and **26**, including STD (a), waterLOGSY (b) and CPMG (c) experiments, with a focus on peaks from aromatic protons.

Comparison of the fragment-only ligand-observed NMR experiments with those in the presence of *Mtb fumarase* was supportive of fragment-protein interaction for both **22** and **26**, with the addition of protein resulting in the appearance of fragment peaks by STD (Figure 20a), the replacement of negative peaks with positive peaks by waterLOGSY (Figure 20b), and a clear attenuation of peak intensity by CPMG (Figure 20c). **2** was also added as a competitor ligand in the CPMG experiments, however this did not result in a

difference in peak intensity for either **22** or **26** (Figure 21), suggesting that the fragments did not possess the same binding mode as **2** with the protein. As a result, the acquisition of structural information on the fragment-protein interactions was sought.

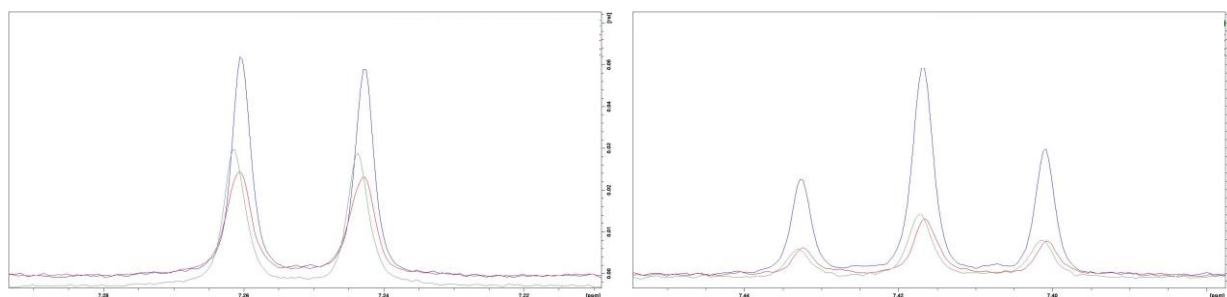


Figure 21: Ligand-observed CPMG experiments (fragment-only = blue, fragment + protein = red, fragment + protein + **2** = green) for **22** and **26**, with a focus on peaks from the highlighted protons (red).

Based on the prior work of recreating the X-ray crystal structure of **2**-bound *Mtb* fumarase, crystals of *Mtb* fumarase were produced by the application of 10,000x seed stock solution to a sitting drop plate with a 3 : 1 : 0.5 ratio by volume of protein (14 mg mL⁻¹ *Mtb* fumarase, 0.15 M NaCl, 10 mM Tris pH 8.0 and 0.5 mM TCEP), reservoir (10% w/v PEG3350, 5% DMSO and 0.30 M magnesium formate) and seed stock solution. Fragments **15**, **20** and **22** were soaked overnight into wells with the highest quality crystals, with the application of high concentration ligand solutions (50 mM ligand, 7.5% DMSO, 26.25% w/v PEG3350 and 0.20 M magnesium formate), with subsequent mounting and flash freezing, and the collection of X-ray data at the Diamond Light Source synchrotron or European Synchrotron Radiation Facility (Grenoble, France). Crystals soaked with **22** failed to diffract sufficiently for full data collection, however data were collected for crystals soaked with **15** or **20**. Molecular replacement with these datasets, using PHASER,¹¹⁸ was best performed with formate-bound *Mtb* fumarase (PDB code 5F92) as a search model.⁴¹ Analysis of the resultant electron density contour map failed to reveal evidence of a bound fragment. In the absence

of structural information from X-ray crystallography, the pursuit of a deconstruction-reconstruction approach with **2** and *Mtb* fumarase was not further prioritised.

2.3: Structure-activity Relationship Study of **2**

Following the defragmentation strategy with **2**, a structure-activity relationship (SAR) study was explored to develop inhibitors of *Mtb* fumarase more potent than **2**. This SAR study focused on modification of the phthalazinone and azepane rings of **2** in addition to the methoxy and sulfonyl groups on the central phenyl ring (Figure 22).

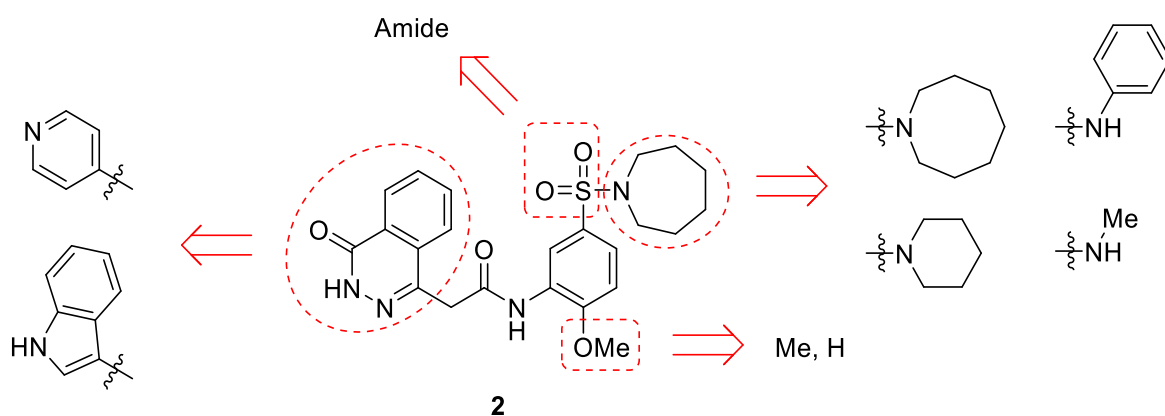
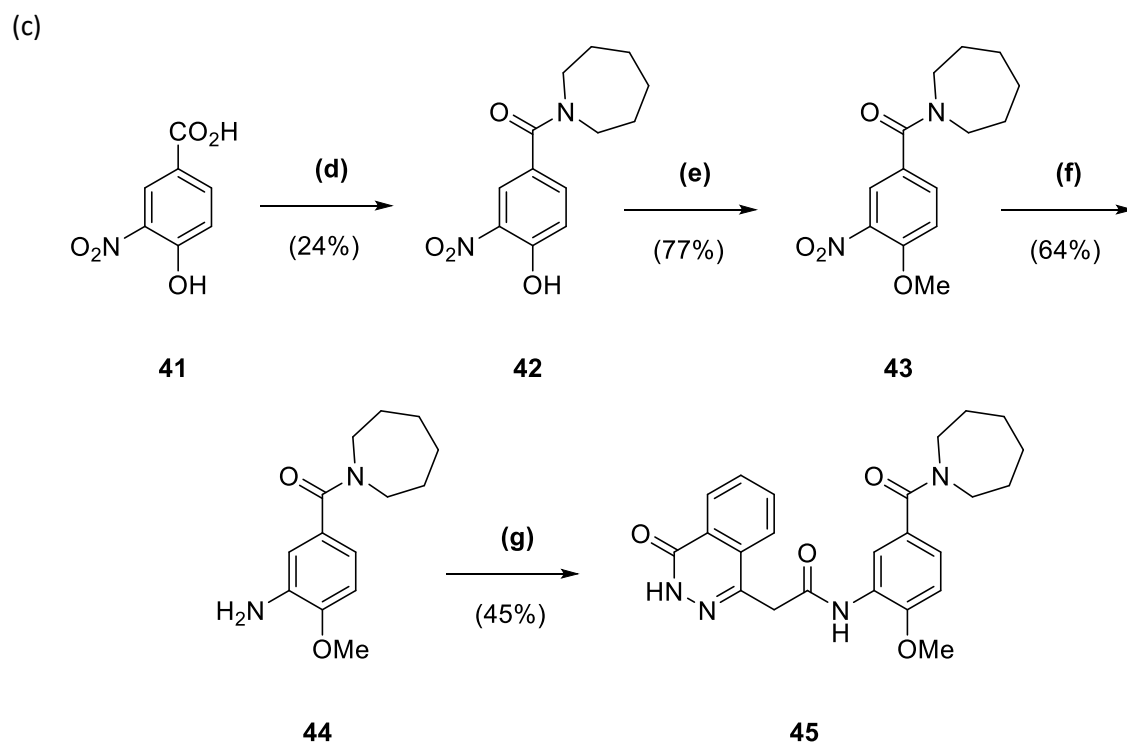
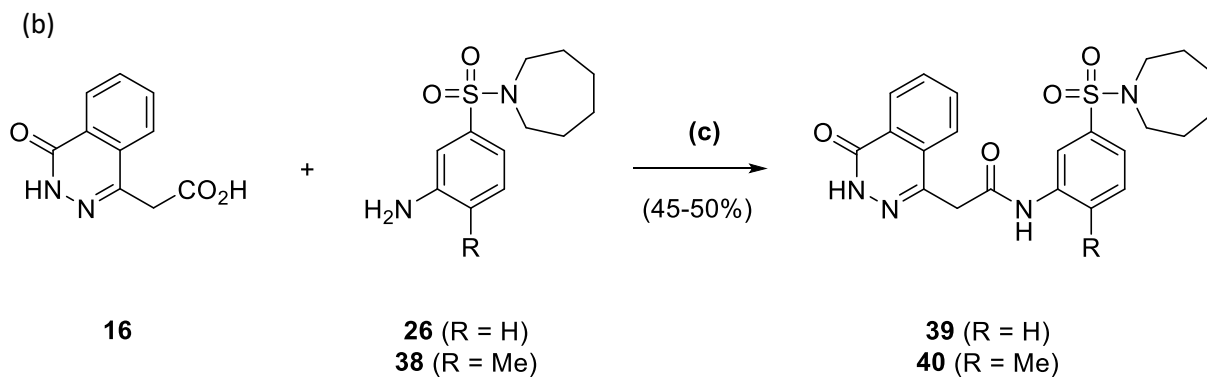
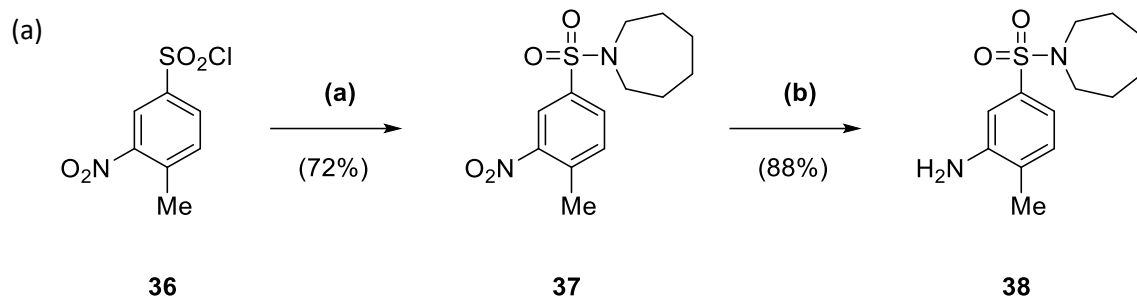


Figure 22: Areas of focus for the SAR study on **2**, the phthalazinone and azepane rings and the methoxy and sulfonyl substituents on the central phenyl ring, with initial ideas for modification.

2.3.1: Analogue Synthesis

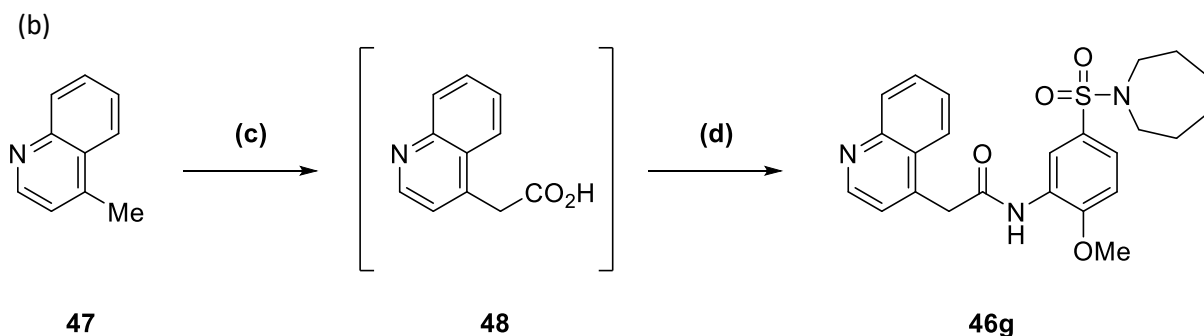
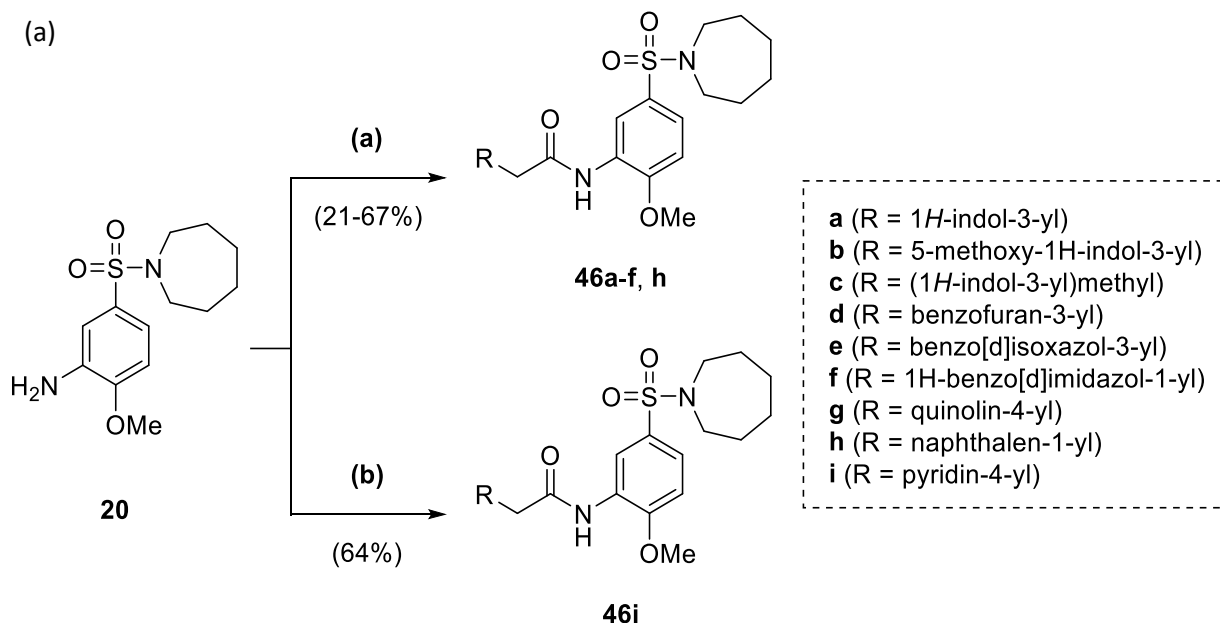
The synthesis of the analogues of **2** with alternative substituents to the methoxy group required the coupling of the corresponding anilines **26** and **38** with **16** by T3P® (45-50% yield) (Scheme 4b). Aniline **26** was available as a member of the focused library, however **38** required synthesis, which was achieved through the application of the synthetic route for **26** to sulfonyl chloride **36** (Scheme 4a). The amide analogue of **2**, **45**, was synthesised in four steps with the initial coupling of carboxylic acid **41** to azepane with T3P® to afford **42** (24% yield), whose phenolic functionality was methylated by dimethyl sulfate (77% yield). The product, **43**, was reduced by NaBH₄ and NiCl₂ to give aniline **44** (64% yield), which was coupled to **16** with T3P® (45% yield) (Scheme 4c).



Reagents and Conditions: (a) hexamethyleneimine, NaH, DMF, 0 °C to rt, 1 h; (b) NaBH₄, NiCl₂, MeOH, 0 °C to rt, 45 min; (c) T3P® (50 wt. % in EtOAc), DIPEA, DMF, 70 °C, 2 h; (d) hexamethyleneimine, T3P® (50 wt. % in DMF), DIPEA, DMF, 1 d; (e) Me₂SO₄, K₂CO₃, acetone, reflux, 2 h; (f) NaBH₄, NiCl₂·6H₂O, MeOH, 0 °C to rt, 90 min; (g) **16**, T3P® (50 wt. % in EtOAc), DIPEA, DMF, 70 °C, 2 h.

Scheme 4: Synthesis of (a) 38 in two steps from 36, (b) 39 and 40 in one step from 16 and 26 or 38, and (c) 45 in four steps from 41, including 16.

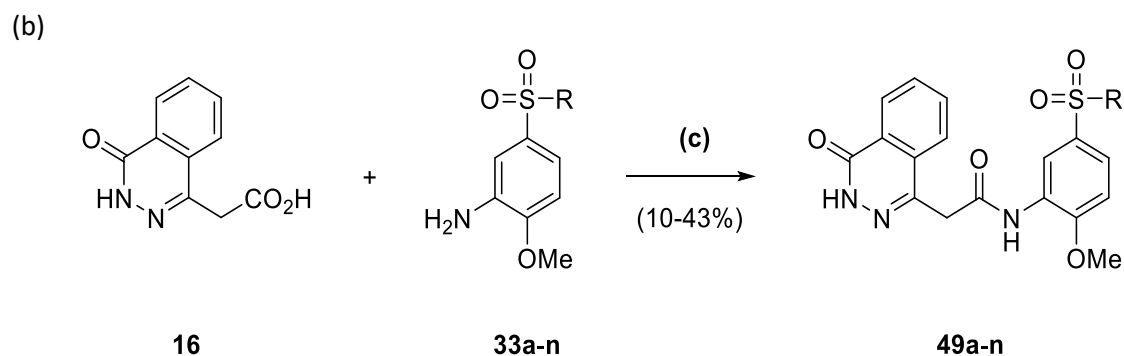
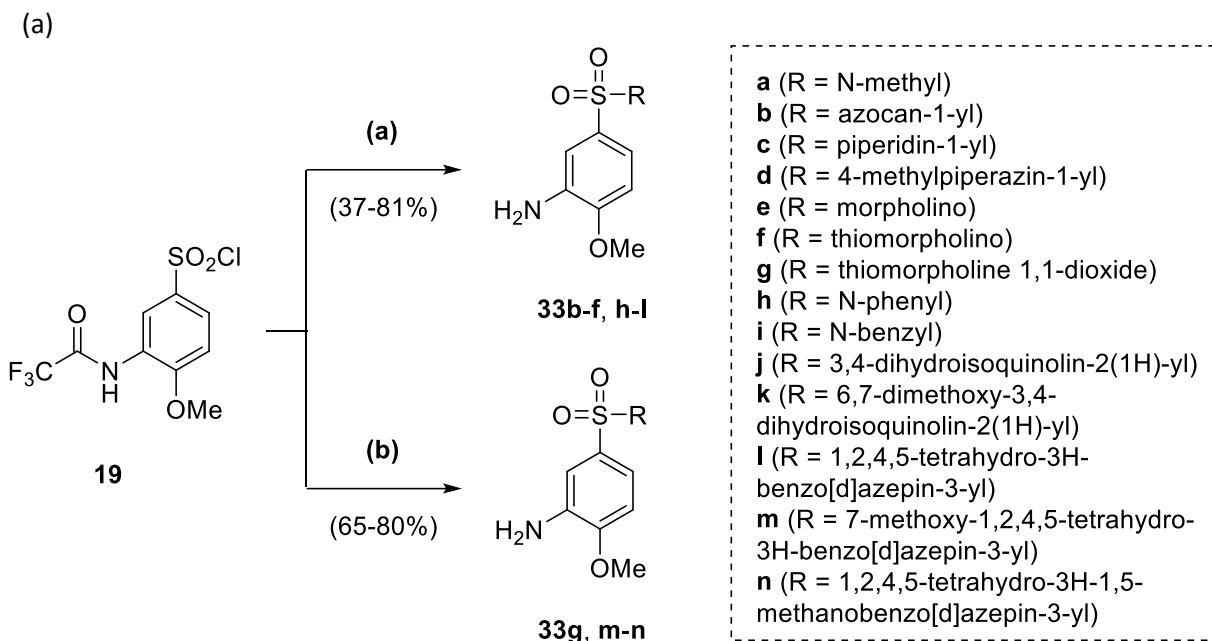
In contrast to **45**, the synthesis of **2** analogues **46a-f** and **46h** required only one reaction with the T3P[®]-mediated coupling of **20** to various carboxylic acids (21-67% yield) (Scheme 5a). The application of T3P[®] in coupling **20** and 4-pyridylacetic acid to synthesise **46i** was unsuccessful, however the use of an EDC-mediated reaction did afford the desired product (64% yield).



Reagents and Conditions: (a) RCH₂CO₂H, T3P[®] (50 wt. % in EtOAc), DIPEA, DMF, 70 °C, 1 to 4 h; (b) 4-pyridylacetic acid HCl, EDC.HCl, DIPEA, DMAP, DCM, 90 min; (c) CO₂ (s), LDA (2 M in THF/ heptane/ ethylbenzene), THF, -78 °C to rt, 1 h; (d) **20**, T3P[®] (50 wt. % in EtOAc), DIPEA, DMF, 70 °C, 40 min.

Scheme 5: Synthesis of (a) 46a-f and 46h-i in one step from 20, and (b) 46g in two steps from 47, including 20.

In the synthesis of **46g**, 4-methylquinoline **47** was deprotonated with LDA and treated with solid carbon dioxide to yield carboxylic acid **48**. However, due to difficulties in extracting this compound from the aqueous phase during workup, the solution was concentrated and the resultant solid taken forward crude with inorganic impurities for T3P[®]-mediated amide coupling with **20** (5% yield overall) (Scheme 5b).



Reagents and Conditions: (a) (i) RH, NaH, DMF, 0 °C to rt, 30 min to 20 h (ii) EtOH, HCl (37.5% w/v), H₂O, reflux, 4 h to 1 d; (b) (i) RH, NEt₃, DMAP, DCM, 30 min to 1 h (ii) EtOH, HCl (37.5% w/v), H₂O, reflux, 3 to 16 h; (c) T3P® (50 wt. % in EtOAc), DIPEA, DMF, 70 °C, 45 min to 5 h.

Scheme 6: Synthesis of (a) 33b-n in one step from 19, and (b) 49a-n in one step from 16 and 33a-n.

In the case of analogues **49a-n** of **2** with alternative amine substituents attached to the sulfonamide, a two step synthetic route was utilised. The second step for all analogues involved the T3P®-mediated coupling of the corresponding aniline with **16** (10-43% yield) (Scheme 6b). Anilines **33b-f** and **33h-l** were made from **19** using the same procedure as **20** with commercially available amines and NaH, followed by acidic trifluoroacetyl deprotection (37-73% yield) (Scheme 6a). However, milder reaction conditions were employed in the synthesis of **33g** due to concern about deprotonation adjacent to the sulfone group of thiomorpholine 1,1-dioxide by NaH, and these were subsequently applied to the last synthesised anilines **33m-n** due to greater ease of use (65-80% yield).

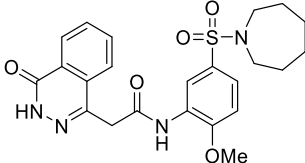
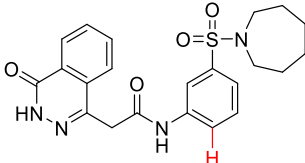
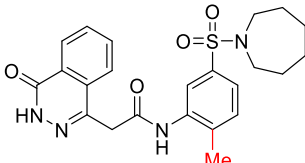
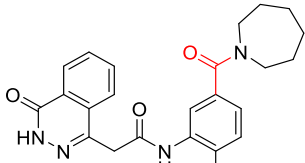
2.3.2: Screening against Target Protein

The synthesised analogues in the SAR study were initially screened at a single concentration of 50 μM using the *Mtb* fumarase biochemical assay (Figure 16b), with full dose-response curves also obtained to determine IC_{50} values, when allowed by solubility and potency. Structural information on ligand interactions with the target protein was also sought, with seventeen of the described analogues soaked into crystals of *Mtb* fumarase. Soaking was performed as described with fragments **15**, **20** and **22**, albeit with solutions including a lower concentration of ligand (0.5 – 5 mM).

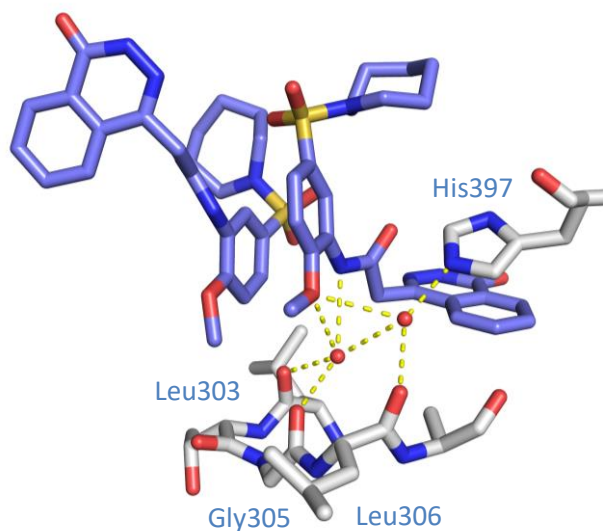
X-ray data were collected at the Diamond Light Source synchrotron or European Synchrotron Radiation Facility, with datasets obtained for all soaked analogues. Molecular replacement was initially carried out with a dataset from the soaking of **49b** into *Mtb* fumarase, due to its high resolution of 1.42 Å, using the previously published **2**-bound *Mtb* fumarase structure as a search model (PDB code 5F91) with PHASER.^{41, 118} Cycles of model building and refinement were then performed, using COOT and REFMAC5 respectively,^{120, 121} until improvements in model quality were judged to be unforthcoming. This model, with ligands and water molecules removed, was then used for molecular replacement with datasets obtained from the soaking of other **2** analogues into *Mtb* fumarase. Whilst an initial cycle of model building and refinement was performed for all analogues, full model building was only carried out with six further compounds of interest due to time constraints from the size of *Mtb* fumarase.

Beginning with modification of the substituents on the central phenyl ring of **2** (> 90% Inhibition at 50 μM), the SAR study showed that removal of the methoxy group in **39** (16% inhibition at 50 μM) was not tolerated. The potency of **39** was not restored with the addition of a methyl group at the same position of the phenyl ring in **40** (< 10% inhibition at 50 μM) (Figure 23a). It is possible that the replacement of the methoxy group of **2** reflects a negative impact on the π -stacking interaction between the central phenyl rings of the two binding molecules in the allosteric site of *Mtb* fumarase. However, **39** and **40** would also have not been able to recapitulate the complex water-mediated hydrogen-bonding network of **2** with the imidazole side chain of His397 and the backbone carbonyls of residues Leu303, Gly305 and Leu306 (Figure 23b).

(a)

| | Compound | Inhibition (%) at 50 μM |
|----|---|------------------------------------|
| 2 |  | > 90 |
| 39 |  | 16 \pm 1 |
| 40 |  | < 10 |
| 45 |  | 14 \pm 1 |

(b)



(c)

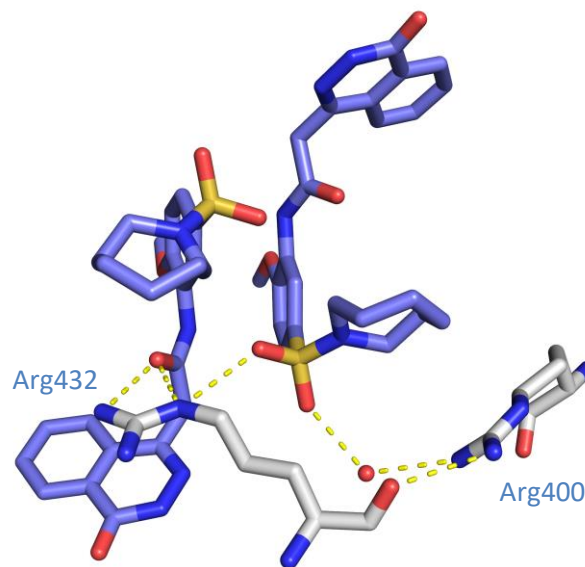


Figure 23: (a) Inhibition at 50 μM concentration afforded by compounds **39**, **40** and **45** in contrast to **2**; X-ray crystal structure of *Mtb* fumarase bound to **2** (PDB code 5F91, 2.00 Å, subunit A = white, subunit C = cyan, **2** = lilac, subunits B and D not visible), illustrating through rotation and the inclusion of interacting residues the interactions of (b) the methoxy group of one of the molecules of **2** and (c) the sulfonamide group of one of the molecules of **2**.⁴¹

The sulfonamide of **2** was shown to be sensitive to replacement, with the amide analogue **45** (14% inhibition at 50 μ M) affording significantly reduced inhibition of *Mtb* fumarase (Figure 23a). As with the methoxy group, this result is likely to be due to disruption of hydrogen bonds with adjacent residues, including the water-mediated interaction with Arg400 and the hydrogen bond with the guanidyl functional group of Arg432. This would have consequences for the dual binding mode of **2** in the allosteric site of *Mtb* fumarase, with the side chain of Arg432 interacting with the second molecule through both a hydrogen bond with the amide carbonyl and a cation- π interaction with the phthalazinone ring system (Figure 23c). The replacement of the sulfonamide of **2** with an amide would also introduce additional rigidification of the scaffold and could orientate the azepanyl ring in an unfavourable conformation in the allosteric site. With these key findings obtained the central phenyl ring of **2** was left unmodified throughout the rest of the study, with focus shifted to other regions including the phthalazinone ring (Figure 24).

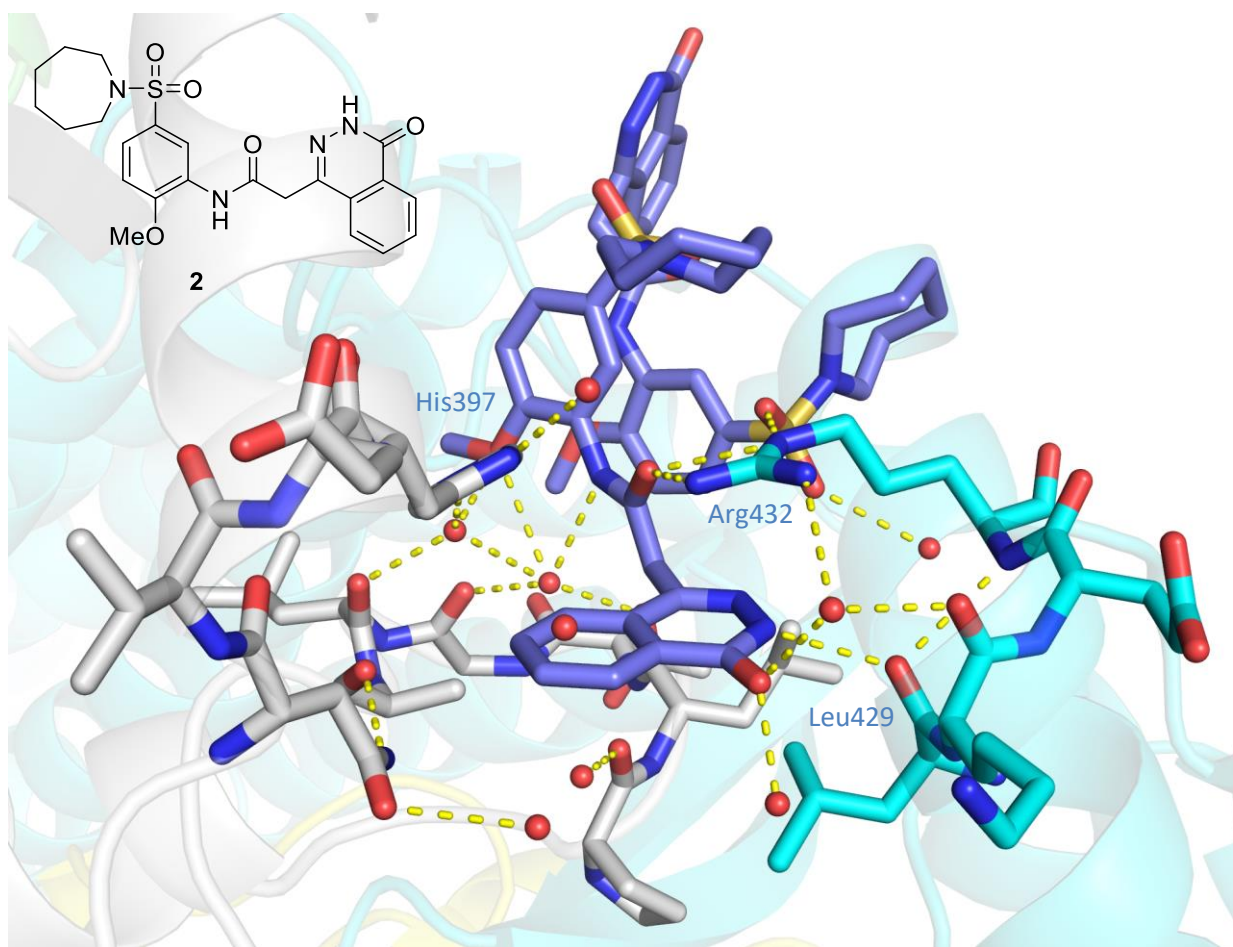
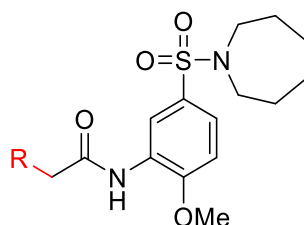


Figure 24: X-ray crystal structure of *Mtb* fumarase bound to **2** (PDB code 5F91, 2.00 Å, subunit A = white, subunit B = green, subunit C = cyan, subunit D = yellow, **2** = lilac), illustrating the interactions of the phthalazinone ring of **2**.⁴¹

Whilst fragment **2** showed that the absence of the phthalazinone ring had a detrimental impact on *Mtb* fumarase inhibition, it was unknown whether it could be replaced with alternative ring systems. In the 2-bound *Mtb* fumarase X-ray crystal structure, the phthalazinone ring is surrounded by networks of hydrogen-bonded water molecules and interacts with residues from both subunits at the head-to-head interface, including the backbone carbonyl of Leu429 as a hydrogen bond donor. As previously mentioned, the phthalazinone ring of **2** also participates in a cation- π interaction with Arg432, with which it additionally interacts through a hydrogen-bonded water molecule (Figure 24).⁴¹



| Compound | R | Inhibition (%) at 50 μ M | Compound | R | Inhibition (%) at 50 μ M |
|------------|---|---------------------------------|------------------------|---|---------------------------------|
| 2 | | > 90 | 46e | | < 10 |
| 46a | | 27 \pm 6 | 46f | | < 10 |
| 46b | | 38 \pm 5 | 46g^a | | 86 \pm 2 |
| 46c | | 12 \pm 9 | 46h | | 21 \pm 17 |
| 46d | | < 10 | 46i | | < 10 |

^a IC₅₀ determined to be 4.1 \pm 0.3 μ M.

Table 2: Inhibition at 50 μ M concentration afforded by derivatives of **2** with alternative aromatic substituents attached to the amide, compounds **46a-i**, in contrast to **2**.

A 3-substituted indole ring was initially explored as a replacement for the phthalazinone ring of **2**, based on a consideration of the available space in the binding pocket, however **46a** (27% inhibition at 50 μM) did not inhibit *Mtb* fumarase significantly at the screened concentration (Table 2). The soaking of *Mtb* fumarase crystals with **46a** afforded visible electron density corresponding to ligand in the allosteric site (Figure 25). The water networks and conformations of residues surrounding the indole ring of **46a** were not significantly changed relative to the **2**-bound *Mtb* fumarase structure, with the indole nitrogen also acting as a hydrogen bond donor to the backbone carbonyl of Leu429. In addition to the altered electronic profile of the indole relative to a phthalazinone ring system and its impact on the interaction with Arg432, it is possible that the loss of inhibitory capability was linked to the movement of the phenyl portion of the indole ring away from His397 relative to the phthalazinone of **2**, and its impact on a potential π - π stacking interaction (Figure 24 and Figure 25).

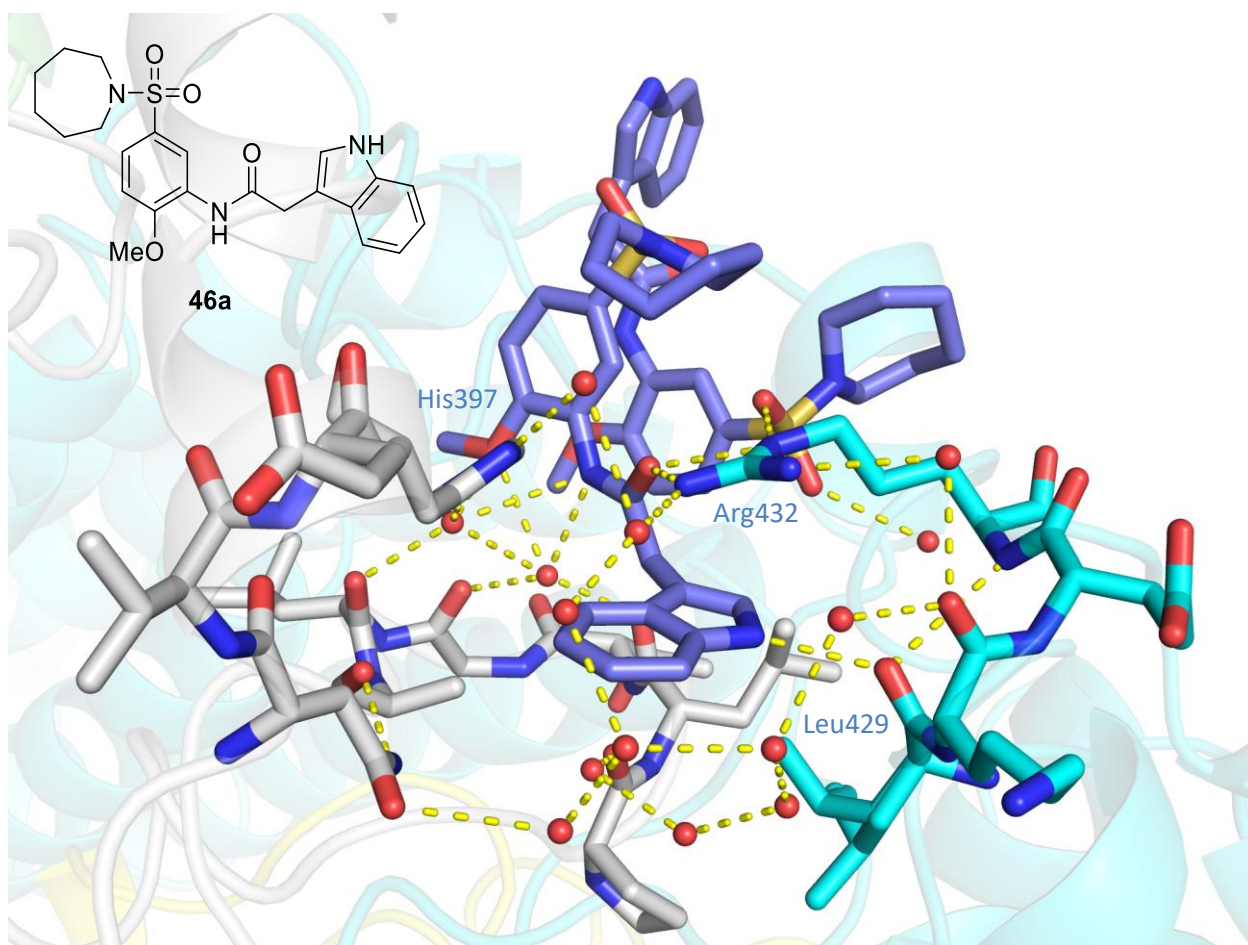


Figure 25: X-ray crystal structure of *Mtb* fumarase bound to **46a** (PDB code 6S7U, 1.48 \AA , subunit A = white, subunit B = green, subunit C = cyan, subunit D = yellow, **46a** = lilac), illustrating the interactions of the indole ring of **46a**.

Several derivatives of **46a** were synthesised to explore further SAR on this series, this includes the modification of the electronic properties of the indole ring through the substitution of a methoxy group in **46b** (38% inhibition at 50 μ M), and the addition of another methylene unit between the indole and amide functional groups of **46a** to provide further flexibility in **46c** (12% inhibition at 50 μ M) (Table 2). Analogues **46d-f**, possessing alternative 5-6 fused rings including benzofuran, benzisoxazole and benzimidazole, were also trialed however none of these offered observable inhibition in the biochemical assay (< 10% inhibition at 50 μ M). Therefore, 6-6 fused rings were explored due to their shape similarity to the phthalazinone ring. The use of a quinoline ring in **46g** (86% inhibition at 50 μ M) inhibited *Mtb* fumarase sufficiently at the tested concentration that a full dose-response curve was determinable (IC_{50} 4.1 μ M), and in addition an X-ray crystal structure of this compound was solved (Figure 26).

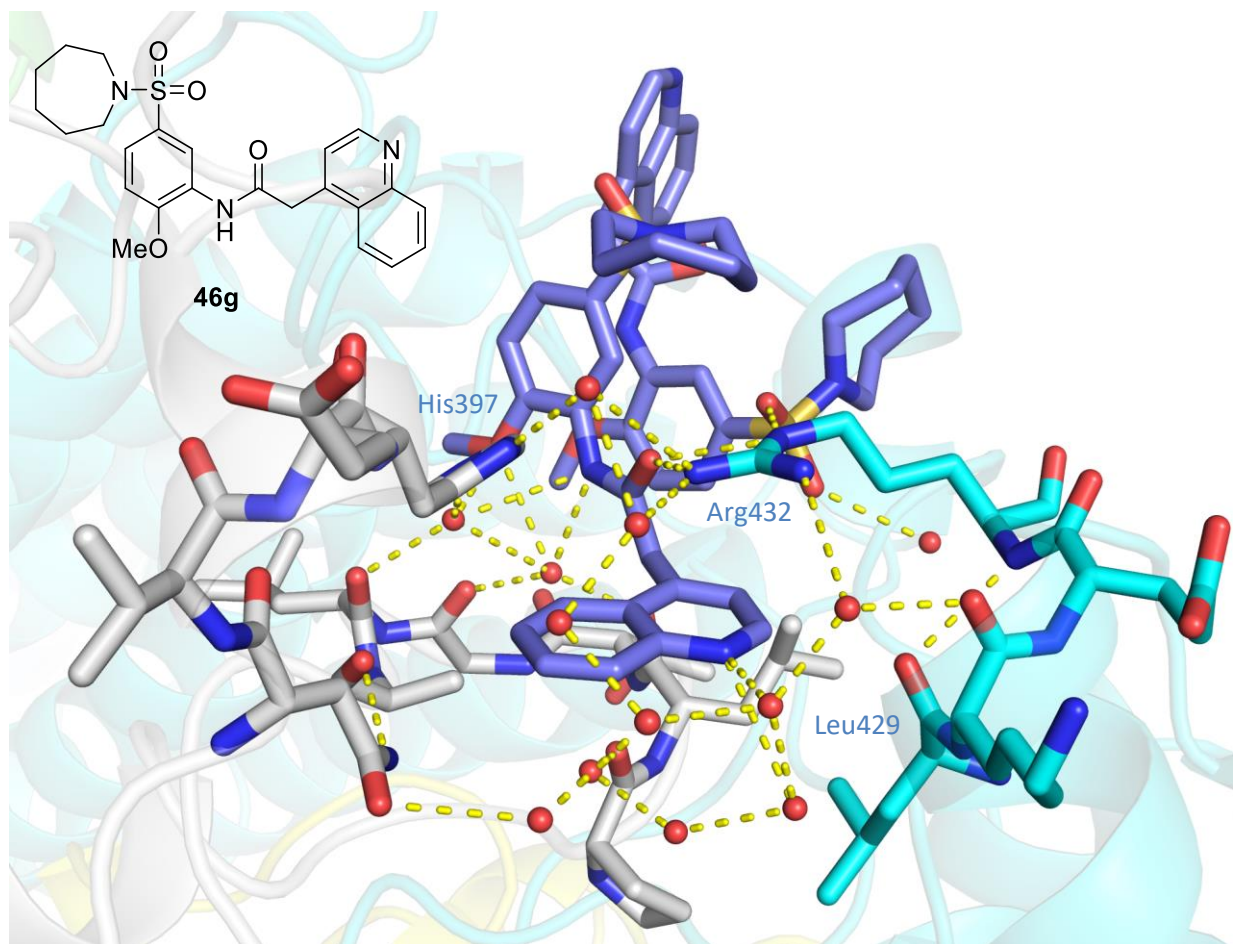


Figure 26: X-ray crystal structure of *Mtb* fumarase bound to **46g** (PDB code 6S7W, 1.44 Å, subunit A = white, subunit B = green, subunit C = cyan, subunit D = yellow, **46g** = lilac), illustrating the interactions of the quinoline ring of **46g**.

The X-ray crystal structure of **46g**-bound *Mtb* fumarase did not show significant movement in the conformations of the residues of the allosteric site relative to **2**, as with **46a**. However, due to the

improved overlap of the quinoline ring with the phthalazinone of **2**, it also exhibited the same relative orientation with His397 (Figure 24 and Figure 26). Whilst the quinoline ring of **46g** did not interact with the carbonyl of Leu429, it did hydrogen bond to two water molecules in an extensive hydrogen-bonded network (Figure 26). The loss of this nitrogen atom in **46h** (21% inhibition at 50 μ M), which possessed a naphthalene ring instead of a quinoline, resulted in a loss of inhibitory capability that prevented the measurement of an IC_{50} value (Table 2). Further, the introduction of a smaller pyridine ring in **46i** (< 10% inhibition at 50 μ M), which retained the hydrogen-bonding capability of the quinoline **46g**, illustrated the importance of full occupation of this portion of the allosteric site and the interaction with His397.

In addition to the phthalazinone ring of **2**, its azepanyl ring, occupying an 'azepane binding pocket' defined by His397, Arg400, Leu401 and Arg432 (Figure 27), was the focus of the majority of the SAR study. As this portion of the molecule made no hydrogen-bonding interactions with *Mtb* fumarase, it was judged that replacement of this ring with alternative moieties would be tolerated better than the phthalazinone ring system.

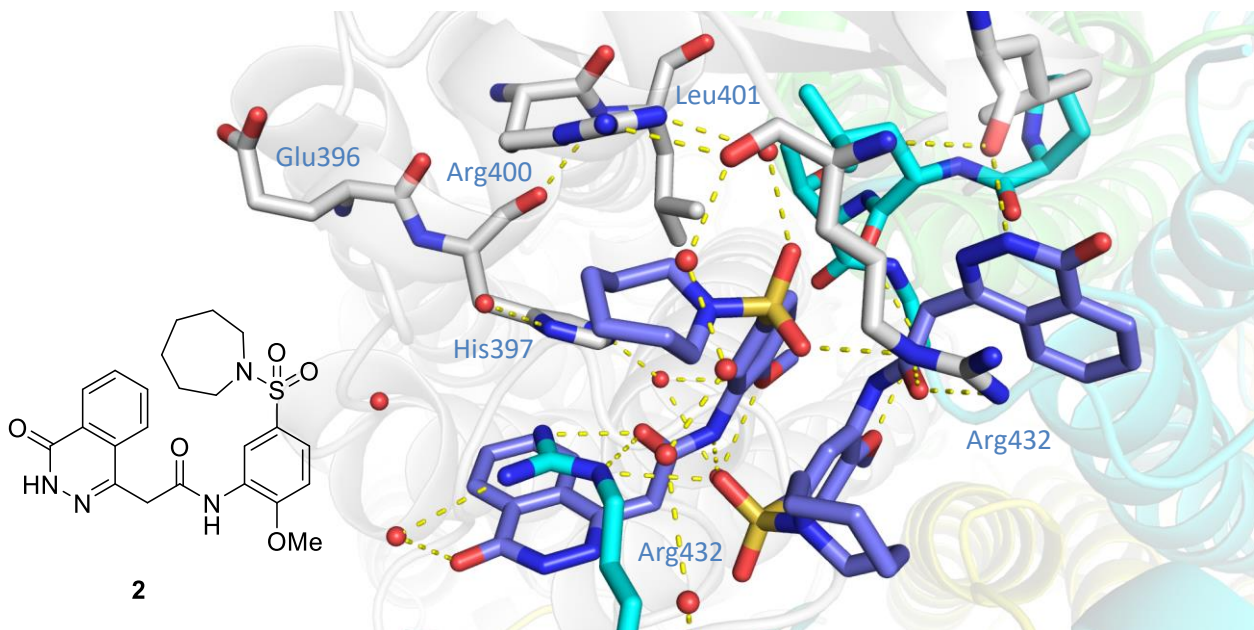
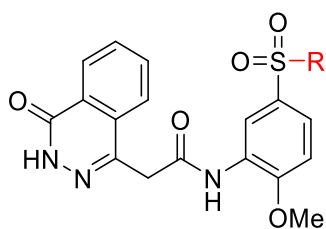


Figure 27: X-ray crystal structure of *Mtb* fumarase bound to **2** (PDB code 5F91, 2.00 Å, subunit A = white, subunit B = green, subunit C = cyan, subunit D = yellow, **2** = lilac), illustrating the azepane binding pocket of the allosteric site.⁴¹

The first modification was to produce a truncated derivative of **2**, **49a** (IC_{50} 57 μ M), with an *N*-methyl sulfonamide. In comparison to **21**, which lacked the sulfonamide of **2**, **49a** gave a measurable IC_{50} value that was only one order of magnitude higher than **2** (IC_{50} 2.0 μ M) (Table 3).



| Compound | R | IC ₅₀ | Compound | R | IC ₅₀ |
|------------|---|------------------|------------|---|------------------|
| 2 | | 2.0 ± 0.1 | 49h | | 17 ± 3 |
| 49a | | 57 ± 3 | 49i | | ND ^a |
| 49b | | 4.0 ± 0.1 | 49j | | 2.2 ± 0.2 |
| 49c | | 4.4 ± 0.1 | 49k | | 3.4 ± 0.2 |
| 49d | | 38 ± 2 | 49l | | 0.67 ± 0.03 |
| 49e | | 12 ± 1 | 49m | | 0.67 ± 0.01 |
| 49f | | 4.7 ± 0.2 | 49n | | ND ^b |
| 49g | | 13 ± 1 | | | |

^a 53 ± 3% inhibition at 50 μM concentration.

^b 44 ± 5% inhibition at 50 μM concentration.

Table 3: Half-maximal inhibitory concentrations (IC₅₀) afforded by derivatives of **2** with alternative amine substituents attached to the sulfonamide, compounds **49a-n**, in contrast to **2**.

An X-ray crystal structure of **49a**-bound *Mtb* fumarase was obtained, illustrating a 5 Å movement of the side chain of Arg400 (at Cε) relative to the structure with **2** to engage Glu396 in a salt bridge and form a hydrogen-bonded water network with Arg432, His397 and the amide carbonyl of **49a**, shrinking the apparent volume for elaboration in the azepane binding pocket (Figure 27 and Figure 28a).

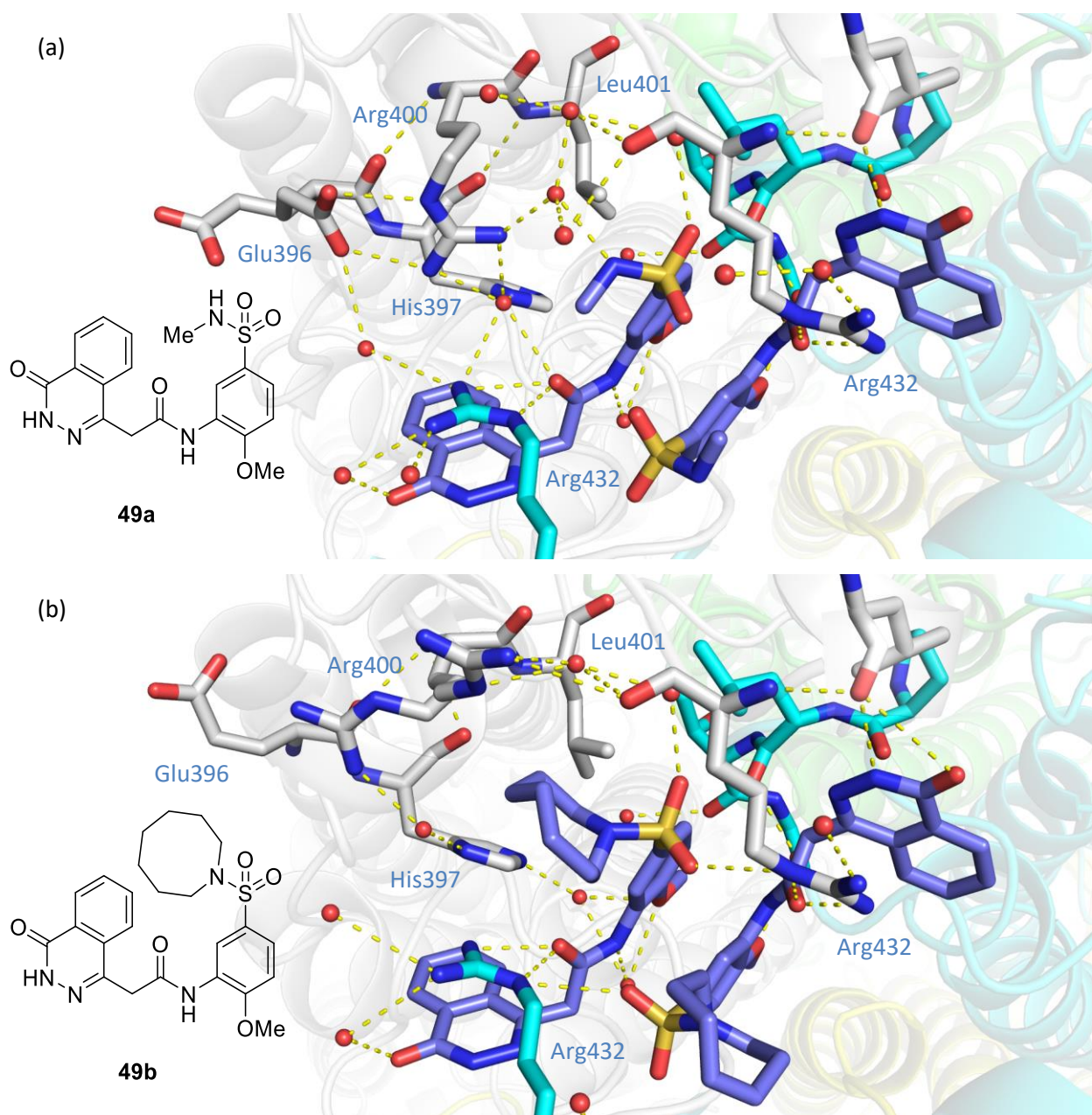


Figure 28: X-ray crystal structures of *Mtb* fumarase (subunit A = white, subunit B = green, subunit C = cyan, subunit D = yellow, ligand = lilac) bound to (a) **49a** (PDB code 6S7K, 1.55 Å), and (b) **49b** (PDB code 6S43, 1.42 Å), illustrating the azepane binding pocket of the allosteric site.

X-ray crystallography also shows the *N*-methyl sulfonamide of **49a** acting as a hydrogen bond donor, interacting with a water molecule hydrogen-bonded to Arg400 (Figure 28a). Following **49a**, derivatives of **2** were synthesised with alternative saturated heterocyclic rings attached to the sulfonamide to probe the azepane binding pocket. The larger 8-membered azocanyl analogue **49b** (IC₅₀ 4.0 μM) possessed a slightly attenuated IC₅₀ value relative to **2** (IC₅₀ 2.0 μM) (Table 3), showing that whilst larger ring sizes were

tolerated to an extent in the azepane binding pocket, they might not afford improvements in inhibition of *Mtb* fumarase. The X-ray crystal structure of **49b**-bound *Mtb* fumarase showed a similar binding pose for **49b** relative to **2** (Figure 27 and Figure 28b). A difference was seen with residue Arg400, adjacent to the azocanyl ring, which displayed greater uncertainty in its orientation, possibly due to a steric impact from the larger size of the ring system. The screening of the smaller 6-membered piperidinyl derivative **49c** (IC_{50} 4.4 μ M) afforded a similar IC_{50} value to **49b** (IC_{50} 4.0 μ M) (Table 3), supporting the status of the 7-membered azepanyl ring system as the ideal size for occupation of this pocket. The inhibition was sufficiently low to justify the exploration of further 6-membered heterocyclic analogues. The thiomorpholino derivative **49f** (IC_{50} 4.7 μ M) afforded the best inhibition out of these analogues, however it was not an improvement on **49c** (IC_{50} 4.4 μ M). In comparison, the *N*-methyl piperazinyl derivative **49d** (IC_{50} 38 μ M) was worse than **49c** (IC_{50} 4.4 μ M), possibly due to the insertion of a basic nitrogen atom between the two positively charged residues Arg400 and Arg432. Surprisingly, the morpholino and thiomorpholine dioxide analogues **49e** (IC_{50} 12 μ M) and **49g** (IC_{50} 13 μ M), which were expected to successfully engage these residues with their oxygen atoms acting as hydrogen bond acceptors, afforded inhibition intermediate between **49d** (IC_{50} 38 μ M) and **49c** (IC_{50} 4.4 μ M).

With several saturated heterocyclic ring systems explored, the tolerance of the azepane binding pocket to aromatic rings was examined, with the goal of engagement of residues Arg400 and Arg432 in cation- π interactions, beginning with **49h** (Figure 29).

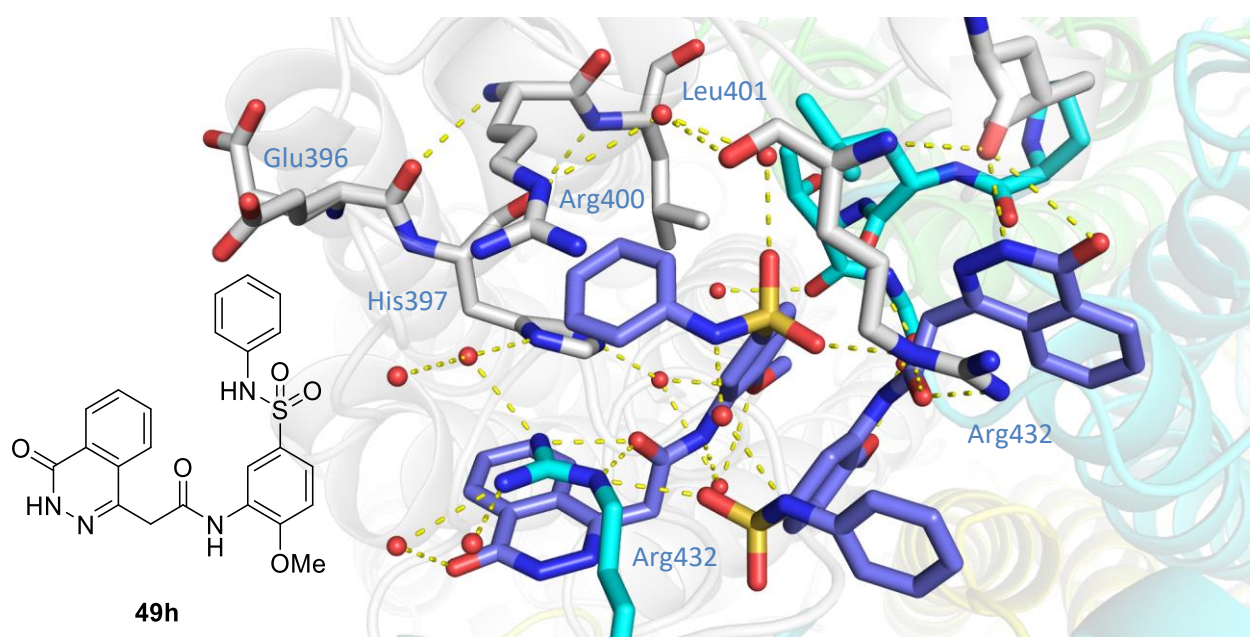


Figure 29: X-ray crystal structure of *Mtb* fumarase bound to **49h** (PDB code 6S7S, 1.70 Å, subunit A = white, subunit B = green, subunit C = cyan, subunit D = yellow, **49h** = lilac), illustrating the interactions of the *N*-phenyl substituent of **49h**.

The attachment of a phenyl ring to the sulfonamide in **49h** (IC_{50} 17 μ M) did not lead to an improvement in inhibition (Table 3), despite the X-ray crystal structure of **49h**-bound *Mtb* fumarase revealing a coplanar arrangement of the guanidyl functional group of Arg400, 4 Å above the phenyl ring (Figure 29). Notably, the sulfonamide nitrogen atoms of the two **49h** molecules in the allosteric site were found sharing a water molecule in an indirect hydrogen-bonded interaction (Figure 29), which was not observed in **49a** (Figure 28a). The drop in inhibition of **49h** (IC_{50} 17 μ M) may be due to a combination of insufficient extension into the azepane binding pocket and a lack of flexibility, however the benzyl derivative with a methylene linker between the sulfonamide and phenyl ring, **49i** (53% inhibition at 50 μ M), performed worse in the biochemical assay (Table 3).

Rigidification of **49i** through the incorporation of the benzyl group into a tetrahydroisoquinolyl ring system in **49j** (IC_{50} 2.2 μ M) improved inhibition, with a comparable IC_{50} to **2** (IC_{50} 2.0 μ M) (Table 3). The X-ray crystal structure showed a 3 Å movement of the phenyl portion of the tetrahydroisoquinolyl ring system of **49j** relative to the phenyl ring of **49h** (Figure 29 and Figure 30a), reaching further into the azepane binding pocket and lying between the guanidyl functional groups of Arg400 and Arg432 (Figure 30a). The movement of the phenyl portion of the tetrahydroisoquinolyl ring system of **49j** through ring expansion to the tetrahydrobenzoazepane analogue **49l** (IC_{50} 0.67 μ M) (Table 3 and Figure 30b), afforded the first sub-micromolar inhibitor with an improved IC_{50} value against *Mtb* fumarase relative to **2** (IC_{50} 2.0 μ M). This was hypothesised to be the result of more efficient coverage of the azepane binding pocket and better tolerated interactions with Arg400 and Arg432.

Modifications were made to **49j** and **49l** to afford further improvements in binding, with the addition of methoxy substituents in **49k** (IC_{50} 3.4 μ M) and **49m** (IC_{50} 0.67 μ M), however this did not significantly alter the values obtained from the biochemical assay (Table 3). A methylene bridge was also added to the tetrahydrobenzoazepane ring system of **49l** in **49n** (44% inhibition at 50 μ M), however this was not tolerated, presumably due to steric effects in the azepane binding pocket and the movement of the phenyl portion of the ring system.

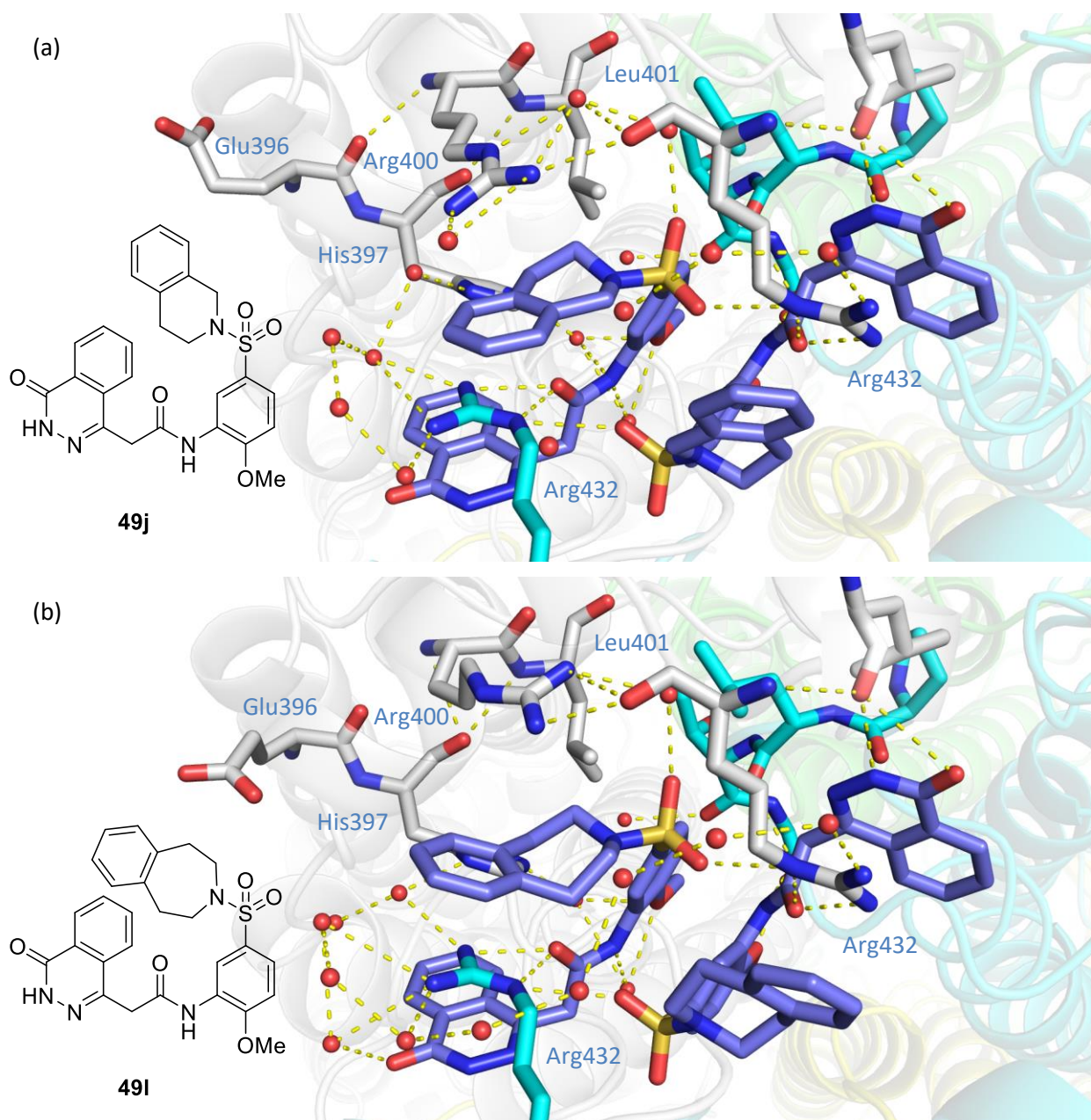


Figure 30: X-ray crystal structures of *Mtb* fumarase (subunit A = white, subunit B = green, subunit C = cyan, subunit D = yellow, ligand = lilac) bound to (a) **49j** (PDB code 6S7Z, 1.85 Å), and (b) **49i** (PDB code 6S88, 1.59 Å), illustrating the azepane binding pocket of the allosteric site.

2.3.3: Screening against *Mycobacterium tuberculosis*

With a significant amount of SAR explored with this series, twenty of the **2** analogues were sent to collaborators Dr Daben Libardo and Dr Helena Boshoff (Tuberculosis Research Section, National Institutes of Health) for testing against *Mtb* in liquid culture (Table 4).

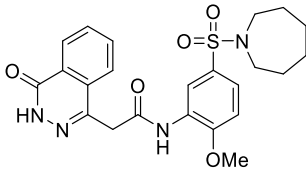
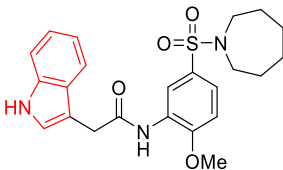
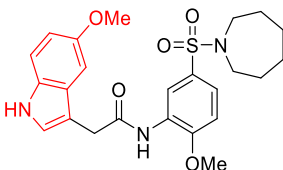
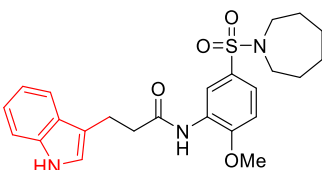
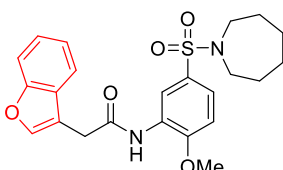
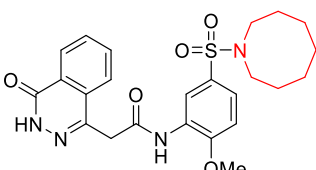
| Compound | H37Rv <i>Mtb</i> MIC (μM) | | | |
|---|--|---------|-------------|----------|
| | GAST-Fe | 7H9/BSA | 7H9/glucose | 7H9/DPPC |
| 2  | > 100 | > 100 | > 100 | > 100 |
| 46a  | > 100 | > 100 | 100 | 9.4 |
| 46b  | > 100 | > 100 | > 100 | 12.5 |
| 46c  | > 100 | > 100 | 25 | 9.4 |
| 46d  | > 100 | > 100 | 9.4 | 6.3 |
| 49b  | > 100 | > 100 | 25 | 18.8 |

Table 4: MIC values afforded by compounds **46a-d** and **49b** in contrast to **2** against H37Rv *Mtb*, performed by Dr. Daben Libardo.

The compounds were tested against *Mtb* in four different growth media (Table 4), which included low-iron glycerol-alanine-salts (GAST-Fe) and Middlebrook 7H9 broth (7H9). GAST-Fe is a minimal medium that is used to test compound efficacy when the majority of the *de novo* biosynthetic pathways in *Mtb* are active, whereas 7H9 is a commercially available medium that supports mycobacterial growth when supplemented with other nutrients. In this study three 7H9-based media were tested, supplemented with mixtures defined by inclusion of either bovine serum albumin (BSA), glucose or dipalmitoylphosphatidylcholine (DPPC). 7H9/BSA is used to investigate plasma protein binding, whereas

7H9/glucose and 7H9/DPPC test compound efficacy with *Mtb* utilising either glucose or a fatty acid as a carbon source, which are both predicted to be relevant during *in vivo* pathogenesis.¹²²

To enable direct comparisons with **2**, the compound was also sent with its analogues for *in vitro* tests but did not afford an MIC value in any media at the tested concentrations (Table 4), consistent with the previous study.⁴¹ Whilst no compounds afforded MIC values with GAST-Fe or 7H9/BSA media, values were obtained for 5 compounds in 7H9/glucose and 7H9/DPPC media (Table 4). Three compounds afforded MIC values against *Mtb* with glucose as a carbon source, however the best results were seen with 7H9/DPPC. In this medium, the testing of **49b** gave an MIC value of 18.8 μM , whilst the values from **2** analogues with 5-6 fused rings ranged from 9.4 to 12.5 μM . As negative results were obtained at the screened concentrations with 7H9/BSA as a medium, it is possible that plasma protein binding could be an issue for this series.

Out of the compounds with observable MIC values against *Mtb* (Table 4), **49b** is the only **2** analogue for which an IC_{50} value was also determinable (IC_{50} 4.0 μM) and possesses the greatest structural similarity to **2**, differing only by its possession of a larger ring attached to the sulfonamide (8- vs 7-membered). It is possible that the difference in behavior of **49b** relative to **2** in the *Mtb in vitro* growth assay is related to differing physicochemical properties, such as its increased lipophilicity (cLogP 3.1 vs 2.7), however it is not guaranteed that this result is from on-target engagement. Further study on this series is required to optimise the physicochemical properties of these molecules to develop potent compounds to kill *Mtb*.

2.4: Summary and Future Work

The exploration of a deconstruction-reconstruction approach with *Mtb* fumarase and **2** proved challenging, with fragments affording negative ΔT_m values by DSF and their soaking into crystals failing to afford ligand density by X-ray crystallography. This is likely due to the multiple interactions that **2** makes across the allosteric site with two subunits from the protein, in addition to itself through its dual binding mode. The subsequent application of a SAR study on **2** was fruitful, with the development of a sub-micromolar inhibitor of *Mtb* fumarase with an IC_{50} three-fold lower than the original HTS hit. Multiple X-ray crystal structures were obtained of ligand-bound *Mtb* fumarase that could be utilised in the further improvement of ligand-target interactions. Further, the screening of a range of analogues of **2** against *Mtb in vitro* identified several compounds that afford measurable MIC values, in contrast to the original HTS

hit. These results represent a significant improvement on the starting point and encourage further work on *Mtb* fumarase as a target for the development of bactericidal compounds.

With the reassuring results from the screening of **2** analogues in the *Mtb in vitro* growth assay, it would be useful to determine whether the MIC values are the result of successful target engagement or off-target effects. This could be achieved through the screening of compounds against *Mtb* strains with modified fumarase expression, which have already been developed in the recent study on fumarase deficiency in *Mtb*.³⁷ In the event that *in vitro* effects are the result of successful target engagement, a physicochemical study on the compounds could be initiated to improve the bactericidal activity of this series of *Mtb* fumarase inhibitors.

3: tRNA (m¹G37) methyltransferase

3.1: Fragment Hits and Initial Elaboration Approaches

The screening of the Abell research group fragment library against *Mab* TrmD was performed by Dr Sherine Thomas (Department of Biochemistry, University of Cambridge) using a two-stage biophysical screening cascade.⁵⁰ This consisted of the initial use of DSF as a first-line screen, where 53 fragment hits (5.6% hit rate) were identified affording ΔT_m values greater than the cut-off of 3 standard deviations. These hits were then validated by X-ray crystallography on soaking into crystals of *Mab* TrmD, of which 27 showed evidence of binding to the active site. These fragments, representing a variety of scaffolds, possessed binding modes that occupied different regions of the active site defined by the X-ray crystal structure of *Mab* TrmD with SAM bound (Figure 9b).⁵⁰

The adenine ring system of SAM ‘anchors’ the molecule in the active site, hydrogen-bonding to the backbone amides of Ile133, Gly134, Tyr136 and Leu138 with the ring system ‘sandwiched’ between Pro85 and the side chains of Leu138 and Ala144, in a volume that can be defined as the ‘adenine binding region’ (Figure 31). All 27 fragment hits were shown in their X-ray crystal structures with *Mab* TrmD to occupy the adenine binding region to an extent, with most recreating at least some of the hydrogen-bonding interactions of the adenine moiety of SAM in this region.⁵⁰

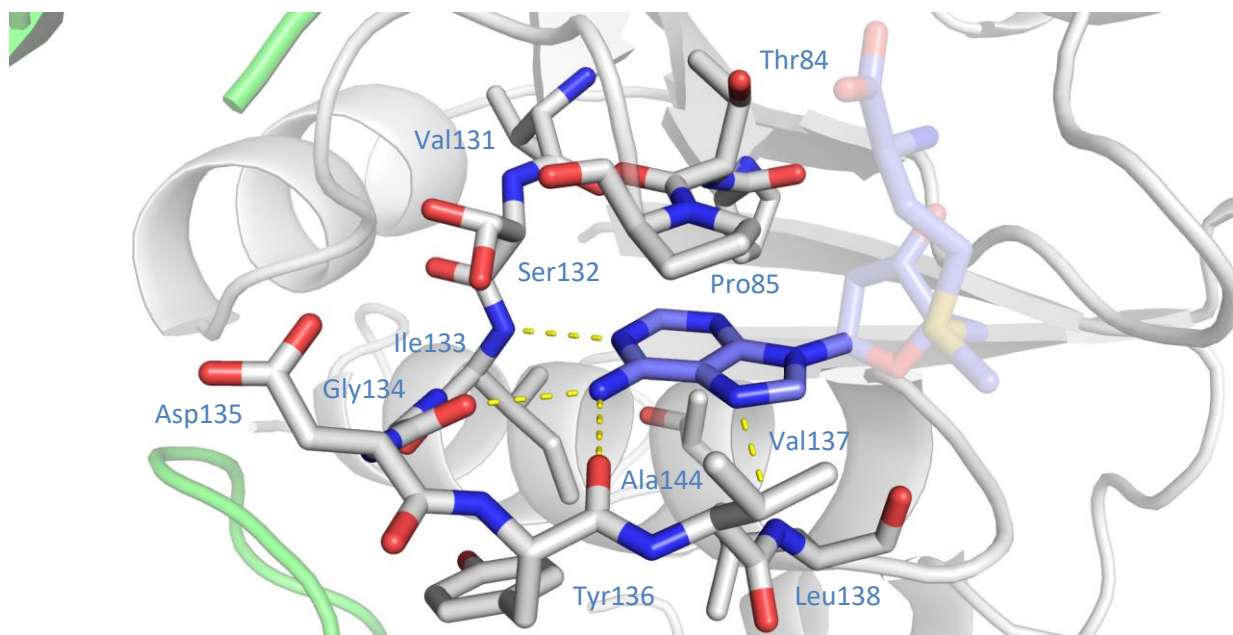


Figure 31: X-ray crystal structure of *Mab* TrmD bound to SAM (PDB code 6NW6, 1.67 Å, subunit A = white, subunit B = green, SAM = lilac), illustrating the binding of the adenine motif in one of the active sites.⁵⁰

The ribose moiety of SAM is enclosed by three loops of the trefoil knot, oriented above residues Gly140 and Gly141, interacting on either side with the backbone amides of residues Pro83 and Gly109 respectively and behind with an ordered water molecule in the ‘ribose binding region’ (Figure 32a).⁵⁰

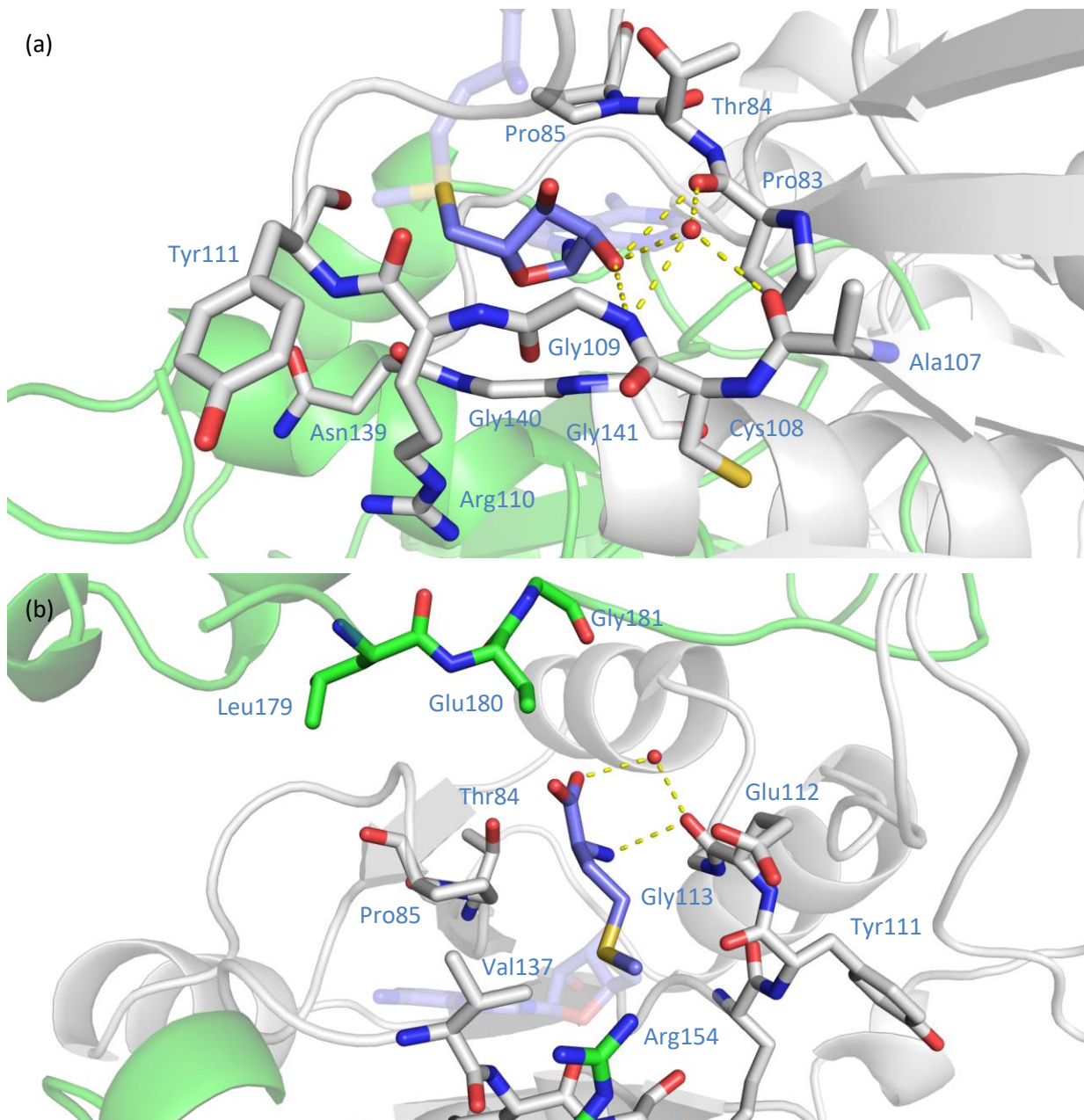


Figure 32: X-ray crystal structure of Mab TrmD bound to SAM (PDB code 6NW6, 1.67 Å, subunit A = white, subunit B = green, SAM = lilac), illustrating (a) the binding of the ribose motif in one of the active sites, and (b) the binding of the methionine motif in one of the active sites.⁵⁰

Finally, despite only interacting directly with the backbone carbonyl of Glu112, the methionine portion of SAM occupies a large volume in the active site. This ‘methionine binding region’ encompasses the volume

bordered by Thr84 to Pro85, Tyr111 to Gly113, the side chains of Val137 and Arg154, Glu180 to Gly181, and a portion of the interdomain linker that is not visible in the X-ray crystal structure (Figure 32b). Most of the fragment hits were shown to extend at least partially into the ribose binding region in their X-ray crystal structures, however only a few were shown to venture into the methionine binding region.⁵⁰

The fragment hits were prioritised for elaboration by consideration of both synthetic tractability and binding pose in X-ray crystal structures with *Mab* TrmD, including the available unoccupied volume in the active site and the suitability of vectors from positions on the scaffold for future elaboration. Fragment hits of interest were subjected to further screening by ITC to obtain K_d values, in addition to SAR by catalogue studies with structurally-related compounds.

3.1.1: Fragment-growth Approach with Hit **50**

Fragment hit **50** (K_d 89 μ M, LE 0.55), which primarily binds in the adenine binding region with its pyrazole ring and ester carbonyl, was initially selected for elaboration due to its high LE and the volume remaining for elaboration in the active site (Figure 33). Further, the ester functional group provided a vector for growth that was judged to be desirable, in addition to offering attractive synthetic tractability.⁵⁰

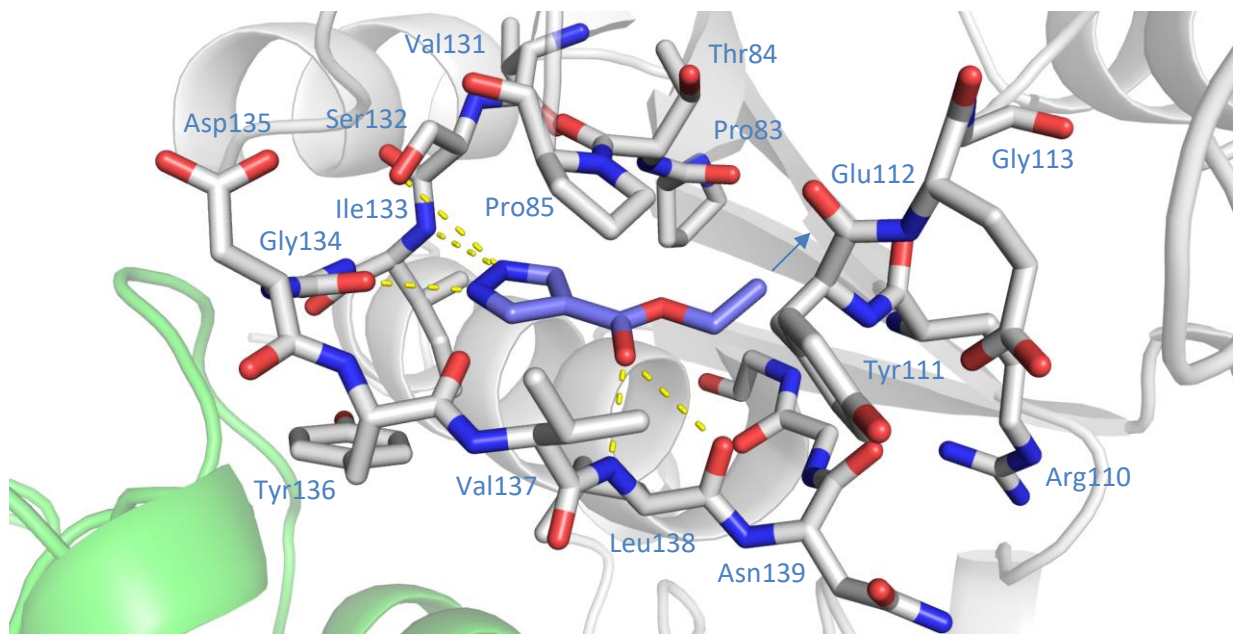


Figure 33: X-ray crystal structure of *Mab* TrmD bound to **50** (PDB code 6QOS, 2.05 Å, subunit A = white, subunit B = green, **50** = lilac), illustrating one of the active sites.⁵⁰

This fragment hit was used as a starting point for the design of a number of analogues, that were elaborated into the ribose and methionine binding regions using a benzyl ester motif (Figure 34).¹²³

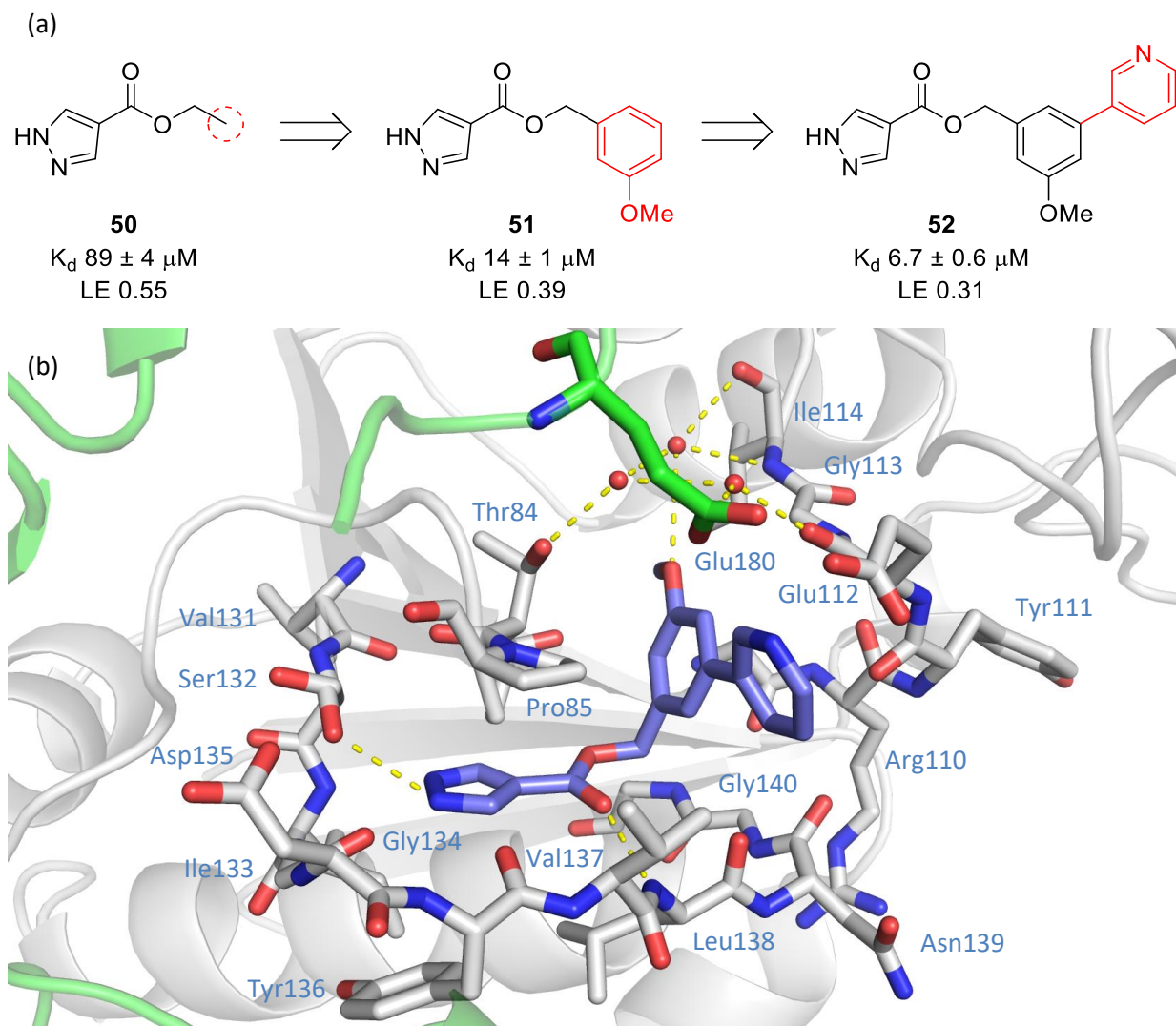


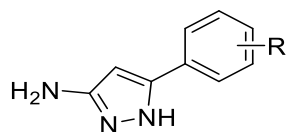
Figure 34: (a) Highlights of fragment-growth strategy applied to fragment hit **50**;¹²³ (b) X-ray crystal structure of Mab TrmD bound to **52** (PDB code 6QQQ, 1.85 Å, subunit A = white, subunit B = green, **52** = lilac), illustrating one of the active sites.¹²³

The application of a fragment-growth approach with **50** was carried out in conjunction with Alexander Fanourakis (Part III student, Department of Chemistry, University of Cambridge), who carried out ~70% of the published synthetic chemistry under the supervision of the author. Unfortunately, attempts to improve the affinity of **50** in a ligand-efficient manner proved challenging, with the best compound in this lead series **52** (K_d 6.7 μM , LE 0.31) only affording a 13-fold improvement in affinity with a significantly attenuated LE (Figure 34).¹²³ As a result, an alternative fragment elaboration strategy focused on fragment hits **53** and **59** was prioritised.

3.1.2: Fragment-merging Approach with Hits **53** and **59**

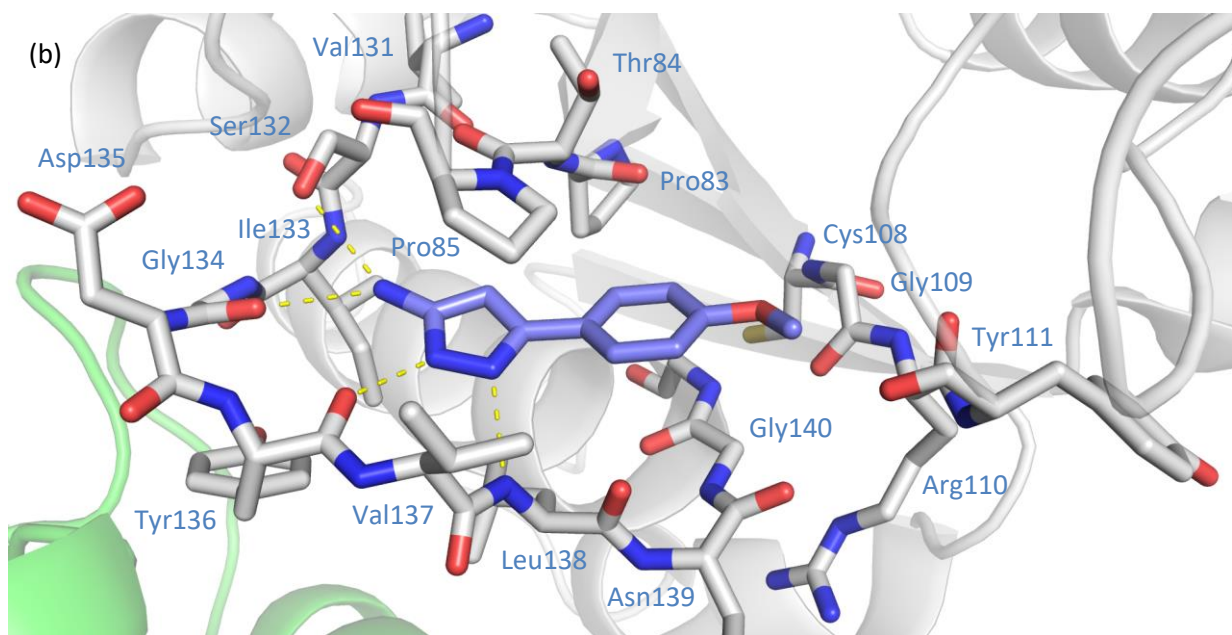
The fragment hit **53** (K_d 170 μ M, LE 0.37) was shown in its X-ray crystal structure to span the active site, with its 3-aminopyrazole ring system anchoring the molecule in place through hydrogen bonds in the adenine binding region to the backbone amides of Gly134, Tyr136 and Leu138, in addition to the side chain of Ser132 (Figure 35).

(a)



| Compound | R | ΔT_m^a ($^{\circ}$ C) | K_d (μ M) | LE ^b |
|-----------|-------|--------------------------------|------------------|-----------------|
| 53 | 4-OMe | +3.0 | 170 \pm 14 | 0.37 |
| 54 | H | +1.5 | ND | - |
| 55 | 4-Me | +1.4 | ND | - |
| 56 | 3-OMe | -0.5 | ND | - |

(b)



^a 5 mM ligand and 10 μ M Mab TrmD, measured by Dr Sherine Thomas (Department of Biochemistry, University of Cambridge) for **53-55**.

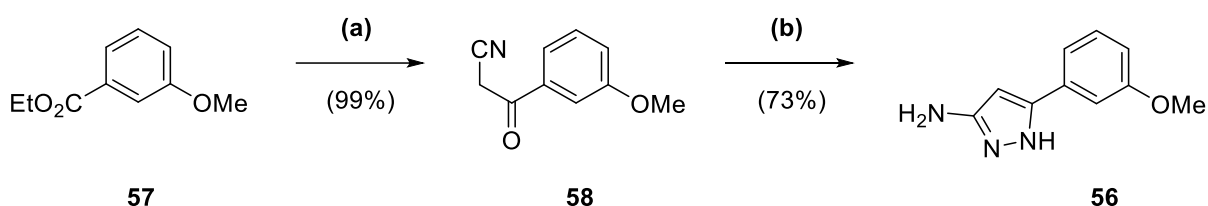
^b kcal mol⁻¹ HA⁻¹.

Figure 35: (a) The change in the melting temperatures (ΔT_m), affinities (K_d) and ligand efficiencies of fragment hit **53** and its structural analogues; (b) X-ray crystal structure of Mab TrmD bound to **53** (PDB code 6QOT, 1.62 \AA , subunit A = white, subunit B = green, **53** = lilac), illustrating one of the active sites.⁵⁰

Extending from the 5-position of the pyrazole ring, the 4-methoxyphenyl ring system of **53** occupies the ribose binding region where it makes no further hydrogen-bonding interactions. However, this portion of the fragment hit was shown to be sensitive to modification, with the phenyl **54** and 4-tolyl **55** derivatives

in the fragment library affording smaller ΔT_m values of +1.5 and +1.4 °C respectively in comparison to **53** (ΔT_m +3.0 °C) (Figure 35).

Further SAR on the 4-methoxyphenyl ring system of **53** was provided by the synthesis of the 3-methoxyphenyl analogue **56** (Scheme 7). This was achieved through the conversion of methyl ester **57** to the corresponding β -ketonitrile **58** through treatment with *n*-butyllithium and acetonitrile (99% yield). Compound **58** was then heated under reflux with hydrazine in ethanol to afford **56** (73% yield).¹²⁴ The screening of **56** afforded a ΔT_m of -0.5 °C, suggesting a preference for 4-substitution on the phenyl ring of **53** (Figure 35a).



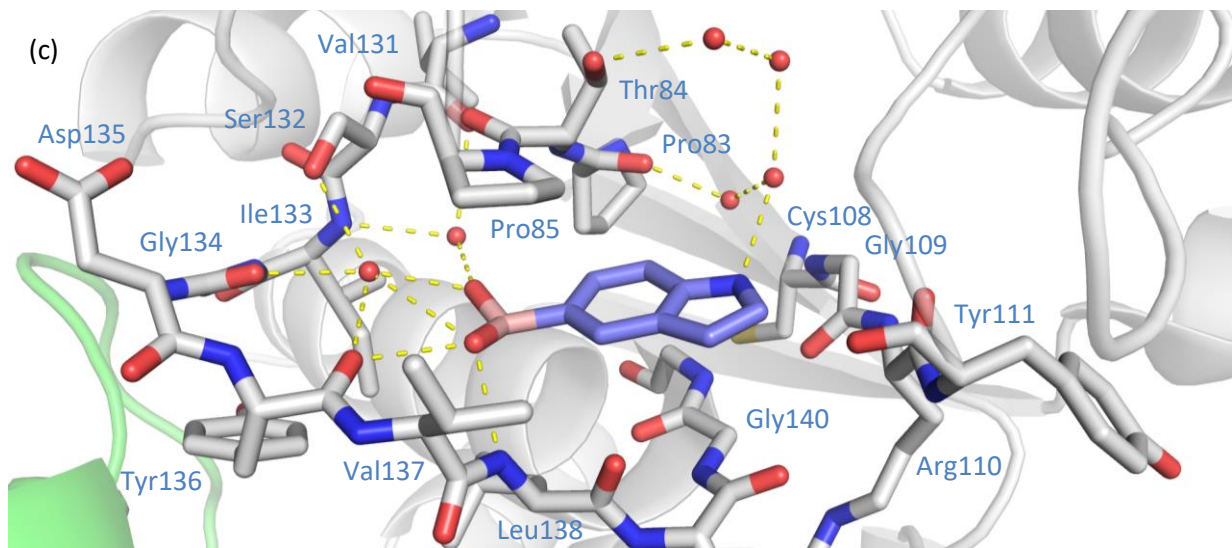
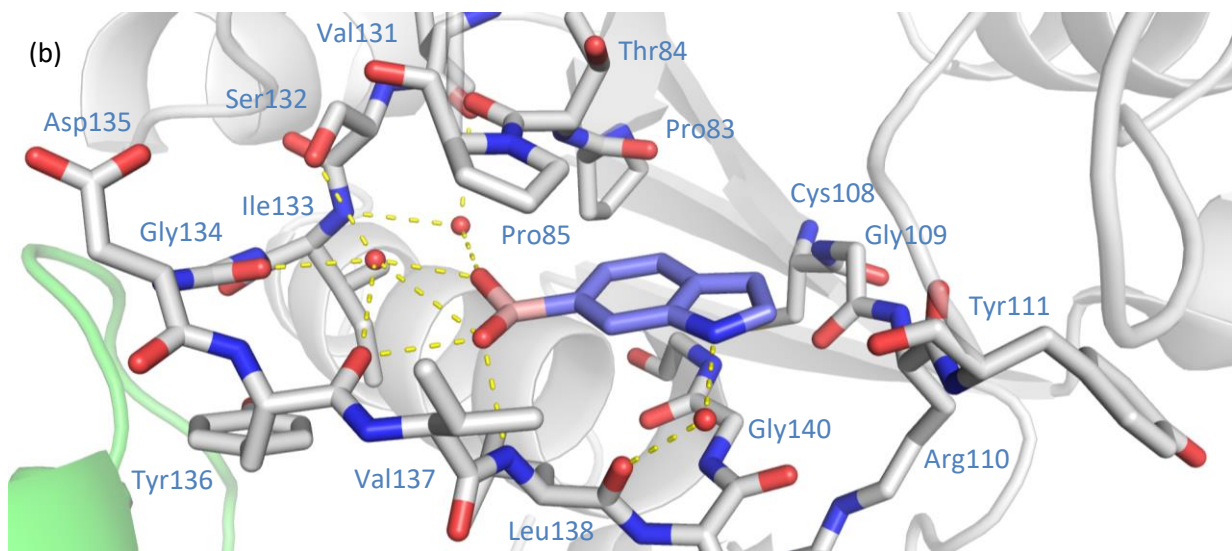
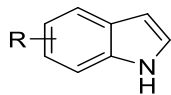
Reagents and Conditions: (a) *n*-butyllithium (1.6 M in hexanes), acetonitrile, THF, -78 °C, 30 min; (b) N₂H₄·H₂O, EtOH, reflux, 6 h.

Scheme 7: Synthesis of 56 in two steps from 57.

With fragment hit **59** (K_d 260 μ M, LE 0.41) the ribose binding region is occupied by an indole ring, oriented with its nitrogen atom facing the opening of the active site and forming a water-mediated interaction with the backbone carbonyl of Leu138 (Figure 36a and b). This fragment is held in the active site through its 6-substituted boronic acid, which extends into the adenine binding region and hydrogen bonds to the backbone amides of Tyr136 and Leu138 in addition to two water molecules, not present in the X-ray crystal structure with **53**, through which it interacts with residues Val131, Ser132, Ile133 and Gly134. The indole ring was demonstrated to possess a preference for presentation of the nitrogen atom towards Leu138 through screening of the 5-substituted isomer **61**. The X-ray crystal structure of **61** in complex with *Mab* TrmD showed the indole ring ‘flipping’ to present the boronic acid anchor in an identical position as **53** in the adenine binding region with the same direct and water-mediated interactions (Figure 36c). To achieve this, the indole ring is oriented to present its nitrogen atom towards the rear of the ribose binding region, where it hydrogen bonds to an ordered water network, however the screening of **61** by DSF gave a lower ΔT_m of +1.3 °C in comparison to **53** (ΔT_m +3.0 °C) (Figure 36a).

(a)

| Compound | R | ΔT_m^a (°C) | K_d (μM) | LE ^b |
|-----------|----------------------|---------------------|-------------------------|-----------------|
| 59 | 6-B(OH) ₂ | +4.0 | 260 ± 15 | 0.41 |
| 60 | 6-CO ₂ H | -0.6 | ND | - |
| 61 | 5-B(OH) ₂ | +1.3 | ND | - |



^a 5 mM ligand and 10 μM Mab TrmD, measured by Dr Sherine Thomas (Department of Biochemistry, University of Cambridge) for **59** and **60**.

^b kcal mol⁻¹ HA⁻¹.

Figure 36: (a) The change in the melting temperatures (ΔT_m), affinities (K_d) and ligand efficiencies of fragment hit **59** and its structural analogues; X-ray crystal structures of Mab TrmD (subunit A = white, subunit B = green, ligand = lilac) bound to (b) **59** (PDB code 6QOU, 1.56 Å),⁵⁰ and **61** (PDB code 6QQR, 1.56 Å),¹²³ illustrating one of the active sites.

Further, through comparison with the corresponding carboxylic acid fragment **60**, which afforded a negative ΔT_m in the initial fragment screen, it appeared that such a replacement of the boronic acid of **59** was not a good way to proceed (Figure 36a).

An overlay of the X-ray crystal structures of **53** and **59** in complex with *Mab* TrmD revealed significant overlap of their respective 4-methoxyphenyl and indole ring systems (Figure 37a). This suggested that a fragment-merging strategy could be used (Figure 37b). The replacement of the 4-methoxyphenyl ring system of **53**, which had shown sensitivity to alternative substitution profiles in **54-56**, with an indole in **62** was believed to provide improved vectors for future elaboration into the methionine binding region. Similarly, the 3-aminopyrazole ring system in **62** offered more promise for elaboration in comparison to the boronic acid of **59**, specifically from the 4-position of the ring system.

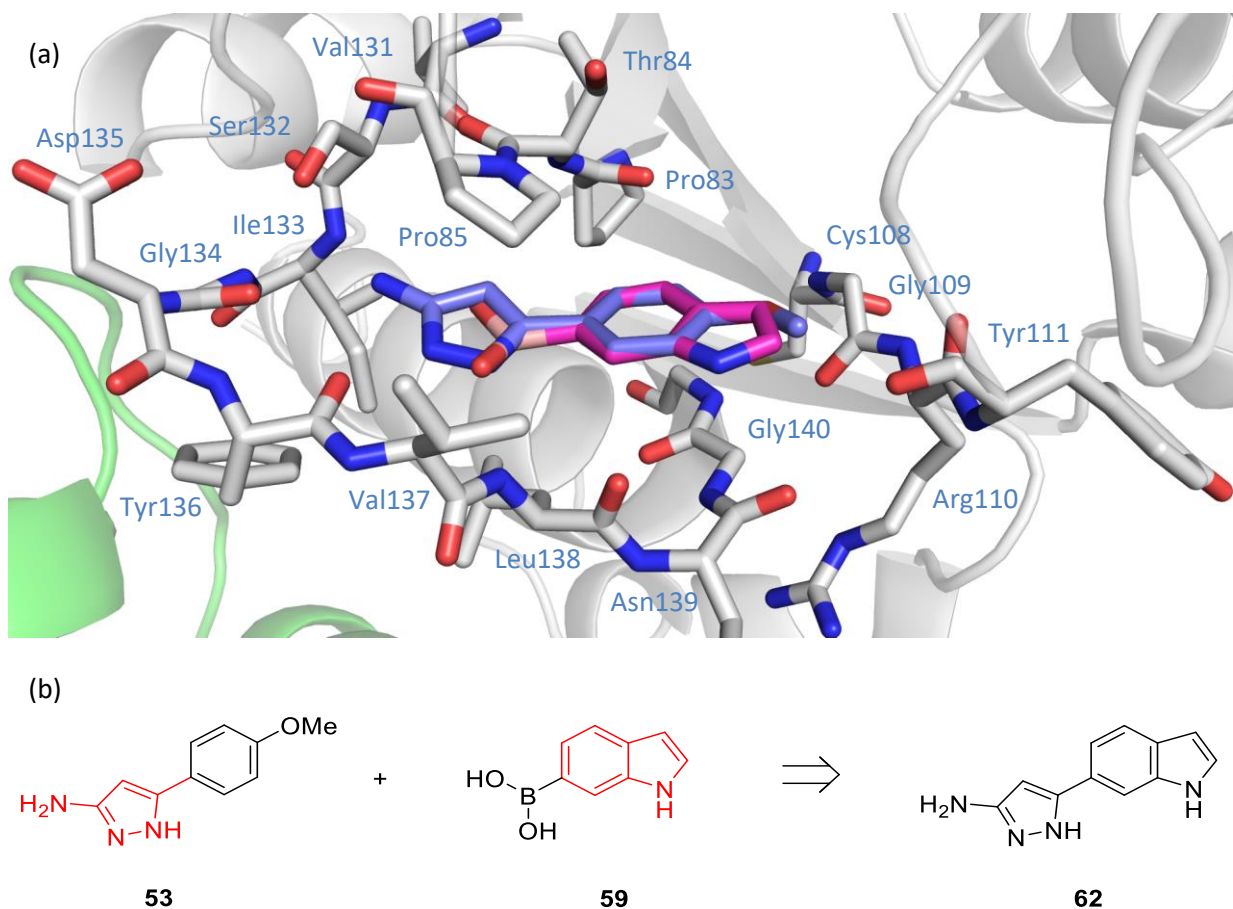
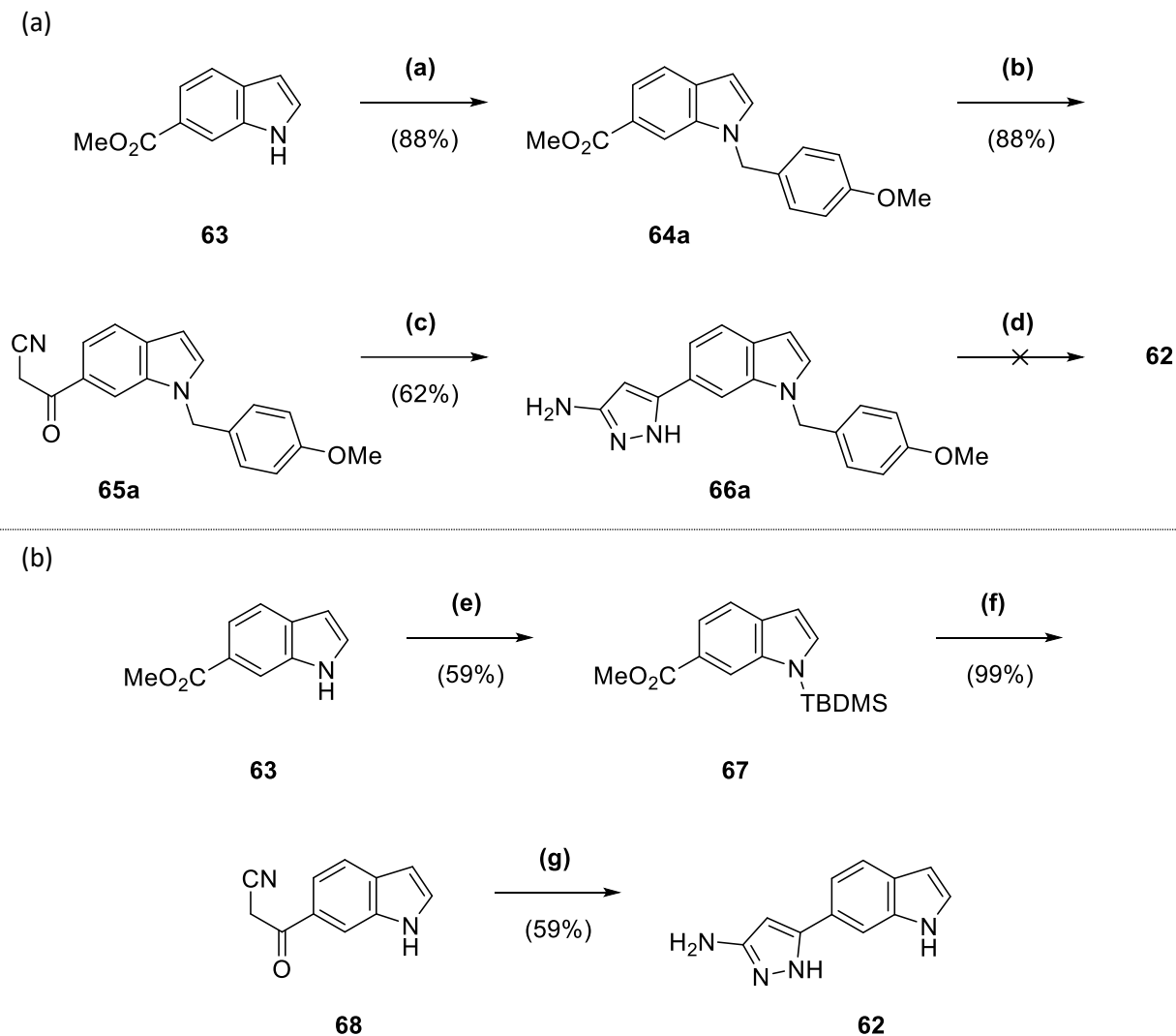


Figure 37: (a) Overlay of X-ray crystal structures of *Mab* TrmD bound to **53** or **59** (overlay of PDB code 6QOT and PDB code 6QOU, subunit A = white, subunit B = green, **53** = lilac, **59** = pink), illustrating one of the active sites;⁵⁰ (b) proposed fragment-merging strategy with **53** and **59**.

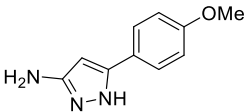
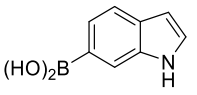
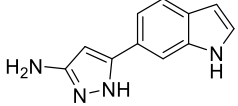
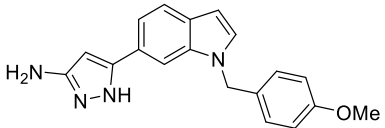
3.1.3: Synthesis and Screening of **62** and **66a**

The initial route explored for the synthesis of **62** was based around the protection of the indole nitrogen with a *p*-methoxybenzyl protecting group (Scheme 8a). The installation of this group on **63** was achieved by heating under reflux with 4-methoxybenzyl chloride and Cs₂CO₃ in acetonitrile (88% yield), with **64a** converted to the corresponding β -ketonitrile **65a** through treatment with *n*-butyllithium and acetonitrile (88% yield).



Scheme 8: Synthesis of (a) **66a** in three steps from **63**, with attempted deprotection to **62**, and (b) **62** in three steps from **63**.

Compound **65a** was then heated under reflux with hydrazine in ethanol to afford *p*-methoxybenzyl-protected **62**, **66a** (62% yield) (Scheme 8a). However, TFA-mediated deprotection of **66a** in the presence of anisole predominantly afforded byproducts with only trace amounts of the desired product **62** by LCMS analysis.¹²⁵ Therefore, an alternative route was initiated with the protection of **63** using a TBDMS group (59% yield) (Scheme 8b). Ester **67** was then converted to the corresponding β -ketonitrile, with the silyl protecting group removed by TBAF following aqueous work up (99% yield overall). Compound **68** was then heated under reflux with hydrazine in ethanol to afford **62** (59% yield).

| Compound | ΔT_m^a (°C) | ΔT_m^b (°C) | K_d (μ M) | LE ^c |
|---|---------------------|---------------------|------------------|-----------------|
| 53  | +3.0 | +0.2 | 170 \pm 14 | 0.37 |
| 59  | +4.0 | -0.1 | 260 \pm 15 | 0.41 |
| 62  | +4.8 | +1.1 | 110 \pm 11 | 0.36 |
| 66a  | +4.3 | +3.4 | 59 \pm 17 | 0.24 |

^a 5 mM ligand and 10 μ M *Mab* TrmD, measured by Dr Sherine Thomas for **53** and **59**.

^b 100 μ M ligand and 10 μ M *Mab* TrmD.

^c kcal mol⁻¹ HA⁻¹.

Table 5: The change in the melting temperatures (ΔT_m), affinities (K_d) and ligand efficiencies of fragment hits **53** and **59**, and compounds **62** and **66a**.

Screening of **62** (K_d 110 μ M, LE 0.36) by ITC revealed an improved binding affinity relative to **53** (K_d 170 μ M, LE 0.37) and **59** (K_d 260 μ M, LE 0.41), with a comparable LE (Table 5). The X-ray crystal structure of **62** in complex with *Mab* TrmD showed its 3-aminopyrazole and indole ring systems adopting the same binding poses as the respective moieties in **53** and **59** (Figure 38a). Further, **62** replicates the hydrogen bond interactions of **53** and **59**, with its 3-aminopyrazole ring system interacting with Ser132, Gly134, Tyr136 and Leu138, and the indole nitrogen interacting with the backbone carbonyl of Leu138 through a water molecule.

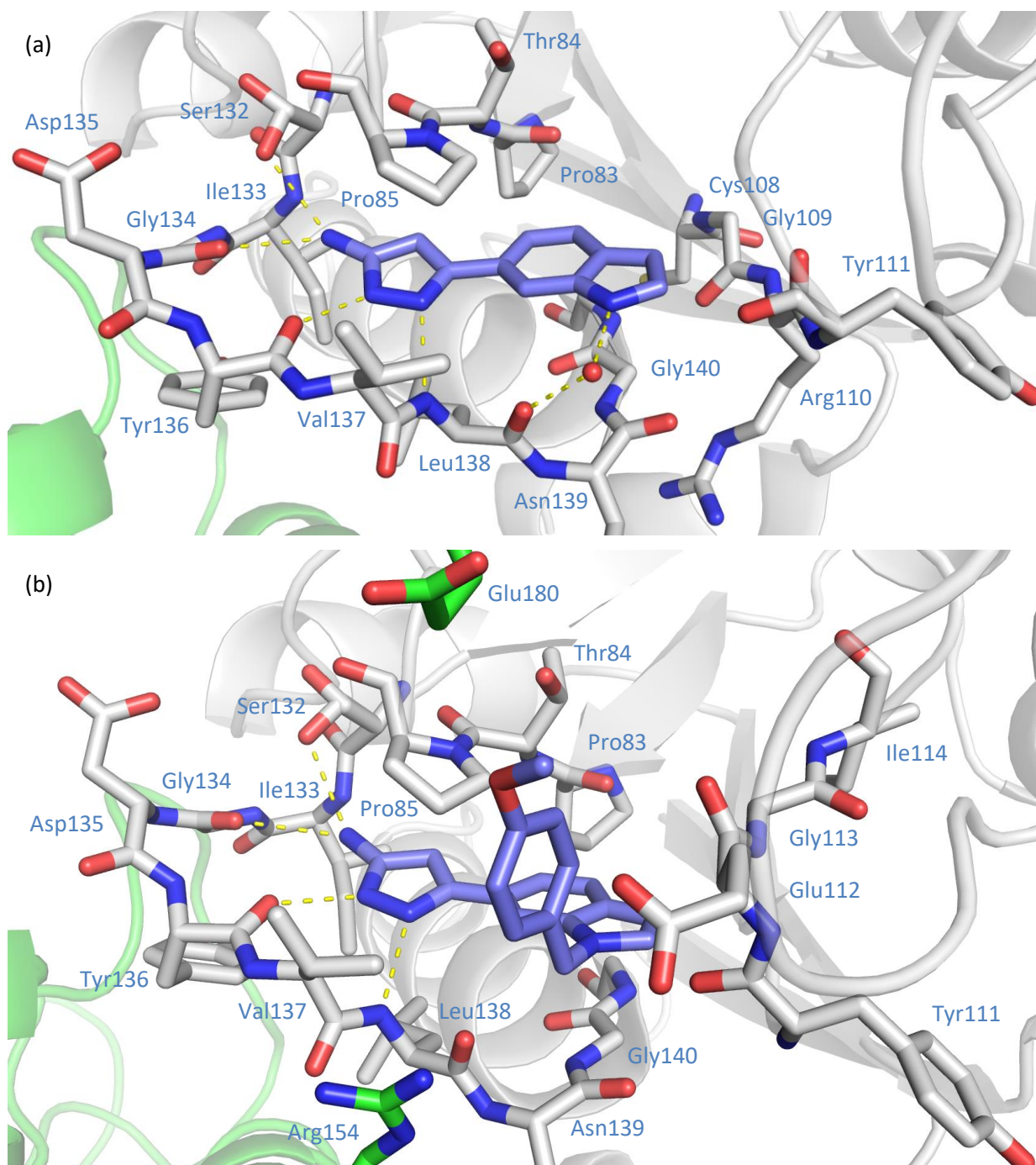


Figure 38: X-ray crystal structures of Mab TrmD (subunit A = white, subunit B = green, ligand = lilac) bound to (a) **62** (PDB code 6QQS, 1.76 Å), and (b) **66a** (PDB code 6QQT, 1.67 Å), illustrating one of the active sites.¹²³

Intermediate **66a** (K_d 59 μM , LE 0.24), the analogue of **62** with a *p*-methoxybenzyl group attached to the indole nitrogen from the first attempted synthetic route, was also screened to reveal a smaller K_d than **62** (K_d 110 μM , LE 0.36) (Table 5). The X-ray crystal structure of **66a** in complex with *Mab* TrmD showed no significant shift in the aminopyrazole-indole portion of the molecule relative to **62**, with the same

hydrogen-bonding interactions visible between the 3-aminopyrazole ring system and residues Ser132, Gly134, Tyr136 and Leu138 (Figure 38b). The methylene linker in the *p*-methoxybenzyl group allows the phenyl ring of **66a** to reach up the active site to the methionine binding region, where it is surrounded by Pro85, Glu112, Val137 and Arg154, with its methoxy group lying 3.2 Å below the carboxylate side chain of Glu180.

The improvement in binding affinity from **62** to the synthetic intermediate was encouraging, however the LE of **66a** (0.24) was significantly below the recommended threshold of 0.3 kcal mol⁻¹ HA⁻¹.¹⁰⁹ Consequently, further work based on **66a** would have to focus on improvement of binding affinity without a corresponding increase in molecular weight.

3.2: Development of the 3-Aminopyrazole Lead Series

Based on the successful screening of compounds **62** and **66a**, the 3-aminopyrazole lead series derived from the application of a fragment-merging strategy to fragment hits **53** and **59** was continued, with the synthesis and screening of further analogues. Throughout the development of this lead series, DSF was generally used as a first-line screen followed by ITC. This biophysical screening cascade was supported by comparison of ΔT_m values and binding affinities from the lead series against *Mab TrmD*, which revealed a good correlation between ΔT_m and the order of magnitude of the K_d (Figure 39).

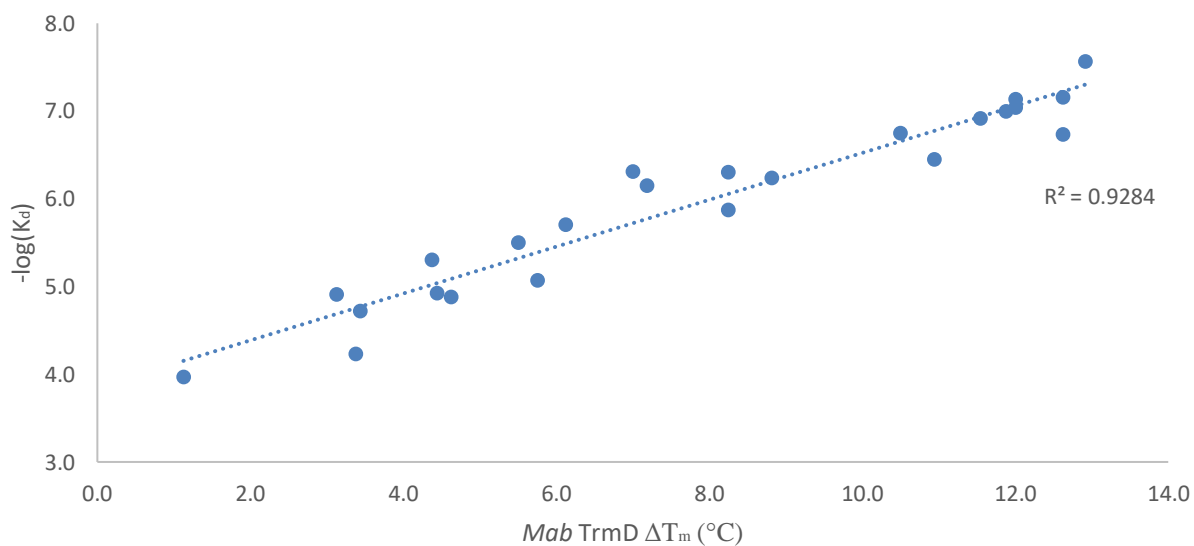


Figure 39: Comparison of melting temperatures (ΔT_m), measured at 100 μ M ligand and 10 μ M *Mab TrmD*, and the logarithm of the affinities (K_d) for synthesised compounds in the 3-aminopyrazole lead series.

3.2.1: Optimisation of the Phenyl Ring of **66a**

Preliminary SAR with **66a** was focused on the phenyl ring and methoxy group (Figure 40). Due to the proximity of its methoxy group to Glu180 (Figure 38b), the impact of its removal or movement to an adjacent position on the phenyl ring to binding affinity was explored, in addition to the use of alternate substituents on the phenyl ring (Figure 40). With the second position of the phenyl ring of **66a** lying 4.1 Å from the side chain of the catalytic residue Arg154 (Figure 38b), the investigation of alternate substituents was focused on its engagement from this position. Finally, investigation of the tolerance of the scaffold of **66a** to replacement of the phenyl ring with alternate heterocycles was sought (Figure 40).

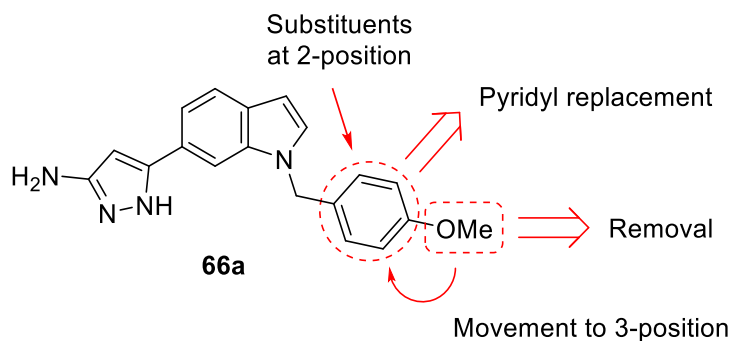
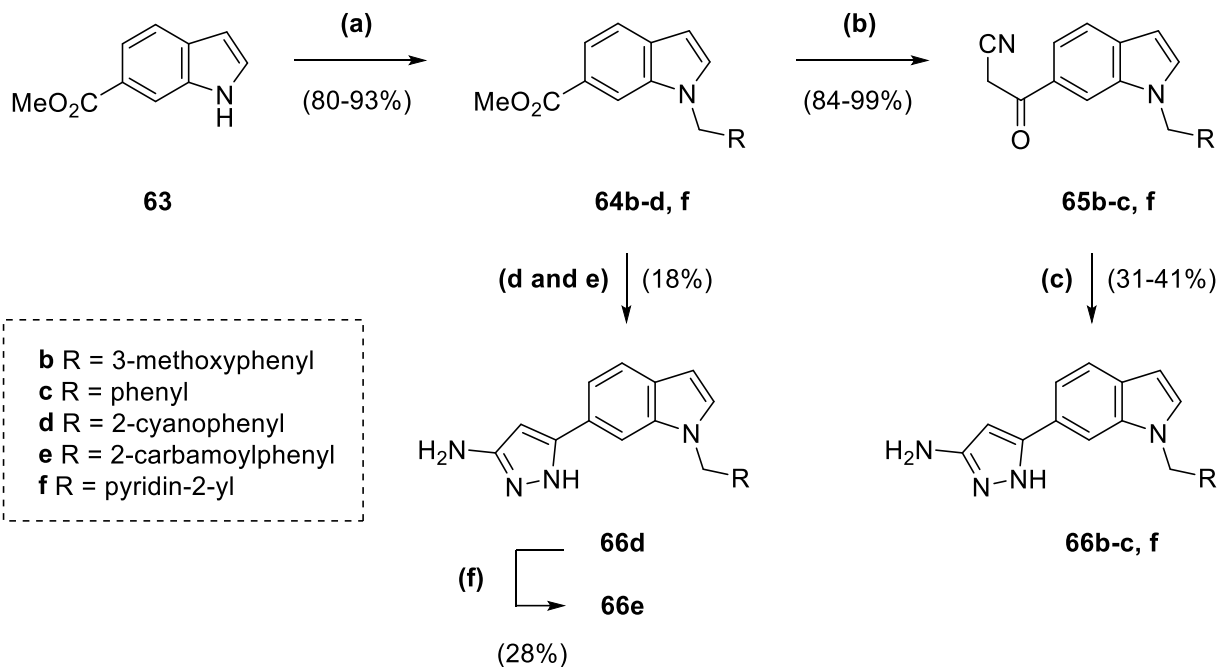


Figure 40: Areas of focus for the SAR study on **66a**, the phenyl ring and methoxy group, with initial ideas for modification.

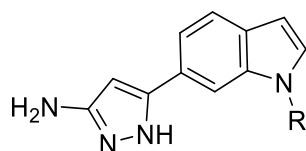
Derivatives of **66a** with either alternately-substituted phenyl rings or a pyridyl ring attached through a methylene linker to the indole in place of the *p*-methoxybenzyl group were synthesised. The first step involved the heating under reflux of **63** with benzyl or picolyl halides and Cs₂CO₃ in acetonitrile (80-93% yield) (Scheme 9). Esters **64b-c** and **64f** were converted to the corresponding β -ketonitriles **65b-c** and **65f** through treatment with *n*-butyllithium and acetonitrile (84-99% yield), which were then heated under reflux with hydrazine in ethanol (31-41% yield). Due to challenges in the purification of the corresponding β -ketonitrile of **64d**, the material was taken forwards crude for the reaction with hydrazine (18% yield overall). The nitrile group of the resultant compound **66d** was hydrolysed to an amide through heating under reflux in aqueous sodium hydroxide (28% yield).



Reagents and Conditions: (a) RCH_2X (.HX), CS_2CO_3 , acetonitrile, reflux, 1 to 15 h; (b) *n*-butyllithium (1.6 M in hexanes), acetonitrile, toluene/THF, -78 °C, 30 min to 1 h; (c) $N_2H_4 \cdot H_2O$, EtOH, reflux, 5 to 13 h; (d) *n*-butyllithium (1.6 M in hexanes), acetonitrile, toluene, -78 °C, 1 h; (e) $N_2H_4 \cdot H_2O$, EtOH, reflux, 5 h; (f) NaOH, H_2O , 100 °C, 7 h.

Scheme 9: Synthesis of 66b-d and 66f in three steps from 63, and 66e in one step from 66d.

Screening of the 3-methoxyphenyl analogue of **66a**, **66b** (K_d 13 μ M, LE 0.28), revealed a greater than four-fold improvement in binding affinity (Table 6). The X-ray crystal structure of **66b** in complex with *Mab* TrmD showed the phenyl ring of **66b** oriented with the methoxy group facing the interior of the active site, away from Glu112 and Arg154 (Figure 41a). Removal of the methoxy group in **66c** (K_d 19 μ M, LE 0.29) afforded a similar 3-fold improvement in binding affinity relative to **66a** (Table 6 and Figure 41b). From the 2-substituted phenyl compounds, **66d** (K_d 12 μ M, LE 0.28) did not give a significant improvement in K_d over **66b** and **66c**, whilst **66e** afforded a ΔT_m of $+1.4$ °C but was not screened by ITC (Table 6). The X-ray crystal structure of **66d** in complex with *Mab* TrmD showed a similar binding mode to **66b**, with the nitrile group oriented towards the interior of the active site above the indole ring (Figure 42a).



| Compound | R | ΔT_m^a (°C) | K_d (μM) | LE ^b | GE ^b (R) |
|------------|---|---------------------|-------------------------|-----------------|---------------------|
| 66a | | +3.4 | 59 ± 17 | 0.24 | 0.04 |
| 66b | | +4.6 | 13 ± 2 | 0.28 | 0.14 |
| 66c | | +3.4 | 19 ± 1 | 0.29 | 0.15 |
| 66d | | +4.4 | 12 ± 2 | 0.28 | 0.15 |
| 66e | | +1.4 | ND | - | - |
| 66f | | +3.1 | 12 ± 1 | 0.30 | 0.18 |

^a 100 μM ligand and 10 μM Mab TrmD.

^b kcal mol⁻¹ HA⁻¹.

Table 6: The change in the melting temperatures (ΔT_m), affinities (K_d) and efficiency metrics of compounds **66a-f**.

Out of the screened **66a** analogues, the pyridyl compound **66f** (K_d 12 μM , LE 0.30) possessed the highest LE (Table 6), despite its X-ray crystal structure not demonstrating any additional hydrogen-bonding interactions by the ring nitrogen (Figure 42b). The improved LE of **66f** was represented in the GE of 0.18 from its pyridyl ring and methylene linker, in comparison the low value of 0.04 from the *p*-methoxybenzyl group of **66a**.

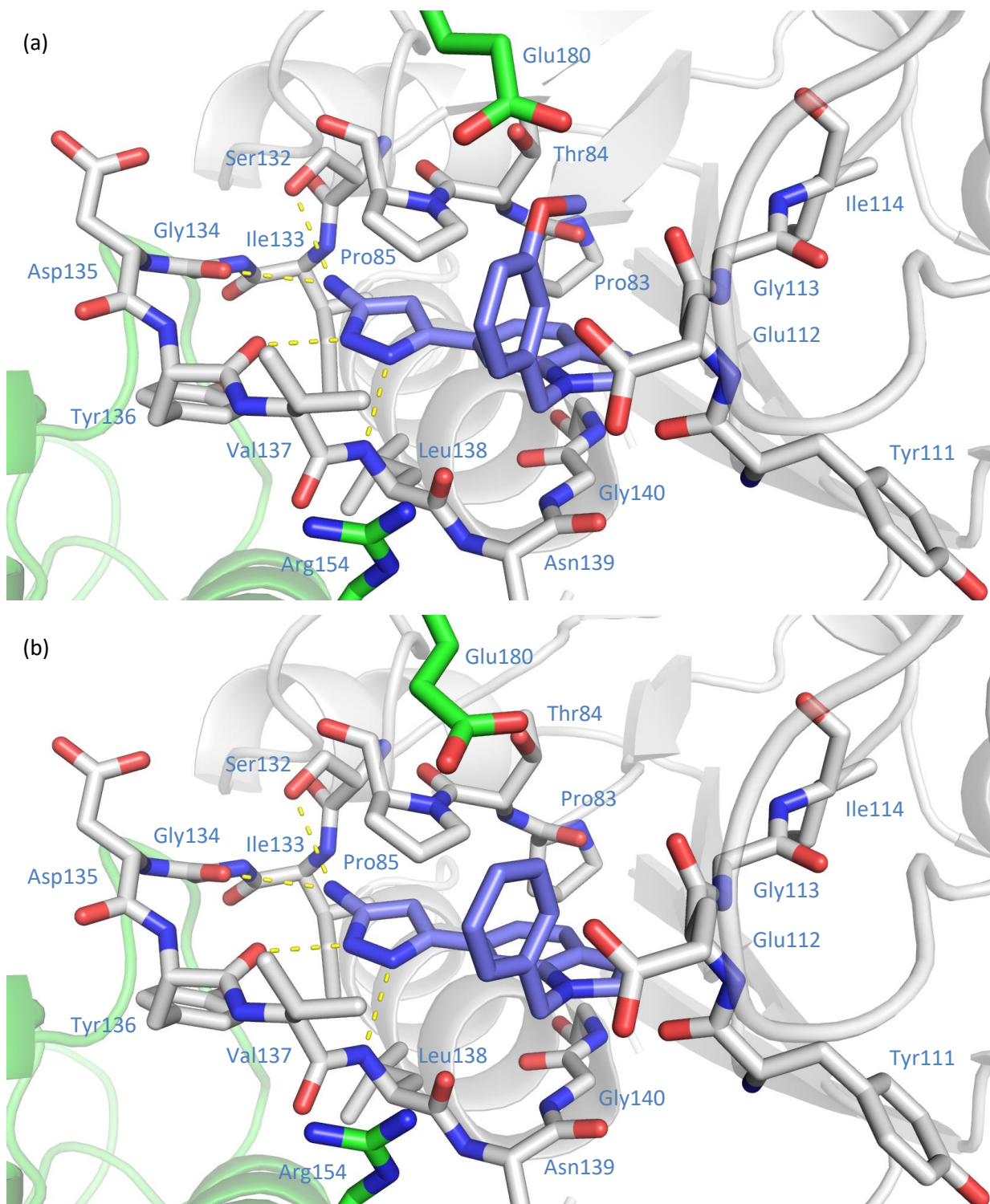


Figure 41: X-ray crystal structures of Mab TrmD (subunit A = white, subunit B = green, ligand = lilac) bound to (a) **66b** (PDB code 6QRC, 1.73 Å), and (b) **66c** (PDB code 6QQW, 1.80 Å), illustrating one of the active sites.¹²³

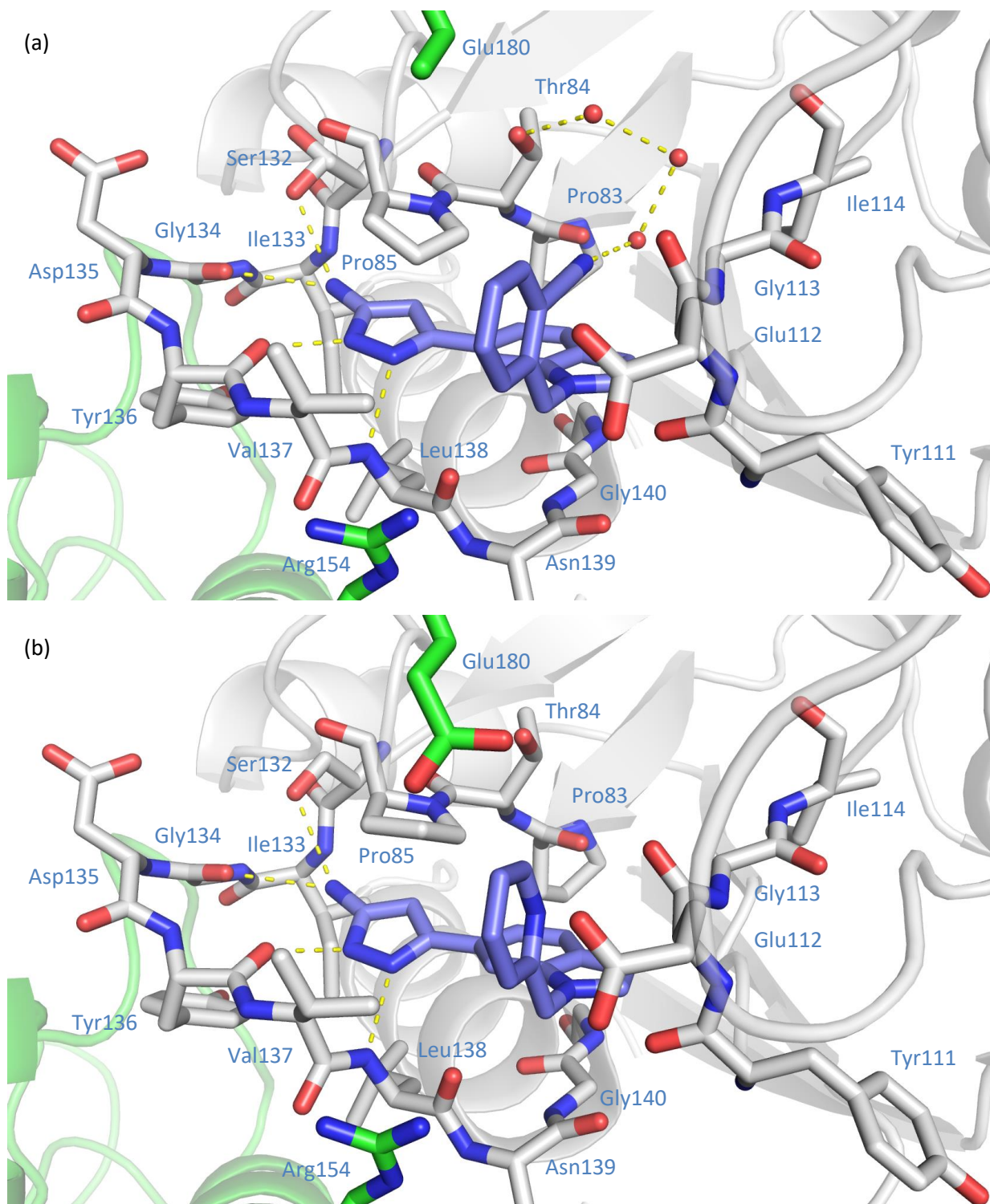


Figure 42: X-ray crystal structures of Mab TrmD (subunit A = white, subunit B = green, ligand = lilac) bound to (a) **66d** (PDB code 6QQV, 1.71 Å),¹²³ and (b) **66f** (PDB code 6QQX, 2.69 Å),⁵⁰ illustrating one of the active sites.

3.2.2: Exploration of Substitution from the Pyrazole 4-Position

In addition to the SAR study on the phenyl ring of **66a**, elaboration was also performed on the 3-aminopyrazole ring system of the lead series. The 4-position of this ring system was shown in the X-ray crystal structure of **62** in complex with *Mab* TrmD to face an elongated narrow pocket, bordered by residues Pro83, Thr84, Val131, Ser132, Ile133 and Ala144 (Figure 43). Hence, the substitution from this position of the pyrazole ring into the pocket was proposed.

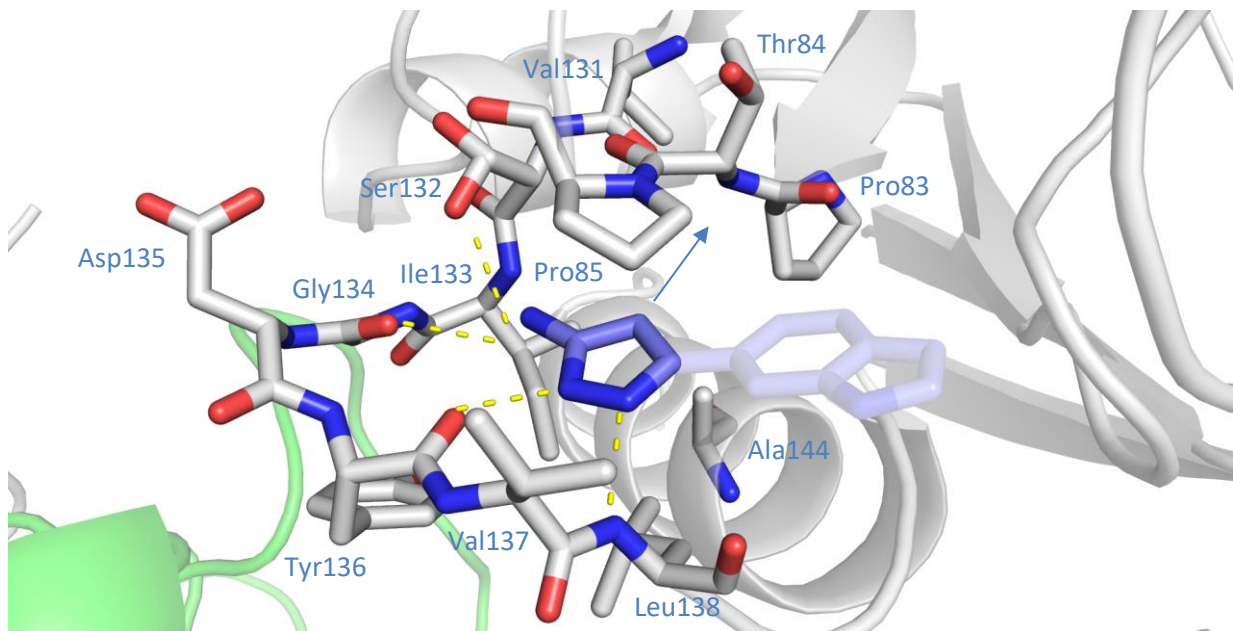
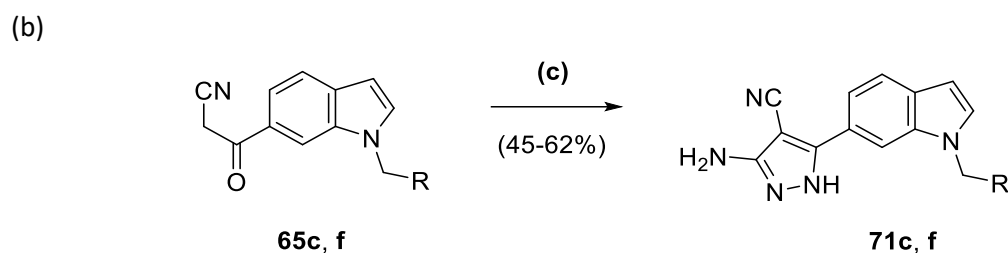
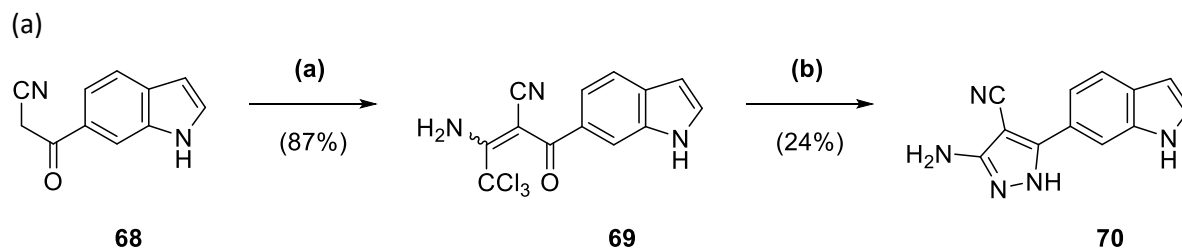


Figure 43: X-ray crystal structure of *Mab* TrmD bound to **62** (PDB code 6QQS, 1.76 Å, subunit A = white, subunit B = green, **62** = lilac), illustrating the 3-aminopyrazole ring system in one of the active sites.⁵⁰

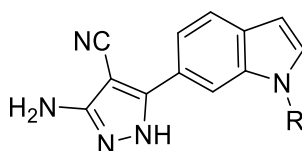
From consideration of the shape of the pocket, the addition of a nitrile group was selected. The synthesis of an analogue of **62** with a nitrile group attached to the 4-position of its 3-aminopyrazole ring system was carried out using β -ketonitrile **68** (Scheme 10), taken from the synthetic route for **62** (Scheme 8b). The methylene group of **68** was reacted with trichloroacetonitrile and sodium acetate to form enone **69** (87% yield) (Scheme 10), using a literature procedure previously utilised with another β -ketonitrile.¹²⁶ Enone **69** was then heated under reflux with hydrazine in ethanol to afford **70** (24% yield). This route was also adapted for the synthesis of nitrile analogues of compounds from the SAR study with **66a**, compounds **66c** and **66f** (Scheme 10), using β -ketonitriles **65c** and **65f** from their respective synthetic routes (Scheme 9). However, the enones produced from these β -ketonitriles were taken forwards without purification, after an aqueous workup, for heating under reflux with hydrazine in ethanol (45-62% yield overall) (Scheme 10).



Reagents and Conditions: (a) CCl_3CN , NaOAc, EtOH, 90 min; (b) $\text{N}_2\text{H}_4\cdot\text{H}_2\text{O}$, EtOH, reflux, 22 h; (c) (i) CCl_3CN , NaOAc, EtOH, 90 min to 9 h (ii) $\text{N}_2\text{H}_4\cdot\text{H}_2\text{O}$, EtOH, reflux, 5 to 15 h.

Scheme 10: Synthesis of (a) 70 in two steps from 68 and (b) 71c and 71f in one step from 65c or 65f.

The screening of the nitrile analogue **70** by ITC (K_d 5.0 μM , LE 0.43) revealed a greater than 20-fold improvement in binding affinity relative to **62** (K_d 110 μM , LE 0.36), with the nitrile group possessing a GE of 0.91 (Table 7).



| Compound | R | ΔT_m^a ($^\circ\text{C}$) | K_d (μM) | LE ^b | GE ^b (R) | GE ^b (CN) |
|------------|---|-------------------------------------|-------------------------|-----------------|---------------------|----------------------|
| 70 | H | +4.4 | 5.0 \pm 2.1 | 0.43 | - | 0.91 |
| 71c | | +10.1 | ND ^c | - | - | - |
| 71f | | +8.3 | 0.50 \pm 0.14 | 0.36 | 0.20 | 0.95 |

^a 100 μM ligand and 10 μM *Mab* TrmD.

^b kcal mol⁻¹ HA⁻¹.

^c Not determined due to aqueous solubility.

Table 7: The change in the melting temperatures (ΔT_m), affinities (K_d) and efficiency metrics of compounds 70, 71c and 71f.

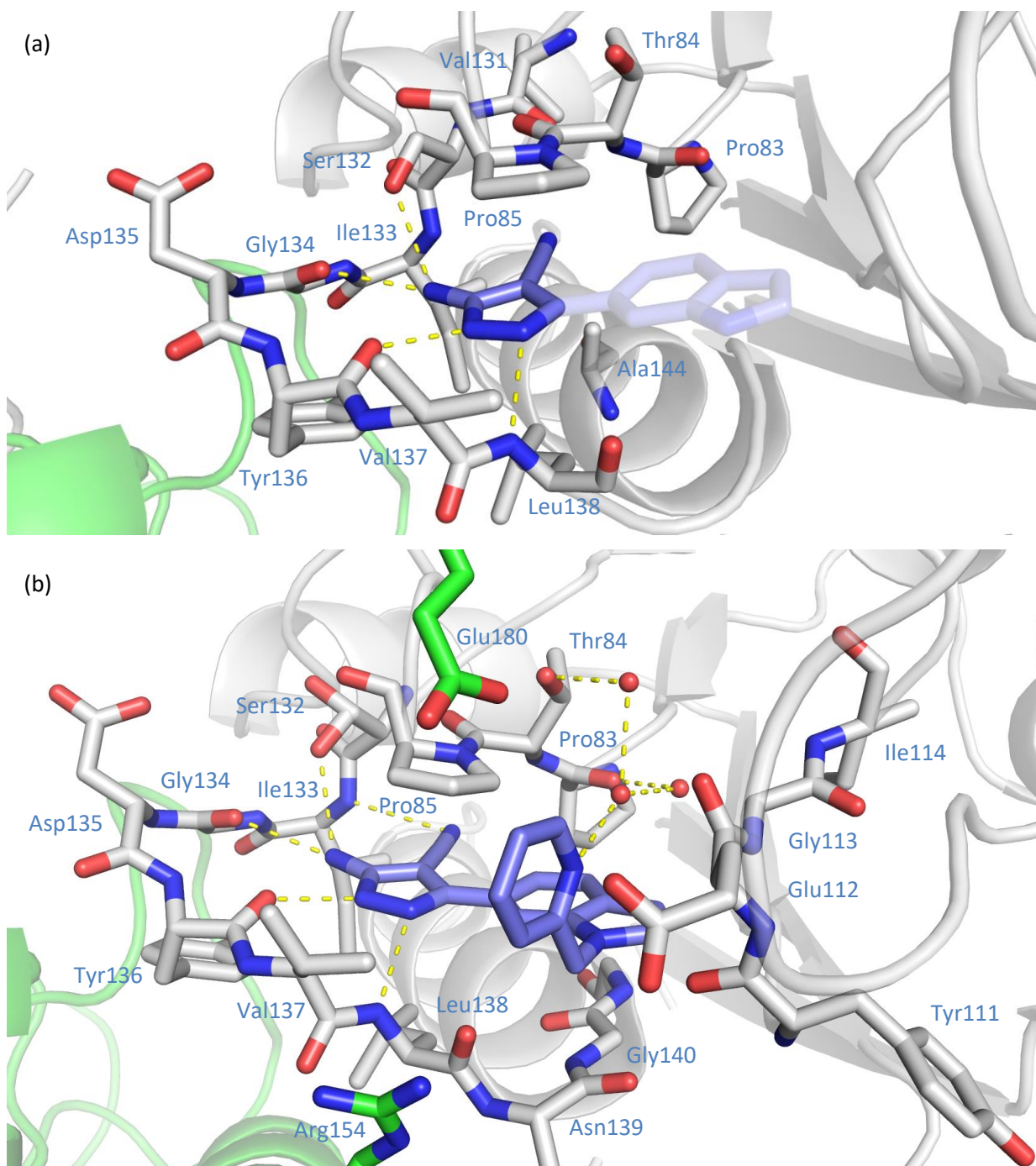


Figure 44: X-ray crystal structures of Mab TrmD (subunit A = white, subunit B = green, ligand = lilac) bound to (a) **70** (PDB code 6QQU, 1.59 Å),¹²³ illustrating the 4-nitrile 3-aminopyrazole ring system in one of the active sites, and (b) **71f** (PDB code 6QQY, 1.49 Å),⁵⁰ illustrating one of the active sites.

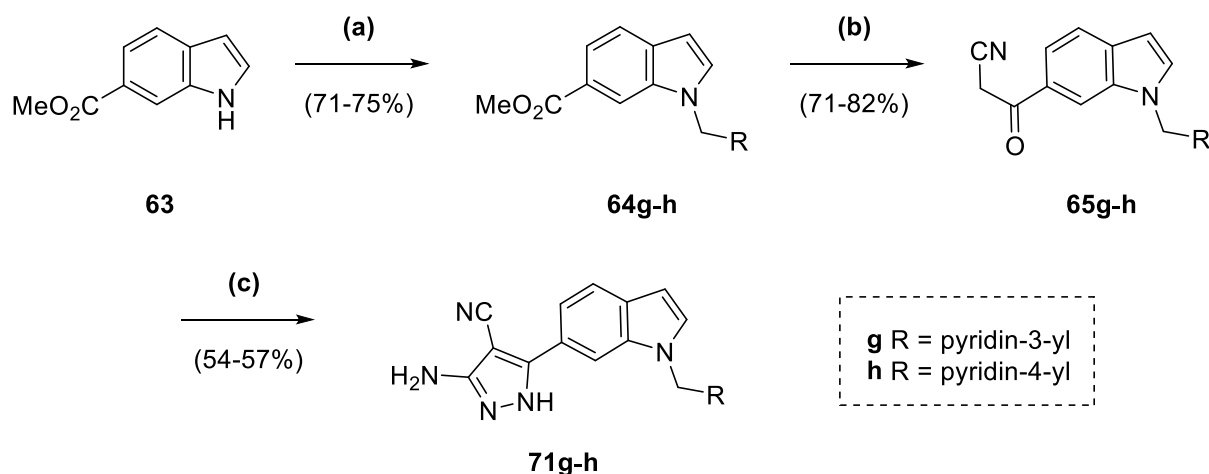
The X-ray crystal structure of **70** in complex with Mab TrmD showed the nitrile group extending into the desired pocket, with rest of the scaffold not shifted significantly in the active site relative to **62** (Figure 44a). A similar improvement in binding affinity and retention of binding mode was seen with **71f** (K_d 0.50

μM , LE 0.36) in comparison to **66f** (K_d 12 μM , LE 0.30) (Table 7 and Figure 44b). However, with **71c** (ΔT_m +10.1 $^\circ\text{C}$) a K_d was not determined due to poor solubility in the ITC buffer. Whilst the ΔT_m of **71c** was large relative to **66c** (ΔT_m +3.4 $^\circ\text{C}$), subsequent SAR study was focused on **71f** due to its improved aqueous solubility.

3.2.3: Structure-activity Relationship Study of **71f** and Pyridyl Isomers

Whilst the submicromolar K_d of **71f** (K_d 0.50 μM , LE 0.36) represented a greater than 200-fold improvement relative to **62** (K_d 110 μM , LE 0.36), achieved with the maintenance of LE, further improvement was sought. This was initially attempted with the exploration of the other isomers of **71f** with the pyridyl ring attached to the methylene linker from the 3- and 4-positions.

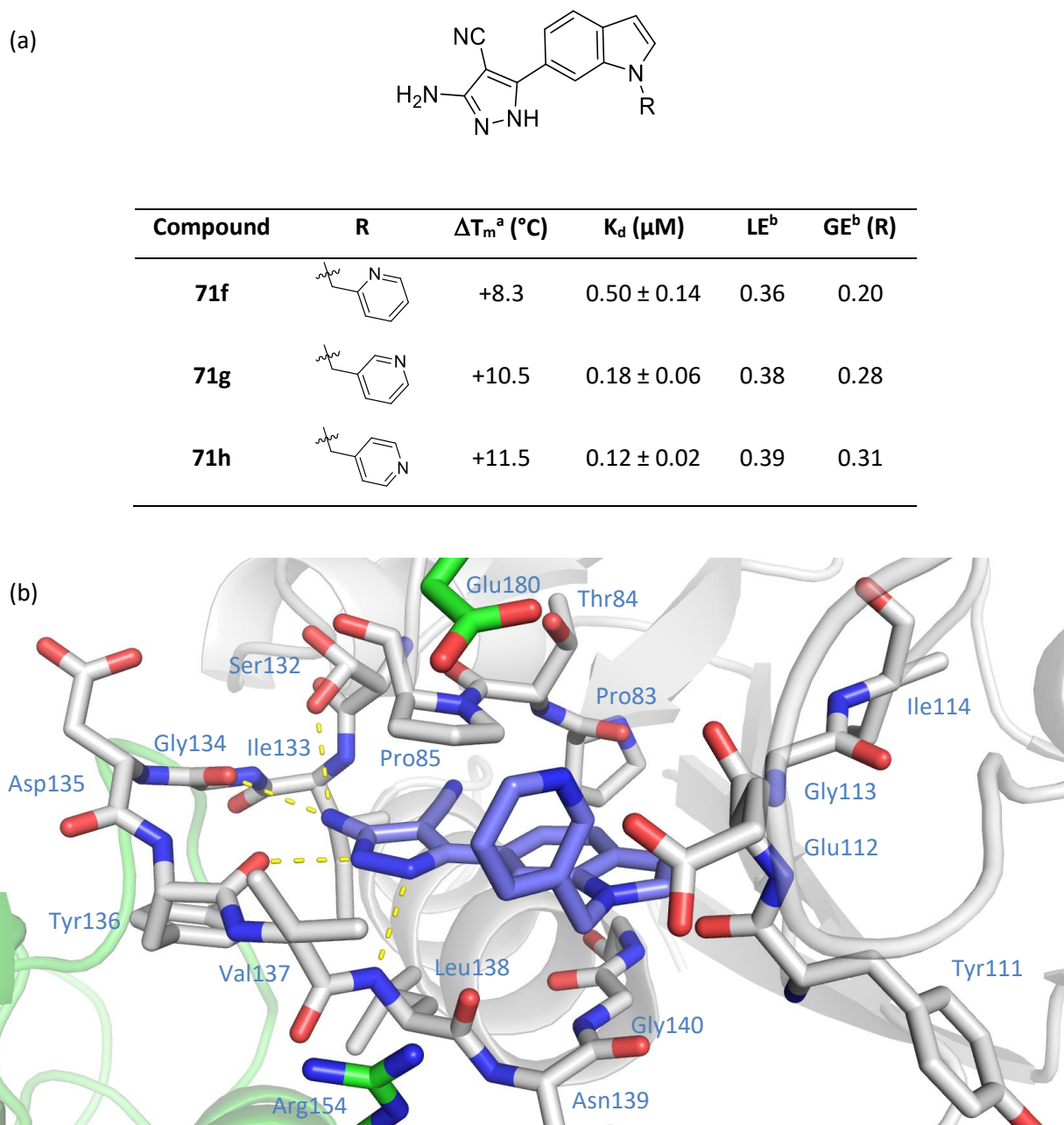
The synthesis of the 3- and 4-pyridyl analogues of **71f** was achieved by a route beginning with the deprotonation of indole **63** by NaH and treatment with the respective picolyl halides. Following consumption of starting material, methanol and sulfuric acid were added to the reaction mixture, which was heated under reflux to recover the carboxylic acid side-product and afford esters **64g-h** (71-75% yield) (Scheme 11). These esters were then converted to the corresponding β -ketonitriles **65g-h** (71-82% yield), which were used to synthesise the 4-cyanopyrazole compounds **71g-h** in the same manner as **71c** and **71f** (54-57% yield overall) (Scheme 10b).



Reagents and Conditions: (a) (i) $\text{RCH}_2\text{X.HX}$, NaH, DMF, 0 $^\circ\text{C}$ to rt, 45 min (ii) MeOH, H_2SO_4 , reflux, 16 h; (b) *n*-butyllithium (1.6 M in hexanes), acetonitrile, THF, -78 $^\circ\text{C}$, 45 min; (c) (i) CCl_3CN , NaOAc, EtOH, 13 h (ii) $\text{N}_2\text{H}_4\cdot\text{H}_2\text{O}$, EtOH, reflux, 21 h.

*Scheme 11: Synthesis of **71g** and **71h** in three steps from **63**.*

The screening of the 3- and 4-pyridyl isomers **71g** (K_d 0.18 μM , LE 0.38) and **71h** (K_d 0.12 μM , LE 0.39) demonstrated 3- and 4-fold improvements in binding affinity relative to **71f** (K_d 0.50 μM , LE 0.36) (Figure 45a).



^a 100 μM ligand and 10 μM *Mab* TrmD.

^b $\text{kcal mol}^{-1} \text{HA}^{-1}$.

Figure 45: (a) The change in the melting temperatures (ΔT_m), affinities (K_d) and efficiency metrics of compounds **71f-h**; X-ray crystal structure of *Mab* TrmD bound to **71g** (PDB code 6QQZ, 1.70 \AA , subunit A = white, subunit B = green, **71g** = lilac), illustrating one of the active sites.¹²³

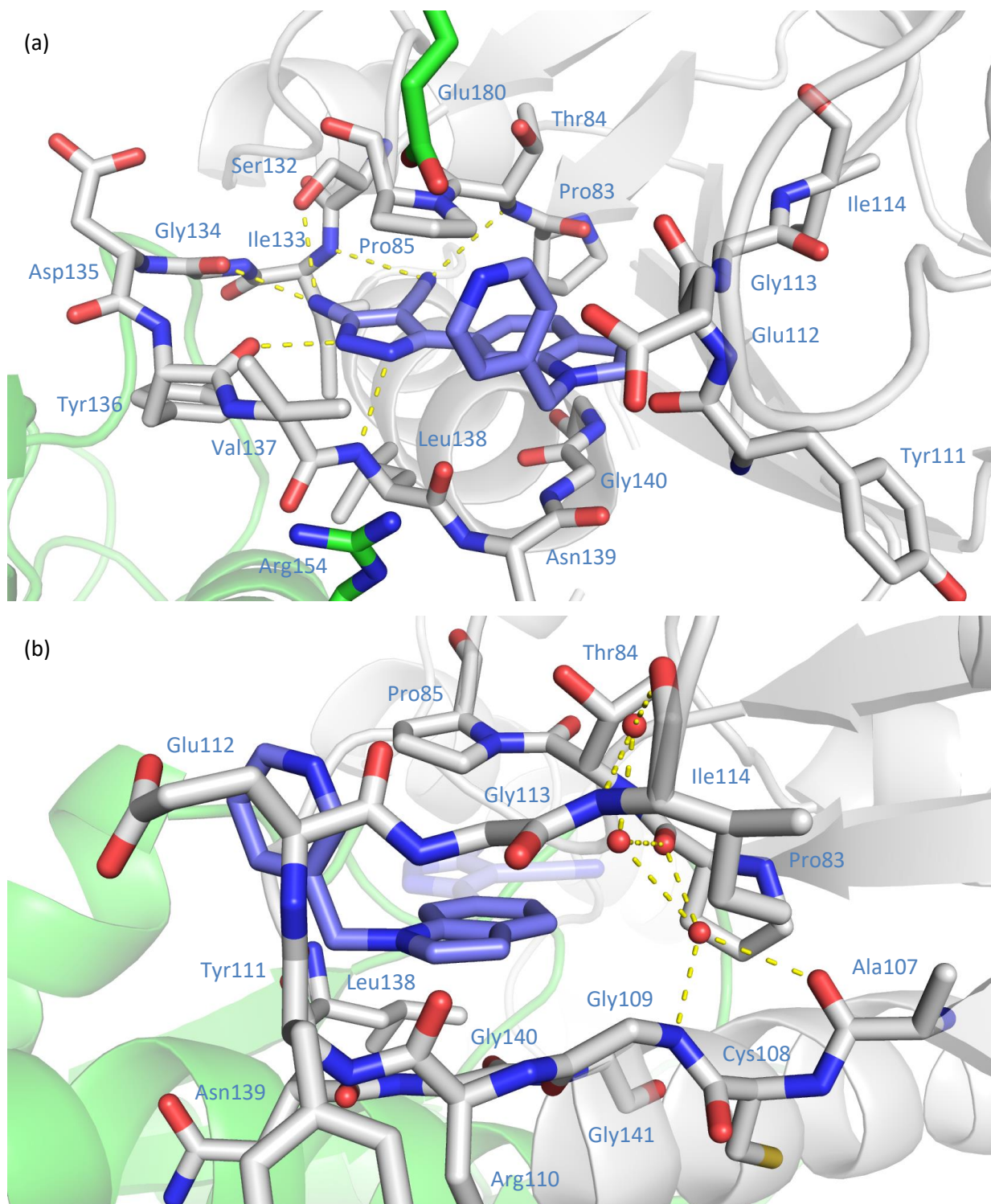


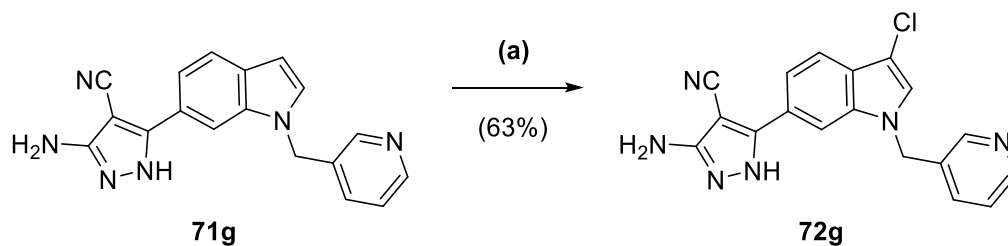
Figure 46: X-ray crystal structures of Mab TrmD (subunit A = white, subunit B = green, ligand = lilac) bound to (a) **71h** (PDB code 6QR0, 1.59 Å), illustrating one of the active sites, and (b) **71g** (PDB code 6QQZ, 1.70 Å), illustrating the indole ring in one of the active sites.¹²³

The X-ray crystal structures of **71g** and **71h** in complex with *Mab* TrmD did not reveal significant differences in the binding poses or hydrogen-bonding interactions of these ligands in comparison to **71f**, with the exception of the 2.9 Å distance between the pyridyl nitrogen of **71h** and the carboxylate side chain of Glu180 that could represent an electrostatic interaction (Figure 45b and Figure 46a).

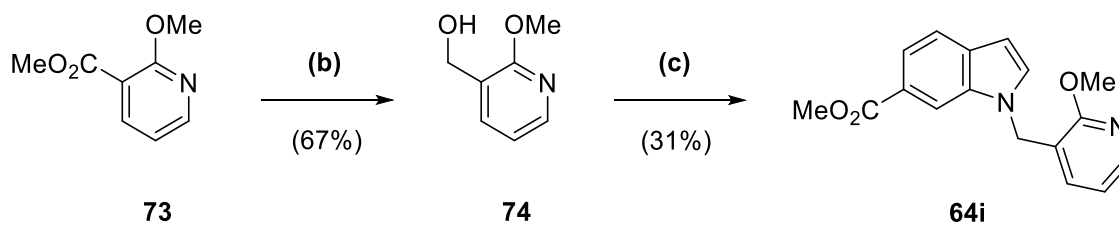
With their improved binding affinities relative to **71f**, **71g** and **71h** were then used as the starting point for three elaboration strategies to further explore the active site. Firstly, it was unknown whether the 3- or 4-positions of the indole ring in the lead series, which were shown in X-ray crystal structures to face a region lined by residues Pro83 to Thr84 and Cys108 to Gly109 to the side and Gly141 beneath, could tolerate substitution (Figure 46b). Hence, the synthesis of at least one analogue with a conservative substitution from one of these positions on the indole ring was sought. Secondly, further investigation on the engagement of the side chains of residues Arg154, Glu112 and Glu180 adjacent to the pyridyl ring was desired, building on the screening of **66d-e**. An idea for the engagement of these residues was the screening of derivatives of **71g** incorporating the heterocycle 2-pyridone, which exhibits keto/enol tautomerism in the presence of water,¹²⁷ with the intention of the 2-hydroxy isomer engaging Arg154 and the 6-hydroxy isomer engaging Glu112 and Glu180 (Figure 45b). Finally, the further probing of the methionine binding region into the volume defined by Glu112 to Gly113 and Thr84 to Pro85, above the indole ring of the lead series and adjacent to the pyridyl rings of **71g** and **71h** was sought (Figure 45b and Figure 46a). Hence, the development of a larger quinolyl analogue that would extend into this volume was selected.

The synthesis of an analogue with a substituent on the rear of the indole ring was achieved through late-stage functionalisation of **71g** with *N*-chlorosuccinimide in DMF, resulting in the installation of a chloride group from the indole 3-position in **72g** (63% yield). Synthesis of the 2-pyridone and quinoline analogues required longer synthetic routes than **71g** or **71h**, all involving the synthesis of methyl esters **64i**, **64k** and **64m** from reaction of the corresponding electrophile with indole **63** and NaH, followed by heating under reflux with methanol and sulfuric acid in the same manner as **64g-h** (Scheme 12b-d). In contrast to **64g-h** however, the corresponding electrophiles required further synthesis. With methyl ester **64i**, this began with the reduction of ester **73** by NaBH₄ to alcohol **74** (67% yield), which was treated with *p*-toluenesulfonyl chloride and DMAP before being taken forwards crude for reaction with indole **63** (31% yield overall) (Scheme 12b).

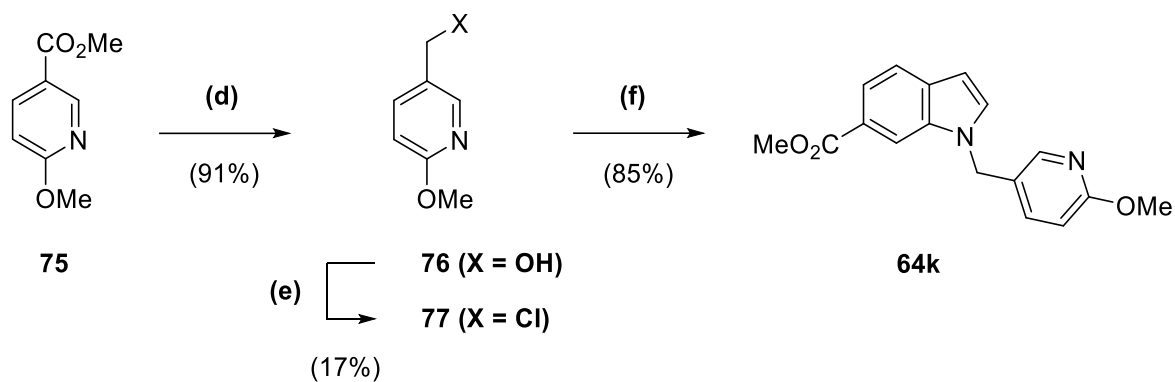
(a)



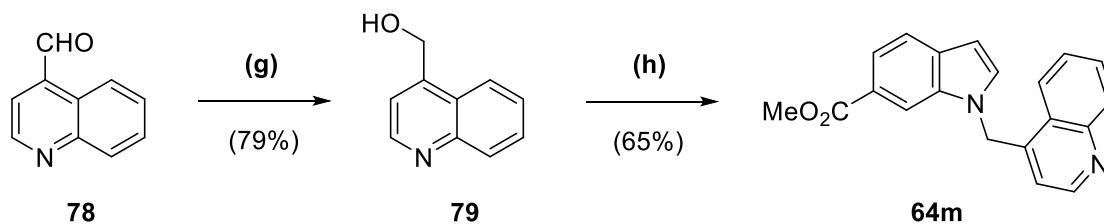
(b)



(c)



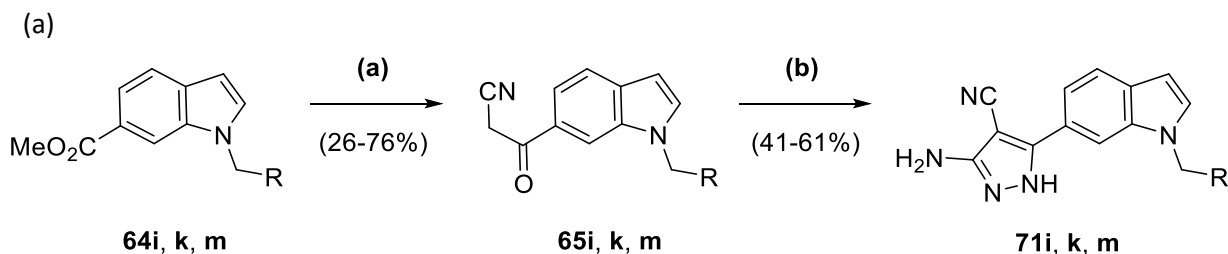
(d)



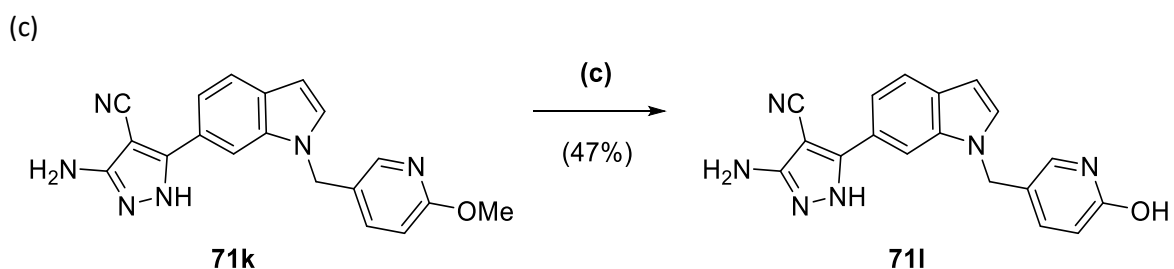
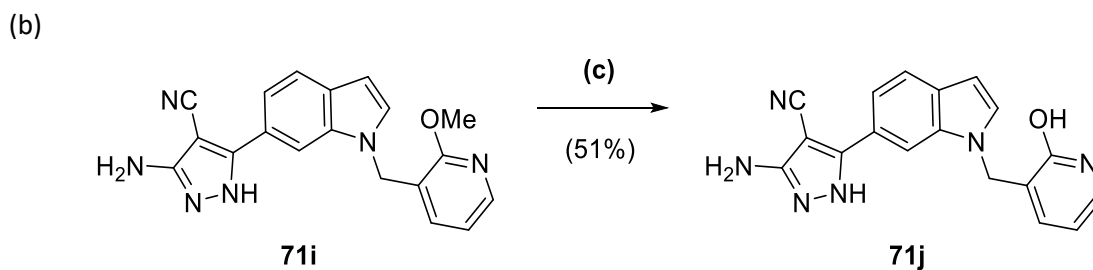
Reagents and Conditions: (a) NCS, DMF, 7 h 30 min; (b) NaBH₄, EtOH, 0 °C to rt, 1 d; (c) (i) TsCl, DMAP, NEt₃, DCM, 2 h (ii) **63**, NaH, DMF, 0 °C to rt, 30 min (iii) MeOH, H₂SO₄, reflux, 90 min; (d) LiAlH₄, THF, 0 °C, 1 h; (e) TsCl, DMAP, NEt₃, DCM, 18 h; (f) (i) **63**, NaH, DMF, 0 °C to rt, 1 h (ii) MeOH, H₂SO₄, reflux, 1 h; (g) NaBH₄, MeOH, 0 °C, 90 min; (h) (i) aqueous HBr (48%), reflux, 90 min (ii) **63**, NaH, DMF, 0 °C to rt, 15 min (iii) MeOH, H₂SO₄, reflux, 2 h.

Scheme 12: Synthesis of (a) **72g** in one step from **71g**, (b) **64i** in two steps from **73**, including **63**, (c) **64k** in three steps from **75**, including **63**, and (d) **64m** in two steps from **78**, including **63**.

A similar approach was taken with methyl ester **64k**, with the reduction of ester **75** by LiAlH₄ to alcohol **76** (91% yield), however the resultant alkyl halide **77** from treatment with *p*-toluenesulfonyl chloride and DMAP was isolated (17% yield) before reaction with indole **63** (85% yield) (Scheme 12c). With methyl ester **64m**, aldehyde **78** was reduced by NaBH₄ to alcohol **79** (79% yield),¹²⁸ which was heated under reflux in aqueous hydrobromic acid. Concentration of the reaction mixture *in vacuo* afforded a crude solid that was reacted with indole **63** (65% yield overall) (Scheme 12d).



i R = 2-methoxypyridin-3-yl
k R = 6-methoxypyridin-3-yl
m R = quinolin-4-yl



Reagents and Conditions: (a) *n*-butyllithium (1.6 M in hexanes), acetonitrile, THF (+ toluene for **64m**), -78 °C, 30 min to 1 h; (b) (i) CCl₃CN, NaOAc, EtOH, 15 to 36 h (ii) N₂H₄·H₂O, EtOH, reflux, 6 to 18 h; (c) LiCl, TsOH·H₂O, DMF, 120 °C, 25 min.

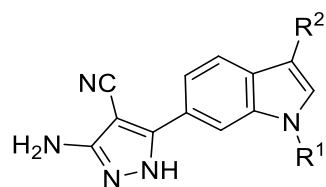
Scheme 13: Synthesis of (a) 71i, 71k and 71m in two steps from 64i, 64k or 64m, (b) 71j in one step from 71i, and (c) 71l in one step from 71k.

Methyl esters **64i**, **64k** and **64m** were converted to the corresponding β-ketonitriles **65i**, **65k** and **65m** (26-76% yield), which were used to synthesise the 4-cyanopyrazole compounds **71i**, **71k** and **71m** in the same

manner as **71c** and **71f** (41-61% yield overall) (Scheme 13a). 2-Pyridone compounds **71j** and **71l** were synthesised from the methoxypyridyl analogues **71i** and **71k** respectively by heating at 125 °C with LiCl and *p*-toluenesulfonic acid in DMF (47-51% yield) (Scheme 13b and c), using a literature procedure previously utilised with other methoxypyridyl compounds.¹²⁹

Screening of the 3-chloroindole analogue **72g** (K_d 8.6 μ M, LE 0.28) afforded an almost 50-fold attenuation of binding affinity in comparison to **71g** (Table 8), suggesting that substitution from the rear of the indole into the adjacent region was not tolerated. Hence, further analogues with alternate substitution from the indole ring were not developed. Comparison of the X-ray crystal structure of **72g** in complex with *Mab* TrmD to that from **71g** did not show significant movement by the indole ring (Figure 46b and Figure 47a). The change in binding affinity could be related to disruption of a hydrogen-bonded water network visible in the X-ray crystal structure of **71g** in complex with *Mab* TrmD (Figure 46b), with the closest water molecule to the indole 3-position bound to the backbone carbonyl of Pro83 not present in the X-ray crystal structure with **72g** (Figure 47a).

2-Pyridone analogues **71j** (K_d 3.2 μ M, LE 0.30) and **71l** (K_d 1.3 μ M, LE 0.32) both possessed worse binding affinities than **71g** (K_d 0.18 μ M, LE 0.38) (Table 8), despite the X-ray crystal structure of **71j** in complex with *Mab* TrmD showing evidence of a water-mediated hydrogen-bonding interaction between the 2-pyridone oxygen and both the guanidyl group of Arg154 and backbone carbonyl of Leu138 (Figure 47b). The ΔT_m values for the methoxypyridyl intermediates **71i** (ΔT_m +5.6 °C) and **71k** (ΔT_m +9.9 °C) were also measured, which suggested similar behaviour to **71j** (ΔT_m +5.5 °C) and **71l** (ΔT_m +8.3 °C) respectively (Table 8), however K_d values could not be obtained by ITC due to poor aqueous solubility in a similar manner to **71c**. Unfavourable aqueous solubility was also seen in the quinolyl analogue **71m** (ΔT_m +10.3 °C), precluding affinity determination by ITC.



| Compound | R ¹ | R ² | ΔT_m^a (°C) | K_d (μM) | LE ^b | GE ^b (R ¹) |
|------------|----------------|----------------|---------------------|-------------------------|-----------------|-----------------------------------|
| 71g | | H | +10.5 | 0.18 ± 0.06 | 0.38 | 0.28 |
| 71h | | H | +11.5 | 0.12 ± 0.02 | 0.39 | 0.31 |
| 71i | | H | +5.6 | ND ^c | - | - |
| 71j | | H | +5.5 | 3.2 ± 0.3 | 0.30 | 0.03 |
| 71k | | H | +9.9 | ND ^c | - | - |
| 71l | | H | +8.3 | 1.3 ± 0.1 | 0.32 | 0.10 |
| 71m | | H | +10.3 | ND ^c | - | - |
| 72g | | Cl | +5.8 | 8.6 ± 1.0 | 0.28 | - |

^a 100 μM ligand and 10 μM *Mab* TrmD.

^b kcal mol⁻¹ HA⁻¹.

^c Not determined due to aqueous solubility.

*Table 8: The change in the melting temperatures (ΔT_m), affinities (K_d) and efficiency metrics of compounds **71g-m** and **72g**.*

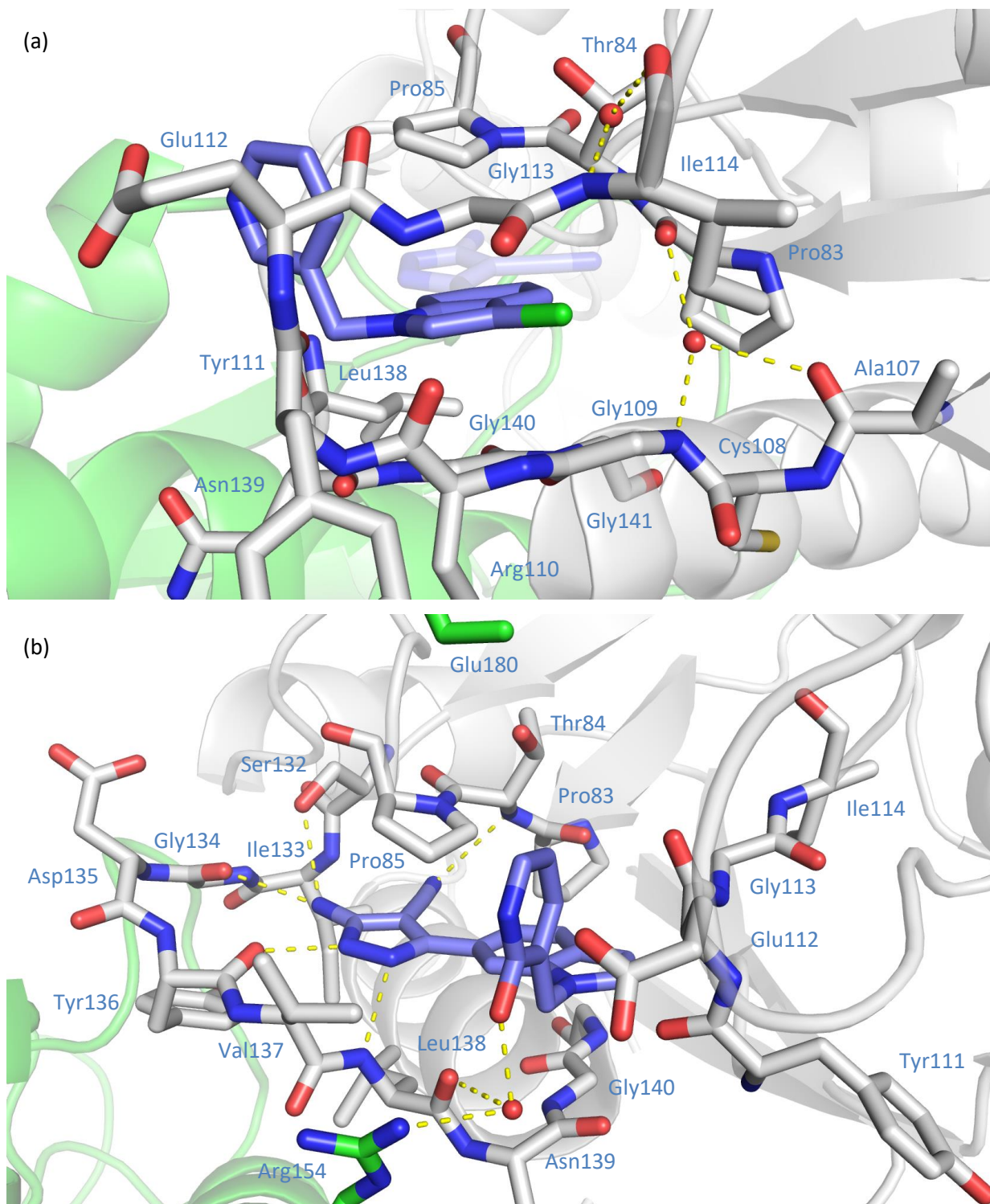


Figure 47: X-ray crystal structures of Mab TrmD (subunit A = white, subunit B = green, ligand = lilac) bound to (a) **72g** (PDB code 6QR1, 1.67 Å), illustrating the indole ring in one of the active sites, and (b) **71j** (PDB code 6QR2, 1.55 Å), illustrating one of the active sites.¹²³

3.2.4: Incorporation of Increased sp³-content in the Scaffold

In light of the reduced aqueous solubility possessed by a number of analogues of **71g** and **71h**, focus was shifted to the screening of compounds with higher sp³ content due to its association with improved aqueous solubility.¹³⁰ Further, due to the presentation of a positively-charged sulfur atom by SAM adjacent to the volume occupied by the phenyl and pyridyl rings of recent analogues in the lead series (Figure 48), and the nearby presence of the carboxylate side chains of residues Glu112 and Glu180, it was believed that their replacement by a saturated amine, protonated under physiological conditions, would be tolerated. Hence, piperidinyl analogues were explored.

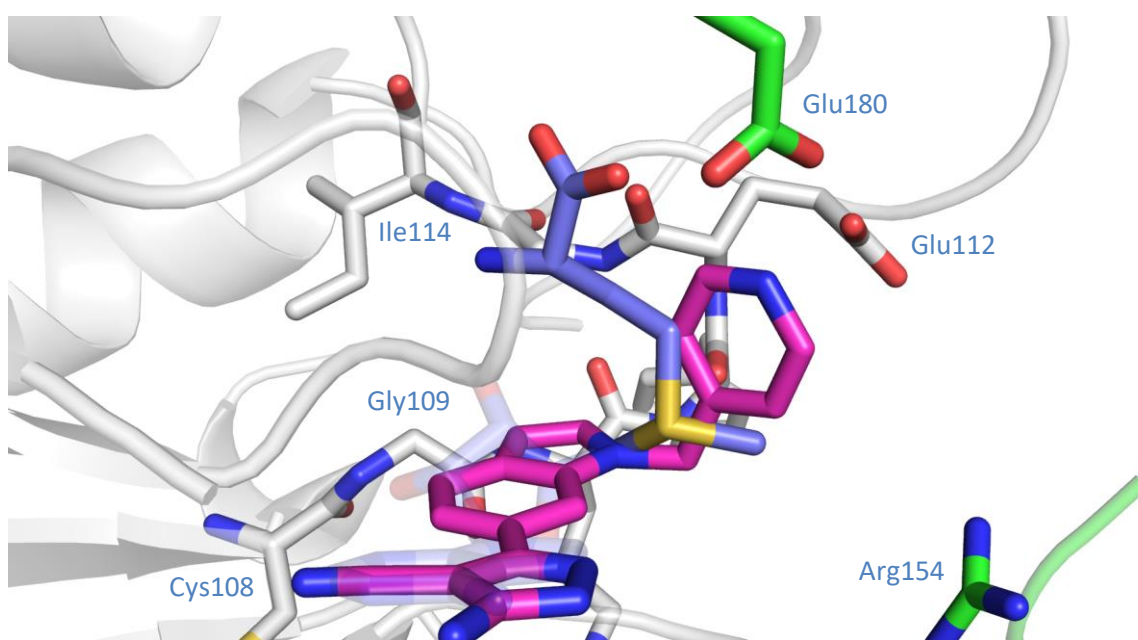
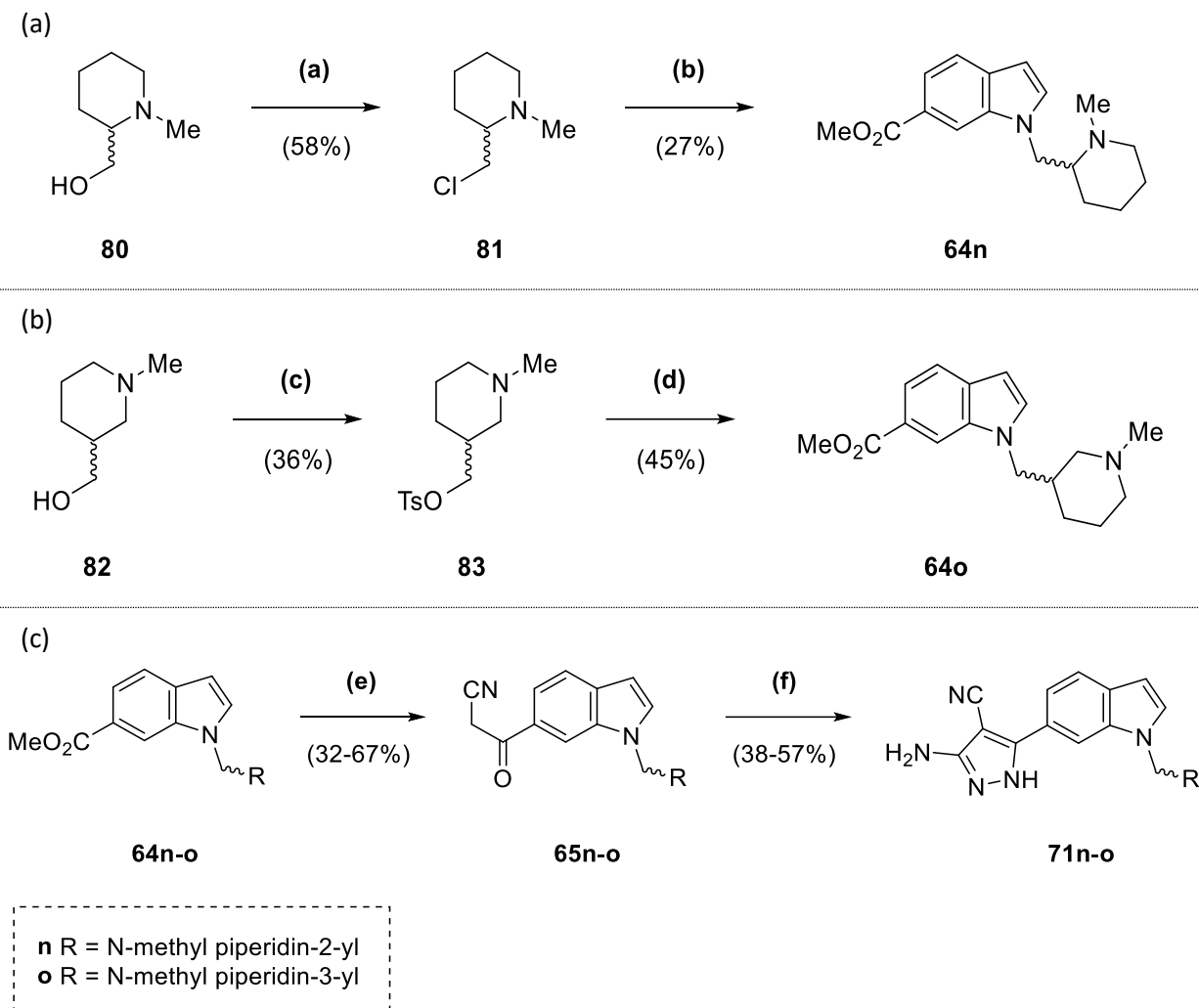


Figure 48: Overlay of X-ray crystal structures of Mab TrmD bound to SAM or **71h** (overlay of PDB code 6NW6 and PDB code 6QR0, subunit A = white, subunit B = green, SAM = lilac, **71h** = pink), illustrating the overlap between **71h** (representing the 3-aminopyrazole lead series) and the methionine portion of SAM in one of the active sites.^{50, 123}

The routes for the synthesis of the piperidinyl analogues involved the synthesis of methyl esters **64n-o** from reaction of the corresponding electrophile with indole **63** and NaH in a similar manner to **64g-h** (27-45% yield) (Scheme 14a and b). However, to achieve conversion of starting material for **64n-o**, the reaction mixture in DMF was heated to 60 °C, with NaI added as a catalyst in the case of **64o**. As with **64i**, **64k** and **64m**, the corresponding electrophiles required further synthesis. This was achieved through the treatment of racemic alcohols **80** and **82** with thionyl chloride or a mixture of *p*-toluenesulfonyl chloride and DMAP respectively (36-58% yield). Methyl esters **64n-o** were converted to the corresponding β -ketonitriles **65n-o** (32-67% yield), which were used to synthesise the 4-cyanopyrazole compounds **71n-o** in the same manner as **71c** and **71f** (38-57% yield overall) (Scheme 14c).

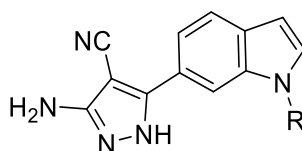


Reagents and Conditions: (a) SOCl_2 , DCM, reflux, 7 h; (b) **63**, NaH, DMF, 0 to 60 °C, 1 h (ii) MeOH, H_2SO_4 , reflux, 1 h; (c) TsCl, DMAP, NEt_3 , DCM, 4 h; (d) (i) **63**, NaH, NaI, DMF, 0 to 60 °C, 1 h; (e) *n*-butyllithium (1.6 M in hexanes), acetonitrile, THF, -78 °C, 30 min to 1 h; (f) (i) CCl_3CN , NaOAc, EtOH, 3 h 30 min to 18 h (ii) $\text{N}_2\text{H}_4 \cdot \text{H}_2\text{O}$, EtOH, reflux, 15 h to 1 d.

Scheme 14: Synthesis of (a) **64n** in two steps from **80**, including **63**, (b) **64o** in two steps from **82**, including **63**, and (c) **71n-o** in two steps from **64n-o**.

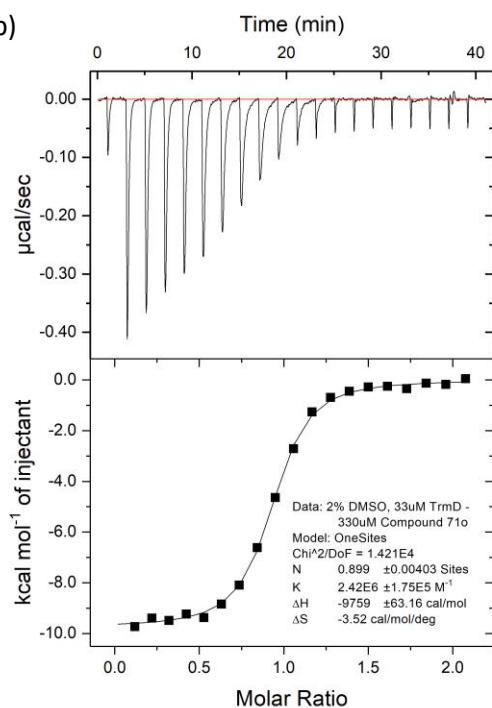
Screening of the piperidinyl analogues **71n** (K_d 0.59 μM , LE 0.34) and **71o** (K_d 0.36 μM , LE 0.35) as racemic mixtures afforded sigmoidal ITC isotherms that suggest binding affinities at the level of **71f** (K_d 0.50 μM , LE 0.36) (Figure 49a). Whilst these K_d values are not as low as **71g** (K_d 0.18 μM , LE 0.38) and **71h** (K_d 0.12 μM , LE 0.39), they demonstrate a tolerance of the methionine binding site for three-dimensional moieties with a protonated group, as expected from the X-ray crystal structure of SAM in complex with *Mab* TrmD (Figure 48), and encouraged further exploration.

(a)

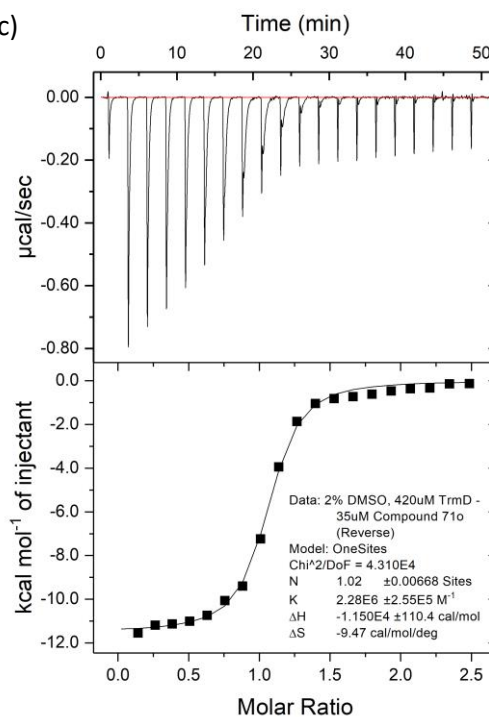


| Compound | R | ΔT_m^a (°C) | K_d (μM) | LE ^b | GE ^b (R) |
|------------|---|---------------------|-------------------------|-----------------|---------------------|
| 71n | | +8.8 | 0.59 ± 0.23 | 0.34 | 0.16 |
| 71o | | +10.9 | 0.36 ± 0.05 | 0.35 | 0.20 |

(b)



(c)



^a 100 μM ligand and 10 μM *Mab* TrmD.

^b kcal mol⁻¹ HA⁻¹.

Figure 49: (a) the change in the melting temperatures (ΔT_m), affinities (K_d) and efficiency metrics of compounds **71n-o**; ITC traces for **71o** from (b) injection of ligand into sample cell ('forward titration'), and (c) injection of protein into sample cell ('reverse titration').

As compounds **71n** and **71o** were screened as racemic mixtures, care must be taken in the interpretation of the results. Mixtures of two compounds with equivalent enthalpies of binding but differing affinity values can afford deceptively simple isotherms by ITC, with curvatures that reflect the affinity of the weaker compound, masking the binding of the most potent compound.¹³¹ Hence, a ‘reverse titration’ ITC experiment, with the injection of an excess of protein into the racemic mixture to separate out the binding of the two enantiomers, was performed with **71o** (Figure 49c). The resultant isotherm could be fitted by a one-site binding model using similar parameters to the ‘forward titration’ (Figure 49b), suggesting that the two enantiomers are equipotent.

X-ray crystal structures obtained by the soaking of racemic mixtures of **71n** or **71o** into *Mab* TrmD crystals were successfully refined using the individual enantiomers. For **71n**, the piperidiny rings of both enantiomers were shown to orient with their *N*-methyl group facing out of the active site, interacting with the backbone carbonyl of Tyr111 (Figure 50).

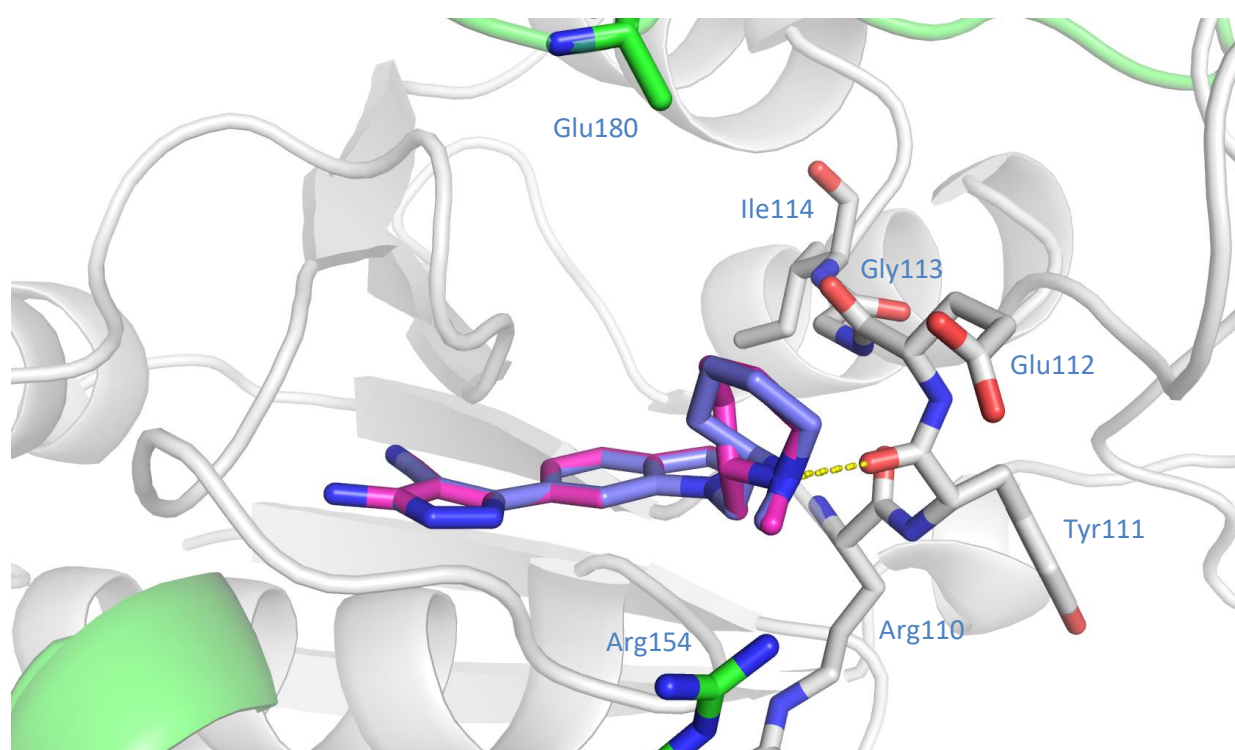


Figure 50: Overlay of X-ray crystal structures of *Mab* TrmD soaked with racemic **71n** solution and refined with individual enantiomers (1.52 Å, subunit A = white, subunit B = green, (**R**)-**71n** = lilac, (**S**)-**71n** = pink), illustrating one of the active sites.¹³²

In contrast to **71n**, the piperidiny rings of both (**R**) and (**S**)-**71o** could be modelled in one site with the *N*-methyl group oriented to form an electrostatic interaction with the carboxylate side chain of Glu112 (Figure 51a). In the other site however, (**S**)-**71o** was shown to interact with Glu180 (Figure 51b).

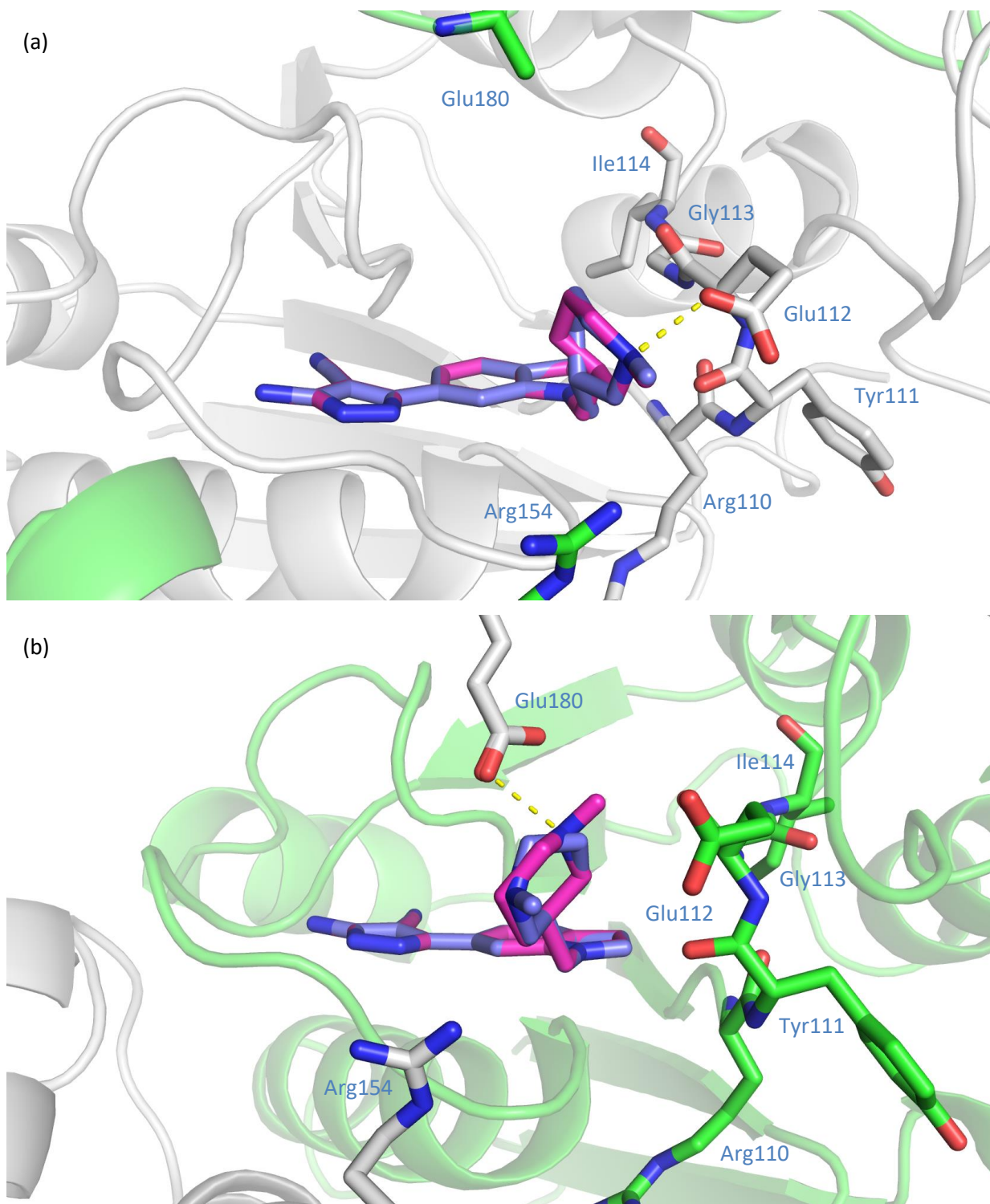


Figure 51: Overlay of X-ray crystal structures of Mab TrmD soaked with racemic **71o** solution and refined with individual enantiomers (1.61 Å, subunit A = white, subunit B = green, (*R*)-**71o** = lilac, (*S*)-**71o** = pink), illustrating active sites 1 (a) and 2 (b).¹³²

The results from the screening of compounds **71n-o**, with the presentation of piperidiny ring systems in the methionine binding region affording comparable binding affinities to the pyridyl analogue **71f**,

encouraged further targeting of the carboxylate side chains of Glu112 and Glu180 by electrostatic interactions with similar saturated motifs. However, whilst the chiral nature of **71o** was addressed in ITC screening, challenges in the acquisition of pure enantiomers encouraged a return to the screening of achiral analogues. To improve affinity, the design of these analogues was focused on the presentation of a protonated amine closer to the side chains of Glu112 and Glu180.

In the previous study on *H. influenzae* TrmD (Figure 11), the addition of basic motifs to a phenyl ring through a methylene linker was used, as represented by aminomethyl analogue **85** which afforded a 5-fold improvement in IC₅₀ relative to the unsubstituted compound **84** (0.56 vs 2.6 μM) (Figure 52).⁶³

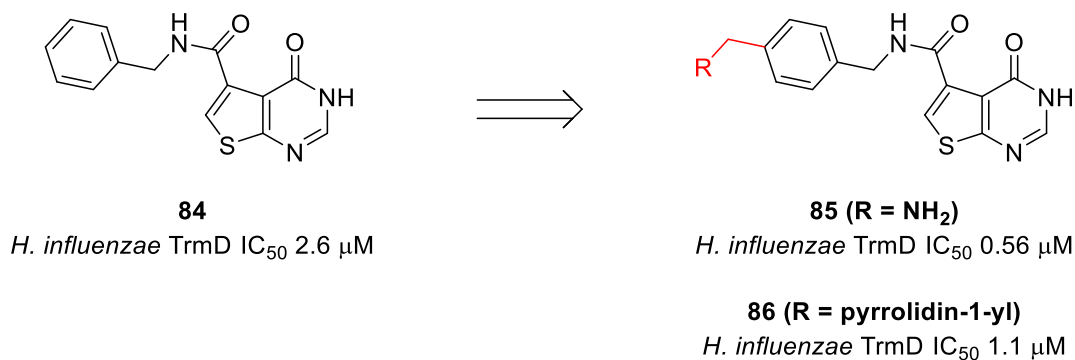


Figure 52: The addition of aminomethylene-based motifs to starting point **84** in the study against *H. influenzae* TrmD, with analogues **85** and **86** shown.⁶³

Similarly to **71o** (Figure 51a), the X-ray crystal structure of **85** with *H. influenzae* TrmD showed an electrostatic interaction between the aminomethyl group of **85** and the carboxylate side chain of Glu116 (Figure 53a), corresponding to Glu112 in *Mab* TrmD. Due to the proximity of the phenyl ring of **85** and the phenyl and pyridyl rings of analogues **66a-f** and **71f-m** in X-ray crystal structures with TrmD from *H. influenzae* and *Mab* respectively as represented with **71f** and **85**, in addition to residues Glu112 and Glu116 (Figure 53b), it was believed that the strategy could be incorporated into the 3-aminopyrazole lead series.

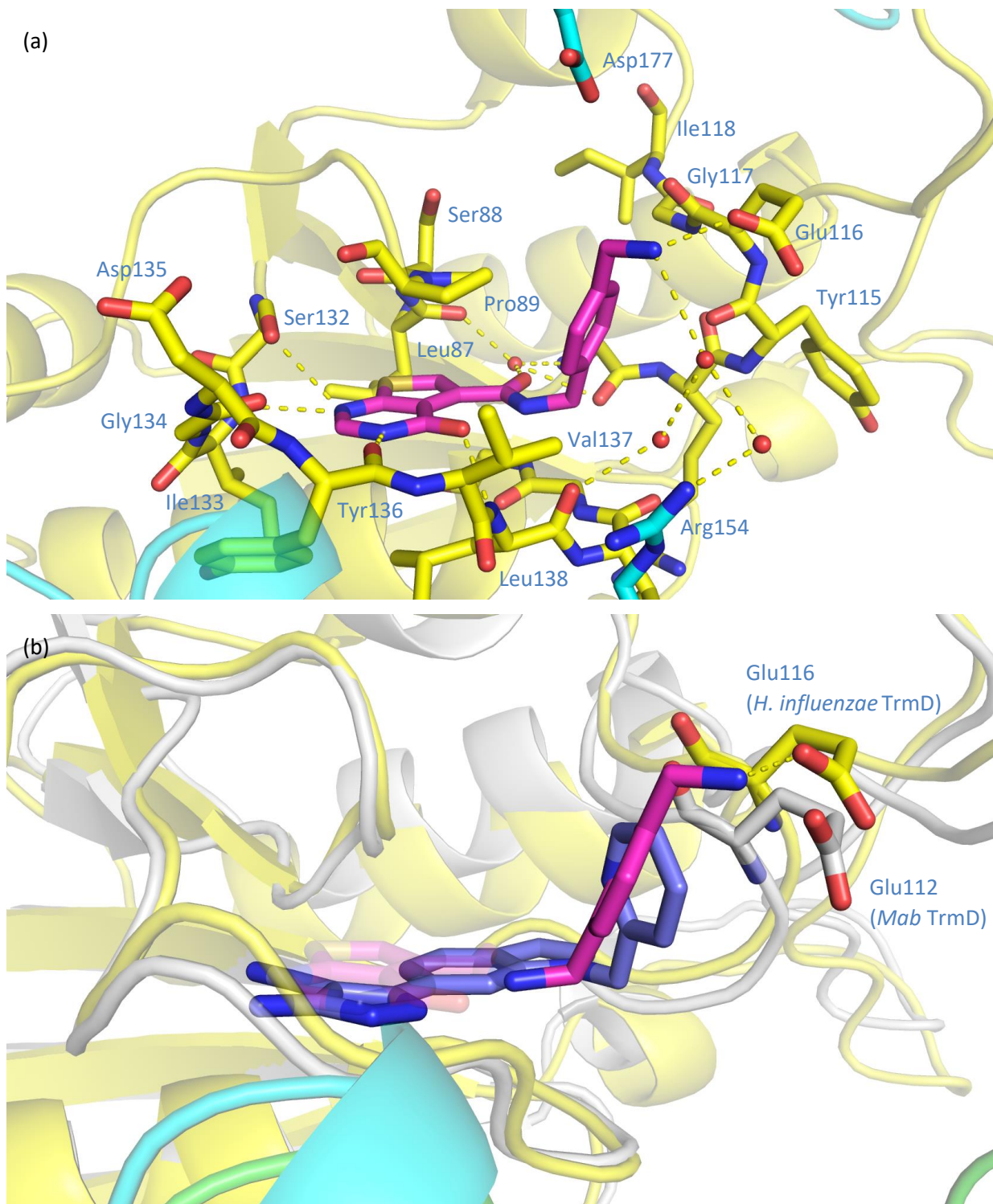


Figure 53: (a) X-ray crystal structure of *H. influenzae* TrmD bound to **85** (PDB code 4MCC, 1.95 Å, subunit A = yellow, subunit B = cyan, **85** = pink), illustrating one of the active sites;⁶³ (b) overlay of X-ray crystal structures of *H. influenzae* TrmD (subunit A = yellow, subunit B = cyan) and Mab TrmD (subunit A = white, subunit B = green) bound to **85** and **71f** respectively (overlay of PDB code 4MCC and PDB code 6QQY, **85** = pink, **71f** = lilac), illustrating one of the active sites.^{50, 63}

From the compounds described in the *H. influenzae* study the pyrrolidinyl ring from **86** (Figure 52), which possessed a comparable IC₅₀ to **85** (1.1 vs 0.56 μM), was selected for incorporation into the lead series due to its small steric profile relative to other screened moieties.⁶³ The scaffolds of both **71f** and **66c** were used for the design of analogues incorporating the pyrrolidinyl ring and methylene linker of **86** for GE analysis (Figure 54).

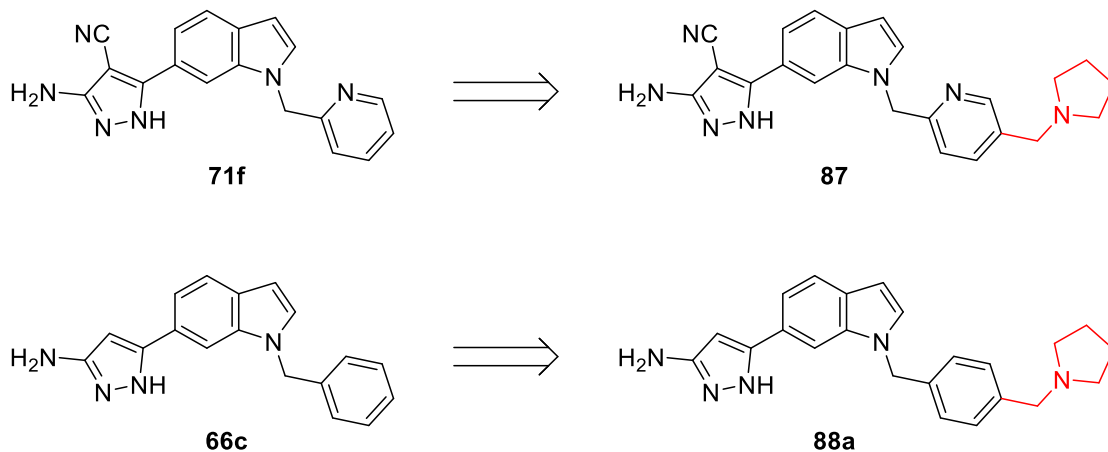
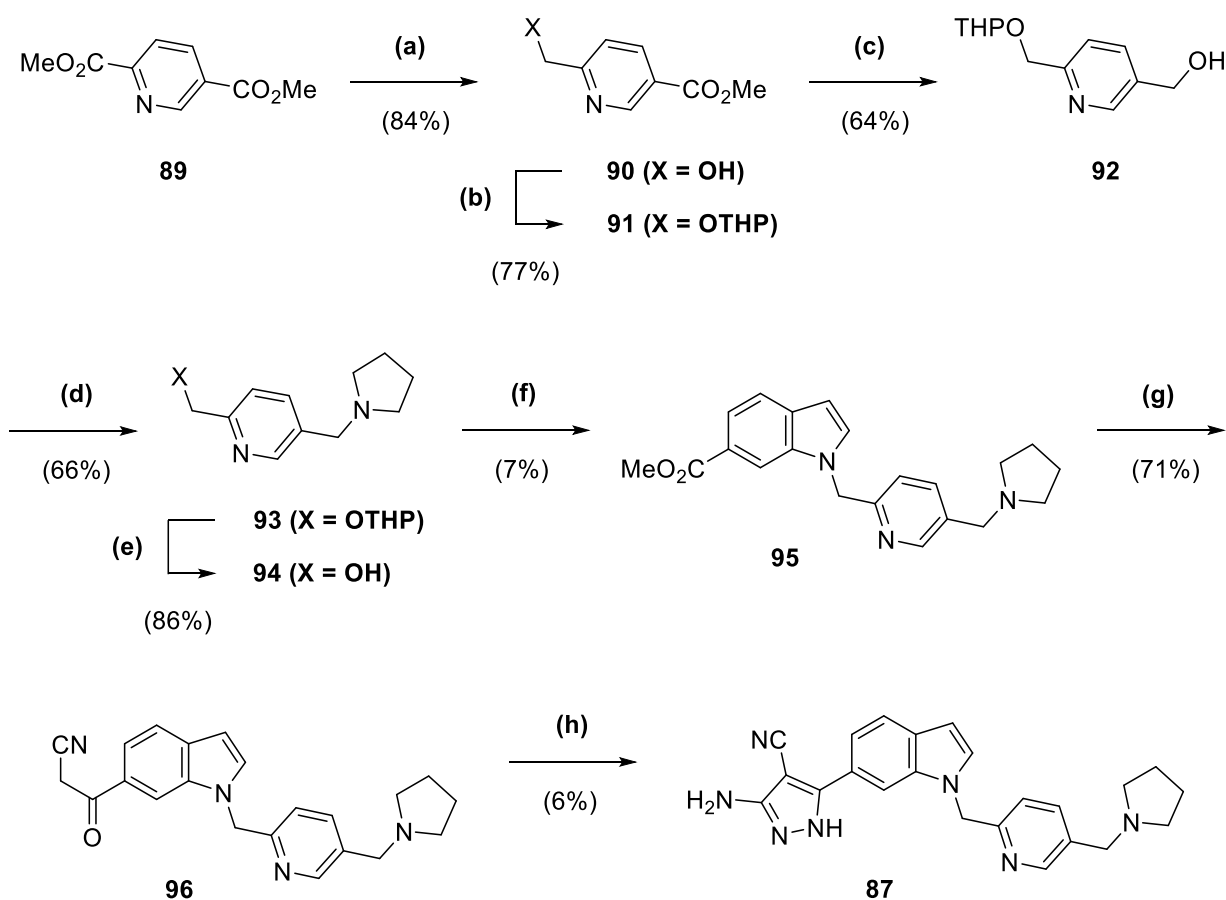


Figure 54: Idea for incorporation of the pyrrolidinyl ring and methylene linker of **86** to the scaffolds of **71f** and **66c**.

The eight-step route for the synthesis of the pyridyl analogue **87** began with the regioselective reduction of one of the ester groups of **89** by a mixture of NaBH₄ and CaCl₂ (84% yield),¹³³ with the resultant alcohol of **90** protected as a THP ether (77% yield) (Scheme 15). The remaining ester group of **91** was reduced by LiAlH₄ (64% yield), with the resultant alcohol of **92** converted to the corresponding mesylate by treatment with methanesulfonyl chloride. The mesylate was taken forwards crude after aqueous workup and stirred with pyrrolidine and Cs₂CO₃ in DMF to afford **93** (66% yield overall). The THP protecting group of **93** was removed by heating at 50 °C with *p*-toluenesulfonic acid in ethanol (86% yield), with the resultant alcohol of **94** treated with methanesulfonyl chloride as with **92**. Following aqueous workup, the crude material was reacted with indole **63** at 60 °C using NaH and NaI in DMF (7% yield overall). Methyl ester **95** was converted to the corresponding β-ketonitrile **96** (71% yield), which was used to synthesise the 4-cyanopyrazole compound **87** in the same manner as **71c** and **71f** (6% yield overall).



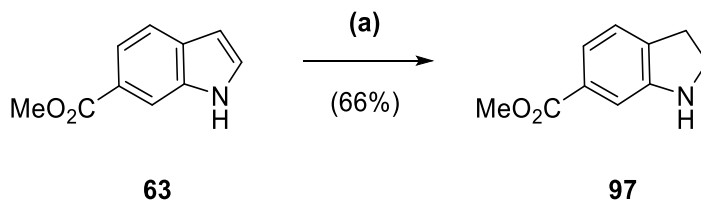
Reagents and Conditions: (a) NaBH₄, CaCl₂, MeOH, THF, 0 °C, 90 min; (b) MeSO₃H, 3,4-dihydro-2H-pyran, DCM, 150 min; (c) LiAlH₄, THF, 0 °C, 45 min; (d) (i) MeSO₂Cl, NEt₃, DCM, 0 °C to rt, 1 h (ii) pyrrolidine, Cs₂CO₃, DMF, 14 h; (e) TsOH·H₂O, ethanol, 50 °C, 30 min; (f) (i) MeSO₂Cl, NEt₃, DCM, 0 °C to rt, 150 min; (ii) **63**, NaH, NaI, DMF, 0 to 60 °C, 75 min (iii) MeOH, H₂SO₄, reflux, 14 h; (g) *n*-butyllithium (1.6 M in hexanes), acetonitrile, THF, -78 °C, 1 h; (h) (i) CCl₃CN, NaOAc, EtOH, 36 h (ii) N₂H₄·H₂O, EtOH, reflux, 1 d.

Scheme 15: Synthesis of **87** in eight steps from **89**.

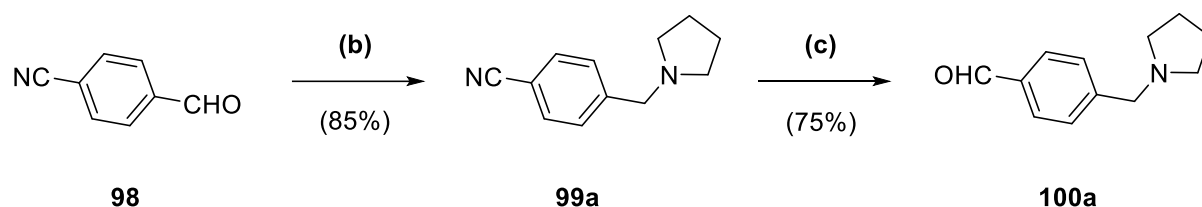
With the synthesis of the phenyl analogue **88a** a convergent six-step route was utilised, beginning with the reduction of indole **63** to indoline **97** by sodium cyanoborohydride in acetic acid (66% yield) (Scheme 16a).¹³⁴ In parallel, 4-formylbenzonitrile **98** was reacted with pyrrolidine in a reductive amination reaction with sodium triacetoxyborohydride and acetic acid (85% yield), with the nitrile group of **99a** reduced by DIBAL-H to afford aldehyde **100a** (75% yield) (Scheme 16b). Compounds **97** and **100a** were used to produce methyl ester **101a** by microwave-assisted condensation with benzoic acid in toluene (53% yield) (Scheme 16c), using a literature procedure previously utilised with other indolines and aromatic aldehydes.¹³⁵ Methyl ester **101a** was converted to the corresponding β -ketonitrile **102a** (87% yield), which was used to synthesise the 3-aminopyrazole compound **88a** in the same manner as **66b-d** and **66f**

(22% yield). β -ketonitrile **102a** was also subsequently used to synthesise the 4-cyanopyrazole compound **103a** in the same manner as **71c** and **71f** (51% yield overall).

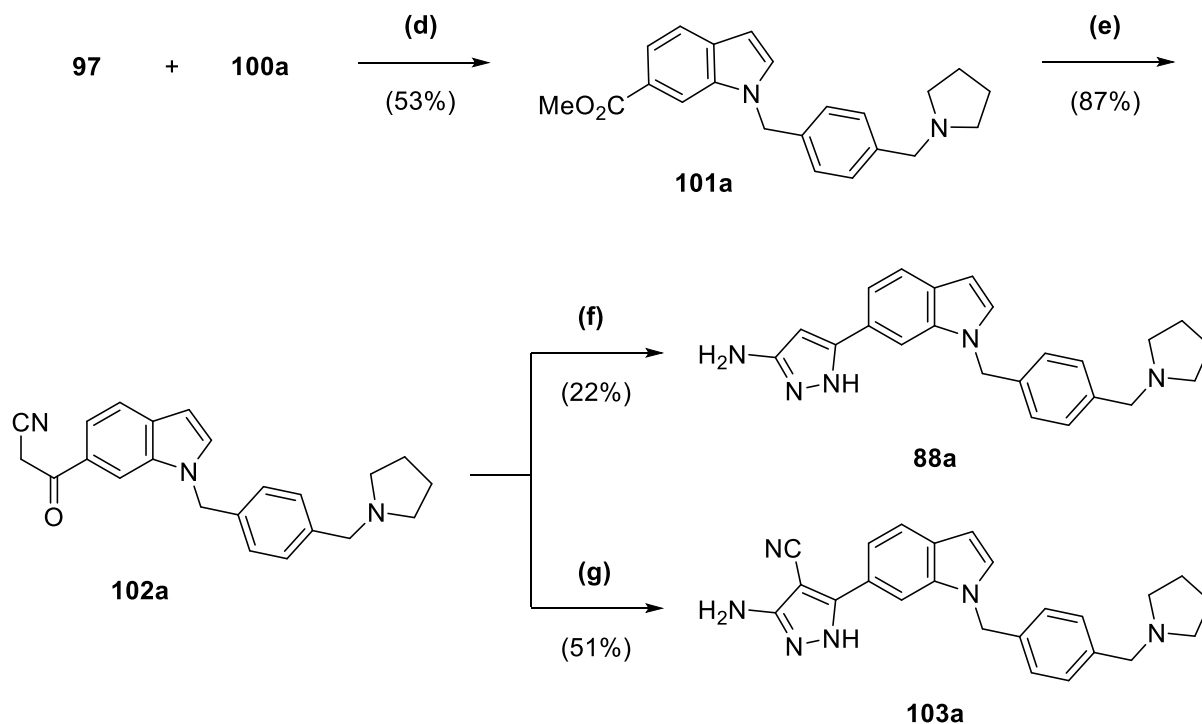
(a)



(b)



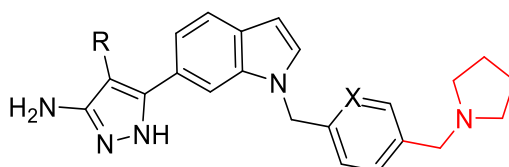
(c)



Reagents and Conditions: (a) NaCNBH₃, AcOH, 0 °C to rt, 7 h; (b) Na(OAc)₃BH, pyrrolidine, AcOH, DCM, 15 h; (c) DIBAL-H, THF, 0 °C to rt, 1 h; (d) PhCO₂H, toluene, 200 °C μ W, 20 min; (e) *n*-butyllithium (1.6 M in hexanes), acetonitrile, THF, -78 °C, 1 h; (f) N₂H₄·H₂O, EtOH, reflux, 12 h; (g) (i) CCl₃CN, NaOAc, EtOH, 4 h (ii) N₂H₄·H₂O, EtOH, reflux, 18 h.

Scheme 16: Synthesis of (a) **97** in one step from **63**, (b) **100a** in two steps from **98**, and (c) **88a** and **103a** in three steps from **97** and **100a**.

The screening of **87** (K_d 92 nM, LE 0.32) revealed a greater than 5-fold improvement in binding affinity in comparison to **71f** (K_d 0.50 μ M, LE 0.36) (Table 9), supporting the adopted strategy. However, with **88a** (K_d 0.49 μ M, LE 0.31) the change in binding affinity from the parent compound **66c** (K_d 19 μ M, LE 0.29) was more beneficial with a 40-fold improvement. This is reflected in the differing GE values for the added pyrrolidin-1-ylmethyl moiety in **87** (GE 0.17) and **88a** (GE 0.36), which could reflect intramolecular interactions between the pyrrolidinyl and pyridyl ring systems in **87**. The high GE value for the added moiety in **88a** was reflected in the nitrile analogue **103a** (K_d 27 nM, LE 0.34), which did not exhibit the poor aqueous solubility of **71c** that precluded screening.



| Compound | X | R | ΔT_m^a ($^{\circ}$ C) | K_d (nM) | LE ^b | GE ^b |
|-------------|----|----|--------------------------------|---------------|-----------------|-----------------|
| 87 | N | CN | +12.0 | 92 \pm 18 | 0.32 | 0.17 |
| 88a | CH | H | +7.0 | 490 \pm 210 | 0.31 | 0.36 |
| 103a | CH | CN | +12.9 | 27 \pm 4 | 0.34 | - |

^a 100 μ M ligand and 10 μ M *Mab* TrmD.

^b kcal mol⁻¹ HA⁻¹, determined for the pyrrolidin-1-ylmethyl moiety highlighted in red.

Table 9: The change in the melting temperatures (ΔT_m), affinities (K_d) and efficiency metrics of compounds **87**, **88a** and **103a**.

The X-ray crystal structure of **103a** in complex with *Mab* TrmD showed the molecule adopting different conformations depending on the active site, with the pyrrolidinyl ring either oriented towards Pro57 and forming an electrostatic interaction with Glu112 (Figure 55a) or oriented towards Ser177 (Figure 55b), reflecting communication between the sites.⁵⁵

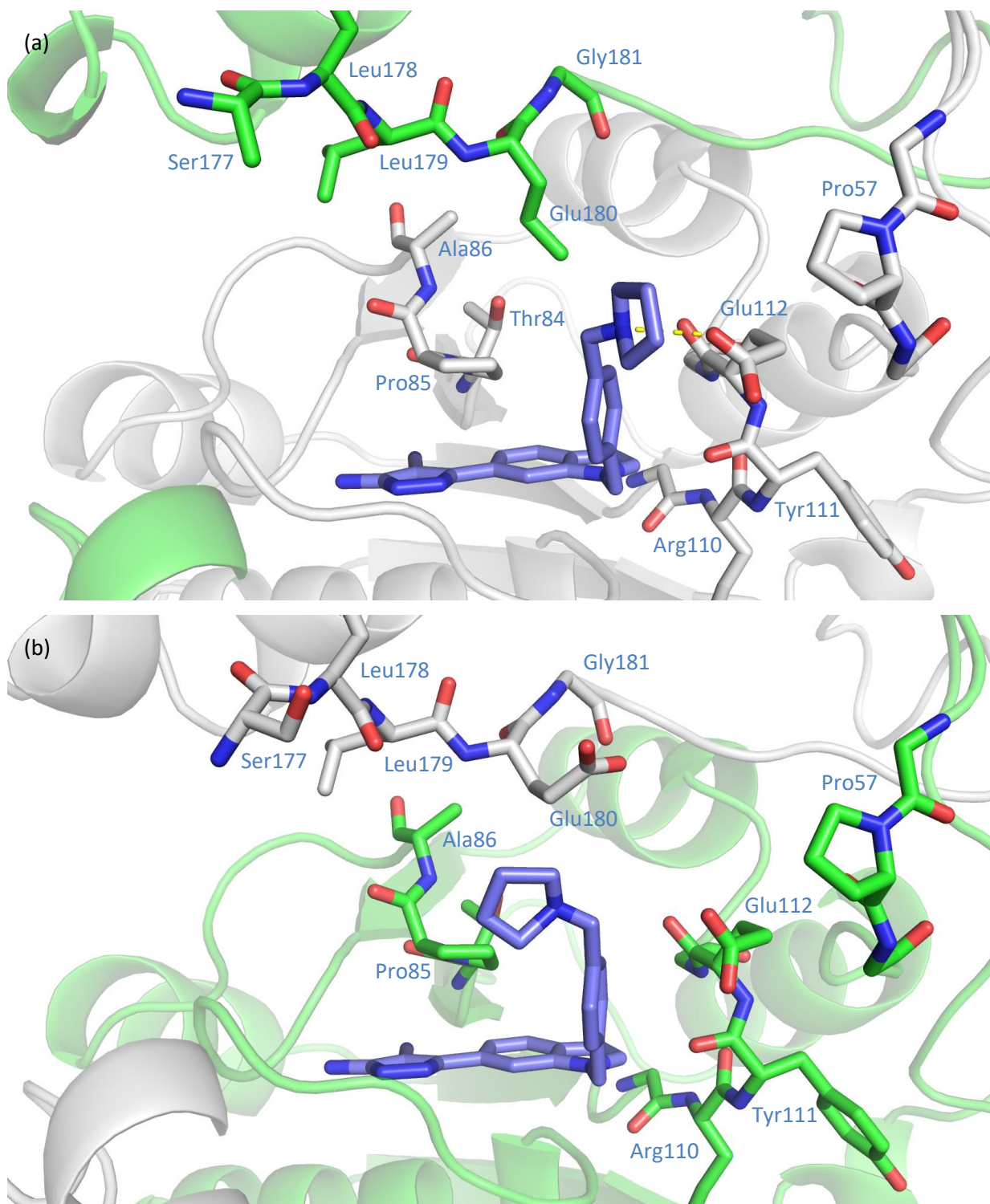
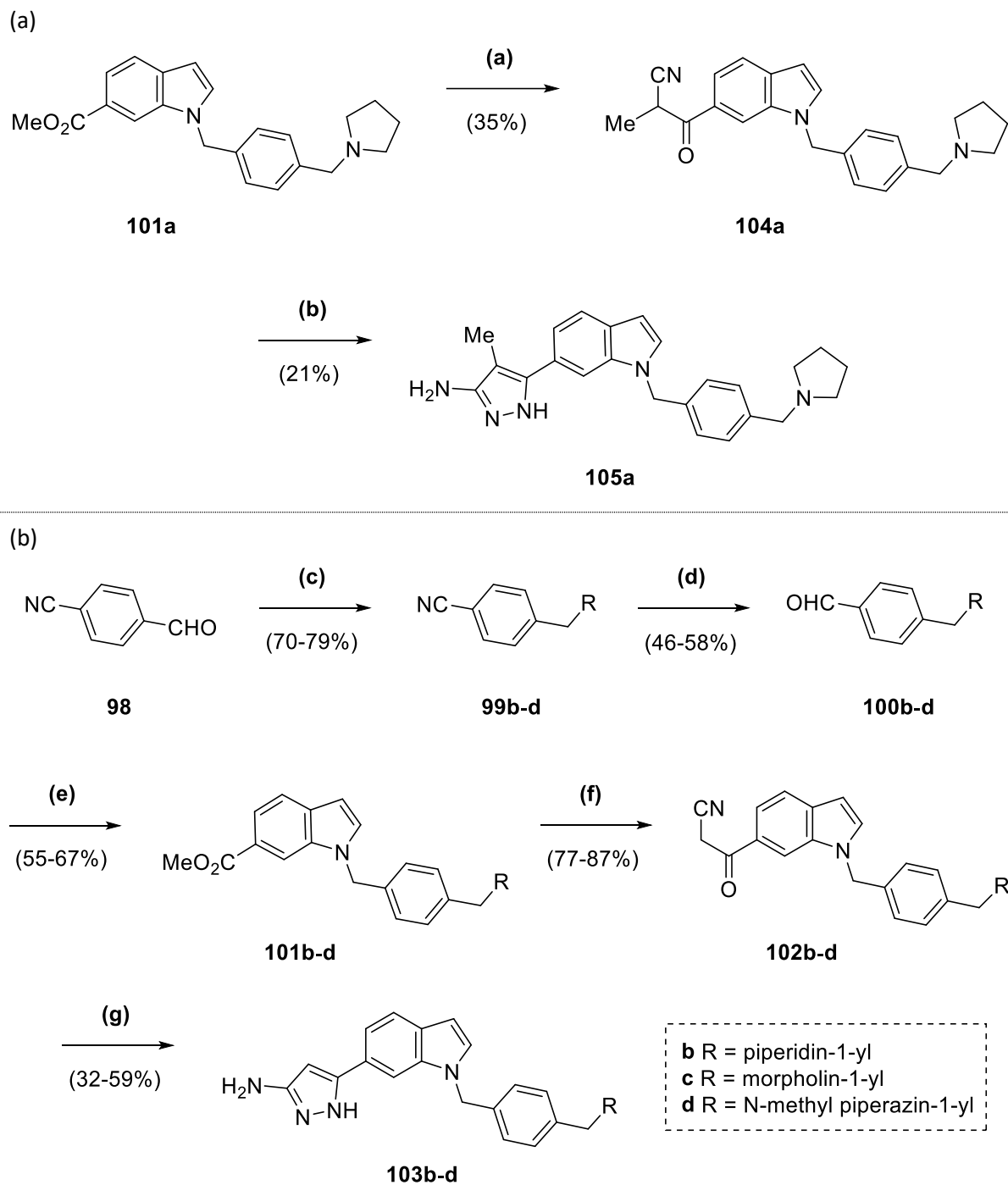


Figure 55: X-ray crystal structure of Mab TrmD bound to **103a** (PDB code 6QR6, 1.71 Å, subunit A = white, subunit B = green, **103a** = lilac), illustrating active sites 1 (a) and 2 (b).⁵⁰

3.2.5: Structure-activity Relationship Study of **103a**

Following the screening of **103a** (K_d 27 nM, LE 0.34), an exploration of SAR was carried out around the nitrile group and pyrrolidinyl ring. In the lead series, analogues had previously only been synthesised with the 4-position of the pyrazole ring either unsubstituted or bearing a nitrile group. Therefore, the tolerance of this position to substitution with other functional groups was sought, with the 4-methylpyrazole analogue of **103a** a focus for synthesis. In the study on *H. influenzae* TrmD, 15 analogues were reported in addition to **86** (IC₅₀ 1.1 μ M) with alternatives to the pyrrolidinyl ring, which varied in IC₅₀ from 0.33 to 9.3 μ M.⁶³ However, *H. influenzae* and *Mab* TrmD only share 42% sequence identity overall and 58% similarity. Further, whilst an X-ray crystal structure was provided for one analogue of **86** with *H. influenzae* TrmD, the lack of observable density for the interdomain linker in the X-ray crystal structure of **103a** in complex with *Mab* TrmD (Figure 55b and c), which surrounds one side of the pyrrolidinyl ring of **103a**, makes direct comparisons challenging. Hence, SAR with the pyrrolidinyl ring of **103a** was sought. Three analogues of **103a** were proposed, including replacement of the pyrrolidinyl ring with a piperidinyl ring to explore the tolerance of the binding pocket for larger ring sizes, and a morpholinyl ring to investigate the impact of reduced basicity on the pyrrolidinyl nitrogen atom and its interaction with the carboxylate side chain of Glu112. Finally, an analogue of **103a** with a piperazinyl ring was desired, whose second nitrogen atom could later be used as a synthetic handle to further explore the active site towards Ser177.

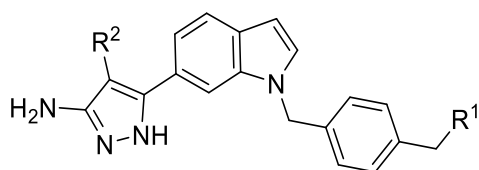
4-Methylpyrazole analogue **105a** was synthesised in two steps from the previously made methyl ester **101a** (Scheme 16), which was treated with *n*-butyllithium and propionitrile to afford β -ketonitrile **104a** (35% yield) (Scheme 17a). Compound **104a** was then heated under reflux with hydrazine in ethanol to afford **105a** (21% yield). Analogues of **103a** with alternate heterocyclic rings in place of the pyrrolidinyl ring were synthesised by the same convergent route as **103a**, using indoline **97** (Scheme 16). For each analogue the corresponding heterocycle was reacted with **98** using sodium triacetoxyborohydride and acetic acid (70-79% yield), with the nitrile group of **99b-d** reduced by DIBAL-H to afford aldehydes **100b-d** (46-58% yield) (Scheme 17b). Compounds **97** and **100b-d** were then used to produce methyl esters **101b-d** in the same manner as **101a** (55-67% yield). Methyl esters **101b-d** were converted to the corresponding β -ketonitriles **102b-d** (77-87% yield), which were used to synthesise the 4-cyanopyrazole compounds **103b-d** in the same manner as **71c** and **71f** (32-59% yield overall).



Reagents and Conditions: (a) *n*-butyllithium (1.6 M in hexanes), propionitrile, toluene, -78 to 0 °C, 2 h; (b) N₂H₄·H₂O, EtOH, reflux, 1 d; (c) Na(OAc)₃BH, RH, AcOH, DCM, 80 min to 5 h; (d) DIBAL-H, THF, 0 °C to rt, 90 min to 1 h; (e) **97**, PhCO₂H, toluene, 200 °C μW, 30 min; (f) *n*-butyllithium (1.6 M in hexanes), acetonitrile, THF, -78 °C, 20 min to 1 h; (g) (i) CCl₃CN, NaOAc, EtOH, 14 h to 2 d (ii) N₂H₄·H₂O, EtOH, reflux, 22 h to 1 d.

Scheme 17: Synthesis of (a) **105a** in two steps from **101a**, and (b) **103b-d** in five steps from **98**, including **97**.

The 4-methylpyrazole analogue **105a** (K_d 2.0 μ M, LE 0.27) showed a significantly attenuated binding affinity on screening in comparison to the 4-cyanopyrazole derivative **103a** (K_d 27 nM, LE 0.34), illustrating a preference for nitrile over methyl substitution from the 4-position of the pyrazole ring of the lead series (Table 10). Further, comparison of **105a** (K_d 2.0 μ M, LE 0.27) with the unsubstituted analogue **88a** (K_d 0.49 μ M, LE 0.31) shows that 4-methyl substitution is less preferable than a lack of substitution from the 3-aminopyrazole ring system of the lead series. It is possible that the greater steric bulk of the methyl group is not tolerated by the residues lining the binding pocket normally occupied by the nitrile group (Figure 43), however it could also be due to an impact on the dihedral angle between the indole and pyrazole rings that is detrimental to binding in the active site.



| Compound | R ¹ | R ² | ΔT_m^a (°C) | K_d (nM) | LE ^b |
|-------------|----------------|----------------|---------------------|------------|-----------------|
| 88a | | H | +7.0 | 490 ± 210 | 0.31 |
| 103a | | CN | +12.9 | 27 ± 4 | 0.34 |
| 103b | | CN | +12.6 | 70 ± 29 | 0.31 |
| 103c | | CN | +12.6 | 190 ± 23 | 0.30 |
| 103d | | CN | +12.0 | 73 ± 30 | 0.30 |
| 105a | | Me | +6.1 | 2000 ± 300 | 0.27 |

^a 100 μ M ligand and 10 μ M *Mab TrmD*.

^b kcal mol⁻¹ HA⁻¹.

Table 10: The change in the melting temperatures (ΔT_m), affinities (K_d) and efficiency metrics of compounds **88a**, **103a-d** and **105a**.

From the screening of the heterocyclic analogues of **103a** (K_d 27 nM, LE 0.34), it was shown that expansion from a pyrrolidinyl to piperidinyl ring in **103b** (K_d 70 nM, LE 0.31) resulted in an almost 3-fold weaker binding affinity (Table 10), suggesting constraints on ring size in this portion of the methionine binding

region. This was reflected in the X-ray crystal structure of **103b** in complex with *Mab* TrmD, which did not show the orientation exhibited by the pyrrolidinyl ring of **103a** towards Ser177, with the piperidinyl ring oriented towards Pro57 in both active sites (Figure 56).

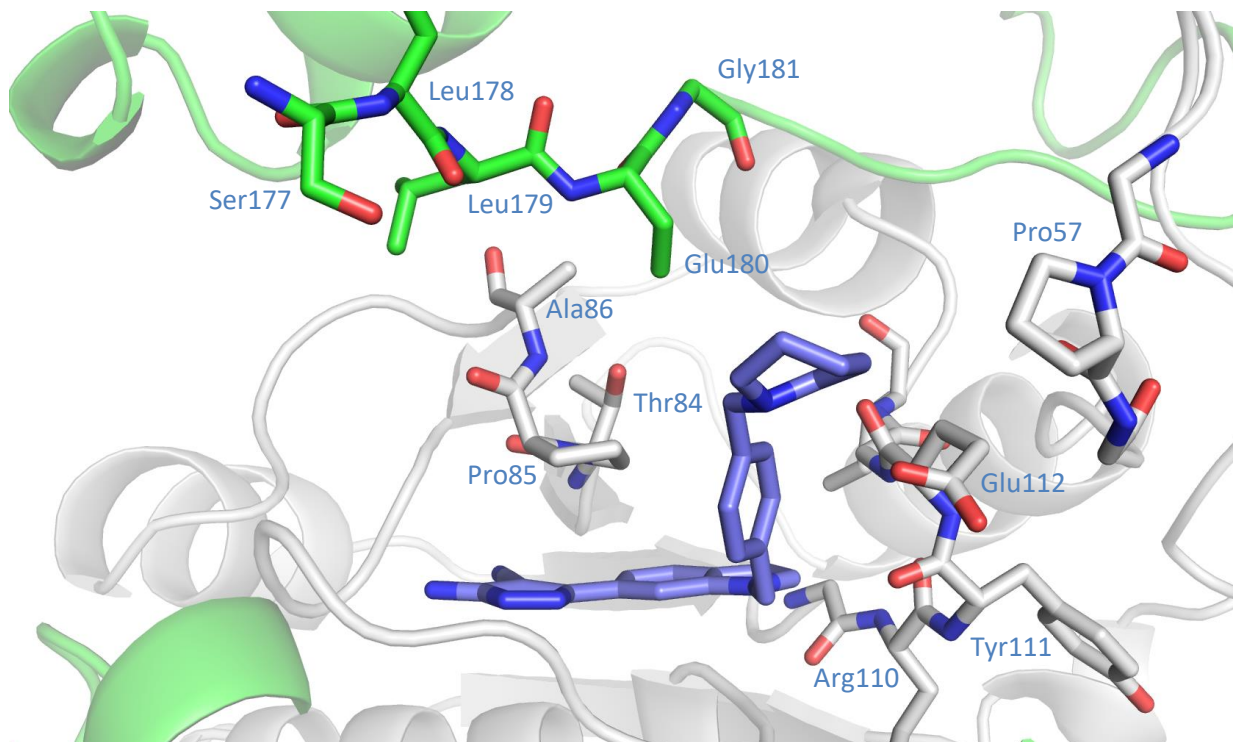


Figure 56: X-ray crystal structure of *Mab* TrmD bound to **103b** (PDB code 6QR7, 2.03 Å, subunit A = white, subunit B = green, **103b** = lilac), illustrating one of the active sites.¹²³

A further almost 3-fold weakening of binding affinity was observed in the morpholinyl analogue **103c** (K_d 0.19 μ M, LE 0.30) in comparison to **103b** (K_d 70 nM, LE 0.31) (Table 10), which is likely due to the impact of the reduced basicity of the nitrogen atom in the ring and its electrostatic interaction with the carboxylate side chain of Glu112. The X-ray crystal structure of **103c** in complex with *Mab* TrmD did not show the oxygen atom of the morpholinyl ring forming any hydrogen-bonding interactions in the active site, however the ring system was rotated significantly in comparison to the piperidinyl ring of **103b** (Figure 57a).

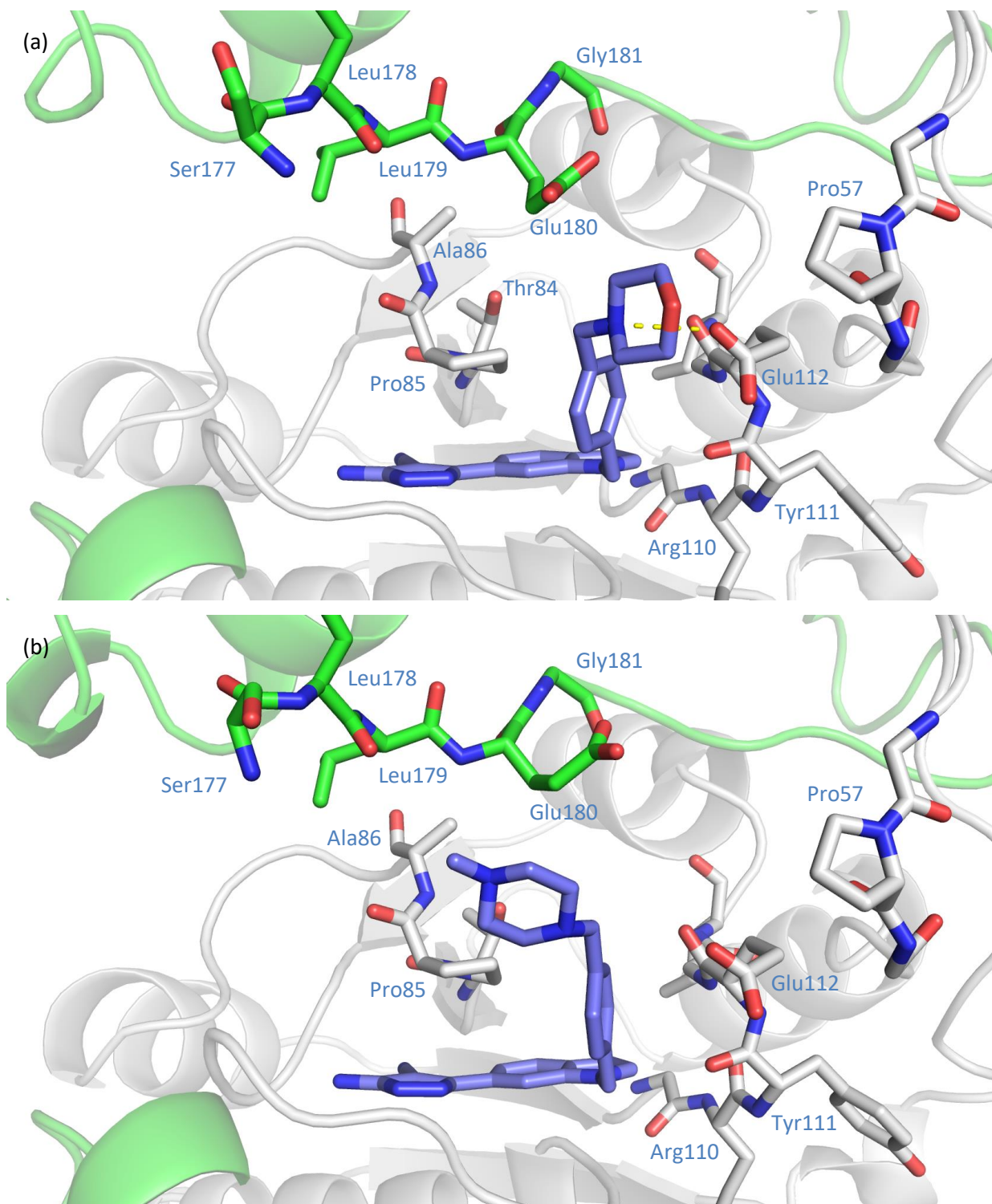


Figure 57: X-ray crystal structures of Mab TrmD (subunit A = white, subunit B = green, ligand = lilac) bound to (a) **103c** (PDB code 6QR9, 2.42 Å),¹²³ and (b) **103d** (PDB code 6QR8, 2.15 Å),⁵⁰ illustrating one of the active sites.

In contrast to **103c** (K_d 0.19 μ M, LE 0.30), screening of the 4-methylpiperazinyl analogue **103d** (K_d 73 nM, LE 0.30) afforded a comparable binding affinity to **103b** (K_d 70 nM, LE 0.31), with the added *N*-methyl

group tolerated by the active site (Table 10). However, the *N*-methyl piperazinyl ring system showed different behaviour to the corresponding heterocyclic rings in analogues **103a-c** in its X-ray crystal structure in complex with *Mab* TrmD, with both active sites showing the ring oriented towards Ser177 (Figure 57b). As no additional hydrogen-bonding interactions were witnessed with the piperazinyl ring, it is likely that this is due to its larger steric bulk in comparison to the other heterocycles with its added methyl group.

3.2.6: Screening against Mycobacteria and Optimisation for Activity

Compounds from the lead series were sent to Dr Karen Brown (Department of Medicine, University of Cambridge) for testing against *Mab* in liquid culture up to a concentration of 400 μ M.^{50, 123} Whilst MIC values were determined for compounds, a lack of correlation between activity against *Mab* and target binding affinity was observed (Table 11). This could be attributed to a number of factors, including the impact of differential metabolism, retention or permeability on activity. Further experiments by Dr Karen Brown and fellow researchers in the Floto research group (Department of Medicine, University of Cambridge) to evaluate the effects of key compounds from the lead series on *Mab* are ongoing.

Select compounds from the lead series were also sent to collaborators Dr Daben Libardo and Dr Helena Boshoff (Tuberculosis Research Section, National Institutes of Health) for testing against *Mtb* in liquid culture.¹²³ The compounds were tested against *Mtb* in the four growth media previously described (2.3.3: Screening against *Mycobacterium tuberculosis*). Promising results were observed for several compounds when applied to *Mtb* in 7H9 growth media in the absence of BSA, with compounds **88a** and **103d** affording MIC values of 12.5 and 6.3 μ M with glucose or DPPC utilised as a carbon source respectively (Table 11). Similarly to the **2**-based lead series (Table 4), the relatively poor activity afforded by compounds in the presence of BSA suggests that plasma protein binding could be an issue for this series (Table 11).

| Compound | | <i>Mab</i> | <i>H37Rv Mtb</i> MIC (μM) | | | | |
|-------------|--|--------------------|--|-------------|-------------|-----------------|--------------|
| | | TrmD K_d (nM) | <i>Mab</i> MIC (μM) | GAST -Fe | 7H9/ BSA | 7H9/ glucose | 7H9/ DPPC |
| 71h | | 120 \pm 15 | 50 | 50 | >100 | ND | |
| 87 | | 92 \pm 18 | 50 | | | ND | |
| 88a | | 490 \pm 210 | 50 | 25 | 100 | 12.5 | 6.3 |
| 103a | | 27 \pm 4 | 50 | 50 | >100 | 25 | 12.5 |
| 103b | | 70 \pm 29 | 50 | 50 | 100 | 25 | 12.5 |
| 103c | | 190 \pm 23 | 50 | 50 | >100 | 100 | 50 |
| 103d | | 73 \pm 30 | 50 | 25 | 50 | 12.5 | 6.3 |
| 105a | | 2000 \pm 300 | 50 | | | ND | |

Table 11: MIC values afforded by compounds **71h**, **87**, **88a**, **103a-d** and **105a** against *Mab*, performed by Dr Karen Brown, and *H37Rv Mtb*, performed by Dr. Daben Libardo.

The promising results for key compounds against *Mtb* encouraged optimisation of activity through a consideration of physicochemical properties, in parallel with experiments by collaborators focused on *Mab*. Due to the low MIC values afforded by **103d** against *Mtb* in comparison to other analogues (Table 11), its scaffold was selected for the design of further compounds. An initial idea for modification of **103d** was the replacement of its *N*-methyl group with an *N*-isopropyl group in **103e** (Figure 58), which was

intended to increase lipophilicity (cLogP 4.06 to 4.90) without significantly impacting either aqueous solubility or the steric profile, avoiding disruption of ligand-target interactions.

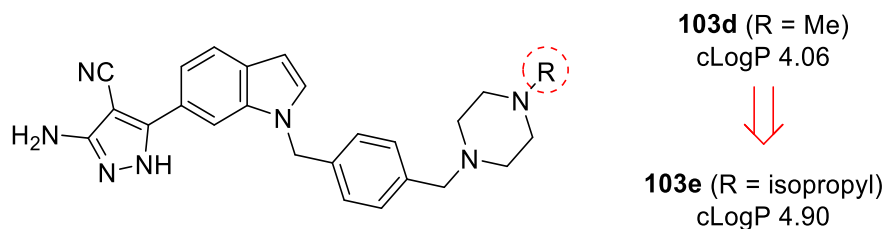
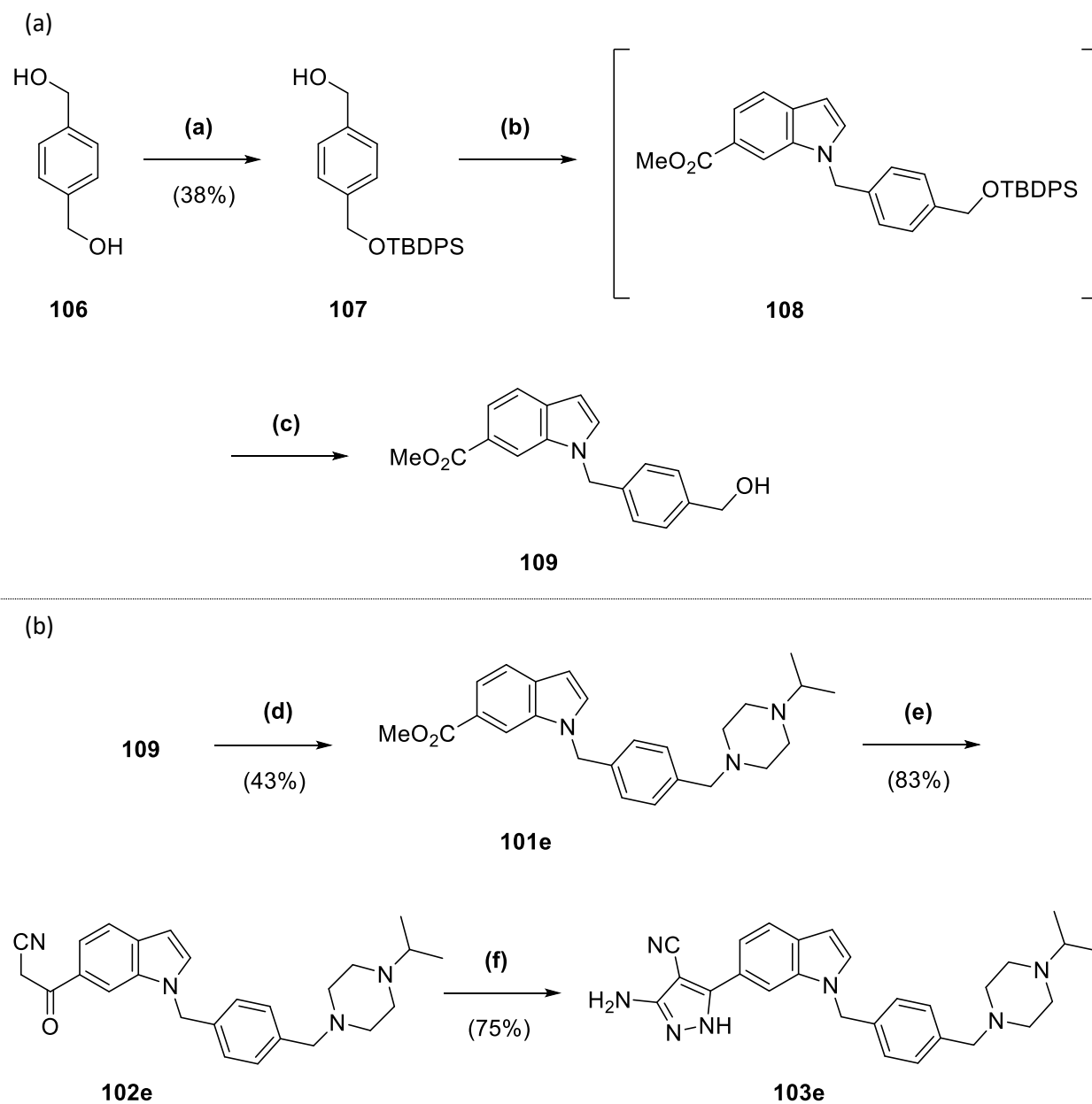


Figure 58: Idea for modification of **103d** with replacement of the *N*-methyl group.

The synthetic route used for compounds **103a-d** (Scheme 16 and Scheme 17b) required five steps for the synthesis of each analogue, excluding the synthesis of indoline **97**. With the *N*-isopropyl piperazinyl analogue **103e** there was a desire to reduce the synthetic burden, facilitating the rapid synthesis of analogues in future physicochemical studies. This was achieved through the synthesis of methyl ester **109**, which could then be used to produce 4-cyanopyrazole analogues with alternate heterocyclic rings attached in place of its alcohol in three steps. Methyl ester **109** was synthesised in three steps (Scheme 18a), beginning with the protection of one of the alcohols of 1,4-benzenedimethanol **106** with a TBDPS group to afford **107** (38% yield). The remaining alcohol of **107** was reacted initially with methanesulfonyl chloride, then with indole **63** and NaH. The silyl protecting group of the resultant product **108**, which was not purified, was removed following aqueous workup by the addition of TBAF (72% yield overall). The deprotected alcohol of methyl ester **109** was reacted initially with methanesulfonyl chloride as with **107**, then stirred with 1-isopropylpiperazine and Cs₂CO₃ in DMF to afford **101e** (43% yield overall) (Scheme 18b). Methyl ester **101e** was converted to the corresponding β -ketonitrile **102e** (83% yield), which was used to synthesise the 4-cyanopyrazole compound **103e** in the same manner as **71c** and **71f** (75% yield overall).

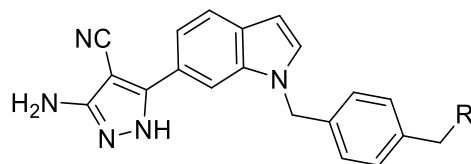


Reagents and Conditions: (a) TBDPSCI, imidazole, DMF, 21 h; (b) (i) MeSO₂Cl, NEt₃, DCM, 0 °C to rt, 1 h (ii) **63**, NaH, DMF, 0 °C to rt, 45 min; (c) TBAF (1 M in THF), 30 min; (d) (i) MeSO₂Cl, NEt₃, DCM, 0 °C to rt, 90 min (ii) 1-isopropylpiperazine, Cs₂CO₃, DMF, 12 h; (e) *n*-butyllithium (1.6 M in hexanes), acetonitrile, THF, -78 °C, 30 min; (f) (i) CCl₃CN, NaOAc, EtOH, 10 h (ii) N₂H₄·H₂O, EtOH, reflux, 7 h.

Scheme 18: Synthesis of (a) 109 in three steps from 106, and (b) 103e in three steps from 109.

Compound **103e** was sent to our collaborators as with previous compounds in the lead series for testing against both *Mab* and *Mtb* in liquid culture.¹²³ Whilst **103e** did not afford an improved MIC value against *Mab* in comparison to **103a** and **103d**, lower values were observed with *Mtb* across all media types (Table 12). Four-fold improvements in MIC were witnessed for **103e** in contrast to **103d** with *Mtb* in GAST-Fe and

7H9/DPPC media, whilst a greater than five-fold improvement was seen with *Mtb* in 7H9 media utilising glucose as a carbon source. Further, a four-fold improvement in comparison to **103d** was demonstrated with *Mtb* in 7H9 media supplemented with BSA, implying a reduction of plasma protein binding.



| Compound | R | <i>Mab</i> TrmD K_d (nM) | <i>Mab</i> MIC (μ M) | H37Rv <i>Mtb</i> MIC (μ M) | | | |
|-------------|---|-------------------------------|------------------------------|---------------------------------|-------------|-----------------|--------------|
| | | | | GAST- Fe | 7H9/ BSA | 7H9/ glucose | 7H9/ DPPC |
| 103a | | 27 \pm 4 | 50 | 50 | >100 | 25 | 12.5 |
| 103d | | 73 \pm 30 | 50 | 25 | 50 | 12.5 | 6.3 |
| 103e | | 100 \pm 24 | 50 | 6.3 | 12.5 | 2.3 | 1.6 |

Table 12: MIC values afforded by compound **103e** in contrast to **103a** and **103d** against *Mab*, performed by Dr Karen Brown, and H37Rv *Mtb*, performed by Dr. Daben Libardo.

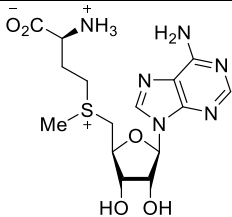
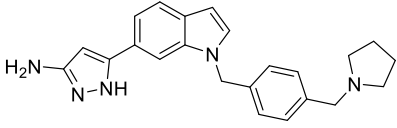
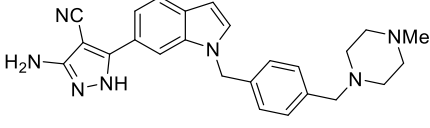
The activity of **103e** against *Mtb* across multiple media types encouraged the synthesis of further derivatives (Table 12), utilising the newly developed shorter synthetic route starting from methyl ester **109** (Scheme 18b). However, this was not possible due to time constraints.

3.3: Investigation of *Mycobacterium tuberculosis* tRNA (m^1G37) methyltransferase

In addition to the synthesis and screening of **103e**, following the screening of compounds **88a** and **103a-d** against *Mtb*, the evaluation of the applicability of the lead series to the *Mtb* TrmD homolog was sought. *Mab* and *Mtb* TrmD share 77% sequence identity overall and 86% similarity.

3.3.1: Protein Expression and Screening by Isothermal Titration Calorimetry

An *E. coli* colony on agar was kindly provided by the Gründling research group (MRC Centre for Molecular Bacteriology and Infection, Imperial College London).¹³⁶ This was grown and processed to afford the pET23b plasmid for *Mtb* TrmD. The isolated plasmid was used to transform *E. coli* BL21(DE3) strain, with the target protein expressed and purified to a yield of 5.0 mg L⁻¹. The *Mtb* TrmD was used to screen several compounds by ITC, including its substrate SAM (K_d 40 μ M, LE 0.22) whose binding affinity was equivalent to that determined for *Mab* TrmD (K_d 47 μ M, LE 0.22) by Dr Sherine Thomas (Table 13).

| Compound | <i>Mab</i> TrmD | | <i>Mtb</i> TrmD | |
|--|-------------------------|-----------------|------------------|-----------------|
| | K_d (μ M) | LE ^a | K_d (μ M) | LE ^a |
| SAM  | 40 \pm 2 ^b | 0.22 | 47 \pm 1 | 0.22 |
| 88a  | 0.49 \pm 0.21 | 0.31 | 0.90 \pm 0.10 | 0.29 |
| 103d  | 0.073 \pm 0.030 | 0.30 | 0.33 \pm 0.06 | 0.28 |

^a kcal mol⁻¹ HA⁻¹.

^b Measured by Dr Sherine Thomas.

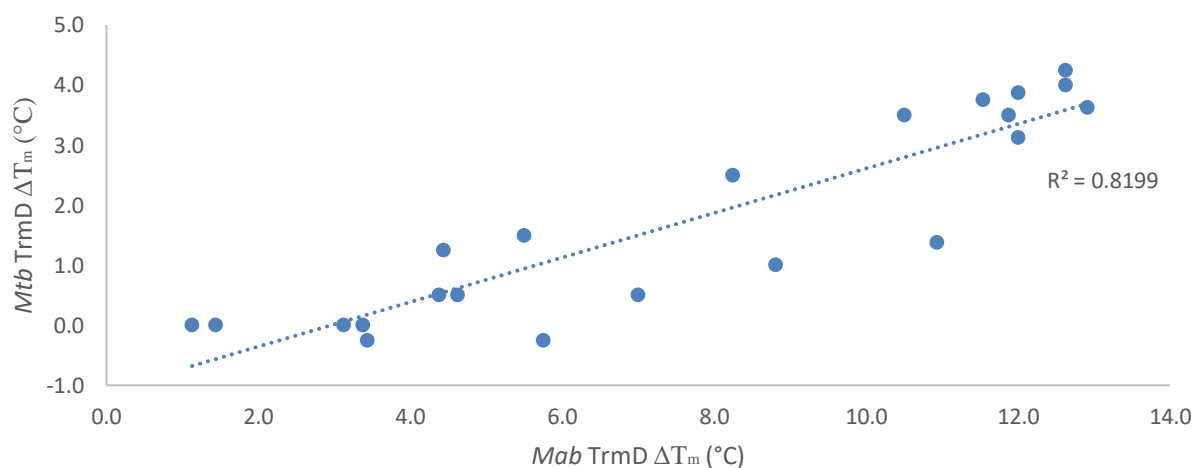
Table 13: The affinities (K_d) and efficiency metrics of SAM and compounds **88a** and **103d** with *Mab* and *Mtb* TrmD.

Based on a consideration of activity against *Mtb*, compounds **88a** (K_d 0.90 μ M, LE 0.29) and **103d** (K_d 0.33 μ M, LE 0.28) were selected for screening against *Mtb* TrmD by ITC (Table 13). The binding affinities afforded by these compounds against *Mtb* TrmD were of the same order of magnitude as the corresponding K_d values for *Mab* TrmD with less than a 2-fold difference for **88a**, demonstrating the broader applicability of the lead series.

3.3.2: Screening by Differential Scanning Fluorimetry

A larger selection of compounds from the lead series was also screened against *Mtb* TrmD by DSF. Under the same experimental conditions as used with *Mab* TrmD, an apo T_m of 57 °C was measured with ΔT_m values varying from -0.3 to +4.3 °C for compounds in the lead series (Figure 59).

| Compound | ΔT_m^a (°C) | | Compound | ΔT_m^a (°C) | |
|------------|---------------------|-----------------|-------------|---------------------|-----------------|
| | <i>Mab</i> TrmD | <i>Mtb</i> TrmD | | <i>Mab</i> TrmD | <i>Mtb</i> TrmD |
| 62 | +1.1 | 0.0 | 71j | +5.5 | +1.5 |
| 66a | +3.4 | 0.0 | 71n | +8.8 | +1.0 |
| 66b | +4.6 | +0.5 | 71o | +10.9 | +1.4 |
| 66c | +3.4 | -0.3 | 72g | +5.8 | -0.3 |
| 66d | +4.4 | +1.3 | 87 | +12.0 | +3.1 |
| 66e | +1.4 | 0.0 | 88a | +7.0 | +0.5 |
| 66f | +3.1 | 0.0 | 103a | +12.9 | +3.6 |
| 70 | +4.4 | +0.5 | 103b | +12.6 | +4.0 |
| 71f | +8.3 | +2.5 | 103c | +12.6 | +4.3 |
| 71g | +10.5 | +3.5 | 103d | +12.0 | +3.9 |
| 71h | +11.5 | +3.8 | 103e | +11.9 | +3.5 |



^a 100 μ M ligand and 10 μ M protein.

Figure 59: The melting temperatures (ΔT_m) of compounds in the 3-aminopyrazole lead series determined against both *Mab* and *Mtb* TrmD.

Whilst the range of ΔT_m values against *Mtb* TrmD was smaller than for *Mab* TrmD, attributed to differing thermodynamics of protein unfolding as demonstrated by its higher apo T_m in contrast to *Mab* TrmD (40.5 - 42.5 °C) under the screened conditions,⁸⁸ the results broadly correlated (Figure 59). Analogues of **103d** with comparable ΔT_m values (>10 °C) against *Mab* TrmD, associated with submicromolar K_d values, generally afforded the highest ΔT_m values against *Mtb* TrmD (>3 °C).

3.4: Summary and Future Work

The screening of a fragment library provided a number of fragment hits with associated ΔT_m values and structural information for elaboration.⁵⁰ Whilst the application of a structure-guided fragment-growth strategy to a highly ligand-efficient starting point did not afford the desired gains in binding affinity,¹²³ a fragment-merging strategy based on fragment hits with overlapping binding modes resulted in the development of a lead series based on the 3-aminopyrazole-indole scaffold of **62** (K_d 110 μ M, LE 0.36) that proved amenable to elaboration. The optimisation of the phenyl ring of a *p*-methoxybenzyl-protected synthetic intermediate **66a** led to a 10-fold improvement in binding affinity in **66f** (K_d 12 μ M, LE 0.30), with the addition of a nitrile group to a position on the pyrazole ring facing a narrow pocket affording a further 25-fold improvement in **71f** (K_d 0.50 μ M, LE 0.36). Further gains were realised in the exploration of isomers and structurally-related analogues, with **71h** (K_d 0.12 μ M, LE 0.39) possessing a ligand efficiency higher than the original 3-aminopyrazole fragment hit **53** (K_d 170 μ M, LE 0.37). Due to poorer aqueous solubility that precluded the screening of a number of analogues by ITC, moieties with greater sp^3 content were incorporated into the lead series that, in combination with a consideration of findings from a prior study on the homolog to *Mab* TrmD in *H. influenzae*,⁶³ enabled the design of a low-nanomolar binding affinity compound **103a** (K_d 27 nM, LE 0.34). Whilst **103a** and its analogs did not perform as desired against *Mab* *in vitro*, promising results were found against *Mtb* that were improved in the more lipophilic derivative **103e**, which afforded low-micromolar activity against *Mtb* across different media types and carbon sources (MIC 1.6 – 12.5 μ M).

In light of these results, the homolog to *Mab* TrmD in *Mtb* was expressed and screened against the lead series to afford positive results illustrating the wider applicability of the compounds beyond the initial target of interest. This encourages further screening and development of the lead series. In a similar manner to **103e**, the design and synthesis of further analogues would be based on a consideration of physicochemical properties and activity against mycobacteria, in addition to binding affinity for TrmD. The determination of the underlying causes behind the lack of correlation between binding affinity and activity

against *Mab in vitro* is important, and experiments are currently ongoing by collaborators focused on an analysis of target engagement, compound retention in the organism and the susceptibility of *Mab* TrmD as a target to inhibition.

4: Experimental Methods

4.1: Synthetic Chemistry

4.1.1: General Chemistry

All reactions were carried out in oven-dried glassware under a positive pressure of dry nitrogen atmosphere. Temperatures of 0 and -78 °C were obtained by submerging the reaction vessel in a bath containing either ice or a mixture of solid CO₂ pellets and acetone respectively. The solvents DCM, EtOAc, acetonitrile, methanol, PET and toluene were distilled over CaH₂ under a dry nitrogen atmosphere prior to use, with THF distilled over a mixture of CaH₂, LiAlH₄ and triphenylphosphine. DMF was purchased as anhydrous from commercial suppliers, with ethanol and acetic acid obtained in the absolute and glacial forms respectively. All purchased chemicals were used as received. Solutions of Na₂CO₃, NaHCO₃, NaCl (brine) and NH₄Cl were aqueous and saturated. Solutions of LiCl were aqueous and 5% w/v.

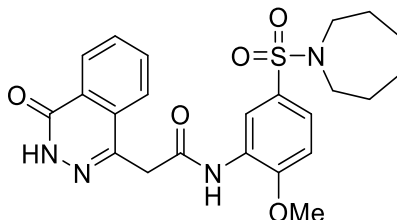
Flash chromatography was performed using automated Biotage® Isolera™ Spektra purification systems with appropriately sized Biotage® SNAP cartridges, containing either KP 50 µm silica (default) or HP-sphere 25 µm C18 silica ('reverse phase'). Analytical thin layer chromatography (TLC) was performed using Merck glass-backed silica plates, with visualization by 254 or 365 nm ultraviolet light.

Liquid chromatography mass spectrometry (LCMS) was carried out using a Waters® Acquity UPLC® H-Class system, with samples run on a solvent gradient from 0 to 95% acetonitrile in water (+ 0.1% formic acid) over 4 minutes. Peaks corresponding to desired product are described, including the retention time (rt) and % purity by integration. High resolution mass spectrometry (HRMS) was mainly performed using ThermoFinnigan Orbitrap Classic, Waters® LCT Premier™ or Waters® Vion™ IMS QToF systems. A Perkin-Elmer® Spectrum One FT-IR spectrometer fitted with a universal attenuated total reflectance accessory was used to record infrared spectra, with wavelengths of maximum absorbance (ν_{\max}) quoted in wavenumbers (cm⁻¹) for signals outside of the fingerprint region (br = broad). Only peaks corresponding to key functional groups were characterized. Nuclear magnetic resonance (NMR) spectra were recorded in the indicated deuterated solvents with Avance™ III HD (400 MHz), QNP Cryoprobe (400 MHz) or DCH Cryoprobe (500 MHz) Bruker spectrometers. ¹H NMR data are presented in the following order: chemical shift (in ppm on a δ scale relative to the residual solvent resonance peak), integration, multiplicity (s = singlet, d = doublet, t = triplet, q = quartet, quin = quintet, sep = septet, m = multiplet) and coupling constant (J, in Hz). ¹³C NMR spectra were proton-decoupled, with chemical shifts recorded and further description provided for certain peaks (br = broad).

A combination of TLC and LCMS analysis was used to monitor reactions. All tested compounds possessed a purity of at least 95% as determined by LCMS analysis.

4.1.2: Methods and Characterisation Data for Screened Compounds

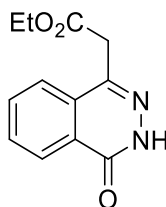
N-(5-(Azepan-1-ylsulfonyl)-2-methoxyphenyl)-2-(4-oxo-3,4-dihydrophthalazin-1-yl)acetamide (**2**)



T3P® (50 wt. % in DMF, 1.3 mL, 2.2 mmol) and DIPEA (0.64 mL, 3.7 mmol) were added to a solution of 2-(4-oxo-3,4-dihydrophthalazin-1-yl)acetic acid **16** (0.150 g, 0.735 mmol) and 5-(azepan-1-ylsulfonyl)-2-methoxyaniline **20** (0.209 g, 0.735 mmol) in DMF (2 mL). The reaction mixture was heated to 70 °C over 1 hour. The reaction mixture was diluted with water (15 mL), adjusted to pH 1 and extracted into EtOAc (3 x 20 mL). The combined organic extracts were dried (MgSO₄) and concentrated in vacuo. Purification by flash chromatography (0 – 20% methanol in DCM) afforded **2** (0.206 g, 60% yield).

LCMS (ESI+): m/z 471.3 [M + H]⁺, (ESI-): m/z 469.1 [M - H]⁻, rt 1.92 minutes, >99%; ¹H NMR (400 MHz, (CD₃)₂SO) 12.62 (1H, s), 9.86 (1H, s), 8.45 (1H, d, J = 2.1 Hz), 8.27 (1H, d, J = 7.9 Hz), 7.99-7.91 (2H, m), 7.90-7.82 (1H, m), 7.49 (1H, dd, J = 8.5, 2.2 Hz), 7.24 (1H, d, J = 8.8 Hz), 4.21 (2H, s), 3.96 (3H, s), 3.12 (4H, t, J = 5.9 Hz), 1.64-1.51 (4H, m), 1.50-1.39 (4H, m); ¹³C NMR (125 MHz, (CD₃)₂SO) 168.4, 159.5, 152.0, 142.1, 133.5, 131.6, 130.4, 129.8, 127.7, 127.6, 125.9, 125.5, 123.4, 119.1, 111.2, 56.3, 47.6, 28.5, 26.3 (1 peak missing); spectroscopic data consistent with literature.⁴¹

Ethyl 2-(4-oxo-3,4-dihydrophthalazin-1-yl)acetate (**15**)^{41, 137}

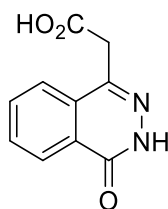


Hydrazine monohydrate (0.47 mL, 9.0 mmol) was added dropwise to a solution of ethyl (E)-2-(3-oxoisobenzofuran-1(3H)-ylidene)acetate **14** (1.97 g, 9.03 mmol) in ethanol (10 mL). The reaction mixture

was stirred at 50 °C over 2 hours. The reaction mixture was cooled to rt and left to stand for 12 hours. The resulting precipitate was obtained by vacuum filtration and washed with ethanol (10 mL) to afford **15** (2.21 g, 99% yield).

LCMS (ESI+): m/z 233.2 [M + H]⁺, rt 1.53 minutes, >99%; ¹H NMR (400 MHz, (CD₃)₂SO) 12.63 (1H, s), 8.30-8.24 (1H, m), 7.98-7.91 (1H, m), 7.90-7.83 (2H, m), 4.11 (2H, q, J = 7.1 Hz), 4.05 (2H, s), 1.17 (3H, t, J = 7.1 Hz); ¹³C NMR (100 MHz, (CD₃)₂SO) 169.8, 159.4, 140.9, 133.6, 131.7, 129.4, 127.5, 125.9, 125.5, 60.7, 37.9, 14.0; ¹H NMR spectroscopic data consistent with literature.¹³⁷

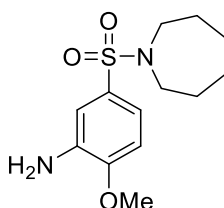
2-(4-Oxo-3,4-dihydrophthalazin-1-yl)acetic acid (**16**)⁴¹



Ethyl 2-(4-oxo-3,4-dihydrophthalazin-1-yl)acetate **15** (0.260 g, 1.12 mmol) was dissolved in a mixture of aqueous NaOH (10% w/v, 10 mL) and THF (10 mL). The reaction mixture was heated under reflux for 1 hour. The reaction mixture was adjusted to pH 1 by the addition of aqueous HCl (2 M) at 0 °C, then extracted into diethyl ether (3 x 100 mL). The combined organic extracts were washed (brine), dried (MgSO₄) and concentrated *in vacuo*. Purification by flash chromatography (0 – 10% methanol in DCM) afforded **16** (0.101 g, 44% yield).

¹H NMR (400 MHz, (CD₃)₂SO) 12.61 (1H, s), 8.26 (1H, d, J = 7.7 Hz), 7.94 (1H, ddd, J = 8.3, 6.9, 1.4 Hz), 7.90-7.82 (2H, m), 3.95 (2H, s); ¹³C NMR (100 MHz, (CD₃)₂SO) 171.4, 159.5, 141.5, 133.5, 131.6, 129.6, 127.5, 125.9, 125.6, 38.2; ¹H NMR spectroscopic data consistent with literature.¹³⁷

5-(Azepan-1-ylsulfonyl)-2-methoxyaniline (**20**)⁴¹

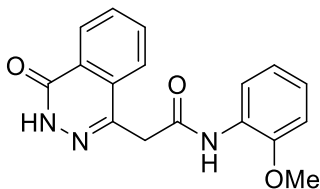


Hexamethyleneimine (0.212 mL, 1.89 mmol) was added dropwise at 0 °C to a suspension of NaH (60% in mineral oil, 0.189 g, 4.72 mmol) in DMF (2 mL). The reaction mixture was stirred at 0 °C over 30 minutes.

A solution of 4-methoxy-3-(2,2,2-trifluoroacetamido)benzenesulfonyl chloride **19** (0.500 g, 1.57 mmol) in DMF (3 mL) was added dropwise at 0 °C to the reaction mixture. The reaction mixture was warmed to rt and stirred over 3 hours. Ethanol (10 mL) was added dropwise at 0 °C to the reaction mixture, followed by water (10 mL) and aqueous HCl (37.5% w/v, 10 mL). The reaction mixture was heated under reflux for 20 hours. The reaction mixture was concentrated *in vacuo* to remove ethanol, then adjusted to pH 9 by the dropwise addition of aqueous NaOH (10% w/v). The mixture was diluted with EtOAc (50 mL), and the resultant aqueous layer discarded. The organic layer was washed with water (3 x 50 mL) and brine (50 mL), dried (MgSO₄) and concentrated *in vacuo*. Purification by flash chromatography (20 – 50% EtOAc in PET) afforded **20** (0.373 g, 83% yield).

LCMS (ESI+): m/z 285.2 [M + H]⁺, rt 1.85 minutes, >99%; ¹H NMR (400 MHz, CDCl₃) 7.17 (1H, dd, J = 8.4, 2.3 Hz), 7.09 (1H, d, J = 2.2 Hz), 6.81 (1H, d, J = 8.4 Hz), 3.98 (2H, br s), 3.90 (3H, s), 3.23 (4H, t, J = 5.9 Hz), 1.75-1.64 (4H, m), 1.62-1.53 (4H, m); ¹³C NMR (100 MHz, CDCl₃) 150.1, 136.7, 131.6, 118.1, 112.7, 109.7, 55.8, 48.3, 29.3, 27.1; ν_{max}/cm⁻¹ 3484 (N-H), 3379 (N-H), 2932, 2849, 1610, 1577, 1513; HRMS (ESI)+: m/z calculated for [C₁₃H₂₀N₂O₃S + K]⁺ = 323.0826, observed 323.0835.

N-(2-Methoxyphenyl)-2-(4-oxo-3,4-dihydrophthalazin-1-yl)acetamide (**21**)

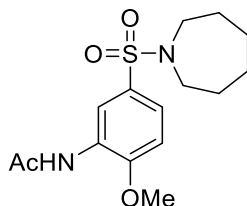


T3P® (50 wt. % in DMF, 0.35 mL, 0.59 mmol) and DIPEA (0.10 mL, 0.59 mmol) were added to a solution of 2-(4-oxo-3,4-dihydrophthalazin-1-yl)acetic acid **16** (40 mg, 0.20 mmol) and *o*-anisidine **17** (33 μL, 0.29 mmol) in DMF (1 mL). The reaction mixture was heated to 40 °C over 2 hours. The reaction mixture was diluted with water (15 mL) and extracted into DCM (3 x 20 mL). The combined organic extracts were dried (MgSO₄) and concentrated *in vacuo*. The residue was dissolved in toluene (10 mL) and concentrated *in vacuo*. Purification by flash chromatography (50 – 100% EtOAc in PET, 0 – 20% methanol in DCM) afforded **21** (50 mg, 82% yield).

LCMS (ESI+): m/z 332.1 [M + Na]⁺, rt 1.64 minutes, >99%; ¹H NMR (500 MHz, (CD₃)₂SO) 12.61 (1H, s), 9.56 (1H, s), 8.27 (1H, d, J = 7.9 Hz), 8.01-7.79 (4H, m), 7.11-7.00 (2H, m), 6.92-6.83 (1H, m), 4.16 (2H, s), 3.86 (3H, s); ¹³C NMR (125 MHz, (CD₃)₂SO) 167.6, 159.5, 149.6, 142.3, 133.5, 131.5, 129.8, 127.6, 127.2, 125.8,

125.6, 124.6, 121.8, 120.2, 111.2, 55.7 (1 peak missing); $\nu_{\max}/\text{cm}^{-1}$ 2905, 1665 (C=O), 1646, 1597, 1539; HRMS (ESI)+: m/z calculated for $[\text{C}_{17}\text{H}_{15}\text{N}_3\text{O}_3 + \text{H}]^+ = 310.1186$, observed 310.1175.

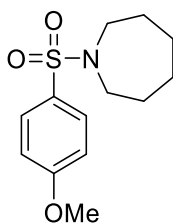
N-(5-(Azepan-1-ylsulfonyl)-2-methoxyphenyl)acetamide (**22**)



Acetic anhydride (10 μL , 0.11 mmol) was added to a solution of 5-(azepan-1-ylsulfonyl)-2-methoxyaniline **20** (15 mg, 0.053 mmol) and pyridine (8.5 μL , 0.11 mmol) in DCM (2 mL). The reaction mixture was stirred over 90 minutes. The reaction mixture was diluted with water (10 mL) and extracted into DCM (3 x 15 mL). The combined organic extracts were dried (MgSO_4) and concentrated *in vacuo*. Purification by flash chromatography (50 – 80% EtOAc in PET) afforded **22** (14 mg, 79% yield).

LCMS (ESI+): m/z 327.3 $[\text{M} + \text{H}]^+$, (ESI-): m/z 325.2 $[\text{M} - \text{H}]^-$; rt 1.90 minutes, 96%; ^1H NMR (400 MHz, CDCl_3) 8.78 (1H, d, $J = 1.8$ Hz), 7.76 (1H, br s), 7.53 (1H, dd, $J = 8.5, 2.3$ Hz), 6.91 (1H, d, $J = 8.6$ Hz), 3.94 (3H, s), 3.30 (4H, t, $J = 6.0$ Hz), 2.22 (3H, s), 1.80-1.67 (4H, m), 1.65-1.53 (4H, m); ^{13}C NMR (125 MHz, CDCl_3) 168.4, 150.4, 132.1, 128.2, 123.5, 118.0, 109.5, 56.2, 48.5, 29.3, 27.1, 25.0; $\nu_{\max}/\text{cm}^{-1}$ 3349, 2930, 2855, 1673 (C=O), 1592, 1518; HRMS (ESI)+: m/z calculated for $[\text{C}_{15}\text{H}_{22}\text{N}_2\text{O}_4\text{S} + \text{H}]^+ = 327.1373$, observed 327.1375.

1-((4-Methoxyphenyl)sulfonyl)azepane (**23**)

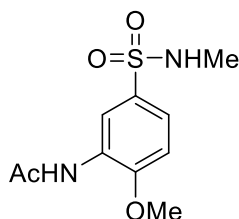


Hexamethyleneimine (0.141 mL, 1.26 mmol) was added dropwise at 0 $^\circ\text{C}$ to a suspension of NaH (60% in mineral oil, 0.137 g, 3.43 mmol) in DMF (1 mL). The reaction mixture was stirred at 0 $^\circ\text{C}$ over 20 minutes. A solution of 4-methoxybenzenesulfonyl chloride **29** (0.236 g, 1.14 mmol) in DMF (2 mL) was added dropwise at 0 $^\circ\text{C}$ to the reaction mixture. The reaction mixture was warmed to rt and stirred over 1 hour. Water (15 mL) was added dropwise at 0 $^\circ\text{C}$ to the reaction mixture. The product was extracted into DCM (3 x 20 mL). The combined organic extracts were washed (brine), dried (MgSO_4) and concentrated *in*

vacuo. The residue was dissolved in toluene (5 mL) and concentrated *in vacuo*. Purification by flash chromatography (0 – 35% EtOAc in PET) afforded **23** (0.243 g, 79% yield).

LCMS (ESI+): m/z 270.2 $[M + H]^+$, rt 2.15 minutes, >99%; 1H NMR (400 MHz, $CDCl_3$) 7.75-7.70 (2H, m), 6.99-6.93 (2H, m), 3.86 (3H, s), 3.25 (4H, t, $J = 5.9$ Hz), 1.75-1.66 (4H, m), 1.62-1.53 (4H, m); ^{13}C NMR (100 MHz, $CDCl_3$) 162.6, 131.5, 129.1, 114.2, 55.7, 48.3, 29.2, 27.1; ν_{max}/cm^{-1} 2929, 2848, 1595, 1579, 1501; HRMS (ESI)+: m/z calculated for $[C_{13}H_{19}NO_3S + H]^+ = 270.1158$, observed 270.1153.

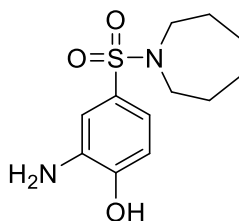
N-(2-Methoxy-5-(*N*-methylsulfonyl)phenyl)acetamide (**24**)



Acetic anhydride (18 μ L, 0.19 mmol) was added to a solution of 3-amino-4-methoxy-*N*-methylbenzenesulfonamide **33a** (42 mg, 0.19 mmol) and pyridine (16 μ L, 0.19 mmol) in DCM (2 mL). The reaction mixture was stirred over 2 days. The reaction mixture was diluted with water (15 mL) and extracted into DCM (3 x 20 mL). The combined organic extracts were dried ($MgSO_4$) and concentrated *in vacuo*. Purification by flash chromatography (50 – 100% EtOAc in PET) afforded **24** (28 mg, 56% yield).

LCMS (ESI+): m/z 259.2 $[M + H]^+$, (ESI-): m/z 257.2 $[M - H]^-$, rt 1.31 minutes, >99%; 1H NMR (400 MHz, CD_3CN) 8.74 (1H, d, $J = 2.0$ Hz), 8.30 (1H, br s), 7.51 (1H, dd, $J = 8.5, 2.2$ Hz), 7.10 (1H, d, $J = 8.6$ Hz), 5.43-5.27 (1H, m), 3.94 (3H, s), 2.47 (3H, d, $J = 5.3$ Hz), 2.14 (3H, s); ^{13}C NMR (100 MHz, CD_3CN) 170.0, 152.2, 131.6, 129.5, 124.0, 118.7, 111.2, 56.9, 29.5, 24.7; ν_{max}/cm^{-1} 3422 (N-H), 3168, 1672 (C=O), 1594, 1530; HRMS (ESI)+: m/z calculated for $[C_{10}H_{14}N_2O_4S + Na]^+ = 281.0566$, observed 281.0569.

2-Amino-4-(azepan-1-ylsulfonyl)phenol (**25**)

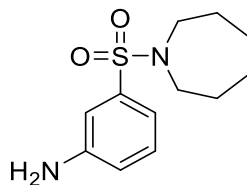


$NaBH_4$ (28 mg, 0.75 mmol) was added portionwise at 0 $^{\circ}C$ to a suspension of $NiCl_2 \cdot 6H_2O$ (59 mg, 0.25 mmol) in methanol (2 mL). The reaction mixture was warmed to rt and stirred over 20 minutes. A solution

of 4-(azepan-1-ylsulfonyl)-2-nitrophenol **32** (0.170 g, 0.498 mmol) in methanol (2 mL) was added at 0 °C to the reaction mixture, followed by further NaBH₄ (94 mg, 2.5 mmol). The reaction mixture was warmed to rt and stirred over 2 hours. Water (15 mL) was added at 0 °C and the reaction mixture filtered through celite. The product was extracted into DCM (3 x 25 mL). The combined organic extracts were washed (brine), dried (MgSO₄) and concentrated *in vacuo*. Purification by flash chromatography (20 – 50% EtOAc in PET) afforded **25** (83 mg, 62% yield).

LCMS (ESI+): m/z 271.2 [M + H]⁺, (ESI-): m/z 269.2 [M - H]⁻, rt 1.71 minutes, >99%; ¹H NMR (400 MHz, CD₃CN) 7.45 (1H, br s), 7.04 (1H, d, J = 2.3 Hz), 6.94 (1H, dd, J = 8.2, 2.2 Hz), 6.80 (1H, d, J = 8.3 Hz), 4.26 (2H, br s), 3.18 (4H, t, J = 5.9 Hz), 1.74-1.60 (4H, m), 1.59-1.50 (4H, m); ¹³C NMR (100 MHz, CD₃CN) 148.0, 137.6, 131.9, 117.8, 114.8, 113.6, 48.9, 29.8, 27.6; ν_{max}/cm⁻¹ 3397, 3350, 3320, 3285, 2927, 2855, 1593, 1510; HRMS (ESI-): m/z calculated for [C₁₂H₁₈N₂O₃S - H]⁻ = 269.0965, observed 269.0965.

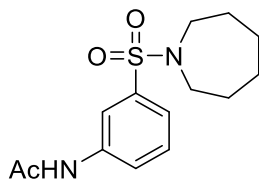
3-(Azepan-1-ylsulfonyl)aniline (**26**)



NaBH₄ (51 mg, 1.4 mmol) was added portionwise at 0 °C to a suspension of NiCl₂ (59 mg, 0.45 mmol) in methanol (2 mL). The reaction mixture was warmed to rt and stirred over 30 minutes. 1-((3-Nitrophenyl)sulfonyl)azepane **35** (0.257 g, 0.904 mmol) was added at 0 °C to the reaction mixture, followed by further methanol (4 mL) and NaBH₄ (0.171 g, 4.52 mmol). The reaction mixture was warmed to rt and stirred over 45 minutes. Water (10 mL) was added at 0 °C and the mixture filtered through celite, eluted with methanol (10 mL) and water (15 mL). The filtrate was concentrated *in vacuo* to remove methanol, then extracted into EtOAc (3 x 25 mL). The combined organic extracts were washed (brine), dried (MgSO₄) and concentrated *in vacuo*. Purification by flash chromatography (20 – 50% EtOAc in PET) afforded **26** (0.188 g, 82% yield).

LCMS (ESI+): m/z 255.2 [M + H]⁺, rt 1.77 minutes, >99%; ¹H NMR (400 MHz, CDCl₃) 7.24 (1H, t, J = 7.8 Hz), 7.15-7.10 (1H, m), 7.08 (1H, t, J = 2.0 Hz), 6.81 (1H, ddd, J = 7.9, 2.3, 0.7 Hz), 3.89 (2H, br s), 3.26 (4H, t, J = 5.9 Hz), 1.77-1.65 (4H, m), 1.63-1.54 (4H, m); ¹³C NMR (100 MHz, CDCl₃) 147.2, 140.4, 130.0, 118.6, 116.7, 113.0, 48.4, 29.3, 27.0; ν_{max}/cm⁻¹ 3391 (N-H), 3326 (N-H), 2928, 2851, 1639, 1596; HRMS (ESI+): m/z calculated for [C₁₂H₁₈N₂O₂S + H]⁺ = 255.1162, observed 255.1166.

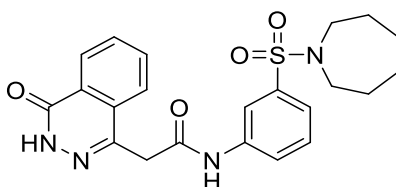
N-(3-(Azepan-1-ylsulfonyl)phenyl)acetamide (**27**)



Acetic anhydride (11 μ L, 0.12 mmol) was added to a solution of 3-(azepan-1-ylsulfonyl)aniline **26** (15 mg, 0.059 mmol) and pyridine (10 μ L, 0.12 mmol) in DCM (2 mL). The reaction mixture was stirred over 5 hours. The reaction mixture was diluted with water (10 mL) and extracted into DCM (3 x 15 mL). The combined organic extracts were dried (MgSO_4) and concentrated *in vacuo*. Purification by flash chromatography (35 – 70% EtOAc in PET) afforded **27** (15 mg, 86% yield).

LCMS (ESI+): m/z 297.2 [$\text{M} + \text{H}$]⁺, (ESI-): m/z 295.2 [$\text{M} - \text{H}$]⁻, *rt* 1.87 minutes, >99%; ¹H NMR (500 MHz, CDCl_3) 7.98 (1H, d, $J = 7.9$ Hz), 7.91 (1H, br s), 7.83-7.78 (1H, m), 7.52-7.47 (1H, m), 7.45 (1H, t, $J = 7.9$ Hz), 3.27 (4H, t, $J = 6.0$ Hz), 2.21 (3H, s), 1.76-1.66 (4H, m), 1.65-1.53 (4H, m); ¹³C NMR (125 MHz, CDCl_3) 169.0, 139.9, 139.1, 130.0, 123.7, 122.2, 117.9, 48.5, 29.3, 27.0, 24.7; $\nu_{\text{max}}/\text{cm}^{-1}$ 3305, 3257, 3192, 3117, 2929, 2851, 1670 (C=O), 1592, 1545; HRMS (ESI+): m/z calculated for [$\text{C}_{14}\text{H}_{20}\text{N}_2\text{O}_3\text{S} + \text{H}$]⁺ = 297.1267, observed 297.1268.

N-(3-(Azepan-1-ylsulfonyl)phenyl)-2-(4-oxo-3,4-dihydrophthalazin-1-yl)acetamide (**39**)

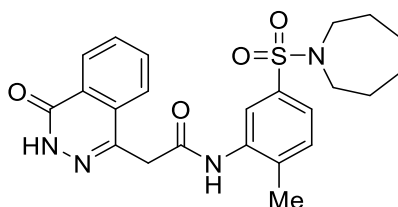


T3P[®] (50 wt. % in EtOAc, 0.35 mL, 0.59 mmol) and DIPEA (0.17 mL, 0.98 mmol) were added to a solution of 2-(4-oxo-3,4-dihydrophthalazin-1-yl)acetic acid **16** (47 mg, 0.20 mmol) and 3-(azepan-1-ylsulfonyl)aniline **26** (50 mg, 0.20 mmol) in DMF (2 mL). The reaction mixture was heated to 70 °C over 2 hours. The reaction mixture was diluted with EtOAc (25 mL), washed with water (3 x 25 mL) and brine (25 mL), dried (MgSO_4) and concentrated *in vacuo*. Purification by flash chromatography (50 – 90% EtOAc in PET) afforded **39** (40 mg, 45% yield).

LCMS (ESI+): m/z 441.3 [$\text{M} + \text{H}$]⁺, (ESI-): m/z 439.2 [$\text{M} - \text{H}$]⁻, *rt* 1.82 minutes, 98%; ¹H NMR (500 MHz, $(\text{CD}_3)_2\text{SO}$) 12.63 (1H, s), 10.67 (1H, s), 8.30-8.25 (1H, m), 8.13 (1H, t, $J = 1.8$ Hz), 7.98-7.92 (2H, m), 7.86 (1H, ddd, $J = 8.1, 5.7, 2.4$ Hz), 7.78 (1H, dq, $J = 8.2, 1.0$ Hz), 7.54 (1H, t, $J = 8.0$ Hz), 7.44 (1H, dq, $J = 7.8, 0.9$

Hz), 4.10 (2H, s), 3.18 (4H, t, J = 5.9 Hz), 1.66-1.56 (4H, m), 1.53-1.44 (4H, m); ^{13}C NMR (125 MHz, $(\text{CD}_3)_2\text{SO}$) 168.1, 159.5, 141.8, 139.7, 139.5, 133.6, 131.6, 130.0, 129.8, 127.6, 125.8, 125.6, 122.6, 121.2, 116.7, 47.7, 28.5, 26.3 (1 peak missing); $\nu_{\text{max}}/\text{cm}^{-1}$ 2929, 2852, 1644 (C=O), 1591, 1541; HRMS (ESI)+: m/z calculated for $[\text{C}_{22}\text{H}_{24}\text{N}_4\text{O}_4\text{S} + \text{H}]^+ = 441.1591$, observed 441.1613.

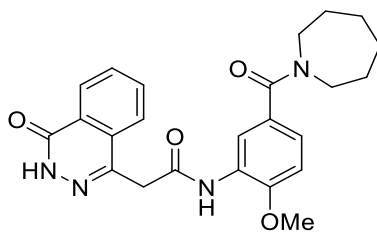
N-(5-(Azepan-1-ylsulfonyl)-2-methylphenyl)-2-(4-oxo-3,4-dihydrophthalazin-1-yl)acetamide (**40**)



T3P® (50 wt. % in EtOAc, 0.33 mL, 0.56 mmol) and DIPEA (0.16 mL, 0.93 mmol) were added to a solution of 2-(4-oxo-3,4-dihydrophthalazin-1-yl)acetic acid **16** (44 mg, 0.19 mmol) and 5-(azepan-1-ylsulfonyl)-2-methylaniline **38** (50 mg, 0.19 mmol) in DMF (2 mL). The reaction mixture was heated to 70 °C over 2 hours. The reaction mixture was diluted with EtOAc (25 mL), washed with water (3 x 25 mL) and brine (25 mL), dried (MgSO_4) and concentrated *in vacuo*. Purification by flash chromatography (50 – 90% EtOAc in PET, 0 – 5% methanol in DCM) afforded **40** (42 mg, 50% yield).

LCMS (ESI+): m/z 455.3 $[\text{M} + \text{H}]^+$, (ESI-): m/z 453.2 $[\text{M} - \text{H}]^-$, rt 1.82 minutes, >99%; ^1H NMR (500 MHz, $(\text{CD}_3)_2\text{SO}$) 12.64 (1H, s), 9.84 (1H, s), 8.28 (1H, d, J = 7.7 Hz), 8.02-7.92 (3H, m), 7.87 (1H, ddd, J = 8.0, 6.7, 1.5 Hz), 7.49-7.41 (2H, m), 4.15 (2H, s), 3.14 (4H, t, J = 6.0 Hz), 2.33 (3H, s), 1.65-1.53 (4H, m), 1.51-1.42 (4H, m); ^{13}C NMR (125 MHz, $(\text{CD}_3)_2\text{SO}$) 168.0, 159.5, 142.0, 136.8, 136.5, 135.8, 133.5, 131.6, 131.3, 129.8, 127.6, 125.9, 125.5, 122.8, 122.1, 47.7, 28.5, 26.3, 18.0 (1 peak missing); $\nu_{\text{max}}/\text{cm}^{-1}$ 3177, 3045, 2915, 2853, 1651 (C=O), 1612, 1600, 1582, 1553; HRMS (ESI)+: m/z calculated for $[\text{C}_{23}\text{H}_{26}\text{N}_4\text{O}_4\text{S} + \text{H}]^+ = 455.1748$, observed 455.1769.

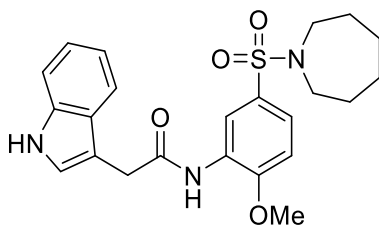
N-(5-(Azepane-1-carbonyl)-2-methoxyphenyl)-2-(4-oxo-3,4-dihydrophthalazin-1-yl)acetamide (**45**)



T3P® (50 wt. % in EtOAc, 0.12 mL, 0.20 mmol) and DIPEA (58 µL, 0.33 mmol) were added to a solution of 2-(4-oxo-3,4-dihydrophthalazin-1-yl)acetic acid **16** (14 mg, 0.067 mmol) and (3-amino-4-methoxyphenyl)(azepan-1-yl)methanone **44** (17 mg, 0.067 mmol) in DMF (1 mL). The reaction mixture was heated to 70 °C over 2 hours. The reaction mixture was diluted with EtOAc (25 mL), washed with water (3 x 10 mL) and brine (25 mL), dried (MgSO₄) and concentrated *in vacuo*. Purification by flash chromatography (50 – 100% EtOAc in PET, 0 – 10% methanol in DCM) afforded **45** (13 mg, 45% yield).

LCMS (ESI+): m/z 435.3 [M + H]⁺, (ESI-): m/z 433.3 [M - H]⁻, rt 1.68 minutes, >99%; ¹H NMR (400 MHz, (CD₃)₂CO) 11.69 (1H, br s), 9.01 (1H, br s), 8.39-8.32 (2H, m), 8.04 (1H, d, J = 8.1 Hz), 7.94 (1H, td, J = 7.7, 1.5 Hz), 7.89-7.82 (1H, m), 7.09 (1H, dd, J = 8.4, 2.0 Hz), 7.04 (1H, d, J = 8.4 Hz), 4.21 (2H, s), 3.91 (3H, s), 3.56 (2H, br s), 3.40 (2H, br s), 1.81-1.47 (8H, m); ¹³C NMR (125 MHz, (CD₃)₂SO) 169.9, 167.9, 159.5, 149.7, 142.2, 133.5, 131.5, 129.8, 129.1, 127.6, 126.8, 125.8, 125.5, 122.9, 119.9, 110.8, 55.9, 49.2, 45.5, 28.9, 27.2, 26.8, 25.8 (1 peak missing); ν_{max}/cm⁻¹ 3191, 2929, 2856, 1674, 1648, 1618, 1548; HRMS (ESI)+: m/z calculated for [C₂₄H₂₆N₄O₄ + H]⁺ = 435.2027, observed 435.2025.

N-(5-(Azepan-1-ylsulfonyl)-2-methoxyphenyl)-2-(1H-indol-3-yl)acetamide (**46a**)

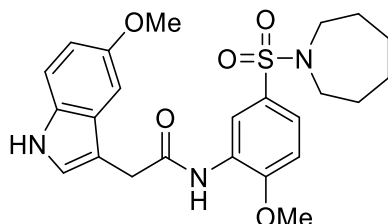


T3P® (50 wt. % in EtOAc, 0.15 mL, 0.26 mmol) and DIPEA (75 µL, 0.43 mmol) were added to a solution of 3-indoleacetic acid (15 mg, 0.086 mmol) and 5-(azepan-1-ylsulfonyl)-2-methoxyaniline **20** (24 mg, 0.086 mmol) in DMF (1 mL). The reaction mixture was heated to 70 °C over 4 hours. The reaction mixture was diluted with EtOAc (25 mL), washed with water (3 x 10 mL) and brine (25 mL), dried (MgSO₄) and concentrated *in vacuo*. Purification by flash chromatography (40 – 80% EtOAc in PET) afforded **46a** (8 mg, 21% yield).

LCMS (ESI+): m/z 442.3 [M + H]⁺, (ESI-): m/z 440.2 [M - H]⁻, rt 2.13 minutes, 97%; ¹H NMR (400 MHz, (CD₃)₂SO) 10.98 (1H, s), 9.34 (1H, s), 8.50 (1H, d, J = 2.2 Hz), 7.61 (1H, d, J = 7.9 Hz), 7.45 (1H, dd, J = 8.6, 2.4 Hz), 7.37 (1H, d, J = 8.1 Hz), 7.30 (1H, d, J = 2.3 Hz), 7.18 (1H, d, J = 8.8 Hz), 7.09 (1H, ddd, J = 8.1, 7.0, 1.1 Hz), 6.99 (1H, ddd, J = 7.9, 7.0, 1.0 Hz), 3.87 (2H, s), 3.85 (3H, s), 3.12 (4H, t, J = 5.9 Hz), 1.65-1.52 (4H, m), 1.51-1.38 (4H, m); ¹³C NMR (100 MHz, (CD₃)₂SO) 170.4, 151.7, 136.2, 130.4, 127.9, 127.2, 124.3, 123.1,

121.2, 118.7, 118.6, 118.5, 111.5, 111.1, 108.2, 56.3, 47.7, 33.5, 28.5, 26.4; $\nu_{\max}/\text{cm}^{-1}$ 3345 (br, N-H), 2928, 2856, 1673 (C=O), 1594, 1524; HRMS (ESI)+: m/z calculated for $[\text{C}_{23}\text{H}_{27}\text{N}_3\text{O}_4\text{S} + \text{Na}]^+ = 464.1614$, observed 464.1615.

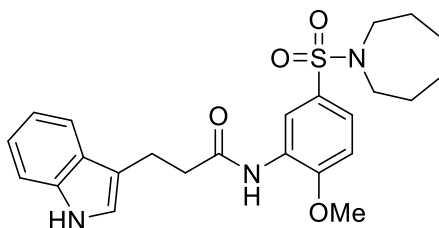
N-(5-(Azepan-1-ylsulfonyl)-2-methoxyphenyl)-2-(5-methoxy-1H-indol-3-yl)acetamide (**46b**)



T3P® (50 wt. % in EtOAc, 0.31 mL, 0.53 mmol) and DIPEA (0.15 mL, 0.88 mmol) were added to a solution of 5-methoxy-3-indoleacetic acid (36 mg, 0.18 mmol) and 5-(azepan-1-ylsulfonyl)-2-methoxyaniline **20** (50 mg, 0.18 mmol) in DMF (2 mL). The reaction mixture was heated to 70 °C over 2 hours. The reaction mixture was diluted with EtOAc (100 mL), washed with water (3 x 100 mL) and brine (100 mL), dried (MgSO_4) and concentrated *in vacuo*. Purification by flash chromatography (30 – 70% EtOAc in PET) afforded **46b** (32 mg, 38% yield).

LCMS (ESI+): m/z 472.3 $[\text{M} + \text{H}]^+$, (ESI-): m/z 470.2 $[\text{M} - \text{H}]^-$, *rt* 2.09 minutes, 98%; ^1H NMR (500 MHz, $(\text{CD}_3)_2\text{SO}$) 10.81 (1H, d, $J = 1.6$ Hz), 9.29 (1H, s), 8.51 (1H, d, $J = 2.1$ Hz), 7.45 (1H, dd, $J = 8.7, 2.3$ Hz), 7.29-7.24 (2H, m), 7.17 (1H, d, $J = 8.8$ Hz), 7.13 (1H, d, $J = 2.4$ Hz), 6.74 (1H, dd, $J = 8.7, 2.4$ Hz), 3.84 (3H, s), 3.83 (2H, s), 3.74 (3H, s), 3.13 (4H, t, $J = 6.0$ Hz), 1.64-1.54 (4H, m), 1.51-1.42 (4H, m); ^{13}C NMR (125 MHz, $(\text{CD}_3)_2\text{SO}$) 170.4, 153.2, 151.6, 131.3, 130.4, 127.8, 127.4, 124.9, 123.0, 118.5, 112.1, 111.2, 111.0, 107.9, 100.5, 56.2, 55.3, 47.7, 33.6, 28.4, 26.3; $\nu_{\max}/\text{cm}^{-1}$ 3350 (br, N-H), 2933, 1719, 1675 (C=O), 1593, 1522; HRMS (ESI)+: m/z calculated for $[\text{C}_{24}\text{H}_{29}\text{N}_3\text{O}_5\text{S} + \text{H}]^+ = 472.1901$, observed 472.1890.

N-(5-(Azepan-1-ylsulfonyl)-2-methoxyphenyl)-3-(1H-indol-3-yl)propanamide (**46c**)

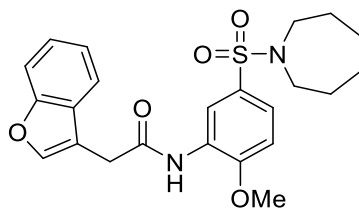


T3P® (50 wt. % in EtOAc, 0.25 mL, 0.42 mmol) and DIPEA (0.12 mL, 0.70 mmol) were added to a solution of 3-indolepropionic acid (27 mg, 0.14 mmol) and 5-(azepan-1-ylsulfonyl)-2-methoxyaniline **20** (40 mg,

0.14 mmol) in DMF (2 mL). The reaction mixture was heated to 70 °C over 1 hour. The reaction mixture was diluted with EtOAc (25 mL), washed with water (3 x 25 mL) and brine (25 mL), dried (MgSO₄) and concentrated *in vacuo*. Purification by flash chromatography (30 – 70% EtOAc in PET) afforded **46c** (26 mg, 41% yield).

LCMS (ESI+): m/z 456.3 [M + H]⁺, (ESI-): m/z 454.3 [M - H]⁻, rt 2.17 minutes, >99%; ¹H NMR (400 MHz, (CD₃)₂SO) 10.78 (1H, s), 9.37 (1H, s), 8.51 (1H, d, J = 1.9 Hz), 7.57 (1H, d, J = 7.8 Hz), 7.47 (1H, dd, J = 8.7, 2.4 Hz), 7.33 (1H, d, J = 8.0 Hz), 7.19 (1H, d, J = 8.7 Hz), 7.14 (1H, d, J = 2.0 Hz), 7.06 (1H, t, J = 7.5 Hz), 6.97 (1H, t, J = 7.4 Hz), 3.89 (3H, s), 3.16 (4H, t, J = 5.9 Hz), 3.01 (2H, t, J = 7.5 Hz), 2.82 (2H, t, J = 7.5 Hz), 1.70-1.56 (4H, m), 1.55-1.41 (4H, m); ¹³C NMR (100 MHz, (CD₃)₂SO) 171.8, 152.0, 136.2, 130.3, 127.8, 127.0, 123.1, 122.3, 120.9, 119.4, 118.5, 118.2, 113.6, 111.3, 111.0, 56.2, 47.7, 36.8, 28.5, 26.4, 20.7; ν_{max}/cm⁻¹ 3360 (br, N-H), 2927, 2856, 1674 (C=O), 1594, 1524; HRMS (ESI)+: m/z calculated for [C₂₄H₂₉N₃O₄S + H]⁺ = 456.1952, observed 456.1970.

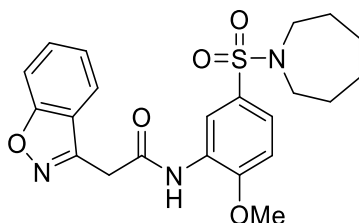
N-(5-(Azepan-1-ylsulfonyl)-2-methoxyphenyl)-2-(benzofuran-3-yl)acetamide (**46d**)



T3P® (50 wt. % in EtOAc, 0.31 mL, 0.53 mmol) and DIPEA (0.15 mL, 0.88 mmol) were added to a solution of benzo[b]furan-3-ylacetic acid (31 mg, 0.18 mmol) and 5-(azepan-1-ylsulfonyl)-2-methoxyaniline **20** (50 mg, 0.18 mmol) in DMF (2 mL). The reaction mixture was heated to 70 °C over 90 minutes. The reaction mixture was diluted with EtOAc (25 mL), washed with water (3 x 25 mL) and brine (25 mL), dried (MgSO₄) and concentrated *in vacuo*. Purification by flash chromatography (30 – 60% EtOAc in PET) afforded **46d** (50 mg, 64% yield).

LCMS (ESI+): m/z 443.3 [M + H]⁺, (ESI-): m/z 441.3 [M - H]⁻, rt 2.24 minutes, >99%; ¹H NMR (500 MHz, (CD₃)₂SO) 9.70 (1H, s), 8.46 (1H, d, J = 2.0 Hz), 7.92 (1H, s), 7.69 (1H, d, J = 7.6 Hz), 7.57 (1H, d, J = 8.2 Hz), 7.49 (1H, dd, J = 8.5, 2.3 Hz), 7.32 (1H, td, J = 7.7, 1.1 Hz), 7.27 (1H, t, J = 7.5 Hz), 7.22 (1H, d, J = 8.7 Hz), 3.94 (3H, s), 3.92 (2H, s), 3.13 (4H, t, J = 5.9 Hz), 1.64-1.53 (4H, m), 1.51-1.42 (4H, m); ¹³C NMR (125 MHz, (CD₃)₂SO) 169.0, 154.5, 152.1, 143.5, 130.4, 127.8, 127.6, 124.4, 123.4, 122.6, 120.2, 119.3, 114.6, 111.3, 111.2, 56.3, 47.6, 31.2, 28.4, 26.3; ν_{max}/cm⁻¹ 3353, 2929, 2855, 1680 (C=O), 1593, 1523; HRMS (ESI)+: m/z calculated for [C₂₃H₂₆N₂O₅S + H]⁺ = 443.1635, observed 443.1652.

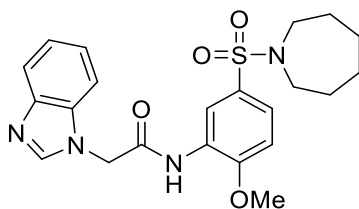
N-(5-(Azepan-1-ylsulfonyl)-2-methoxyphenyl)-2-(benzo[d]isoxazol-3-yl)acetamide (**46e**)



T3P® (50 wt. % in EtOAc, 81 μ L, 0.14 mmol) and DIPEA (39 μ L, 0.23 mmol) were added to a solution of 2-(1,2-benzisoxazol-3-yl)acetic acid (8 mg, 0.05 mmol) and 5-(azepan-1-ylsulfonyl)-2-methoxyaniline **20** (13 mg, 0.045 mmol) in DMF (1 mL). The reaction mixture was heated to 70 °C over 3 hours. The reaction mixture was diluted with EtOAc (25 mL), washed with water (3 x 15 mL) and brine (25 mL), dried (MgSO₄) and concentrated *in vacuo*. Purification by flash chromatography (30 – 70% EtOAc in PET) followed by reverse phase flash chromatography (0 – 100% acetonitrile in water (+ 0.1% NH₃)) afforded **46e** (11 mg, 55% yield).

LCMS (ESI+): m/z 444.3 [M + H]⁺, (ESI-): m/z 442.2 [M - H]⁻, rt 2.15 minutes, >99%; ¹H NMR (400 MHz, (CD₃)₂SO) 10.03 (1H, s), 8.44 (1H, d, J = 1.9 Hz), 7.91 (1H, d, J = 8.0 Hz), 7.75 (1H, d, J = 8.5 Hz), 7.66 (1H, t, J = 7.7 Hz), 7.52 (1H, dd, J = 8.6, 2.2 Hz), 7.41 (1H, t, J = 7.4 Hz), 7.25 (1H, d, J = 8.7 Hz), 4.34 (2H, s), 3.97 (3H, s), 3.13 (4H, t, J = 5.9 Hz), 1.67-1.52 (4H, m), 1.51-1.39 (4H, m); ¹³C NMR (100 MHz, (CD₃)₂SO) 166.8, 162.4, 154.2, 152.2, 130.4, 127.4, 123.7, 122.6, 121.5, 119.5, 111.3, 109.7, 56.3, 47.6, 32.8, 28.5, 26.3 (2 peaks missing); $\nu_{\max}/\text{cm}^{-1}$ 2923, 2856, 1689 (C=O), 1595, 1527; HRMS (ESI)+: m/z calculated for [C₂₂H₂₅N₃O₅S + H]⁺ = 444.1588, observed 444.1592.

N-(5-(Azepan-1-ylsulfonyl)-2-methoxyphenyl)-2-(1H-benzo[d]imidazol-1-yl)acetamide (**46f**)

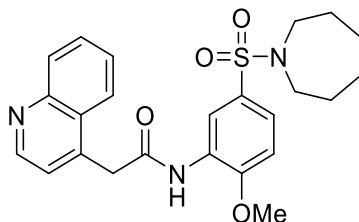


T3P® (50 wt. % in EtOAc, 0.25 mL, 0.42 mmol) and DIPEA (0.12 mL, 0.70 mmol) were added to a solution of 2-(1H-benzimidazol-1-yl)acetic acid (25 mg, 0.14 mmol) and 5-(azepan-1-ylsulfonyl)-2-methoxyaniline **20** (40 mg, 0.14 mmol) in DMF (2 mL). The reaction mixture was heated to 70 °C over 1 hour. The reaction mixture was diluted with EtOAc (25 mL), washed with water (3 x 25 mL) and brine (25 mL), dried (MgSO₄)

and concentrated *in vacuo*. Purification by flash chromatography (50 – 100% EtOAc in PET, 0 – 5% methanol in DCM) afforded **46f** (33 mg, 53% yield).

LCMS (ESI+): m/z 443.3 [M + H]⁺, (ESI-): m/z 441.2 [M - H]⁻, *rt* 1.62 minutes, >99%; ¹H NMR (500 MHz, (CD₃)₂SO) 10.00 (1H, s), 8.45 (1H, d, *J* = 2.2 Hz), 8.23 (1H, s), 7.70-7.65 (1H, m), 7.54 (1H, d, *J* = 7.8 Hz), 7.51 (1H, dd, *J* = 8.7, 2.3 Hz), 7.29-7.19 (3H, m), 5.31 (2H, s), 3.98 (3H, s), 3.11 (4H, t, *J* = 5.9 Hz), 1.62-1.51 (4H, m), 1.49-1.40 (4H, m); ¹³C NMR (125 MHz, (CD₃)₂SO) 166.5, 152.0, 145.0, 143.2, 134.4, 130.4, 127.3, 123.7, 122.4, 121.6, 119.4, 119.1, 111.3, 110.3, 56.4, 47.6, 47.3, 28.4, 26.3; $\nu_{\max}/\text{cm}^{-1}$ 2930, 2853, 1694 (C=O), 1596, 1533; HRMS (ESI)+: m/z calculated for [C₂₂H₂₆N₄O₄S + H]⁺ = 443.1748, observed 443.1769.

N-(5-(Azepan-1-ylsulfonyl)-2-methoxyphenyl)-2-(quinolin-4-yl)acetamide (**46g**)

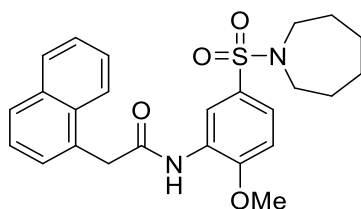


Lithium diisopropylamide (2 M in THF/heptane/ethylbenzene, 1.5 mL, 3.0 mmol) was added dropwise over 30 minutes at -78 °C to a mixture of 4-methylquinoline **47** (0.33 mL, 2.5 mmol) and THF (5 mL). The reaction mixture was stirred at -78 °C over 1 hour, then solid CO₂ pellets (1 g) were added. The reaction mixture was stirred at -78 °C over 10 minutes, then warmed to *rt* and stirred over 1 hour. Water (20 mL) was added dropwise at 0 °C, followed by aqueous NaOH (10% w/v, 5 mL). The mixture was washed with DCM (3 x 25 mL), then adjusted to pH 6 and washed with DCM/methanol (9:1, 3 x 50 mL). The aqueous phase was concentrated *in vacuo* to afford a crude residue. 5-(azepan-1-ylsulfonyl)-2-methoxyaniline **20** (0.140 g, 0.492 mmol) and DMF (10 mL) were added to the crude residue, followed by T3P® (50 wt. % in EtOAc, 3.5 mL, 5.9 mmol) and DIPEA (1.7 mL, 9.9 mmol). The reaction mixture was heated to 70 °C over 40 minutes. The reaction mixture was diluted with EtOAc (100 mL), washed with water (3 x 100 mL) and brine (100 mL), dried (MgSO₄) and concentrated *in vacuo*. Purification by flash chromatography (50 – 100% EtOAc in PET, 0 – 10% methanol in DCM) followed by reverse phase flash chromatography (0 – 50% acetonitrile in water (+ 0.1% NH₃)) afforded **46g** (11 mg, 5% yield).

LCMS (ESI+): m/z 454.3 [M + H]⁺, (ESI-): m/z 452.3 [M - H]⁻, *rt* 1.70 minutes, >99%; ¹H NMR (400 MHz, (CD₃)₂SO) 9.90 (1H, s), 8.85 (1H, d, *J* = 4.3 Hz), 8.42 (1H, d, *J* = 2.2 Hz), 8.19 (1H, d, *J* = 8.4 Hz), 8.05 (1H, dd, *J* = 8.4, 0.7 Hz), 7.77 (1H, ddd, *J* = 8.4, 6.9, 1.4 Hz), 7.65 (1H, ddd, *J* = 8.4, 6.9, 1.3 Hz), 7.53-7.46 (2H, m),

7.24 (1H, d, J = 8.8 Hz), 4.39 (2H, s), 3.97 (3H, s), 3.11 (4H, t, J = 5.9 Hz), 1.63-1.51 (4H, m), 1.50-1.39 (4H, m); ¹³C NMR (125 MHz, CDCl₃) 167.1, 150.6, 150.5, 148.8, 140.2, 132.2, 130.6, 130.0, 127.63, 127.58, 127.4, 124.0, 123.7, 122.8, 118.1, 109.6, 56.2, 48.5, 42.1, 29.3, 27.0; $\nu_{\max}/\text{cm}^{-1}$ 3295, 2923, 1663 (C=O), 1593, 1537; HRMS (ESI)+: m/z calculated for [C₂₄H₂₇N₃O₄S + H]⁺ = 454.1795, observed 454.1781.

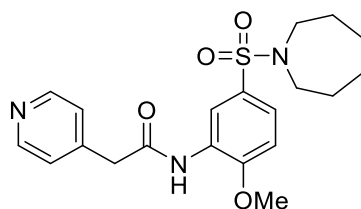
N-(5-(Azepan-1-ylsulfonyl)-2-methoxyphenyl)-2-(naphthalen-1-yl)acetamide (**46h**)



T3P® (50 wt. % in EtOAc, 0.31 mL, 0.53 mmol) and DIPEA (0.15 mL, 0.88 mmol) were added to a solution of 1-naphthaleneacetic acid (33 mg, 0.18 mmol) and 5-(azepan-1-ylsulfonyl)-2-methoxyaniline **20** (50 mg, 0.18 mmol) in DMF (2 mL). The reaction mixture was heated to 70 °C over 2 hours. The reaction mixture was diluted with EtOAc (25 mL), washed with water (3 x 25 mL) and brine (25 mL), dried (MgSO₄) and concentrated *in vacuo*. Purification by flash chromatography (0 – 50% EtOAc in PET) afforded **46h** (53 mg, 67% yield).

LCMS (ESI+): m/z 453.3 [M + H]⁺, (ESI-): m/z 451.3 [M - H]⁻, rt 2.37 minutes, >99%; ¹H NMR (400 MHz, (CD₃)₂SO) 9.69 (1H, s), 8.44 (1H, d, J = 2.3 Hz), 8.12 (1H, d, J = 7.9 Hz), 7.98-7.91 (1H, m), 7.86 (1H, dd, J = 7.2, 2.2 Hz), 7.59-7.44 (5H, m), 7.22 (1H, d, J = 8.8 Hz), 4.30 (2H, s), 3.94 (3H, s), 3.11 (4H, t, J = 5.9 Hz), 1.62-1.51 (4H, m), 1.49-1.40 (4H, m); ¹³C NMR (125 MHz, CDCl₃) 169.0, 150.6, 134.2, 132.2, 132.1, 130.6, 129.0, 128.9, 128.6, 127.9, 127.1, 126.4, 125.8, 123.9, 123.6, 117.9, 109.4, 56.0, 48.5, 43.1, 29.4, 27.0; $\nu_{\max}/\text{cm}^{-1}$ 3360, 2925, 2862, 1675 (C=O), 1592, 1519; HRMS (ESI)+: m/z calculated for [C₂₅H₂₈N₂O₄S + Na]⁺ = 475.1662, observed 475.1652.

N-(5-(Azepan-1-ylsulfonyl)-2-methoxyphenyl)-2-(pyridin-4-yl)acetamide (**46i**)

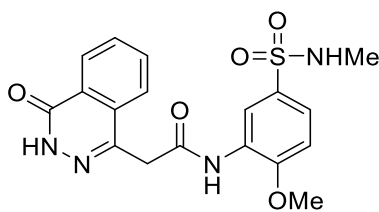


EDC.HCl (83 mg, 0.43 mmol), DIPEA (0.15 mL, 0.86 mmol) and DMAP (5 mg, 0.04 mmol) were added to a solution of 4-pyridylacetic acid hydrochloride (50 mg, 0.29 mmol) and 5-(azepan-1-ylsulfonyl)-2-

methoxyaniline **20** (98 mg, 0.35 mmol) in DCM (2 mL). The reaction mixture was stirred over 90 minutes, then diluted with water (25 mL) and extracted into DCM (3 x 25 mL). The combined organic extracts were washed (brine), dried (MgSO₄) and concentrated *in vacuo*. Purification by flash chromatography (50 – 100% EtOAc in PET, 0 – 5% methanol in DCM) afforded **46i** (74 mg, 64% yield).

LCMS (ESI+): m/z 404.3 [M + H]⁺, (ESI-): m/z 402.2 [M - H]⁻, rt 1.54 minutes, >99%; ¹H NMR (400 MHz, (CD₃)₂SO) 9.73 (1H, s), 8.54-8.48 (2H, m), 8.45 (1H, d, J = 2.2 Hz), 7.49 (1H, dd, J = 8.6, 2.3 Hz), 7.38-7.31 (2H, m), 7.23 (1H, d, J = 8.8 Hz), 3.94 (3H, s), 3.86 (2H, s), 3.14 (4H, t, J = 5.9 Hz), 1.66-1.54 (4H, m), 1.52-1.41 (4H, m); ¹³C NMR (125 MHz, CDCl₃) 167.2, 150.6, 150.5, 143.1, 132.3, 127.6, 124.7, 124.0, 118.2, 109.6, 56.3, 48.5, 44.2, 29.3, 27.0; ν_{max}/cm⁻¹ 3300, 2931, 2858, 1658 (C=O), 1596, 1536; HRMS (ESI)+: m/z calculated for [C₂₀H₂₅N₃O₄S + Na]⁺ = 426.1458, observed 426.1447.

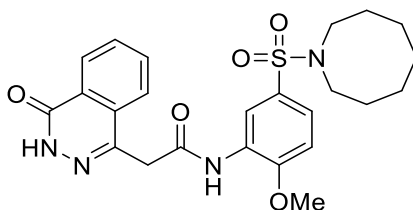
N-(2-Methoxy-5-(*N*-methylsulfamoyl)phenyl)-2-(4-oxo-3,4-dihydrophthalazin-1-yl)acetamide (**49a**)



T3P® (50 wt. % in EtOAc, 93 μL, 0.16 mmol) and DIPEA (46 μL, 0.26 mmol) were added to a solution of 2-(4-oxo-3,4-dihydrophthalazin-1-yl)acetic acid **16** (11 mg, 0.052 mmol) and 3-amino-4-methoxy-*N*-methylbenzenesulfonamide **33a** (11 mg, 0.052 mmol) in DMF (1 mL). The reaction mixture was heated to 70 °C over 5 hours. The reaction mixture was diluted with EtOAc (25 mL), washed with water (3 x 15 mL) and brine (15 mL), dried (MgSO₄) and concentrated *in vacuo*. Purification by flash chromatography (50 – 100% EtOAc in PET, 0 – 10% methanol in DCM) afforded **49a** (6 mg, 29% yield).

LCMS (ESI+): m/z 403.2 [M + H]⁺, (ESI-): m/z 401.1 [M - H]⁻, rt 1.44 minutes, >99%; ¹H NMR (500 MHz, (CD₃)₂SO) 12.61 (1H, s), 9.83 (1H, s), 8.47 (1H, d, J = 2.2 Hz), 8.27 (1H, d, J = 7.5 Hz), 8.00-7.92 (2H, m), 7.86 (1H, ddd, J = 8.0, 6.3, 1.9 Hz), 7.50 (1H, dd, J = 8.7, 2.3 Hz), 7.31-7.22 (2H, m), 4.21 (2H, s), 3.96 (3H, s), 2.35 (3H, d, J = 5.0 Hz); ¹³C NMR (125 MHz, (CD₃)₂SO) 168.2, 159.5, 152.0, 142.2, 133.5, 131.6, 130.7, 129.8, 127.6, 127.5, 125.8, 125.6, 123.5, 119.5, 111.1, 56.3, 28.6 (1 peak missing); ν_{max}/cm⁻¹ 3277, 3173, 3016, 2904, 1660 (C=O), 1594, 1537; HRMS (ESI)+: m/z calculated for [C₁₈H₁₈N₄O₅S + H]⁺ = 403.1071, observed 403.1064.

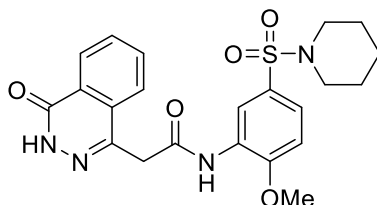
N-(5-(Azocan-1-ylsulfonyl)-2-methoxyphenyl)-2-(4-oxo-3,4-dihydrophthalazin-1-yl)acetamide (**49b**)



T3P® (50 wt. % in EtOAc, 0.24 mL, 0.40 mmol) and DIPEA (0.12 mL, 0.67 mmol) were added to a solution of 2-(4-oxo-3,4-dihydrophthalazin-1-yl)acetic acid **16** (32 mg, 0.13 mmol) and 5-(azocan-1-ylsulfonyl)-2-methoxyaniline **33b** (40 mg, 0.13 mmol) in DMF (2 mL). The reaction mixture was heated to 70 °C over 2 hours. The reaction mixture was diluted with EtOAc (25 mL), washed with water (3 x 25 mL) and brine (25 mL), dried (MgSO₄) and concentrated *in vacuo*. Purification by flash chromatography (50 – 100% EtOAc in PET, 0 – 5% methanol in DCM) afforded **49b** (24 mg, 37% yield).

LCMS (ESI+): *m/z* 485.3 [M + H]⁺, (ESI-): *m/z* 483.2 [M - H]⁻, *rt* 1.94 minutes, >99%; ¹H NMR (500 MHz, (CD₃)₂SO) 12.62 (1H, s), 9.86 (1H, s), 8.45 (1H, d, *J* = 2.2 Hz), 8.30-8.25 (1H, m), 7.98-7.92 (2H, m), 7.89-7.83 (1H, m), 7.48 (1H, dd, *J* = 8.6, 2.3 Hz), 7.24 (1H, d, *J* = 8.8 Hz), 4.21 (2H, s), 3.97 (3H, s), 3.01 (4H, t, *J* = 5.8 Hz), 1.67-1.44 (10H, m); ¹³C NMR (125 MHz, (CD₃)₂SO) 168.4, 159.5, 152.1, 142.1, 133.5, 131.6, 129.8, 129.5, 127.7, 127.6, 125.9, 125.5, 123.5, 119.2, 111.2, 56.3, 48.0, 27.2, 26.2, 24.6 (1 peak missing); *v*_{max}/cm⁻¹ 3307, 2923, 1693, 1644 (C=O), 1596, 1530; HRMS (ESI)+: *m/z* calculated for [C₂₄H₂₈N₄O₅S + H]⁺ = 485.1853, observed 485.1848.

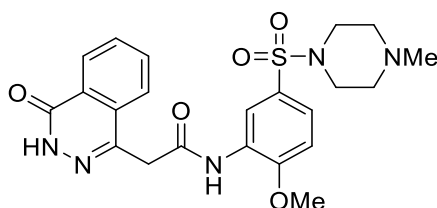
N-(2-Methoxy-5-(piperidin-1-ylsulfonyl)phenyl)-2-(4-oxo-3,4-dihydrophthalazin-1-yl)acetamide (**49c**)



T3P® (50 wt. % in EtOAc, 0.14 mL, 0.23 mmol) and DIPEA (66 μL, 0.38 mmol) were added to a solution of 2-(4-oxo-3,4-dihydrophthalazin-1-yl)acetic acid **16** (16 mg, 0.076 mmol) and 2-methoxy-5-(piperidin-1-ylsulfonyl)aniline **33c** (21 mg, 0.076 mmol) in DMF (1 mL). The reaction mixture was heated to 70 °C over 2 hours. The reaction mixture was diluted with EtOAc (25 mL), washed with water (3 x 10 mL) and brine (25 mL), dried (MgSO₄) and concentrated *in vacuo*. Purification by flash chromatography (50 – 100% EtOAc in PET, 0 – 10% methanol in DCM) afforded **49c** (14 mg, 40% yield).

LCMS (ESI+): m/z 457.3 $[M + H]^+$, (ESI-): m/z 455.2 $[M - H]^-$, rt 1.76 minutes, 98%; 1H NMR (500 MHz, $(CD_3)_2SO$) 12.62 (1H, s), 9.88 (1H, s), 8.39 (1H, d, $J = 2.2$ Hz), 8.28 (1H, d, $J = 7.9$ Hz), 7.99-7.92 (2H, m), 7.86 (1H, ddd, $J = 8.0, 5.7, 2.5$ Hz), 7.45 (1H, dd, $J = 8.6, 2.3$ Hz), 7.28 (1H, d, $J = 8.7$ Hz), 4.22 (2H, s), 3.98 (3H, s), 2.81 (4H, t, $J = 5.2$ Hz), 1.50 (4H, quin, $J = 5.7$ Hz), 1.39-1.28 (2H, m); ^{13}C NMR (125 MHz, $(CD_3)_2SO$) 168.4, 159.5, 152.4, 142.1, 133.5, 131.6, 129.8, 127.59, 127.56, 126.7, 125.9, 125.5, 124.3, 119.9, 111.2, 56.4, 46.5, 24.6, 22.8 (1 peak missing); ν_{max}/cm^{-1} 3176, 3057, 2923, 1674, 1646 (C=O), 1594, 1542; HRMS (ESI)+: m/z calculated for $[C_{22}H_{24}N_4O_5S + H]^+ = 457.1540$, observed 457.1537.

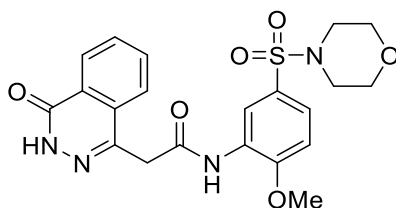
N-(2-Methoxy-5-((4-methylpiperazin-1-yl)sulfonyl)phenyl)-2-(4-oxo-3,4-dihydrophthalazin-1-yl)acetamide
(49d)



T3P® (50 wt. % in EtOAc, 0.24 mL, 0.41 mmol) and DIPEA (0.12 mL, 0.68 mmol) were added to a solution of 2-(4-oxo-3,4-dihydrophthalazin-1-yl)acetic acid **16** (32 mg, 0.14 mmol) and 2-methoxy-5-((4-methylpiperazin-1-yl)sulfonyl)aniline **33d** (40 mg, 0.14 mmol) in DMF (2 mL). The reaction mixture was heated to 70 °C over 2 hours. The reaction mixture was diluted with EtOAc (25 mL), washed with water (3 x 25 mL) and brine (25 mL), dried ($MgSO_4$) and concentrated *in vacuo*. Purification by flash chromatography (50 – 100% EtOAc in PET, 0 - 10% methanol in DCM) followed by reverse phase flash chromatography (0 – 30% acetonitrile in water (+ 0.1% NH_3)) afforded **49d** (10 mg, 16% yield).

LCMS (ESI+): m/z 472.3 $[M + H]^+$, (ESI-): m/z 470.2 $[M - H]^-$, rt 1.23 minutes, >99%; 1H NMR (500 MHz, $(CD_3)_2SO$) 12.62 (1H, s), 9.91 (1H, s), 8.40 (1H, d, $J = 2.2$ Hz), 8.30-8.25 (1H, m), 7.99-7.92 (2H, m), 7.86 (1H, ddd, $J = 8.0, 5.8, 2.4$ Hz), 7.46 (1H, dd, $J = 8.6, 2.3$ Hz), 7.30 (1H, d, $J = 8.7$ Hz), 4.22 (2H, s), 3.99 (3H, s), 2.81 (4H, br s), 2.38-2.28 (4H, m), 2.10 (3H, s); ^{13}C NMR (125 MHz, $(CD_3)_2SO$) 168.4, 159.4, 152.6, 142.1, 133.5, 131.6, 129.8, 127.62, 127.56, 126.0, 125.8, 125.5, 124.5, 120.0, 111.3, 56.4, 53.5, 45.7, 45.2 (1 peak missing); ν_{max}/cm^{-1} 3376, 2922, 1684, 1655 (C=O), 1594, 1533; HRMS (ESI)+: m/z calculated for $[C_{22}H_{25}N_5O_5S + H]^+ = 472.1649$, observed 472.1662.

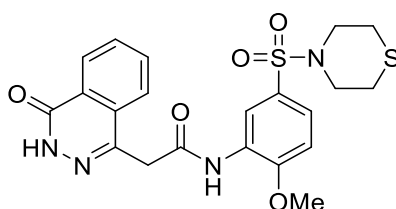
N-(2-Methoxy-5-(morpholinosulfonyl)phenyl)-2-(4-oxo-3,4-dihydrophthalazin-1-yl)acetamide (**49e**)



T3P® (50 wt. % in EtOAc, 0.26 mL, 0.44 mmol) and DIPEA (0.13 mL, 0.73 mmol) were added to a solution of 2-(4-oxo-3,4-dihydrophthalazin-1-yl)acetic acid **16** (35 mg, 0.15 mmol) and 2-methoxy-5-(morpholinosulfonyl)aniline **33e** (40 mg, 0.15 mmol) in DMF (2 mL). The reaction mixture was heated to 70 °C over 2 hours. The reaction mixture was diluted with EtOAc (25 mL), washed with water (3 x 25 mL) and brine (25 mL), dried (MgSO₄) and concentrated *in vacuo*. Purification by flash chromatography (50 – 100% EtOAc in PET, 0 - 10% methanol in DCM) followed by reverse phase flash chromatography (0 – 60% acetonitrile in water (+ 0.1% NH₃)) afforded **49e** (7 mg, 10% yield).

LCMS (ESI+): m/z 459.3 [M + H]⁺, (ESI-): m/z 457.3 [M - H]⁻, rt 1.55 minutes, >99%; ¹H NMR (400 MHz, (CD₃)₂SO) 12.62 (1H, s), 9.93 (1H, s), 8.41 (1H, d, J = 2.0 Hz), 8.27 (1H, d, J = 7.8 Hz), 8.01-7.91 (2H, m), 7.86 (1H, ddd, J = 8.0, 5.7, 2.5 Hz), 7.47 (1H, dd, J = 8.7, 2.2 Hz), 7.31 (1H, d, J = 8.7 Hz), 4.23 (2H, s), 3.99 (3H, s), 3.59 (4H, t, J = 4.5 Hz), 2.79 (4H, t, J = 4.4 Hz); ¹³C NMR (100 MHz, (CD₃)₂SO) 168.5, 159.5, 152.7, 142.1, 133.6, 131.6, 129.8, 127.7, 127.6, 125.9, 125.6, 125.5, 124.6, 120.1, 111.4, 65.2, 56.4, 45.9 (1 peak missing); ν_{max}/cm⁻¹ 3175, 3027, 2924, 2854, 1672, 1646 (C=O), 1593, 1538; HRMS (ESI)+: m/z calculated for [C₂₁H₂₂N₄O₆S + Na]⁺ = 481.1152, observed 481.1143.

N-(2-Methoxy-5-(thiomorpholinosulfonyl)phenyl)-2-(4-oxo-3,4-dihydrophthalazin-1-yl)acetamide (**49f**)

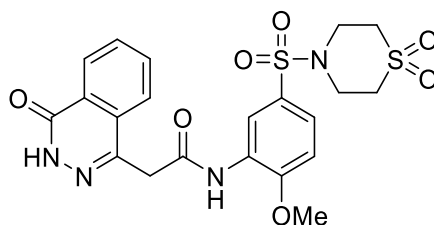


T3P® (50 wt. % in EtOAc, 0.24 mL, 0.40 mmol) and DIPEA (0.12 mL, 0.67 mmol) were added to a solution of 2-(4-oxo-3,4-dihydrophthalazin-1-yl)acetic acid **16** (32 mg, 0.13 mmol) and 2-methoxy-5-(thiomorpholinosulfonyl)aniline **33f** (40 mg, 0.13 mmol) in DMF (2 mL). The reaction mixture was heated to 70 °C over 2 hours. The reaction mixture was diluted with EtOAc (25 mL), washed with water (3 x 25

mL) and brine (25 mL), dried (MgSO₄) and concentrated *in vacuo*. Purification by flash chromatography (50 – 100% EtOAc in PET, 0 – 10% methanol in DCM) afforded **49f** (23 mg, 36% yield).

LCMS (ESI+): m/z 475.2 [M + H]⁺, (ESI-): m/z 473.2 [M - H]⁻, rt 1.72 minutes, >99%; ¹H NMR (500 MHz, (CD₃)₂SO) 12.62 (1H, s), 9.92 (1H, s), 8.41 (1H, d, J = 2.3 Hz), 8.27 (1H, d, J = 7.9 Hz), 8.00-7.92 (2H, m), 7.86 (1H, ddd, J = 8.0, 5.8, 2.3 Hz), 7.47 (1H, dd, J = 8.7, 2.3 Hz), 7.29 (1H, d, J = 8.7 Hz), 4.23 (2H, s), 3.99 (3H, s), 3.13 (4H, t, J = 4.7 Hz), 2.63 (4H, t, J = 5.1 Hz); ¹³C NMR (125 MHz, (CD₃)₂SO) 168.4, 159.5, 152.6, 142.1, 133.6, 131.6, 129.8, 127.8, 127.6, 127.2, 125.9, 125.6, 124.2, 119.6, 111.4, 56.4, 47.8, 26.3 (1 peak missing); ν_{max}/cm⁻¹ 3391, 2929, 2849, 1674, 1645, 1607, 1516; HRMS (ESI)+: m/z calculated for [C₂₁H₂₂N₄O₅S₂ + H]⁺ = 475.1104, observed 475.1104.

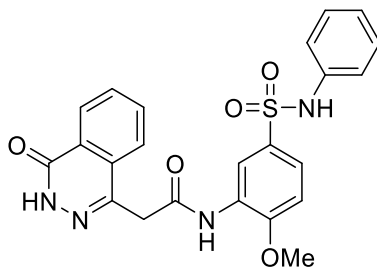
N-(5-((1,1-Dioxidothiomorpholino)sulfonyl)-2-methoxyphenyl)-2-(4-oxo-3,4-dihydrophthalazin-1-yl)acetamide (**49g**)



T3P® (50 wt. % in EtOAc, 0.67 mL, 1.1 mmol) and DIPEA (0.33 mL, 1.9 mmol) were added to a solution of 2-(4-oxo-3,4-dihydrophthalazin-1-yl)acetic acid **16** (89 mg, 0.38 mmol) and 4-((3-amino-4-methoxyphenyl)sulfonyl)thiomorpholine 1,1-dioxide **33g** (0.120 g, 0.375 mmol) in DMF (2 mL). The reaction mixture was heated to 70 °C over 1 hour. The reaction mixture was diluted with EtOAc (25 mL), washed with water (3 x 25 mL) and brine (25 mL), dried (MgSO₄) and concentrated *in vacuo*. Purification by flash chromatography (50 – 100% EtOAc in PET, 0 – 20% methanol in DCM) followed by reverse phase flash chromatography (0 – 60% acetonitrile in water (+ 0.1% NH₃)) afforded **49g** (55 mg, 28% yield).

LCMS (ESI+): m/z 507.2 [M + H]⁺, (ESI-): m/z 505.2 [M - H]⁻, rt 1.61 minutes, 97%; ¹H NMR (500 MHz, (CD₃)₂SO) 12.62 (1H, s), 9.96 (1H, s), 8.47 (1H, s), 8.27 (1H, d, J = 7.8 Hz), 8.02-7.82 (3H, m), 7.55 (1H, d, J = 8.8 Hz), 7.32 (1H, d, J = 8.7 Hz), 4.23 (2H, s), 4.00 (3H, s), 3.27-3.19 (4H, m) (1 peak suspected to be obscured by H₂O signal); ¹³C NMR (125 MHz, (CD₃)₂SO) 168.6, 159.5, 152.9, 142.1, 133.6, 131.6, 129.8, 128.0, 127.6, 126.8, 125.9, 125.6, 124.2, 119.5, 111.7, 56.5, 49.9, 45.1 (1 peak missing); ν_{max}/cm⁻¹ 3403, 3001, 2933, 1663 (C=O), 1597, 1525; HRMS (ESI)-: m/z calculated for [C₂₁H₂₂N₄O₇S₂ - H]⁻ = 505.0857, observed 505.0851.

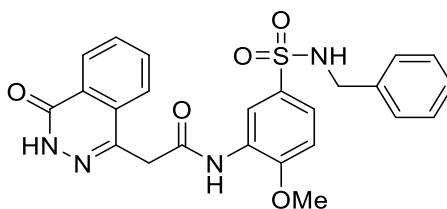
N-(2-Methoxy-5-(*N*-phenylsulfamoyl)phenyl)-2-(4-oxo-3,4-dihydrophthalazin-1-yl)acetamide (**49h**)



T3P® (50 wt. % in EtOAc, 0.16 mL, 0.27 mmol) and DIPEA (79 μ L, 0.45 mmol) were added to a solution of 2-(4-oxo-3,4-dihydrophthalazin-1-yl)acetic acid **16** (19 mg, 0.090 mmol) and 3-amino-4-methoxy-*N*-phenylbenzenesulfonamide **33h** (25 mg, 0.090 mmol) in DMF (1 mL). The reaction mixture was heated to 70 °C over 2 hours. The reaction mixture was diluted with EtOAc (25 mL), washed with water (3 x 10 mL) and brine (25 mL), dried (MgSO₄) and concentrated *in vacuo*. Purification by flash chromatography (50 – 100% EtOAc in PET, 0 – 10% methanol in DCM) afforded **49h** (14 mg, 33% yield).

LCMS (ESI+): m/z 465.2 [M + H]⁺, (ESI-): m/z 463.2 [M - H]⁻, *rt* 1.71 minutes, 98%; ¹H NMR (500 MHz, (CD₃)₂SO) 12.61 (1H, s), 10.17 (1H, s), 9.78 (1H, s), 8.55 (1H, d, *J* = 2.2 Hz), 8.31-8.25 (1H, m), 7.98-7.91 (2H, m), 7.90-7.84 (1H, m), 7.47 (1H, dd, *J* = 8.7, 2.4 Hz), 7.22-7.14 (3H, m), 7.07-7.03 (2H, m), 7.00-6.94 (1H, m), 4.20 (2H, s), 3.91 (3H, s); ¹³C NMR (125 MHz, (CD₃)₂SO) 168.2, 159.4, 152.2, 142.1, 137.9, 133.5, 131.6, 131.0, 129.8, 129.1, 127.6, 127.5, 125.8, 125.6, 123.7, 123.6, 119.6, 119.3, 111.0, 56.3 (1 peak missing); $\nu_{\max}/\text{cm}^{-1}$ 3175, 3016, 1674, 1647 (C=O), 1592, 1538; HRMS (ESI+): m/z calculated for [C₂₃H₂₀N₄O₅S + H]⁺ = 465.1227, observed 465.1223.

N-(5-(*N*-Benzylsulfamoyl)-2-methoxyphenyl)-2-(4-oxo-3,4-dihydrophthalazin-1-yl)acetamide (**49i**)

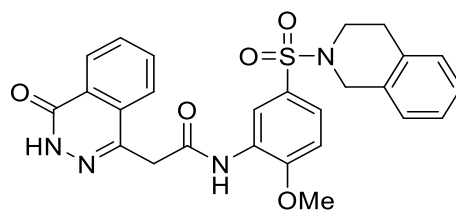


T3P® (50 wt. % in EtOAc, 0.26 mL, 0.43 mmol) and DIPEA (0.12 mL, 0.71 mmol) were added to a solution of 2-(4-oxo-3,4-dihydrophthalazin-1-yl)acetic acid **16** (30 mg, 0.14 mmol) and 3-amino-*N*-benzyl-4-methoxybenzenesulfonamide **33i** (45 mg, 0.14 mmol) in DMF (2 mL). The reaction mixture was heated to 70 °C over 2 hours. The reaction mixture was diluted with EtOAc (25 mL), washed with water (3 x 25 mL)

and brine (25 mL), dried (MgSO₄) and concentrated *in vacuo*. Purification by flash chromatography (50 – 100% EtOAc in PET, 0 – 8% methanol in DCM) afforded **49i** (25 mg, 37% yield).

LCMS (ESI+): *m/z* 479.3 [M + H]⁺, (ESI-): *m/z* 477.2 [M - H]⁻, *rt* 1.74 minutes, >99%; ¹H NMR (500 MHz, (CD₃)₂SO) 12.62 (1H, s), 9.81 (1H, s), 8.51 (1H, d, *J* = 2.2 Hz), 8.27 (1H, d, *J* = 7.8 Hz), 8.03-7.92 (3H, m), 7.86 (1H, ddd, *J* = 8.0, 6.6, 1.6 Hz), 7.53 (1H, dd, *J* = 8.6, 2.3 Hz), 7.28-7.17 (6H, m), 4.22 (2H, s), 3.96 (3H, s), 3.89 (2H, d, *J* = 6.5 Hz); ¹³C NMR (125 MHz, (CD₃)₂SO) 168.1, 159.5, 152.0, 142.2, 137.7, 133.5, 132.1, 131.6, 129.8, 128.2, 127.6, 127.53, 127.49, 127.1, 125.8, 125.6, 123.4, 119.4, 111.1, 56.3, 46.1 (1 peak missing); *v*_{max}/cm⁻¹ 3287, 3176, 3026, 1672, 1647 (C=O), 1593, 1538; HRMS (ESI)+: *m/z* calculated for [C₂₄H₂₂N₄O₅S + H]⁺ = 479.1384, observed 479.1381.

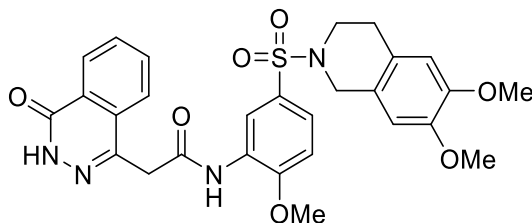
N-(5-((3,4-Dihydroisoquinolin-2(1H)-yl)sulfonyl)-2-methoxyphenyl)-2-(4-oxo-3,4-dihydrophthalazin-1-yl)acetamide (**49j**)



T3P® (50 wt. % in EtOAc, 0.28 mL, 0.47 mmol) and DIPEA (0.14 mL, 0.79 mmol) were added to a solution of 2-(4-oxo-3,4-dihydrophthalazin-1-yl)acetic acid **16** (37 mg, 0.16 mmol) and 5-((3,4-dihydroisoquinolin-2(1H)-yl)sulfonyl)-2-methoxyaniline **33j** (50 mg, 0.16 mmol) in DMF (2 mL). The reaction mixture was heated to 70 °C over 1 hour. The reaction mixture was diluted with EtOAc (25 mL), washed with water (3 x 25 mL) and brine (25 mL), dried (MgSO₄) and concentrated *in vacuo*. Purification by flash chromatography (50 – 100% EtOAc in PET, 0 – 5% methanol in DCM) afforded **49j** (35 mg, 43% yield).

LCMS (ESI-): *m/z* 503.3 [M - H]⁻, *rt* 1.90 minutes, 98%; ¹H NMR (500 MHz, (CD₃)₂SO) 12.62 (1H, s), 9.89 (1H, s), 8.50 (1H, d, *J* = 2.2 Hz), 8.28 (1H, d, *J* = 7.9 Hz), 7.99-7.92 (2H, m), 7.86 (1H, ddd, *J* = 8.0, 5.9, 2.3 Hz), 7.56 (1H, dd, *J* = 8.6, 2.3 Hz), 7.28 (1H, d, *J* = 8.7 Hz), 7.17-7.05 (4H, m), 4.22 (2H, s), 4.11 (2H, s), 3.97 (3H, s), 3.22 (2H, t, *J* = 6.0 Hz), 2.83 (2H, t, *J* = 5.8 Hz); ¹³C NMR (125 MHz, (CD₃)₂SO) 168.4, 159.5, 152.5, 142.1, 133.5, 133.0, 131.6, 131.5, 129.8, 128.6, 127.7, 127.6, 126.9, 126.6, 126.4, 126.1, 125.8, 125.6, 124.4, 119.9, 111.4, 56.4, 47.2, 43.6, 28.0 (1 peak missing); *v*_{max}/cm⁻¹ 3354, 2929, 2853, 1679 (C=O), 1592, 1523; HRMS (ESI)+: *m/z* calculated for [C₂₆H₂₄N₄O₅S + H]⁺ = 505.1540, observed 505.1534.

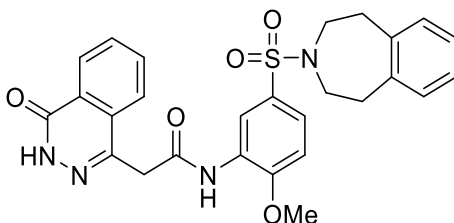
N-(5-((6,7-Dimethoxy-3,4-dihydroisoquinolin-2(1H)-yl)sulfonyl)-2-methoxyphenyl)-2-(4-oxo-3,4-dihydrophthalazin-1-yl)acetamide (**49k**)



T3P® (50 wt. % in EtOAc, 0.38 mL, 0.63 mmol) and DIPEA (0.18 mL, 1.1 mmol) were added to a solution of 2-(4-oxo-3,4-dihydrophthalazin-1-yl)acetic acid **16** (50 mg, 0.21 mmol) and 5-((6,7-dimethoxy-3,4-dihydroisoquinolin-2(1H)-yl)sulfonyl)-2-methoxyaniline **33k** (80 mg, 0.21 mmol) in DMF (2 mL). The reaction mixture was heated to 70 °C over 1 hour. The reaction mixture was diluted with EtOAc (25 mL), washed with water (3 x 25 mL) and brine (25 mL), dried (MgSO₄) and concentrated *in vacuo*. Purification by flash chromatography (50 – 100% EtOAc in PET, 0 – 7% methanol in DCM) followed by reverse phase flash chromatography (0 – 50% acetonitrile in water (+ 0.1% NH₃)) afforded **49k** (48 mg, 40% yield).

LCMS (ESI+): m/z 565.4 [M + H]⁺, (ESI-): m/z 563.2 [M - H]⁻, rt 1.78 minutes, >99%; ¹H NMR (500 MHz, (CD₃)₂SO) 12.62 (1H, s), 9.89 (1H, s), 8.50 (1H, d, J = 2.2 Hz), 8.28 (1H, d, J = 7.7 Hz), 7.99-7.92 (2H, m), 7.86 (1H, ddd, J = 8.0, 6.0, 2.1 Hz), 7.54 (1H, dd, J = 8.6, 2.3 Hz), 7.28 (1H, d, J = 8.9 Hz), 6.71 (1H, s), 6.65 (1H, s), 4.22 (2H, s), 4.01 (2H, s), 3.97 (3H, s), 3.67 (3H, s), 3.65 (3H, s), 3.18 (2H, t, J = 5.9 Hz), 2.74 (2H, t, J = 5.8 Hz); ¹³C NMR (125 MHz, (CD₃)₂SO) 168.4, 159.5, 152.5, 147.5, 147.3, 142.1, 133.5, 131.6, 129.8, 127.7, 127.6, 127.0, 125.8, 125.6, 124.7, 124.4, 123.1, 119.8, 111.7, 111.3, 109.8, 56.4, 55.5, 55.4, 46.9, 43.7, 27.7 (1 peak missing); ν_{max}/cm⁻¹ 3299, 3010, 2938, 2837, 1695, 1641 (C=O), 1596, 1520; HRMS (ESI)+: m/z calculated for [C₂₈H₂₈N₄O₇S + Na]⁺ = 587.1571, observed 587.1543.

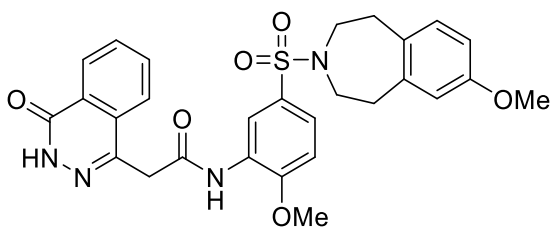
N-(2-Methoxy-5-((1,2,4,5-tetrahydro-3H-benzo[d]azepin-3-yl)sulfonyl)phenyl)-2-(4-oxo-3,4-dihydrophthalazin-1-yl)acetamide (**49l**)



T3P® (50 wt. % in EtOAc, 0.38 mL, 0.63 mmol) and DIPEA (0.18 mL, 1.1 mmol) were added to a solution of 2-(4-oxo-3,4-dihydrophthalazin-1-yl)acetic acid **16** (50 mg, 0.21 mmol) and 2-methoxy-5-((1,2,4,5-tetrahydro-3H-benzo[d]azepin-3-yl)sulfonyl)aniline **33I** (70 mg, 0.21 mmol) in DMF (2 mL). The reaction mixture was heated to 70 °C over 2 hours. The reaction mixture was diluted with EtOAc (25 mL), washed with water (3 x 25 mL) and brine (25 mL), dried (MgSO₄) and concentrated *in vacuo*. Purification by flash chromatography (50 – 80% EtOAc in PET, 0 – 5% methanol in DCM) followed by reverse phase flash chromatography (0 – 100% acetonitrile in water (+ 0.1% NH₃)) afforded **49I** (20 mg, 18% yield).

LCMS (ESI+): m/z 519.3 [M + H]⁺, (ESI-): m/z 517.2 [M - H]⁻, rt 2.06 minutes, >99%; ¹H NMR (500 MHz, (CD₃)₂SO) 12.61 (1H, s), 9.85 (1H, s), 8.42 (1H, d, J = 2.1 Hz), 8.27 (1H, d, J = 7.8 Hz), 7.97-7.90 (2H, m), 7.89-7.83 (1H, m), 7.48 (1H, dd, J = 8.7, 2.3 Hz), 7.23 (1H, d, J = 8.8 Hz), 7.12-7.04 (4H, m), 4.19 (2H, s), 3.94 (3H, s), 3.18-3.04 (4H, m), 2.96-2.83 (4H, m); ¹³C NMR (125 MHz, (CD₃)₂SO) 168.4, 159.4, 152.3, 142.1, 140.4, 133.5, 131.6, 129.8, 129.1, 128.7, 127.7, 127.6, 126.5, 125.9, 125.5, 123.9, 119.3, 111.3, 56.3, 48.1, 35.5 (1 peak missing); ν_{max}/cm⁻¹ 3302, 3173, 3011, 2906, 1687, 1650 (C=O), 1595, 1530; HRMS (ESI)-: m/z calculated for [C₂₇H₂₆N₄O₅S - H]⁻ = 517.1551, observed 517.1549.

N-(2-Methoxy-5-((7-methoxy-1,2,4,5-tetrahydro-3H-benzo[d]azepin-3-yl)sulfonyl)phenyl)-2-(4-oxo-3,4-dihydrophthalazin-1-yl)acetamide (**49m**)

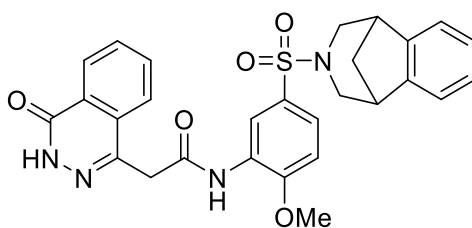


T3P® (50 wt. % in EtOAc, 0.50 mL, 0.84 mmol) and DIPEA (0.24 mL, 1.4 mmol) were added to a solution of 2-(4-oxo-3,4-dihydrophthalazin-1-yl)acetic acid **16** (66 mg, 0.28 mmol) and 2-methoxy-5-((7-methoxy-1,2,4,5-tetrahydro-3H-benzo[d]azepin-3-yl)sulfonyl)aniline **33m** (0.101 g, 0.279 mmol) in DMF (2 mL). The reaction mixture was heated to 70 °C over 1 hour. The reaction mixture was diluted with EtOAc (25 mL), washed with water (3 x 25 mL) and brine (25 mL), dried (MgSO₄) and concentrated *in vacuo*. Purification by flash chromatography (50 – 100% EtOAc in PET, 0 – 7% methanol in DCM) afforded **49m** (48 mg, 30% yield).

LCMS (ESI+): m/z 549.4 [M + H]⁺, (ESI-): m/z 547.3 [M - H]⁻, rt 1.96 minutes, 96%; ¹H NMR (500 MHz, (CD₃)₂SO) 12.61 (1H, s), 9.85 (1H, s), 8.41 (1H, d, J = 2.1 Hz), 8.27 (1H, d, J = 7.9 Hz), 7.97-7.90 (2H, m), 7.89-

7.83 (1H, m), 7.47 (1H, dd, J = 8.7, 2.3 Hz), 7.22 (1H, d, J = 8.8 Hz), 6.98 (1H, d, J = 8.2 Hz), 6.67 (1H, d, J = 2.6 Hz), 6.62 (1H, dd, J = 8.2, 2.8 Hz), 4.20 (2H, s), 3.94 (3H, s), 3.66 (3H, s), 3.15-3.02 (4H, m), 2.91-2.76 (4H, m); ^{13}C NMR (125 MHz, $(\text{CD}_3)_2\text{SO}$) 168.4, 159.5, 157.8, 152.3, 142.1, 141.7, 133.6, 132.4, 131.6, 130.2, 129.8, 128.7, 127.7, 127.6, 125.9, 125.5, 123.9, 119.3, 115.0, 111.3, 111.2, 56.3, 55.0, 48.6, 48.1, 35.7, 34.7 (1 peak missing); $\nu_{\text{max}}/\text{cm}^{-1}$ 3308, 2913, 1691, 1642 (C=O), 1595, 1529; HRMS (ESI)+: m/z calculated for $[\text{C}_{28}\text{H}_{28}\text{N}_4\text{O}_6\text{S} + \text{Na}]^+$ = 571.1622, observed 571.1615.

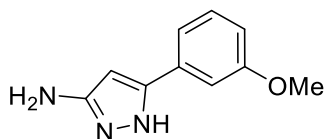
N-(2-Methoxy-5-((1,2,4,5-tetrahydro-3H-1,5-methanobenzo[d]azepin-3-yl)sulfonyl)phenyl)-2-(4-oxo-3,4-dihydrophthalazin-1-yl)acetamide (**49n**)



T3P® (50 wt. % in EtOAc, 0.26 mL, 0.43 mmol) and DIPEA (0.13 mL, 0.72 mmol) were added to a solution of 2-(4-oxo-3,4-dihydrophthalazin-1-yl)acetic acid **16** (34 mg, 0.14 mmol) and 2-methoxy-5-((1,2,4,5-tetrahydro-3H-1,5-methanobenzo[d]azepin-3-yl)sulfonyl)aniline **33n** (55 mg, 0.14 mmol) in DMF (2 mL). The reaction mixture was heated to 70 °C over 45 minutes. The reaction mixture was diluted with EtOAc (25 mL), washed with water (3 x 25 mL) and brine (25 mL), dried (MgSO_4) and concentrated *in vacuo*. Purification by flash chromatography (50 – 80% EtOAc in PET, 0 – 5% methanol in DCM) followed by reverse phase flash chromatography (0 – 50% acetonitrile in water (+ 0.1% NH_3)) afforded **49n** (26 mg, 33% yield).

LCMS (ESI+): m/z 531.3 $[\text{M} + \text{H}]^+$, (ESI-): m/z 529.3 $[\text{M} - \text{H}]^-$; rt 1.98 minutes, 96%; ^1H NMR (500 MHz, $(\text{CD}_3)_2\text{SO}$) 12.64 (1H, s), 9.82 (1H, s), 8.28 (1H, d, J = 7.9 Hz), 8.22 (1H, d, J = 1.6 Hz), 8.01-7.92 (2H, m), 7.87 (1H, ddd, J = 8.0, 6.3, 1.9 Hz), 7.22-7.06 (6H, m), 4.23 (2H, s), 3.97 (3H, s), 3.40 (2H, d, J = 10.6 Hz), 3.18-3.12 (2H, m), 2.80 (2H, d, J = 10.8 Hz), 2.11-2.01 (1H, m), 1.51 (1H, d, J = 10.9 Hz); ^{13}C NMR (125 MHz, $(\text{CD}_3)_2\text{SO}$) 168.2, 159.5, 152.1, 144.3, 142.1, 133.5, 131.6, 129.8, 128.1, 127.6, 127.5, 126.9, 125.9, 125.6, 123.6, 122.4, 119.6, 111.0, 56.3, 49.2, 41.2 (2 peaks missing); $\nu_{\text{max}}/\text{cm}^{-1}$ 3177, 3020, 2937, 2908, 2851, 1673, 1646 (C=O), 1597, 1540; HRMS (ESI)+: m/z calculated for $[\text{C}_{28}\text{H}_{26}\text{N}_4\text{O}_5\text{S} + \text{Na}]^+$ = 553.1516, observed 553.1517.

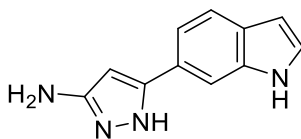
5-(3-Methoxyphenyl)-1H-pyrazol-3-amine (**56**)



Hydrazine monohydrate (1.1 mL, 23 mmol) was added to a suspension of 3-(3-methoxyphenyl)-3-oxopropanenitrile **58** (0.400 g, 2.28 mmol) in ethanol (10 mL). The reaction mixture was heated under reflux for 6 hours, then quenched with excess acetone at rt and concentrated *in vacuo*. Purification by flash chromatography (0 – 50% EtOAc in PET, 0 – 6% methanol in DCM) afforded **56** (0.314 g, 73% yield).

LCMS (ESI+): m/z 190.2 $[M + H]^+$, rt 1.21 minutes, >99%; 1H NMR (500 MHz, $CDCl_3$) 7.28 (1H, t, $J = 8.0$ Hz), 7.13 (1H, dt, $J = 7.7, 1.2$ Hz), 7.09 (1H, t, $J = 2.0$ Hz), 6.86 (1H, ddd, $J = 8.2, 2.6, 0.8$ Hz), 5.89 (1H, s), 3.80 (3H, s); ^{13}C NMR (125 MHz, $CDCl_3$) 160.1, 154.5, 145.7, 131.8, 130.1, 118.0, 114.0, 111.2, 90.7, 55.4; ν_{max}/cm^{-1} 3200 (br, N-H), 2837, 1612, 1589, 1567, 1506; HRMS (ESI+): m/z calculated for $[C_{10}H_{11}N_3O + H]^+$ = 190.0975, observed 190.0972.

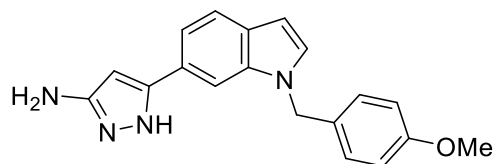
5-(1H-Indol-6-yl)-1H-pyrazol-3-amine (**62**)



Hydrazine monohydrate (0.101 mL, 0.814 mmol) was added to a solution of 3-(1H-indol-6-yl)-3-oxopropanenitrile **68** (50 mg, 0.27 mmol) in ethanol (5 mL). The reaction mixture was heated under reflux for 11 hours. Further hydrazine monohydrate (0.101 mL, 0.814 mmol) was added to the reaction mixture. The reaction mixture was heated under reflux for 1 hour, then concentrated *in vacuo*. Purification by flash chromatography (0 – 10% methanol in DCM) afforded **62** (32 mg, 59% yield).

LCMS (ESI+): m/z 199.1 $[M + H]^+$, (ESI-): m/z 197.0 $[M - H]^-$, rt 1.98 minutes, 100%; 1H NMR (400 MHz, CD_3OD) 7.65 (1H, s), 7.56 (1H, d, $J = 8.3$ Hz), 7.30 (1H, dd, $J = 8.3, 1.5$ Hz), 7.26 (1H, d, $J = 3.1$ Hz), 6.44 (1H, dd, $J = 3.1, 0.7$ Hz), 5.93 (1H, s); ^{13}C NMR (125 MHz, CD_3CN) 155.2, 147.7, 137.1, 128.8, 126.9, 125.5, 121.4, 108.8, 102.5, 89.3 (1 peak missing); ν_{max}/cm^{-1} 3389 (N-H), 3250 (br, N-H), 1616, 1584, 1561, 1516; HRMS (ESI+): m/z calculated for $[C_{11}H_{10}N_4 + H]^+$ = 199.0978, observed 199.0973.

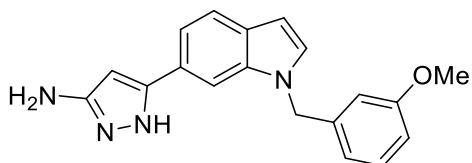
5-(1-(4-Methoxybenzyl)-1H-indol-6-yl)-1H-pyrazol-3-amine (**66a**)



Hydrazine monohydrate (42 μ L, 0.67 mmol) was added to a solution of 3-(1-(4-methoxybenzyl)-1H-indol-6-yl)-3-oxopropanenitrile **65a** (0.200 g, 0.611 mmol) in ethanol (5 mL). The reaction mixture was heated under reflux for 30 minutes, then further hydrazine monohydrate (0.114 mL, 1.83 mmol) was added at rt. The reaction mixture was heated under reflux for 4 hours, then quenched with excess acetone at rt and concentrated *in vacuo*. Purification by flash chromatography (0 – 10% methanol in DCM) afforded **66a** (0.120 g, 62% yield).

LCMS (ESI+): m/z 319.3 [M + H]⁺, rt 1.65 minutes, >99%; ¹H NMR (500 MHz, CDCl₃) 7.63 (1H, d, J = 8.3 Hz), 7.46 (1H, s), 7.30-7.25 (1H, m), 7.12 (1H, d, J = 3.1 Hz), 7.06-7.02 (2H, m), 6.83-6.78 (2H, m), 6.52 (1H, d, J = 3.0 Hz), 5.88 (1H, s), 5.22 (2H, s), 3.74 (3H, s); ¹³C NMR (125 MHz, CDCl₃) 159.3, 155.0, 146.7, 136.5, 129.5, 129.3, 129.1, 128.3, 123.8, 121.6, 117.7, 114.3, 106.8, 101.9, 90.5, 55.4, 49.7; $\nu_{\max}/\text{cm}^{-1}$ 3150 (br, N-H), 2927, 1610, 1585, 1510; HRMS (ESI+): m/z calculated for [C₁₉H₁₈N₄O + H]⁺ = 319.1553, observed 319.1557.

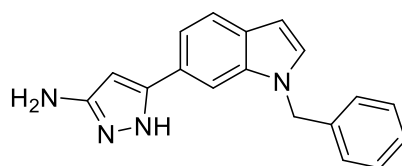
5-(1-(3-Methoxybenzyl)-1H-indol-6-yl)-1H-pyrazol-3-amine (**66b**)



Hydrazine monohydrate (0.104 mL, 2.14 mmol) was added to a solution of 3-(1-(3-methoxybenzyl)-1H-indol-6-yl)-3-oxopropanenitrile **65b** (65 mg, 0.21 mmol) in ethanol (4 mL). The reaction mixture was heated under reflux for 5 hours, then concentrated *in vacuo*. Purification by flash chromatography (0 – 100% EtOAc in PET, 0 – 10% methanol in DCM) was carried out, followed by reverse phase chromatography (0 – 40% acetonitrile in water (+ 0.1% formic acid)) with addition of NaHCO₃ solution (10 mL) to the combined fractions and extraction into DCM (3 x 25 mL). The combined organic extracts were washed (brine), dried (MgSO₄) and concentrated *in vacuo* to afford **66b** (27 mg, 40% yield).

LCMS (ESI+): m/z 319.2 $[M + H]^+$, rt 1.65 minutes, >99%; 1H NMR (500 MHz, $CDCl_3$) 7.66 (1H, d, $J = 8.3$ Hz), 7.42 (1H, s), 7.29-7.25 (1H, m), 7.21 (1H, t, $J = 7.9$ Hz), 7.17 (1H, d, $J = 3.2$ Hz), 6.80 (1H, dd, $J = 8.2, 2.4$ Hz), 6.69 (1H, d, $J = 7.6$ Hz), 6.66-6.63 (1H, m), 6.56 (1H, dd, $J = 3.2, 0.7$ Hz), 5.89 (1H, s), 5.30 (2H, s), 3.72 (3H, s); ^{13}C NMR (125 MHz, $CDCl_3$) 160.2, 155.2, 146.6, 138.9, 136.6, 130.1, 129.8, 129.2, 123.8, 121.7, 119.1, 117.7, 113.0, 112.8, 106.8, 102.1, 90.7, 55.3, 50.2; ν_{max}/cm^{-1} 3150 (br, N-H), 1585, 1505; HRMS (ESI+): m/z calculated for $[C_{19}H_{18}N_4O + H]^+ = 319.1553$, observed 319.1542.

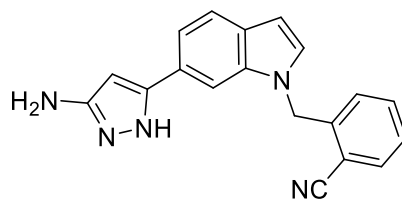
5-(1-Benzyl-1H-indol-6-yl)-1H-pyrazol-3-amine (66c)



Hydrazine monohydrate (0.271 mL, 5.58 mmol) was added to a solution of 3-(1-benzyl-1H-indol-6-yl)-3-oxopropanenitrile **65c** (0.170 g, 0.558 mmol) in ethanol (10 mL). The reaction mixture was heated under reflux for 8 hours, then quenched with excess acetone at rt and concentrated *in vacuo*. Purification by flash chromatography (0 – 10% methanol in DCM) afforded **66c** (50 mg, 31% yield).

LCMS (ESI+): m/z 289.3 $[M + H]^+$, rt 1.65 minutes, >99%; 1H NMR (400 MHz, CD_3OD) 7.63 (1H, s), 7.58 (1H, d, $J = 8.3$ Hz), 7.34 (1H, dd, $J = 8.4, 1.5$ Hz), 7.31-7.20 (4H, m), 7.16 (2H, d, $J = 7.2$ Hz), 6.50 (1H, d, $J = 3.1$ Hz), 5.90 (1H, s), 5.42 (2H, s); ^{13}C NMR (125 MHz, CD_3OD) 155.6, 148.7, 139.5, 137.9, 130.7, 130.4, 129.7, 128.5, 127.9, 125.5, 122.0, 118.5, 107.7, 102.6, 90.2, 50.7; ν_{max}/cm^{-1} 2920, 2849, 1583, 1503; HRMS (ESI+): m/z calculated for $[C_{18}H_{16}N_4 + H]^+ = 289.1448$, observed 289.1446.

2-((6-(3-Amino-1H-pyrazol-5-yl)-1H-indol-1-yl)methyl)benzonitrile (66d)

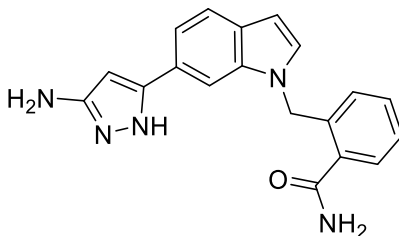


n-Butyllithium (1.6 M in hexanes, 4.09 mL, 6.54 mmol) was added dropwise at -78 °C to a mixture of acetonitrile (0.68 mL, 13 mmol) and toluene (5 mL). The reaction mixture was stirred at -78 °C over 30 minutes. A solution of methyl 1-(2-cyanobenzyl)-1H-indole-6-carboxylate **64d** (0.380 g, 1.31 mmol) in toluene (5 mL) was added dropwise at -78 °C over 30 minutes. The reaction mixture was stirred at -78 °C over 1 hour, then aqueous HCl (1 M, 15 mL) was added dropwise at 0 °C. The product was extracted into

EtOAc (3 x 25 mL). The combined organic extracts were washed (brine), dried (MgSO₄) and concentrated *in vacuo*. Purification by flash chromatography (0 – 80% EtOAc in PET) was attempted. Ethanol (20 mL) was added to the crude residue, followed by hydrazine monohydrate (0.50 mL, 10 mmol). The reaction mixture was heated under reflux for 5 hours, then quenched with excess acetone at rt and concentrated *in vacuo*. Purification by flash chromatography (0 – 10% methanol in DCM) afforded **66d** (73 mg, 18% yield), with 14 mg subjected to further purification by flash chromatography (0 – 100% EtOAc in PET, 0 – 5% methanol in DCM).

LCMS (ESI+): m/z 314.3 [M + H]⁺, rt 1.58 minutes, 96%; ¹H NMR (400 MHz, CD₃OD) 7.77 (1H, dd, J = 7.6, 1.1 Hz), 7.63 (1H, s), 7.61 (1H, d, J = 8.4 Hz), 7.49 (1H, td, J = 7.7, 1.2 Hz), 7.44-7.35 (2H, m), 7.34 (1H, d, J = 3.2 Hz), 6.90 (1H, d, J = 7.9 Hz), 6.56 (1H, d, J = 3.2 Hz), 5.92 (1H, s), 5.64 (2H, s); ¹³C NMR (125 MHz, CD₃OD) 155.5, 148.5, 142.9, 137.9, 134.6, 134.2, 130.8, 130.4, 129.4, 128.8, 126.0, 122.2, 118.8, 118.3, 112.0, 107.5, 103.3, 90.2 (1 peak missing); $\nu_{\max}/\text{cm}^{-1}$ 3200 (br, N-H), 2225 (C≡N), 1585, 1505; HRMS (ESI+): m/z calculated for [C₁₉H₁₅N₅ + H]⁺ = 314.1400, observed 314.1402.

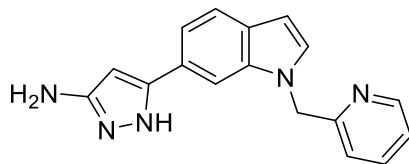
2-((6-(3-Amino-1H-pyrazol-5-yl)-1H-indol-1-yl)methyl)benzamide (66e)



A suspension of 2-((6-(3-amino-1H-pyrazol-5-yl)-1H-indol-1-yl)methyl)benzamide **66d** (50 mg, 0.16 mmol) in aqueous NaOH (10 M, 4 mL) was heated under reflux for 7 hours. The reaction mixture was adjusted to pH 3 and extracted into DCM/methanol (10:1, 3 x 75 mL). The combined organic extracts were washed (brine), dried (MgSO₄) and concentrated *in vacuo*. Purification by reverse phase flash chromatography (0 – 35% acetonitrile in water) afforded **66e** (15 mg, 28% yield).

LCMS (ESI+): m/z 332.3 [M + H]⁺, (ESI-): m/z 330.1 [M - H]⁻, rt 1.47 minutes, >99%; ¹H NMR (500 MHz, CD₃OD) 7.62-7.52 (3H, m), 7.37-7.24 (4H, m), 6.82-6.75 (1H, m), 6.51 (1H, d, J = 3.0 Hz), 5.90 (1H, s), 5.64 (2H, s); ¹³C NMR (125 MHz, CD₃OD) 174.6, 138.0, 137.7, 135.9, 131.6, 131.2, 130.3, 128.7, 128.5, 125.3 (br), 122.0, 118.5, 107.7, 102.7, 90.5 (br), 48.3 (3 peaks missing); $\nu_{\max}/\text{cm}^{-1}$ 3200 (br), 1635 (C=O), 1505; HRMS (ESI+): m/z calculated for [C₁₉H₁₇N₅O + H]⁺ = 332.1506, observed 332.1504.

5-(1-(Pyridin-2-ylmethyl)-1H-indol-6-yl)-1H-pyrazol-3-amine (**66f**)



Hydrazine monohydrate (0.300 mL, 6.17 mmol) was added to a solution of 3-oxo-3-(1-(pyridin-2-ylmethyl)-1H-indol-6-yl)propanenitrile **65f** (0.170 g, 0.617 mmol) in ethanol (15 mL). The reaction mixture was heated under reflux for 13 hours, then concentrated *in vacuo*. Purification by flash chromatography (0 – 20% methanol in DCM) afforded **66f** (73 mg, 41% yield).

LCMS (ESI+): m/z 290.3 $[M + H]^+$, rt 1.43 minutes, 100%; 1H NMR (400 MHz, CD_3OD) 8.56-8.50 (1H, m), 7.68 (1H, td, $J = 7.7, 1.8$ Hz), 7.63-7.58 (2H, m), 7.38-7.33 (2H, m), 7.28 (1H, dd, $J = 7.6, 5.0$ Hz), 6.89 (1H, d, $J = 7.9$ Hz), 6.55 (1H, d, $J = 3.1$ Hz), 5.90 (1H, s), 5.52 (2H, s); ^{13}C NMR (125 MHz, CD_3OD) 158.8, 155.7 (br), 150.0, 148.4 (br), 139.2, 137.9, 130.9, 130.4, 125.8, 124.1, 122.7, 122.2, 118.7, 107.5, 103.1, 90.2, 52.2; ν_{max}/cm^{-1} 3150 (br, N-H), 2916, 1597, 1585, 1504; HRMS (ESI+): m/z calculated for $[C_{17}H_{15}N_5 + H]^+ = 290.1400$, observed 290.1405.

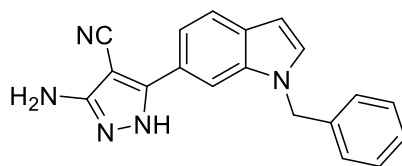
3-Amino-5-(1H-indol-6-yl)-1H-pyrazole-4-carbonitrile (**70**)



Hydrazine monohydrate (0.163 mL, 3.36 mmol) was added to a suspension of 3-amino-4,4,4-trichloro-2-(1H-indole-6-carbonyl)but-2-enenitrile **69** (0.690 g, 2.10 mmol) in ethanol (10 mL). The reaction mixture was heated under reflux for 22 hours, then quenched with excess acetone at rt and concentrated *in vacuo*. Purification by flash chromatography (0 – 100% EtOAc in PET) afforded **70** (0.113 g, 24% yield).

LCMS (ESI+): m/z 224.2 $[M + H]^+$, (ESI-): m/z 222.1 $[M - H]^-$, rt 1.50 minutes, >99%; 1H NMR (400 MHz, CD_3OD) 7.89 (1H, s), 7.63 (1H, d, $J = 8.0$ Hz), 7.45 (1H, d, $J = 7.0$ Hz), 7.33 (1H, d, $J = 2.1$ Hz), 6.50 (1H, d, $J = 2.7$ Hz); ^{13}C NMR (125 MHz, CD_3OD) 137.5, 130.6, 127.8, 121.7, 118.5, 116.9, 110.6, 102.6 (4 peaks missing); ν_{max}/cm^{-1} 3411 (N-H), 3200 (br, N-H), 2221 ($C\equiv N$), 1634, 1584, 1527; HRMS (ESI+): m/z calculated for $[C_{12}H_9N_5 + H]^+ = 224.0931$, observed 224.0935.

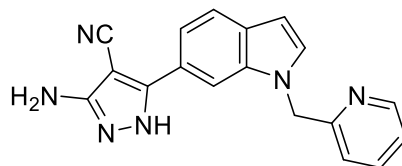
3-Amino-5-(1-benzyl-1H-indol-6-yl)-1H-pyrazole-4-carbonitrile (71c)



Trichloroacetonitrile (0.168 mL, 1.67 mmol) was added to a suspension of 3-(1-benzyl-1H-indol-6-yl)-3-oxopropanenitrile **65c** (0.170 g, 0.558 mmol) and sodium acetate (0.229 g, 2.79 mmol) in ethanol (5 mL). The reaction mixture was stirred over 9 hours, then concentrated *in vacuo*, diluted with water (20 mL) and extracted into DCM (3 x 25 mL). The combined organic extracts were washed (brine), dried (MgSO₄) and concentrated *in vacuo*. The crude residue was dissolved in ethanol (10 mL) and hydrazine monohydrate (0.271 mL, 5.58 mmol) was added. The reaction mixture was heated under reflux for 5 hours, then quenched with excess acetone at rt and concentrated *in vacuo*. Purification by flash chromatography (0 – 100% EtOAc in PET) afforded **71c** (78 mg, 45% yield).

LCMS (ESI+): m/z 314.2 [M + H]⁺, (ESI-): m/z 312.1 [M - H]⁻, rt 1.84 minutes, 100%; ¹H NMR (500 MHz, CDCl₃) 7.72 (1H, s), 7.67 (1H, d, J = 8.3 Hz), 7.41 (1H, dd, J = 8.2, 1.5 Hz), 7.29-7.19 (4H, m), 7.13-7.08 (2H, m), 6.57 (1H, dd, J = 3.1, 0.8 Hz), 5.26 (2H, s), 4.12 (2H, br s); ¹³C NMR (125 MHz, CDCl₃) 157.0, 150.1, 136.9, 136.2, 130.8, 130.4, 129.0, 128.0, 127.1, 122.0, 120.8, 117.6, 115.3, 108.2, 102.3, 76.1, 50.4; ν_{max}/cm⁻¹ 3200 (br, N-H), 2211 (C≡N), 1621, 1582, 1524, 1501; HRMS (ESI+): m/z calculated for [C₁₉H₁₅N₅ + H]⁺ = 314.1400, observed 314.1404.

3-Amino-5-(1-(pyridin-2-ylmethyl)-1H-indol-6-yl)-1H-pyrazole-4-carbonitrile (71f)

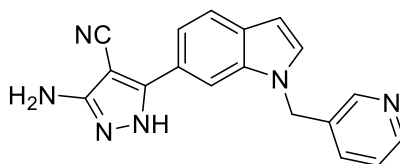


Trichloroacetonitrile (0.186 mL, 1.85 mmol) was added to a suspension of 3-oxo-3-(1-(pyridin-2-ylmethyl)-1H-indol-6-yl) propanenitrile **65f** (0.170 g, 0.617 mmol) and sodium acetate (0.253 g, 3.09 mmol) in ethanol (5 mL). The reaction mixture was stirred over 90 minutes. The reaction mixture was concentrated *in vacuo*, then water (20 mL) was added. The intermediate was extracted into DCM (3 x 25 mL). The combined organic extracts were washed (brine), dried (MgSO₄) and concentrated *in vacuo*. The crude residue was dissolved in ethanol (10 mL) and hydrazine monohydrate (0.300 mL, 6.17 mmol) was added.

The reaction mixture was heated under reflux for 15 hours, then concentrated *in vacuo*. Purification by flash chromatography (0 - 100% EtOAc in PET, 0 – 10% methanol in DCM) afforded **71f** (0.121 g, 62% yield).

LCMS (ESI+): m/z 315.2 $[M + H]^+$, (ESI-): m/z 313.1 $[M - H]^-$, rt 1.53 minutes, 100%; 1H NMR (400 MHz, $CDCl_3$) 8.46 (1H, d, $J = 5.0$ Hz), 7.70 (1H, s), 7.67 (1H, d, $J = 8.3$ Hz), 7.62-7.53 (2H, m), 7.31 (1H, d, $J = 3.1$ Hz), 7.14 (1H, dd, $J = 7.6, 4.9$ Hz), 6.91 (1H, d, $J = 7.8$ Hz), 6.58 (1H, d, $J = 3.2$ Hz), 5.38 (2H, s); ^{13}C NMR (125 MHz, $CDCl_3$) 157.8, 156.7, 149.2, 149.1, 137.8, 136.1, 130.9, 130.4, 123.3, 122.1, 121.8, 121.0, 118.1, 115.6, 107.6, 102.7, 76.2, 52.3; ν_{max}/cm^{-1} 3200 (br, N-H), 2211 ($C\equiv N$), 1621, 1592, 1503; HRMS (ESI+): m/z calculated for $[C_{18}H_{14}N_6 + H]^+ = 315.1353$, observed 315.1338.

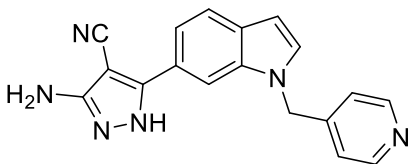
3-Amino-5-(1-(pyridin-3-ylmethyl)-1H-indol-6-yl)-1H-pyrazole-4-carbonitrile (71g)



Trichloroacetonitrile (0.647 mL, 6.45 mmol) was added to a suspension of 3-oxo-3-(1-(pyridin-3-ylmethyl)-1H-indol-6-yl)propanenitrile **65g** (0.592 g, 2.15 mmol) and sodium acetate (0.882 g, 10.8 mmol) in ethanol (20 mL). The reaction mixture was stirred over 13 hours, then concentrated *in vacuo*, diluted with water (20 mL) and extracted into DCM (3 x 25 mL). The combined organic extracts were washed (brine), dried ($MgSO_4$) and concentrated *in vacuo*. The crude residue was dissolved in ethanol (20 mL) and hydrazine monohydrate (1.1 mL, 22 mmol) was added. The reaction mixture was heated under reflux for 21 hours, then quenched with excess acetone at rt and concentrated *in vacuo*. Purification by flash chromatography (0 – 100% EtOAc in DCM, 5% methanol in DCM) afforded **71g** (0.367 g, 54% yield).

LCMS (ESI+): m/z 315.2 $[M + H]^+$, (ESI-): m/z 313.1 $[M - H]^-$, rt 1.38 minutes, >99%; 1H NMR (400 MHz, $(CD_3)_2SO$) 12.09 (1H, br s), 8.56 (1H, s), 8.46 (1H, dd, $J = 4.7, 1.3$ Hz), 7.90 (1H, s), 7.74-7.56 (3H, m), 7.50 (1H, d, $J = 8.2$ Hz), 7.32 (1H, dd, $J = 7.7, 4.8$ Hz), 6.55 (1H, d, $J = 2.8$ Hz), 6.26 (2H, br s), 5.49 (2H, s); ^{13}C NMR (100 MHz, $(CD_3)_2SO$) 148.8, 148.5, 135.4, 135.0, 133.5, 130.6, 128.9, 123.7, 120.9, 117.5, 116.5, 107.4, 101.6, 46.8 (4 peaks missing); ν_{max}/cm^{-1} 3345 (N-H), 3100 (br, N-H), 2215 ($C\equiv N$), 1662, 1600, 1502; HRMS (ESI-): m/z calculated for $[C_{18}H_{14}N_6 - H]^- = 313.1207$, observed 313.1195.

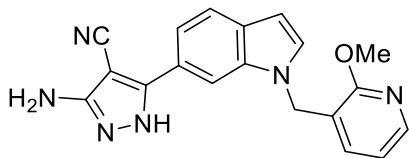
3-Amino-5-(1-(pyridin-4-ylmethyl)-1H-indol-6-yl)-1H-pyrazole-4-carbonitrile (71h)



Trichloroacetonitrile (0.309 mL, 3.08 mmol) was added to a suspension of 3-oxo-3-(1-(pyridin-4-ylmethyl)-1H-indol-6-yl)propanenitrile **65h** (0.283 g, 1.03 mmol) and sodium acetate (0.422 g, 5.14 mmol) in ethanol (20 mL). The reaction mixture was stirred over 13 hours, then concentrated *in vacuo*, diluted with water (20 mL) and extracted into DCM (4 x 25 mL). The combined organic extracts were washed (brine), dried (MgSO₄) and concentrated *in vacuo*. The crude residue was dissolved in ethanol (20 mL) and hydrazine monohydrate (0.500 mL, 10.3 mmol) was added. The reaction mixture was heated under reflux for 21 hours, then quenched with excess acetone at rt and concentrated *in vacuo*. Purification by flash chromatography (0 – 100% EtOAc in DCM, 8% methanol in DCM) afforded **71h** (0.183 g, 57% yield).

LCMS (ESI+): m/z 315.2 [M + H]⁺, (ESI-): m/z 313.1 [M - H]⁻, rt 1.35 minutes, >99%; ¹H NMR (500 MHz, CD₃OD) 8.40-8.36 (2H, m), 7.73 (1H, s), 7.66 (1H, d, J = 8.3 Hz), 7.53 (1H, dd, J = 8.2, 1.1 Hz), 7.37 (1H, d, J = 3.2 Hz), 7.12-7.08 (2H, m), 6.58 (1H, dd, J = 3.2, 0.8 Hz), 5.43 (2H, s); ¹³C NMR (125 MHz, CD₃OD) 157.8, 152.5, 150.3, 149.7, 137.4, 131.7, 131.3, 124.6, 123.3, 122.4, 119.2, 116.9, 108.8, 103.3, 73.9, 49.7; ν_{max}/cm⁻¹ 2204 (C≡N), 1605, 1554, 1500; HRMS (ESI+): m/z calculated for [C₁₈H₁₄N₆ + H]⁺ = 315.1353, observed 315.1350.

3-Amino-5-(1-((2-methoxypyridin-3-yl)methyl)-1H-indol-6-yl)-1H-pyrazole-4-carbonitrile (71i)

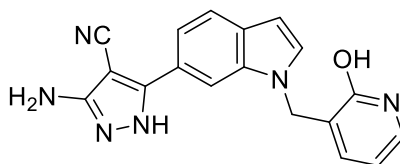


Trichloroacetonitrile (0.122 mL, 1.22 mmol) was added to a suspension of 3-(1-((2-methoxypyridin-3-yl)methyl)-1H-indol-6-yl)-3-oxopropanenitrile **65i** (0.124 g, 0.406 mmol) and sodium acetate (0.167 g, 2.03 mmol) in ethanol (5 mL). The reaction mixture was stirred over 15 hours, then concentrated *in vacuo*, diluted with NaHCO₃ solution (25 mL) and extracted into DCM (3 x 25 mL). The combined organic extracts were washed (brine), dried (MgSO₄) and concentrated *in vacuo*. The crude residue was dissolved in ethanol (10 mL) and hydrazine monohydrate (0.198 mL, 4.06 mmol) was added. The reaction mixture was

heated under reflux for 18 hours, then quenched with excess acetone at rt and concentrated *in vacuo*. Purification by flash chromatography (0 – 70% EtOAc in PET) afforded **71i** (85 mg, 61% yield).

LCMS (ESI+): m/z 345.2 $[M + H]^+$, (ESI-): m/z 343.1 $[M - H]^-$, rt 1.83 minutes, 97%; 1H NMR (400 MHz, $(CD_3)_2SO$) 12.00 (1H, br s), 8.07 (1H, dd, $J = 5.0, 1.6$ Hz), 7.93-7.79 (1H, m), 7.76-7.42 (3H, m), 7.15 (1H, dd, $J = 7.3, 1.8$ Hz), 6.88 (1H, dd, $J = 7.2, 5.0$ Hz), 6.62-6.48 (1H, m), 6.39 (1H, br s), 5.37 (2H, s), 3.95 (3H, s); ^{13}C NMR (100 MHz, $(CD_3)_2SO$) 160.7, 154.6, 151.2, 145.9, 136.8, 135.6, 130.8, 128.5, 125.6, 120.6, 120.1, 117.5, 117.2, 116.7, 107.3, 101.2, 69.6, 53.4, 44.2; ν_{max}/cm^{-1} 3200 (br, N-H), 2918, 2210 ($C\equiv N$), 1622, 1599, 1584, 1526, 1500; HRMS (ESI+): m/z calculated for $[C_{19}H_{16}N_6O + Na]^+ = 367.1278$, observed 367.1277.

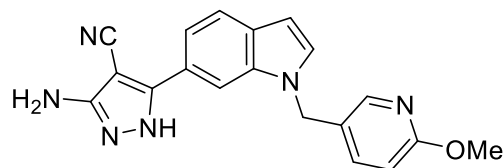
3-Amino-5-(1-((2-hydroxypyridin-3-yl)methyl)-1H-indol-6-yl)-1H-pyrazole-4-carbonitrile (71j)



LiCl (12 mg, 0.29 mmol) and *p*-toluenesulfonic acid monohydrate (55 mg, 0.29 mmol) were added to a solution of 3-amino-5-(1-((2-methoxypyridin-3-yl)methyl)-1H-indol-6-yl)-1H-pyrazole-4-carbonitrile **71i** (20 mg, 0.058 mmol) in DMF (1 mL). The reaction mixture was heated to 120 °C over 25 minutes, then diluted with EtOAc (100 mL), washed with water (3 x 100 mL) and brine (100 mL), dried ($MgSO_4$) and concentrated *in vacuo*. Purification by flash chromatography (50 – 100% EtOAc in PET, 0 – 10% methanol in DCM) afforded **71j** (10 mg, 51% yield).

LCMS (ESI+): m/z 331.2 $[M + H]^+$, (ESI-): m/z 329.1 $[M - H]^-$, rt 1.55 minutes, 97%; 1H NMR (500 MHz, CD_3OD) 7.82 (1H, s), 7.66 (1H, d, $J = 8.1$ Hz), 7.51 (1H, d, $J = 7.5$ Hz), 7.45 (1H, s), 7.32 (1H, dd, $J = 6.5, 2.0$ Hz), 7.08 (1H, d, $J = 4.8$ Hz), 6.55 (1H, d, $J = 2.8$ Hz), 6.25 (1H, t, $J = 6.7$ Hz), 5.28 (2H, s); ^{13}C NMR (125 MHz, CD_3OD) 164.1, 140.1, 137.4, 135.0, 132.1, 131.4, 129.6, 122.3, 119.0, 116.9, 109.0, 108.0, 102.7, 46.2 (4 peaks missing); ν_{max}/cm^{-1} 3150 (br, N-H/O-H), 2925, 2207 ($C\equiv N$), 1647, 1611, 1564, 1529, 1501; HRMS (ESI+): m/z calculated for $[C_{18}H_{14}N_6O + Na]^+ = 353.1121$, observed 353.1105.

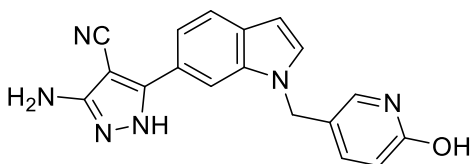
3-Amino-5-(1-((6-methoxypyridin-3-yl)methyl)-1H-indol-6-yl)-1H-pyrazole-4-carbonitrile (71k)



Trichloroacetonitrile (0.114 mL, 1.14 mmol) was added to a suspension of 3-(1-((6-methoxypyridin-3-yl)methyl)-1H-indol-6-yl)-3-oxopropanenitrile **65k** (0.121 g, 0.380 mmol) and sodium acetate (0.156 g, 1.90 mmol) in ethanol (5 mL). The reaction mixture was stirred over 18 hours, then concentrated *in vacuo*, diluted with NaHCO₃ solution (20 mL) and extracted into DCM (3 x 25 mL). The combined organic extracts were washed (brine), dried (MgSO₄) and concentrated *in vacuo*. The crude residue was dissolved in ethanol (10 mL) and hydrazine monohydrate (0.185 mL, 3.80 mmol) was added. The reaction mixture was heated under reflux for 7 hours, then quenched with excess acetone at rt and concentrated *in vacuo*. Purification by flash chromatography (0 – 100% EtOAc in PET) afforded **71k** (62 mg, 47% yield).

LCMS (ESI+): m/z 345.2 [M + H]⁺, (ESI-): m/z 343.1 [M - H]⁻, rt 1.75 minutes, >99%; ¹H NMR (500 MHz, CD₃OD) 8.07 (1H, d, J = 2.5 Hz), 7.91-7.87 (1H, m), 7.64 (1H, dd, J = 8.3, 0.5 Hz), 7.55 (1H, dd, J = 8.8, 2.5 Hz), 7.51 (1H, dd, J = 8.2, 1.5 Hz), 7.40 (1H, d, J = 3.2 Hz), 6.72 (1H, dd, J = 8.6, 0.5 Hz), 6.55 (1H, dd, J = 3.1, 0.8 Hz), 5.36 (2H, s), 3.85 (3H, s); ¹³C NMR (125 MHz, CD₃OD) 165.3, 157.9, 152.6, 146.4, 139.8, 137.3, 131.4, 131.2, 127.9, 124.3, 122.3, 118.9, 117.0, 111.9, 108.9, 103.0, 74.0, 54.2, 47.9; $\nu_{\max}/\text{cm}^{-1}$ 2942, 2211 (C≡N), 1676, 1608, 1573; HRMS (ESI+): m/z calculated for [C₁₉H₁₆N₆O + Na]⁺ = 367.1278, observed 367.1278.

3-Amino-5-(1-((6-hydroxypyridin-3-yl)methyl)-1H-indol-6-yl)-1H-pyrazole-4-carbonitrile (71l)

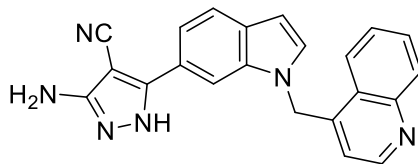


LiCl (26 mg, 0.61 mmol) and *p*-toluenesulfonic acid monohydrate (0.116 g, 0.610 mmol) were added to a solution of 3-amino-5-(1-((6-methoxypyridin-3-yl)methyl)-1H-indol-6-yl)-1H-pyrazole-4-carbonitrile **71k** (42 mg, 0.12 mmol) in DMF (1 mL). The reaction mixture was heated to 120 °C over 25 minutes, then diluted with EtOAc (100 mL), washed with water (3 x 100 mL) and brine (100 mL), dried (MgSO₄) and concentrated *in vacuo*. Purification by flash chromatography (50 – 100% EtOAc in PET, 0 – 12% methanol in DCM) afforded **71l** (19 mg, 47% yield).

LCMS (ESI+): m/z 331.2 [M + H]⁺, (ESI-): m/z 329.1 [M - H]⁻, rt 1.47 minutes, >99%; ¹H NMR (500 MHz, (CD₃)₂SO) 12.01 (1H, br s), 11.54 (1H, br s), 7.94 (1H, s), 7.73-7.29 (5H, m), 6.51 (1H, d, J = 2.4 Hz), 6.39 (1H, br s), 6.26 (1H, d, J = 9.3 Hz), 5.15 (2H, s); ¹³C NMR (125 MHz, (CD₃)₂SO) 161.9, 141.0, 135.3, 133.9, 130.3, 128.8, 125.6, 120.8, 120.3, 117.4, 116.6, 114.6, 107.5, 101.4, 45.7 (3 peaks missing); $\nu_{\max}/\text{cm}^{-1}$ 3436,

3340, 3231, 2941, 2211 (C≡N), 1661, 1614, 1533; HRMS (ESI)⁺: m/z calculated for [C₁₈H₁₄N₆O + H]⁺ = 331.1302, observed 331.1289.

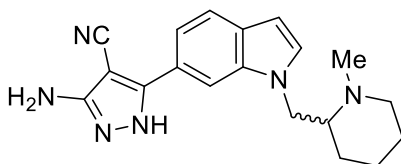
3-Amino-5-(1-(quinolin-4-ylmethyl)-1H-indol-6-yl)-1H-pyrazole-4-carbonitrile (71m)



Trichloroacetonitrile (92 μ L, 0.91 mmol) was added to a suspension of 3-oxo-3-(1-(quinolin-4-ylmethyl)-1H-indol-6-yl)propanenitrile **65m** (99 mg, 0.30 mmol) and sodium acetate (0.125 g, 1.52 mmol) in ethanol (10 mL). The reaction mixture was stirred over 36 hours, then diluted with water (50 mL) and extracted into DCM (3 x 50 mL). The combined organic extracts were washed (brine), dried (MgSO₄) and concentrated *in vacuo*. The crude residue was dissolved in ethanol (10 mL) and hydrazine monohydrate (0.148 mL, 3.04 mmol) was added. The reaction mixture was heated under reflux for 6 hours, then concentrated *in vacuo*. Purification by flash chromatography (50 – 100% EtOAc in PET) afforded **71m** (45 mg, 41% yield).

LCMS (ESI⁺): m/z 365.3 [M + H]⁺, (ESI⁻): m/z 363.2 [M - H]⁻, rt 1.55 minutes, >99%; ¹H NMR (400 MHz, CD₃OD) 8.61 (1H, d, J = 4.6 Hz), 8.23 (1H, d, J = 8.3 Hz), 8.07 (1H, d, J = 8.6 Hz), 7.81 (1H, t, J = 7.9 Hz), 7.76-7.65 (3H, m), 7.57 (1H, d, J = 7.9 Hz), 7.41 (1H, s), 6.65 (1H, d, J = 2.9 Hz), 6.62 (1H, d, J = 4.6 Hz), 5.99 (2H, s); ¹³C NMR (125 MHz, CD₃OD) 151.2, 148.5, 146.2, 137.8, 131.6, 131.2, 129.9, 128.6, 127.3, 124.3, 122.4, 119.6, 119.5, 117.0, 108.8, 103.6, 47.7 (5 peaks missing); ν_{\max} /cm⁻¹ 3150 (br, N-H), 2210 (C≡N), 1621, 1595, 1504; HRMS (ESI⁺): m/z calculated for [C₂₂H₁₆N₆ + Na]⁺ = 387.1329, observed 387.1328.

3-Amino-5-(1-((1-methylpiperidin-2-yl)methyl)-1H-indol-6-yl)-1H-pyrazole-4-carbonitrile (71n)

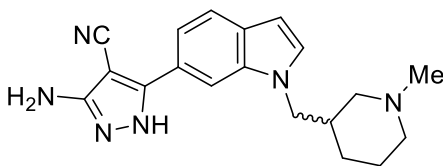


Trichloroacetonitrile (42 μ L, 0.42 mmol) was added to a suspension of 3-(1-((1-methylpiperidin-2-yl)methyl)-1H-indol-6-yl)-3-oxopropanenitrile **65n** (43 mg, 0.14 mmol) and sodium acetate (58 mg, 0.71 mmol) in ethanol (5 mL). The reaction mixture was stirred over 18 hours, then diluted with NaHCO₃ solution (12.5 mL) and water (12.5 mL) and extracted into DCM (3 x 25 mL). The combined organic extracts

were washed (brine), dried (MgSO₄) and concentrated *in vacuo*. The crude residue was dissolved in ethanol (5 mL) and hydrazine monohydrate (69 μL, 1.4 mmol) was added. The reaction mixture was heated under reflux for 24 hours, then concentrated *in vacuo*. Purification by flash chromatography (50 – 100% EtOAc in PET, 0 – 16% methanol in DCM) afforded **71n** (27 mg, 57% yield).

LCMS (ESI+): m/z 335.3 [M + H]⁺, (ESI-): m/z 333.2 [M - H]⁻, rt 1.22 minutes, >99%; ¹H NMR (500 MHz, CD₃OD) 7.90 (1H, s), 7.64 (1H, d, J = 8.4 Hz), 7.50 (1H, dd, J = 8.4, 0.9 Hz), 7.31 (1H, d, J = 3.2 Hz), 6.52 (1H, dd, J = 3.2, 0.6 Hz), 4.74 (1H, dd, J = 14.3, 4.7 Hz), 4.07 (1H, dd, J = 14.4, 9.5 Hz), 3.11-3.03 (1H, m), 2.97-2.87 (1H, m), 2.66 (3H, s), 2.51 (1H, td, J = 11.3, 3.4 Hz), 1.74-1.58 (3H, m), 1.41-1.18 (3H, m); ¹³C NMR (125 MHz, CD₃OD) 157.9 (br), 152.8 (br), 137.5, 131.8, 131.3, 124.4 (br), 122.4, 119.0, 117.2, 109.1, 102.9, 74.3 (br), 64.2, 57.7, 42.8, 29.5, 25.5, 23.7 (1 peak missing); ν_{max}/cm⁻¹ 3150 (br, N-H), 2927, 2210 (C≡N), 1623, 1589, 1525, 1503; HRMS (ESI+): m/z calculated for [C₁₉H₂₂N₆ + H]⁺ = 335.1979, observed 335.1971.

3-Amino-5-(1-((1-methylpiperidin-3-yl)methyl)-1H-indol-6-yl)-1H-pyrazole-4-carbonitrile (71o)

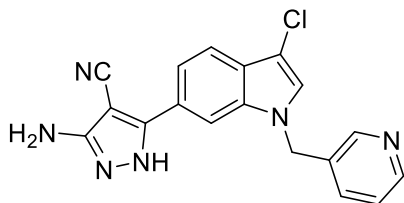


Trichloroacetonitrile (0.143 mL, 1.42 mmol) was added to a suspension of 3-(1-((1-methylpiperidin-3-yl)methyl)-1H-indol-6-yl)-3-oxopropanenitrile **65o** (0.140 g, 0.474 mmol) and sodium acetate (0.194 g, 2.37 mmol) in ethanol (3 mL). The reaction mixture was stirred over 3 hours 30 minutes, then diluted with NaHCO₃ solution (10 mL) and extracted into DCM (3 x 25 mL). The combined organic extracts were washed (brine), dried (MgSO₄) and concentrated *in vacuo*. The crude residue was dissolved in ethanol (5 mL) and hydrazine monohydrate (0.231 mL, 4.74 mmol) was added. The reaction mixture was heated under reflux for 15 hours, then concentrated *in vacuo*. Purification by flash chromatography (50 – 100% EtOAc in PET, 0 – 20% methanol in DCM) was carried out, followed by reverse phase chromatography (0 – 8% acetonitrile in water (+ 0.1% formic acid)) with addition of NaHCO₃ solution (40 mL) to the combined fractions and extraction into DCM/methanol (9:1, 4 x 50 mL). The combined organic extracts were washed (brine), dried (MgSO₄) and concentrated *in vacuo* to afford **71o** (61 mg, 38% yield).

LCMS (ESI+): m/z 335.3 [M + H]⁺, (ESI-): m/z 333.2 [M - H]⁻, rt 1.23 minutes, >99%; ¹H NMR (500 MHz, CDCl₃) 7.78 (1H, s), 7.63 (1H, d, J = 8.3 Hz), 7.41 (1H, dd, J = 8.2, 1.4 Hz), 7.11 (1H, d, J = 3.2 Hz), 6.49 (1H, dd, J = 3.0, 0.6 Hz), 4.44 (2H, br s), 4.05-3.91 (2H, m), 2.68 (1H, d, J = 9.6 Hz), 2.61 (1H, d, J = 10.4 Hz), 2.32-2.21 (1H, m), 2.17 (3H, s), 2.05-1.88 (1H, m), 1.77 (1H, t J = 10.2 Hz), 1.69-1.45 (3H, m), 1.06-0.92 (1H, m);

^{13}C NMR (125 MHz, CDCl_3) 157.1, 150.2, 136.2, 130.8, 130.1, 121.8, 121.1, 117.6, 115.7, 108.2, 101.7, 76.0, 59.4, 56.1, 50.4, 46.4, 37.0, 28.0, 24.5; $\nu_{\text{max}}/\text{cm}^{-1}$ 3200 (br, N-H), 2932, 2788, 2209 ($\text{C}\equiv\text{N}$), 1622, 1590, 1524, 1501; HRMS (ESI+): m/z calculated for $[\text{C}_{19}\text{H}_{22}\text{N}_6 + \text{H}]^+ = 335.1979$, observed 335.1983.

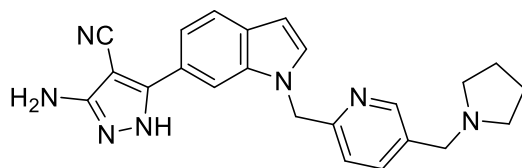
3-Amino-5-(3-chloro-1-(pyridin-3-ylmethyl)-1H-indol-6-yl)-1H-pyrazole-4-carbonitrile (72g)



N-Chlorosuccinimide (21 mg, 0.16 mmol) was added to a solution of 3-amino-5-(1-(pyridin-3-ylmethyl)-1H-indol-6-yl)-1H-pyrazole-4-carbonitrile **71g** (50 mg, 0.16 mmol) in DMF (1 mL). The reaction mixture was stirred over 6 hours, then further *N*-chlorosuccinimide (7 mg, 0.05 mmol) was added. The reaction mixture was stirred over 90 minutes, then diluted with EtOAc (100 mL), washed with NaHCO_3 solution (2 x 100 mL) and brine (100 mL), dried (MgSO_4) and concentrated *in vacuo*. Purification by flash chromatography (0 – 100% EtOAc in PET, 0 – 7% methanol in DCM), followed by reverse phase flash chromatography (0 – 50% acetonitrile in water), afforded **72g** (35 mg, 63% yield).

LCMS (ESI+): m/z 349.2 [$\text{M} + \text{H}$] $^+$, (ESI-): m/z 347.1 [$\text{M} - \text{H}$] $^-$, r_t 1.57 minutes, >99%; ^1H NMR (500 MHz, $(\text{CD}_3)_2\text{SO}$) 8.60 (1H, d, $J = 1.8$ Hz), 8.47 (1H, dd, $J = 4.8, 1.6$ Hz), 7.97 (1H, s), 7.88 (1H, s), 7.67 (1H, dt, $J = 7.9, 1.9$ Hz), 7.61 (1H, dd, $J = 8.4, 1.3$ Hz), 7.58 (1H, d, $J = 8.4$ Hz), 7.33 (1H, ddd, $J = 7.9, 4.7, 0.8$ Hz), 6.22 (2H, br s), 5.48 (2H, s); ^{13}C NMR (125 MHz, $(\text{CD}_3)_2\text{SO}$) 155.7, 149.6, 149.0, 148.6, 135.1, 134.6, 133.0, 127.2, 126.0, 125.4, 123.8, 118.4, 118.0, 116.5, 108.0, 103.5, 70.8, 47.0; $\nu_{\text{max}}/\text{cm}^{-1}$ 3344 (N-H), 2218 ($\text{C}\equiv\text{N}$), 1623, 1586, 1525; HRMS (ESI-): m/z calculated for $[\text{C}_{18}\text{H}_{13}\text{ClN}_6 - \text{H}]^- = 347.0817$, observed 347.0804.

3-Amino-5-(1-((5-(pyrrolidin-1-ylmethyl)pyridin-2-yl)methyl)-1H-indol-6-yl)-1H-pyrazole-4-carbonitrile (87)

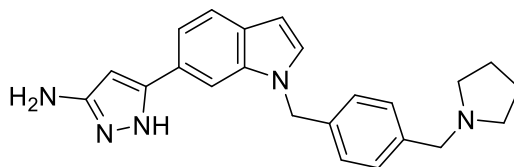


Trichloroacetonitrile (45 μL , 0.45 mmol) was added to a suspension of 3-oxo-3-(1-((5-(pyrrolidin-1-ylmethyl)pyridin-2-yl)methyl)-1H-indol-6-yl)propanenitrile **96** (66 mg, 0.15 mmol) and sodium acetate (61

mg, 0.75 mmol) in ethanol (4 mL). The reaction mixture was stirred over 36 hours, then Na₂CO₃ solution (12.5 mL) and water (12.5 mL) were added. The intermediate was extracted into DCM (2 x 25 mL) and methanol/DCM (9:1, 4 x 25 mL). The combined organic extracts were washed (brine), dried (MgSO₄) and concentrated *in vacuo*. The crude residue was dissolved in ethanol (5 mL) and hydrazine monohydrate (73 μL, 1.5 mmol) was added. The reaction mixture was heated under reflux for 24 hours, then quenched with excess acetone at rt and concentrated *in vacuo*. Purification by flash chromatography (0 – 20% methanol (+ 0.1% NH₃) in DCM) afforded **87** (3.6 mg, 6% yield).

LCMS (ESI+): m/z 398.3 [M + H]⁺, (ESI-): m/z 396.2 [M - H]⁻, rt 1.32 minutes, 100%; ¹H NMR (500 MHz, CD₃OD) 8.41 (1H, d, J = 1.9 Hz), 7.83 (1H, s), 7.66 (1H, d, J = 8.4 Hz), 7.64 (1H, dd, J = 8.1, 2.3 Hz), 7.51 (1H, d, J = 7.9 Hz), 7.47 (1H, d, J = 3.2 Hz), 7.42 (1H, d, J = 8.2 Hz), 6.58 (1H, d, J = 3.1 Hz), 5.49 (2H, s), 3.79 (2H, s), 2.67-2.59 (4H, m), 1.83-1.76 (4H, m); ¹³C NMR (125 MHz, CD₃OD) 158.3, 148.5, 137.5, 137.2, 134.2, 131.5, 125.0, 122.4, 119.0, 117.0, 109.0, 103.2, 61.9, 55.1, 48.2, 24.2 (5 peaks missing); ν_{max}/cm⁻¹ 3150 (br, N-H), 2918, 2209 (C≡N), 1602, 1501; HRMS (ESI+): m/z calculated for [C₂₃H₂₃N₇ + H]⁺ = 398.2088, observed 398.2082.

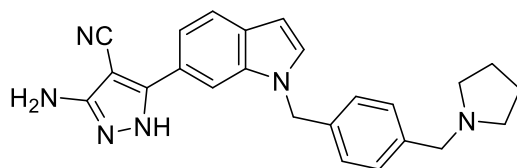
5-(1-(4-(Pyrrolidin-1-ylmethyl)benzyl)-1H-indol-6-yl)-1H-pyrazol-3-amine (88a)



Hydrazine monohydrate (0.157 mL, 3.22 mmol) was added to a solution of 3-oxo-3-(1-(4-(pyrrolidin-1-ylmethyl)benzyl)-1H-indol-6-yl)propanenitrile **102a** (0.115 g, 0.322 mmol) in ethanol (15 mL). The reaction mixture was heated under reflux for 12 hours, then concentrated *in vacuo*. Purification by reverse phase flash chromatography (0 – 100% acetonitrile in water, 0 – 65% methanol in acetonitrile) afforded **88a** (27 mg, 22% yield).

LCMS (ESI+): m/z 372.5 [M + H]⁺, rt 1.22 minutes, 96%; ¹H NMR (500 MHz, CDCl₃) 7.63 (1H, d, J = 8.2 Hz), 7.43 (1H, s), 7.30-7.25 (1H, m), 7.24 (2H, d, J = 8.2 Hz), 7.13 (1H, d, J = 3.1 Hz), 7.03 (2H, d, J = 8.1 Hz), 6.53 (1H, dd, J = 3.1, 0.5 Hz), 5.87 (1H, s), 5.26 (2H, s), 3.68 (2H, br s), 3.55 (2H, s), 2.53-2.38 (4H, m), 1.81-1.67 (4H, m); ¹³C NMR (125 MHz, CDCl₃) 155.0 (br), 146.7 (br), 139.1, 136.6, 135.9, 129.6, 129.5, 129.0, 126.9, 124.0, 121.5, 117.7, 106.8, 102.0, 90.5, 60.4, 54.3, 50.0, 23.5; ν_{max}/cm⁻¹ 3150 (br, N-H), 2963, 2789, 1587, 1505; HRMS (ESI+): m/z calculated for [C₂₃H₂₅N₅ + H]⁺ = 372.2183, observed 372.2173.

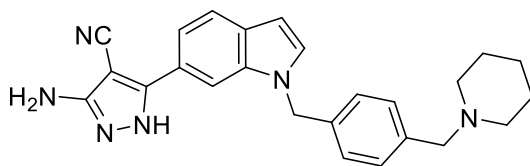
3-Amino-5-(1-(4-(pyrrolidin-1-ylmethyl)benzyl)-1H-indol-6-yl)-1H-pyrazole-4-carbonitrile (103a)



Trichloroacetonitrile (0.201 mL, 2.01 mmol) was added to a suspension of 3-oxo-3-(1-(4-(pyrrolidin-1-ylmethyl)benzyl)-1H-indol-6-yl)propanenitrile **102a** (0.239 g, 0.669 mmol) and sodium acetate (0.274 g, 3.34 mmol) in ethanol (5 mL). The reaction mixture was stirred over 4 hours, then NaHCO₃ solution (7.5 mL) and water (7.5 mL) were added. The intermediate was extracted into DCM (3 x 25 mL). The combined organic extracts were washed (brine), dried (MgSO₄) and concentrated *in vacuo*. The crude residue was dissolved in ethanol (4 mL) and hydrazine monohydrate (0.325 mL, 6.69 mmol) was added. The reaction mixture was heated under reflux for 18 hours, then quenched with excess acetone at rt and concentrated *in vacuo*. Purification by flash chromatography (100% EtOAc, 0 – 7% methanol (+ 0.1% NH₃) in DCM) afforded **103a** (0.135 g, 51% yield).

LCMS (ESI+): m/z 397.3 [M + H]⁺, (ESI-): m/z 395.3 [M - H]⁻, rt 1.35 minutes, 100%; ¹H NMR (500 MHz, CDCl₃) 7.70 (1H, s), 7.62 (1H, d, J = 8.3 Hz), 7.42 (1H, dd, J = 8.2, 1.5 Hz), 7.21 (2H, d, J = 8.2 Hz), 7.17 (1H, d, J = 3.0 Hz), 7.04 (2H, d, J = 8.1 Hz), 6.53 (1H, dd, J = 3.1, 0.8 Hz), 5.18 (2H, s), 4.40 (2H, br s), 3.55 (2H, s), 2.55-2.42 (4H, m), 1.75-1.64 (4H, m); ¹³C NMR (125 MHz, CDCl₃) 156.7, 152.0, 150.4, 138.5, 136.2, 136.0, 130.4, 130.1, 129.7, 127.2, 121.8, 117.9, 115.9, 108.0, 102.2, 75.4, 60.3, 54.2, 50.1, 23.4; ν_{max}/cm⁻¹ 3100 (br, N-H), 2928, 2799, 2208 (C≡N), 1620, 1589, 1501; HRMS (ESI+): m/z calculated for [C₂₄H₂₄N₆ + H]⁺ = 397.2135, observed 397.2132.

3-Amino-5-(1-(4-(piperidin-1-ylmethyl)benzyl)-1H-indol-6-yl)-1H-pyrazole-4-carbonitrile (103b)

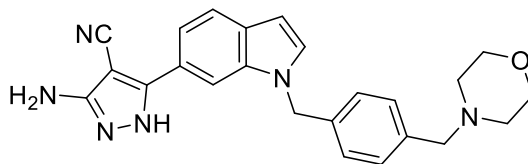


Trichloroacetonitrile (0.138 mL, 1.37 mmol) was added to a suspension of 3-oxo-3-(1-(4-(piperidin-1-ylmethyl)benzyl)-1H-indol-6-yl)propanenitrile **102b** (0.170 g, 0.458 mmol) and sodium acetate (0.188 g, 2.29 mmol) in ethanol (5 mL). The reaction mixture was stirred over 44 hours, then diluted with NaHCO₃ solution (10 mL) and water (10 mL) and extracted into DCM (3 x 20 mL). The combined organic extracts were washed (brine), dried (MgSO₄) and concentrated *in vacuo*. The crude residue was dissolved in

ethanol (10 mL) and hydrazine monohydrate (0.223 mL, 4.58 mmol) was added. The reaction mixture was heated under reflux for 24 hours, then concentrated *in vacuo*. Purification by flash chromatography (0 – 100% EtOAc in PET, 0 – 15% methanol in DCM) was carried out, followed by reverse phase chromatography (0 – 35% acetonitrile in water (+ 0.1% formic acid)) with adjustment of the combined fractions to pH 8 and extraction into DCM/methanol (10:1, 3 x 50 mL). The combined organic extracts were washed (brine), dried (MgSO₄) and concentrated *in vacuo* to afford **103b** (60 mg, 32% yield).

LCMS (ESI+): m/z 411.3 [M + H]⁺, rt 1.44 minutes, >99%; ¹H NMR (500 MHz, CDCl₃) 7.70 (1H, s), 7.63 (1H, d, J = 8.2 Hz), 7.40 (1H, dd, J = 8.2, 1.4 Hz), 7.21 (2H, d, J = 8.1 Hz), 7.19 (1H, d, J = 3.1 Hz), 7.04 (2H, d, J = 7.9 Hz), 6.54 (1H, dd, J = 3.2, 0.6 Hz), 5.20 (2H, s), 4.33 (2H, br s), 3.42 (2H, s), 2.36 (4H, br s), 1.50 (4H, quin, J = 5.6 Hz), 1.42-1.33 (2H, m); ¹³C NMR (125 MHz, CDCl₃) 156.8, 150.2, 137.4, 136.2, 136.0, 130.6, 130.21, 130.17, 127.1, 121.9, 121.4, 117.7, 115.7, 108.1, 102.2, 75.7, 63.3, 54.5, 50.1, 25.6, 24.2; ν_{max}/cm⁻¹ 3200 (br, N-H), 2931, 2211 (C≡N), 1621, 1584, 1502; HRMS (ESI+): m/z calculated for [C₂₅H₂₆N₆ + H]⁺ = 411.2292, observed 411.2287.

3-Amino-5-(1-(4-(morpholinomethyl)benzyl)-1H-indol-6-yl)-1H-pyrazole-4-carbonitrile (103c)

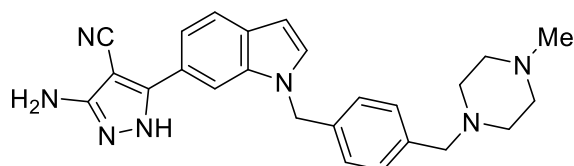


Trichloroacetonitrile (0.142 mL, 1.42 mmol) was added to a suspension of 3-(1-(4-(morpholinomethyl)benzyl)-1H-indol-6-yl)-3-oxopropanenitrile **102c** (0.190 g, 0.473 mmol) and sodium acetate (0.194 g, 2.37 mmol) in ethanol (5 mL). The reaction mixture was stirred over 14 hours, then diluted with NaHCO₃ solution (15 mL) and extracted into DCM (3 x 25 mL). The combined organic extracts were washed (brine), dried (MgSO₄) and concentrated *in vacuo*. The crude residue was dissolved in ethanol (5 mL) and hydrazine monohydrate (0.230 mL, 4.73 mmol) was added. The reaction mixture was heated under reflux for 22 hours, then concentrated *in vacuo*. Purification by flash chromatography (0 – 100% EtOAc in PET, 0 – 10% methanol in DCM) was carried out, followed by reverse phase chromatography (100% water (+ 0.1% formic acid)) with adjustment of the combined fractions to pH 8 and extraction into DCM/methanol (10:1, 3 x 50 mL). The combined organic extracts were washed (brine), dried (MgSO₄) and concentrated *in vacuo* to afford **103c** (81 mg, 42% yield).

LCMS (ESI+): m/z 413.3 [M + H]⁺, rt 1.36 minutes, >99%; ¹H NMR (500 MHz, CDCl₃) 7.73 (1H, s), 7.66 (1H, d, J = 8.2 Hz), 7.39 (1H, dd, J = 8.3, 1.3 Hz), 7.25-7.20 (3H, m), 7.08 (2H, d, J = 8.1 Hz), 6.56 (1H, dd, J = 3.2,

0.6 Hz), 5.26 (2H, s), 4.20 (2H, s), 3.64 (4H, t, J = 4.6 Hz), 3.41 (2H, s), 2.47-2.31 (4H, m); ^{13}C NMR (125 MHz, CDCl_3) 157.0, 150.1, 137.6, 136.2, 135.9, 130.7, 130.4, 129.9, 127.1, 122.0, 121.0, 117.6, 115.4, 108.2, 102.3, 76.1, 67.0, 63.1, 53.7, 50.2; $\nu_{\text{max}}/\text{cm}^{-1}$ 3200 (br, N-H), 2922, 2212 ($\text{C}\equiv\text{N}$), 1740, 1624, 1584, 1502; HRMS (ESI+): m/z calculated for $[\text{C}_{24}\text{H}_{24}\text{N}_6\text{O} + \text{H}]^+ = 413.2084$, observed 413.2079.

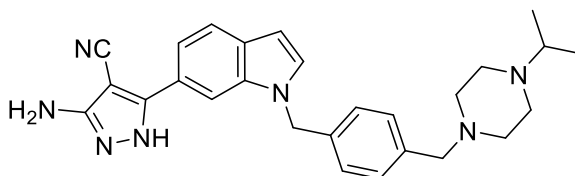
3-Amino-5-(1-(4-((4-methylpiperazin-1-yl)methyl)benzyl)-1H-indol-6-yl)-1H-pyrazole-4-carbonitrile (103d)



Trichloroacetonitrile (0.167 mL, 1.66 mmol) was added to a suspension of 3-(1-(4-((4-methylpiperazin-1-yl)methyl)benzyl)-1H-indol-6-yl)-3-oxopropanenitrile **102d** (0.241 g, 0.555 mmol) and sodium acetate (0.228 g, 2.77 mmol) in ethanol (5 mL). The reaction mixture was stirred over 17 hours, then NaHCO_3 solution (25 mL) was added. The intermediate was extracted into DCM (3 x 25 mL). The combined organic extracts were washed (brine), dried (MgSO_4) and concentrated *in vacuo*. The crude residue was dissolved in ethanol (10 mL) and hydrazine monohydrate (0.270 mL, 5.55 mmol) was added. The reaction mixture was heated under reflux for 24 hours, then concentrated *in vacuo*. Purification by reverse phase flash chromatography (0 – 50% acetonitrile in water (+ 0.1% formic acid)) was attempted, with the resultant fractions combined, adjusted to pH 8, and extracted into DCM/methanol (9:1, 6 x 50 mL). The combined organic extracts were dried (MgSO_4) and concentrated *in vacuo*. Purification by flash chromatography (0 – 20% methanol (+ 0.1% NH_3) in DCM) afforded **103d** (0.140 g, 59% yield).

LCMS (ESI+): m/z 426.4 $[\text{M} + \text{H}]^+$, (ESI-): m/z 424.3 $[\text{M} - \text{H}]^-$, rt 1.36 minutes, 100%; ^1H NMR (500 MHz, CD_3OD) 7.84-7.81 (1H, m), 7.64 (1H, d, J = 8.3 Hz), 7.49 (1H, dd, J = 8.2, 1.4 Hz), 7.39 (1H, d, J = 3.1 Hz), 7.27-7.21 (2H, m), 7.21-7.16 (2H, m), 6.53 (1H, dd, J = 3.1, 0.7 Hz), 5.37 (2H, s), 3.46 (2H, s), 2.44 (8H, br s), 2.24 (3H, s); ^{13}C NMR (125 MHz, CD_3OD) 158.0 (br), 152.5 (br), 138.3, 137.7, 137.4, 131.6, 131.4, 131.1, 128.2, 124.0 (br), 122.2, 118.7, 117.0, 109.1, 102.7, 74.0 (br), 63.3, 55.5, 53.3, 50.8, 45.8; $\nu_{\text{max}}/\text{cm}^{-1}$ 3150 (br, N-H), 2919, 2808, 2207 ($\text{C}\equiv\text{N}$), 1612, 1581; HRMS (ESI+): m/z calculated for $[\text{C}_{25}\text{H}_{27}\text{N}_7 + \text{H}]^+ = 426.2401$, observed 426.2396.

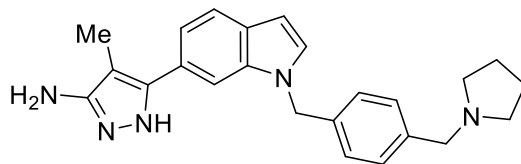
3-Amino-5-(1-(4-((4-isopropylpiperazin-1-yl)methyl)benzyl)-1H-indol-6-yl)-1H-pyrazole-4-carbonitrile
(103e)



Trichloroacetonitrile (0.129 mL, 1.29 mmol) was added to a suspension of 3-(1-(4-((4-isopropylpiperazin-1-yl)methyl)benzyl)-1H-indol-6-yl)-3-oxopropanenitrile **102e** (0.178 g, 0.429 mmol) and sodium acetate (0.176 g, 2.15 mmol) in ethanol (5 mL). The reaction mixture was stirred over 10 hours, then diluted with NaHCO₃ solution (7.5 mL) and water (7.5 mL) and extracted into DCM (3 x 25 mL). The combined organic extracts were washed (brine), dried (MgSO₄) and concentrated *in vacuo*. The crude residue was dissolved in ethanol (3 mL) and hydrazine monohydrate (0.209 mL, 4.29 mmol) was added. The reaction mixture was heated under reflux for 7 hours, then quenched with excess acetone at rt and concentrated *in vacuo*. Purification by flash chromatography (50 – 100% EtOAc in PET, 0 - 20% methanol in DCM (+ 0.1% NH₃)) afforded **103e** (0.147 g, 75% yield).

LCMS (ESI+): m/z 454.3 [M + H]⁺, (ESI-): m/z 452.3 [M - H]⁻, rt 1.40 minutes, >99%; ¹H NMR (500 MHz, CD₃OD) 7.81 (1H, s), 7.63 (1H, d, J = 8.3 Hz), 7.48 (1H, d, J = 8.1 Hz), 7.39 (1H, d, J = 2.6 Hz), 7.25 (2H, d, J = 8.1 Hz), 7.21 (2H, d, J = 8.2 Hz), 6.53 (1H, d, J = 3.2 Hz), 5.36 (2H, s), 3.55 (2H, s), 3.36-3.29 (1H, m), 3.10 (4H, br s), 2.69 (4H, br s), 1.27 (6H, d, J = 6.9 Hz); ¹³C NMR (125 MHz, CD₃OD) 138.6, 137.3, 137.1, 131.6, 131.4, 130.8, 128.5, 122.2, 118.7, 117.0, 109.2, 102.7, 62.3, 59.0, 51.0, 50.8, 49.4, 17.3 (4 peaks missing); ν_{max}/cm⁻¹ 2210 (C≡N), 1623, 1587, 1501; HRMS (ESI)+: m/z calculated for [C₂₇H₃₁N₇ + H]⁺ = 454.2714, observed 454.2715.

4-Methyl-5-(1-(4-(pyrrolidin-1-ylmethyl)benzyl)-1H-indol-6-yl)-1H-pyrazol-3-amine (105a)



Hydrazine monohydrate (0.147 mL, 3.01 mmol) was added to a solution of 2-methyl-3-oxo-3-(1-(4-(pyrrolidin-1-ylmethyl)benzyl)-1H-indol-6-yl)propanenitrile **104a** (0.140 g, 0.301 mmol) in ethanol (5 mL). The reaction mixture was heated under reflux for 28 hours, then quenched with excess acetone at rt and

concentrated *in vacuo*. Purification by flash chromatography (50 – 100% EtOAc in PET, 0 – 20% methanol (+ 0.1% NH₃) in DCM) afforded **105a** (24 mg, 21% yield).

LCMS (ESI+): m/z 386.3 [M + H]⁺, rt 1.25 minutes, >99%; ¹H NMR (500 MHz, CDCl₃) 7.69 (1H, d, J = 8.2 Hz), 7.30 (1H, s), 7.26 (2H, d, J = 8.1 Hz), 7.20 (1H, d, J = 3.2 Hz), 7.18 (1H, dd, J = 8.4, 1.5 Hz), 7.08 (2H, d, J = 8.1 Hz), 6.57 (1H, dd, J = 3.1, 0.7 Hz), 5.31 (2H, s), 3.58 (2H, s), 2.53-2.43 (4H, m), 1.98 (3H, s), 1.81-1.71 (4H, m); ¹³C NMR (125 MHz, CDCl₃) 154.4, 142.7, 139.1, 136.4, 135.8, 129.7, 129.6, 128.8, 126.9, 124.3, 121.5, 119.0, 108.8, 101.9, 99.3, 60.3, 54.2, 50.3, 23.5, 7.9; $\nu_{\text{max}}/\text{cm}^{-1}$ 3200 (br, N-H), 2916, 2788, 1606, 1502; HRMS (ESI)+: m/z calculated for [C₂₄H₂₇N₅ + H]⁺ = 386.2339, observed 386.2354.

4.2: Protein Expression and Purification

4.2.1: *Mycobacterium tuberculosis* fumarate hydratase

A single freshly transformed *E. coli* strain BL21(DE3) colony was transferred to LB media (20 mL) with ampicillin (100 $\mu\text{g mL}^{-1}$) and incubated overnight (37 °C, 200 rpm). The starter culture was used to inoculate 2 flasks, each containing TB media (1 L) with ampicillin (100 $\mu\text{g mL}^{-1}$), with incubation (37 °C, 200 rpm) until an optical density ($A_{600\text{nm}}$) of 1.1 was reached. Protein expression was induced by the addition of IPTG (0.5 mM), followed by overnight incubation (15 °C, 200 rpm). Cells were harvested by centrifugation (4 °C, 4000 g, 20 minutes), then frozen.

The cells were resuspended in 50 mL lysis buffer (50 mM Tris pH 8.0, 150 mM NaCl, 20 mM imidazole) with a tablet of cOmplete™ Protease Inhibitor Cocktail (Roche). The suspension was sonicated (15 minutes, 10 seconds on/ 20 seconds off) and centrifuged (4 °C, 30000 g, 20 minutes). The lysate was loaded onto a 7.5 mL nickel Sepharose™ fast flow column (GE Healthcare), pre-equilibrated with lysis buffer. The column was washed with 5 column volumes of lysis buffer and eluted with buffer B (50 mM Tris pH 8.0, 150 mM NaCl, 300 mM imidazole) in 8 x 5 mL aliquots. Protein-containing aliquots, as determined by SDS-PAGE, were combined and concentrated (30 kDa cutoff), then loaded onto a Superdex 200 HiLoad™ 26/60 column (GE Healthcare) pre-equilibrated with filtration buffer (10 mM Tris pH 8.0, 150 mM NaCl, 0.5 mM TCEP). Chromatography was conducted using an ÄKTA™ FPLC system (GE Healthcare), with protein-containing fractions, as determined by SDS-PAGE, combined and concentrated to 27.9 mg mL⁻¹ (24.3 mg L⁻¹ yield), then flash-frozen in liquid nitrogen and stored at -80 °C. The identity of the protein was confirmed by LCMS analysis.

4.2.2: *Mycobacterium abscessus* tRNA (m¹G37) methyltransferase

Mab TrmD protein was supplied by Dr Sherine Thomas.⁵⁰

4.2.3: *Mycobacterium tuberculosis* tRNA (m¹G37) methyltransferase

A colony of *E. coli* strain ANG3685 (XL1 Blue pET23b-His6-trmDTB) kindly provided by the research group of Professor Angelika Gründling at Imperial College London,¹³⁶ was transferred to LB media (5 mL) with ampicillin (100 µg mL⁻¹) and incubated overnight (37 °C, 160 rpm). The resultant material was processed with a GeneJET™ Plasmid Miniprep Kit (Thermo Scientific™) to obtain plasmid (30 ng µL⁻¹, A_{260nm}/A_{280nm} 1.87), with identity confirmed by Sanger sequencing (DNA Sequencing Facility, Department of Biochemistry, University of Cambridge).

The isolated plasmid was used to transform *E. coli* strain BL21(DE3), with a colony transferred to LB media (20 mL) with ampicillin (100 µg mL⁻¹) and incubated overnight (37 °C, 160 rpm). The starter culture was used to inoculate 2 flasks, each containing LB media (1 L) with ampicillin (100 µg mL⁻¹), with incubation (37 °C, 200 rpm) until an optical density (A_{600nm}) of 0.5 was reached. Protein expression was induced by the addition of IPTG (0.5 mM), followed by overnight incubation (20 °C, 200 rpm). Cells were harvested by centrifugation (4 °C, 4000 g, 20 minutes), then frozen.

The cells were resuspended in 50 mL lysis buffer (50 mM HEPES pH 7.4, 1 M NaCl, 25 mM imidazole, 5 mM mercaptoethanol) with a tablet of cOmplete™ Protease Inhibitor Cocktail (Roche). The suspension was sonicated (10 minutes: 10 seconds on/ 20 seconds off), centrifuged (4 °C, 30000 g, 20 minutes) and filtered (0.45 µm). The resultant lysate was loaded onto a 7.5 mL nickel Sepharose™ fast flow column (GE Healthcare), pre-equilibrated with lysis buffer. The column was washed with 5 column volumes of buffer A (25 mM HEPES pH 7.5, 500 mM NaCl, 20 mM imidazole, 5 mM mercaptoethanol) and eluted with buffer B (25 mM HEPES pH 7.5, 500 mM NaCl, 500 mM imidazole, 5 mM mercaptoethanol) in 7 x 5 mL aliquots. Protein-containing aliquots, as determined by SDS-PAGE, were combined and concentrated (10 kDa cutoff) to a volume of 7 mL, then loaded onto a Superdex 75 Hiload™ 16/60 column (GE Healthcare) pre-equilibrated with filtration buffer (25 mM HEPES pH 7.5, 500 mM NaCl, 5 mM mercaptoethanol). Chromatography was conducted using an ÄKTA™ FPLC system (GE Healthcare), with protein-containing fractions, as determined by SDS-PAGE, combined and concentrated (10 kDa cutoff) to 14.4 mg mL⁻¹ (5.0 mg L⁻¹ yield), then flash-frozen in liquid nitrogen and stored at -80 °C. The identity of the protein was confirmed by LCMS analysis.

4.3: Biochemical Assay with *Mycobacterium tuberculosis* fumarate hydratase

The enzymatic activity of *Mtb* fumarase was followed by a CLARIOstar® microplate spectrometer (BMG Labtech) in a 96-well UV plate (Greiner). 2 µL of DMSO (control) or a solution of the ligand in DMSO was pipetted per well. 150 µL of a solution containing acetyl coenzyme A sodium salt (267 µM), β-nicotinamide adenine dinucleotide hydrate (200 µM), malate dehydrogenase (13.3 units mL⁻¹), citrate synthase (1.33 units mL⁻¹) and *Mtb* fumarase (33.3 nM) in buffer (250 mM Tris pH 8.0, 5 mM MgCl₂) was pipetted per well. The plate was left to equilibrate for 5 minutes at 25 °C, then 48 µL of either buffer (negative control) or fumaric acid (1.67 mM) (positive control or ligand) was pipetted per well. After 2 minutes the plate was read at a wavelength of 340 nm at intervals of 24 seconds over 10 minutes.

Inhibition values for each ligand at a particular concentration were calculated from the gradient of the assay read over the 10 minutes, with correction by the negative control and normalization by the positive control. Inhibition experiments at 50 µM ligand concentration were performed at least twice ($n \geq 2$), with % inhibition and standard error of the mean reported. IC₅₀ experiments ($n = 6$) were performed with 10 ligand concentrations, obtained through serial dilution. Dose-response curves were calculated using Origin software (OriginLab, Northampton, MA, USA), with IC₅₀ and standard error reported, and are presented in appendix A.2 (Figure 60 - Figure 66).

4.4: Biophysical Techniques

4.4.1: Differential Scanning Fluorimetry

DSF was performed using a BioRad CFX Connect™ system, from 25 to 95 °C in 0.5 °C increments of 30 seconds duration. Samples were run in 96-well clear-bottomed plates, with two wells per ligand ($n \geq 2$). In experiments with *Mtb* fumarase each well contained a final volume of 50 µL, consisting of 100 mM Tris pH 7.5, 50 mM NaCl, 2.5x SyproOrange®, 2.5 µM *Mtb* fumarase and either 5% DMSO or 5% ligand stock solution in DMSO. In experiments with *Mab* TrmD each well contained a final volume of 25 µL, consisting of 50 mM HEPES pH 7.5, 500 mM NaCl, 5x SyproOrange®, 10 µM *Mab* TrmD and either 5% DMSO or 5% ligand stock solution in DMSO. Data was processed with Microsoft Excel.

4.4.2: Isothermal Titration Calorimetry

ITC experiments to quantify binding to TrmD were performed using Malvern MicroCal iTC200 or Auto-iTC200 systems at 25 °C. Titrations consisted of an initial injection (0.2 µL), discarded during data processing, followed by either 19 (2 µL) or 39 (1 µL) injections separated by intervals of 60 – 150 seconds duration. Protein was dialysed overnight at 4 °C in storage buffer (*Mab* TrmD: 50 mM HEPES pH 7.5, 500 mM NaCl, 5% glycerol; *Mtb* TrmD: 25 mM HEPES pH 7.5, 500 mM NaCl). Sample cell and syringe solutions were prepared using the same storage buffer, with a final DMSO concentration of 2 – 10% according to ligand solubility in the buffer. TrmD concentrations of either 33 or 100 µM were used, with ligand to protein concentration ratios ranging from 10-20:1. Control titrations without protein were also performed and subtracted from ligand to protein titrations. Titrations were fitted with Origin software (OriginLab, Northampton, MA, USA), using a one-site binding model with N fixed to 1 only for weakly binding ligands. Titrations were typically performed once ($n = 1$), with multiple isotherms obtained ($n > 1$) for key compounds of interest. K_d values are reported to 2 significant figures. Error provided by Origin software due to model fit is reported when $n = 1$, whereas standard deviation is reported when $n > 1$. ITC traces are presented in appendix A.3 (Figure 67 - Figure 73), with the exception of **71o** (Figure 49b and c).

For the reverse ITC titration with **71o** (Figure 49c), protein solution (420 µM *Mab* TrmD) was injected into the sample cell (35 µM ligand). Other aspects of experiment setup and analysis were identical to the forward titrations.

4.5: X-ray Crystallography with *Mycobacterium tuberculosis* fumarate hydratase

Crystals were grown in Intelli-Plate® 24-4 well sitting drop plates (Art Robbins Instruments), incubated at 19 °C in a ROCK IMAGER® 1000 system (FORMULATRIX®) that was used for drop imaging.

4.5.1: Seed Stock

A sitting drop was set up with 2 µL protein solution (14 mg mL⁻¹ *Mtb* fumarase, 0.15 M NaCl, 10 mM Tris pH 8.0 and 0.5 mM TCEP) and 1 µL reservoir solution (10% w/v PEG3350, 5% DMSO and 0.30 M magnesium formate), equilibrated against 400 µL reservoir solution. After 3 weeks the drop was diluted with 5 µL reservoir solution, and the crystals disturbed with a loop before transfer to a Beads-for-Seeds

microcentrifuge tube (Jena Bioscience). Further reservoir solution was added to the tube to a total volume of 50 μL prior to sonication (10 cycles: 30 seconds on/ 30 seconds off). The resultant suspension was diluted both 5,000x and 10,000x in buffer (17% w/v PEG3350, 5% DMSO and 0.30 M magnesium formate), then flash-frozen in liquid nitrogen and stored at $-80\text{ }^{\circ}\text{C}$.

4.5.2: Crystal Growth and Soaking

The recreation of the X-ray crystal structure of **2** in complex with *Mtb* fumarase was achieved with the setting up of a sitting drop with 3 μL protein solution (14 mg mL^{-1} *Mtb* fumarase, 0.15 M NaCl, 10 mM Tris pH 8.0 and 0.5 mM TCEP), 1 μL reservoir solution (12.8% w/v PEG3350, 5% DMSO and 0.30 M magnesium formate) and 0.5 μL 5,000x seed stock, equilibrated against 400 μL reservoir solution. After 6 days, the drop was treated with 2 μL soaking solution (1 mM ligand, 7.5% DMSO, 26.25% w/v PEG3350 and 0.20 M magnesium formate) and incubated overnight.

The determination of the X-ray crystal structure of **49j** in complex with *Mtb* fumarase was achieved with the setting up of a sitting drop with 3 μL protein solution (14 mg mL^{-1} *Mtb* fumarase, 0.15 M NaCl, 10 mM Tris pH 8.0 and 0.5 mM TCEP), 1 μL reservoir solution (11.4% w/v PEG3350, 5% DMSO and 0.30 M magnesium formate) and 0.5 μL 10,000x seed stock, equilibrated against 400 μL reservoir solution. After 6 days the drop was treated with 2 μL soaking solution (1 mM ligand, 7.5% DMSO, 26.25% w/v PEG3350 and 0.2 M magnesium formate) and incubated overnight.

The determination of X-ray crystal structures of **46a**, **46g**, **49a-b**, **49h** and **49i** in complex with *Mtb* fumarase was achieved with the setting up of sitting drops with 3 μL protein solution (14 mg mL^{-1} *Mtb* fumarase, 0.15 M NaCl, 10 mM Tris pH 8.0 and 0.5 mM TCEP), 1 μL reservoir solution (10% w/v PEG3350, 5% DMSO and 0.30 M magnesium formate) and 0.5 μL 10,000x seed stock, equilibrated against 400 μL reservoir solution. After 1 – 2 weeks a drop was treated with 2 μL soaking solution (0.5 – 3 mM ligand, 7.5% DMSO, 26.25% w/v PEG3350 and 0.20 M magnesium formate) and incubated overnight. Ligand concentrations: 0.5 mM (**49i**), 1 mM (**46g** and **49b**), 2 mM (**46a** and **49h**) and 3 mM (**49a**).

Crystals were mounted into loops and flash frozen in liquid nitrogen.

4.5.3: X-ray Data Collection and Processing

X-ray data for **2**, **46a**, **46g**, **49a-b**, **49h** and **49j-l** in complex with *Mtb* fumarase were collected on beamlines i03 and i04 at the Diamond Light Source synchrotron (Oxfordshire, United Kingdom) at wavelengths of 0.9762 – 0.9795 Å, with Ω start 0.0°, Ω oscillation 0.10 – 0.20°, 1500 – 3000 images and an exposure of 0.050 seconds. Data was processed using autoPROC.¹³⁸

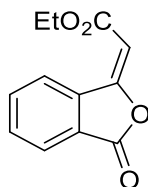
4.5.4: Structure Solution and Refinement

Molecular replacement for structures of *Mtb* fumarase in complex with **2** or **49b** was carried out using PHASER,¹¹⁸ accessed through the CCP4 software suite,¹¹⁹ with the previously published **2**-bound *Mtb* fumarase structure (PDB code 5F91) used as a search model.⁴¹ For structures of *Mtb* fumarase in complex with **46a**, **46g**, **49a**, **49h**, **49j** or **49l**, the solved **49b**-bound structure was used as a search model. Models were manually rebuilt using the COOT molecular graphics software package,¹²⁰ and refined with REFMAC5,¹²¹ accessed through CCP4.¹¹⁹ The statistics for the resultant models, compiled using PHENIX,¹³⁹ are presented in appendix A.4 (Table 14), with the exception of **2** whose model was not fully rebuilt.

Appendix: Supporting Data

A.1: Methods and Characterisation Data for Non-key Compounds

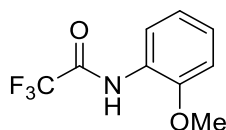
Ethyl-(E)-2-(3-oxoisobenzofuran-1(3H)-ylidene)acetate (**14**)^{41, 137}



A solution of (carbethoxymethylene)triphenylphosphorane (4.70 g, 13.5 mmol) in chloroform (12.5 mL) was added dropwise to a solution of phthalic anhydride **13** (2.00 g, 13.5 mmol) in chloroform (12.5 mL). The reaction mixture was heated under reflux for 3 hours, then concentrated *in vacuo*. Purification by flash chromatography (5% EtOAc in PET) afforded **14** (1.97 g, 67% yield).

¹H NMR (500 MHz, CDCl₃) 9.05 (1H, d, J = 8.0 Hz), 7.96 (1H, dt, J = 7.5, 1.0 Hz), 7.84-7.78 (1H, m), 7.70 (1H, td, J = 7.5, 0.9 Hz), 6.15 (1H, s), 4.30 (2H, q, J = 7.2 Hz), 1.36 (3H, t, J = 7.2 Hz); ¹³C NMR (125 MHz, CDCl₃) 165.9, 165.7, 158.0, 136.3, 135.4, 132.6, 128.4, 126.7, 125.5, 102.6, 61.1, 14.4; ¹H NMR spectroscopic data consistent with literature.¹³⁷

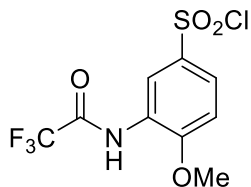
2,2,2-Trifluoro-N-(2-methoxyphenyl)acetamide (**18**)¹⁴⁰



Trifluoroacetic anhydride (0.55 mL, 3.9 mmol) was added dropwise at 0 °C to a mixture of o-anisidine **17** (0.37 mL, 3.3 mmol), pyridine (0.39 mL, 4.9 mmol) and DCM (4 mL). The reaction mixture was warmed to rt and stirred over 3 days. Water (20 mL) was added dropwise at 0 °C to the reaction mixture. The product was extracted into DCM (3 x 20 mL). The combined organic extracts were dried (MgSO₄) and concentrated *in vacuo*. Purification by flash chromatography (0 – 20% EtOAc in PET) afforded **18** (0.713 g, 99% yield).

LCMS (ESI-): m/z 218.1 [M - H]⁻, rt 2.14 minutes, >99%; ¹H NMR (400 MHz, CDCl₃) 8.57 (1H, br s), 8.32 (1H, d, J = 8.0 Hz), 7.17 (1H, t, J = 8.0 Hz), 7.01 (1H, t, J = 7.7 Hz), 6.94 (1H, d, J = 8.2 Hz), 3.93 (3H, s); ¹³C NMR (100 MHz, CDCl₃) 154.5 (q, J = 37 Hz), 148.4, 126.1, 125.2, 121.4, 120.3, 115.8 (q, J = 288 Hz), 110.3, 56.0; ¹H NMR spectroscopic data consistent with literature.¹⁴⁰

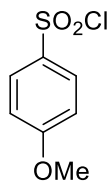
4-Methoxy-3-(2,2,2-trifluoroacetamido)benzenesulfonyl chloride (**19**)¹⁴⁰



Chlorosulfonic acid (0.41 mL, 6.2 mmol) was added dropwise at 0 °C to a solution of 2,2,2-trifluoro-N-(2-methoxyphenyl)acetamide **18** (0.683 g, 3.12 mmol) in DCM (6 mL). The reaction mixture was warmed to rt and stirred over 16 hours. Water (20 mL) was added dropwise at 0 °C to the reaction mixture. The product was extracted into DCM (3 x 20 mL). The combined organic extracts were dried (MgSO₄) and concentrated *in vacuo* to afford **19** (0.767 g, 77% yield).

¹H NMR (400 MHz, CDCl₃) 9.05 (1H, s), 8.59 (1H, br s), 7.90 (1H, d, J = 8.8 Hz), 7.11 (1H, d, J = 8.9 Hz), 4.09 (3H, s); ¹³C NMR (100 MHz, CDCl₃) 154.9 (q, J = 38 Hz), 153.1, 137.1, 126.1, 125.9, 118.9, 115.5 (q, J = 289 Hz), 110.5, 57.1; ¹H NMR spectroscopic data consistent with literature.¹⁴⁰

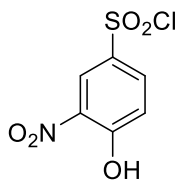
4-Methoxybenzenesulfonyl chloride (**29**)



Chlorosulfonic acid (0.25 mL, 3.7 mmol) was added dropwise at 0 °C to a mixture of anisole **28** (0.201 mL, 1.85 mmol) and chloroform (5 mL). The reaction mixture was warmed to rt and stirred over 30 minutes. Water (15 mL) was added dropwise at 0 °C to the reaction mixture. The product was extracted into DCM (3 x 20 mL). The combined organic extracts were washed (brine), dried (MgSO₄) and concentrated *in vacuo* to afford **29** (0.246 g, 64% yield).

¹H NMR (400 MHz, CDCl₃) 7.98 (2H, d, J = 9.0 Hz), 7.05 (2H, d, J = 8.9 Hz), 3.92 (3H, s); ¹³C NMR (100 MHz, CDCl₃) 165.0, 136.3, 129.7, 114.9, 56.1; spectroscopic data consistent with literature.¹⁴¹

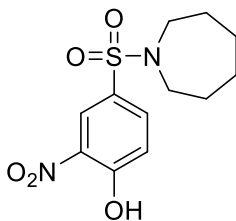
4-Hydroxy-3-nitrobenzenesulfonyl chloride (**31**)



Chlorosulfonic acid (0.96 mL, 14 mmol) was added dropwise at 0 °C to a solution of 2-nitrophenol **30** (1.00 g, 7.19 mmol) in chloroform (5 mL). The reaction mixture was heated under reflux for 90 minutes. Water (15 mL) was added dropwise at 0 °C to the reaction mixture. The product was extracted into DCM (3 x 25 mL). The combined organic extracts were dried (MgSO₄) and concentrated *in vacuo* to afford **31** (1.33 g, 78% yield).

LCMS (ESI-): m/z 236.0 [M - H]⁻, rt 1.89 minutes, >99%; ¹H NMR (400 MHz, CDCl₃) 11.12 (1H, s), 8.84 (1H, d, J = 2.4 Hz), 8.21 (1H, dd, J = 9.0, 2.4 Hz), 7.42 (1H, d, J = 9.0 Hz); ¹³C NMR (100 MHz, CDCl₃) 159.5, 136.2, 134.9, 132.9, 126.0, 122.4; ν_{max}/cm⁻¹ 3249 (br, O-H), 3088, 1615, 1578, 1539 (N=O), 1328 (N=O).

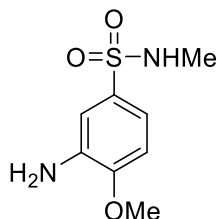
4-(Azepan-1-ylsulfonyl)-2-nitrophenol (**32**)



Hexamethyleneimine (0.108 mL, 0.963 mmol) and DIPEA (0.305 mL, 1.75 mmol) were added to a solution of 4-hydroxy-3-nitrobenzenesulfonyl chloride **31** (0.208 g, 0.875 mmol) in DCM (2 mL). The reaction mixture was stirred over 15 hours, then water (10 mL) and aqueous HCl (37.5% w/v, 5 mL) were added. The product was extracted into DCM (3 x 25 mL). The combined organic extracts were dried (MgSO₄) and concentrated *in vacuo*. Purification by flash chromatography (0 – 40% EtOAc in PET) afforded **32** (0.190 g, 64% yield).

LCMS (ESI+): m/z 301.2 [M + H]⁺, (ESI-): m/z 299.1 [M - H]⁻, rt 2.11 minutes, 88%; ¹H NMR (400 MHz, CDCl₃) 10.85 (1H, s), 8.56 (1H, d, J = 2.4 Hz), 7.96 (1H, dd, J = 8.9, 2.2 Hz), 7.29 (1H, d, J = 8.7 Hz), 3.29 (4H, t, J = 5.9 Hz), 1.79-1.69 (4H, m), 1.65-1.58 (4H, m); ¹³C NMR (100 MHz, CDCl₃) 157.5, 135.2, 133.1, 132.5, 124.8, 121.4, 48.5, 29.3, 27.0; ν_{max}/cm⁻¹ 2939, 1615, 1583, 1528 (N=O), 1330 (N=O); HRMS (ESI)+: m/z calculated for [C₁₂H₁₆N₂O₅S + Na]⁺ = 323.0672, observed 323.0661.

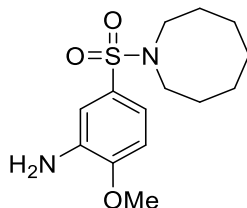
3-Amino-4-methoxy-N-methylbenzenesulfonamide (**33a**)



Methylamine (2 M in THF, 0.33 mL, 0.67 mmol) was added at 0 °C to a solution of 4-methoxy-3-(2,2,2-trifluoroacetamido)benzenesulfonyl chloride **19** (0.106 g, 0.334 mmol) in THF (2 mL). The reaction mixture was warmed to rt and stirred overnight. Further methylamine (2 M in THF, 2.0 mL, 4.0 mmol) was added, and the reaction mixture heated under reflux for 1 hour. Further methylamine (2 M in THF, 1.0 mL, 2.0 mmol) was added at rt, and the reaction mixture heated under reflux for 30 minutes. The reaction mixture was concentrated *in vacuo*, then ethanol (5 mL), water (5 mL) and aqueous HCl (37.5% w/v, 5 mL) were added. The reaction mixture was heated under reflux for 3 hours 30 minutes. The reaction mixture was adjusted to pH 14 by the dropwise addition of aqueous NaOH (10% w/v) at rt, then concentrated *in vacuo* to remove ethanol. The product was extracted into EtOAc (3 x 25 mL). The combined organic extracts were dried (MgSO₄) and concentrated *in vacuo*. Purification by flash chromatography (25 – 75% EtOAc in PET) afforded **33a** (59 mg, 82% yield).

LCMS (ESI+): m/z 217.2 [M + H]⁺, rt 1.23 minutes, >99%; ¹H NMR (400 MHz, CD₃CN) 7.12-7.06 (2H, m), 6.92 (1H, d, J = 8.0 Hz), 5.28-5.07 (1H, m), 4.39 (2H, br s), 3.88 (3H, s), 2.46 (3H, d, J = 5.3 Hz); ¹³C NMR (100 MHz, CD₃CN) 150.8, 138.8, 131.8, 117.8, 112.5, 110.7, 56.5, 29.6; ν_{max}/cm⁻¹ 3388 (N-H), 3306 (N-H), 3043, 2919, 2840, 1590, 1509; HRMS (ESI)+: m/z calculated for [C₈H₁₂N₂O₃S + Na]⁺ = 239.0461, observed 239.0463.

5-(Azocan-1-ylsulfonyl)-2-methoxyaniline (**33b**)

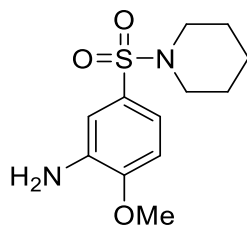


Heptamethyleneimine (95 μL, 0.76 mmol) was added dropwise at 0 °C to a suspension of NaH (60% in mineral oil, 76 mg, 1.9 mmol) in DMF (2 mL). The reaction mixture was stirred at 0 °C over 20 minutes. A solution of 4-methoxy-3-(2,2,2-trifluoroacetamido)benzenesulfonyl chloride **19** (0.200 g, 0.630 mmol) in

DMF (1 mL) was added dropwise at 0 °C to the reaction mixture. The reaction mixture was warmed to rt and stirred over 2 hours. Ethanol (5 mL) was added dropwise at 0 °C to the reaction mixture, followed by water (5 mL) and aqueous HCl (37.5% w/v, 5 mL). The reaction mixture was heated under reflux for 17 hours. The reaction mixture was adjusted to pH 9 by the dropwise addition of aqueous NaOH (10% w/v) at rt, then concentrated *in vacuo* to remove ethanol. The mixture was diluted with EtOAc (25 mL), and the resultant aqueous layer discarded. The organic layer was washed with water (2 x 25 mL) and brine (25 mL), dried (MgSO₄) and concentrated *in vacuo*. Purification by flash chromatography (0 – 50% EtOAc in PET) afforded **33b** (0.130 g, 69% yield).

LCMS (ESI+): m/z 299.2 [M + H]⁺, rt 1.96 minutes, >99%; ¹H NMR (400 MHz, CDCl₃) 7.16 (1H, dd, J = 8.4, 2.2 Hz), 7.09 (1H, d, J = 2.2 Hz), 6.81 (1H, d, J = 8.3 Hz), 3.97 (2H, br s), 3.89 (3H, s), 3.11 (4H, t, J = 5.8 Hz), 1.75-1.57 (10H, m); ¹³C NMR (100 MHz, CDCl₃) 150.1, 136.7, 130.8, 118.2, 112.9, 109.7, 55.8, 48.8, 28.0, 26.8, 25.3; ν_{max}/cm⁻¹ 3488 (N-H), 3383 (N-H), 2914, 2851, 1729, 1611, 1577, 1512; HRMS (ESI)+: m/z calculated for [C₁₄H₂₂N₂O₃S + H]⁺ = 299.1424, observed 299.1429.

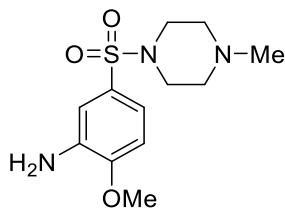
2-Methoxy-5-(piperidin-1-ylsulfonyl)aniline (33c)



Piperidine (62 μL, 0.63 mmol) was added dropwise at 0 °C to a suspension of NaH (60% in mineral oil, 76 mg, 1.9 mmol) in DMF (1 mL). The reaction mixture was stirred at 0 °C over 20 minutes. A solution of 4-methoxy-3-(2,2,2-trifluoroacetamido)benzenesulfonyl chloride **19** (0.200 g, 0.630 mmol) in DMF (2 mL) was added dropwise at 0 °C to the reaction mixture. The reaction mixture was warmed to rt and stirred over 20 hours. Ethanol (5 mL) was added dropwise at 0 °C to the reaction mixture, followed by water (5 mL) and aqueous HCl (37.5% w/v, 5 mL). The reaction mixture was heated under reflux for 9 hours. The reaction mixture was adjusted to pH 7 by the dropwise addition of aqueous NaOH (10% w/v) at rt, then concentrated *in vacuo*. Water (15 mL) was added to the crude residue. The product was extracted into DCM (3 x 20 mL). The combined organic extracts were dried (MgSO₄) and concentrated *in vacuo*. Purification by flash chromatography (20 – 50% EtOAc in PET) afforded **33c** (0.104 g, 61% yield).

LCMS (ESI+): m/z 271.2 $[M + H]^+$, rt 1.86 minutes, >99%; 1H NMR (500 MHz, $CDCl_3$) 7.13 (1H, dd, $J = 8.4, 2.1$ Hz), 7.05 (1H, d, $J = 2.2$ Hz), 6.83 (1H, d, $J = 8.4$ Hz), 3.97 (2H, br s), 3.91 (3H, s), 2.95 (4H, t, $J = 5.4$ Hz), 1.63 (4H, quin, $J = 5.7$ Hz), 1.45-1.36 (2H, m); ^{13}C NMR (125 MHz, $CDCl_3$) 150.3, 136.6, 128.2, 118.9, 113.3, 109.7, 55.9, 47.1, 25.3, 23.7; ν_{max}/cm^{-1} 3475 (N-H), 3372 (N-H), 2939, 2851, 1616, 1581, 1510; HRMS (ESI)+: m/z calculated for $[C_{12}H_{18}N_2O_3S + Na]^+ = 293.0930$, observed 293.0935.

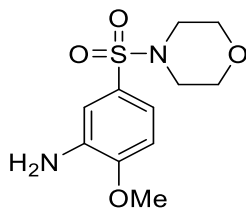
2-Methoxy-5-((4-methylpiperazin-1-yl)sulfonyl)aniline (33d)



1-Methylpiperazine (84 μ L, 0.76 mmol) was added dropwise at 0 °C to a suspension of NaH (60% in mineral oil, 76 mg, 1.9 mmol) in DMF (2 mL). The reaction mixture was stirred at 0 °C over 20 minutes. A solution of 4-methoxy-3-(2,2,2-trifluoroacetamido)benzenesulfonyl chloride **19** (0.200 g, 0.630 mmol) in DMF (1 mL) was added dropwise at 0 °C to the reaction mixture. The reaction mixture was warmed to rt and stirred over 2 hours. Ethanol (5 mL) was added dropwise at 0 °C to the reaction mixture, followed by water (5 mL) and aqueous HCl (37.5% w/v, 5 mL). The reaction mixture was heated under reflux for 18 hours. The reaction mixture was adjusted to pH 9 by the dropwise addition of aqueous NaOH (10% w/v) at rt , then concentrated *in vacuo* to remove ethanol. The mixture was diluted with EtOAc (25 mL), and the resultant aqueous layer discarded. The organic layer was washed with water (2 x 25 mL) and brine (25 mL), dried ($MgSO_4$) and concentrated *in vacuo*. Purification by flash chromatography (0 – 10% methanol in DCM) afforded **33d** (0.120 g, 65% yield).

LCMS (ESI+): m/z 286.3 $[M + H]^+$, rt 0.47 minutes, 97%; 1H NMR (500 MHz, $(CD_3)_2SO$) 6.99-6.95 (2H, m), 6.88 (1H, dd, $J = 8.5, 2.3$ Hz), 5.23 (2H, s), 3.84 (3H, s), 2.82 (4H, br s), 2.34 (4H, t, $J = 4.4$ Hz), 2.13 (3H, s); ^{13}C NMR (125 MHz, $(CD_3)_2SO$) 149.5, 138.3, 126.3, 116.1, 111.5, 109.9, 55.6, 53.6, 45.7, 45.3; ν_{max}/cm^{-1} 3481 (N-H), 3376 (N-H), 2919, 2842, 2795, 1609, 1576, 1516; HRMS (ESI)+: m/z calculated for $[C_{12}H_{19}N_3O_3S + H]^+ = 286.1220$, observed 286.1225.

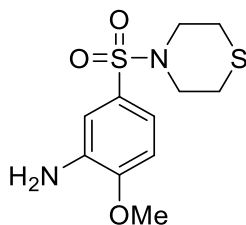
2-Methoxy-5-(morpholinosulfonyl)aniline (**33e**)



Morpholine (66 μ L, 0.76 mmol) was added dropwise at 0 °C to a suspension of NaH (60% in mineral oil, 76 mg, 1.9 mmol) in DMF (2 mL). The reaction mixture was stirred at 0 °C over 20 minutes. A solution of 4-methoxy-3-(2,2,2-trifluoroacetamido)benzenesulfonyl chloride **19** (0.200 g, 0.630 mmol) in DMF (1 mL) was added dropwise at 0 °C to the reaction mixture. The reaction mixture was warmed to rt and stirred over 2 hours. Ethanol (5 mL) was added dropwise at 0 °C to the reaction mixture, followed by water (5 mL) and aqueous HCl (37.5% w/v, 5 mL). The reaction mixture was heated under reflux for 18 hours. The reaction mixture was adjusted to pH 9 by the dropwise addition of aqueous NaOH (10% w/v) at rt, then concentrated *in vacuo* to remove ethanol. The mixture was diluted with EtOAc (25 mL), and the resultant aqueous layer discarded. The organic layer was washed with water (2 x 25 mL) and brine (25 mL), dried (MgSO_4) and concentrated *in vacuo*. Purification by flash chromatography (20 – 60% EtOAc in PET) afforded **33e** (0.117 g, 68% yield).

LCMS (ESI+): m/z 273.2 $[\text{M} + \text{H}]^+$, rt 1.40 minutes, >99%; ^1H NMR (500 MHz, $(\text{CD}_3)_2\text{SO}$) 7.01-6.96 (2H, m), 6.89 (1H, dd, $J = 8.3, 2.3$ Hz), 5.25 (2H, s), 3.85 (3H, s), 3.62 (4H, t, $J = 4.8$ Hz), 2.80 (4H, t, $J = 4.7$ Hz); ^{13}C NMR (125 MHz, $(\text{CD}_3)_2\text{SO}$) 149.6, 138.4, 125.9, 116.2, 111.5, 109.9, 65.3, 55.6, 45.9; $\nu_{\text{max}}/\text{cm}^{-1}$ 3486 (N-H), 3390 (N-H), 2924, 2864, 1691, 1611, 1507; HRMS (ESI)+: m/z calculated for $[\text{C}_{11}\text{H}_{16}\text{N}_2\text{O}_4\text{S} + \text{Na}]^+ = 295.0723$, observed 295.0719.

2-Methoxy-5-(thiomorpholinosulfonyl)aniline (**33f**)

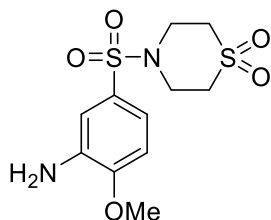


Thiomorpholine (76 μ L, 0.76 mmol) was added dropwise at 0 °C to a suspension of NaH (60% in mineral oil, 76 mg, 1.9 mmol) in DMF (2 mL). The reaction mixture was stirred at 0 °C over 20 minutes. A solution of 4-methoxy-3-(2,2,2-trifluoroacetamido)benzenesulfonyl chloride **19** (0.200 g, 0.630 mmol) in DMF (1

mL) was added dropwise at 0 °C to the reaction mixture. The reaction mixture was warmed to rt and stirred over 2 hours. Ethanol (5 mL) was added dropwise at 0 °C to the reaction mixture, followed by water (5 mL) and aqueous HCl (37.5% w/v, 5 mL). The reaction mixture was heated under reflux for 17 hours. The reaction mixture was adjusted to pH 9 by the dropwise addition of aqueous NaOH (10% w/v) at rt, then concentrated *in vacuo* to remove ethanol. The mixture was diluted with EtOAc (50 mL), washed with water (3 x 25 mL) and brine (25 mL), dried (MgSO₄) and concentrated *in vacuo*. Purification by flash chromatography (0 – 50% EtOAc in PET) afforded **33f** (0.126 g, 67% yield).

LCMS (ESI+): m/z 289.2 [M + H]⁺, rt 1.66 minutes, 96%; ¹H NMR (400 MHz, CDCl₃) 7.11 (1H, dd, J = 8.4, 2.2 Hz), 7.02 (1H, d, J = 2.2 Hz), 6.83 (1H, d, J = 8.4 Hz), 4.02 (2H, br s), 3.91 (3H, s), 3.31 (4H, t, J = 4.9 Hz), 2.69 (4H, t, J = 5.2 Hz); ¹³C NMR (100 MHz, CDCl₃) 150.5, 137.0, 128.6, 118.5, 112.8, 109.8, 55.9, 48.1, 27.5; $\nu_{\max}/\text{cm}^{-1}$ 3489 (N-H), 3389 (N-H), 2970, 2914, 2852, 1730, 1611, 1577, 1512; HRMS (ESI)+: m/z calculated for [C₁₁H₁₆N₂O₃S₂ + H]⁺ = 289.0675, observed 289.0688.

4-((3-Amino-4-methoxyphenyl)sulfonyl)thiomorpholine 1,1-dioxide (**33g**)

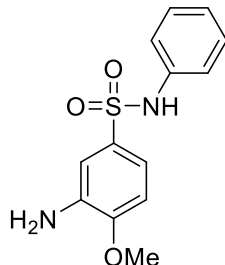


Triethylamine (0.66 mL, 4.7 mmol) and DCM (20 mL) were added to a mixture of thiomorpholine 1,1-dioxide (0.153 g, 1.13 mmol), 4-methoxy-3-(2,2,2-trifluoroacetamido)benzenesulfonyl chloride **19** (0.300 g, 0.944 mmol) and DMAP (35 mg, 0.28 mmol). The reaction mixture was stirred over 30 minutes, then concentrated *in vacuo*. Ethanol (30 mL), water (30 mL) and aqueous HCl (37.5% w/v, 30 mL) were added, and the reaction mixture heated under reflux for 3 hours. The reaction mixture was concentrated *in vacuo* to remove ethanol, then adjusted to pH 14 by the dropwise addition of aqueous NaOH (10% w/v). The product was extracted into DCM (3 x 100 mL). The combined organic extracts were washed (brine), dried (MgSO₄) and concentrated *in vacuo*. Purification by flash chromatography (20 – 70% EtOAc in PET, 0 – 7% methanol in DCM) afforded **33g** (0.250 g, 80% yield).

LCMS (ESI+): m/z 321.2 [M + H]⁺, rt 1.44 minutes, 97%; ¹H NMR (400 MHz, (CD₃)₂SO) 7.03-6.92 (3H, m), 5.27 (2H, s), 3.85 (3H, s), 3.42-3.30 (4H, m), 3.22 (4H, t, J = 5.0 Hz); ¹³C NMR (100 MHz, (CD₃)₂SO) 150.1,

138.9, 127.4, 116.2, 111.0, 110.4, 55.9, 50.2, 45.3; $\nu_{\max}/\text{cm}^{-1}$ 3458 (N-H), 3369 (N-H), 2907, 2849, 1616, 1579, 1510; HRMS (ESI)+: m/z calculated for $[\text{C}_{11}\text{H}_{16}\text{N}_2\text{O}_5\text{S}_2 + \text{Na}]^+ = 343.0393$, observed 343.0394.

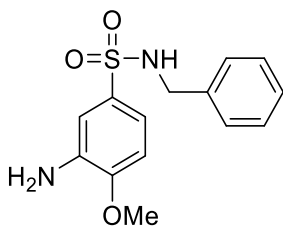
3-Amino-4-methoxy-N-phenylbenzenesulfonamide (33h)



Aniline (43 μL , 0.47 mmol) was added dropwise at 0 °C to a suspension of NaH (60% in mineral oil, 57 mg, 1.4 mmol) in DMF (1 mL). The reaction mixture was stirred at 0 °C over 20 minutes. A solution of 4-methoxy-3-(2,2,2-trifluoroacetamido)benzenesulfonyl chloride **19** (0.150 g, 0.472 mmol) in DMF (2 mL) was added dropwise at 0 °C to the reaction mixture. The reaction mixture was warmed to rt and stirred over 1 hour. Ethanol (5 mL) was added dropwise at 0 °C to the reaction mixture, followed by water (5 mL) and aqueous HCl (37.5% w/v, 5 mL). The reaction mixture was heated under reflux for 10 hours. The reaction mixture was adjusted to pH 9 by the dropwise addition of aqueous NaOH (10% w/v) at rt, then concentrated *in vacuo* to remove ethanol. The product was extracted into DCM (3 x 25 mL). The combined organic extracts were washed (brine), dried (MgSO_4) and concentrated *in vacuo*. Purification by flash chromatography (0 – 75% EtOAc in PET) afforded **33h** (50 mg, 37% yield).

LCMS (ESI+): m/z 279.2 $[\text{M} + \text{H}]^+$, (ESI-): m/z 277.1 $[\text{M} - \text{H}]^-$, rt 1.77 minutes, 97%; ^1H NMR (400 MHz, CDCl_3) 7.25-7.19 (2H, m), 7.16 (1H, dd, $J = 8.4, 2.3$ Hz), 7.12-7.04 (4H, m), 6.82 (1H, s), 6.72 (1H, d, $J = 8.5$ Hz), 3.85 (3H, s), 3.54 (1H, br s); ^{13}C NMR (100 MHz, CDCl_3) 150.7, 136.9, 136.7, 131.0, 129.4, 125.2, 121.6, 118.7, 112.7, 109.6, 55.8; $\nu_{\max}/\text{cm}^{-1}$ 3380 (N-H), 3250 (N-H), 1615, 1598, 1508; HRMS (ESI)+: m/z calculated for $[\text{C}_{13}\text{H}_{14}\text{N}_2\text{O}_3\text{S} + \text{H}]^+ = 279.0798$, observed 279.0796.

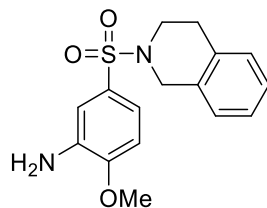
3-Amino-N-benzyl-4-methoxybenzenesulfonamide (33i)



Benzylamine (52 μ L, 0.47 mmol) was added dropwise at 0 $^{\circ}$ C to a suspension of NaH (60% in mineral oil, 57 mg, 1.4 mmol) in DMF (1 mL). The reaction mixture was stirred at 0 $^{\circ}$ C over 20 minutes. A solution of 4-methoxy-3-(2,2,2-trifluoroacetamido)benzenesulfonyl chloride **19** (0.150 g, 0.472 mmol) in DMF (2 mL) was added dropwise at 0 $^{\circ}$ C to the reaction mixture. The reaction mixture was warmed to rt and stirred over 1 hour. Ethanol (5 mL) was added dropwise at 0 $^{\circ}$ C to the reaction mixture, followed by water (5 mL) and aqueous HCl (37.5% w/v, 5 mL). The reaction mixture was heated under reflux for 10 hours. The reaction mixture was adjusted to pH 7 by the dropwise addition of aqueous NaOH (10% w/v) at rt, then concentrated *in vacuo* to remove ethanol. The product was extracted into DCM (3 x 25 mL). The combined organic extracts were washed (brine), dried (MgSO₄) and concentrated *in vacuo*. Purification by flash chromatography (0 – 10% methanol in DCM) afforded **33i** (89 mg, 59% yield).

LCMS (ESI+): m/z 293.2 [M + H]⁺, (ESI-): m/z 291.1 [M - H]⁻, rt 1.80 minutes, 92%; ¹H NMR (400 MHz, CDCl₃) 7.31-7.18 (6H, m), 7.16 (1H, d, J = 2.3 Hz), 6.82 (1H, d, J = 8.5 Hz), 4.59 (1H, t, J = 6.2 Hz), 4.08 (2H, d, J = 6.3 Hz), 3.91 (3H, s); ¹³C NMR (100 MHz, CDCl₃) 150.5, 137.0, 136.6, 131.6, 128.8, 128.1, 128.0, 118.4, 112.6, 109.8, 55.9, 47.5; ¹H NMR spectroscopic data consistent with literature.¹⁴²

5-((3,4-Dihydroisoquinolin-2(1H)-yl)sulfonyl)-2-methoxyaniline (33j)

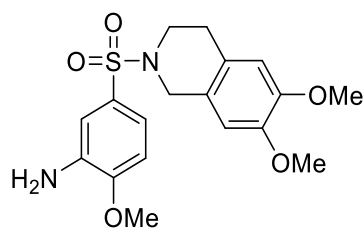


1,2,3,4-Tetrahydroisoquinoline (95 μ L, 0.76 mmol) was added dropwise at 0 $^{\circ}$ C to a suspension of NaH (60% in mineral oil, 76 mg, 1.9 mmol) in DMF (2 mL). The reaction mixture was stirred at 0 $^{\circ}$ C over 20 minutes. A solution of 4-methoxy-3-(2,2,2-trifluoroacetamido)benzenesulfonyl chloride **19** (0.200 g, 0.630 mmol) in DMF (1 mL) was added dropwise at 0 $^{\circ}$ C to the reaction mixture. The reaction mixture was warmed to rt and stirred over 1 hour. Ethanol (5 mL) was added dropwise at 0 $^{\circ}$ C to the reaction mixture, followed by water (5 mL) and aqueous HCl (37.5% w/v, 5 mL). The reaction mixture was heated under reflux for 24 hours, then further ethanol (10 mL), water (10 mL) and aqueous HCl (37.5% w/v, 10 mL) were added. The reaction mixture was heated under reflux for 24 hours. The reaction mixture was adjusted to pH 10 by the dropwise addition of aqueous NaOH (10% w/v) at rt, then concentrated *in vacuo* to remove ethanol. The mixture was diluted with EtOAc (50 mL), and the resultant aqueous layer discarded. The

organic layer was washed with water (2 x 50 mL) and brine (50 mL), dried (MgSO₄) and concentrated *in vacuo*. Purification by flash chromatography (0 – 30% EtOAc in PET) afforded **33j** (0.146 g, 73% yield).

LCMS (ESI+): m/z 319.2 [M + H]⁺, rt 1.94 minutes, >99%; ¹H NMR (400 MHz, (CD₃)₂SO) 7.18-7.09 (4H, m), 7.07 (1H, d, J = 1.9 Hz), 7.02-6.94 (2H, m), 5.23 (2H, s), 4.10 (2H, s), 3.83 (3H, s), 3.20 (2H, t, J = 5.9 Hz), 2.86 (2H, t, J = 5.9 Hz); ¹³C NMR (100 MHz, (CD₃)₂SO) 149.5, 138.4, 133.0, 131.7, 128.7, 127.1, 126.6, 126.4, 126.1, 116.1, 111.4, 110.0, 55.6, 47.3, 43.6, 28.2; ν_{max}/cm⁻¹ 3457 (N-H), 3363 (N-H), 1624, 1583, 1505; HRMS (ESI)+: m/z calculated for [C₁₆H₁₈N₂O₃S + H]⁺ = 319.1111, observed 319.1122.

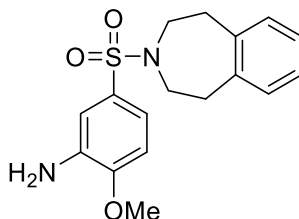
5-((6,7-Dimethoxy-3,4-dihydroisoquinolin-2(1H)-yl)sulfonyl)-2-methoxyaniline (**33k**)



6,7-Dimethoxy-1,2,3,4-tetrahydroisoquinoline hydrochloride (0.174 g, 0.756 mmol) was added portionwise at 0 °C to a suspension of NaH (60% in mineral oil, 0.126 g, 3.15 mmol) in DMF (3 mL). The reaction mixture was stirred at 0 °C over 20 minutes. A solution of 4-methoxy-3-(2,2,2-trifluoroacetamido)benzenesulfonyl chloride **19** (0.200 g, 0.630 mmol) in DMF (2 mL) was added dropwise at 0 °C to the reaction mixture. The reaction mixture was warmed to rt and stirred over 1 hour. Ethanol (15 mL) was added dropwise at 0 °C to the reaction mixture, followed by water (15 mL) and aqueous HCl (37.5% w/v, 15 mL). The reaction mixture was heated under reflux for 20 hours. The reaction mixture was concentrated *in vacuo* to remove ethanol, then adjusted to pH 14 by the dropwise addition of aqueous NaOH (10% w/v). The mixture was diluted with EtOAc (50 mL), and the resultant aqueous layer discarded. The organic layer was washed with water (2 x 50 mL) and brine (50 mL), dried (MgSO₄) and concentrated *in vacuo*. Purification by flash chromatography (0 – 100% EtOAc in PET) afforded **33k** (0.194 g, 81% yield).

LCMS (ESI+): m/z 379.3 [M + H]⁺, rt 1.80 minutes, >99%; ¹H NMR (400 MHz, CDCl₃) 7.21 (1H, dd, J = 8.4, 2.2 Hz), 7.13 (1H, d, J = 2.2 Hz), 6.84 (1H, d, J = 8.4 Hz), 6.55 (1H, s), 6.50 (1H, s), 4.15 (2H, s), 4.01 (2H, br s), 3.90 (3H, s), 3.82 (3H, s), 3.81 (3H, s), 3.31 (2H, t, J = 5.9 Hz), 2.84 (2H, t, J = 5.8 Hz); ¹³C NMR (100 MHz, CDCl₃) 150.5, 147.9, 147.8, 136.8, 128.1, 125.2, 123.8, 118.9, 113.2, 111.4, 109.8, 109.2, 56.1, 56.0, 55.9, 47.5, 44.0, 28.7; ν_{max}/cm⁻¹ 3483 (N-H), 3365 (N-H), 2966, 2930, 2842, 1661, 1611, 1578, 1512; HRMS (ESI)+: m/z calculated for [C₁₈H₂₂N₂O₅S + Na]⁺ = 401.1142, observed 401.1124.

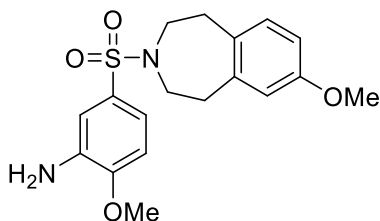
2-Methoxy-5-((1,2,4,5-tetrahydro-3H-benzo[d]azepin-3-yl)sulfonyl)aniline (**33l**)



A solution of 2,3,4,5-tetrahydro-1H-benzo[d]azepine (0.167 g, 1.13 mmol) in DMF (1 mL) was added dropwise at 0 °C to a suspension of NaH (60% in mineral oil, 0.113 g, 2.83 mmol) in DMF (2 mL). The reaction mixture was stirred at 0 °C over 20 minutes. A solution of 4-methoxy-3-(2,2,2-trifluoroacetamido)benzenesulfonyl chloride **19** (0.300 g, 0.944 mmol) in DMF (2 mL) was added dropwise at 0 °C to the reaction mixture. The reaction mixture was warmed to rt and stirred over 30 minutes. Ethanol (30 mL) was added dropwise at 0 °C to the reaction mixture, followed by water (30 mL) and aqueous HCl (37.5% w/v, 30 mL). The reaction mixture was heated under reflux for 15 hours. The reaction mixture was concentrated *in vacuo* to remove ethanol, then adjusted to pH 8 by the dropwise addition of aqueous NaOH (10% w/v). The mixture was diluted with EtOAc (100 mL), and the resultant aqueous layer discarded. The organic layer was washed with water (2 x 100 mL) and brine (100 mL), dried (MgSO₄) and concentrated *in vacuo*. Purification by flash chromatography (0 – 50% EtOAc in PET) afforded **33l** (0.131 g, 42% yield).

LCMS (ESI+): m/z 333.2 [M + H]⁺, rt 2.07 minutes, >99%; ¹H NMR (500 MHz, (CD₃)₂SO) 7.10 (4H, s), 7.00-6.96 (1H, m), 6.93-6.88 (2H, m), 5.17 (2H, s), 3.80 (3H, s), 3.17-3.06 (4H, m), 2.96-2.87 (4H, m); ¹³C NMR (125 MHz, (CD₃)₂SO) 149.3, 140.5, 138.3, 129.1, 129.0, 126.5, 115.5, 110.9, 109.9, 55.5, 48.2, 35.6; ν_{max}/cm⁻¹ 3459 (N-H), 3367 (N-H), 2906, 2850, 1615, 1579, 1509; HRMS (ESI+): m/z calculated for [C₁₇H₂₀N₂O₃S + Na]⁺ = 355.1087, observed 355.1085.

2-Methoxy-5-((7-methoxy-1,2,4,5-tetrahydro-3H-benzo[d]azepin-3-yl)sulfonyl)aniline (**33m**)

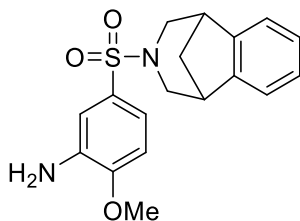


Triethylamine (0.29 mL, 2.1 mmol) and DCM (10 mL) were added to a mixture of 7-methoxy-2,3,4,5-tetrahydro-1H-benzo[d]azepine hydrochloride (96 mg, 0.45 mmol), 4-methoxy-3-(2,2,2-

trifluoroacetamido)benzenesulfonyl chloride **19** (0.130 g, 0.409 mmol) and DMAP (10 mg, 0.082 mmol). The reaction mixture was stirred over 1 hour, then concentrated *in vacuo*. Ethanol (30 mL), water (30 mL) and aqueous HCl (37.5% w/v, 30 mL) were added, and the reaction mixture heated under reflux for 3 hours. The reaction mixture was adjusted to pH 10 by the dropwise addition of Na₂CO₃ solution at 0 °C and extracted into DCM (3 x 100 mL). The combined organic extracts were washed (brine), dried (MgSO₄) and concentrated *in vacuo*. Purification by flash chromatography (20 – 50% EtOAc in PET) afforded **33m** (0.111 g, 75% yield).

LCMS (ESI+): m/z 363.3 [M + H]⁺, rt 2.01 minutes, >99%; ¹H NMR (500 MHz, (CD₃)₂SO) 7.00 (1H, d, J = 8.3 Hz), 6.97 (1H, d, J = 1.9 Hz), 6.93-6.87 (2H, m), 6.69 (1H, d, J = 2.7 Hz), 6.64 (1H, dd, J = 8.3, 2.7 Hz), 5.17 (2H, s), 3.80 (3H, s), 3.67 (3H, s), 3.16-3.02 (4H, m), 2.91-2.77 (4H, m); ¹³C NMR (125 MHz, (CD₃)₂SO) 157.8, 149.3, 141.8, 138.4, 132.5, 130.2, 129.0, 115.6, 115.0, 111.2, 110.9, 109.9, 55.6, 55.0, 48.7, 48.2, 35.8, 34.7; ν_{max}/cm⁻¹ 3474 (N-H), 3443, 3367 (N-H), 2944, 2906, 2845, 1613, 1579, 1506; HRMS (ESI+): m/z calculated for [C₁₈H₂₂N₂O₄S + Na]⁺ = 385.1192, observed 385.1192.

2-Methoxy-5-((1,2,4,5-tetrahydro-3H-1,5-methanobenzo[d]azepin-3-yl)sulfonyl)aniline (33n)

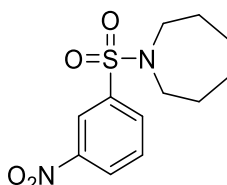


Triethylamine (0.33 mL, 2.4 mmol) and DCM (10 mL) were added to a mixture of 2,3,4,5-tetrahydro-1H-1,5-methano-3-benzazepine hydrochloride (0.102 g, 0.519 mmol), 4-methoxy-3-(2,2,2-trifluoroacetamido)benzenesulfonyl chloride **19** (0.150 g, 0.472 mmol) and DMAP (12 mg, 0.094 mmol). The reaction mixture was stirred over 1 hour, then concentrated *in vacuo*. Ethanol (30 mL), water (30 mL) and aqueous HCl (37.5% w/v, 30 mL) were added, and the reaction mixture heated under reflux for 16 hours. The reaction mixture was adjusted to pH 10 by the dropwise addition of Na₂CO₃ solution at 0 °C and extracted into DCM (3 x 100 mL). The combined organic extracts were washed (brine), dried (MgSO₄) and concentrated *in vacuo*. Purification by flash chromatography (0 – 50% EtOAc in PET) afforded **33n** (0.118 g, 65% yield).

LCMS (ESI+): m/z 345.2 [M + H]⁺, rt 2.05 minutes, >99%; ¹H NMR (500 MHz, (CD₃)₂SO) 7.25-7.14 (4H, m), 6.88 (1H, d, J = 8.5 Hz), 6.84 (1H, d, J = 2.3 Hz), 6.68 (1H, dd, J = 8.3, 2.3 Hz), 5.14 (2H, s), 3.83 (3H, s), 3.46-

3.38 (2H, m), 3.23-3.16 (2H, m), 2.74 (2H, dd, J = 10.7, 1.3 Hz), 2.14-2.04 (1H, m), 1.50 (1H, d, J = 10.8 Hz); ^{13}C NMR (125 MHz, $(\text{CD}_3)_2\text{SO}$) 149.2, 144.4, 138.1, 128.0, 126.9, 122.4, 115.6, 111.2, 109.8, 55.6, 49.3, 41.5 (1 peak missing); $\nu_{\text{max}}/\text{cm}^{-1}$ 3455 (N-H), 3364 (N-H), 2950, 2854, 1733, 1621, 1578, 1509; HRMS (ESI)+: m/z calculated for $[\text{C}_{18}\text{H}_{20}\text{N}_2\text{O}_3\text{S} + \text{Na}]^+$ = 367.1087, observed 367.1092.

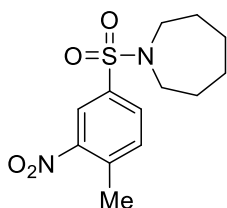
1-((3-Nitrophenyl)sulfonyl)azepane (35)



Hexamethyleneimine (0.303 mL, 2.71 mmol) was added dropwise at 0 °C to a suspension of NaH (60% in mineral oil, 0.271 g, 6.77 mmol) in DMF (3 mL). The reaction mixture was stirred at 0 °C over 20 minutes. A solution of 3-nitrobenzenesulfonyl chloride **34** (0.500 g, 2.26 mmol) in DMF (2 mL) was added dropwise at 0 °C to the reaction mixture. The reaction mixture was warmed to rt and stirred over 90 min. Water (25 mL) was added dropwise at 0 °C to the reaction mixture, followed by EtOAc (25 mL) with the resultant aqueous layer discarded. The organic layer was washed with water (2 x 25 mL) and brine (25 mL), dried (MgSO_4) and concentrated *in vacuo*. Purification by flash chromatography (0 – 20% EtOAc in PET) afforded **35** (0.267 g, 42% yield).

^1H NMR (400 MHz, CDCl_3) 8.61 (1H, t, J = 1.9 Hz), 8.40 (1H, ddd, J = 8.2, 2.2, 1.0 Hz), 8.12 (1H, ddd, J = 7.8, 1.7, 1.1 Hz), 7.73 (1H, t, J = 8.0 Hz), 3.31 (4H, t, J = 5.9 Hz), 1.80-1.68 (4H, m), 1.65-1.55 (4H, m); ^{13}C NMR (100 MHz, CDCl_3) 148.5, 142.0, 132.5, 130.5, 126.8, 122.1, 48.6, 29.3, 26.9; $\nu_{\text{max}}/\text{cm}^{-1}$ 3101, 2937, 2858, 1608, 1523 (N=O), 1338 (N=O); HRMS (ESI)+: m/z calculated for $[\text{C}_{12}\text{H}_{16}\text{N}_2\text{O}_4\text{S} + \text{H}]^+$ = 285.0904, observed 285.0897.

1-((4-Methyl-3-nitrophenyl)sulfonyl)azepane (37)

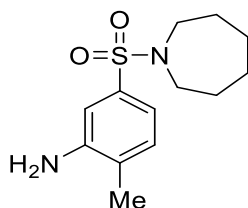


Hexamethyleneimine (0.285 mL, 2.55 mmol) was added dropwise at 0 °C to a suspension of NaH (60% in mineral oil, 0.110 g, 2.76 mmol) in DMF (3 mL). The reaction mixture was stirred at 0 °C over 20 minutes.

A solution of 4-methyl-3-nitrobenzenesulfonyl chloride **36** (0.500 g, 2.12 mmol) in DMF (2 mL) was added dropwise at 0 °C to the reaction mixture. The reaction mixture was warmed to rt and stirred over 1 hour. Water (25 mL) was added dropwise at 0 °C to the reaction mixture, followed by EtOAc (25 mL) with the resultant aqueous layer discarded. The organic layer was washed with water (2 x 25 mL) and brine (25 mL), dried (MgSO₄) and concentrated *in vacuo*. Purification by flash chromatography (0 – 20% EtOAc in PET) afforded **37** (0.453 g, 72% yield).

LCMS (ESI+): m/z 299.2 [M + H]⁺, rt 2.15 minutes, >99%; ¹H NMR (400 MHz, CDCl₃) 8.35 (1H, d, J = 1.9 Hz), 7.89 (1H, dd, J = 8.0, 1.9 Hz), 7.50 (1H, d, J = 8.1 Hz), 3.30 (4H, t, J = 5.9 Hz), 2.67 (3H, s), 1.81-1.68 (4H, m), 1.65-1.54 (4H, m); ¹³C NMR (100 MHz, CDCl₃) 149.3, 139.3, 137.9, 133.9, 130.8, 123.4, 48.5, 29.3, 27.0, 20.6; ν_{max}/cm⁻¹ 2934, 2861, 1608, 1523 (N=O), 1338 (N=O); HRMS (ESI+): m/z calculated for [C₁₃H₁₈N₂O₄S + H]⁺ = 299.1060, observed 299.1065.

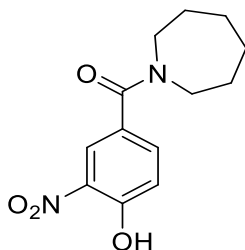
5-(Azepan-1-ylsulfonyl)-2-methylaniline (**38**)



NaBH₄ (83 mg, 2.2 mmol) was added portionwise at 0 °C to a suspension of NiCl₂ (95 mg, 0.74 mmol) in methanol (2 mL). The reaction mixture was warmed to rt and stirred over 30 minutes. 1-((4-Methyl-3-nitrophenyl)sulfonyl)azepane **37** (0.439 g, 1.47 mmol) was added at 0 °C to the reaction mixture, followed by further methanol (8 mL) and NaBH₄ (0.278 g, 7.36 mmol). The reaction mixture was warmed to rt and stirred over 45 minutes. Water (10 mL) was added at 0 °C and the mixture filtered through celite, eluted with methanol (10 mL) and water (15 mL). The filtrate was concentrated *in vacuo* to remove methanol, then extracted into EtOAc (3 x 25 mL). The combined organic extracts were washed (brine), dried (MgSO₄) and concentrated *in vacuo*. Purification by flash chromatography (20 – 50% EtOAc in PET) afforded **38** (0.347 g, 88% yield).

LCMS (ESI+): m/z 269.2 [M + H]⁺, rt 1.90 minutes, >99%; ¹H NMR (400 MHz, CDCl₃) 7.13 (1H, d, J = 8.4 Hz), 7.10-7.04 (2H, m), 3.80 (2H, br s), 3.24 (4H, t, J = 5.9 Hz), 2.19 (3H, s), 1.77-1.65 (4H, m), 1.63-1.53 (4H, m); ¹³C NMR (100 MHz, CDCl₃) 145.2, 137.9, 131.0, 126.7, 116.9, 112.8, 48.4, 29.3, 27.1, 17.6; ν_{max}/cm⁻¹ 3490 (N-H), 3377 (N-H), 2930, 2858, 1625, 1574; HRMS (ESI+): m/z calculated for [C₁₃H₂₀N₂O₂S + H]⁺ = 269.1318, observed 269.1321.

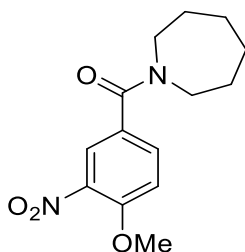
Azepan-1-yl(4-hydroxy-3-nitrophenyl)methanone (42)



T3P® (50 wt. % in DMF, 3.3 mL, 5.5 mmol) and DIPEA (0.95 mL, 5.5 mmol) were added to a solution of 4-hydroxy-3-nitrobenzoic acid **41** (0.500 g, 2.73 mmol) and hexamethyleneimine (0.61 mL, 5.5 mmol) in DMF (2 mL). The reaction mixture was stirred over 1 day, then diluted with water (15 mL), adjusted to pH 2 and extracted into DCM (3 x 20 mL). The combined organic extracts were dried (MgSO₄) and concentrated *in vacuo*. Purification by flash chromatography (0 – 10% methanol in DCM) afforded **42** (0.174 g, 24% yield).

LCMS (ESI+): m/z 265.3 [M + H]⁺, (ESI-): m/z 263.2 [M - H]⁻, rt 1.84 minutes, >99%; ¹H NMR (400 MHz, CD₃CN) 10.34 (1H, br s), 8.10 (1H, d, J = 2.0 Hz), 7.65 (1H, dd, J = 8.7, 2.2 Hz), 7.20 (1H, d, J = 8.6 Hz), 3.58 (2H, t, J = 5.7 Hz), 3.37 (2H, t, J = 5.4 Hz), 1.83-1.71 (2H, m), 1.68-1.51 (6H, m); ¹³C NMR (100 MHz, CD₃CN) 169.3, 155.8, 136.8, 134.5, 130.8, 124.4, 120.9, 50.5, 46.9, 30.0, 28.4, 28.0, 27.0; ν_{max}/cm⁻¹ 2927, 2857, 1623 (C=O), 1531 (N=O), 1350 (N=O); HRMS (ESI)+: m/z calculated for [C₁₃H₁₆N₂O₄ + H]⁺ = 265.1183, observed 265.1184.

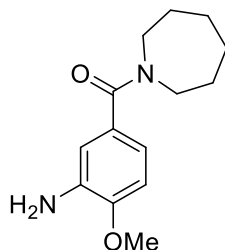
Azepan-1-yl(4-methoxy-3-nitrophenyl)methanone (43)



Dimethyl sulfate (0.115 mL, 1.21 mmol) was added to a suspension of azepan-1-yl(4-hydroxy-3-nitrophenyl)methanone **42** (0.160 g, 0.605 mmol) and K₂CO₃ (0.167 g, 1.21 mmol) in acetone (5 mL). The reaction mixture was heated under reflux for 2 hours. The reaction mixture was diluted with water (15 mL) at 0 °C, then concentrated *in vacuo* to remove acetone. The product was extracted into DCM (3 x 20 mL). The combined organic extracts were dried (MgSO₄) and concentrated *in vacuo*. Purification by flash chromatography (40 – 100% EtOAc in PET) afforded **43** (0.129 g, 77% yield).

LCMS (ESI+): m/z 279.3 $[M + H]^+$, rt 1.90 minutes, >99%; 1H NMR (400 MHz, CD_3CN) 7.83 (1H, d, $J = 2.1$ Hz), 7.62 (1H, dd, $J = 8.6, 2.1$ Hz), 7.27 (1H, d, $J = 8.7$ Hz), 3.96 (3H, s), 3.58 (2H, t, $J = 5.7$ Hz), 3.37 (2H, t, $J = 5.5$ Hz), 1.83-1.71 (2H, m), 1.67-1.50 (6H, m); ^{13}C NMR (100 MHz, CD_3CN) 169.4, 153.9, 140.1, 133.6, 130.7, 124.7, 114.9, 57.6, 50.5, 46.8, 30.0, 28.5, 28.0, 27.0; ν_{max}/cm^{-1} 2928, 2854, 1615 (C=O), 1530 (N=O), 1350 (N=O); HRMS (ESI+): m/z calculated for $[C_{14}H_{18}N_2O_4 + H]^+ = 279.1339$, observed 279.1345.

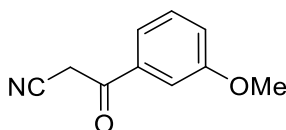
(3-Amino-4-methoxyphenyl)(azepan-1-yl)methanone (44)



$NaBH_4$ (22 mg, 0.59 mmol) was added portionwise at 0 °C to a suspension of $NiCl_2 \cdot 6H_2O$ (47 mg, 0.20 mmol) in methanol (1 mL). The reaction mixture was warmed to rt and stirred over 20 minutes. A solution of azepan-1-yl(4-methoxy-3-nitrophenyl)methanone **43** (0.109 g, 0.392 mmol) in methanol (1 mL) was added at 0 °C to the reaction mixture, followed by $NaBH_4$ (52 mg, 1.4 mmol). The reaction mixture was warmed to rt and stirred over 1 hour, then further $NaBH_4$ (30 mg, 0.78 mmol) was added at 0 °C. The reaction mixture was warmed to rt and stirred over 30 minutes. Water (15 mL) was added at 0 °C, and the reaction mixture filtered through celite. The filtrate was extracted into DCM (3 x 20 mL). The combined organic extracts were dried ($MgSO_4$) and concentrated *in vacuo*. Purification by flash chromatography (20 – 100% EtOAc in PET) afforded **44** (62 mg, 64% yield).

LCMS (ESI+): m/z 249.3 $[M + H]^+$, rt 1.61 minutes, >99%; 1H NMR (500 MHz, CD_3CN) 6.80 (1H, d, $J = 8.1$ Hz), 6.65 (1H, d, $J = 2.0$ Hz), 6.62 (1H, dd, $J = 8.1, 2.1$ Hz), 4.16 (2H, br s), 3.83 (3H, s), 3.61-3.48 (2H, m), 3.44-3.29 (2H, m), 1.82-1.67 (2H, m), 1.66-1.48 (6H, m); ^{13}C NMR (125 MHz, CD_3CN) 172.2, 148.3, 138.0, 131.5, 116.6, 113.3, 110.8, 56.2, 50.4, 46.6, 30.2, 28.5, 28.1, 27.0; ν_{max}/cm^{-1} 3466 (N-H), 3330 (N-H), 2922, 2853, 1608 (C=O), 1584, 1516; HRMS (ESI+): m/z calculated for $[C_{14}H_{20}N_2O_2 + H]^+ = 249.1598$, observed 249.1600.

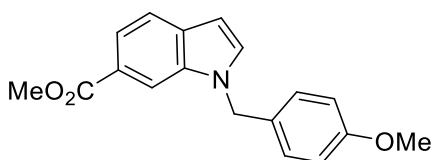
3-(3-Methoxyphenyl)-3-oxopropanenitrile (58)



n-Butyllithium (1.6 M in hexanes, 5.2 mL, 8.3 mmol) was added dropwise at -78 °C to a mixture of acetonitrile (0.87 mL, 17 mmol) and THF (10 mL). The reaction mixture was stirred at -78 °C over 30 minutes. Ethyl 3-methoxybenzoate **57** (0.600 g, 3.33 mmol) was added dropwise at -78 °C, and the reaction mixture stirred at -78 °C over 30 minutes. Water (10 mL) and aqueous HCl (1 M, 20 mL) were added dropwise at 0 °C. The product was extracted into DCM (3 x 25 mL). The combined organic extracts were washed (brine), dried (MgSO₄) and concentrated *in vacuo*. Purification by flash chromatography (0 – 50% EtOAc in PET) afforded **58** (0.599 g, 99% yield).

LCMS (ESI-): m/z 174.1 [M - H]⁻, rt 1.56 minutes, >99%; ¹H NMR (400 MHz, CDCl₃) 7.49-7.39 (3H, m), 7.23-7.17 (1H, m), 4.07 (2H, s), 3.87 (3H, s); ¹³C NMR (100 MHz, CDCl₃) 187.1, 160.3, 135.7, 130.3, 121.4, 121.1, 113.9, 112.8, 55.7, 29.6; spectroscopic data consistent with literature.¹⁴³

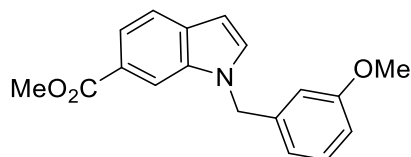
Methyl 1-(4-methoxybenzyl)-1H-indole-6-carboxylate (64a)



4-Methoxybenzyl chloride (0.255 mL, 1.88 mmol) was added to a suspension of methyl 1H-indole-6-carboxylate **63** (0.300 g, 1.71 mmol) and Cs₂CO₃ (1.12 g, 3.42 mmol) in acetonitrile (10 mL). The reaction mixture was heated under reflux for 1 hour, then concentrated *in vacuo*. Water (25 mL) was added to the resultant residue and the product extracted into DCM (3 x 25 mL). The combined organic extracts were washed (brine), dried (MgSO₄) and concentrated *in vacuo*. Purification by flash chromatography (0 – 30% EtOAc in PET) afforded **64a** (0.445 g, 88% yield).

LCMS (ESI+): m/z 296.2 [M + H]⁺, rt 2.16 minutes, >99%; ¹H NMR (400 MHz, CDCl₃) 8.12 (1H, s), 7.81 (1H, dd, J = 8.3, 1.3 Hz), 7.65 (1H, d, J = 8.4 Hz), 7.24 (1H, d, J = 3.1 Hz), 7.12-7.04 (2H, m), 6.87-6.81 (2H, m), 6.57 (1H, dd, J = 3.1, 0.6 Hz), 5.31 (2H, s), 3.92 (3H, s), 3.77 (3H, s); ¹³C NMR (100 MHz, CDCl₃) 168.3, 159.4, 135.8, 132.5, 131.3, 129.1, 128.5, 123.5, 120.7, 120.6, 114.4, 112.1, 102.1, 55.4, 52.1, 49.7; ν_{max}/cm⁻¹ 2951, 2835, 1697 (C=O), 1614, 1585, 1511; HRMS (ESI)+: m/z calculated for [C₁₈H₁₇NO₃ + Na]⁺ = 318.1101, observed 318.1107.

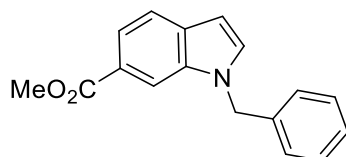
Methyl 1-(3-methoxybenzyl)-1H-indole-6-carboxylate (64b)



3-Methoxybenzyl chloride (0.299 mL, 2.05 mmol) was added to a suspension of methyl 1H-indole-6-carboxylate **63** (0.300 g, 1.71 mmol) and Cs₂CO₃ (1.12 g, 3.42 mmol) in acetonitrile (10 mL). The reaction mixture was heated under reflux for 1 hour, then concentrated *in vacuo*. Water (20 mL) was added to the resultant residue and the product extracted into DCM (3 x 25 mL). The combined organic extracts were washed (brine), dried (MgSO₄) and concentrated *in vacuo*. Purification by flash chromatography (0 – 25% EtOAc in PET) afforded **64b** (0.471 g, 93% yield).

LCMS (ESI+): m/z 296.2 [M + H]⁺, rt 2.18 minutes, 98%; ¹H NMR (500 MHz, CDCl₃) 8.10 (1H, s), 7.81 (1H, dd, J = 8.3, 1.4 Hz), 7.66 (1H, dd, J = 8.4, 0.6 Hz), 7.27 (1H, d, J = 3.2 Hz), 7.22 (1H, t, J = 7.9 Hz), 6.81 (1H, dd, J = 8.1, 2.4 Hz), 6.72-6.68 (1H, m), 6.65-6.62 (1H, m), 6.59 (1H, dd, J = 3.1, 0.9 Hz), 5.35 (2H, s), 3.91 (3H, s), 3.73 (3H, s); ¹³C NMR (125 MHz, CDCl₃) 168.3, 160.2, 138.8, 135.9, 132.4, 131.6, 130.1, 123.6, 120.8, 120.7, 119.2, 113.1, 112.8, 112.1, 102.4, 55.3, 52.1, 50.1; ν_{max}/cm⁻¹ 2913, 1703 (C=O), 1602, 1505; HRMS (ESI+): m/z calculated for [C₁₈H₁₇NO₃ + H]⁺ = 296.1281, observed 296.1277.

Methyl 1-benzyl-1H-indole-6-carboxylate (64c)

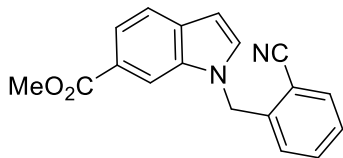


Benzyl bromide (0.244 mL, 2.05 mmol) was added to a suspension of methyl 1H-indole-6-carboxylate **63** (0.300 g, 1.71 mmol) and Cs₂CO₃ (1.12 g, 3.42 mmol) in acetonitrile (15 mL). The reaction mixture was heated under reflux for 2 hours, then concentrated *in vacuo*. Water (15 mL) was added to the resultant residue and the product extracted into DCM (3 x 25 mL). The combined organic extracts were washed (brine), dried (MgSO₄) and concentrated *in vacuo*. Purification by flash chromatography (0 – 25% EtOAc in PET) afforded **64c** (0.436 g, 91% yield).

LCMS (ESI+): m/z 266.2 [M + H]⁺, rt 2.16 minutes, 95%; ¹H NMR (400 MHz, CDCl₃) 8.09 (1H, s), 7.80 (1H, dd, J = 8.3, 1.4 Hz), 7.65 (1H, d, J = 8.3 Hz), 7.34-7.23 (4H, m), 7.13-7.07 (2H, m), 6.58 (1H, dd, J = 3.1, 0.7 Hz), 5.38 (2H, s), 3.90 (3H, s); ¹³C NMR (100 MHz, CDCl₃) 168.3, 137.2, 135.9, 132.4, 131.5, 129.0, 128.0,

126.9, 123.6, 120.8, 120.7, 112.1, 102.3, 52.1, 50.2; $\nu_{\max}/\text{cm}^{-1}$ 2949, 1704 (C=O), 1613; HRMS (ESI)+: m/z calculated for $[\text{C}_{17}\text{H}_{15}\text{NO}_2 + \text{H}]^+ = 266.1176$, observed 266.1182.

Methyl 1-(2-cyanobenzyl)-1H-indole-6-carboxylate (64d)



2-(Bromomethyl)benzotrile (0.403 g, 2.05 mmol) was added to a suspension of methyl 1H-indole-6-carboxylate **63** (0.300 g, 1.71 mmol) and Cs_2CO_3 (1.12 g, 3.42 mmol) in acetonitrile (10 mL). The reaction mixture was heated under reflux for 4 hours, then concentrated *in vacuo*. Water (20 mL) was added to the resultant residue and the product extracted into DCM (3 x 25 mL). The combined organic extracts were washed (brine), dried (MgSO_4) and concentrated *in vacuo*. Purification by flash chromatography (0 – 25% EtOAc in PET) afforded **64d** (0.399 g, 80% yield).

^1H NMR (400 MHz, CDCl_3) 8.04 (1H, s), 7.84 (1H, dd, $J = 8.4, 1.4$ Hz), 7.73 (1H, dd, $J = 7.5, 1.4$ Hz), 7.69 (1H, d, $J = 8.3$ Hz), 7.44 (1H, td, $J = 7.7, 1.4$ Hz), 7.38 (1H, td, $J = 7.6, 1.2$ Hz), 7.33 (1H, d, $J = 3.2$ Hz), 6.78 (1H, dd, $J = 7.7, 0.7$ Hz), 6.65 (1H, dd, $J = 3.2, 0.8$ Hz), 5.62 (2H, s), 3.91 (3H, s); ^{13}C NMR (100 MHz, CDCl_3) 168.1, 140.9, 135.8, 133.6, 133.3, 132.5, 131.6, 128.5, 127.4, 124.1, 121.2, 121.0, 117.2, 111.8, 110.9, 103.2, 52.2, 48.3; $\nu_{\max}/\text{cm}^{-1}$ 2227 (C \equiv N), 1703 (C=O), 1616, 1601, 1502; HRMS (ESI)+: m/z calculated for $[\text{C}_{18}\text{H}_{14}\text{N}_2\text{O}_2 + \text{H}]^+ = 291.1128$, observed 291.1134.

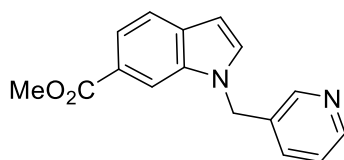
Methyl 1-(pyridin-2-ylmethyl)-1H-indole-6-carboxylate (64f)



2-(Bromomethyl)pyridine hydrobromide (0.476 mg, 1.88 mmol) was added to a suspension of methyl 1H-indole-6-carboxylate **63** (0.300 g, 1.71 mmol) and Cs_2CO_3 (1.39 g, 4.28 mmol) in acetonitrile (15 mL). The reaction mixture was heated under reflux for 15 hours, then concentrated *in vacuo*. Water (20 mL) was added and the product extracted into DCM (3 x 25 mL). The combined organic extracts were washed (brine), dried (MgSO_4) and concentrated *in vacuo*. Purification by flash chromatography (0 – 50% EtOAc in PET) afforded **64f** (0.386 g, 85% yield).

LCMS (ESI+): m/z 267.3 $[M + H]^+$, rt 1.82 minutes, 100%; ^1H NMR (400 MHz, CDCl_3) 8.60 (1H, dq, $J = 4.9, 0.8$ Hz), 8.09-8.05 (1H, m), 7.82 (1H, dd, $J = 8.3, 1.4$ Hz), 7.67 (1H, dd, $J = 8.3, 0.5$ Hz), 7.54 (1H, td, $J = 7.7, 1.8$ Hz), 7.37 (1H, d, $J = 3.2$ Hz), 7.21-7.14 (1H, m), 6.70 (1H, d, $J = 7.8$ Hz), 6.63 (1H, dd, $J = 3.1, 0.8$ Hz), 5.52 (2H, s), 3.90 (3H, s); ^{13}C NMR (100 MHz, CDCl_3) 168.2, 157.1, 149.7, 137.3, 135.8, 132.5, 131.8, 123.8, 122.8, 120.9, 120.8, 112.1, 102.7, 52.10, 52.08 (1 peak missing); $\nu_{\text{max}}/\text{cm}^{-1}$ 1717 (C=O), 1593, 1505; HRMS (ESI)+: m/z calculated for $[\text{C}_{16}\text{H}_{14}\text{N}_2\text{O}_2 + \text{H}]^+ = 267.1128$, observed 267.1136.

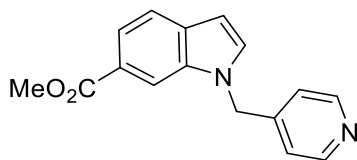
Methyl 1-(pyridin-3-ylmethyl)-1H-indole-6-carboxylate (64g)



Methyl 1H-indole-6-carboxylate **63** (0.600 g, 3.42 mmol) was added portionwise at 0 °C to a suspension of NaH (60% in mineral oil, 0.685 g, 17.1 mmol) in DMF (5 mL). The reaction mixture was warmed to rt and stirred over 1 hour. 3-(Chloromethyl)pyridine hydrochloride (0.674 g, 4.11 mmol) was added portionwise at 0 °C to the reaction mixture. The reaction mixture was warmed to rt and stirred over 45 minutes. Methanol (150 mL) was added dropwise at 0 °C, and the reaction mixture adjusted to pH 1 using sulfuric acid dropwise at 0 °C. The reaction mixture was heated under reflux for 14 hours, then further sulfuric acid (10 mL) was added dropwise at 0 °C. The reaction mixture was heated under reflux for 2 hours, then concentrated *in vacuo*. NaHCO_3 solution (200 mL) was added dropwise at 0 °C. The product was extracted into DCM (3 x 150 mL). The combined organic extracts were washed with NaHCO_3 solution (100 mL) and brine (100 mL), dried (MgSO_4) and concentrated *in vacuo*. Purification by flash chromatography (70% EtOAc in PET) afforded **64g** (0.732 g, 75% yield).

LCMS (ESI+): m/z 267.2 $[M + H]^+$, rt 1.61 minutes, 96%; ^1H NMR (400 MHz, CDCl_3) 8.54 (1H, dd, $J = 4.8, 1.4$ Hz), 8.51 (1H, d, $J = 1.9$ Hz), 8.06 (1H, s), 7.82 (1H, dd, $J = 8.3, 1.4$ Hz), 7.67 (1H, d, $J = 8.3$ Hz), 7.33 (1H, dt, $J = 7.8, 1.9$ Hz), 7.27 (1H, d, $J = 3.2$ Hz), 7.22 (1H, dd, $J = 7.8, 4.9$ Hz), 6.62 (1H, dd, $J = 3.2, 0.8$ Hz), 5.41 (2H, s), 3.91 (3H, s); ^{13}C NMR (100 MHz, CDCl_3) 168.1, 149.4, 148.3, 135.7, 134.7, 132.9, 132.5, 131.2, 124.0, 123.9, 121.1, 120.9, 111.8, 103.0, 52.1, 47.8; $\nu_{\text{max}}/\text{cm}^{-1}$ 3093, 2941, 1696 (C=O), 1613, 1577, 1506; HRMS (ESI)+: m/z calculated for $[\text{C}_{16}\text{H}_{14}\text{N}_2\text{O}_2 + \text{H}]^+ = 267.1128$, observed 267.1122.

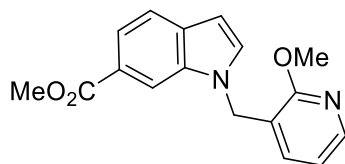
Methyl 1-(pyridin-4-ylmethyl)-1H-indole-6-carboxylate (64h)



Methyl 1H-indole-6-carboxylate **63** (0.400 g, 2.28 mmol) was added portionwise at 0 °C to a suspension of NaH (60% in mineral oil, 0.457 g, 11.4 mmol) in DMF (5 mL). The reaction mixture was warmed to rt and stirred over 1 hour. 4-(Bromomethyl)pyridine hydrobromide (0.635 g, 2.51 mmol) was added portionwise at 0 °C to the reaction mixture. The reaction mixture was warmed to rt and stirred over 45 minutes. Methanol (150 mL) was added dropwise at 0 °C, and the reaction mixture adjusted to pH 1 using sulfuric acid dropwise at 0 °C. The reaction mixture was heated under reflux for 14 hours, then further sulfuric acid (10 mL) was added dropwise at 0 °C. The reaction mixture was heated under reflux for 2 hours, then concentrated *in vacuo*. NaHCO₃ solution (200 mL) was added dropwise at 0 °C. The product was extracted into DCM (3 x 150 mL). The combined organic extracts were washed with NaHCO₃ solution (100 mL) and brine (100 mL), dried (MgSO₄) and concentrated *in vacuo*. Purification by flash chromatography (20 – 80% EtOAc in PET) afforded **64h** (0.474 g, 71% yield).

LCMS (ESI+): m/z 267.2 [M + H]⁺, rt 1.53 minutes, 96%; ¹H NMR (400 MHz, CDCl₃) 8.56-8.49 (2H, m), 7.97 (1H, s), 7.83 (1H, dd, J = 8.4, 1.4 Hz), 7.69 (1H, dd, J = 8.3, 0.5 Hz), 7.28 (1H, d, J = 3.1 Hz), 6.96-6.91 (2H, m), 6.65 (1H, dd, J = 3.2, 0.8 Hz), 5.41 (2H, s), 3.90 (3H, s); ¹³C NMR (100 MHz, CDCl₃) 168.0, 150.3, 146.5, 135.7, 132.4, 131.5, 124.1, 121.4, 121.2, 121.0, 111.7, 103.1, 52.1, 49.1; ν_{max}/cm⁻¹ 2948, 1699 (C=O), 1602, 1562, 1504; HRMS (ESI+): m/z calculated for [C₁₆H₁₄N₂O₂ + Na]⁺ = 289.0947, observed 289.0940.

Methyl 1-((2-methoxypyridin-3-yl)methyl)-1H-indole-6-carboxylate (64i)

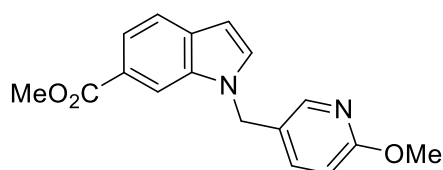


p-Toluenesulfonyl chloride (1.11 g, 5.80 mmol) and DMAP (6 mg, 0.05 mmol) were added to a solution of (2-methoxypyridin-3-yl)methanol **74** (0.673 g, 4.84 mmol) and triethylamine (1.35 mL, 9.67 mmol) in DCM (7 mL). The reaction mixture was stirred over 2 hours, then diluted with NaHCO₃ solution (25 mL) and extracted into DCM (3 x 25 mL). The combined organic extracts were washed (brine), dried (MgSO₄) and concentrated *in vacuo*. Purification by flash chromatography (0 – 15% EtOAc in PET) was attempted,

affording a crude residue. A solution of methyl 1H-indole-6-carboxylate **63** (0.710 g, 4.05 mmol) in DMF (2 mL) was added dropwise at 0 °C to a suspension of NaH (60% in mineral oil, 0.405 g, 10.1 mmol) in DMF (2 mL). The reaction mixture was warmed to rt and stirred over 30 minutes. A solution of the crude residue in DMF (1 mL) was added dropwise at 0 °C to the reaction mixture. The reaction mixture was warmed to rt and stirred over 30 minutes. Methanol (200 mL) was added dropwise at 0 °C to the reaction mixture followed by sulfuric acid (15 mL). The reaction mixture was heated under reflux for 90 minutes, then concentrated *in vacuo*. The reaction mixture was diluted with EtOAc (200 mL), washed with NaHCO₃ solution (2 x 200 mL) and brine (200 mL), dried (MgSO₄) and concentrated *in vacuo*. Purification by flash chromatography (10% EtOAc in PET) afforded **64i** (0.455 g, 31% yield).

LCMS (ESI+): m/z 297.2 [M + H]⁺, rt 2.14 minutes, 97%; ¹H NMR (400 MHz, CDCl₃) 8.10-8.05 (2H, m), 7.81 (1H, dd, J = 8.3, 1.4 Hz), 7.66 (1H, dd, J = 8.4, 0.6 Hz), 7.31 (1H, d, J = 3.2 Hz), 6.89-6.84 (1H, m), 6.73 (1H, dd, J = 7.3, 5.1 Hz), 6.60 (1H, dd, J = 3.1, 0.9 Hz), 5.34 (2H, s), 4.06 (3H, s), 3.91 (3H, s); ¹³C NMR (100 MHz, CDCl₃) 168.3, 161.1, 146.1, 136.1, 135.8, 132.4, 131.8, 123.7, 120.8, 120.7, 120.1, 117.1, 112.1, 102.4, 53.7, 52.1, 45.1; ν_{max}/cm⁻¹ 2948, 1711 (C=O), 1617, 1595, 1584, 1501; HRMS (ESI)+: m/z calculated for [C₁₇H₁₆N₂O₃ + Na]⁺ = 319.1053, observed 319.1056.

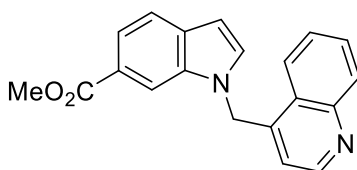
1-((6-Methoxypyridin-3-yl)methyl)-1H-indole-6-carboxylate (64k)



A solution of methyl 1H-indole-6-carboxylate **63** (0.237 g, 1.36 mmol) in DMF (1 mL) was added dropwise at 0 °C to a suspension of NaH (60% in mineral oil, 0.108 g, 2.71 mmol) in DMF (1 mL). The reaction mixture was warmed to rt and stirred over 30 minutes. A solution of 5-(chloromethyl)-2-methoxypyridine **77** (0.160 g, 0.904 mmol) in DMF (1 mL) was added dropwise at 0 °C to the reaction mixture. The reaction mixture was warmed to rt and stirred over 1 hour. Methanol (150 mL) was added dropwise at 0 °C to the reaction mixture followed by sulfuric acid (5 mL). The reaction mixture was heated under reflux for 1 hour, then concentrated *in vacuo*. The reaction mixture was diluted with EtOAc (100 mL), washed with NaHCO₃ solution (2 x 100 mL) and brine (100 mL), dried (MgSO₄) and concentrated *in vacuo*. Purification by flash chromatography (0 – 15% EtOAc in PET) afforded **64k** (0.227 g, 85% yield).

LCMS (ESI+): m/z 297.2 $[M + H]^+$, rt 2.09 minutes, >99%; 1H NMR (400 MHz, $CDCl_3$) 8.13-8.10 (1H, m), 8.05 (1H, dd, $J = 2.5, 0.6$ Hz), 7.81 (1H, dd, $J = 8.4, 1.4$ Hz), 7.65 (1H, dd, $J = 8.3, 0.6$ Hz), 7.31 (1H, dd, $J = 8.5, 2.5$ Hz), 7.23 (1H, d, $J = 3.2$ Hz), 6.67 (1H, d, $J = 8.5$ Hz), 6.58 (1H, dd, $J = 3.2, 0.8$ Hz), 5.29 (2H, s), 3.92 (3H, s), 3.91 (3H, s); ^{13}C NMR (100 MHz, $CDCl_3$) 168.2, 164.1, 145.6, 137.8, 135.6, 132.5, 131.0, 125.4, 123.7, 120.9, 120.8, 111.9, 111.5, 102.6, 53.7, 52.1, 47.3; ν_{max}/cm^{-1} 2948, 1704 (C=O), 1610, 1572; HRMS (ESI+): m/z calculated for $[C_{17}H_{16}N_2O_3 + H]^+ = 297.1234$, observed 297.1235.

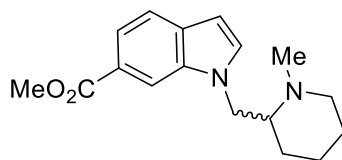
Methyl 1-(quinolin-4-ylmethyl)-1H-indole-6-carboxylate (64m)



A suspension of quinolin-4-ylmethanol **79** (0.378 g, 2.37 mmol) in aqueous HBr (48%, 5 mL) was heated under reflux for 90 minutes, then concentrated *in vacuo* to afford a crude residue. A solution of methyl 1H-indole-6-carboxylate **63** (0.400 g, 2.28 mmol) in DMF (2 mL) was added dropwise at 0 °C to a suspension of NaH (60% in mineral oil, 0.457 g, 11.4 mmol) in DMF (5 mL). The reaction mixture was warmed to rt and stirred over 30 minutes. The crude residue was added portionwise at 0 °C to the reaction mixture. The reaction mixture was warmed to rt and stirred over 15 minutes. Methanol (150 mL) was added dropwise at 0 °C to the reaction mixture followed by sulfuric acid (10 mL). The reaction mixture was heated under reflux for 2 hours, then concentrated *in vacuo*. The reaction mixture was diluted with EtOAc (200 mL), washed with $NaHCO_3$ solution (2 x 100 mL), water (2 x 200 mL) and brine (100 mL), dried ($MgSO_4$) and concentrated *in vacuo*. Purification by flash chromatography (0 – 30% EtOAc in PET) afforded **64m** (0.497 g, 65% yield).

LCMS (ESI+): m/z 317.2 $[M + H]^+$, rt 1.83 minutes, 94%; 1H NMR (400 MHz, $(CD_3)_2SO$) 8.69 (1H, d, $J = 4.4$ Hz), 8.30 (1H, d, $J = 8.4$ Hz), 8.12-8.04 (2H, m), 7.85 (1H, ddd, $J = 8.3, 7.0, 1.2$ Hz), 7.79-7.67 (4H, m), 6.72 (1H, dd, $J = 3.1, 0.7$ Hz), 6.34 (1H, d, $J = 4.4$ Hz), 6.20 (2H, s), 3.77 (3H, s); ^{13}C NMR (100 MHz, $(CD_3)_2SO$) 167.0, 150.5, 147.5, 144.0, 135.5, 133.4, 132.0, 129.7, 129.6, 126.9, 125.4, 123.7, 122.7, 120.7, 120.2, 117.4, 112.0, 102.2, 51.8, 46.3; ν_{max}/cm^{-1} 3112, 3095, 1700 (C=O), 1618, 1599, 1570, 1508; HRMS (ESI+): m/z calculated for $[C_{20}H_{16}N_2O_2 + Na]^+ = 339.1104$, observed 339.1100.

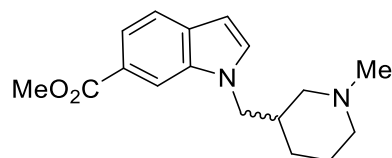
Methyl 1-((1-methylpiperidin-2-yl)methyl)-1H-indole-6-carboxylate (64n)



A solution of methyl 1H-indole-6-carboxylate **63** (0.392 g, 2.24 mmol) in DMF (2 mL) was added dropwise at 0 °C to a suspension of NaH (60% in mineral oil, 0.122 g, 3.05 mmol) in DMF (2 mL). The reaction mixture was warmed to rt and stirred over 30 minutes. A solution of 2-(chloromethyl)-1-methylpiperidine **81** (0.300 g, 2.03 mmol) in DMF (2 mL) was added at 0 °C to the reaction mixture. The reaction mixture was heated to 60 °C over 1 hour. Methanol (150 mL) was added dropwise at 0 °C to the reaction mixture followed by sulfuric acid (10 mL). The reaction mixture was heated under reflux for 1 hour, then concentrated *in vacuo*. The reaction mixture was diluted with EtOAc (200 mL), washed with NaHCO₃ solution (2 x 200 mL) and brine (200 mL), dried (MgSO₄) and concentrated *in vacuo*. Purification by flash chromatography (0 – 100% EtOAc in PET, 0 – 10% methanol in DCM) afforded **64n** (0.172 g, 27% yield).

LCMS (ESI+): m/z 287.3 [M + H]⁺, rt 1.32 minutes, 90%; ¹H NMR (400 MHz, CDCl₃) 8.11 (1H, s), 7.78 (1H, dd, J = 8.3, 1.4 Hz), 7.61 (1H, d, J = 8.3 Hz), 7.24 (1H, d, J = 3.1 Hz), 6.52 (1H, dd, J = 3.0, 0.8 Hz), 4.56 (1H, dd, J = 14.2, 4.4 Hz), 4.01-3.90 (4H, m), 2.95-2.83 (1H, m), 2.47 (3H, s), 2.44-2.34 (1H, m), 2.14 (1H, td, J = 11.3, 3.6 Hz), 1.67-1.46 (3H, m), 1.28-1.02 (3H, m); ¹³C NMR (100 MHz, CDCl₃) 168.3, 135.9, 132.2, 132.0, 123.3, 120.5, 120.4, 112.1, 101.8, 63.4, 57.3, 52.0, 49.4, 43.6, 29.5, 25.7, 23.6; ν_{max}/cm⁻¹ 2938, 2855, 2784, 1707 (C=O), 1614, 1505; HRMS (ESI)+: m/z calculated for [C₁₇H₂₂N₂O₂ + H]⁺ = 287.1754, observed 287.1751.

Methyl 1-((1-methylpiperidin-3-yl)methyl)-1H-indole-6-carboxylate (64o)

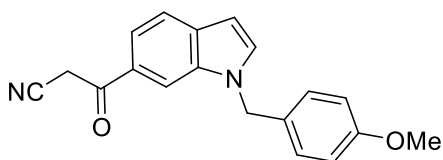


A solution of methyl 1H-indole-6-carboxylate **63** (0.568 g, 3.24 mmol) in DMF (2 mL) was added dropwise at 0 °C to a suspension of NaH (60% in mineral oil, 0.151 g, 3.78 mmol) in DMF (2 mL). The reaction mixture was warmed to rt and stirred over 30 minutes. A solution of (1-methylpiperidin-3-yl)methyl 4-methylbenzenesulfonate **83** (0.797 g, 2.70 mmol) in DMF (2 mL) was added at 0 °C to the reaction mixture, followed by NaI (81 mg, 0.54 mmol). The reaction mixture was heated to 60 °C over 1 hour, then diluted with EtOAc (200 mL), washed with NaHCO₃ solution (2 x 200 mL) and brine (200 mL), dried (MgSO₄) and

concentrated *in vacuo*. Purification by flash chromatography (0 – 8% methanol in DCM), followed by reverse phase chromatography (40 – 60% acetonitrile in water (+ 0.1% NH₃)), afforded **64o** (0.348 g, 45% yield).

LCMS (ESI+): m/z 287.3 [M + H]⁺, rt 1.49 minutes, >99%; ¹H NMR (400 MHz, CDCl₃) 8.10 (1H, s), 7.78 (1H, d, J = 8.3 Hz), 7.62 (1H, d, J = 8.4 Hz), 7.22 (1H, d, J = 3.0 Hz), 6.52 (1H, d, J = 2.9 Hz), 4.12 (1H, dd, J = 14.3, 7.9 Hz), 4.04 (1H, dd, J = 14.2, 7.2 Hz), 3.94 (3H, s), 2.73-2.61 (1H, m), 2.56 (1H, d, J = 10.2 Hz), 2.30-2.16 (4H, m), 2.06-1.93 (1H, m), 1.78 (1H, t, J = 10.1 Hz), 1.74-1.47 (3H, m), 1.12-0.97 (1H, m); ¹³C NMR (100 MHz, CDCl₃) 168.4, 135.8, 132.2, 131.6, 123.3, 120.6, 120.5, 112.1, 101.7, 59.6, 56.3, 52.1, 50.3, 46.8, 37.5, 28.1, 24.7; ν_{max}/cm⁻¹ 2934, 2780, 1707 (C=O), 1615, 1504; HRMS (ESI)+: m/z calculated for [C₁₇H₂₂N₂O₂ + H]⁺ = 287.1754, observed 287.1748.

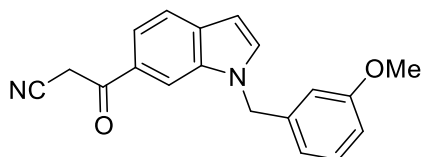
3-(1-(4-Methoxybenzyl)-1H-indol-6-yl)-3-oxopropanenitrile (65a)



n-Butyllithium (1.6 M in hexanes, 1.8 mL, 2.9 mmol) was added dropwise at -78 °C to a mixture of acetonitrile (0.23 mL, 4.3 mmol) and THF (4 mL). The reaction mixture was stirred at -78 °C over 30 minutes. A solution of methyl 1-(4-methoxybenzyl)-1H-indole-6-carboxylate **64a** (0.425 g, 1.44 mmol) in THF (2 mL) was added dropwise at -78 °C over 30 minutes. The reaction mixture was stirred at -78 °C over 15 minutes. Aqueous HCl (1 M, 25 mL) was added dropwise at 0 °C. The product was extracted into DCM (3 x 25 mL). The combined organic extracts were washed (brine), dried (MgSO₄) and concentrated *in vacuo*. Purification by flash chromatography (0 – 50% EtOAc in PET) afforded **65a** (0.387 g, 88% yield).

LCMS (ESI+): m/z 327.2 [M + Na]⁺, (ESI-): m/z 303.1 [M - H]⁻, rt 2.01 minutes, >99%; (400 MHz, (CD₃)₂SO) 8.22 (1H, s), 7.79 (1H, d, J = 3.0 Hz), 7.67 (1H, d, J = 8.3 Hz), 7.60 (1H, dd, J = 8.3, 1.5 Hz), 7.25-7.19 (2H, m), 6.91-6.84 (2H, m), 6.59 (1H, d, J = 3.1 Hz), 5.45 (2H, s), 4.77 (2H, s), 3.69 (3H, s); ¹³C NMR (100 MHz, (CD₃)₂SO) 189.2, 158.7, 135.0, 133.8, 132.7, 129.8, 128.7, 128.0, 120.5, 119.1, 116.3, 114.0, 111.9, 101.8, 55.1, 48.6, 29.9; ν_{max}/cm⁻¹ 2943, 1679 (C=O), 1607, 1511; HRMS (ESI)+: m/z calculated for [C₁₉H₁₆N₂O₂ + Na]⁺ = 327.1104, observed 327.1096.

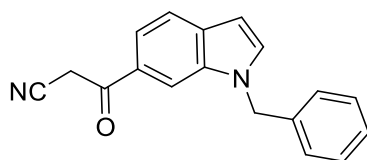
3-(1-(3-Methoxybenzyl)-1H-indol-6-yl)-3-oxopropanenitrile (**65b**)



n-Butyllithium (1.6 M in hexanes, 2.9 mL, 4.6 mmol) was added dropwise at -78 °C to a mixture of acetonitrile (0.40 mL, 7.6 mmol) and THF (5 mL). The reaction mixture was stirred at -78 °C over 45 minutes. A solution of methyl 1-(3-methoxybenzyl)-1H-indole-6-carboxylate **64b** (0.450 g, 1.52 mmol) in THF (5 mL) was added dropwise at -78 °C over 30 minutes. The reaction mixture was stirred at -78 °C over 1 hour. Aqueous HCl (1 M, 15 mL) was added dropwise at 0 °C. The product was extracted into DCM (3 x 25 mL). The combined organic extracts were washed (brine), dried (MgSO₄) and concentrated *in vacuo*. Purification by flash chromatography (0 – 50% EtOAc in PET) afforded **65b** (0.465 g, 99% yield).

LCMS (ESI-): *m/z* 303.2 [M - H]⁻, *rt* 2.01 minutes, >99%; ¹H NMR (400 MHz, CDCl₃) 7.97 (1H, s), 7.70 (1H, d, *J* = 8.4 Hz), 7.59 (1H, dd, *J* = 8.4, 1.6 Hz), 7.37 (1H, d, *J* = 3.1 Hz), 7.24 (1H, t, *J* = 7.9 Hz), 6.81 (1H, dd, *J* = 8.3, 2.5 Hz), 6.73-6.67 (1H, m), 6.64-6.60 (2H, m), 5.37 (2H, s), 4.09 (2H, s), 3.74 (3H, s); ¹³C NMR (100 MHz, CDCl₃) 187.1, 160.2, 138.2, 136.0, 133.8, 133.4, 130.2, 128.1, 121.3, 119.7, 119.2, 114.5, 113.2, 112.9, 111.3, 102.7, 55.4, 50.4, 29.6; *v*_{max}/cm⁻¹ 2942, 1677 (C=O), 1606, 1585; HRMS (ESI)⁺: *m/z* calculated for [C₁₉H₁₆N₂O₂ + Na]⁺ = 327.1104, observed 327.1089.

3-(1-(Benzyl)-1H-indol-6-yl)-3-oxopropanenitrile (**65c**)



n-Butyllithium (1.6 M in hexanes, 4.7 mL, 7.5 mmol) was added dropwise at -78 °C to a mixture of acetonitrile (0.78 mL, 15 mmol) and toluene (7 mL). The reaction mixture was stirred at -78 °C over 30 minutes. A solution of methyl 1-benzyl-1H-indole-6-carboxylate **64c** (0.418 g, 1.50 mmol) in toluene (5 mL) was added dropwise at -78 °C over 30 minutes. The reaction mixture was stirred at -78 °C over 1 hour, then warmed to 0 °C and stirred over 20 minutes. Aqueous HCl (3 M, 15 mL) was added dropwise at 0 °C. The product was extracted into EtOAc (3 x 25 mL). The combined organic extracts were washed (brine), dried (MgSO₄) and concentrated *in vacuo*. Purification by flash chromatography (0 – 30% EtOAc in PET, 0 – 20% methanol in DCM) afforded **65c** (0.384 g, 84% yield).

LCMS (ESI-): m/z 273.2 $[M - H]^-$, rt 1.99 minutes, >99%; 1H NMR (400 MHz, $(CD_3)_2SO$) 8.21 (1H, s), 7.81 (1H, d, $J = 3.0$ Hz), 7.69 (1H, d, $J = 8.3$ Hz), 7.61 (1H, dd, $J = 8.4, 1.2$ Hz), 7.39-7.18 (5H, m), 6.63 (1H, d, $J = 2.9$ Hz), 5.55 (2H, s), 4.76 (2H, s); ^{13}C NMR (100 MHz, $(CD_3)_2SO$) 189.2, 138.0, 135.1, 134.0, 132.7, 128.7, 128.1, 127.5, 127.1, 120.6, 119.2, 116.3, 111.8, 101.9, 49.1, 29.9; ν_{max}/cm^{-1} 1679, 1663, 1606, 1504; HRMS (ESI)+: m/z calculated for $[C_{18}H_{14}N_2O + H]^+$ = 275.1179, observed 275.1179.

3-Oxo-3-(1-(pyridin-2-ylmethyl)-1H-indol-6-yl)propanenitrile (65f)



n-Butyllithium (1.6 M in hexanes, 2.6 mL, 4.2 mmol) was added dropwise at -78 °C to a mixture of acetonitrile (0.369 mL, 7.06 mmol) and THF (5 mL). The reaction mixture was stirred at -78 °C over 30 minutes. A solution of methyl 1-(pyridin-2-ylmethyl)-1H-indole-6-carboxylate **64f** (0.376 g, 1.41 mmol) in THF (5 mL) was added dropwise at -78 °C over 30 minutes. The reaction mixture was stirred at -78 °C over 30 minutes. Aqueous HCl (1 M, 15 mL) was added dropwise at 0 °C. The product was extracted into DCM (3 x 50 mL). The combined organic extracts were washed (brine), dried ($MgSO_4$) and concentrated *in vacuo* to afford **65f** (0.363 g, 93% yield).

LCMS (ESI+): m/z 276.2 $[M + H]^+$, (ESI-): m/z 274.2 $[M - H]^-$, rt 1.65 minutes, 100%; 1H NMR (400 MHz, $(CD_3)_2SO$) 8.55 (1H, d, $J = 4.8$ Hz), 8.19 (1H, s), 7.81 (1H, d, $J = 3.1$ Hz), 7.76 (1H, td, $J = 7.6, 1.7$ Hz), 7.70 (1H, d, $J = 8.4$ Hz), 7.61 (1H, dd, $J = 8.4, 1.4$ Hz), 7.31 (1H, dd, $J = 7.5, 4.9$ Hz), 7.06 (1H, d, $J = 7.8$ Hz), 6.64 (1H, d, $J = 3.1$ Hz), 5.66 (2H, s), 4.74 (2H, s); ^{13}C NMR (100 MHz, $(CD_3)_2SO$) 189.2, 156.8, 149.1, 137.6, 135.3, 134.3, 132.7, 128.1, 122.9, 121.3, 120.5, 119.3, 116.3, 111.8, 102.0, 50.8, 29.9; ν_{max}/cm^{-1} 1673 (C=O), 1606, 1590, 1502; HRMS (ESI)+: m/z calculated for $[C_{17}H_{13}N_3O + H]^+$ = 276.1131, observed 276.1126.

3-Oxo-3-(1-(pyridin-3-ylmethyl)-1H-indol-6-yl)propanenitrile (65g)



n-Butyllithium (1.6 M in hexanes, 5.1 mL, 8.1 mmol) was added dropwise at -78 °C to a mixture of acetonitrile (0.71 mL, 14 mmol) and THF (6 mL). The reaction mixture was stirred at -78 °C over 30 minutes. A solution of methyl 1-(pyridin-3-ylmethyl)-1H-indole-6-carboxylate **64g** (0.721 g, 2.71 mmol) in THF (4

mL) was added dropwise at $-78\text{ }^{\circ}\text{C}$ over 30 minutes. The reaction mixture was stirred at $-78\text{ }^{\circ}\text{C}$ over 45 minutes. Water (20 mL) was added dropwise at $0\text{ }^{\circ}\text{C}$, and the reaction mixture adjusted to pH 7. The product was extracted into DCM (3 x 25 mL). The combined organic extracts were washed (brine), dried (MgSO_4) and concentrated *in vacuo*. Purification by flash chromatography (0 – 4% methanol in DCM) afforded **65g** (0.612 g, 82% yield).

LCMS (ESI+): m/z 276.2 $[\text{M} + \text{H}]^+$, (ESI-): m/z 274.1 $[\text{M} - \text{H}]^-$, rt 1.41 minutes, >99%; ^1H NMR (500 MHz, $(\text{CD}_3)_2\text{SO}$) 8.55 (1H, d, $J = 1.9$ Hz), 8.47 (1H, dd, $J = 4.8, 1.6$ Hz), 8.25 (1H, s), 7.85 (1H, d, $J = 3.1$ Hz), 7.69 (1H, d, $J = 8.2$ Hz), 7.64-7.59 (2H, m), 7.34 (1H, ddd, $J = 7.8, 4.8, 0.8$ Hz), 6.64 (1H, d, $J = 3.0$ Hz), 5.60 (2H, s), 4.76 (2H, s); ^{13}C NMR (125 MHz, $(\text{CD}_3)_2\text{SO}$) 189.2, 148.9, 148.5, 135.0, 134.9, 133.8, 133.5, 132.7, 128.2, 123.8, 120.7, 119.3, 116.3, 111.8, 102.3, 46.6, 29.9; $\nu_{\text{max}}/\text{cm}^{-1}$ 3089, 2952, 2926, 2267 ($\text{C}\equiv\text{N}$), 1677 ($\text{C}=\text{O}$), 1611, 1577, 1561, 1502; HRMS (ESI-): m/z calculated for $[\text{C}_{17}\text{H}_{13}\text{N}_3\text{O} - \text{H}]^- = 274.0986$, observed 274.0976.

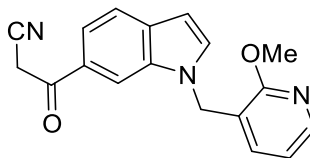
3-Oxo-3-(1-(pyridin-4-ylmethyl)-1H-indol-6-yl)propanenitrile (**65h**)



n-Butyllithium (1.6 M in hexanes, 2.9 mL, 4.7 mmol) was added dropwise at $-78\text{ }^{\circ}\text{C}$ to a mixture of acetonitrile (0.41 mL, 7.8 mmol) and THF (6 mL). The reaction mixture was stirred at $-78\text{ }^{\circ}\text{C}$ over 30 minutes. A solution of methyl 1-(pyridin-4-ylmethyl)-1H-indole-6-carboxylate **64h** (0.454 g, 1.55 mmol) in THF (4 mL) was added dropwise at $-78\text{ }^{\circ}\text{C}$ over 30 minutes. The reaction mixture was stirred at $-78\text{ }^{\circ}\text{C}$ over 45 minutes. Water (20 mL) was added dropwise at $0\text{ }^{\circ}\text{C}$, and the reaction mixture adjusted to pH 7. The product was extracted into DCM (3 x 25 mL). The combined organic extracts were washed (brine), dried (MgSO_4) and concentrated *in vacuo*. Purification by flash chromatography (0 – 4% methanol in DCM) afforded **65h** (0.303 g, 71% yield).

LCMS (ESI+): m/z 276.2 $[\text{M} + \text{H}]^+$, (ESI-): m/z 274.2 $[\text{M} - \text{H}]^-$, rt 1.37 minutes, >99%; ^1H NMR (500 MHz, $(\text{CD}_3)_2\text{SO}$) 8.51-8.47 (2H, m), 8.15 (1H, s), 7.83 (1H, d, $J = 3.1$ Hz), 7.72 (1H, d, $J = 8.4$ Hz), 7.63 (1H, dd, $J = 8.4, 1.4$ Hz), 7.11-7.06 (2H, m), 6.68 (1H, d, $J = 2.9$ Hz), 5.63 (2H, s), 4.74 (2H, s); ^{13}C NMR (125 MHz, $(\text{CD}_3)_2\text{SO}$) 189.2, 149.9, 146.9, 135.2, 134.1, 132.6, 128.3, 121.7, 120.7, 119.4, 116.2, 111.7, 102.3, 47.9, 29.8; $\nu_{\text{max}}/\text{cm}^{-1}$ 3076, 2918, 2258 ($\text{C}\equiv\text{N}$), 1664 ($\text{C}=\text{O}$), 1599, 1560; HRMS (ESI-): m/z calculated for $[\text{C}_{17}\text{H}_{13}\text{N}_3\text{O} - \text{H}]^- = 274.0986$, observed 274.0976.

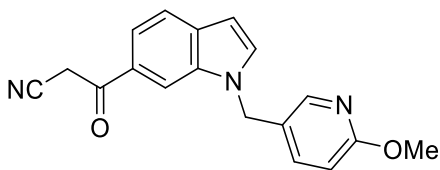
3-(1-((2-Methoxypyridin-3-yl)methyl)-1H-indol-6-yl)-3-oxopropanenitrile (**65i**)



n-Butyllithium (1.6 M in hexanes, 1.1 mL, 1.7 mmol) was added dropwise at -78 °C to a mixture of acetonitrile (0.15 mL, 2.9 mmol) and THF (4 mL). The reaction mixture was stirred at -78 °C over 30 minutes. A solution of methyl 1-((2-methoxypyridin-3-yl)methyl)-1H-indole-6-carboxylate **64i** (0.177 g, 0.579 mmol) in THF (1 mL) was added dropwise at -78 °C. The reaction mixture was stirred at -78 °C over 1 hour, then NH₄Cl solution (25 mL) was added dropwise at 0 °C. The product was extracted into DCM (3 x 25 mL). The combined organic extracts were washed (brine), dried (MgSO₄) and concentrated *in vacuo*. Purification by flash chromatography (0 – 50% EtOAc in PET) afforded **65i** (0.134 g, 76% yield).

LCMS (ESI+): *m/z* 306.2 [M + H]⁺, (ESI-): *m/z* 304.1 [M - H]⁻, *rt* 1.94 minutes, >99%; ¹H NMR (400 MHz, CDCl₃) 8.09 (1H, dd, *J* = 5.0, 1.8 Hz), 8.02 (1H, s), 7.70 (1H, d, *J* = 8.3 Hz), 7.59 (1H, dd, *J* = 8.5, 1.5 Hz), 7.41 (1H, d, *J* = 3.1 Hz), 6.97-6.92 (1H, m), 6.76 (1H, dd, *J* = 7.3, 5.0 Hz), 6.63 (1H, dd, *J* = 3.1, 0.6 Hz), 5.35 (2H, s), 4.12 (2H, s), 4.04 (3H, s); ¹³C NMR (100 MHz, CDCl₃) 187.1, 161.2, 146.5, 136.3, 135.9, 133.7, 133.6, 128.2, 121.4, 119.8, 119.5, 117.1, 114.4, 111.2, 102.7, 53.8, 45.3, 29.6; *v*_{max}/cm⁻¹ 2953, 2261 (C≡N), 1683 (C=O), 1589; HRMS (ESI)+: *m/z* calculated for [C₁₈H₁₅N₃O₂ + H]⁺ = 306.1237, observed 306.1237.

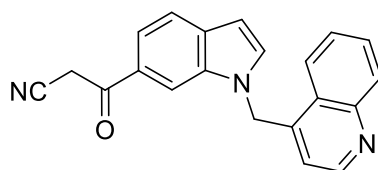
3-(1-((6-Methoxypyridin-3-yl)methyl)-1H-indol-6-yl)-3-oxopropanenitrile (**65k**)



n-Butyllithium (1.6 M in hexanes, 1.3 mL, 2.1 mmol) was added dropwise at -78 °C to a mixture of acetonitrile (0.18 mL, 3.5 mmol) and THF (4 mL). The reaction mixture was stirred at -78 °C over 20 minutes. A solution of methyl 1-((6-methoxypyridin-3-yl)methyl)-1H-indole-6-carboxylate **64k** (0.206 g, 0.695 mmol) in THF (2 mL) was added dropwise at -78 °C over 20 minutes. The reaction mixture was stirred at -78 °C over 30 minutes. NH₄Cl solution (25 mL) was added dropwise at 0 °C. The product was extracted into DCM (3 x 25 mL). The combined organic extracts were washed (brine), dried (MgSO₄) and concentrated *in vacuo*. Purification by flash chromatography (0 – 50% EtOAc in PET) afforded **65k** (0.137 g, 62% yield).

LCMS (ESI+): m/z 306.2 $[M + H]^+$, (ESI-): m/z 304.1 $[M - H]^-$, rt 1.86 minutes, 96%; 1H NMR (400 MHz, $CDCl_3$) 8.06-8.00 (2H, m), 7.69 (1H, d, $J = 8.4$ Hz), 7.58 (1H, dd, $J = 8.3, 1.0$ Hz), 7.36-7.30 (2H, m), 6.69 (1H, d, $J = 8.6$ Hz), 6.61 (1H, d, $J = 3.0$ Hz), 5.32 (2H, s), 4.11 (2H, s), 3.90 (3H, s); ^{13}C NMR (100 MHz, $CDCl_3$) 187.1, 164.3, 145.7, 137.8, 135.8, 133.9, 132.9, 128.2, 124.8, 121.4, 119.9, 114.5, 111.6, 111.0, 103.0, 53.7, 47.5, 29.6; ν_{max}/cm^{-1} 2940, 2249 ($C\equiv N$), 1676 ($C=O$), 1607, 1572; HRMS (ESI+): m/z calculated for $[C_{18}H_{15}N_3O_2 + H]^+ = 306.1237$, observed 306.1234.

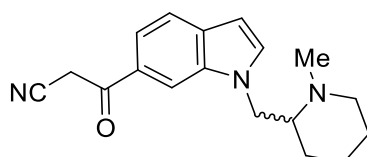
3-Oxo-3-(1-(quinolin-4-ylmethyl)-1H-indol-6-yl)propanenitrile (65m)



n-Butyllithium (1.6 M in hexanes, 1.7 mL, 2.8 mmol) was added dropwise at -78 °C to a mixture of acetonitrile (0.22 mL, 4.2 mmol) and toluene (3 mL). The reaction mixture was stirred at -78 °C over 30 minutes. A suspension of methyl 1-(quinolin-4-ylmethyl)-1H-indole-6-carboxylate **64m** (0.467 g, 1.39 mmol) in toluene/THF (3:1, 12 mL) was added dropwise at -78 °C. The reaction mixture was stirred at -78 °C over 30 minutes. Water (50 mL) was added dropwise at 0 °C, and the reaction mixture adjusted to pH 8. The product was extracted into EtOAc (50 mL) and DCM/methanol (9:1, 3 x 50 mL). The combined organic extracts were dried ($MgSO_4$) and concentrated *in vacuo*. Purification by flash chromatography (0 – 60% EtOAc in PET) afforded **65m** (0.119 g, 26% yield).

LCMS (ESI+): m/z 326.2 $[M + H]^+$, (ESI-): m/z 324.1 $[M - H]^-$, rt 1.65 minutes, >99%; 1H NMR (400 MHz, $(CD_3)_2SO$) 8.70 (1H, d, $J = 4.4$ Hz), 8.31 (1H, d, $J = 8.2$ Hz), 8.20 (1H, s), 8.09 (1H, d, $J = 8.2$ Hz), 7.90-7.71 (4H, m), 7.67 (1H, d, $J = 8.3$ Hz), 6.75 (1H, d, $J = 2.7$ Hz), 6.36 (1H, d, $J = 4.4$ Hz), 6.21 (2H, s), 4.70 (2H, s); ^{13}C NMR (100 MHz, $(CD_3)_2SO$) 189.2, 150.5, 147.5, 144.0, 135.6, 134.3, 132.6, 129.66, 129.64, 128.4, 126.9, 125.4, 123.6, 120.8, 119.4, 117.4, 116.2, 111.9, 102.5, 46.3, 29.8; ν_{max}/cm^{-1} 2948, 2845, 2252 ($C\equiv N$), 1673 ($C=O$), 1610, 1597, 1570, 1560, 1504; HRMS (ESI+): m/z calculated for $[C_{21}H_{15}N_3O + Na]^+ = 348.1107$, observed 348.1106.

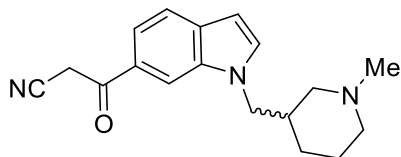
3-(1-((1-Methylpiperidin-2-yl)methyl)-1H-indol-6-yl)-3-oxopropanenitrile (65n)



n-Butyllithium (1.6 M in hexanes, 0.62 mL, 0.99 mmol) was added dropwise at -78 °C to a mixture of acetonitrile (78 μ L, 1.5 mmol) and THF (3 mL). The reaction mixture was stirred at -78 °C over 30 minutes. A solution of methyl 1-((1-methylpiperidin-2-yl)methyl)-1H-indole-6-carboxylate **64n** (0.158 g, 0.497 mmol) in THF (3 mL) was added dropwise at -78 °C over 30 minutes. The reaction mixture was stirred at -78 °C over 1 hour. Water (50 mL) was added dropwise at 0 °C, and the reaction mixture adjusted to pH 10. The product was extracted into DCM/methanol (10:1, 4 x 50 mL). The combined organic extracts were washed (brine), dried (MgSO₄) and concentrated *in vacuo*. Purification by flash chromatography (50 – 100% EtOAc in PET, 0 – 5% methanol in DCM), followed by reverse phase chromatography (0 – 50% acetonitrile in water (+ 0.1% NH₃)), afforded **65n** (48 mg, 32% yield).

LCMS (ESI+): *m/z* 296.3 [M + H]⁺, (ESI-): *m/z* 294.2 [M - H]⁻, *rt* 1.21 minutes, 97%; ¹H NMR (400 MHz, CDCl₃) 8.02 (1H, s), 7.65 (1H, d, *J* = 8.5 Hz), 7.55 (1H, dd, *J* = 8.4, 1.1 Hz), 7.35 (1H, d, *J* = 3.1 Hz), 6.55 (1H, d, *J* = 2.7 Hz), 4.55 (1H, dd, *J* = 14.2, 4.3 Hz), 4.12 (2H, br s), 3.99 (1H, dd, *J* = 14.3, 8.7 Hz), 2.88 (1H, d, *J* = 11.6 Hz), 2.46 (3H, s), 2.42-2.32 (1H, m), 2.15 (1H, td, *J* = 11.5, 3.2 Hz), 1.72-1.42 (3H, m), 1.31-1.01 (3H, m); ¹³C NMR (100 MHz, CDCl₃) 187.1, 136.1, 133.8, 133.4, 127.9, 121.1, 119.4, 114.6, 111.2, 102.2, 63.3, 57.2, 49.3, 43.6, 29.6, 29.4, 25.5, 23.5; $\nu_{\text{max}}/\text{cm}^{-1}$ 2939, 2855, 2787, 2168 (C≡N), 1676 (C=O), 1606, 1500; HRMS (ESI)+: *m/z* calculated for [C₁₈H₂₁N₃O + H]⁺ = 296.1757, observed 296.1747.

3-(1-((1-Methylpiperidin-3-yl)methyl)-1H-indol-6-yl)-3-oxopropanenitrile (65o)

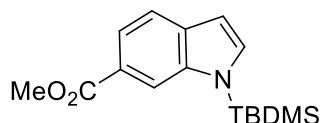


n-Butyllithium (1.6 M in hexanes, 1.4 mL, 2.2 mmol) was added dropwise at -78 °C to a mixture of acetonitrile (0.17 mL, 3.3 mmol) and THF (3 mL). The reaction mixture was stirred at -78 °C over 30 minutes. A suspension of methyl 1-((1-methylpiperidin-3-yl)methyl)-1H-indole-6-carboxylate **64o** (0.318 g, 1.11 mmol) in THF (10 mL) was added dropwise at -78 °C. The reaction mixture was stirred at -78 °C over 30 minutes. Water (50 mL) was added dropwise at 0 °C, and the reaction mixture adjusted to pH 8. The product was extracted into DCM/methanol (10:1, 4 x 50 mL). The combined organic extracts were washed (brine), dried (MgSO₄) and concentrated *in vacuo*. Purification by flash chromatography (50 – 100% EtOAc in PET, 0 – 10% methanol in DCM) afforded **65o** (0.221 g, 67% yield).

LCMS (ESI+): *m/z* 296.3 [M + H]⁺, (ESI-): *m/z* 294.2 [M - H]⁻, *rt* 1.37 minutes, >99%; ¹H NMR (400 MHz, CDCl₃) 8.03 (1H, s), 7.66 (1H, d, *J* = 8.4 Hz), 7.57 (1H, d, *J* = 8.4 Hz), 7.31 (1H, d, *J* = 3.1 Hz), 6.56 (1H, d, *J* =

2.8 Hz), 4.34-3.96 (4H, m), 2.74-2.61 (1H, m), 2.55 (1H, d, $J = 10.5$ Hz), 2.31-2.14 (4H, m), 2.13-1.99 (1H, m), 1.83 (1H, t, $J = 10.1$ Hz), 1.78-1.68 (1H, m), 1.67-1.50 (2H, m), 1.15-1.01 (1H, m); ^{13}C NMR (100 MHz, CDCl_3) 187.2, 136.0, 133.5, 133.4, 127.9, 121.2, 119.5, 114.6, 111.2, 102.2, 59.3, 56.1, 50.1, 46.6, 37.3, 29.7, 27.8, 24.4; $\nu_{\text{max}}/\text{cm}^{-1}$ 2936, 2782, 2166 ($\text{C}\equiv\text{N}$), 1675 ($\text{C}=\text{O}$), 1607, 1564; HRMS (ESI)+: m/z calculated for $[\text{C}_{18}\text{H}_{21}\text{N}_3\text{O} + \text{H}]^+ = 296.1757$, observed 296.1753.

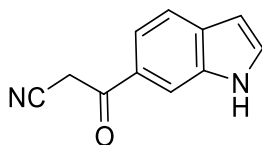
Methyl 1-(tert-butyldimethylsilyl)-1H-indole-6-carboxylate (67)



A solution of methyl 1H-indole-6-carboxylate **63** (0.500 g, 2.71 mmol) in THF (10 mL) was added dropwise at 0 °C to a stirred suspension of NaH (60% in mineral oil, 0.141 g, 3.52 mmol) in THF (10 mL). The reaction mixture was warmed to rt and stirred over 30 minutes. *tert*-Butyldimethylsilyl chloride (1 M in DCM, 4.1 mL, 4.1 mmol) was added dropwise at 0 °C to the reaction mixture. The reaction mixture was warmed to rt and stirred over 10 hours. NH_4Cl solution (20 mL) was added dropwise at 0 °C. The product was extracted into diethyl ether (2 x 50 mL). The combined organic extracts were washed (brine), dried (MgSO_4) and concentrated *in vacuo*. Purification by flash chromatography (0 – 20% EtOAc in PET) afforded **67** (0.462 g, 59% yield).

LCMS (ESI+): m/z 290.2 $[\text{M} + \text{H}]^+$, rt 3.05 minutes, 100%; ^1H NMR (500 MHz, CDCl_3) 8.29-8.27 (1H, m), 7.80 (1H, dd, $J = 8.3, 1.4$ Hz), 7.63 (1H, d, $J = 8.4$ Hz), 7.34 (1H, d, $J = 3.2$ Hz), 6.65 (1H, dd, $J = 3.1, 0.9$ Hz), 3.93 (3H, s), 0.93 (9H, s), 0.65 (6H, s); ^{13}C NMR (125 MHz, CDCl_3) 168.5, 140.5, 135.3, 134.6, 123.2, 121.0, 120.2, 116.2, 105.2, 52.1, 26.4, 19.5, -3.8; spectroscopic data consistent with literature.¹⁴⁴

3-(1H-Indol-6-yl)-3-oxopropanenitrile (68)

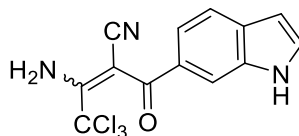


n-Butyllithium (1.6 M in hexanes, 3.0 mL, 4.8 mmol) was added dropwise at -78 °C to a mixture of acetonitrile (0.180 mL, 3.45 mmol) and toluene (3 mL). The reaction mixture was stirred at -78 °C over 30 minutes. A solution of methyl 1-(*tert*-butyldimethylsilyl)-1H-indole-6-carboxylate **67** (0.200 g, 0.691 mmol) in toluene (2 mL) was added dropwise at -78 °C over 30 minutes. The reaction mixture was stirred

at -78 °C over 1 hour, then warmed to rt over 1 hour. Aqueous HCl (3 M, 20 mL) was added dropwise at 0 °C. The intermediate was extracted into EtOAc (2 x 25 mL). The combined organic extracts were washed (brine), dried (MgSO₄) and concentrated *in vacuo*. The crude residue was dissolved in THF (2 mL) and TBAF (1 M in THF, 0.760 mL, 0.760 mmol) was added dropwise. The reaction mixture was stirred over 20 minutes, then NaHCO₃ solution (30 mL) was added dropwise. The product was extracted into DCM (3 x 25 mL). The combined organic extracts were washed (brine), dried (MgSO₄) and concentrated *in vacuo*. Purification by flash chromatography (0 – 20% methanol in DCM) afforded **68** (0.131 g, 99% yield).

LCMS (ESI-): m/z 183.1 [M - H]⁻, rt 1.91 minutes, 100%; ¹H NMR (500 MHz, CD₃CN) 9.74 (1H, br s), 8.07 (1H, s), 7.69 (1H, d, J = 8.4 Hz), 7.62 (1H, dd, J = 8.4, 1.5 Hz), 7.53 (1H, t, J = 2.8 Hz), 6.61-6.57 (1H, m), 4.36 (2H, s); ¹³C NMR (125 MHz, CD₃CN) 189.5, 136.2, 133.6, 131.0, 129.3, 121.3, 120.1, 116.4, 113.9, 103.2, 30.6; ν_{max}/cm⁻¹ 3326 (N-H), 1675 (C=O), 1611, 1501; HRMS (ESI)+: m/z calculated for [C₁₁H₈N₂O + H]⁺ = 185.0709, observed 185.0708.

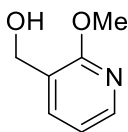
3-Amino-4,4,4-trichloro-2-(1H-indole-6-carbonyl)but-2-enitrile (**69**)



Trichloroacetonitrile (0.738 mL, 7.36 mmol) was added to a suspension of 3-(1H-indol-6-yl)-3-oxopropanenitrile **68** (0.491 g, 2.45 mmol) and sodium acetate (1.01 g, 12.3 mmol) in ethanol (15 mL). The reaction mixture was stirred over 90 minutes. The reaction mixture was concentrated *in vacuo*, then NaHCO₃ solution (20 mL) was added. The product was extracted into DCM/methanol (10:1, 3 x 50 mL). The combined organic extracts were washed (brine), dried (MgSO₄) and concentrated *in vacuo*. Purification by flash chromatography (0 – 8% methanol in DCM) afforded **69** (0.717 g, 87% yield).

¹H NMR (500 MHz, (CD₃)₂SO) 11.88 (1H, br s), 11.49 (1H, s), 9.72 (1H, br s), 7.92-7.88 (1H, m), 7.62 (1H, d, J = 8.3 Hz), 7.58 (1H, t, J = 2.8 Hz), 7.38 (1H, dd, J = 8.3, 1.6 Hz), 6.55-6.51 (1H, m); ¹³C NMR (125 MHz, (CD₃)₂SO) 193.6, 167.9, 134.5, 131.1, 130.4, 129.0, 119.5, 119.0, 118.8, 112.5, 101.5, 91.3, 77.2; ν_{max}/cm⁻¹ 3389 (N-H), 3280 (N-H), 2205 (C≡N), 1597 (C=O), 1508; HRMS (ESI)+: m/z calculated for [C₁₃H₈Cl₃N₃O + H]⁺ = 327.9806, observed 327.9812.

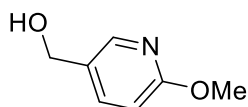
(2-Methoxypyridin-3-yl)methanol (74)



NaBH₄ (1.02 g, 26.9 mmol) was added portionwise at 0 °C to a solution of methyl 2-methoxynicotinate **73** (1.50 g, 8.97 mmol) in ethanol (24 mL). The reaction mixture was warmed to rt and stirred over 24 hours, then diluted with NaHCO₃ solution (50 mL) and extracted into DCM (4 x 50 mL). The combined organic extracts were washed (brine), dried (MgSO₄) and concentrated *in vacuo*. Purification by flash chromatography (0 – 10% methanol in DCM) afforded **74** (0.840 g, 67% yield).

¹H NMR (400 MHz, CDCl₃) 8.09 (1H, dd, J = 5.1, 2.0 Hz), 7.62-7.55 (1H, m), 6.88 (1H, dd, J = 7.2, 5.1 Hz), 4.64 (2H, s), 3.99 (3H, s), 2.41 (1H, br s); ¹³C NMR (100 MHz, CDCl₃) 161.7, 145.8, 136.7, 123.5, 117.0, 61.1, 53.6; spectroscopic data consistent with literature.¹⁴⁵

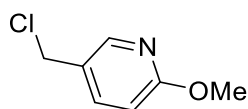
(6-Methoxypyridin-3-yl)methanol (76)



LiAlH₄ (2.4 M in THF, 1.25 mL, 2.99 mmol) was added dropwise at 0 °C to a solution of methyl 6-methoxynicotinate **75** (1.00 g, 5.98 mmol) in THF (10 mL). The reaction mixture was stirred at 0 °C over 1 hour. Aqueous potassium sodium tartrate (1 M, 25 mL) was added dropwise at 0 °C to the reaction mixture. The product was extracted into EtOAc (3 x 25 mL). The combined organic extracts were washed (brine), dried (MgSO₄) and concentrated *in vacuo*. Purification by flash chromatography (0 – 5% methanol in DCM) afforded **76** (0.759 g, 91% yield).

¹H NMR (400 MHz, CDCl₃) 8.07 (1H, d, J = 2.3 Hz), 7.60 (1H, dd, J = 8.5, 2.3 Hz), 6.73 (1H, d, J = 8.5 Hz), 4.59 (2H, s), 3.91 (3H, s), 2.38 (1H, s); ¹³C NMR (100 MHz, CDCl₃) 164.0, 145.7, 138.7, 129.2, 111.1, 62.5, 53.7; spectroscopic data consistent with literature.¹⁴⁶

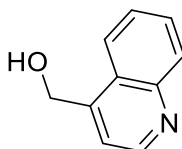
5-(Chloromethyl)-2-methoxypyridine (77)



p-Toluenesulfonyl chloride (1.21 g, 6.37 mmol) and DMAP (6 mg, 0.05 mmol) were added to a solution of (6-methoxypyridin-3-yl)methanol **76** (0.739 g, 5.31 mmol) and triethylamine (1.48 mL, 10.6 mmol) in DCM (10 mL). The reaction mixture was stirred over 18 hours, then diluted with water (20 mL). The product was extracted into DCM (3 x 25 mL). The combined organic extracts were washed (brine), dried (MgSO₄) and concentrated *in vacuo*. Purification by flash chromatography (0 – 30% EtOAc in PET) afforded **77** (0.160 g, 17% yield).

LCMS (ESI+): *m/z* 158.2 [M + H]⁺, *rt* 1.71 minutes, 89%; ¹H NMR (400 MHz, CDCl₃) 8.15 (1H, d, *J* = 2.4 Hz), 7.62 (1H, dd, *J* = 8.6, 2.5 Hz), 6.75 (1H, d, *J* = 8.5 Hz), 4.55 (2H, s), 3.94 (3H, s); spectroscopic data consistent with literature.¹⁴⁶

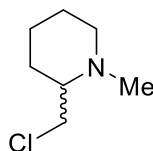
Quinolin-4-ylmethanol (**79**)¹²⁸



NaBH₄ (0.144 g, 3.82 mmol) was added at 0 °C to a solution of 4-quinolinecarboxaldehyde **78** (0.500 g, 3.18 mmol) in methanol (10 mL). The reaction mixture was stirred at 0 °C over 90 minutes, then diluted with water (50 mL) and extracted into DCM (3 x 50 mL). The combined organic extracts were washed (brine), dried (MgSO₄) and concentrated *in vacuo*. Purification by flash chromatography (0 – 7% methanol in DCM) afforded **79** (0.398 g, 79% yield).

¹H NMR (400 MHz, CD₃OD) 8.82 (1H, d, *J* = 4.4 Hz), 8.11-7.99 (2H, m), 7.77 (1H, ddd, *J* = 8.4, 7.0, 1.4 Hz), 7.69-7.59 (2H, m), 5.17 (2H, s); ¹³C NMR (100 MHz, CD₃OD) 151.2, 150.0, 148.3, 130.8, 129.6, 128.0, 127.3, 124.4, 119.3, 61.5; spectroscopic data consistent with literature.¹²⁸

2-(Chloromethyl)-1-methylpiperidine (**81**)

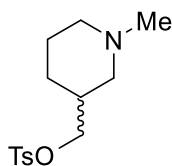


Thionyl chloride (3 mL) was added dropwise to a solution of (1-methylpiperidin-2-yl)methanol **80** (1.02 mL, 7.74 mmol) in DCM (15 mL). The reaction mixture was heated under reflux for 7 hours, then diluted

with NaHCO₃ solution (100 mL) and extracted into DCM (3 x 100 mL). The combined organic extracts were washed (brine), dried (MgSO₄) and concentrated *in vacuo* to afford **81** (0.658 g, 58% yield).

¹H NMR (400 MHz, CDCl₃) 3.63 (1H, dd, J = 11.5, 5.2 Hz), 3.50 (1H, dd, J = 11.5, 2.6 Hz), 2.84 (1H, dtd, J = 11.5, 3.5, 1.5 Hz), 2.27 (3H, s), 2.14-2.02 (2H, m), 1.78-1.48 (5H, m), 1.34-1.18 (1H, m); ¹³C NMR (100 MHz, CDCl₃) 64.2, 57.0, 46.9, 43.0, 29.6, 25.8, 24.0; ν_{max}/cm⁻¹ 2936, 2855, 2780, 2712.

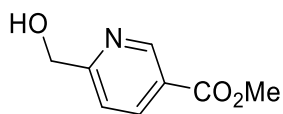
(1-Methylpiperidin-3-yl)methyl 4-methylbenzenesulfonate (83)



DMAP (47 mg, 0.39 mmol), triethylamine (2.2 mL, 16 mmol) and *p*-toluenesulfonyl chloride (1.62 g, 8.51 mmol) were added to a solution of (1-methylpiperidin-3-yl)methanol **82** (0.987 mL, 7.74 mmol) in DCM (15 mL). The reaction mixture was stirred over 4 hours, then diluted with water (25 mL) and extracted into DCM (3 x 25 mL). The combined organic extracts were washed (brine), dried (MgSO₄) and concentrated *in vacuo*. Purification by flash chromatography (0 – 20% methanol in DCM) afforded **83** (0.815 g, 36% yield).

LCMS (ESI⁺): m/z 284.2 [M + H]⁺, rt 1.36 minutes, 96%; ¹H NMR (500 MHz, CDCl₃) 7.80-7.75 (2H, m), 7.36-7.31 (2H, m), 3.91 (1H, dd, J = 9.7, 5.8 Hz), 3.86 (1H, dd, J = 9.6, 7.1 Hz), 2.74 (1H, d, J = 10.2 Hz), 2.68 (1H, d, J = 10.8 Hz), 2.44 (3H, s), 2.22 (3H, s), 2.02-1.93 (1H, m), 1.90 (1H, t, J = 11.3 Hz), 1.72 (1H, t, J = 10.5 Hz), 1.67-1.48 (3H, m), 1.03-0.90 (1H, m); ¹³C NMR (125 MHz, CDCl₃) 144.9, 133.1, 130.0, 128.0, 73.0, 58.3, 56.0, 46.6, 35.9, 26.1, 24.4, 21.8; ν_{max}/cm⁻¹ 2938, 2783, 1598; HRMS (ESI⁺): m/z calculated for [C₁₄H₂₁NO₃S + H]⁺ = 284.1315, observed 284.1315.

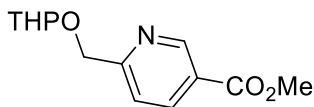
Methyl 6-(hydroxymethyl)nicotinate (90) ¹³³



NaBH₄ (0.727 g, 19.2 mmol) was added portionwise at 0 °C to a suspension of dimethyl pyridine-2,5-dicarboxylate **89** (2.50 g, 12.8 mmol) and CaCl₂ (5.69 g, 51.2 mmol) in methanol/THF (2:1, 90 mL). The reaction mixture was stirred at 0 °C over 90 minutes, then diluted with water (50 mL) dropwise at 0 °C. The product was extracted into chloroform (3 x 50 mL). The combined organic extracts were washed (brine), dried (MgSO₄) and concentrated *in vacuo* to afford **90** (1.80 g, 84% yield).

^1H NMR (400 MHz, CDCl_3) 9.15 (1H, d, $J = 1.4$ Hz), 8.29 (1H, dd, $J = 8.2, 2.1$ Hz), 7.36 (1H, d, $J = 8.2$ Hz), 4.83 (2H, d, $J = 3.6$ Hz), 3.95 (3H, s), 3.75-3.65 (1H, m); ^{13}C NMR (100 MHz, CDCl_3) 165.8, 163.7, 150.1, 137.9, 125.1, 120.1, 64.4, 52.6; spectroscopic data consistent with literature.¹³³

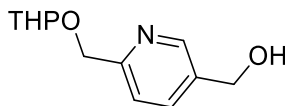
Methyl 6-(((tetrahydro-2H-pyran-2-yl)oxy)methyl)nicotinate (91)



Methanesulfonic acid (0.763 mL, 11.8 mmol) was added to a solution of methyl 6-(hydroxymethyl)nicotinate **90** (1.79 g, 10.7 mmol) and 3,4-dihydro-2H-pyran (1.95 mL, 21.4 mmol) in DCM (20 mL). The reaction mixture was stirred over 150 minutes, then washed with NaHCO_3 solution (2 x 15 mL) and brine (15 mL), dried (MgSO_4) and concentrated *in vacuo*. Purification by flash chromatography (0 – 20% EtOAc in PET) afforded **91** (2.07 g, 77% yield).

^1H NMR (400 MHz, CDCl_3) 9.14 (1H, d, $J = 2.1$ Hz), 8.29 (1H, dd, $J = 8.1, 2.2$ Hz), 7.58 (1H, dd, $J = 8.2, 0.7$ Hz), 4.95 (1H, d, $J = 14.6$ Hz), 4.78 (1H, t, $J = 3.5$ Hz), 4.70 (1H, d, $J = 14.5$ Hz), 3.94 (3H, s), 3.93-3.84 (1H, m), 3.60-3.52 (1H, m), 1.97-1.47 (6H, m); ^{13}C NMR (100 MHz, CDCl_3) 166.0, 163.5, 150.5, 137.8, 124.7, 120.7, 98.8, 69.7, 62.5, 52.5, 30.6, 25.5, 19.5; $\nu_{\text{max}}/\text{cm}^{-1}$ 2946, 2926, 2876, 2848, 1714 (C=O), 1596; HRMS (ESI)+: m/z calculated for $[\text{C}_{13}\text{H}_{17}\text{NO}_4 + \text{Na}]^+ = 274.1050$, observed 274.1045.

(6-(((Tetrahydro-2H-pyran-2-yl)oxy)methyl)pyridin-3-yl)methanol (92)

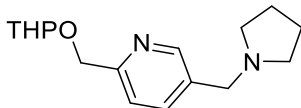


LiAlH_4 (2.4 M in THF, 5.1 mL, 12 mmol) was added dropwise at 0 °C to a solution of methyl 6-(((tetrahydro-2H-pyran-2-yl)oxy)methyl)nicotinate **91** (2.06 g, 8.20 mmol) in THF (20 mL). The reaction mixture was stirred at 0 °C for 45 minutes. Isopropanol (5 mL) was added dropwise at 0 °C to the reaction mixture, followed by water (50 mL). The product was extracted into DCM/methanol (9:1, 3 x 100 mL). The combined organic extracts were washed (brine), dried (MgSO_4) and concentrated *in vacuo*. Purification by flash chromatography (60 – 90% EtOAc in PET) afforded **92** (1.16 g, 64% yield).

^1H NMR (400 MHz, CDCl_3) 8.50 (1H, d, $J = 1.7$ Hz), 7.74 (1H, dd, $J = 7.9, 2.2$ Hz), 7.48 (1H, d, $J = 8.1$ Hz), 4.90 (1H, d, $J = 13.3$ Hz), 4.78 (1H, t, $J = 3.6$ Hz), 4.73 (2H, s), 4.65 (1H, d, $J = 13.3$ Hz), 3.97-3.88 (1H, m), 3.61-3.53 (1H, m), 2.60 (1H, br s), 1.91-1.49 (6H, m); ^{13}C NMR (100 MHz, CDCl_3) 158.0, 148.0, 135.7, 135.0,

121.5, 98.7, 69.8, 62.7, 62.4, 30.7, 25.5, 19.5; $\nu_{\max}/\text{cm}^{-1}$ 3300 (br, O-H), 2939, 2869, 1604, 1574; HRMS (ESI)+: m/z calculated for $[\text{C}_{12}\text{H}_{17}\text{NO}_3 + \text{H}]^+ = 224.1281$, observed 224.1284.

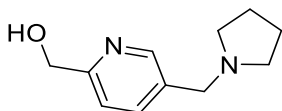
5-(Pyrrolidin-1-ylmethyl)-2-(((tetrahydro-2H-pyran-2-yl)oxy)methyl)pyridine (93)



Methanesulfonyl chloride (0.478 mL, 6.18 mmol) was added dropwise at 0 °C to a solution of (6-(((tetrahydro-2H-pyran-2-yl)oxy)methyl)pyridin-3-yl)methanol **92** (1.15 g, 5.15 mmol) and triethylamine (0.933 mL, 6.70 mmol) in DCM (10 mL). The reaction mixture was warmed to rt and stirred over 1 hour. The reaction was diluted with NaHCO_3 solution (25 mL) and extracted into DCM (3 x 50 mL). The combined organic extracts were washed (brine), dried (MgSO_4) and concentrated *in vacuo*. The crude residue was dissolved in DMF (10 mL), then pyrrolidine (0.516 mL, 6.18 mmol) and Cs_2CO_3 (2.18 g, 6.70 mmol) were added. The reaction mixture was stirred over 14 hours, then diluted with EtOAc (100 mL), washed with Na_2CO_3 solution (2 x 100 mL) and brine (100 mL), dried (MgSO_4) and concentrated *in vacuo*. Purification by flash chromatography (0 – 8% methanol in DCM) afforded **93** (0.970 g, 66% yield).

LCMS (ESI+): m/z 277.3 $[\text{M} + \text{H}]^+$, rt 0.65 minutes, 97%; ^1H NMR (400 MHz, CDCl_3) 8.48 (1H, s), 7.68 (1H, dd, $J = 7.9, 1.7$ Hz), 7.42 (1H, d, $J = 7.9$ Hz), 4.88 (1H, d, $J = 13.2$ Hz), 4.77 (1H, t, $J = 3.4$ Hz), 4.62 (1H, d, $J = 13.3$ Hz), 3.96-3.85 (1H, m), 3.61 (2H, s), 3.58-3.51 (1H, m), 2.55-2.43 (4H, m), 1.95-1.48 (10H, m); ^{13}C NMR (100 MHz, CDCl_3) 157.3, 149.6, 137.3, 133.4, 121.3, 98.6, 69.9, 62.3, 57.8, 54.2, 30.7, 25.5, 23.5, 19.5; $\nu_{\max}/\text{cm}^{-1}$ 2939, 2783, 1602, 1572; HRMS (ESI)+: m/z calculated for $[\text{C}_{16}\text{H}_{24}\text{N}_2\text{O}_2 + \text{H}]^+ = 277.1911$, observed 277.1906.

(5-(Pyrrolidin-1-ylmethyl)pyridin-2-yl)methanol (94)

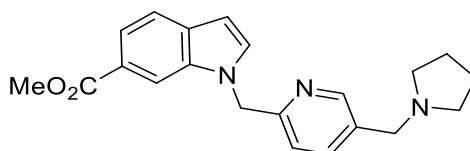


p-Toluenesulfonic acid monohydrate (1.28 g, 6.74 mmol) was added to a solution of 5-(pyrrolidin-1-ylmethyl)-2-(((tetrahydro-2H-pyran-2-yl)oxy)methyl)pyridine **93** (0.960 g, 3.37 mmol) in ethanol (10 mL). The reaction mixture was heated to 50 °C over 30 minutes, then diluted with water (15 mL), adjusted to pH 14 using aqueous NaOH (10% w/v) and extracted into DCM (6 x 25 mL). The combined organic extracts

were washed (brine), dried (MgSO₄) and concentrated *in vacuo*. Purification by flash chromatography (0 – 15% methanol (+ 0.1% NH₃) in DCM) afforded **94** (0.560 g, 86% yield).

¹H NMR (400 MHz, CDCl₃) 8.48 (1H, d, J = 1.5 Hz), 7.69 (1H, dd, J = 7.9, 2.0 Hz), 7.21 (1H, d, J = 8.1 Hz), 4.74 (2H, s), 3.62 (2H, s), 2.57-2.44 (4H, m), 1.85-1.73 (4H, m); ¹³C NMR (100 MHz, CDCl₃) 158.0, 148.9, 137.5, 133.6, 120.3, 64.2, 57.7, 54.2, 23.6; $\nu_{\max}/\text{cm}^{-1}$ 3200 (br, O-H), 2963, 2794, 1603, 1572; HRMS (ESI)+: m/z calculated for [C₁₁H₁₆N₂O + H]⁺ = 193.1335, observed 193.1335.

Methyl 1-((5-(pyrrolidin-1-ylmethyl)pyridin-2-yl)methyl)-1H-indole-6-carboxylate (95)

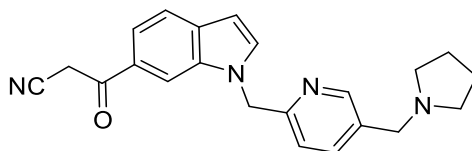


Methanesulfonyl chloride (0.242 mL, 3.12 mmol) was added dropwise at 0 °C to a solution of (5-(pyrrolidin-1-ylmethyl)pyridin-2-yl)methanol **94** (0.500 g, 2.60 mmol) and triethylamine (0.471 mL, 3.38 mmol) in DCM (10 mL). The reaction mixture was warmed to rt and stirred over 150 minutes. Na₂CO₃ solution (15 mL) was added dropwise at 0 °C to the reaction mixture. The intermediate was extracted into DCM (4 x 25 mL). The combined organic extracts were washed (brine), dried (MgSO₄) and concentrated *in vacuo* to afford the intermediate as a crude residue. A solution of methyl 1H-indole-6-carboxylate **63** (0.547 g, 3.12 mmol) in DMF (3 mL) was added dropwise at 0 °C to a suspension of NaH (60% in mineral oil, 0.520 g, 13.0 mmol) in DMF (2 mL). The reaction mixture was warmed to rt over 30 minutes. The crude residue was dissolved in DMF (5 mL) and added dropwise at 0 °C to the reaction mixture. The reaction mixture was warmed to rt and stirred over 45 minutes. NaI (39 mg, 0.26 mmol) was added to the reaction mixture, and it was heated to 60 °C over 30 minutes. Methanol (150 mL) was added dropwise at 0 °C to the reaction mixture followed by sulfuric acid (10 mL). The reaction mixture was heated under reflux for 14 hours, then concentrated *in vacuo*. Na₂CO₃ solution (200 mL) was added dropwise to the reaction mixture, followed by water (50 mL). The product was extracted into EtOAc (2 x 200 mL), followed by DCM/methanol (9:1, 3 x 200 mL). The combined organic extracts were washed (brine), dried (MgSO₄) and concentrated *in vacuo*. Purification by flash chromatography (0 – 100% EtOAc in PET, 0 – 10% methanol in DCM) afforded **95** (95 mg, 7% yield).

LCMS (ESI+): m/z 350.3 [M + H]⁺, rt 1.39 minutes, 84%; ¹H NMR (400 MHz, CDCl₃) 8.46 (1H, d, J = 1.6 Hz), 8.07 (1H, s), 7.82 (1H, dd, J = 8.4, 1.4 Hz), 7.66 (1H, d, J = 8.4 Hz), 7.36 (1H, d, J = 7.9 Hz), 7.31 (1H, dd, J = 8.0, 2.2 Hz), 7.27-7.24 (1H, m), 6.61 (1H, dd, J = 3.1, 0.8 Hz), 5.39 (2H, s), 3.92 (3H, s), 3.79 (2H, s), 2.61

(4H, br s), 1.87-1.75 (4H, m); ^{13}C NMR (100 MHz, CDCl_3) 168.0, 158.4, 147.6, 135.5, 135.1, 132.4, 131.10, 131.08, 123.6, 123.4, 120.9, 120.7, 111.7, 102.7, 61.5, 54.1, 52.0, 47.4, 23.5; $\nu_{\text{max}}/\text{cm}^{-1}$ 2951, 2799, 1705 (C=O), 1615, 1602, 1569, 1505; HRMS (ESI) $^+$: m/z calculated for $[\text{C}_{21}\text{H}_{23}\text{N}_3\text{O}_2 + \text{H}]^+ = 350.1863$, observed 350.1863.

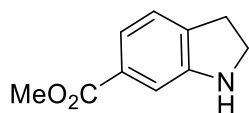
3-Oxo-3-(1-((5-(pyrrolidin-1-ylmethyl)pyridin-2-yl)methyl)-1H-indol-6-yl)propanenitrile (96)



n-Butyllithium (1.6 M in hexanes, 0.42 mL, 0.67 mmol) was added dropwise at $-78\text{ }^\circ\text{C}$ to a mixture of acetonitrile (58 μL , 1.1 mmol) and THF (2 mL). The reaction mixture was stirred at $-78\text{ }^\circ\text{C}$ over 30 minutes. A solution of methyl 1-((5-(pyrrolidin-1-ylmethyl)pyridin-2-yl)methyl)-1H-indole-6-carboxylate **95** (92 mg, 0.22 mmol) in THF (3 mL) was added dropwise at $-78\text{ }^\circ\text{C}$ over 30 minutes. The reaction mixture was stirred at $-78\text{ }^\circ\text{C}$ over 1 hour. Water (15 mL) was added dropwise at $0\text{ }^\circ\text{C}$, and the reaction mixture adjusted to pH 8. The product was extracted into DCM (3 x 25 mL), followed by DCM/methanol (9:1, 3 x 25 mL). The combined organic extracts were washed (brine), dried (MgSO_4) and concentrated *in vacuo*. Purification by flash chromatography (0 – 20% methanol in DCM) afforded **96** (69 mg, 71% yield).

LCMS (ESI $^+$): m/z 359.2 $[\text{M} + \text{H}]^+$, (ESI $^-$): m/z 357.1 $[\text{M} - \text{H}]^-$, rt 1.30 minutes, 81%; ^1H NMR (400 MHz, CDCl_3) 8.38 (1H, s), 7.96 (1H, s), 7.66 (1H, d, $J = 8.4\text{ Hz}$), 7.56 (1H, d, $J = 8.3\text{ Hz}$), 7.42-7.29 (3H, m), 6.60 (1H, d, $J = 2.8\text{ Hz}$), 5.37 (2H, s), 4.13 (2H, br s), 3.79 (2H, s), 2.70-2.55 (4H, m), 1.85-1.70 (4H, m); ^{13}C NMR (100 MHz, CDCl_3) 187.1, 158.3, 147.8, 135.7, 135.2, 133.7, 132.9, 130.8, 128.3, 123.5, 121.4, 119.8, 114.6, 110.9, 103.1, 61.4, 54.2, 47.7, 29.8, 23.5; $\nu_{\text{max}}/\text{cm}^{-1}$ 2919, 2799, 2168 (C \equiv N), 1675 (C=O), 1605; HRMS (ESI) $^+$: m/z calculated for $[\text{C}_{22}\text{H}_{22}\text{N}_4\text{O} + \text{H}]^+ = 359.1866$, observed 359.1866.

Methyl indoline-6-carboxylate (97) ¹³⁴

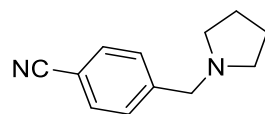


Sodium cyanoborohydride (1.61 g, 25.7 mmol) was added portionwise at $0\text{ }^\circ\text{C}$ to a solution of methyl 1H-indole-6-carboxylate **63** (1.50 g, 8.56 mmol) in acetic acid (15 mL) over 30 minutes. The reaction mixture was warmed to rt and stirred over 7 hours. The reaction was diluted with EtOAc (100 mL), washed with

NaHCO₃ solution (3 x 100 mL) and brine (100 mL), dried (MgSO₄) and concentrated *in vacuo*. Purification by flash chromatography (0 – 30% EtOAc in PET) afforded **97** (1.11 g, 66% yield).

LCMS (ESI+): m/z 178.2 [M + H]⁺, rt 1.00 minutes, 90%; ¹H NMR (400 MHz, CDCl₃) 7.40 (1H, dd, J = 7.6, 1.4 Hz), 7.23 (1H, d, J = 1.4 Hz), 7.12 (1H, d, J = 7.6 Hz), 3.90 (1H, br s), 3.86 (3H, s), 3.57 (2H, t, J = 8.4 Hz), 3.04 (2H, t, J = 8.4 Hz); ¹³C NMR (100 MHz, CDCl₃) 167.6, 151.9, 135.0, 129.4, 124.3, 120.7, 109.6, 52.0, 47.5, 29.9; ¹H NMR spectroscopic data consistent with literature.¹³⁴

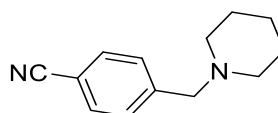
4-(Pyrrolidin-1-ylmethyl)benzonitrile (**99a**)



Sodium triacetoxyborohydride (1.29 g, 6.10 mmol) was added to a solution of 4-formylbenzonitrile **98** (0.500 g, 3.81 mmol), pyrrolidine (0.318 mL, 3.81 mmol) and acetic acid (0.262 mL, 4.58 mmol) in DCM (10 mL). The reaction mixture was stirred over 15 hours. The reaction was diluted with water (25 mL), adjusted to pH 14 using aqueous NaOH (6 M) and extracted into DCM (3 x 25 mL). The combined organic extracts were dried (MgSO₄) and concentrated *in vacuo*. Purification by flash chromatography (0 – 5% methanol in DCM) afforded **99a** (0.645 g, 85% yield).

¹H NMR (400 MHz, CDCl₃) 7.62-7.56 (2H, m), 7.47-7.41 (2H, m), 3.65 (2H, s), 2.55-2.44 (4H, m), 1.84-1.73 (4H, m); ¹³C NMR (100 MHz, CDCl₃) 145.4, 132.2, 129.4, 119.2, 110.8, 60.3, 54.4, 23.6; spectroscopic data consistent with literature.¹⁴⁷

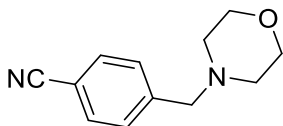
4-(Piperidin-1-ylmethyl)benzonitrile (**99b**)



Sodium triacetoxyborohydride (2.59 g, 12.2 mmol) was added to a solution of 4-formylbenzonitrile **98** (1.00 g, 7.63 mmol), piperidine (0.753 mL, 7.63 mmol) and acetic acid (0.524 mL, 9.15 mmol) in DCM (10 mL). The reaction mixture was stirred over 5 hours, then diluted with water (10 mL), adjusted to pH 14 and extracted into DCM (3 x 25 mL). The combined organic extracts were dried (MgSO₄) and concentrated *in vacuo*. Purification by flash chromatography (0 – 25% EtOAc in PET) afforded **99b** (1.21 g, 79% yield).

^1H NMR (400 MHz, CDCl_3) 7.62-7.55 (2H, m), 7.44 (2H, d, $J = 8.3$ Hz), 3.49 (2H, s), 2.43-2.27 (4H, m), 1.57 (4H, quin, $J = 5.6$ Hz), 1.48-1.38 (2H, m); ^{13}C NMR (100 MHz, CDCl_3) 145.0, 132.1, 129.6, 119.2, 110.7, 63.4, 54.7, 26.1, 24.3; spectroscopic data consistent with literature.¹⁴⁸

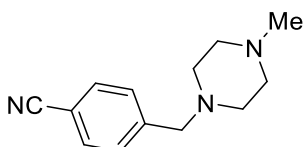
4-(Morpholinomethyl)benzonitrile (99c)



Sodium triacetoxyborohydride (1.42 g, 6.71 mmol) was added to a solution of 4-formylbenzonitrile **98** (0.550 g, 4.19 mmol), morpholine (0.367 mL, 4.19 mmol) and acetic acid (0.288 mL, 5.03 mmol) in DCM (6 mL). The reaction mixture was stirred over 90 minutes, then diluted with water (10 mL), adjusted to pH 14 and extracted into DCM (3 x 25 mL). The combined organic extracts were dried (MgSO_4) and concentrated *in vacuo*. Purification by flash chromatography (0 – 60% EtOAc in PET) afforded **99c** (0.738 g, 77% yield).

^1H NMR (400 MHz, CDCl_3) 7.62-7.57 (2H, m), 7.45 (2H, d, $J = 8.2$ Hz), 3.70 (4H, t, $J = 4.6$ Hz), 3.53 (2H, s), 2.43 (4H, t, $J = 4.6$ Hz); ^{13}C NMR (100 MHz, CDCl_3) 143.9, 132.3, 129.6, 119.0, 111.1, 67.0, 62.9, 53.7; spectroscopic data consistent with literature.¹⁴⁹

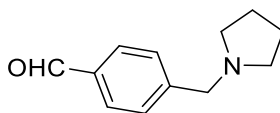
4-((4-Methylpiperazin-1-yl)methyl)benzonitrile (99d)



Sodium triacetoxyborohydride (2.59 g, 12.2 mmol) was added to a solution of 4-formylbenzonitrile **98** (1.00 g, 7.63 mmol), 1-methylpiperazine (0.846 mL, 7.63 mmol) and acetic acid (0.524 mL, 9.15 mmol) in DCM (10 mL). The reaction mixture was stirred over 80 minutes. The reaction was diluted with water (10 mL), adjusted to pH 14 using aqueous NaOH (10% w/v) and extracted into DCM (3 x 25 mL). The combined organic extracts were dried (MgSO_4) and concentrated *in vacuo*. Purification by flash chromatography (0 – 4% methanol in DCM) afforded **99d** (1.28 g, 70% yield).

^1H NMR (400 MHz, CDCl_3) 7.61-7.56 (2H, m), 7.44 (2H, d, $J = 8.2$ Hz), 3.53 (2H, s), 2.45 (8H, br s), 2.27 (3H, s); ^{13}C NMR (100 MHz, CDCl_3) 144.4, 132.2, 129.6, 119.1, 111.0, 62.5, 55.2, 53.3, 46.1; spectroscopic data consistent with literature.¹⁵⁰

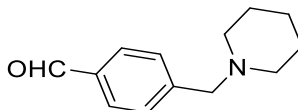
4-(Pyrrolidin-1-ylmethyl)benzaldehyde (**100a**)



DIBAL-H (1 M in THF, 2.2 mL, 2.2 mmol) was added dropwise at 0 °C to a solution of 4-(pyrrolidin-1-ylmethyl)benzotrile **99a** (0.408 g, 2.19 mmol) in THF (5 mL). The reaction mixture was warmed to rt and stirred over 45 minutes. Further DIBAL-H (2.2 mL, 2.2 mmol) was added dropwise at 0 °C to the reaction mixture. The reaction mixture was warmed to rt and stirred over 15 minutes, then NaHCO₃ solution (50 mL) was added dropwise at 0 °C. The product was extracted into DCM/methanol (10:1, 3 x 50 mL). The combined organic extracts were washed (brine), dried (MgSO₄) and concentrated *in vacuo*. Purification by flash chromatography (0 – 4% methanol (+ 0.1% NH₃) in DCM) afforded **100a** (0.313 g, 75% yield).

¹H NMR (400 MHz, CDCl₃) 9.99 (1H, s), 7.83 (2H, d, J = 8.2 Hz), 7.50 (2H, d, J = 8.0 Hz), 3.68 (2H, s), 2.56-2.48 (4H, m), 1.84-1.75 (4H, m); ¹³C NMR (100 MHz, CDCl₃) 192.2, 147.0, 135.5, 129.9, 129.4, 60.6, 54.4, 23.7; spectroscopic data consistent with literature.¹⁵¹

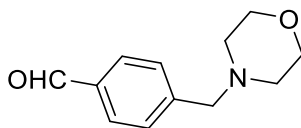
4-(Piperidin-1-ylmethyl)benzaldehyde (**100b**)



DIBAL-H (1 M in THF, 5.9 mL, 5.9 mmol) was added dropwise at 0 °C to a solution of 4-(piperidin-1-ylmethyl)benzotrile **99b** (1.19 g, 5.94 mmol) in THF (10 mL). The reaction mixture was warmed to rt and stirred over 90 minutes, then NaHCO₃ solution (50 mL) was added dropwise at 0 °C. The product was extracted into DCM/methanol (10:1, 3 x 50 mL). The combined organic extracts were washed (brine), dried (MgSO₄) and concentrated *in vacuo*. Purification by flash chromatography (0 – 18% EtOAc in PET) afforded **100b** (0.877 g, 58% yield).

¹H NMR (400 MHz, CDCl₃) 9.97 (1H, s), 7.80 (2H, d, J = 8.1 Hz), 7.48 (2H, d, J = 8.1 Hz), 3.53 (2H, s), 2.48-2.26 (4H, m), 1.64-1.51 (4H, m), 1.47-1.37 (2H, m); ¹³C NMR (100 MHz, CDCl₃) 192.1, 146.3, 135.5, 129.8, 129.6, 63.5, 54.6, 26.0, 24.3; spectroscopic data consistent with literature.¹⁵²

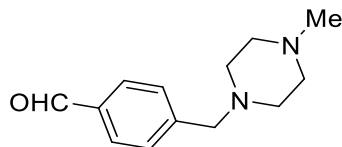
4-(Morpholinomethyl)benzaldehyde (**100c**)



DIBAL-H (1 M in THF, 3.1 mL, 3.1 mmol) was added dropwise at 0 °C to a solution of 4-(morpholinomethyl)benzotrile **99c** (0.717 g, 3.12 mmol) in THF (6 mL). The reaction mixture was warmed to rt and stirred over 30 minutes, then further DIBAL-H (1 M in THF, 3.1 mL, 3.1 mmol) was added dropwise at 0 °C. The reaction mixture was warmed to rt and stirred over 30 minutes, then NaHCO₃ solution (50 mL) was added dropwise at 0 °C. The product was extracted into DCM/methanol (10:1, 3 x 50 mL). The combined organic extracts were washed (brine), dried (MgSO₄) and concentrated *in vacuo*. Purification by flash chromatography (0 – 50% EtOAc in PET) afforded **100c** (0.297 g, 46% yield).

¹H NMR (400 MHz, CDCl₃) 9.99 (1H, s), 7.87-7.81 (2H, m), 7.51 (2H, d, J = 8.1 Hz), 3.71 (4H, t, J = 4.6 Hz), 3.57 (2H, s), 2.45 (4H, t, J = 4.5 Hz); ¹³C NMR (100 MHz, CDCl₃) 192.1, 145.5, 135.7, 129.9, 129.6, 67.1, 63.2, 53.8; spectroscopic data consistent with literature.¹⁵²

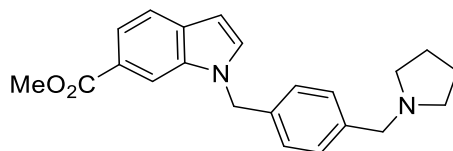
4-((4-Methylpiperazin-1-yl)methyl)benzaldehyde (**100d**)



DIBAL-H (1 M in THF, 5.3 mL, 5.3 mmol) was added dropwise at 0 °C to a solution of 4-((4-methylpiperazin-1-yl)methyl)benzotrile **99d** (1.26 g, 5.27 mmol) in THF (10 mL). The reaction mixture was warmed to rt and stirred over 30 minutes. Further DIBAL-H (5.3 mL, 5.3 mmol) was added dropwise at 0 °C to the reaction mixture. The reaction mixture was warmed to rt and stirred over 30 minutes, then NaHCO₃ solution (50 mL) was added dropwise at 0 °C. The product was extracted into DCM/methanol (9:1, 3 x 50 mL). The combined organic extracts were washed (brine), dried (MgSO₄) and concentrated *in vacuo*. Purification by flash chromatography (0 – 4% methanol (+ 0.1% NH₃) in DCM) afforded **100d** (0.576 g, 50% yield).

¹H NMR (400 MHz, CDCl₃) 9.98 (1H, s), 7.85-7.79 (2H, m), 7.50 (2H, d, J = 8.0 Hz), 3.57 (2H, s), 2.47 (8H, br s), 2.28 (3H, s); ¹³C NMR (100 MHz, CDCl₃) 192.1, 146.0, 135.6, 129.9, 129.6, 62.8, 55.2, 53.3, 46.2; spectroscopic data consistent with literature.¹⁵²

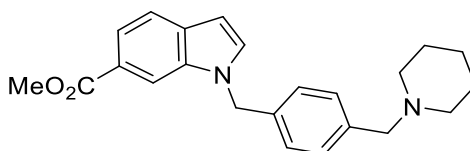
Methyl 1-(4-(pyrrolidin-1-ylmethyl)benzyl)-1H-indole-6-carboxylate (101a)



A solution of 4-(pyrrolidin-1-ylmethyl)benzaldehyde **100a** (0.302 g, 1.60 mmol) in toluene (3 mL) was added to a mixture of methyl indoline-6-carboxylate **97** (0.377 g, 1.91 mmol) and benzoic acid (39 mg, 0.32 mmol). The reaction mixture was heated to 200 °C by microwave for 20 minutes. The reaction was diluted with EtOAc (50 mL), washed with NaHCO₃ solution (3 x 50 mL) and brine (50 mL), dried (MgSO₄) and concentrated *in vacuo*. Purification by flash chromatography (40 – 80% EtOAc in PET) afforded **101a** (0.297 g, 53% yield).

LCMS (ESI+): m/z 349.3 [M + H]⁺, rt 1.51 minutes, 100%; ¹H NMR (400 MHz, CDCl₃) 8.11 (1H, s), 7.81 (1H, dd, J = 8.3, 1.3 Hz), 7.66 (1H, d, J = 8.4 Hz), 7.32-7.23 (3H, m), 7.07 (2H, d, J = 7.9 Hz), 6.59 (1H, dd, J = 3.1, 0.5 Hz), 5.37 (2H, s), 3.92 (3H, s), 3.58 (2H, s), 2.52-2.44 (4H, m), 1.80-1.73 (4H, m); ¹³C NMR (100 MHz, CDCl₃) 168.3, 139.3, 135.9, 135.6, 132.4, 131.5, 129.5, 126.9, 123.5, 120.72, 120.65, 112.1, 102.2, 60.4, 54.3, 52.0, 50.0, 23.6; ν_{max}/cm⁻¹ 2951, 2782, 1706 (C=O), 1615, 1505; HRMS (ESI)+: m/z calculated for [C₂₂H₂₄N₂O₂ + H]⁺ = 349.1911, observed 349.1913.

Methyl 1-(4-(piperidin-1-ylmethyl)benzyl)-1H-indole-6-carboxylate (101b)

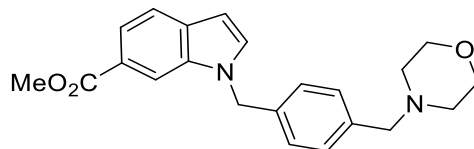


A solution of 4-(piperidin-1-ylmethyl)benzaldehyde **100b** (0.400 g, 1.57 mmol) in toluene (3 mL) was added to a mixture of methyl indoline-6-carboxylate **97** (0.360 g, 1.89 mmol) and benzoic acid (38 mg, 0.32 mmol). The reaction mixture was heated to 200 °C by microwave for 30 minutes, then diluted with EtOAc (25 mL), washed with NaHCO₃ solution (3 x 15 mL) and brine (15 mL), dried (MgSO₄) and concentrated *in vacuo*. Purification by flash chromatography (20 – 41% EtOAc in PET) afforded **101b** (0.393 g, 67% yield).

LCMS (ESI+): m/z 363.4 [M + H]⁺, rt 1.50 minutes, 97%; ¹H NMR (400 MHz, CDCl₃) 8.10 (1H, s), 7.83-7.77 (1H, m), 7.65 (1H, d, J = 8.4 Hz), 7.29-7.22 (3H, m), 7.05 (2H, d, J = 7.6 Hz), 6.61-6.55 (1H, m), 5.36 (2H, s), 3.91 (3H, s), 3.42 (2H, s), 2.34 (4H, br s), 1.62-1.50 (4H, m), 1.46-1.36 (2H, m); ¹³C NMR (100 MHz, CDCl₃)

168.3, 138.6, 135.9, 135.6, 132.4, 131.5, 129.8, 126.8, 123.5, 120.72, 120.66, 112.2, 102.2, 63.6, 54.6, 52.1, 50.0, 26.1, 24.5; $\nu_{\max}/\text{cm}^{-1}$ 2933, 2851, 2793, 2754, 1707 (C=O), 1615, 1505; HRMS (ESI)+: m/z calculated for $[\text{C}_{23}\text{H}_{26}\text{N}_2\text{O}_2 + \text{H}]^+ = 363.2067$, observed 363.2051.

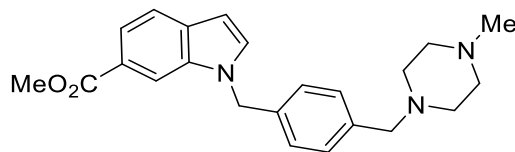
Methyl 1-(4-(morpholinomethyl)benzyl)-1H-indole-6-carboxylate (101c)



Toluene (3 mL) was added to a mixture of 4-(morpholinomethyl)benzaldehyde **100c** (0.282 g, 1.37 mmol), methyl indole-6-carboxylate **97** (0.325 g, 1.65 mmol) and benzoic acid (34 mg, 0.28 mmol). The reaction mixture was heated to 200 °C by microwave for 30 minutes, then diluted with EtOAc (25 mL), washed with NaHCO_3 solution (3 x 15 mL) and brine (15 mL), dried (MgSO_4) and concentrated *in vacuo*. Purification by flash chromatography (0 – 55% EtOAc in PET) afforded **101c** (0.330 g, 59% yield).

LCMS (ESI+): m/z 365.3 $[\text{M} + \text{H}]^+$, rt 1.45 minutes, >99%; ^1H NMR (400 MHz, CDCl_3) 8.10 (1H, s), 7.81 (1H, dd, $J = 8.3, 1.4$ Hz), 7.66 (1H, d, $J = 8.3$ Hz), 7.31-7.23 (3H, m), 7.06 (2H, d, $J = 7.9$ Hz), 6.59 (1H, dd, $J = 3.1, 0.7$ Hz), 5.37 (2H, s), 3.91 (3H, s), 3.69 (4H, t, $J = 4.7$ Hz), 3.45 (2H, s), 2.41 (4H, t, $J = 4.4$ Hz); ^{13}C NMR (100 MHz, CDCl_3) 168.3, 137.7, 136.0, 135.9, 132.4, 131.5, 129.8, 126.9, 123.6, 120.73, 120.68, 112.1, 102.3, 67.1, 63.1, 53.7, 52.1, 50.0; $\nu_{\max}/\text{cm}^{-1}$ 2950, 2854, 2808, 1706 (C=O), 1615, 1504; HRMS (ESI)+: m/z calculated for $[\text{C}_{22}\text{H}_{24}\text{N}_2\text{O}_3 + \text{H}]^+ = 365.1860$, observed 365.1848.

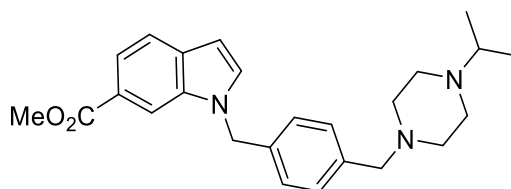
Methyl 1-(4-((4-methylpiperazin-1-yl)methyl)benzyl)-1H-indole-6-carboxylate (101d)



Toluene (3 mL) was added to a mixture of 4-((4-methylpiperazin-1-yl)methyl)benzaldehyde **100d** (0.300 g, 1.37 mmol), methyl indole-6-carboxylate **97** (0.314 g, 1.65 mmol) and benzoic acid (34 mg, 0.28 mmol). The reaction mixture was heated to 200 °C by microwave for 30 minutes. The reaction was diluted with EtOAc (25 mL), washed with NaHCO_3 solution (3 x 15 mL) and brine (15 mL), dried (MgSO_4) and concentrated *in vacuo*. Purification by flash chromatography (0 – 10% methanol in DCM) afforded **101d** (0.329 g, 55% yield).

LCMS (ESI+): m/z 378.3 [M + H]⁺, rt 1.46 minutes, 100%; ¹H NMR (400 MHz, CDCl₃) 8.12 (1H, s), 7.83 (1H, dd, J = 8.4, 1.4 Hz), 7.68 (1H, d, J = 8.4 Hz), 7.30-7.24 (3H, m), 7.08 (2H, d, J = 8.2 Hz), 6.61 (1H, dd, J = 3.1, 0.7 Hz), 5.38 (2H, s), 3.93 (3H, s), 3.49 (2H, s), 2.49 (8H, br s), 2.31 (3H, s); ¹³C NMR (100 MHz, CDCl₃) 168.1, 137.9, 135.8, 135.7, 132.3, 131.3, 129.6, 126.7, 123.4, 120.6, 120.5, 112.0, 102.1, 62.5, 55.0, 52.8, 51.9, 49.8, 45.8; ν_{max}/cm⁻¹ 2937, 2794, 1706 (C=O), 1614, 1504; HRMS (ESI)+: m/z calculated for [C₂₃H₂₇N₃O₂ + H]⁺ = 378.2176, observed 378.2159.

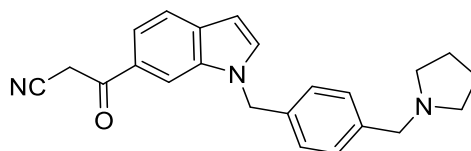
Methyl 1-(4-((4-isopropylpiperazin-1-yl)methyl)benzyl)-1H-indole-6-carboxylate (101e)



Methanesulfonyl chloride (0.126 mL, 1.63 mmol) was added dropwise at 0 °C to a solution of methyl 1-(4-(hydroxymethyl)benzyl)-1H-indole-6-carboxylate **109** (0.400 g, 1.35 mmol) and triethylamine (0.245 mL, 1.76 mmol) in DCM (4 mL). The reaction mixture was warmed to rt and stirred over 90 minutes. Water (15 mL) was added dropwise at 0 °C. The intermediate was extracted into DCM (3 x 25 mL). The combined organic extracts were washed (brine), dried (MgSO₄) and concentrated *in vacuo*. The crude residue was dissolved in DMF (4 mL), then 1-isopropylpiperazine (0.233 mL, 1.63 mmol) and Cs₂CO₃ (0.574 g, 1.76 mmol) were added. The reaction mixture was stirred over 11 hours, then further 1-isopropylpiperazine (0.233 mL, 1.63 mmol) and Cs₂CO₃ (0.574 g, 1.76 mmol) were added. The reaction mixture was stirred over 1 hour, then diluted with EtOAc (100 mL), washed with water (3 x 100 mL) and brine (100 mL), dried (MgSO₄) and concentrated *in vacuo*. Purification by flash chromatography (50 – 100% EtOAc in PET) afforded **101e** (0.254 g, 43% yield).

LCMS (ESI+): m/z 406.3 [M + H]⁺, rt 1.54 minutes, 92%; ¹H NMR (400 MHz, CDCl₃) 8.10 (1H, s), 7.80 (1H, dd, J = 8.4, 1.4 Hz), 7.65 (1H, d, J = 8.4 Hz), 7.29-7.22 (3H, m), 7.06 (2H, d, J = 8.1 Hz), 6.58 (1H, dd, J = 3.2, 0.8 Hz), 5.36 (2H, s), 3.91 (3H, s), 3.47 (2H, s), 2.62 (1H, sept, J = 6.5 Hz), 2.62-2.32 (8H, m), 1.03 (6H, d, J = 6.5 Hz); ¹³C NMR (100 MHz, CDCl₃) 168.3, 138.1, 135.9, 135.8, 132.4, 131.5, 129.8, 126.9, 123.6, 120.74, 120.67, 112.1, 102.3, 62.8, 54.6, 53.6, 52.1, 50.0, 48.8, 18.8; ν_{max}/cm⁻¹ 2964, 2929, 2875, 2808, 1709 (C=O), 1618, 1571, 1505; HRMS (ESI)+: m/z calculated for [C₂₅H₃₁N₃O₂ + H]⁺ = 406.2489, observed 406.2481.

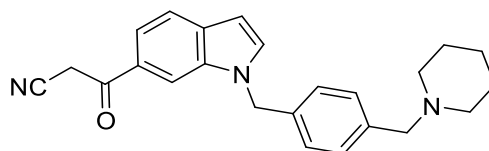
3-Oxo-3-(1-(4-(pyrrolidin-1-ylmethyl)benzyl)-1H-indol-6-yl)propanenitrile (102a)



n-Butyllithium (1.6 M in hexanes, 2.7 mL, 4.3 mmol) was added dropwise at -78 °C to a mixture of acetonitrile (0.375 mL, 7.17 mmol) and THF (6 mL). The reaction mixture was stirred at -78 °C over 30 minutes. A solution of methyl 1-(4-(pyrrolidin-1-ylmethyl)benzyl)-1H-indole-6-carboxylate **101a** (0.500 g, 1.43 mmol) in THF (4 mL) was added dropwise at -78 °C over 30 minutes. The reaction mixture was stirred at -78 °C over 1 hour. Water (15 mL) was added dropwise at 0 °C, and the reaction mixture adjusted to pH 8. The product was extracted into DCM (3 x 25 mL). The combined organic extracts were washed (brine), dried (MgSO₄) and concentrated *in vacuo*. Purification by flash chromatography (50 – 100% EtOAc in PET, 0 – 10% methanol in DCM) afforded **102a** (0.448 g, 87% yield).

LCMS (ESI+): *m/z* 358.3 [M + H]⁺, (ESI-): *m/z* 356.2 [M - H]⁻, *rt* 1.38 minutes, 100%; ¹H NMR (400 MHz, CDCl₃) 7.98 (1H, s), 7.70 (1H, d, *J* = 8.3 Hz), 7.59 (1H, dd, *J* = 8.4, 1.3 Hz), 7.36 (1H, d, *J* = 3.1 Hz), 7.29 (2H, d, *J* = 8.1 Hz), 7.07 (2H, d, *J* = 7.9 Hz), 6.61 (1H, d, *J* = 3.1 Hz), 5.38 (2H, s), 4.09 (2H, br s), 3.59 (2H, s), 2.55-2.44 (4H, m), 1.83-1.71 (4H, m); ¹³C NMR (100 MHz, CDCl₃) 187.0, 139.4, 136.0, 135.2, 133.9, 133.4, 129.7, 128.1, 127.0, 121.3, 119.7, 114.5, 111.3, 102.6, 60.3, 54.3, 50.3, 29.6, 23.5; *v*_{max}/cm⁻¹ 2960, 2786, 2165 (C≡N), 1680 (C=O), 1607, 1503.

3-Oxo-3-(1-(4-(piperidin-1-ylmethyl)benzyl)-1H-indol-6-yl)propanenitrile (102b)

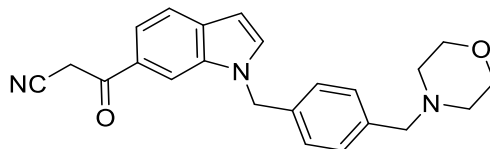


n-Butyllithium (1.6 M in hexanes, 1.3 mL, 2.0 mmol) was added dropwise at -78 °C to a mixture of acetonitrile (0.16 mL, 3.0 mmol) and THF (3 mL). The reaction mixture was stirred at -78 °C over 30 minutes. A solution of methyl 1-(4-(piperidin-1-ylmethyl)benzyl)-1H-indole-6-carboxylate **101b** (0.377 g, 1.01 mmol) in THF (3 mL) was added dropwise at -78 °C over 30 minutes. The reaction mixture was stirred at -78 °C over 1 hour. Water (20 mL) was added dropwise at 0 °C, and the reaction mixture adjusted to pH 8. The product was extracted into DCM (4 x 50 mL). The combined organic extracts were dried (MgSO₄)

and concentrated *in vacuo*. Purification by flash chromatography (50 – 90% EtOAc in PET) afforded **102b** (0.289 g, 77% yield).

LCMS (ESI+): m/z 372.4 $[M + H]^+$, rt 1.43 minutes, >99%; 1H NMR (400 MHz, $CDCl_3$) 7.99 (1H, s), 7.70 (1H, d, $J = 8.4$ Hz), 7.60 (1H, dd, $J = 8.3, 1.5$ Hz), 7.37 (1H, d, $J = 3.2$ Hz), 7.27 (2H, d, $J = 7.5$ Hz), 7.06 (2H, d, $J = 8.2$ Hz), 6.62 (1H, d, $J = 3.1$ Hz), 5.38 (2H, s), 4.09 (2H, s), 3.43 (2H, s), 2.34 (4H, br s), 1.55 (4H, quin, $J = 5.6$ Hz), 1.47-1.36 (2H, m); ^{13}C NMR (100 MHz, $CDCl_3$) 187.0, 138.9, 136.0, 135.1, 133.8, 133.4, 129.9, 128.1, 126.8, 121.3, 119.7, 114.5, 111.3, 102.6, 63.5, 54.6, 50.3, 29.6, 26.1, 24.5; ν_{max}/cm^{-1} 2914, 2805, 2252 ($C\equiv N$), 1682 ($C=O$), 1608, 1503; HRMS (ESI+): m/z calculated for $[C_{24}H_{25}N_3O + H]^+ = 372.2070$, observed 372.2053.

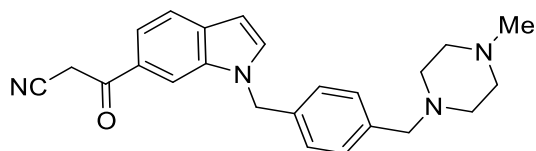
3-(1-(4-(Morpholinomethyl)benzyl)-1H-indol-6-yl)-3-oxopropanenitrile (102c)



n-Butyllithium (1.6 M in hexanes, 1.5 mL, 2.3 mmol) was added dropwise at -78 °C to a mixture of acetonitrile (0.20 mL, 3.9 mmol) and THF (3 mL). The reaction mixture was stirred at -78 °C over 30 minutes. A solution of methyl 1-(4-(morpholinomethyl)benzyl)-1H-indole-6-carboxylate **101c** (0.315 g, 0.778 mmol) in THF (3 mL) was added dropwise at -78 °C over 30 minutes. The reaction mixture was stirred at -78 °C over 20 minutes. Water (10 mL) was added dropwise at 0 °C, and the reaction mixture adjusted to pH 8. The product was extracted into DCM (3 x 25 mL). The combined organic extracts were washed (brine), dried ($MgSO_4$) and concentrated *in vacuo*. Purification by flash chromatography (20 – 80% EtOAc in PET) afforded **102c** (0.272 g, 87% yield).

LCMS (ESI+): m/z 374.2 $[M + H]^+$, rt 1.36 minutes, 93%; 1H NMR (400 MHz, $CDCl_3$) 7.99 (1H, s), 7.70 (1H, d, $J = 8.3$ Hz), 7.59 (1H, dd, $J = 8.4, 1.5$ Hz), 7.37 (1H, d, $J = 3.2$ Hz), 7.28 (2H, d, $J = 8.1$ Hz), 7.07 (2H, d, $J = 7.9$ Hz), 6.62 (1H, d, $J = 3.2$ Hz), 5.38 (2H, s), 4.09 (2H, s), 3.68 (4H, t, $J = 4.6$ Hz), 3.45 (2H, s), 2.45-2.36 (4H, m); ^{13}C NMR (100 MHz, $CDCl_3$) 187.1, 138.0, 136.0, 135.5, 133.9, 133.4, 129.9, 128.1, 126.9, 121.3, 119.8, 114.4, 111.3, 102.7, 67.1, 63.1, 53.7, 50.3, 29.6; ν_{max}/cm^{-1} 2940, 2846, 2251 ($C\equiv N$), 1681 ($C=O$), 1607, 1503; HRMS (ESI)-: m/z calculated for $[C_{23}H_{23}N_3O_2 - H]^- = 372.1718$, observed 372.1723.

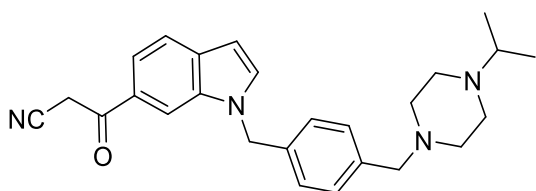
3-(1-(4-((4-Methylpiperazin-1-yl)methyl)benzyl)-1H-indol-6-yl)-3-oxopropanenitrile (**102d**)



n-Butyllithium (1.6 M in hexanes, 1.4 mL, 2.2 mmol) was added dropwise at -78 °C to a mixture of acetonitrile (0.188 mL, 3.61 mmol) and THF (3 mL). The reaction mixture was stirred at -78 °C over 30 minutes. A solution of methyl 1-(4-((4-methylpiperazin-1-yl)methyl)benzyl)-1H-indole-6-carboxylate **101d** (0.313 g, 0.721 mmol) in THF (3 mL) was added dropwise at -78 °C over 30 minutes. The reaction mixture was stirred at -78 °C over 30 minutes. Water (20 mL) was added dropwise at 0 °C, and the reaction mixture adjusted to pH 8. The product was extracted into DCM (3 x 25 mL). The combined organic extracts were washed (brine), dried (MgSO₄) and concentrated *in vacuo*. Purification by flash chromatography (50 – 100% EtOAc in PET, 0 – 10% methanol in DCM) afforded **102d** (0.258 g, 82% yield).

LCMS (ESI+): *m/z* 387.2 [M + H]⁺, *rt* 1.38 minutes, 89%; ¹H NMR (400 MHz, CDCl₃) 7.98 (1H, s), 7.69 (1H, d, *J* = 8.3 Hz), 7.58 (1H, dd, *J* = 8.4, 1.6 Hz), 7.36 (1H, d, *J* = 3.2 Hz), 7.26 (2H, d, *J* = 8.1 Hz), 7.06 (2H, d, *J* = 8.2 Hz), 6.61 (1H, dd, *J* = 3.1, 0.7 Hz), 5.37 (2H, s), 4.09 (2H, br s), 3.47 (2H, s), 2.44 (8H, br s), 2.27 (3H, s); ¹³C NMR (100 MHz, CDCl₃) 187.0, 138.4, 136.0, 135.3, 133.8, 133.4, 129.9, 128.1, 126.9, 121.3, 119.7, 114.5, 111.3, 102.6, 62.6, 55.2, 53.1, 50.3, 46.1, 29.7; *v*_{max}/cm⁻¹ 2934, 2790, 2165 (C≡N), 1680 (C=O), 1607, 1502; HRMS (ESI)-: *m/z* calculated for [C₂₄H₂₆N₄O - H]⁻ = 385.2034, observed 385.2029.

3-(1-(4-((4-Isopropylpiperazin-1-yl)methyl)benzyl)-1H-indol-6-yl)-3-oxopropanenitrile (**102e**)

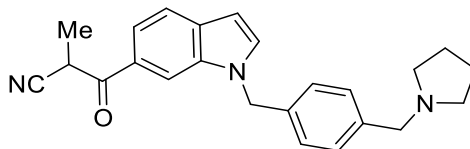


n-Butyllithium (1.6 M in hexanes, 1.0 mL, 1.6 mmol) was added dropwise at -78 °C to a mixture of acetonitrile (0.14 mL, 2.7 mmol) and THF (2 mL). The reaction mixture was stirred at -78 °C over 30 minutes. A solution of methyl 1-(4-((4-isopropylpiperazin-1-yl)methyl)benzyl)-1H-indole-6-carboxylate **101e** (0.241 g, 0.547 mmol) in THF (4 mL) was added dropwise at -78 °C over 30 minutes. The reaction mixture was stirred at -78 °C over 30 minutes. Water (15 mL) was added dropwise at 0 °C, and the reaction mixture adjusted to pH 8. The product was extracted into DCM/methanol (9:1, 3 x 25 mL). The combined

organic extracts were washed (brine), dried (MgSO₄) and concentrated *in vacuo*. Purification by flash chromatography (50 – 100% EtOAc in PET, 0 – 8% methanol in DCM) afforded **102e** (0.187 g, 83% yield).

LCMS (ESI+): m/z 415.3 [M + H]⁺, (ESI-): m/z 413.2 [M - H]⁻, rt 1.45 minutes, >99%; ¹H NMR (400 MHz, CDCl₃) 7.98 (1H, s), 7.70 (1H, d, J = 8.4 Hz), 7.59 (1H, dd, J = 8.4, 1.5 Hz), 7.37 (1H, d, J = 3.2 Hz), 7.26 (2H, d, J = 8.2 Hz), 7.06 (2H, d, J = 8.1 Hz), 6.62 (1H, d, J = 3.2 Hz), 5.38 (2H, s), 4.10 (2H, s), 3.48 (2H, s), 2.76-2.41 (9H, m), 1.06 (6H, d, J = 6.6 Hz); ¹³C NMR (100 MHz, CDCl₃) 187.0, 138.2, 136.0, 135.4, 133.9, 133.4, 130.0, 128.1, 126.9, 121.3, 119.7, 114.5, 111.3, 102.6, 62.6, 54.8, 53.1, 50.3, 48.7, 29.6, 18.6; ν_{max}/cm⁻¹ 2934, 2810, 2162 (C≡N), 1681 (C=O), 1607, 1502; HRMS (ESI)+: m/z calculated for [C₂₆H₃₀N₄O + H]⁺ = 415.2492, observed 415.2479.

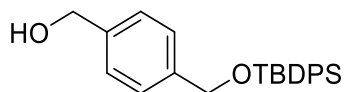
2-Methyl-3-oxo-3-(1-(4-(pyrrolidin-1-ylmethyl)benzyl)-1H-indol-6-yl)propanenitrile (104a)



n-Butyllithium (1.6 M in hexanes, 1.1 mL, 1.7 mmol) was added dropwise at -78 °C to a mixture of propionitrile (0.123 mL, 1.72 mmol) and toluene (4 mL). The reaction mixture was stirred at -78 °C over 30 minutes. A solution of methyl 1-(4-(pyrrolidin-1-ylmethyl)benzyl)-1H-indole-6-carboxylate **101a** (0.300 g, 0.861 mmol) in toluene (2 mL) was added dropwise at -78 °C over 30 minutes. The reaction mixture was stirred at -78 °C over 1 hour, then warmed to 0 °C and stirred over 1 hour. Water (15 mL) was added dropwise at 0 °C, and the reaction mixture adjusted to pH 8. The product was extracted into EtOAc (3 x 25 mL). The combined organic extracts were washed (brine), dried (MgSO₄) and concentrated *in vacuo*. Purification by flash chromatography (50 – 100% EtOAc in PET) afforded **104a** (0.140 g, 35% yield).

¹H NMR (400 MHz, CDCl₃) 8.03 (1H, s), 7.70 (2H, s), 7.36 (1H, d, J = 3.1 Hz), 7.29 (2H, d, J = 8.1 Hz), 7.09 (2H, d, J = 7.9 Hz), 6.61 (1H, d, J = 2.9 Hz), 5.38 (2H, s), 4.42 (1H, q, J = 7.2 Hz), 3.58 (2H, s), 2.54-2.40 (4H, m), 1.80-1.70 (4H, m), 1.64 (3H, d, J = 7.2 Hz).

4-(((Tert-butyl)diphenylsilyloxy)methyl)phenyl)methanol (107)

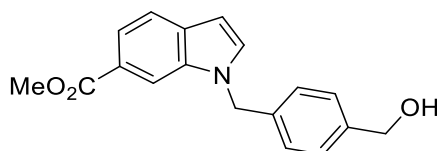


tert-Butyldiphenylchlorosilane (3.8 mL, 15 mmol) was added to a solution of 1,4-benzenedimethanol **106** (4.02 g, 29.1 mmol) and imidazole (1.09 g, 16.0 mmol) in DMF (20 mL). The reaction mixture was stirred

over 21 hours. The reaction was diluted with EtOAc (100 mL), washed with water (3 x 100 mL) and brine (100 mL), dried (MgSO₄) and concentrated *in vacuo*. Purification by flash chromatography (0 – 20% EtOAc in PET) afforded **107** (4.14 g, 38% yield).

¹H NMR (400 MHz, CDCl₃) 7.73-7.68 (4H, m), 7.47-7.32 (10H, m), 4.78 (2H, s), 4.70 (2H, d, J = 5.7 Hz), 1.66 (1H, t, J = 5.9 Hz), 1.10 (9H, s); ¹³C NMR (100 MHz, CDCl₃) 140.8, 139.6, 135.7, 133.6, 129.8, 127.9, 127.2, 126.4, 65.5, 65.4, 27.0, 19.5; spectroscopic data consistent with literature.¹⁵³

Methyl 1-(4-(hydroxymethyl)benzyl)-1H-indole-6-carboxylate (109)



Methanesulfonyl chloride (1.0 mL, 13 mmol) was added dropwise at 0 °C to a solution of 4-(((*tert*-butyldiphenylsilyloxy)methyl)phenyl)methanol **107** (4.12 g, 11.0 mmol) and triethylamine (2.0 mL, 14 mmol) in DCM (20 mL). The reaction mixture was warmed to rt and stirred over 1 hour. Water (1 mL) was added dropwise at 0 °C. The mixture was diluted with DCM (30 mL), washed with water (3 x 50 mL) and brine (50 mL), dried (MgSO₄) and concentrated *in vacuo* to afford a crude residue. A solution of methyl 1H-indole-6-carboxylate **63** (1.88 g, 10.7 mmol) in DMF (6 mL) was added dropwise at 0 °C to a suspension of NaH (60% in mineral oil, 0.514 g, 12.8 mmol) in DMF (4 mL). The reaction mixture was warmed to rt over 30 minutes. A solution of the crude residue in DMF (10 mL) was added dropwise at 0 °C to the reaction mixture. The reaction mixture was warmed to rt and stirred over 45 minutes. Water (10 mL) was added dropwise at 0 °C. The mixture was diluted with EtOAc (200 mL), washed with water (3 x 200 mL) and brine (200 mL), dried (MgSO₄) and concentrated *in vacuo*. TBAF (1 M in THF, 14 mL, 14 mmol) was added to the resultant residue. The mixture was stirred over 30 minutes, then water (50 mL) was added. The product was extracted into DCM (3 x 50 mL). The combined organic extracts were washed (brine), dried (MgSO₄) and concentrated *in vacuo*. Purification by flash chromatography (10 – 50% EtOAc in PET) afforded **109** (2.33 g, 72% yield).

LCMS (ESI+): m/z 296.2 [M + H]⁺, rt 1.96 minutes, 100%; ¹H NMR (400 MHz, CDCl₃) 8.08 (1H, s), 7.80 (1H, dd, J = 8.4, 1.4 Hz), 7.66 (1H, d, J = 8.4 Hz), 7.30 (2H, d, J = 8.2 Hz), 7.26 (1H, d, J = 3.2 Hz), 7.10 (2H, d, J = 8.2 Hz), 6.59 (1H, dd, J = 3.1, 0.8 Hz), 5.37 (2H, s), 4.65 (2H, d, J = 2.8 Hz), 3.90 (3H, s), 1.82-1.72 (1H, m); ¹³C NMR (100 MHz, CDCl₃) 168.3, 140.7, 136.5, 135.8, 132.5, 131.5, 127.6, 127.2, 123.6, 120.8, 120.7,

112.1, 102.4, 65.0, 52.1, 50.0; $\nu_{\max}/\text{cm}^{-1}$ 3295 (br, O-H), 2949, 1705 (C=O), 1618, 1500; HRMS (ESI)+: m/z calculated for $[\text{C}_{18}\text{H}_{17}\text{NO}_3 + \text{Na}]^+ = 318.1101$, observed 318.1094.

A.2: Biochemical Assay Dose-response Curves

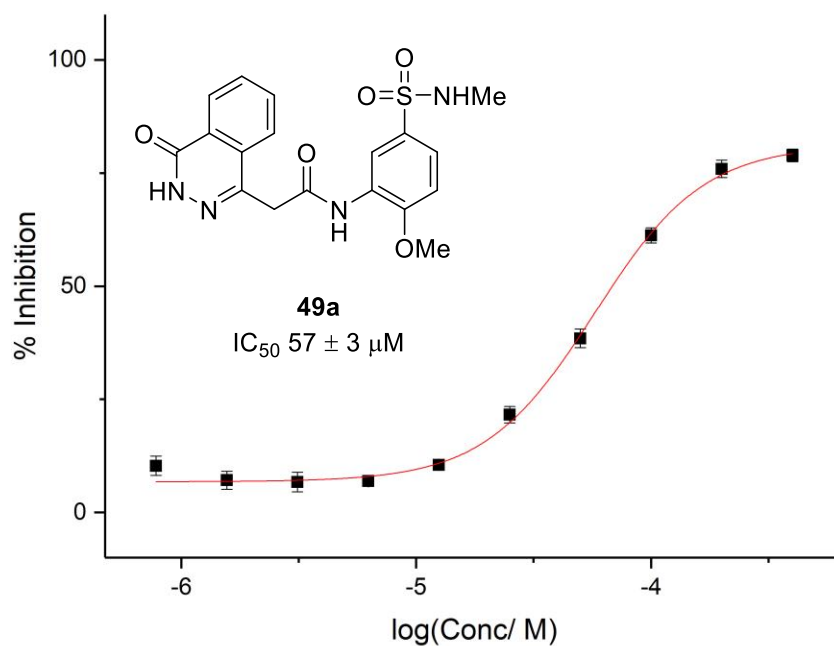
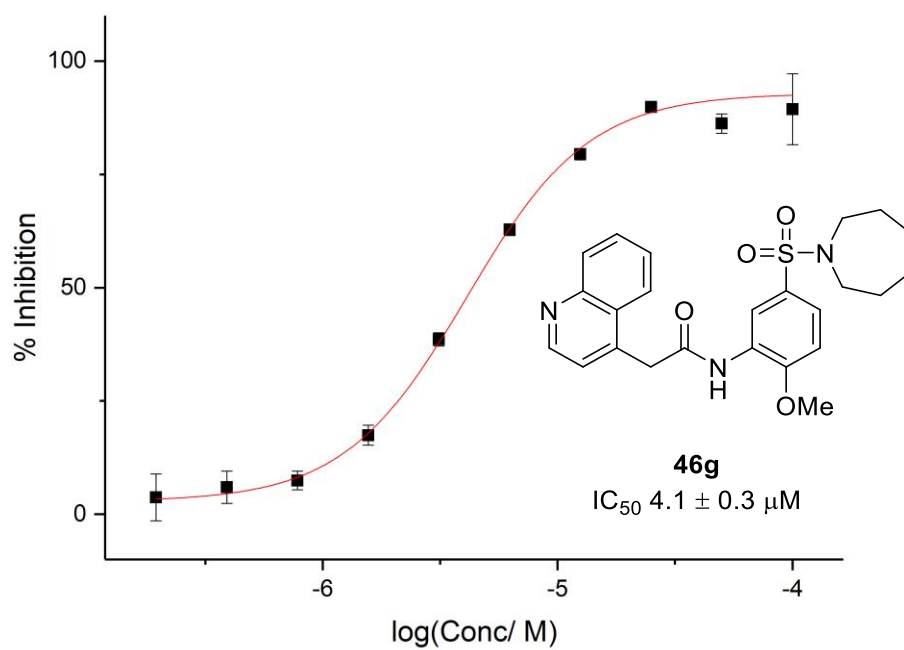


Figure 60: Dose-response curves for **46g** and **49a**, with data points representing an average of replicates ($n = 6$) and error bars indicating standard errors of the mean.

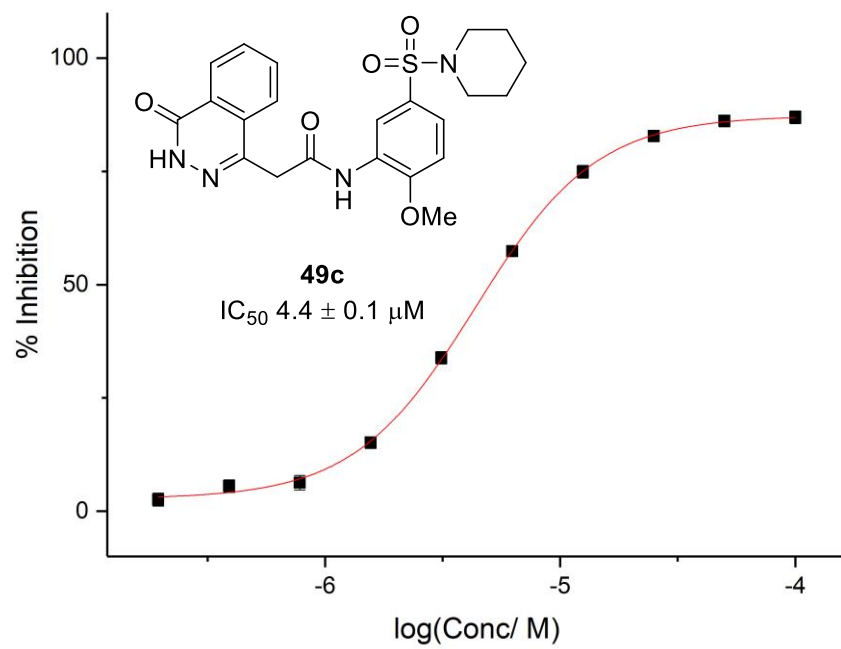
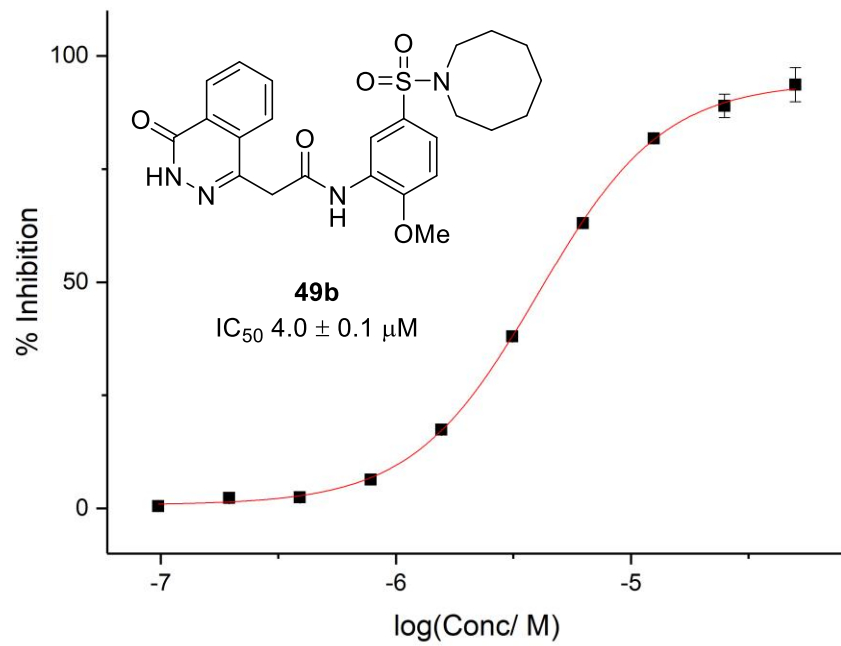


Figure 61: Dose-response curves for **49b-c**, with data points representing an average of replicates ($n = 6$) and error bars indicating standard errors of the mean.

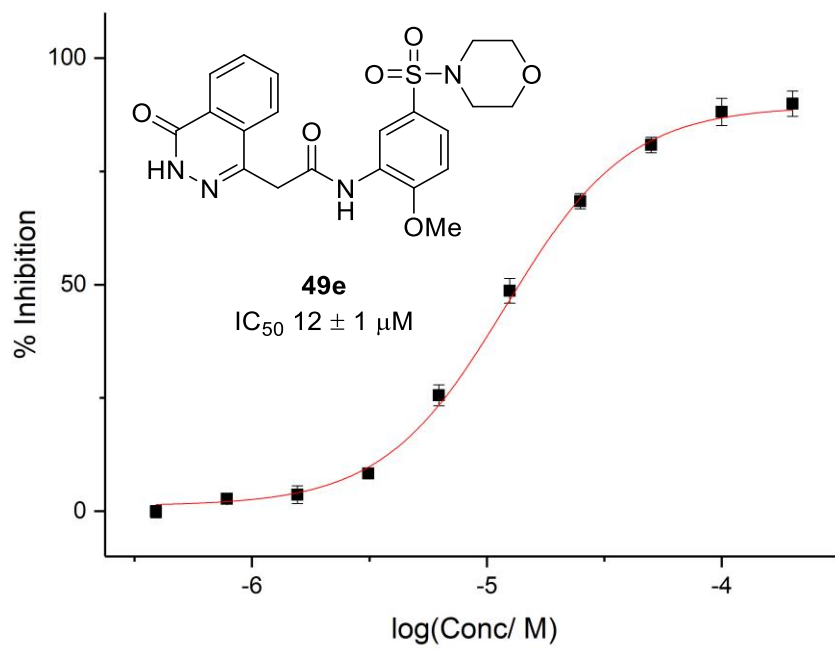
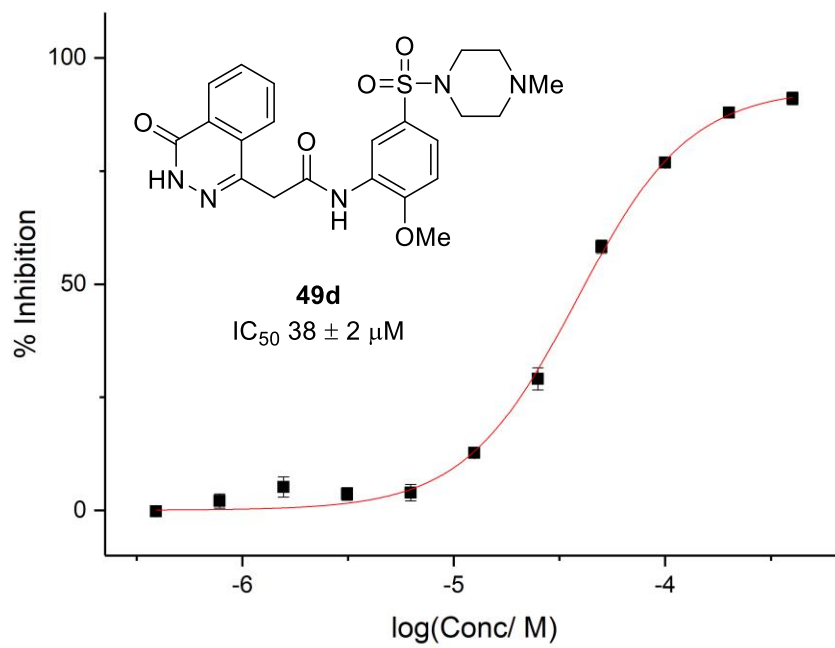


Figure 62: Dose-response curves for **49d-e**, with data points representing an average of replicates ($n = 6$) and error bars indicating standard errors of the mean.

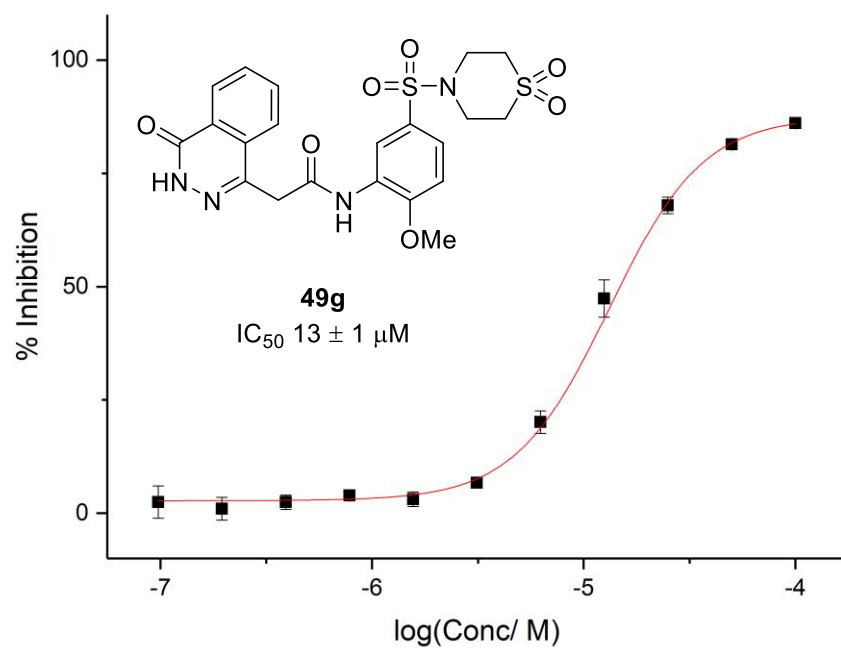
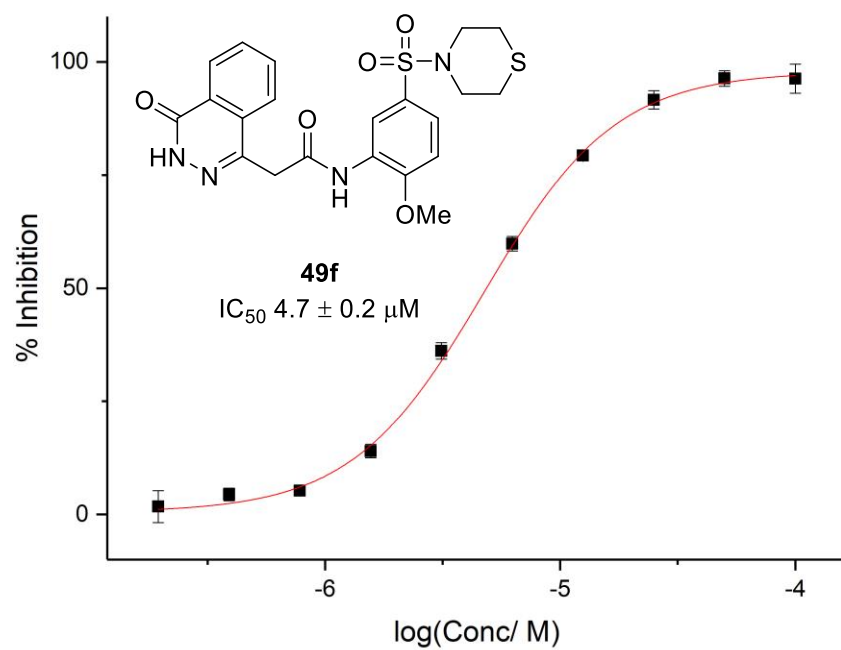


Figure 63: Dose-response curves for **49f-g**, with data points representing an average of replicates ($n = 6$) and error bars indicating standard errors of the mean.

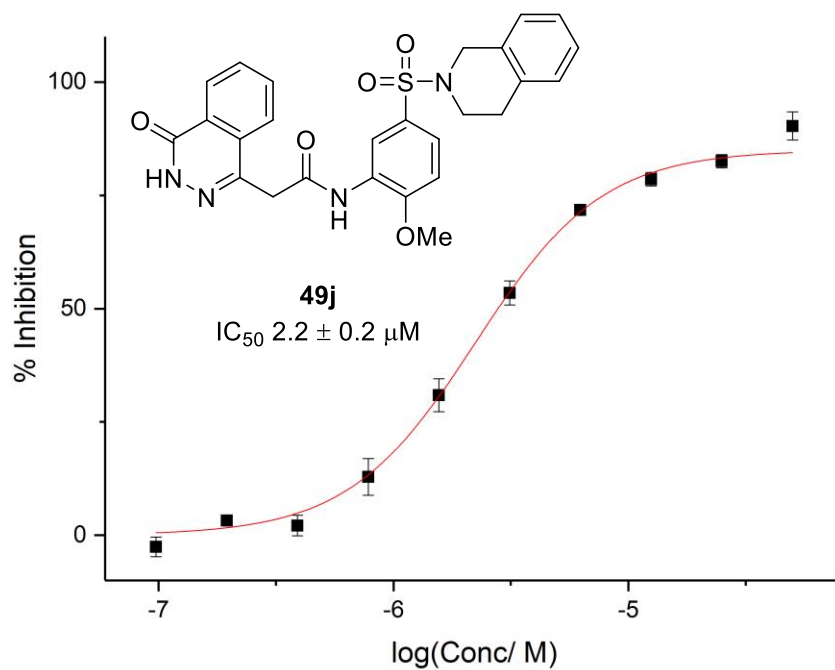
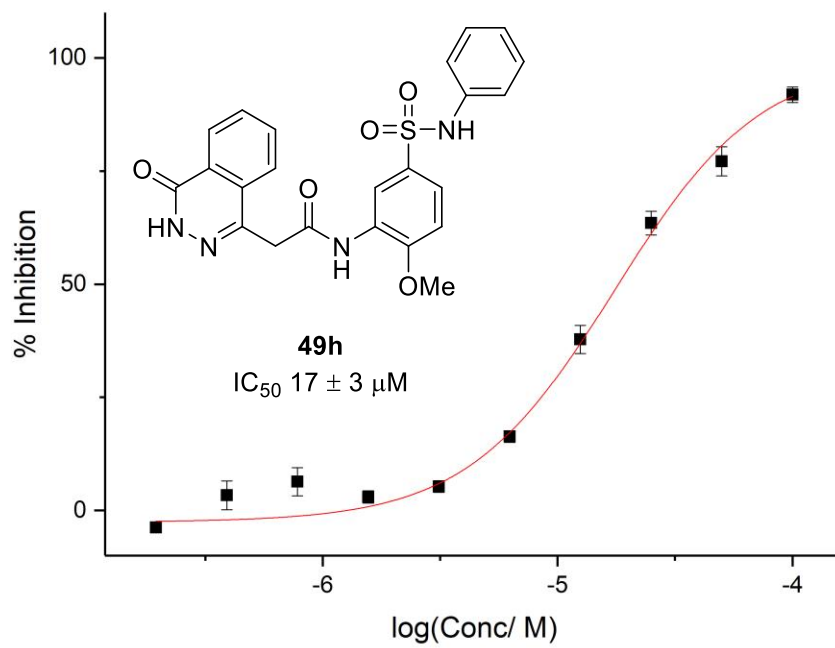


Figure 64: Dose-response curves for **49h** and **49j**, with data points representing an average of replicates ($n = 6$) and error bars indicating standard errors of the mean.

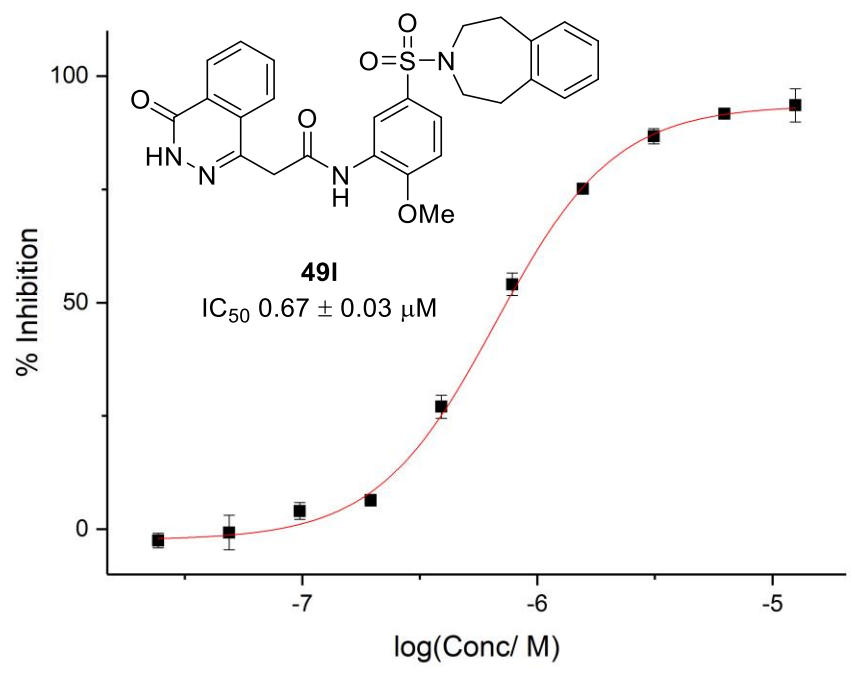
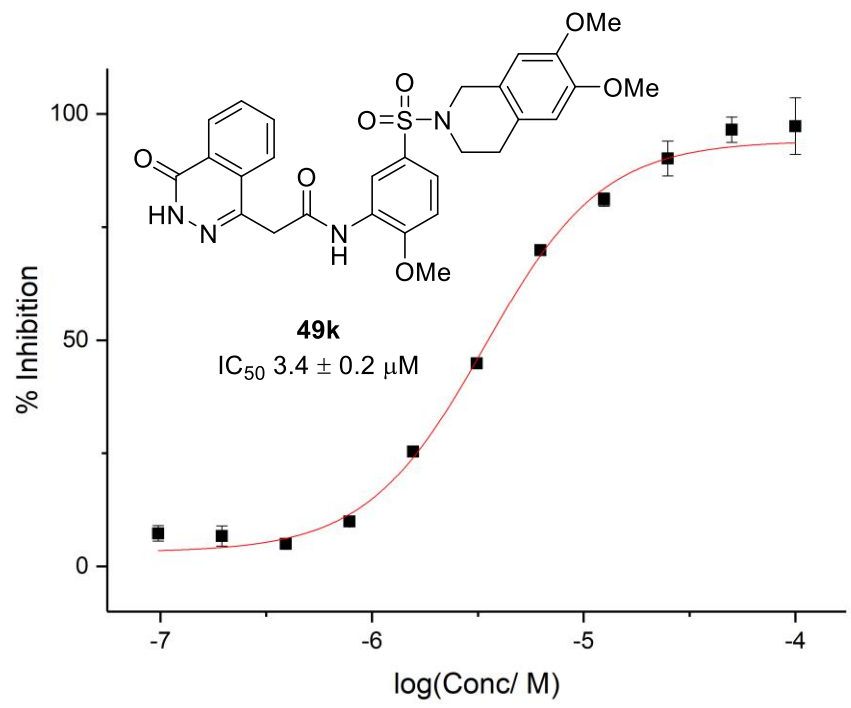


Figure 65: Dose-response curves for **49k-l**, with data points representing an average of replicates ($n = 6$) and error bars indicating standard errors of the mean.

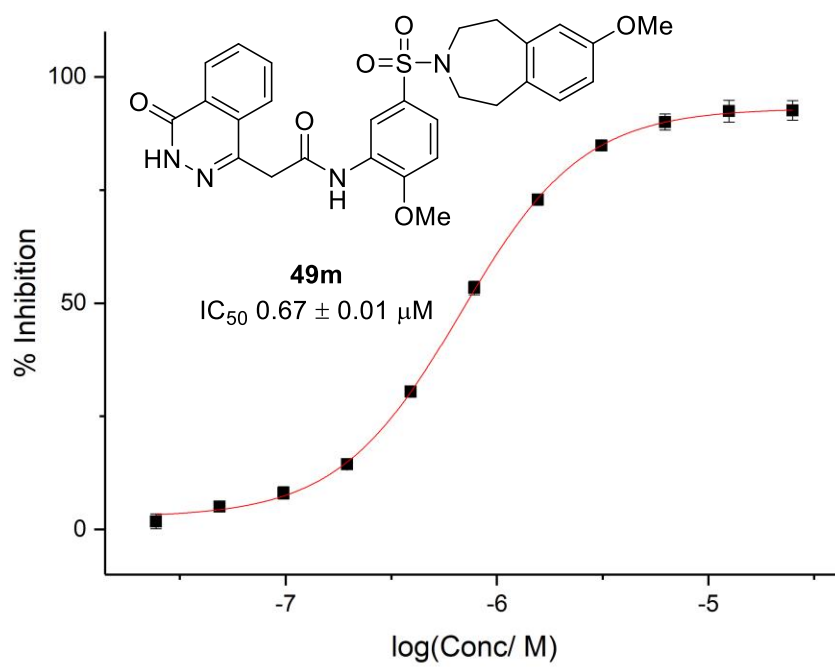


Figure 66: Dose-response curves for **49m**, with data points representing an average of replicates ($n = 6$) and error bars indicating standard errors of the mean.

A.3: Isothermal Titration Calorimetry Traces

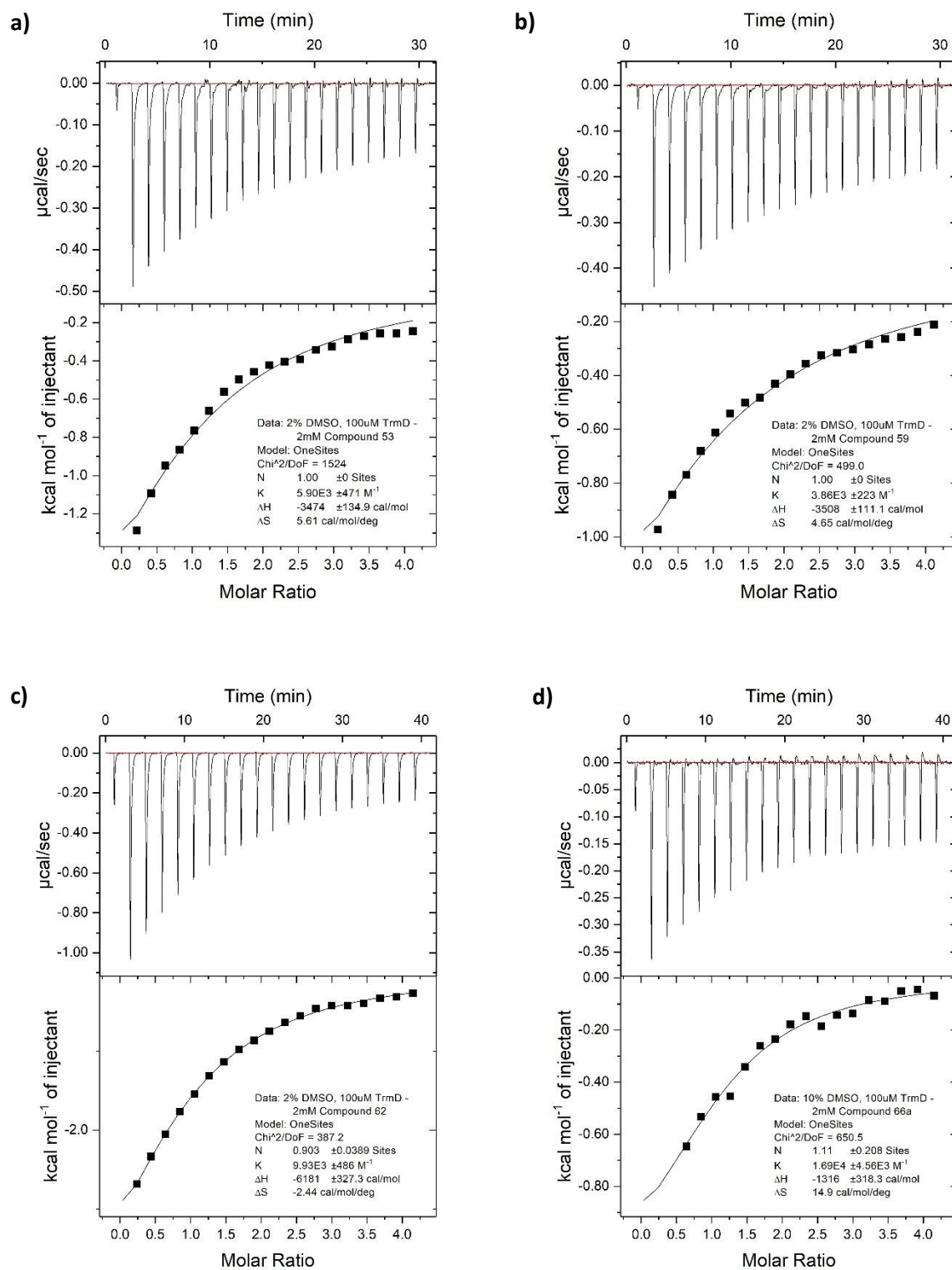


Figure 67: ITC traces with Mab TrmD for a) 53 ($n = 1$), b) 59 ($n = 1$), c) 62 ($n = 2$), and d) 66a ($n = 1$).

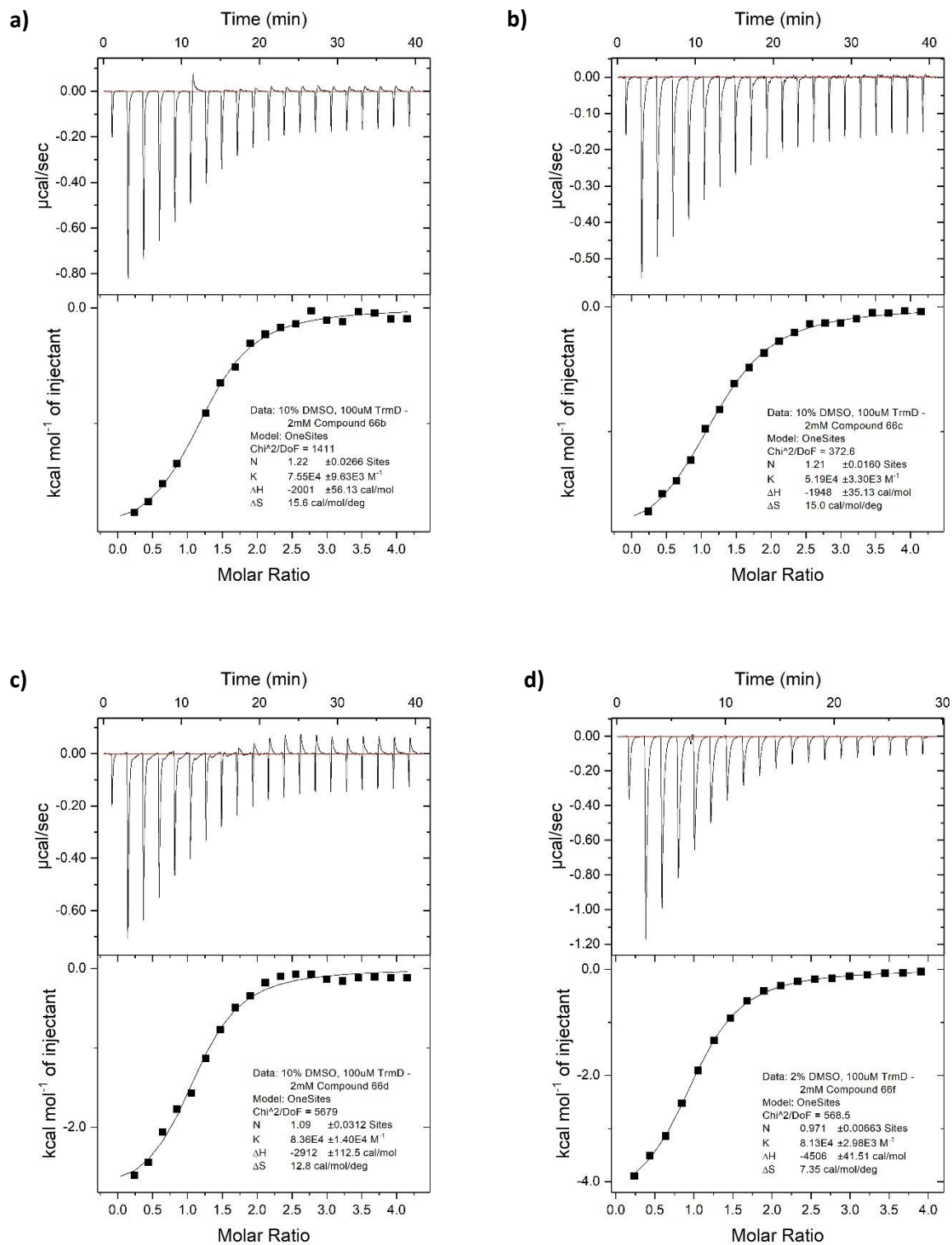


Figure 68: ITC traces with Mab TrmD ($n = 1$) for a) 66b, b) 66c, c) 66d, and d) 66f.

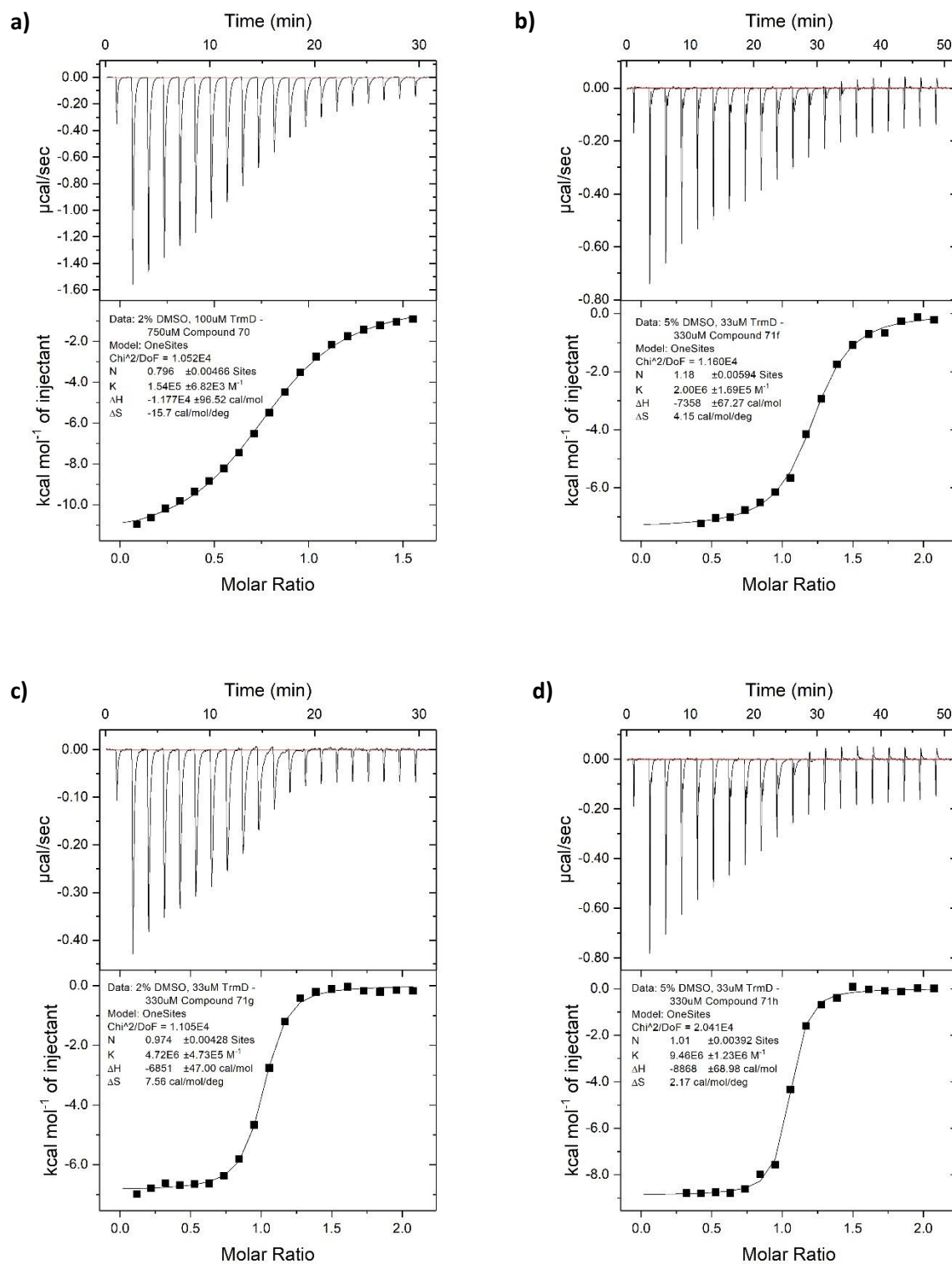


Figure 69: ITC traces with Mab TrmD for a) 70 ($n = 2$), b) 71f ($n = 3$), c) 71g ($n = 3$), and d) 71h ($n = 3$).

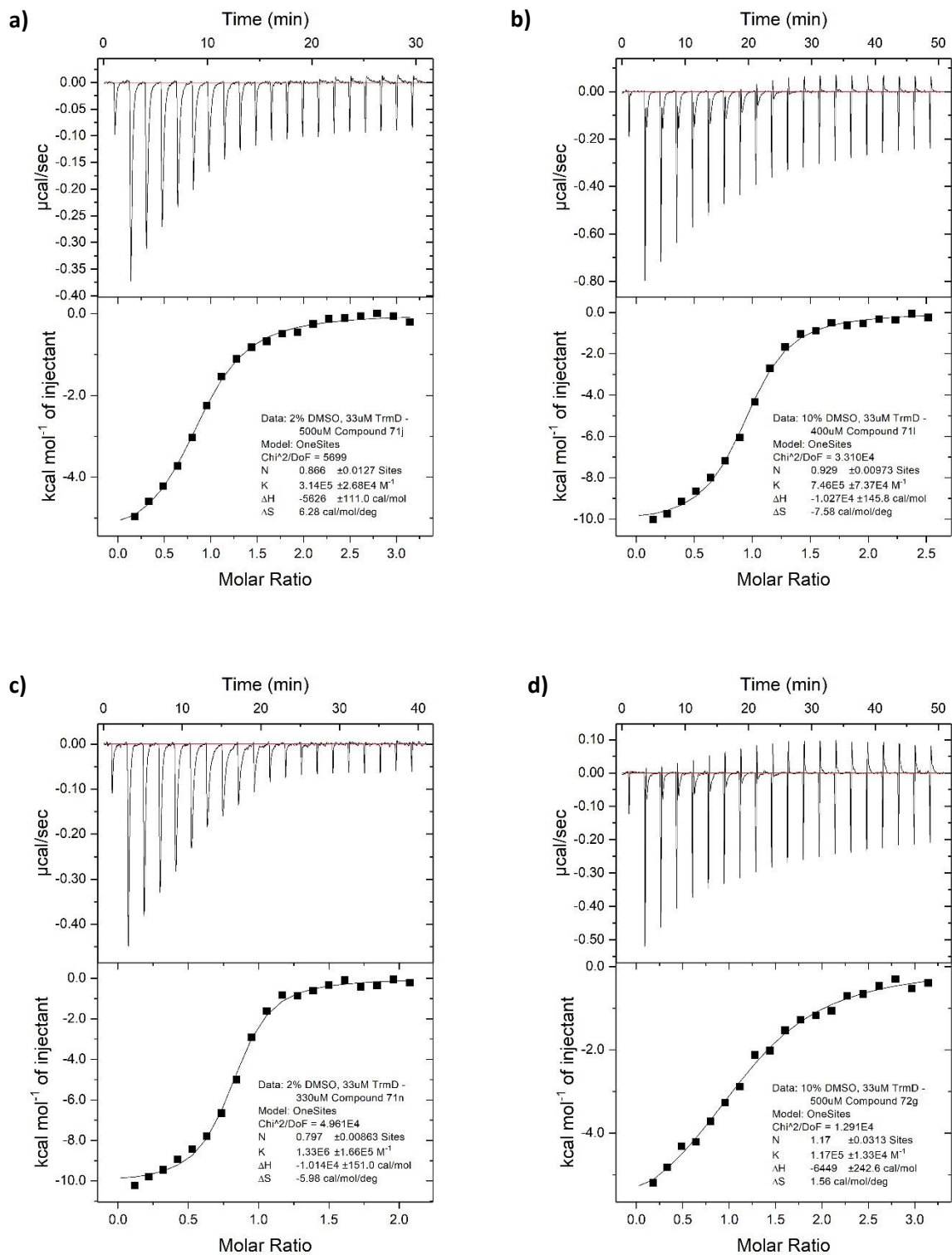


Figure 70: ITC traces with Mab TrmD for a) 71j ($n = 1$), b) 71l ($n = 1$), c) 71n ($n = 2$), and d) 72g ($n = 1$).

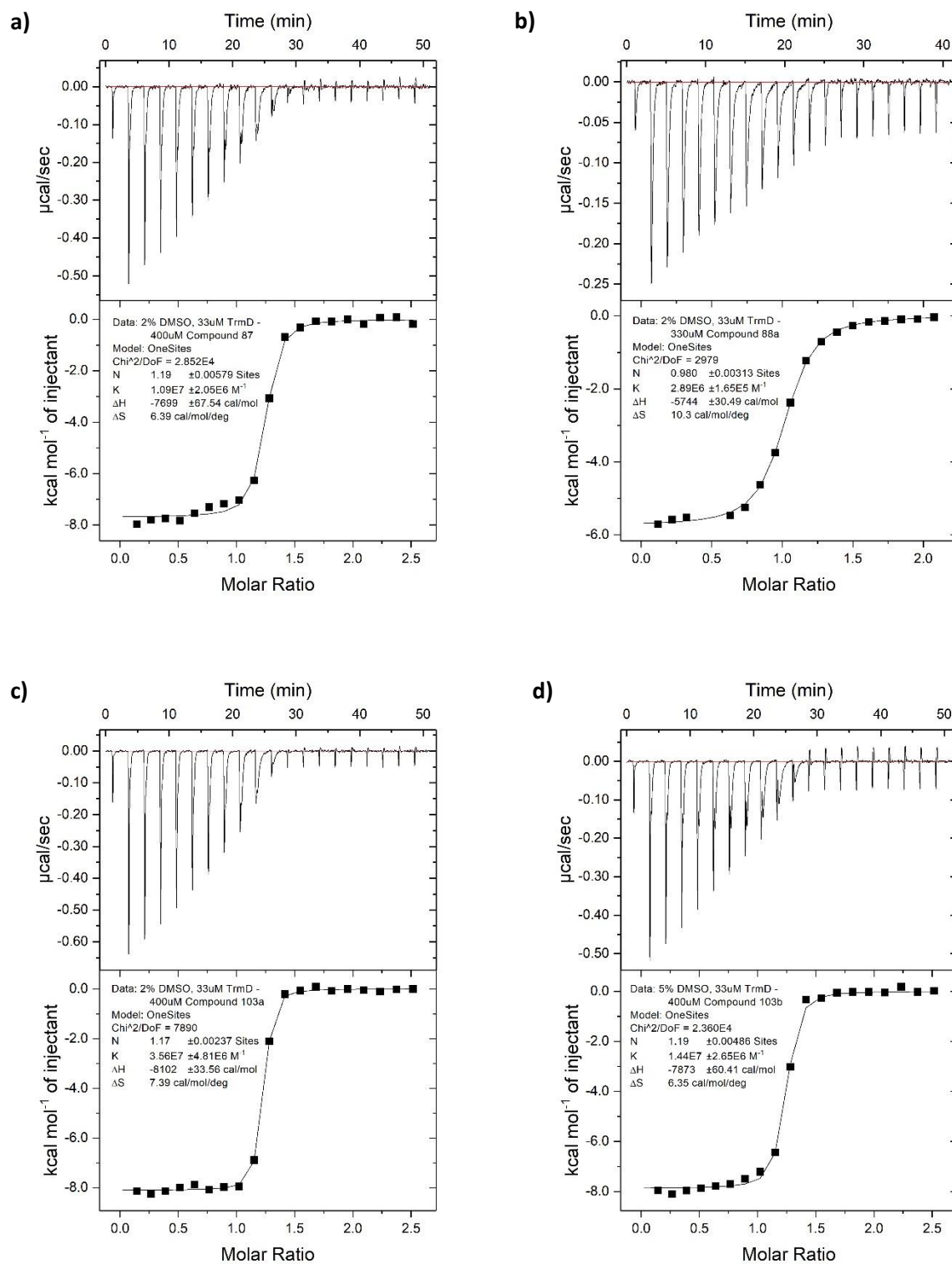


Figure 71: ITC traces with Mab TrmD for a) **87** ($n = 1$), b) **88a** ($n = 2$), c) **103a** ($n = 3$), and d) **103b** ($n = 3$).

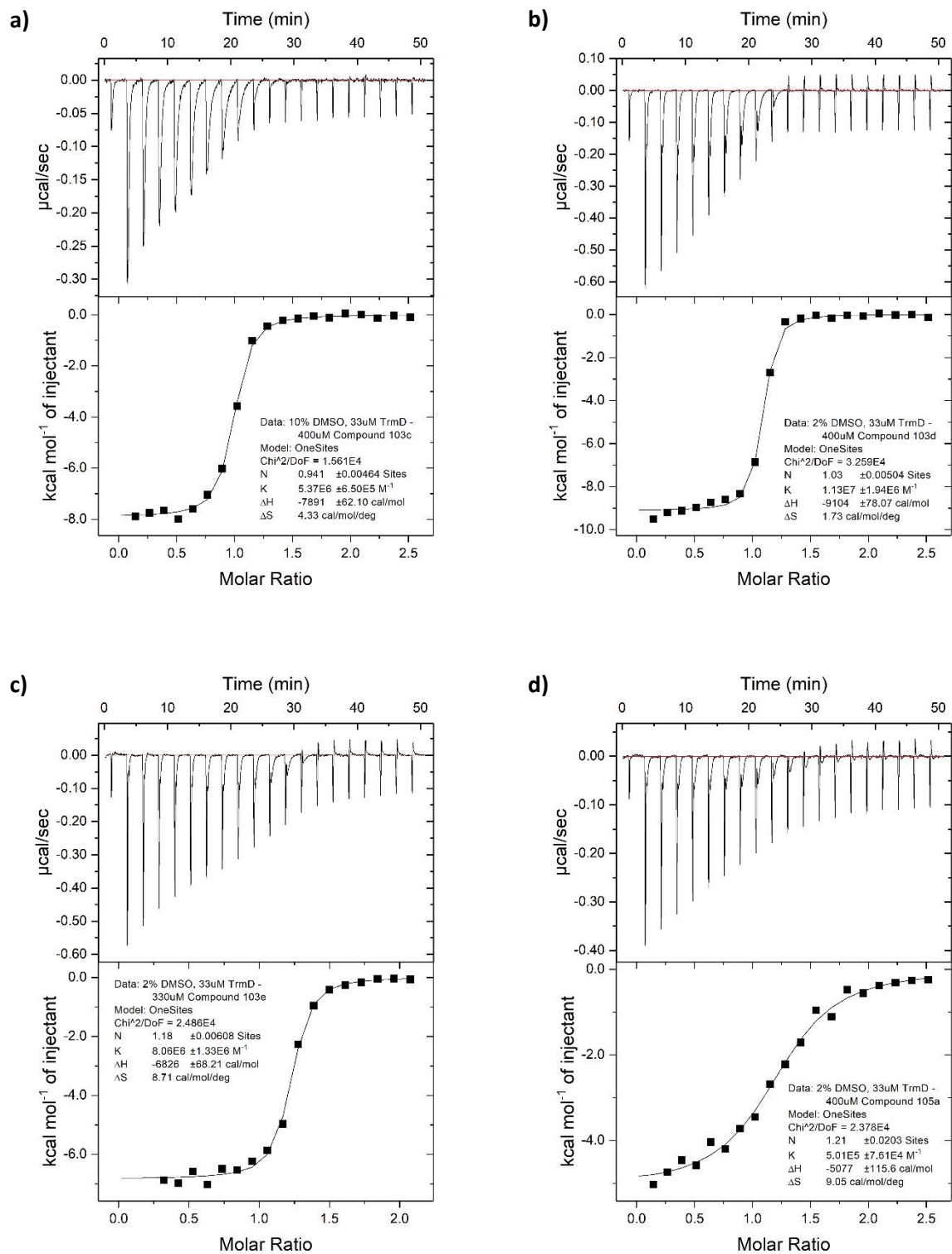


Figure 72: ITC traces with Mab TrmD for a) **103c** ($n = 1$), b) **103d** ($n = 3$), c) **103e** ($n = 3$), and d) **105a** ($n = 1$).

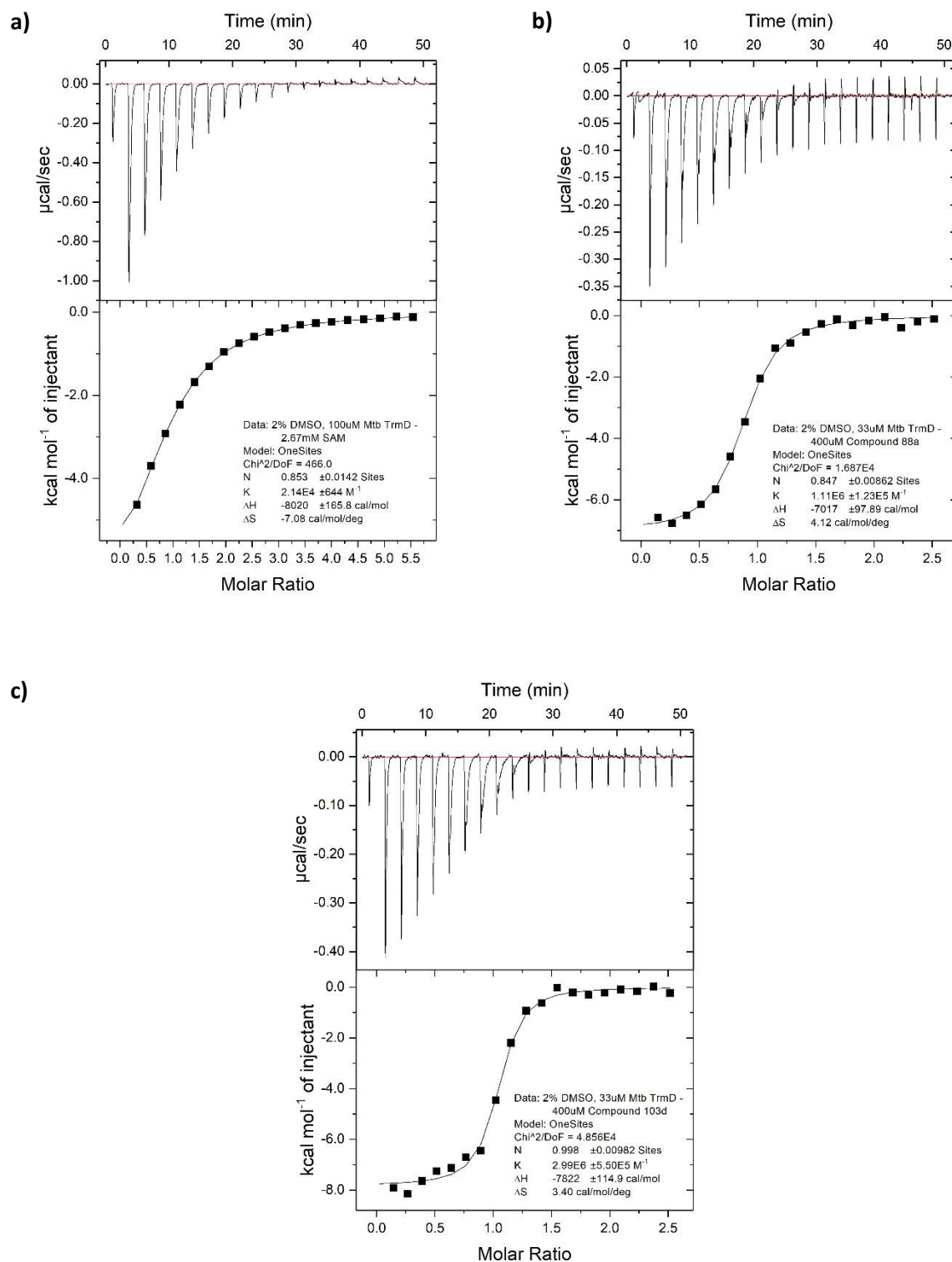


Figure 73: ITC traces with Mtb TrmD ($n = 1$) for a) SAM, b) 88a, and c) 103d.

A.4: X-ray Crystallography Statistics

| Ligand | 46a | 46g | 49a | 49b |
|--------------------------------|--------------------------------------|--------------------------------------|--------------------------------------|--------------------------------------|
| Wavelength (Å) | 0.9763 | 0.9762 | 0.9763 | 0.9763 |
| Resolution range | 85.47 - 1.48 (1.533 - 1.48) | 48.97 - 1.44 (1.491 - 1.44) | 48.67 - 1.552 (1.607 - 1.552) | 63.61 - 1.424 (1.475 - 1.424) |
| Space group | C 1 2 1 | C 1 2 1 | C 1 2 1 | C 1 2 1 |
| Unit cell | 175.258 96.662 124.259 90 102.746 90 | 175.682 96.963 124.736 90 102.706 90 | 174.669 96.388 123.707 90 102.655 90 | 175.313 96.567 124.349 90 102.701 90 |
| Total reflections | 2395184 (366843) | 1836514 (276801) | 1955581 (307235) | 2627362 (403102) |
| Unique reflections | 322623 (33323) | 349365 (35951) | 269929 (28745) | 359386 (37498) |
| Multiplicity | 7.4 (7.5) | 5.2 (5.2) | 7.2 (7.3) | 7.3 (7.4) |
| Completeness (%) | 96.17 (99.80) | 91.55 (86.20) | 93.67 (99.90) | 95.48 (99.97) |
| Mean I/sigma(I) | 8.4 (1.1) | 6.8 (0.9) | 9.5 (1.1) | 9.6 (1.1) |
| Wilson B-factor | 16.95 | 12.88 | 19 | 16.99 |
| R-merge | 0.141 (1.856) | 0.131 (2.001) | 0.118 (1.626) | 0.106 (1.682) |
| R-meas | 0.151 (1.993) | 0.146 (2.248) | 0.127 (1.753) | 0.114 (1.811) |
| R-pim | 0.055 (0.719) | 0.064 (1.004) | 0.047 (0.647) | 0.042 (0.663) |
| CC1/2 | 0.998 (0.442) | 0.995 (0.806) | 0.998 (0.449) | 0.998 (0.465) |
| Reflections used in refinement | 322588 (33319) | 336514 (31625) | 269859 (28716) | 359347 (37494) |
| Reflections used for R-free | 16113 (1588) | 16825 (1562) | 13407 (1433) | 17870 (1773) |
| R-work | 0.1702 (0.2911) | 0.2069 (0.5116) | 0.1694 (0.3211) | 0.1669 (0.3075) |
| R-free | 0.1941 (0.2859) | 0.2256 (0.5191) | 0.1935 (0.3376) | 0.1878 (0.3061) |
| Number of non-hydrogen atoms | 15798 | 15337 | 15613 | 15622 |
| macromolecules | 14032 | 13882 | 14060 | 13888 |
| ligands | 67 | 68 | 61 | 73 |
| solvent | 1699 | 1387 | 1492 | 1661 |
| Protein residues | 1805 | 1807 | 1808 | 1805 |
| RMS(bonds) | 0.016 | 0.016 | 0.015 | 0.016 |
| RMS(angles) | 1.89 | 1.9 | 1.85 | 1.88 |
| Ramachandran favored (%) | 97.54 | 97.82 | 97.65 | 97.76 |
| Ramachandran allowed (%) | 2.35 | 2.18 | 2.23 | 2.24 |
| Ramachandran outliers (%) | 0.11 | 0 | 0.11 | 0 |
| Rotamer outliers (%) | 1.1 | 1.18 | 1.3 | 0.97 |
| Clashscore | 2.82 | 2.42 | 3.34 | 3.06 |
| Average B-factor | 24.35 | 23.58 | 25.42 | 24.16 |
| macromolecules | 23.27 | 22.85 | 24.63 | 23.15 |
| ligands | 28.42 | 23.87 | 21.93 | 24.72 |
| solvent | 33.11 | 30.83 | 32.99 | 32.57 |

| Ligand | 49h | 49j | 49l |
|--------------------------------|--------------------------------------|-------------------------------------|-------------------------------------|
| Wavelength (Å) | 0.9763 | 0.9795 | 0.9762 |
| Resolution range | 48.96 - 1.7 (1.761 - 1.7) | 52.14 - 1.85 (1.916 - 1.85) | 46.98 - 1.59 (1.647 - 1.59) |
| Space group | C 1 2 1 | C 1 2 1 | C 1 2 1 |
| Unit cell | 175.566 96.924 124.753 90 102.858 90 | 175.465 97.132 124.78 90 102.744 90 | 175.71 96.775 124.796 90 102.745 90 |
| Total reflections | 1365156 (210332) | 915578 (105262) | 1357807 (225699) |
| Unique reflections | 190941 (22175) | 172935 (16430) | 244289 (26216) |
| Multiplicity | 7.1 (6.4) | 5.3 (4.3) | 5.5 (5.8) |
| Completeness (%) | 84.65 (99.30) | 99.20 (93.56) | 89.04 (96.36) |
| Mean I/sigma(I) | 10.3 (0.9) | 6.8 (1.2) | 8.0 (1.2) |
| Wilson B-factor | 22.7 | 21.18 | 19.45 |
| R-merge | 0.119 (1.874) | 0.185 (1.187) | 0.123 (1.431) |
| R-meas | 0.129 (2.039) | 0.206 (1.349) | 0.137 (1.572) |
| R-pim | 0.048 (0.791) | 0.088 (0.622) | 0.058 (0.645) |
| CC1/2 | 0.999 (0.412) | 0.991 (0.477) | 0.997 (0.434) |
| Reflections used in refinement | 189157 (22140) | 172623 (16212) | 243039 (26216) |
| Reflections used for R-free | 9479 (1118) | 8588 (794) | 12256 (1309) |
| R-work | 0.1835 (0.3330) | 0.1960 (0.3629) | 0.1781 (0.2936) |
| R-free | 0.2136 (0.3348) | 0.2288 (0.3801) | 0.1996 (0.3070) |
| Number of non-hydrogen atoms | 15135 | 15112 | 15230 |
| macromolecules | 13859 | 13811 | 13838 |
| ligands | 69 | 76 | 78 |
| solvent | 1207 | 1225 | 1314 |
| Protein residues | 1807 | 1804 | 1807 |
| RMS(bonds) | 0.015 | 0.016 | 0.015 |
| RMS(angles) | 1.82 | 1.87 | 1.84 |
| Ramachandran favored (%) | 97.48 | 97.81 | 97.32 |
| Ramachandran allowed (%) | 2.35 | 2.19 | 2.63 |
| Ramachandran outliers (%) | 0.17 | 0 | 0.06 |
| Rotamer outliers (%) | 1.39 | 0.91 | 0.84 |
| Clashscore | 2.71 | 3.19 | 2.72 |
| Average B-factor | 31.45 | 27.05 | 26.52 |
| macromolecules | 31.08 | 26.74 | 26 |
| ligands | 29.47 | 22.54 | 21.9 |
| solvent | 35.75 | 30.81 | 32.18 |

Table 14: Data collection and refinement statistics for X-ray crystal structures of Mtb fumarase in complex with 46a, 46g, 49a-b, 49h, 49j and 49l.

References

1. Fedrizzi, T.; Meehan, C. J.; Grottola, A.; Giacobazzi, E.; Serpini, G. F.; Tagliazucchi, S.; Fabio, A.; Bettua, C.; Bertorelli, R.; De Sanctis, V.; Rumpianesi, F.; Pecorari, M.; Jousson, O.; Tortoli, E.; Segata, N. Genomic characterization of nontuberculous mycobacteria. *Sci. Rep.* **2017**, *7*, 45258.
2. Jankute, M.; Cox, J. A. G.; Harrison, J.; Besra, G.. Assembly of the mycobacterial cell wall. *Annu. Rev. Microbiol.* **2015**, *69*, 405-423.
3. Bansal-Mutalik, R.; Nikaido, H. Mycobacterial outer membrane is a lipid bilayer and the inner membrane is unusually rich in diacyl phosphatidylinositol dimannosides. *Proc. Natl. Acad. Sci. U. S. A.* **2014**, *111*, 4958-4963.
4. Chiaradia, L.; Lefebvre, C.; Parra, J.; Marcoux, J.; Burlet-Schiltz, O.; Etienne, G.; Tropis, M.; Daffé, M. Dissecting the mycobacterial cell envelope and defining the composition of the native mycomembrane. *Sci. Rep.* **2017**, *7*, 12807.
5. da Silva, P. E. A.; Von Groll, A.; Martin, A.; Palomino, J. C. Efflux as a mechanism for drug resistance in *Mycobacterium tuberculosis*. *FEMS Immunol. Med. Microbiol.* **2011**, *63*, 1-9.
6. Pule, C. M.; Sampson, S. L.; Warren, R. M.; Black, P. A.; van Helden, P. D.; Victor, T. C.; Louw, G. E. Efflux pump inhibitors: targeting mycobacterial efflux systems to enhance TB therapy. *J. Antimicrob. Chemother.* **2016**, *71*, 17-26.
7. *Global tuberculosis report 2018*; World Health Organization: Geneva, 2018.
8. Pai, M.; Behr, M. A.; Dowdy, D.; Dheda, K.; Divangahi, M.; Boehme, C. C.; Ginsberg, A.; Swaminathan, S.; Spigelman, M.; Getahun, H.; Menzies, D.; Raviglione, M. Tuberculosis. *Nat. Rev. Dis. Primers* **2016**, *2*, Article Number 16076.
9. Ramakrishnan, L. Revisiting the role of the granuloma in tuberculosis. *Nat. Rev. Immunol.* **2012**, *12*, 352-366.
10. Getahun, H.; Matteelli, A.; Chaisson, R. E.; Raviglione, M. Latent *Mycobacterium tuberculosis* infection. *N. Engl. J. Med.* **2015**, *372*, 2127-2135.
11. Houben, R. M. G. J.; Dodd, P. J. The global burden of latent tuberculosis: A re-estimation using mathematical modelling. *PLoS Med.* **2016**, *13*, e1002152.
12. Tiemersma, E. W.; van der Werf, M. J.; Borgdorff, M. W.; Williams, B. G.; Nagelkerke, N. J. D. Natural history of tuberculosis: Duration and fatality of untreated pulmonary tuberculosis in HIV negative patients: A systematic review. *PLoS One* **2011**, *6*, e17601.
13. *Guidelines for treatment of drug-susceptible tuberculosis and patient care, 2017 update*; World Health Organization: Geneva, 2017.

14. WHO treatment guidelines for drug-resistant tuberculosis, 2016 update; World Health Organization: Geneva, 2016.
15. Libardo, M. D. J.; Boshoff, H. I. M.; Barry, C. E. The present state of the tuberculosis drug development pipeline. *Curr. Opin. Pharmacol.* **2018**, *42*, 81-94.
16. Moore, M.; Frerichs, J. B. An unusual acid-fast infection of the knee with subcutaneous, abscess-like lesions of the gluteal region; report of a case with a study of the organism, *Mycobacterium abscessus*, n. sp. *J. Invest. Dermatol.* **1953**, *20*, 133-169.
17. Kusunoki, S.; Ezaki, T. Proposal of *Mycobacterium peregrinum* sp. nov., nom. rev., and elevation of *Mycobacterium chelonae* subsp. *abscessus* (Kubica et al.) to species status: *Mycobacterium abscessus* comb. nov. *Int. J. Syst. Bacteriol.* **1992**, *42*, 240-245.
18. Macheras, E.; Roux, A.-L.; Bastian, S.; Leão, S. C.; Palaci, M.; Sivadon-Tardy, V.; Gutierrez, C.; Richter, E.; Rüsç-Gerdes, S.; Pfyffer, G.; Bodmer, T.; Cambau, E.; Gaillard, J.-L.; Heym, B. Multilocus sequence analysis and *rpoB* sequencing of *Mycobacterium abscessus* (sensu lato) strains. *J. Clin. Microbiol.* **2011**, *49*, 491-499.
19. Koh, W.-J.; Jeon, K.; Lee, N. Y.; Kim, B.-J.; Kook, Y.-H.; Lee, S.-H.; Park, Y. K.; Kim, C. K.; Shin, S. J.; Huitt, G. A.; Daley, C. L.; Kwon, O. J. Clinical significance of differentiation of *Mycobacterium massiliense* from *Mycobacterium abscessus*. *Am. J. Respir. Crit. Care Med.* **2011**, *183*, 405-410.
20. Ripoll, F.; Pasek, S.; Schenowitz, C.; Dossat, C.; Barbe, V.; Rottman, M.; Macheras, E.; Heym, B.; Herrmann, J.-L.; Daffé, M.; Brosch, R.; Risler, J.-L.; Gaillard, J.-L. Non mycobacterial virulence genes in the genome of the emerging pathogen *Mycobacterium abscessus*. *PLoS One* **2009**, *4*, e5660.
21. Lee, M.-R.; Sheng, W.-H.; Hung, C.-C.; Yu, C.-J.; Lee, L.-N.; Hsueh, P.-R. *Mycobacterium abscessus* complex infections in humans. *Emerging Infect. Dis.* **2015**, *21*, 1638-1646.
22. Griffith, D. E.; Aksamit, T.; Brown-Elliott, B. A.; Catanzaro, A.; Daley, C.; Gordin, F.; Holland, S. M.; Horsburgh, R.; Huitt, G.; Iademarco, M. F.; Iseman, M.; Olivier, K.; Ruoss, S.; Fordham von Reyn, C.; Wallace Jr, R. J.; Winthrop, K. An official ATS/IDSA statement: Diagnosis, treatment, and prevention of nontuberculous mycobacterial diseases. *Am. J. Respir. Crit. Care Med.* **2007**, *175*, 367-416.
23. Han, D.; Lee, K. S.; Koh, W.-J.; Yi, C. A.; Kim, T. S.; Kwon, O. J. Radiographic and CT findings of nontuberculous mycobacterial pulmonary infection caused by *Mycobacterium abscessus*. *Am. J. Roentgenol.* **2003**, *181*, 513-517.
24. Esther Jr, C. R.; Esserman, D. A.; Gilligan, P.; Kerr, A.; Noone, P. G. Chronic *Mycobacterium abscessus* infection and lung function decline in cystic fibrosis. *J. Cystic Fibrosis* **2010**, *9*, 117-123.
25. Qvist, T.; Taylor-Robinson, D.; Waldmann, E.; Olesen, H. V.; Hansen, C. R.; Mathiesen, I. H.; Højby, N.; Katzenstein, T. L.; Smyth, R. L.; Diggle, P. J.; Pressler, T. Comparing the harmful effects of nontuberculous mycobacteria and gram negative bacteria on lung function in patients with cystic fibrosis. *J. Cystic Fibrosis* **2016**, *15*, 380-385.

26. Bryant, J. M.; Grogono, D. M.; Greaves, D.; Foweraker, J.; Roddick, I.; Inns, T.; Reacher, M.; Haworth, C. S.; Curran, M. D.; Harris, S. R.; Peacock, S. J.; Parkhill, J.; Floto, R. A. Whole-genome sequencing to identify transmission of *Mycobacterium abscessus* between patients with cystic fibrosis: A retrospective cohort study. *Lancet* **2013**, *381*, 1551-1560.
27. Bryant, J. M.; Grogono, D. M.; Rodriguez-Rincon, D.; Overall, I.; Brown, K. P.; Moreno, P.; Verma, D.; Hill, E.; Drijkoningen, J.; Gilligan, P.; Esther, C. R.; Noone, P. G.; Giddings, O.; Bell, S. C.; Thomson, R.; Wainwright, C. E.; Coulter, C.; Pandey, S.; Wood, M. E.; Stockwell, R. E.; Ramsay, K. A.; Sherrard, L. J.; Kidd, T. J.; Jabbour, N.; Johnson, G. R.; Knibbs, L. D.; Morawska, L.; Sly, P. D.; Jones, A.; Bilton, D.; Laurenson, I.; Ruddy, M.; Bourke, S.; Bowler, I. C. J. W.; Chapman, S. J.; Clayton, A.; Cullen, M.; Dempsey, O.; Denton, M.; Desai, M.; Drew, R. J.; Edenborough, F.; Evans, J.; Folb, J.; Daniels, T.; Humphrey, H.; Isalska, B.; Jensen-Fangel, S.; Jönsson, B.; Jones, A. M.; Katzenstein, T. L.; Lillebaek, T.; MacGregor, G.; Mayell, S.; Millar, M.; Modha, D.; Nash, E. F.; O'Brien, C.; O'Brien, D.; Ohri, C.; Pao, C. S.; Peckham, D.; Perrin, F.; Perry, A.; Pressler, T.; Prtak, L.; Qvist, T.; Robb, A.; Rodgers, H.; Schaffer, K.; Shafi, N.; van Ingen, J.; Walshaw, M.; Watson, D.; West, N.; Whitehouse, J.; Haworth, C. S.; Harris, S. R.; Ordway, D.; Parkhill, J.; Floto, R. A. Emergence and spread of a human-transmissible multidrug-resistant nontuberculous mycobacterium. *Science* **2016**, *354*, 751-757.
28. Nessar, R.; Cambau, E.; Reyrat, J. M.; Murray, A.; Gicquel, B. *Mycobacterium abscessus*: A new antibiotic nightmare. *J. Antimicrob. Chemother.* **2012**, *67*, 810-818.
29. Floto, R. A.; Olivier, K. N.; Saiman, L.; Daley, C. L.; Herrmann, J.-L.; Nick, J. A.; Noone, P. G.; Bilton, D.; Corris, P.; Gibson, R. L.; Hempstead, S. E.; Koetz, K.; Sadoski, K. A.; Sermet-Gaudelus, I.; Smyth, A. R.; van Ingen, J.; Wallace, R. J.; Winthrop, K. L.; Marshall, B. C.; Haworth, C. S. US Cystic Fibrosis Foundation and European Cystic Fibrosis Society consensus recommendations for the management of non-tuberculous mycobacteria in individuals with cystic fibrosis. *Thorax* **2016**, *71*, i1-i22.
30. Novosad, S. A.; Beekmann, S. E.; Polgreen, P. M.; Mackey, K.; Winthrop, K. L.; M. abscessus Study Team. Treatment of *Mycobacterium abscessus* infection. *Emerging Infect. Dis.* **2016**, *22*, 511-514.
31. Cole, S. T.; Brosch, R.; Parkhill, J.; Garnier, T.; Churcher, C.; Harris, D.; Gordon, S. V.; Eiglmeier, K.; Gas, S.; Barry, C. E.; Tekaia, F.; Badcock, K.; Basham, D.; Brown, D.; Chillingworth, T.; Connor, R.; Davies, R.; Devlin, K.; Feltwell, T.; Gentles, S.; Hamlin, N.; Holroyd, S.; Hornsby, T.; Jagels, K.; Krogh, A.; McLean, J.; Moule, S.; Murphy, L.; Oliver, K.; Osborne, J.; Quail, M. A.; Rajandream, M. -A.; Rogers, J.; Rutter, S.; Seeger, K.; Skelton, J.; Squares, R.; Squares, S.; Sulston, J. E.; Taylor, K.; Whitehead, S.; Barrell, B. G. Deciphering the biology of *Mycobacterium tuberculosis* from the complete genome sequence. *Nature* **1998**, *393*, 537-544.
32. Tian, J.; Bryk, R.; Itoh, M.; Suematsu, M.; Nathan, C. Variant tricarboxylic acid cycle in *Mycobacterium tuberculosis*: Identification of alpha-ketoglutarate decarboxylase. *Proc. Natl. Acad. Sci. U. S. A.* **2005**, *102*, 10670-10675.
33. Watanabe, S.; Zimmermann, M.; Goodwin, M. B.; Sauer, U.; Barry, C. E.; Boshoff, H. I. Fumarate reductase activity maintains an energized membrane in anaerobic *Mycobacterium tuberculosis*. *PLoS Pathog.* **2011**, *7*, e1002287.

34. Eoh, H.; Rhee, K. Y. Multifunctional essentiality of succinate metabolism in adaptation to hypoxia in *Mycobacterium tuberculosis*. *Proc. Natl. Acad. Sci. U. S. A.* **2013**, *110*, 6554-6559.
35. Woods, S. A.; Schwartzbach, S. D.; Guest, J. R. Two biochemically distinct classes of fumarase in *Escherichia coli*. *Biochim. Biophys. Acta, Protein Struct. Mol. Enzymol.* **1988**, *954*, 14-26.
36. Sasseti, C. M.; Boyd, D. H.; Rubin, E. J. Genes required for mycobacterial growth defined by high density mutagenesis. *Mol. Microbiol.* **2003**, *48*, 77-84.
37. Ruecker, N.; Jansen, R.; Trujillo, C.; Puckett, S.; Jayachandran, P.; Piroli, G. G.; Frizzell, N.; Molina, H.; Rhee, K. Y.; Ehrt, S. Fumarase deficiency causes protein and metabolite succination and intoxicates *Mycobacterium tuberculosis*. *Cell Chem. Biol.* **2017**, *24*, 306-315.
38. Mechaly, A. E.; Haouz, A.; Miras, I.; Barilone, N.; Weber, P.; Shepard, W.; Alzari, P. M.; Bellinzoni, M. Conformational changes upon ligand binding in the essential class II fumarase Rv1098c from *Mycobacterium tuberculosis*. *FEBS Lett.* **2012**, *586*, 1606-1611.
39. Weaver, T. M.; Levitt, D. G.; Donnelly, M. I.; Wilkens Stevens, P. P.; Banaszak, L. J. The multisubunit active site of fumarase C from *Escherichia coli*. *Nat. Struct. Biol.* **1995**, *2*, 654-662.
40. Weaver, T.; Banaszak, L. Crystallographic studies of the catalytic and a second site in fumarase C from *Escherichia coli*. *Biochemistry* **1996**, *35*, 13955-13965.
41. Kasbekar, M.; Fischer, G.; Mott, B. T.; Yasgar, A.; Hyvönen, M.; Boshoff, H. I. M.; Abell, C.; Barry, C. E.; Thomas, C. J. Selective small molecule inhibitor of the *Mycobacterium tuberculosis* fumarate hydratase reveals an allosteric regulatory site. *Proc. Natl. Acad. Sci. U. S. A.* **2016**, *113*, 7503-7508.
42. Fibriansah, G.; Veetil, V. P.; Poelarends, G. J.; Thunnissen, A.-M. W. H. Structural basis for the catalytic mechanism of aspartate ammonia lyase. *Biochemistry* **2011**, *50*, 6053-6062.
43. Takeuchi, T.; Schumacker, P. T.; Kozmin, S. A. Identification of fumarate hydratase inhibitors with nutrient-dependent cytotoxicity. *J. Am. Chem. Soc.* **2015**, *137*, 564-567.
44. de Pádua, R. A. P.; Nonato, M. C. Cloning, expression, purification, crystallization and preliminary X-ray diffraction analysis of recombinant human fumarase. *Acta Crystallogr., Sect. F: Struct. Biol. Commun.* **2014**, *70*, 120-122.
45. Anantharaman, V.; Koonin, E. V.; Aravind, L. SPOUT: A class of methyltransferases that includes spoU and trmD RNA methylase superfamilies, and novel superfamilies of predicted prokaryotic RNA methylases. *J. Mol. Microbiol. Biotechnol.* **2002**, *4*, 71-75.
46. Holmes, W. M.; Andraos-Selim, C.; Roberts, I.; Wahab, S. Z. Structural requirements for tRNA methylation. Action of *Escherichia coli* tRNA(guanosine-1)methyltransferase on tRNA(1Leu) structural variants. *J. Biol. Chem.* **1992**, *267*, 13440-13445.
47. Björk, G. R.; Wikström, P. M.; Byström, A. S. Prevention of translational frameshifting by the modified nucleoside 1-methylguanosine. *Science* **1989**, *244*, 986-989.

48. Gamper, H. B.; Masuda, I.; Frenkel-Morgenstern, M.; Hou, Y.-M. Maintenance of protein synthesis reading frame by EF-P and m1G37-tRNA. *Nat. Commun.* **2015**, *6*, 7226.
49. Maehigashi, T.; Dunkle, J. A.; Miles, S. J.; Dunham, C. M. Structural insights into +1 frameshifting promoted by expanded or modification-deficient anticodon stem loops. *Proc. Natl. Acad. Sci. U. S. A.* **2014**, *111*, 12740-12745.
50. Thomas, S. E.; Whitehouse, A. J.; Brown, K.; Belardinelli, J. M.; Lahiri, R.; Libardo, M. D. J.; Gupta, P.; Malhotra, S.; Boshoff, H. I. M.; Jackson, M.; Abell, C.; Coyne, A. G.; Blundell, T. L.; Floto, R. A.; Mendes, V. Fragment-based discovery of a new class of inhibitors targeting mycobacterial tRNA modification. **2019**, doi: <https://doi.org/10.1101/564013>. bioRxiv. <https://www.biorxiv.org/content/10.1101/564013v2> (accessed May 29, 2019).
51. Tkaczuk, K. L.; Dunin-Horkawicz, S.; Purta, E.; Bujnicki, J. M. Structural and evolutionary bioinformatics of the SPOUT superfamily of methyltransferases. *BMC Bioinf.* **2007**, *8*, 73.
52. Ahn, H. J.; Kim, H.-W.; Yoon, H.-J.; Lee, B. I.; Suh, S. W.; Yang, J. K. Crystal structure of tRNA(m1G37)methyltransferase: Insights into tRNA recognition. *EMBO J.* **2003**, *22*, 2593-2603.
53. Elkins, P. A.; Watts, J. M.; Zalacain, M.; van Thiel, A.; Vitazka, P. R.; Redlak, M.; Andraos-Selim, C.; Rastinejad, F.; Holmes, W. M. Insights into catalysis by a knotted TrmD tRNA methyltransferase. *J. Mol. Biol.* **2003**, *333*, 931-949.
54. Baugh, L.; Phan, I.; Begley, D. W.; Clifton, M. C.; Armour, B.; Dranow, D. M.; Taylor, B. M.; Muruthi, M. M.; Abendroth, J.; Fairman, J. W.; Fox III, D.; Dieterich, S. H.; Staker, B. L.; Gardberg, A. S.; Choi, R.; Hewitt, S. N.; Napuli, A. J.; Myers, J.; Barrett, L. K.; Zhang, Y.; Ferrell, M.; Mundt, E.; Thompkins, K.; Tran, N.; Lyons-Abbott, S.; Abramov, A.; Sekar, A.; Serbzhinskiy, D.; Lorimer, D.; Buchko, G. W.; Stacy, R.; Stewart, L. J.; Edwards, T. E.; Van Voorhis, W. C.; Myler, P. J. Increasing the structural coverage of tuberculosis drug targets. *Tuberculosis (Oxford, U. K.)* **2015**, *95*, 142-148.
55. Christian, T.; Sakaguchi, R.; Perlinska, A. P.; Lahoud, G.; Ito, T.; Taylor, E. A.; Yokoyama, S.; Sulkowska, J. I.; Hou, Y.-M. Methyl transfer by substrate signaling from a knotted protein fold. *Nat. Struct. Mol. Biol.* **2016**, *23*, 941-948.
56. Christian, T.; Lahoud, G.; Liu, C.; Hou, Y.-M. Control of catalytic cycle by a pair of analogous tRNA modification enzymes. *J. Mol. Biol.* **2010**, *400*, 204-217.
57. Ito, T.; Masuda, I.; Yoshida, K.-i.; Goto-Ito, S.; Sekine, S.-i.; Suh, S. W.; Hou, Y.-M.; Yokoyama, S. Structural basis for methyl-donor-dependent and sequence-specific binding to tRNA substrates by knotted methyltransferase TrmD. *Proc. Natl. Acad. Sci. U. S. A.* **2015**, *112*, E4197-E4205.
58. Sakaguchi, R.; Lahoud, G.; Christian, T.; Gamper, H.; Hou, Y.-M. A divalent metal ion-dependent N1 transfer to G37-tRNA. *Chem. Biol. (Oxford, U. K.)* **2014**, *21*, 1351-1360.
59. Björk, G. R.; Jacobsson, K.; Nilsson, K.; Johansson, M. J. O.; Byström, A. S.; Persson, O. P. A primordial tRNA modification required for the evolution of life? *EMBO J.* **2001**, *20*, 231-239.

60. Goto-Ito, S.; Ito, T.; Kuratani, M.; Bessho, Y.; Yokoyama, S. Tertiary structure checkpoint at anticodon loop modification in tRNA functional maturation. *Nat. Struct. Mol. Biol.* **2009**, *16*, 1109-1115.
61. Christian, T.; Gamper, H.; Hou, Y.-M. Conservation of structure and mechanism by Trm5 enzymes. *RNA* **2013**, *19*, 1192-1199.
62. Lahoud, G.; Goto-Ito, S.; Yoshida, K.-i.; Ito, T.; Yokoyama, S.; Hou, Y.-M. Differentiating analogous tRNA methyltransferases by fragments of the methyl donor. *RNA* **2011**, *17*, 1236-1246.
63. Hill, P. J.; Abibi, A.; Albert, R.; Andrews, B.; Gagnon, M. M.; Gao, N.; Grebe, T.; Hajec, L. I.; Huang, J.; Livchak, S.; Lahiri, S. D.; McKinney, D. C.; Thresher, J.; Wang, H.; Olivier, N.; Buurman, E. T. Selective inhibitors of bacterial t-RNA-(N(1)G37) methyltransferase (TrmD) that demonstrate novel ordering of the lid domain. *J. Med. Chem.* **2013**, *56*, 7278-7288.
64. Bohacek, R. S.; McMartin, C.; Guida, W. C. The art and practice of structure-based drug design: A molecular modeling perspective. *Med. Res. Rev.* **1996**, *16*, 3-50.
65. Shuker, S. B.; Hajduk, P. J.; Meadows, R. P.; Fesik, S. W. Discovering high-affinity ligands for proteins: SAR by NMR. *Science* **1996**, *274*, 1531-1534.
66. Erlanson, D. A.; Fesik, S. W.; Hubbard, R. E.; Jahnke, W.; Jhoti, H. Twenty years on: The impact of fragments on drug discovery. *Nat. Rev. Drug Discovery* **2016**, *15*, 605-619.
67. Bollag, G.; Tsai, J.; Zhang, J.; Zhang, C.; Ibrahim, P.; Nolop, K.; Hirth, P. Vemurafenib: The first drug approved for BRAF-mutant cancer. *Nat. Rev. Drug Discovery* **2012**, *11*, 873-886.
68. Mullard, A. Pioneering apoptosis-targeted cancer drug poised for FDA approval. *Nat. Rev. Drug Discovery* **2016**, *15*, 147-149.
69. Peplow, M. Astex shapes CDK4/6 inhibitor for approval. *Nat. Biotechnol.* **2017**, *35*, 395-396.
70. O'Leary, B.; Finn, R. S.; Turner, N. C. Treating cancer with selective CDK4/6 inhibitors. *Nat. Rev. Clin. Oncol.* **2016**, *13*, 417-430.
71. Souers, A. J.; Levenson, J. D.; Boghaert, E. R.; Ackler, S. L.; Catron, N. D.; Chen, J.; Dayton, B. D.; Ding, H.; Enschede, S. H.; Fairbrother, W. J.; Huang, D. C. S.; Hymowitz, S. G.; Jin, S.; Khaw, S. L.; Kovar, P. J.; Lam, L. T.; Lee, J.; Maecker, H. L.; Marsh, K. C.; Mason, K. D.; Mitten, M. J.; Nimmer, P. M.; Oleksijew, A.; Park, C. H.; Park, C.-M.; Phillips, D. C.; Roberts, A. W.; Sampath, D.; Seymour, J. F.; Smith, M. L.; Sullivan, G. M.; Tahir, S. K.; Tse, C.; Wendt, M. D.; Xiao, Y.; Xue, J. C.; Zhang, H.; Humerickhouse, R. A.; Rosenberg, S. H.; Elmore, S. W. ABT-199, a potent and selective BCL-2 inhibitor, achieves antitumor activity while sparing platelets. *Nat. Med. (N. Y., NY, U. S.)* **2013**, *19*, 202-208.
72. Scott, D. E.; Coyne, A. G.; Hudson, S. A.; Abell, C. Fragment-based approaches in drug discovery and chemical biology. *Biochemistry* **2012**, *51*, 4990-5003.

73. Jhoti, H.; Williams, G.; Rees, D. C.; Murray, C. W. The 'rule of three' for fragment-based drug discovery: Where are we now? *Nat. Rev. Drug Discovery* **2013**, *12*, 644-645.
74. Lipinski, C. A.; Lombardo, F.; Dominy, B. W.; Feeney, P. J. Experimental and computational approaches to estimate solubility and permeability in drug discovery and development settings. *Adv. Drug Delivery Rev.* **1997**, *23*, 3-25.
75. Congreve, M.; Carr, R.; Murray, C.; Jhoti, H. A 'rule of three' for fragment-based lead discovery? *Drug Discovery Today* **2003**, *8*, 876-877.
76. Ruddigkeit, L.; van Deursen, R.; Blum, L. C.; Reymond, J.-L. Enumeration of 166 billion organic small molecules in the chemical universe database GDB-17. *J. Chem. Inf. Model.* **2012**, *52*, 2864-2875.
77. Hall, R. J.; Mortenson, P. N.; Murray, C. W. Efficient exploration of chemical space by fragment-based screening. *Prog. Biophys. Mol. Biol.* **2014**, *116*, 82-91.
78. Keserű, G. M.; Erlanson, D. A.; Ferenczy, G. G.; Hann, M. M.; Murray, C. W.; Pickett, S. D. Design principles for fragment libraries: Maximizing the value of learnings from pharma fragment-based drug discovery (FBDD) programs for use in academia. *J. Med. Chem.* **2016**, *59*, 8189-8206.
79. Hann, M. M.; Leach, A. R.; Harper, G. Molecular complexity and its impact on the probability of finding leads for drug discovery. *J. Chem. Inf. Model.* **2001**, *41*, 856-864.
80. Murray, C. W.; Verdonk, M. L. The consequences of translational and rotational entropy lost by small molecules on binding to proteins. *J. Comput.-Aided Mol. Des.* **2002**, *16*, 741-753.
81. Leeson, P. D.; St-Gallay, S. A. The influence of the 'organizational factor' on compound quality in drug discovery. *Nat. Rev. Drug Discovery* **2011**, *10*, 749-765.
82. Renaud, J.-P.; Chung, C.-w.; Danielson, U. H.; Egner, U.; Hennig, M.; Hubbard, R. E.; Nar, H. Biophysics in drug discovery: Impact, challenges and opportunities. *Nat. Rev. Drug Discovery* **2016**, *15*, 679-698.
83. Schiebel, J.; Radeva, N.; Krimmer, S. G.; Wang, X.; Stieler, M.; Ehrmann, F. R.; Fu, K.; Metz, A.; Huschmann, F. U.; Weiss, M. S.; Mueller, U.; Heine, A.; Klebe, G. Six biophysical screening methods miss a large proportion of crystallographically discovered fragment hits: A case study. *ACS Chem. Biol.* **2016**, *11*, 1693-1701.
84. Mashalidis, E. H.; Śledź, P.; Lang, S.; Abell, C. A three-stage biophysical screening cascade for fragment-based drug discovery. *Nat. Protoc.* **2013**, *8*, 2309-2324.
85. Silvestre, H. L.; Blundell, T. L.; Abell, C.; Ciulli, A. Integrated biophysical approach to fragment screening and validation for fragment-based lead discovery. *Proc. Natl. Acad. Sci. U. S. A.* **2013**, *110*, 12984-12989.
86. Chilton, M.; Clennell, B.; Edfeldt, F.; Geschwindner, S. Hot-spotting with thermal scanning: A ligand- and structure- independent assessment of target ligandability. *J. Med. Chem.* **2017**, *60*, 4923-4931.

87. Niesen, F. H.; Berglund, H.; Vedadi, M. The use of differential scanning fluorimetry to detect ligand interactions that promote protein stability. *Nat. Protoc.* **2007**, *2*, 2212-2221.
88. Scott, D. E.; Spry, C.; Abell, C. *Fragment-based drug discovery lessons and outlook*, Ch. 7.; Wiley-VCH, 2016; Vol. 34, Methods and principles in medicinal chemistry, pp 139-170.
89. Dai, R.; Wilson, D. J.; Geders, T. W.; Aldrich, C. C.; Finzel, B. C. Inhibition of Mycobacterium tuberculosis transaminase BioA by aryl hydrazines and hydrazides. *ChemBioChem* **2014**, *15*, 575-586.
90. Seetoh, W.-G.; Abell, C. Disrupting the constitutive, homodimeric protein-protein interface in CK2 β using a biophysical fragment-based approach. *J. Am. Chem. Soc.* **2016**, *138*, 14303-14311.
91. Ślędź, P.; Abell, C.; Ciulli, A. *NMR of biomolecules: Towards mechanistic systems biology*, Ch. 15.; Wiley-VCH, 2012; pp 265-280.
92. Mayer, M.; Meyer, B. Characterization of ligand binding by saturation transfer difference NMR spectroscopy. *Angew. Chem., Int. Ed.* **1999**, *38*, 1784-1788.
93. Dalvit, C.; Pevarello, P.; Tatò, M.; Veronesi, M.; Vulpetti, A.; Sundström, M. Identification of compounds with binding affinity to proteins via magnetization transfer from bulk water. *J. Biomol. NMR* **2000**, *18*, 65-68.
94. Hajduk, P. J.; Olejniczak, E. T.; Fesik, S. W. One-dimensional relaxation- and diffusion-edited NMR methods for screening compounds that bind to macromolecules. *J. Am. Chem. Soc.* **1997**, *119*, 12257-12261.
95. Davies, T. G.; Wixted, W. E.; Coyle, J. E.; Griffiths-Jones, C.; Hearn, K.; McMenamin, R.; Norton, D.; Rich, S. J.; Richardson, C.; Saxty, G.; Willems, H. M. G.; Woolford, A. J.-A.; Cottom, J. E.; Kou, J.-P.; Yonchuk, J. G.; Feldser, H. G.; Sanchez, Y.; Foley, J. P.; Bolognese, B. J.; Logan, G.; Podolin, P. L.; Yan, H.; Callahan, J. F.; Heightman, T. D.; Kerns, J. K. Monoacidic inhibitors of the Kelch-like ECH-associated protein 1: Nuclear factor erythroid 2-related factor 2 (KEAP1:NRF2) protein-protein interaction with high cell potency identified by fragment-based discovery. *J. Med. Chem.* **2016**, *59*, 3991-4006.
96. Holdgate, G. A.; Ward, W. H. J. Measurements of binding thermodynamics in drug discovery. *Drug Discovery Today* **2005**, *10*, 1543-1550.
97. Ladbury, J. E.; Klebe, G.; Freire, E. Adding calorimetric data to decision making in lead discovery: A hot tip. *Nat. Rev. Drug Discovery* **2010**, *9*, 23-27.
98. Geschwindner, S.; Ulander, J.; Johansson, P. Ligand binding thermodynamics in drug discovery: Still a hot tip? *J. Med. Chem.* **2015**, *58*, 6321-6335.

99. Williams, G.; Ferenczy, G. G.; Ulander, J.; Keserű, G. M. Binding thermodynamics discriminates fragments from druglike compounds: A thermodynamic description of fragment-based drug discovery. *Drug Discovery Today* **2017**, *22*, 681-689.
100. Trapero, A.; Pacitto, A.; Singh, V.; Sabbah, M.; Coyne, A. G.; Mizrahi, V.; Blundell, T. L.; Ascher, D. B.; Abell, C. Fragment-based approach to targeting inosine-5'-monophosphate dehydrogenase (IMPDH) from *Mycobacterium tuberculosis*. *J. Med. Chem.* **2018**, *61*, 2806-2822.
101. Jencks, W. P. On the attribution and additivity of binding energies. *Proc. Natl. Acad. Sci. U. S. A.* **1981**, *78*, 4046-4050.
102. Hung, A. W.; Silvestre, H. L.; Wen, S.; Ciulli, A.; Blundell, T. L.; Abell, C. Application of fragment growing and fragment linking to the discovery of inhibitors of *Mycobacterium tuberculosis* pantothenate synthetase. *Angew. Chem., Int. Ed.* **2009**, *48*, 8452-8456.
103. Woolford, A. J.-A.; Pero, J. E.; Aravapalli, S.; Berdini, V.; Coyle, J. E.; Day, P. J.; Dodson, A. M.; Grondin, P.; Holding, F. P.; Lee, L. Y. W.; Li, P.; Manas, E. S.; Marino, J.; Martin, A. C. L.; McClelland, B. W.; McMenamin, R. L.; Murray, C. W.; Neipp, C. E.; Page, L. W.; Patel, V. K.; Potvain, F.; Rich, S.; Rivero, R. A.; Smith, K.; Somers, D. O.; Trottet, L.; Velagaleti, R.; Williams, G.; Xie, R. Exploitation of a novel binding pocket in human lipoprotein-associated phospholipase A2 (Lp-PLA2) discovered through X-ray fragment screening. *J. Med. Chem.* **2016**, *59*, 5356-5367.
104. Hudson, S. A.; McLean, K. J.; Surade, S.; Yang, Y.-Q.; Leys, D.; Ciulli, A.; Munro, A. W.; Abell, C. Application of fragment screening and merging to the discovery of inhibitors of the *Mycobacterium tuberculosis* cytochrome P450 CYP121. *Angew. Chem., Int. Ed.* **2012**, *51*, 9311-9316.
105. Hudson, S. A.; Surade, S.; Coyne, A. G.; McLean, K. J.; Leys, D.; Munro, A. W.; Abell, C. Overcoming the limitations of fragment merging: Rescuing a strained merged fragment series targeting *Mycobacterium tuberculosis* CYP121. *ChemMedChem* **2013**, *8*, 1451-1456.
106. Drwal, M. N.; Bret, G.; Perez, C.; Jacquemard, C.; Desaphy, J.; Kellenberger, E. Structural insights on fragment binding mode conservation. *J. Med. Chem.* **2018**, *61*, 5963-5973.
107. Mortenson, P. N.; Erlanson, D. A.; de Esch, I. J. P.; Jahnke, W.; Johnson, C. N. Fragment-to-lead medicinal chemistry publications in 2017. *J. Med. Chem.* **2019**, *62*, 3857-3872.
108. Hopkins, A.; Keseru, G.; Leeson, P.; Rees, D.; Reynolds, C. The role of ligand efficiency metrics in drug discovery. *Nat. Rev. Drug Discov.* **2014**, *13*, 105-121.
109. Hopkins, A. L.; Groom, C. R.; Alex, A. Ligand efficiency: A useful metric for lead selection. *Drug Discovery Today* **2004**, *9*, 430-431.
110. Verdonk, M. L.; Rees, D. C. Group efficiency: A guideline for hits-to-leads chemistry. *ChemMedChem* **2008**, *3*, 1179-1180.

111. Hung, A. W.; Silvestre, H. L.; Wen, S.; George, G. P. C.; Boland, J.; Blundell, T. L.; Ciulli, A.; Abell, C. Optimization of inhibitors of Mycobacterium tuberculosis pantothenate synthetase based on group efficiency analysis. *ChemMedChem* **2016**, *11*, 38-42.
112. Kavanagh, M. E.; Coyne, A. G.; McLean, K. J.; James, G. G.; Levy, C. W.; Marino, L. B.; de Carvalho, L. P. S.; Chan, D. S. H.; Hudson, S. A.; Surade, S.; Leys, D.; Munro, A. W.; Abell, C. Fragment-based approaches to the development of Mycobacterium tuberculosis CYP121 inhibitors. *J. Med. Chem.* **2016**, *59*, 3272-3302.
113. Chen, H.; Zhou, X.; Wang, A.; Zheng, Y.; Gao, Y.; Zhou, J. Evolutions in fragment-based drug design: The deconstruction–reconstruction approach. *Drug Discovery Today* **2015**, *20*, 105-113.
114. Hoegenauer, K.; Soldermann, N.; Stauffer, F.; Furet, P.; Graveleau, N.; Smith, A. B.; Hebach, C.; Hollingworth, G. J.; Lewis, I.; Gutmann, S.; Rummel, G.; Knapp, M.; Wolf, R. M.; Blanz, J.; Feifel, R.; Burkhart, C.; Zécri, F. Discovery and pharmacological characterization of novel quinazoline-based PI3K delta-selective inhibitors. *ACS Med. Chem. Lett.* **2016**, *7*, 762-767.
115. Babaoglu, K.; Shoichet, B. K. Deconstructing fragment-based inhibitor discovery. *Nat. Chem. Biol.* **2006**, *2*, 720-723.
116. Wissmann, H.; Kleiner, H. New peptide synthesis. *Angew. Chem., Int. Ed. Engl.* **1980**, *19*, 133-134.
117. Kasbekar, M. *Thesis*; Department of Chemistry, University of Cambridge, 2016.
118. McCoy, A. J.; Grosse-Kunstleve, R. W.; Adams, P. D.; Winn, M. D.; Storoni, L. C.; Read, R. J. Phaser crystallographic software. *J. Appl. Crystallogr.* **2007**, *40*, 658-674.
119. Winn, M. D.; Ballard, C. C.; Cowtan, K. D.; Dodson, E. J.; Emsley, P.; Evans, P. R.; Keegan, R. M.; Krissinel, E. B.; Leslie, A. G. W.; McCoy, A.; McNicholas, S. J.; Murshudov, G. N.; Pannu, N. S.; Potterton, E. A.; Powell, H. R.; Read, R. J.; Vagin, A.; Wilson, K. S. Overview of the CCP4 suite and current developments. *Acta Crystallogr., Sect. D: Biol. Crystallogr.* **2011**, *67*, 235-242.
120. Emsley, P.; Cowtan, K. Coot: Model-building tools for molecular graphics. *Acta Crystallogr., Sect. D: Biol. Crystallogr.* **2004**, *60*, 2126-2132.
121. Murshudov, G. N.; Skubák, P.; Lebedev, A. A.; Pannu, N. S.; Steiner, R. A.; Nicholls, R. A.; Winn, M. D.; Long, F.; Vagin, A. A. REFMAC5 for the refinement of macromolecular crystal structures. *Acta Crystallogr., Sect. D: Biol. Crystallogr.* **2011**, *67*, 355-367.
122. Ehrst, S.; Rhee, K. Mycobacterium tuberculosis metabolism and host interaction: Mysteries and paradoxes. *Curr. Top. Microbiol. Immunol.* **2013**, *374*, 163-188.
123. Whitehouse, A. J.; Thomas, S. E.; Brown, K.; Fanourakis, A.; Chan, D. S. H.; Libardo, M. D. J.; Mendes, V.; Boshoff, H. I. M.; Floto, R. A.; Abell, C.; Blundell, T. L.; Coyne, A. G. Development of inhibitors against Mycobacterium abscessus tRNA (m1G37) methyltransferase (TrmD) using fragment-based approaches. *J. Med. Chem.* **2019**, *62*, 7210-7232.

124. Zanaletti, R.; Bettinetti, L.; Castaldo, C.; Cocconcelli, G.; Comery, T.; Dunlop, J.; Gaviraghi, G.; Ghiron, C.; Haydar, S. N.; Jow, F.; Maccari, L.; Micco, I.; Nencini, A.; Scali, C.; Turlizzi, E.; Valacchi, M. Discovery of a novel alpha-7 nicotinic acetylcholine receptor agonist series and characterization of the potent, selective, and orally efficacious agonist 5-(4-acetyl[1,4]diazepan-1-yl)pentanoic acid [5-(4-methoxyphenyl)-1H-pyrazol-3-yl] amide. *J. Med. Chem.* **2012**, *55*, 4806-4823.
125. Wuts, P. G. M.; Greene, T. W. *Greene's protective groups in organic synthesis*, 4th ed.; John Wiley & Sons: Hoboken, New Jersey, 2007; p 882.
126. Hassaneen, H. M. E. New approach to 4- and 5-aminopyrazole derivatives. *Synth. Commun.* **2007**, *37*, 3579-3588.
127. Mata, S.; Cortijo, V.; Caminati, W.; Alonso, J. L.; Sanz, M. E.; López, J. C.; Blanco, S. Tautomerism and microsolvation in 2-hydroxypyridine/2-pyridone. *J. Phys. Chem.* **2010**, *114*, 11393-11398.
128. Wender, P. A.; Beckham, S.; O'Leary, J. G. A second generation photochemically activatable dymemicin analog: A concise synthesis and DNA cleavage studies. *Synthesis* **1994**, 1278-1282.
129. Soni, A.; Dutt, A.; Sattigeri, V.; Cliffe, I. A. Efficient and selective demethylation of heteroaryl methyl ethers in the presence of aryl methyl ethers. *Synth. Commun.* **2011**, *41*, 1852-1857.
130. Lovering, F.; Bikker, J.; Humblet, C. Escape from flatland: Increasing saturation as an approach to improving clinical success. *J. Med. Chem.* **2009**, *52*, 6752-6756.
131. Lundbäck, T.; O'Brien, R.; Williams, G. *In The Mix: Simultaneous Affinity Determination for Isomers and Enantiomers*; MicroCal: Northampton, MA, USA, 2006.
132. Thomas, S. E. *Unpublished work*; Department of Biochemistry, University of Cambridge.
133. Soler, M.; Figueras, E.; Serrano-Plana, J.; González-Bártulos, M.; Massaguer, A.; Company, A.; Martínez, A.; Malina, J.; Brabec, V.; Feliu, L.; Planas, M.; Ribas, X.; Costas, M. Design, preparation, and characterization of Zn and Cu metallopeptides based on tetradentate aminopyridine ligands showing enhanced DNA cleavage activity. *Inorg. Chem.* **2015**, *54*, 10542-10558.
134. Doebelin, C.; Patouret, R.; Garcia-Ordóñez, R. D.; Chang, M. R.; Dharmarajan, V.; Kuruvilla, D. S.; Novick, S. J.; Lin, L.; Cameron, M. D.; Griffin, P. R.; Kamenecka, T. M. N-Arylsulfonyl indolines as retinoic acid receptor-related orphan receptor γ (ROR γ) agonists. *ChemMedChem* **2016**, *11*, 2607-2620.
135. Deb, I.; Das, D.; Seidel, D. Redox isomerization via azomethine ylide intermediates: N-Alkyl indoles from indolines and aldehydes. *Org. Lett.* **2011**, *13*, 812-815.
136. Zhang, Y.; Agrebi, R.; Bellows, L. E.; Collet, J.-F.; Kaeffer, V.; Gründling, A. Evolutionary Adaptation of the Essential tRNA Methyltransferase TrmD to the Signaling Molecule 3',5' -cAMP in Bacteria. *J. Biol. Chem.* **2017**, *292*, 313-327.

137. Agrawal, M.; Kharkar, P.; Moghe, S.; Mahajan, T.; Deka, V.; Thakkar, C.; Nair, A.; Mehta, C.; Bose, J.; Kulkarni-Almeida, A.; Bhedi, D.; Vishwakarma, R. A. Discovery of thiazolyl-phthalazinone acetamides as potent glucose uptake activators via high-throughput screening. *Bioorg. Med. Chem. Lett.* **2013**, *23*, 5740-5743.
138. Vonrhein, C.; Flensburg, C.; Keller, P.; Sharff, A.; Smart, O.; Paciorek, W.; Womack, T.; Bricogne, G. Data processing and analysis with the autoPROC toolbox. *Acta Crystallogr., Sect. D: Biol. Crystallogr.* **2011**, *67*, 293-302.
139. Adams, P. D.; Afonine, P. V.; Bunkóczi, G.; Chen, V. B.; Davis, I. W.; Echols, N.; Headd, J. J.; Hung, L.-W.; Kapral, G. J.; Grosse-Kunstleve, R. W.; McCoy, A. J.; Moriarty, N. W.; Oeffner, R.; Read, R. J.; Richardson, D. C.; Richardson, J. S.; Terwilliger, T. C.; Zwart, P. H. PHENIX: A comprehensive Python-based system for macromolecular structure solution. *Acta Crystallogr., Sect. D: Biol. Crystallogr.* **2010**, *66*, 213-221.
140. Nirogi, R.; Shinde, A.; Daulatabad, A.; Kambhampati, R.; Gudla, P.; Shaik, M.; Gampa, M.; Balasubramaniam, S.; Gangadasari, P.; Reballi, V.; Badange, R.; Bojja, K.; Subramanian, R.; Bhyrapuneni, G.; Muddana, N.; Jayarajan, P. Design, synthesis, and pharmacological evaluation of piperidin-4-yl amino aryl sulfonamides: Novel, potent, selective, orally active, and brain penetrant 5-HT₆ receptor antagonists. *J. Med. Chem.* **2012**, *55*, 9255-9269.
141. Kirihaara, M.; Naito, S.; Nishimura, Y.; Ishizuka, Y.; Iwai, T.; Takeuchi, H.; Ogata, T.; Hanai, H.; Kinoshita, Y.; Kishida, M.; Yamazaki, K.; Noguchi, T.; Yamashoji, S. Oxidation of disulfides with electrophilic halogenating reagents: Concise methods for preparation of thiosulfonates and sulfonyl halides. *Tetrahedron* **2014**, *70*, 2464-2471.
142. Nirogi, R. V. S.; Daulatabad, A. V.; Parandhama, G.; Mohammad, S.; Sastri, K. R.; Shinde, A. K.; Dubey, P. K. Synthesis and pharmacological evaluation of aryl aminosulfonamide derivatives as potent 5-HT(6) receptor antagonists. *Bioorg. Med. Chem. Lett.* **2010**, *20*, 4440-4443.
143. Park, A.; Lee, S. Synthesis of benzoylacetone nitriles from Pd-catalyzed carbonylation of aryl iodides and trimethylsilylacetone nitrile. *Org. Lett.* **2012**, *14*, 1118-1121.
144. Islam, S.; Larrosa, I. "On water", phosphine-free palladium-catalyzed room temperature C-H arylation of indoles. *Chem. - Eur. J.* **2013**, *19*, 15093-15096.
145. Yamamoto, T.; Furusawa, T.; Zhumagazin, A.; Yamakawa, T.; Oe, Y.; Ohta, T. Palladium-catalyzed arylation of aldehydes with bromo-substituted 1,3-diaryl-imidazoline carbene ligand. *Tetrahedron* **2015**, *19-26*, 71.
146. Slowinski, F.; Ayad, O. B.; Vache, J.; Saady, M.; Leclerc, O.; Lochead, A. Synthesis of new bridgehead substituted azabicyclo-[2.2.1]heptane and -[3.3.1]nonane derivatives as potent and selective $\alpha 7$ nicotinic ligands. *Org. Lett.* **2010**, *12*, 5004-5007.
147. Chusov, D.; List, B. Reductive amination without an external hydrogen source. *Angew. Chem., Int. Ed.* **2014**, *53*, 5199-5201.

148. Molander, G. A.; Sandrock, D. L. Aminomethylations via cross-coupling of potassium organotrifluoroborates with aryl bromides. *Org. Lett.* **2007**, *9*, 1597-1600.
149. Lueng, S. C.; Gibbons, P.; Amewu, R.; Nixon, G. L.; Pidathala, C.; Hong, W. D.; Pacorel, B.; Berry, N. G.; Sharma, R.; Stocks, P. A.; Srivastava, A.; Shone, A. E.; Charoensutthivarakul, S.; Taylor, L.; Berger, O.; Mbekeani, A.; Hill, A.; Fisher, N. E.; Warman, A. J.; Biagini, G. A.; Ward, S. A.; O'Neill, P. M. Identification, design and biological evaluation of heterocyclic quinolones targeting Plasmodium falciparum type II NADH:quinone oxidoreductase (PfNDH2). *J. Med. Chem.* **2012**, *55*, 1844-1857.
150. Reeves, J. T.; Malapit, C. A.; Buono, F. G.; Sidhu, K. P.; Marsini, M. A.; Sader, C. A.; Frandrick, K. R.; Busacca, C. A.; Senanayake, C. H. Transnitration from dimethylmalononitrile to aryl grignard and lithium reagents: A practical method for aryl nitrile synthesis. *J. Am. Chem. Soc.* **2015**, *137*, 9481-9488.
151. Leicht, H.; Huber, S.; Göttker-Schnetmann, I.; Mecking, S. Allylboration as a versatile tool for the in situ post-polymerization functionalization of 1,4-cis-poly(butadiene). *Polym. Chem.* **2016**, *7*, 7195-7198.
152. Prati, F.; Simone, A. D.; Armirotti, A.; Summa, M.; Pizzirani, D.; Scarpelli, R.; Bertozzi, S. M.; Perez, D. I.; Andrisano, V.; Perez-Castillo, A.; Monti, B.; Massenzio, F.; Polito, L.; Racchi, M.; Sabatino, P.; Bottegoni, G.; Martinez, A.; Cavalli, A.; Bolognesi, M. L. 3,4-Dihydro-1,3,5-triazin-2(1H)-ones as the first dual BACE-1/GSK-3 β fragment hits against alzheimer's disease. *ACS Chem. Neurosci.* **2015**, *6*, 1665-1682.
153. Saisaha, P.; Buettner, L.; van der Meer, M.; Hage, R.; Feringa, L.; Browne, W. R.; de Boer, J. W. Selective catalytic oxidation of alcohols, aldehydes, alkanes and alkenes employing manganese catalysts and hydrogen peroxide. *Adv. Synth. Catal.* **2013**, *355*, 2591-2603.